ISSN 1007-9327 (print)
ISSN 2219-2840 (online)

World Journal of *Gastroenterology*

World J Gastroenterol 2020 October 21; 26(39): 5911-6110

Published by Baishideng Publishing Group Inc

World Journal of Gastroenterology

Contents

Weekly Volume 26 Number 39 October 21, 2020

OPINION REVIEW

5911 Use of artificial intelligence in improving adenoma detection rate during colonoscopy: Might both endoscopists and pathologists be further helped

Sinagra E, Badalamenti M, Maida M, Spadaccini M, Maselli R, Rossi F, Conoscenti G, Raimondo D, Pallio S, Repici A, Anderloni A

REVIEW

5919 Clinical assessment and management of liver fibrosis in non-alcoholic fatty liver disease

Campos-Murguía A, Ruiz-Margáin A, González-Regueiro JA, Macías-Rodríguez RU

MINIREVIEWS

5944 Enteroscopy in children and adults with inflammatory bowel disease

Di Nardo G, Esposito G, Ziparo C, Micheli F, Masoni L, Villa MP, Parisi P, Manca MB, Baccini F, Corleto VD

5959 Artificial intelligence technique in detection of early esophageal cancer

Huang LM, Yang WJ, Huang ZY, Tang CW, Li J

ORIGINAL ARTICLE

Basic Study

5970 Polyethylene glycol 35 ameliorates pancreatic inflammatory response in cerulein-induced acute pancreatitis in rats

Ferrero-Andrés A, Panisello-Roselló A, Roselló-Catafau J, Folch-Puy E

5983 Identification of differentially expressed genes in ulcerative colitis and verification in a colitis mouse model by bioinformatics analyses

Shi L, Han X, Li JX, Liao YT, Kou FS, Wang ZB, Shi R, Zhao XJ, Sun ZM, Hao Y

5997 Herbal cake-partitioned moxibustion inhibits colonic autophagy in Crohn's disease *via* signaling involving distinct classes of phosphatidylinositol 3-kinases

Wang SY, Zhao JM, Zhou CL, Zheng HD, Huang Y, Zhao M, Zhang ZY, Wu LY, Wu HG, Liu HR

Case Control Study

6015 Single access laparoscopic total colectomy for severe refractory ulcerative colitis

Burke J, Toomey D, Reilly F, Cahill R

Retrospective Study

6027 Real-world treatment attrition rates in advanced esophagogastric cancer

Tsang ES, Lim HJ, Renouf DJ, Davies JM, Loree JM, Gill S

6037 Metastatic pattern in esophageal and gastric cancer: Influenced by site and histology

Verstegen MHP, Harker M, van de Water C, van Dieren J, Hugen N, Nagtegaal ID, Rosman C, van der Post RS

6047 Relationships of early esophageal cancer with human papillomavirus and alcohol metabolism

Inoue M, Shimizu Y, Ishikawa M, Abiko S, Shimoda Y, Tanaka I, Kinowaki S, Ono M, Yamamoto K, Ono S, Sakamoto N

6057 Dynamic contrast-enhanced magnetic resonance imaging and diffusion-weighted imaging in the activity staging of terminal ileum Crohn's disease

Wu YC, Xiao ZB, Lin XH, Zheng XY, Cao DR, Zhang ZS

Observational Study

6074 Relationship of meteorological factors and air pollutants with medical care utilization for gastroesophageal reflux disease in urban area

Seo HS, Hong J, Jung J

6087 Acute gastrointestinal injury in critically ill patients with COVID-19 in Wuhan, China

Sun JK, Liu Y, Zou L, Zhang WH, Li JJ, Wang Y, Kan XH, Chen JD, Shi QK, Yuan ST

Randomized Controlled Trial

6098 Impact of cap-assisted colonoscopy during transendoscopic enteral tubing: A randomized controlled trial

Wen Q, Liu KJ, Cui BT, Li P, Wu X, Zhong M, Wei L, Tu H, Yuan Y, Lin D, Hsu WH, Wu DC, Yin H, Zhang FM

ABOUT COVER

Editorial Board Member of *World Journal of Gastroenterology*, Dr. Sung-Chul Lim is a Distinguished Professor at the Chosun University School of Medicine. Having received his Bachelor's degree from Chosun University College of Medicine in 1987, Dr. Lim undertook his postgraduate training, first at the Graduate School of Chosun University, receiving his Master's degree in 1990, and then at the Graduate School of Chungnam National University, receiving his PhD in 1995. He became Professor and Pathologist in the Department of Pathology of Chosun University School of Medicine and Chosun University Hospital in 1996, rising to Head of the Department of Pathology in 2019. His ongoing research interests involve chemoresistance and apoptotic cell death of gastric cancer cells and inhibition of hepatic fibrogenesis. Currently, he serves as Chairperson of the Certification Committee of the Korean Society of Pathologists and Director of the Biobank of Chosun University Hospital. (L-Editor: Filipodia)

AIMS AND SCOPE

The primary aim of *World Journal of Gastroenterology* (*WJG*, *World J Gastroenterol*) is to provide scholars and readers from various fields of gastroenterology and hepatology with a platform to publish high-quality basic and clinical research articles and communicate their research findings online. *WJG* mainly publishes articles reporting research results and findings obtained in the field of gastroenterology and hepatology and covering a wide range of topics including gastroenterology, hepatology, gastrointestinal endoscopy, gastrointestinal surgery, gastrointestinal oncology, and pediatric gastroenterology.

INDEXING/ABSTRACTING

The *WJG* is now indexed in Current Contents®/Clinical Medicine, Science Citation Index Expanded (also known as SciSearch®), Journal Citation Reports®, Index Medicus, MEDLINE, PubMed, PubMed Central, and Scopus. The 2020 edition of Journal Citation Report® cites the 2019 impact factor (IF) for *WJG* as 3.665; IF without journal self cites: 3.534; 5-year IF: 4.048; Ranking: 35 among 88 journals in gastroenterology and hepatology; and Quartile category: Q2.

RESPONSIBLE EDITORS FOR THIS ISSUE

Production Editor: *Yu-Jie Ma*; **Production Department Director:** *Xiang Li*; **Editorial Office Director:** *Ze-Mao Gong*.

NAME OF JOURNAL
World Journal of Gastroenterology

ISSN
ISSN 1007-9327 (print) ISSN 2219-2840 (online)

LAUNCH DATE
October 1, 1995

FREQUENCY
Weekly

EDITORS-IN-CHIEF
Andrzej S Tarnawski, Subrata Ghosh

EDITORIAL BOARD MEMBERS
http://www.wjgnet.com/1007-9327/editorialboard.htm

PUBLICATION DATE
October 21, 2020

INSTRUCTIONS TO AUTHORS
https://www.wjgnet.com/bpg/gerinfo/204

GUIDELINES FOR ETHICS DOCUMENTS
https://www.wjgnet.com/bpg/GerInfo/287

GUIDELINES FOR NON-NATIVE SPEAKERS OF ENGLISH
https://www.wjgnet.com/bpg/gerinfo/240

PUBLICATION ETHICS
https://www.wjgnet.com/bpg/GerInfo/288

PUBLICATION MISCONDUCT
https://www.wjgnet.com/bpg/gerinfo/208

ARTICLE PROCESSING CHARGE
https://www.wjgnet.com/bpg/gerinfo/242

STEPS FOR SUBMITTING MANUSCRIPTS
https://www.wjgnet.com/bpg/GerInfo/239

ONLINE SUBMISSION
https://www.f6publishing.com

E-mail: bpgoffice@wjgnet.com https://www.wjgnet.com

World Journal of Gastroenterology

Submit a Manuscript: https://www.f6publishing.com

World J Gastroenterol 2020 October 21; 26(39): 5911-5918

DOI: 10.3748/wjg.v26.i39.5911

ISSN 1007-9327 (print) ISSN 2219-2840 (online)

OPINION REVIEW

Use of artificial intelligence in improving adenoma detection rate during colonoscopy: Might both endoscopists and pathologists be further helped

Emanuele Sinagra, Matteo Badalamenti, Marcello Maida, Marco Spadaccini, Roberta Maselli, Francesca Rossi, Giuseppe Conoscenti, Dario Raimondo, Socrate Pallio, Alessandro Repici, Andrea Anderloni

ORCID number: Emanuele Sinagra 0000-0002-8528-0384; Matteo Badalamenti 0000-0002-95439862; Marcello Maida 0000-0002-4992-9289; Marco Spadaccini 0000-0003-3909-9012; Roberta Maselli 0000000172919110; Francesca Rossi 0000-0003-3213-2617; Giuseppe Conoscenti 0000-0002-0349-5235; Dario Raimondo 0000-0003-4156-3435; Socrate Pallio 0000-0002-0787-2640; Alessandro Repici 0000-0002-1621-6450; Andrea Anderloni 0000-0002-1021-0031.

Author contributions: Sinagra E designed the study; Sinagra E, Badalamenti M, Maida M, Spadaccini M, Maselli R, Rossi F and Conoscenti G wrote the paper; Pallio S, Raimondo D, Anderloni A and Repici A supervised the work.

Conflict-of-interest statement: Authors declare no conflict of interests for this article.

Emanuele Sinagra, Francesca Rossi, Giuseppe Conoscenti, Dario Raimondo, Gastroenterology and Endoscopy Unit, Fondazione Istituto San Raffaele Giglio, Cefalù 90015, Italy

Matteo Badalamenti, Marco Spadaccini, Roberta Maselli, Alessandro Repici, Andrea Anderloni, Digestive Endoscopy Unit, Division of Gastroenterology, Humanitas Clinical and Research Center IRCCS, Rozzano 20089, Italy

Marcello Maida, Gastroenterology and Endoscopy Unit, S. Elia-Raimondi Hospital, Caltanissetta 93100, Italy

Socrate Pallio, Endoscopy Unit, AOUP Policlinico G. Martino, Messina 98125, Italy

Corresponding author: Emanuele Sinagra, MD, PhD, Senior Researcher, Gastroenterology and Endoscopy Unit, Fondazione Istituto San Raffaele Giglio, Contrada Pietra Pollastra Pisciotto, Cefalù 90015, Italy. emanuelesinagra83@googlemail.com

Abstract

Colonoscopy remains the standard strategy for screening for colorectal cancer around the world due to its efficacy in both detecting adenomatous or pre-cancerous lesions and the capacity to remove them intra-procedurally. Computer-aided detection and diagnosis (CAD), thanks to the brand new developed innovations of artificial intelligence, and especially deep-learning techniques, leads to a promising solution to human biases in performance by guarantying decision support during colonoscopy. The application of CAD on real-time colonoscopy helps increasing the adenoma detection rate, and therefore contributes to reduce the incidence of interval cancers improving the effectiveness of colonoscopy screening on critical outcome such as colorectal cancer related mortality. Furthermore, a significant reduction in costs is also expected. In addition, the assistance of the machine will lead to a reduction of the examination time and therefore an optimization of the endoscopic schedule. The aim of this opinion review is to analyze the clinical applications of CAD and artificial intelligence in colonoscopy, as it is reported in literature, addressing evidence, limitations, and future prospects.

Key Words: Colonoscopy; Artificial intelligence; Adenoma detection rate; Pathology;

Manuscript source: Invited manuscript

Received: July 27, 2020
Peer-review started: July 27, 2020
First decision: August 8, 2020
Revised: August 18, 2020
Accepted: September 23, 2020
Article in press: September 23, 2020
Published online: October 21, 2020

P-Reviewer: Cheng X, Coghlan E
S-Editor: Zhang L
L-Editor: A
P-Editor: Ma YJ

Endoscopy; Computer-aided detection and diagnosis

Core Tip: Artificial intelligence is an emerging technology which application is rapidly increasingin numerous medical fields. The several applications of artificial intelligence in gastroenterology are showing promising results, especially in the setting of gastrointestinal oncology. Among these, the techniques able to increase the Adenoma detection rate will play a key role in reducing the colorectal cancer incidence and its related mortality caused by undetected or missclassified interval cancers. Furthermore, a significant reduction in costs is also expected. In addition the assistance of the Computer-aided detection and diagnosis systems will lead to a reduction of the examination time and therefore an optimization of the endoscopic schedule.

Citation: Sinagra E, Badalamenti M, Maida M, Spadaccini M, Maselli R, Rossi F, Conoscenti G, Raimondo D, Pallio S, Repici A, Anderloni A. Use of artificial intelligence in improving adenoma detection rate during colonoscopy: Might both endoscopists and pathologists be further helped. *World J Gastroenterol* 2020; 26(39): 5911-5918
URL: https://www.wjgnet.com/1007-9327/full/v26/i39/5911.htm
DOI: https://dx.doi.org/10.3748/wjg.v26.i39.5911

INTRODUCTION

Colorectal cancer (CRC) is a major healthcare issue all over the world. It is the third most common cancer in males and second in females, and the fourth cause for cancer death worldwide[1-3]. As of now, almost 60%-70% of recognized cases in symptomatic patients are diagnosed at an advanced stage[4]. Early stage detection would offer better outcome in terms of decreasing the disease burden[5].

Globally, colonoscopy remains the standard strategy for CRC screening due to its efficacy in both detecting adenomatous or pre-cancerous lesions and the possibility to remove them intra-procedurally[5,6]. However, the identification as well as the classification of lesions are strictly operator-dependent, human errors in this setting increases the chances of progression to CRC[6]. Although uncertain, indirect evidence highlights that endoscopists might fail to detect lesions even when within the endoscopic field of view[7-11], therefore increasing the occurrence of interval colorectal cancer, defined as a CRC diagnosed within 60 mo after a negative colonoscopy.

Computer-aided detection and diagnosis (CAD), thanks to the brand new developed innovations of artificial intelligence (AI), and especially deep-learning techniques, leads to a promising solution to human biases in performance by guarantying decision support during colonoscopy[11]. The aim of this opinion review is to analyze the clinical applications of CAD and AI in colonoscopy, as it is reported in literature, addressing evidence, limitations, and future prospects.

WHAT IS AI

CAD systems by the use of advanced AI techniques represent an innovative technology that will likely lead to a paradigm move in the field of diagnostic colonoscopy[12,13]. Since endoscopy is generally related to computer vision technology, this technique allows computers to "see" and decipher visual content[14]. Through processes of machine learning, and more recently deep learning, AI systems can be trained to recognise "normal" characteristics by connecting a gold standard to suitable images[14] (Figure 1).

Deep learning is a recent machine learning method that utilizes a deep neural network automatically extracting specific features from data without human power if a very high numbers of learning samples are available[15,16].

Initial AI development is based on creating an algorithm that uses highly accurate datasets, coded in an independently organized manner by a group of specialists[16]. This process is called the "ground-truth" setting, where the computer is prepared to

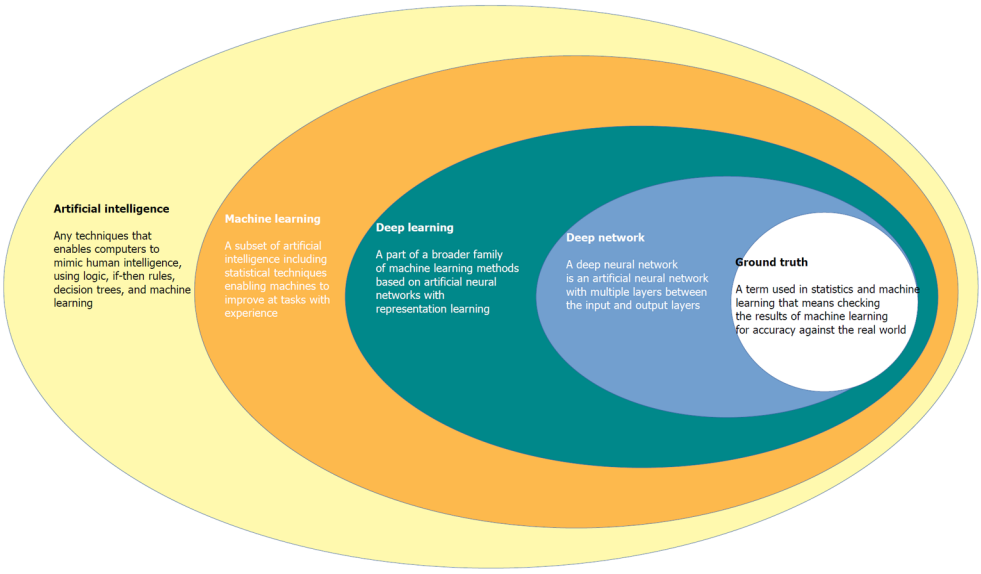

Figure 1 Interlacing of the main concept involved in the filed of artificial intelligence.

distinguish between 'abnormal' and 'normal' tissue[16]. Once an algorithm is made, deep convoluted neural networks use vast datasets to enable the algorithm to become more skilled[16]. This intelligence can extend to the algorithm becoming agnostic to manual data input and it can learn by developing its own rules and classifiers[16,17]. AI is expected to have at least 2 major roles in colonoscopy practice: Polyp detection (CADe) and polyp characterization (CADx). CADe has the potential to decrease the polyp miss rate, contributing to improve adenoma detection, whereas CADx can improve the accuracy of colorectal polyp optical diagnosis, leading to reduction of unnecessary removal of non-neoplastic lesions, potential implementation of a resect-and-discard strategy, and proper application of advanced resection techniques[17-20].

HOW COULD AI HELP IN POLYP DETECTION

Adenoma detection rate (ADR) is defined as the proportion of patients with at least one colorectal adenoma detected at first-time screening colonoscopy, among all the patients examined by an endoscopist[21]. The benchmark for ADRs is 25% overall (30% in males, 20% in females)[22] and it is reported that a 1% increase in the ADR is associated with a 3% decrease in interval CRC incidence[20]. A recent systematic review with Meta-Analysis reported that about 25% of colorectal neoplasm are missed at screening colonoscopy[18], resulting in an unacceptable variability in the key quality indicator ADR, among endoscopists[19,20].

The rationale on the working process and therefore on the aid of AI CADe system is the Deep Learning properties. CADe systems are fed with data derived from video recordings of colonoscopies that are post-hoc revised by experts. Among them, a Convolutional Neural Network (GI-genius, Medtronic) for instance was trained and validated (99.7% sensitivity, 0.9% of activation noise due to false-positive frames)[23] using a video library of 2684 Lesions that were confirmed at histology, in a high-quality clinical trial[24]. This CAD system collects input from the digital frames of the standard endoscopic processor and outputs the coordinates of a signal box only when instance of the target lesions are recognized in the image. Real-time assessment is conceived thanks to the fact that this input-output process, leading to the CADe signal on the endoscopy display, is not perceivable as a matter of time by the endoscopist, because it appears immediately (1.52 ± 0.08 μs *i.e.*, 1.52 millionth of a second)[25].

The average video recording of a 30 min colonoscopy is made of approximately 50000 frames, corresponding to 25-30 frames per second, and one polyp may be recognizable even only in few frames, explaining how failure in polyp recognition is likely to occur, irrespectively of the endoscopy setting. In this way this cutting-edge new technology could provide the essential help in decreasing the CRC incidence and related mortality. In fact, CADe systems have been recently introduced in the real-time

endoscopic setting to overcome the colossal miss lesions rate. The outcomes reported by differentmono- and multi-centric randomized clinical trials (RCTs) seem to be stronglypromising: The overall ADR of these studies was significantly higher while aided by CADe systems as shown in Table 1[25-29]. Repici *et al*[25] conducted in 2019 a multicentered study in which 700 consecutive 40 to 80 years old patients were randomized 1: 1 in CADe arm and Control. ADR was significantly higher in the CADe arm 54.8% *vs* 40.4%. They also reported the Adenoma Per Colonoscopy, that still was higher in the CADe group (1.05 ± 1.55 *vs* 0.7 ± 1.19)[25]. Wang *et al*[26] in 2019 performed an open, non-blinded trial, in which 1058 consecutive patients were prospectively randomized to undergo diagnostic colonoscopy with (n = 522) or without (n = 536) assistance of a real-time automatic polyp detection system. Thanks to the aid of AI, ADR increased from 20% to 29%[26]. Wang *et al*[26] in 2020 performed a double blind monocenter RCT enrolling 1010 patients that were randomized in a CAD aided arm (n = 508) and a Control one (n = 502), reporting an higher ADR in the CAD assisted arm: 34.1% *vs* 28%. Gong *et al*[28] in 2020 performed and RCT in which 704 patients were randomly allocated with the ENDOANGEL CADe system (n = 355) or unassisted (control) colonoscopy (n = 349). ADR was significantly higher in the CADe group: 16.7% *vs* 8.2%. Liu *et al*[29] enrolled 1026 patients in a RCT and randomized them in a Control arm (n = 518) and a CADe assisted one (n = 508), also in this case ADR was reported to be significantly higher on the CADe assisted group: 39.2% *vs* 24%. This type of AI could also help in standardizing colonoscopy regardless the operator and the endoscopic setting by eliminating the subjective biases.

HOW COULD AI HELP IN POLYP CHARACTERIZATION

In order to reduce the incidence and related mortality of CRC, there is also a major factor other than missing-lesions that need to be demolished: The accuracy of characterizing and classifying small (< 5 mm) polyps by trained endoscopists is reported to be < 80%[30]. Furthermore, the resection of non-neoplastic/hyperplastic polyps, that are almost never evolving in a malignant form, represent a financial burden, an unnecessary intervention performed on an healthy tissue, and both the resection or/and the observation of these irrelevant polyps represent an unnecessary waste of time[31]. Recently, CADx system AI for polyp characterization and diagnosis, optical biopsy and histology prediction classificationhas been developed by multiple groups that used computational analysis to predict polyp histology[32-34]. CADx are applications of AI where the system helps the physician in interpreting the content of a medical image by assigning a label to the image itself. Consequently, AI systems that support the real time optical biopsy by providing the classification of a colon polyp into a category (*e.g.*, adenoma, hyperplastic, *etc.*) are CADx. The Convolutional Neural Networks that are able to perform such task are called image classifiers, and the research in this field has been extremely active in the past five years. Both accuracy, sensitivity, specificity, positive predictive value and negative predictive value (NPV) as well as feasibility of these systems have been recently described: Aihara *et al*[35] initially published a prospective study of 32 patients with 102 colorectal lesions, with the use of CAD to differentiate neoplastic from non-neoplastic lesions using a CADx system that enables "real-time" color analysis of colorectal lesions when applied to autofluorescence endoscopy to perform color-tone sampling aiming to the reduction of unnecessary treatments for non-neoplastic lesions; all lesions greater than 5 mm were endoscopically removed and lesions less than 5 mm were biopsied. They concluded that lesions with a green/red ratio of less than 1.01 were neoplastic while those above that cut-off were considered non-neoplastic, with sensitivity, specificity and NPV of 94.2%, 88.9% and 85.2% respectively[35]. Kuiper *et al*[36] used a system called WavSTAT for real-time optical diagnosis based on laser-induced autofluorescence spectroscopy on 87 patients with 207 small (< 10 mm) colorectal lesions. During colonoscopy, the endoscopists tried to differenciate real-time adenomas *vs* non-adenomas as a low or high confidence call. Then, all lesions were analyzed using the system. Histopathology was used as the reference standard. The accuracy and NPV of WavSTAT were 74.4% and 73.5% respectively for WavSTAT alone, while they were 79.2% and 73.9% respectively combining WavSTAT with high resolution endoscopy[36]. The study concluded that it did not fulfill the American Society of Gastrointestinal Endoscopy (ASGE) performance thresholds for the assessment of diminutive and small lesions. Rath *et al*[37] used the WavSTAT4 optical biopsy forceps system designed by Spectrascience Inc, San Diego, California, United States. For prediction of histology using laser-induced autofluorescence spectroscopy on 27 patients with 137 diminutive

Table 1 The overall adenoma detection rate of these studies was significantly higher while aided by computer aided detection systems

Ref.	Study type	CADe system	ARM	ADR
Repici *et al*[25], 2020	Multicenter RCT	GI Genius	WL	40, 40%
			CADe	54, 80%
Wang *et al*[26], 2019	Monocenter RCT	Endoscreener	WL	20%
			CADe	29%
Wang *et al*[27], 2020	Monocenter RCT	Endoscreener	WL	28%
			CADe	34, 10%
Gong *et al*[28], 2020	Monocenter RCT	ENDOANGEL	WL	8, 20%
			CADe	16, 70%
Liu *et al*[29], 2020	Monocenter RCT	HenanTongyu	WL	24%
			CADe	39, 20%

WL: White light; RCT: Randomized clinical trial; CADe: Computer aided detection; ADR: Adenoma detection rate.

(≤ 5 mm) polyps[37]. The accuracy was 84.7% along with sensitivity of 81.8%, specificity of 85.2% and NPV of 96.1%. They concluded that this new WavSTAT4 systemhad the potential to meet the ASGE thresholds for the "resect and discard" strategy. Kominami *et al*[38] used a narrow band imaging (NBI) magnification colonoscopy system for CAD real-time image recognition system with a support vector machine outputof colorectal polyps histology on 41 patients with 118 colorectal lesions[38]. Concordance between the endoscopists and CAD was 97.5%. The accuracy, sensitivity, specificity, positive predictive value and NPV were 93.2%, 93%, 93.3%, 93% and 93.3% respectively, concluding that this CAD system may satisfy the Preservation and Incorporation of Valuable Endoscopic Innovations committee recommendations of ASGE for the resect and discard strategy. Mori *et al*[39] used × 520 ultramagnifying colonoscopes providing microvascular and cellular visualization of colorectal polyps after application of NBI and methylene blue staining modes to assess the performance of real-time CAD. To assist with CAD and characterization in 325 patients with 466 diminutive polyps. The accuracy was 98.1% with a NPV of 96.4% and 96.5% for methylene blue staining modes and NBI modes respectively. They concluded that their CAD system can achieve the thresholds of preservation and incorporation of valuable endoscopic innovations for diminutive, non-neoplastic rectosigmoid polyps[39]. Study data are reported in Table 2. Given the novelty of this type of AI, there is still a lack of Randomized Clinical Trials that would be needed to define the exact efficacy of CADx system.

Anyhow, these technologies are rapidly evolving andare expected also to lead to a reduction of the costs related to unnecessary polypectomy, "resect and discard" and perhaps, in the future, to substitute completely the pathological examination of the resected tissue, therefore defining the specific histological characteristic and related malignancy potential as well as potential consequent follow ups immediately, during colonoscopy itself. In addition, most of the proposed AI are aiming to create a system which is able to write automatic endoscopic report. The main advantages of developing this aspect would increase the accuracy of the report itself that nowadays can stillbe compromised by the subjectivity bias of different endoscopists both in describing location and characteristics of the polyps, such as dimensions or pit pattern *etc*. In this way, we would expect that this technology would help standardizing characterization real-time of the lesions, and the endoscopic reports as well. The automatic report would also help the endoscopist to avoid time wasting in the writing of the report and could therefore also increase the rate of endoscopic exams and interventions performed by the digestive endoscopic unit.

CONCLUSION

AI is an emerging technology which application is rapidly increasing in numerous medical fields. The several applications of AI in gastroenterology are showing promising results, especially in the setting of gastrointestinal oncology. Among these,

Table 2 Computer-aided detection and diagnosis system can achieve the thresholds of preservation and incorporation of valuable endoscopic innovations for diminutive, non-neoplastic rectosigmoid polyps

Ref.	Target	System	Performance	Year	Country
Aihara *et al*[35]	All polyps (*n* = 102)	AFE	Sensitivity: 94.2 % Specificity: 88.9% NPV: 85.2%	2013	Japan
Kuiper *et al*[36]	< 10 mm polyps (*n* = 207)	WAVSTAT, WAVSTAT + HRE	Accuracy: 74.4% Accuracy + HRE: 79.2% NPV: 73.5% NPV + HRE: 73.9 %	2015	Netherlands
Rath *et al*[37]	≤ 5 mm polyps (*n* = 137)	WAVSTAT4 + LIFS	Accuracy: 84.7% Sensitivity: 81.8% Specificity: 85.2% NPV: 96.1%	2016	Germany
Kominami *et al*[38]	All polyps (*n* = 118)	NBI	Concordance: 97.5% Accuracy: 93.2 % Sensitivity: 93% Specificity: 93.3% PPV: 93% NPV: 93.3%	2016	Japan
Mori *et al*[39]	≤ 5 mm polyps (*n* = 466)	EC-NBI-CAD EC-MB-CAD	Accuracy: 98.1% NPV EC-NBI-CAD:96.5% NPV EC-MB-CAD: 96.4%	2018	Japan

NBI: Narrow band imaging; CAD: Computer-aided detection and diagnosis; NPV: Negative predictive value.

the techniques able to increase the ADR will play a key role in reducing the CRC incidence and its related mortality caused by undetected or misclassified interval cancers. Furthermore, a significant reduction in costs is also expected. In addition, the assistance of the machine will lead to a reduction of the examination time and therefore an optimization of the endoscopic schedule.

Moreover, the resect and discharge policy, supported by good sensitivity and specificity, will lead to decrease the direct costs of unnecessary polypectomies. Furthermore, greater diagnostic accuracy in identifying pre-neoplastic and neoplastic lesions will lead to a reduction in the secondary costs of the prevented neoplasms.

Despite the promising results, AI techniques for detection and identification of colorectal lesions, need to be furtherly investigated in the near future. In particular, since most of results come from trials performed in highly specialized centers, representing a limitation for the generalizability of results, they must be also confirmed in clinical practice.

Finally, the integration of AI in a human-base medicine setting has to be taken into consideration: AI is not conceived, nor now, not ever, to substitute the endoscopist, on the contrary, it seems to be an extremely helpful tool to be used from the endoscopist himself that, given his ability and skills, is the only one able to process and interpret all the AI information to make decisions on the patient management.

REFERENCES

1 **Global Burden of Disease Cancer Collaboration**, Fitzmaurice C, Dicker D, Pain A, Hamavid H, Moradi-Lakeh M, MacIntyre MF, Allen C, Hansen G, Woodbrook R, Wolfe C, Hamadeh RR, Moore A, Werdecker A, Gessner BD, Te Ao B, McMahon B, Karimkhani C, Yu C, Cooke GS, Schwebel DC, Carpenter DO, Pereira DM, Nash D, Kazi DS, De Leo D, Plass D, Ukwaja KN, Thurston GD, Yun Jin K, Simard EP, Mills E, Park EK, Catalá-López F, deVeber G, Gotay C, Khan G, Hosgood HD 3rd, Santos IS, Leasher JL, Singh J, Leigh J, Jonas JB, Sanabria J, Beardsley J, Jacobsen KH, Takahashi K, Franklin RC, Ronfani L, Montico M, Naldi L, Tonelli M, Geleijnse J, Petzold M, Shrime MG, Younis M, Yonemoto N, Breitborde N, Yip P, Pourmalek F, Lotufo PA, Esteghamati A, Hankey GJ, Ali R, Lunevicius R, Malekzadeh R, Dellavalle R, Weintraub R, Lucas R, Hay R, Rojas-Rueda D, Westerman R, Sepanlou SG, Nolte S, Patten S, Weichenthal S, Abera SF, Fereshtehnejad SM, Shiue I, Driscoll T, Vasankari T, Alsharif U, Rahimi-Movaghar V, Vlassov VV, Marcenes WS, Mekonnen W, Melaku YA, Yano Y, Artaman A, Campos I, MacLachlan J, Mueller U, Kim D, Trillini M, Eshrati B, Williams HC, Shibuya K, Dandona R, Murthy K, Cowie B, Amare AT, Antonio CA, Castañeda-Orjuela C, van Gool CH, Violante F, Oh IH, Deribe K, Soreide K, Knibbs L, Kereselidze M, Green M, Cardenas R, Roy N, Tillmann T, Li Y, Krueger H, Monasta L, Dey S, Sheikhbahaei S, Hafezi-Nejad N, Kumar GA, Sreeramareddy CT, Dandona L, Wang H, Vollset SE, Mokdad A, Salomon JA, Lozano R, Vos T, Forouzanfar M, Lopez A, Murray C, Naghavi M. The Global Burden of Cancer 2013. *JAMA Oncol* 2015; **1**: 505-527 [PMID: 26181261 DOI: 10.1001/jamaoncol.2015.0735]

2 **Torre LA**, Bray F, Siegel RL, Ferlay J, Lortet-Tieulent J, Jemal A. Global cancer statistics, 2012. *CA Cancer J Clin* 2015; **65**: 87-108 [PMID: 25651787 DOI: 10.3322/caac.21262]

3 **Maida M**, Morreale G, Sinagra E, Ianiro G, Margherita V, Cirrone Cipolla A, Camilleri S. Quality measures improving endoscopic screening of colorectal cancer: a review of the literature. *Expert Rev Anticancer Ther* 2019; **19**: 223-235 [PMID: 30614284 DOI: 10.1080/14737140.2019.1565999]

4 **Mandel JS**, Bond JH, Church TR, Snover DC, Bradley GM, Schuman LM, Ederer F. Reducing mortality from colorectal cancer by screening for fecal occult blood. Minnesota Colon Cancer Control Study. *N Engl J Med* 1993; **328**: 1365-1371 [PMID: 8474513 DOI: 10.1056/NEJM199305133281901]

5 **Maida M**, Macaluso FS, Ianiro G, Mangiola F, Sinagra E, Hold G, Maida C, Cammarota G, Gasbarrini A, Scarpulla G. Screening of colorectal cancer: present and future. *Expert Rev Anticancer Ther* 2017; **17**: 1131-1146 [PMID: 29022408 DOI: 10.1080/14737140.2017.1392243]

6 **Corley DA**, Jensen CD, Marks AR, Zhao WK, Lee JK, Doubeni CA, Zauber AG, de Boer J, Fireman BH, Schottinger JE, Quinn VP, Ghai NR, Levin TR, Quesenberry CP. Adenoma detection rate and risk of colorectal cancer and death. *N Engl J Med* 2014; **370**: 1298-1306 [PMID: 24693890 DOI: 10.1056/NEJMoa1309086]

7 **Thakkar S**, Carleton NM, Rao B, Syed A. Use of Artificial Intelligence-Based Analytics From Live Colonoscopies to Optimize the Quality of the Colonoscopy Examination in Real Time: Proof of Concept. *Gastroenterology* 2020; **158**: 1219-1221. e2 [PMID: 31945357 DOI: 10.1053/j.gastro.2019.12.035]

8 **Crockett SD**, Gourevitch RA, Morris M, Carrell DS, Rose S, Shi Z, Greer JB, Schoen RE, Mehrotra A. Endoscopist factors that influence serrated polyp detection: a multicenter study. *Endoscopy* 2018; **50**: 984-992 [PMID: 29689571 DOI: 10.1055/a-0597-1740]

9 **McGill SK**, Kaltenbach T, Friedland S, Soetikno R. The learning curve for detection of non-polypoid (flat and depressed) colorectal neoplasms. *Gut* 2015; **64**: 184-185 [PMID: 23946382 DOI: 10.1136/gutjnl-2013-305743]

10 **Coe SG**, Crook JE, Diehl NN, Wallace MB. An endoscopic quality improvement program improves detection of colorectal adenomas. *Am J Gastroenterol* 2013; **108**: 219-26; quiz 227 [PMID: 23295274 DOI: 10.1038/ajg.2012.417]

11 **Ahmad OF**, Soares AS, Mazomenos E, Brandao P, Vega R, Seward E, Stoyanov D, Chand M, Lovat LB. Artificial intelligence and computer-aided diagnosis in colonoscopy: current evidence and future directions. *Lancet Gastroenterol Hepatol* 2019; **4**: 71-80 [PMID: 30527583 DOI: 10.1016/S2468-1253(18)30282-6]

12 **Byrne MF**, Shahidi N, Rex DK. Will Computer-Aided Detection and Diagnosis Revolutionize Colonoscopy? *Gastroenterology* 2017; **153**: 1460-1464.e1 [PMID: 29100847 DOI: 10.1053/j.gastro.2017.10.026]

13 **Ahmad OF**, Stoyanov D, Lovat LB. Human-machine collaboration: bringing artificial intelligence into colonoscopy. *Frontline Gastroenterol* 2019; **10**: 198-199 [PMID: 31205664 DOI: 10.1136/flgastro-2018-101047]

14 **Misawa M**, Kudo SE, Mori Y, Cho T, Kataoka S, Yamauchi A, Ogawa Y, Maeda Y, Takeda K, Ichimasa K, Nakamura H, Yagawa Y, Toyoshima N, Ogata N, Kudo T, Hisayuki T, Hayashi T, Wakamura K, Baba T, Ishida F, Itoh H, Roth H, Oda M, Mori K. Artificial Intelligence-Assisted Polyp Detection for Colonoscopy: Initial Experience. *Gastroenterology* 2018; **154**: 2027-2029. e3 [PMID: 29653147 DOI: 10.1053/j.gastro.2018.04.003]

15 **Tran D**, Bourdev L, Fergus R, Torresani L, Paluri M. Learning spatiotemporal features with 3d convolutional networks. Proceedings of the IEEE International Conference on Computer Vision. 2015: 4489-4497 [DOI: 10.1109/ICCV.2015.510]

16 **Alagappan M**, Brown JRG, Mori Y, Berzin TM. Artificial intelligence in gastrointestinal endoscopy: The future is almost here. *World J Gastrointest Endosc* 2018; **10**: 239-249 [PMID: 30364792 DOI: 10.4253/wjge.v10.i10.239]

17 **Vinsard DG**, Mori Y, Misawa M, Kudo SE, Rastogi A, Bagci U, Rex DK, Wallace MB. Quality assurance of computer-aided detection and diagnosis in colonoscopy. *Gastrointest Endosc* 2019; **90**: 55-63 [PMID: 30926431 DOI: 10.1016/j.gie.2019.03.019]

18 **Wieszczy P**, Regula J, Kaminski MF. Adenoma detection rate and risk of colorectal cancer. *Best Pract Res Clin Gastroenterol* 2017; **31**: 441-446 [PMID: 28842054 DOI: 10.1016/j.bpg.2017.07.002]

19 **Rex DK**, Schoenfeld PS, Cohen J, Pike IM, Adler DG, Fennerty MB, Lieb JG 2nd, Park WG, Rizk MK, Sawhney MS, Shaheen NJ, Wani S, Weinberg DS. Quality indicators for colonoscopy. *Gastrointest Endosc* 2015; **81**: 31-53 [PMID: 25480100 DOI: 10.1016/j.gie.2014.07.058]

20 **Corley DA**, Levin TR, Doubeni CA. Adenoma detection rate and risk of colorectal cancer and death. *N Engl J Med* 2014; **370**: 2541 [PMID: 24963577 DOI: 10.1056/NEJMc1405329]

21 **Zhao S**, Wang S, Pan P, Xia T, Chang X, Yang X, Guo L, Meng Q, Yang F, Qian W, Xu Z, Wang Y, Wang Z, Gu L, Wang R, Jia F, Yao J, Li Z, Bai Y. Magnitude, Risk Factors, and Factors Associated With Adenoma Miss Rate of Tandem Colonoscopy: A Systematic Review and Meta-analysis. *Gastroenterology* 2019; **156**: 1661-1674. e11 [PMID: 30738046 DOI: 10.1053/j.gastro.2019.01.260]

22 **Rex DK**, Cutler CS, Lemmel GT, Rahmani EY, Clark DW, Helper DJ, Lehman GA, Mark DG. Colonoscopic miss rates of adenomas determined by back-to-back colonoscopies. *Gastroenterology* 1997; **112**: 24-28 [PMID: 8978338 DOI: 10.1016/s0016-5085(97)70214-2]

23 **Hassan C**, Wallace MB, Sharma P, Maselli R, Craviotto V, Spadaccini M, Repici A. New artificial intelligence system: first validation study versus experienced endoscopists for colorectal polyp detection. *Gut* 2020; **69**: 799-800 [PMID: 31615835 DOI: 10.1136/gutjnl-2019-319914]

24 **Repici A**, Wallace MB, East JE, Sharma P, Ramirez FC, Bruining DH, Young M, Gatof D, Irene Mimi Canto M, Marcon N, Cannizzaro R, Kiesslich R, Rutter M, Dekker E, Siersema PD, Spaander M, Kupcinskas L, Jonaitis L, Bisschops R, Radaelli F, Bhandari P, Wilson A, Early D, Gupta N, Vieth M, Lauwers GY, Rossini M, Hassan C. Efficacy of Per-oral Methylene Blue Formulation for Screening Colonoscopy. *Gastroenterology* 2019; **156**: 2198-2207. e1 [PMID: 30742834 DOI: 10.1053/j.gastro.2019.02.001]

25 **Repici A**, Badalamenti M, Maselli R, Correale L, Radaelli F, Rondonotti E, Ferrara E, Spadaccini M, Alkandari A, Fugazza A, Anderloni A, Galtieri PA, Pellegatta G, Carrara S, Di Leo M, Craviotto V, Lamonaca L, Lorenzetti R, Andrealli A, Antonelli G, Wallace M, Sharma P, Rosch T, Hassan C. Efficacy of Real-Time Computer-Aided Detection of Colorectal Neoplasia in a Randomized Trial. *Gastroenterology* 2020; **159**: 512-520. e7 [PMID: 32371116 DOI: 10.1053/j.gastro.2020.04.062]

26 **Wang P**, Berzin TM, Glissen Brown JR, Bharadwaj S, Becq A, Xiao X, Liu P, Li L, Song Y, Zhang D, Li Y, Xu G, Tu M, Liu X. Real-time automatic detection system increases colonoscopic polyp and adenoma detection rates: a prospective randomised controlled study. *Gut* 2019; **68**: 1813-1819 [PMID: 30814121 DOI: 10.1136/gutjnl-2018-317500]

27 **Wang P**, Liu X, Berzin TM, Glissen Brown JR, Liu P, Zhou C, Lei L, Li L, Guo Z, Lei S, Xiong F, Wang H,

Song Y, Pan Y, Zhou G. Effect of a deep-learning computer-aided detection system on adenoma detection during colonoscopy (CADe-DB trial): a double-blind randomised study. *Lancet Gastroenterol Hepatol* 2020; **5**: 343-351 [PMID: 31981517 DOI: 10.1016/S2468-1253(19)30411-X]

28 **Gong D**, Wu L, Zhang J, Mu G, Shen L, Liu J, Wang Z, Zhou W, An P, Huang X, Jiang X, Li Y, Wan X, Hu S, Chen Y, Hu X, Xu Y, Zhu X, Li S, Yao L, He X, Chen D, Huang L, Wei X, Wang X, Yu H. Detection of colorectal adenomas with a real-time computer-aided system (ENDOANGEL): a randomised controlled study. *Lancet Gastroenterol Hepatol* 2020; **5**: 352-361 [PMID: 31981518 DOI: 10.1016/S2468-1253(19)30413-3]

29 **Liu WN**, Zhang YY, Bian XQ, Wang LJ, Yang Q, Zhang XD, Huang J. Study on detection rate of polyps and adenomas in artificial-intelligence-aided colonoscopy. *Saudi J Gastroenterol* 2020; **26**: 13-19 [PMID: 31898644 DOI: 10.4103/sjg.SJG_377_19]

30 **Rees CJ**, Rajasekhar PT, Wilson A, Close H, Rutter MD, Saunders BP, East JE, Maier R, Moorghen M, Muhammad U, Hancock H, Jayaprakash A, MacDonald C, Ramadas A, Dhar A, Mason JM. Narrow band imaging optical diagnosis of small colorectal polyps in routine clinical practice: the Detect Inspect Characterise Resect and Discard 2 (DISCARD 2) study. *Gut* 2017; **66**: 887-895 [PMID: 27196576 DOI: 10.1136/gutjnl-2015-310584]

31 **El Hajjar A**, Rey JF. Artificial intelligence in gastrointestinal endoscopy: general overview. *Chin Med J (Engl)* 2020; **133**: 326-334 [PMID: 31929362 DOI: 10.1097/CM9.0000000000000623]

32 **Puig I**, Kaltenbach T. Optical Diagnosis for Colorectal Polyps: A Useful Technique Now or in the Future? *Gut Liver* 2018; **12**: 385-392 [PMID: 29278867 DOI: 10.5009/gnl17137]

33 **Mori Y**, Kudo SE, Chiu PW, Singh R, Misawa M, Wakamura K, Kudo T, Hayashi T, Katagiri A, Miyachi H, Ishida F, Maeda Y, Inoue H, Nimura Y, Oda M, Mori K. Impact of an automated system for endocytoscopic diagnosis of small colorectal lesions: an international web-based study. *Endoscopy* 2016; **48**: 1110-1118 [PMID: 27494455 DOI: 10.1055/s-0042-113609]

34 **Lee BI**, Matsuda T. Estimation of Invasion Depth: The First Key to Successful Colorectal ESD. *Clin Endosc* 2019; **52**: 100-106 [PMID: 30914629 DOI: 10.5946/ce.2019.012]

35 **Aihara H**, Saito S, Inomata H, Ide D, Tamai N, Ohya TR, Kato T, Amitani S, Tajiri H. Computer-aided diagnosis of neoplastic colorectal lesions using 'real-time' numerical color analysis during autofluorescence endoscopy. *Eur J Gastroenterol Hepatol* 2013; **25**: 488-494 [PMID: 23249604 DOI: 10.1097/MEG.0b013e32835c6d9a]

36 **Kuiper T**, Alderlieste YA, Tytgat KM, Vlug MS, Nabuurs JA, Bastiaansen BA, Löwenberg M, Fockens P, Dekker E. Automatic optical diagnosis of small colorectal lesions by laser-induced autofluorescence. *Endoscopy* 2015; **47**: 56-62 [PMID: 25264763 DOI: 10.1055/s-0034-1378112]

37 **Rath T**, Tontini GE, Vieth M, Nägel A, Neurath MF, Neumann H. In vivo real-time assessment of colorectal polyp histology using an optical biopsy forceps system based on laser-induced fluorescence spectroscopy. *Endoscopy* 2016; **48**: 557-562 [PMID: 27009081 DOI: 10.1055/s-0042-102251]

38 **Kominami Y**, Yoshida S, Tanaka S, Sanomura Y, Hirakawa T, Raytchev B, Tamaki T, Koide T, Kaneda K, Chayama K. Computer-aided diagnosis of colorectal polyp histology by using a real-time image recognition system and narrow-band imaging magnifying colonoscopy. *Gastrointest Endosc* 2016; **83**: 643-649 [PMID: 26264431 DOI: 10.1016/j.gie.2015.08.004]

39 **Mori Y**, Kudo SE, Misawa M, Saito Y, Ikematsu H, Hotta K, Ohtsuka K, Urushibara F, Kataoka S, Ogawa Y, Maeda Y, Takeda K, Nakamura H, Ichimasa K, Kudo T, Hayashi T, Wakamura K, Ishida F, Inoue H, Itoh H, Oda M, Mori K. Real-Time Use of Artificial Intelligence in Identification of Diminutive Polyps During Colonoscopy: A Prospective Study. *Ann Intern Med* 2018; **169**: 357-366 [PMID: 30105375 DOI: 10.7326/M18-0249]

World Journal of Gastroenterology

Submit a Manuscript: https://www.f6publishing.com

World J Gastroenterol 2020 October 21; 26(39): 5919-5943

DOI: 10.3748/wjg.v26.i39.5919

ISSN 1007-9327 (print) ISSN 2219-2840 (online)

REVIEW

Clinical assessment and management of liver fibrosis in non-alcoholic fatty liver disease

Alejandro Campos-Murguía, Astrid Ruiz-Margáin, José A González-Regueiro, Ricardo U Macías-Rodríguez

ORCID number: Alejandro Campos-Murguía 0000-0002-2178-302X; Astrid Ruiz-Margáin 0000-0003-2779-8641; José A González-Regueiro 0000-0001-5211-4710; Ricardo U Macías-Rodríguez 0000-0002-7637-4477.

Author contributions: Macías-Rodríguez RU contributed to conception and design of the review; Campos-Murguía A, Ruiz-Margáin A, González-Regueiro JA and Macías-Rodríguez RU contributed with literature review, writing and analysis of data; Campos-Murguía A, Ruiz-Margáin A and Macías-Rodríguez RU contributed with drafting, critical revision, supervision and editing of the content of the manuscript; Campos-Murguía A, Ruiz-Margáin A, González-Regueiro JA and Macías-Rodríguez RU contributed to writing the final version of the manuscript.

Conflict-of-interest statement: All authors declare no conflicts of interest related to this article.

Alejandro Campos-Murguía, Astrid Ruiz-Margáin, José A González-Regueiro, Ricardo U Macías-Rodríguez, Department of Gastroenterology, Instituto Nacional de Ciencias Médicas y Nutrición Salvador Zubirán, Mexico City 14080, Mexico

Corresponding author: Ricardo U Macías-Rodríguez, MD, MSc, PhD, Assistant Professor, Department of Gastroenterology, Instituto Nacional de Ciencias Médicas y Nutrición Salvador Zubirán, Liver Fibrosis and Nutrition lab (LFN-Lab). MICTLÁN Network: mechanisms of liver injury, cell death and translational nutrition in liver diseases-research network. Vasco de Quiroga 15, Col. Belisario Domínguez Sección XVI, Mexico City 14080, Mexico. ricardomacro@yahoo.com.mx

Abstract

Non-alcoholic fatty liver disease (NAFLD) is among the most frequent etiologies of cirrhosis worldwide, and it is associated with features of metabolic syndrome; the key factor influencing its prognosis is the progression of liver fibrosis. This review aimed to propose a practical and stepwise approach to the evaluation and management of liver fibrosis in patients with NAFLD, analyzing the currently available literature. In the assessment of NAFLD patients, it is important to identify clinical, genetic, and environmental determinants of fibrosis development and its progression. To properly detect fibrosis, it is important to take into account the available methods and their supporting scientific evidence to guide the approach and the sequential selection of the best available biochemical scores, followed by a complementary imaging study (transient elastography, magnetic resonance elastography or acoustic radiation force impulse) and finally a liver biopsy, when needed. To help with the selection of the most appropriate method a Fagan's nomogram analysis is provided in this review, describing the diagnostic yield of each method and their post-test probability of detecting liver fibrosis. Finally, treatment should always include diet and exercise, as well as controlling the components of the metabolic syndrome, +/- vitamin E, considering the presence of sleep apnea, and when available, allocate those patients with advanced fibrosis or high risk of progression into clinical trials. The final end of this approach should be to establish an opportune diagnosis and treatment of liver fibrosis in patients with NAFLD, aiming to decrease/stop its progression and improve their prognosis.

Key Words: Non-alcoholic fatty liver disease; Liver fibrosis; Clinical assessment; Diagnosis; Treatment; Test accuracy

Manuscript source: Invited manuscript

Received: May 15, 2020
Peer-review started: May 15, 2020
First decision: May 21, 2020
Revised: May 24, 2020
Accepted: September 22, 2020
Article in press: September 22, 2020
Published online: October 21, 2020

P-Reviewer: Bodenheimer HC, Chen GX
S-Editor: Huang P
L-Editor: A
P-Editor: Wang LL

Core Tip: The most important liver-related factor associated with adverse clinical outcomes and mortality in patients with non-alcoholic fatty liver disease (NAFLD) is the presence and progression of fibrosis; its progression depends upon genetic, clinical, and biochemical risk factors, that must be assessed in order to identify patients at risk. To be able to accurately identify fibrosis we must take into account the diagnostic ability of each method and its possible variations according to the local prevalence and the selected cutoffs. This review summarizes the available data on assessment and management of NAFLD with a comprehensive analysis of the current diagnostic methods.

Citation: Campos-Murguía A, Ruiz-Margáin A, González-Regueiro JA, Macías-Rodríguez RU. Clinical assessment and management of liver fibrosis in non-alcoholic fatty liver disease. *World J Gastroenterol* 2020; 26(39): 5919-5943
URL: https://www.wjgnet.com/1007-9327/full/v26/i39/5919.htm
DOI: https://dx.doi.org/10.3748/wjg.v26.i39.5919

INTRODUCTION

Non-alcoholic fatty liver disease (NAFLD) is one of the main etiologies of cirrhosis worldwide[1], given its close relationship with features of the metabolic syndrome, including obesity and insulin resistance, NAFLD is becoming one of the most frequent and the fastest-growing cause of chronic liver disease in the world, and it is expected to grow exponentially in the following years, thus increasing the health system and economic burden[2,3].

NAFLD is defined as the accumulation of fat in the liver (> 5%), after the exclusion of other potential causes such as alcohol, viral infections, and drugs, among others. The next entity in the spectrum of the disease is non-alcoholic steatohepatitis (NASH) which is defined as the presence of hepatocellular injury and cell death, with lobular and portal inflammation. The final stages, fibrosis and cirrhosis arise as a consequence of the deposition of collagen and subsequent vascular remodeling[4,5]. Finally, within the spectrum of the disease, hepatocellular carcinoma should be included as a complication after this series of pathophysiological events.

The frequency of hepatic steatosis varies significantly according to ethnicity, being more frequent in Hispanics (45%) than in Caucasians (10%-33%) and African Americans (24%), which is probably related to the higher prevalence of obesity and insulin resistance in this ethnic group, as well as the influence of genetic factors[3,6,7]. Genetic polymorphisms in NAFLD have been identified as associated with the presence of features of the metabolic syndrome (glucose and lipid metabolism, as well as hypertension) and inflammation[8]. The prevalence of NAFLD in high-risk groups, like type 2 diabetes mellitus (T2DM) is even higher, being present in almost 70% of this group[9]. Other high-risk populations include those with hypertension, obesity, and dyslipidemia[2,10]. In terms of fibrosis, according to the National Health and Nutrition Examination Survey up to 10.3% of the patients with NAFLD have advanced fibrosis[11].

The presence of fibrosis rather than the diagnosis of steatohepatitis is the most relevant feature associated with liver-related events and overall mortality. This effect is seen even in the early stages of fibrosis, showing a stepwise increase in adverse outcomes as the stage of fibrosis progresses[11-14]. Fibrosis parallels the development of the two major components of chronic liver diseases: Portal hypertension and functional hepatocyte insufficiency. However, the importance of liver fibrosis is beyond "liver prognosis" itself, as it is associated with other adverse clinical outcomes, including cardiovascular events[15], ischemic stroke[16], metabolic complications[17], and all-cause and cardiovascular mortality[18,19]. This could be explained by a more pronounced systemic inflammation profile influencing different organs and systems, and the interaction between them leading to further inflammation and activation of the immune response.

Therefore, early recognition and proper management of liver fibrosis in NAFLD are of major importance. In this review, we will address the risk factors for NAFLD and

the risk of progression, as well as the currently available methods used to assess liver fibrosis and the new treatments available. This will help the clinicians to early recognize liver fibrosis in patients with NAFLD and use the best available methods for its evaluation and management.

DETERMINANTS OF FIBROSIS PROGRESSION

It is important to note that both biopsy-proven NASH and simple steatosis can progress to liver fibrosis, which contradicts the classic theory in which NAFLD has a benign curse while NASH has a more aggressive one[20]. Significant fibrosis can be observed in approximately one-third of patients with NAFLD in the absence of NASH[21]. The etiology of fibrosis in non-NASH patients is not entirely clear, although there are several theories; it has been hypothesized that these cases represent a form of NASH in remission as aminotransferase levels improve regardless of whether or not fibrosis progress or that T2DM by itself could be fibrogenic[22-24].

The progression of fibrosis in patients with NAFLD and NASH is variable, on average 40% have progression of fibrosis over a mean period of 3-6 years. Despite the incidence of fibrosis, the change is slow, being about 0.02 stages overall per year. There is considerable variability, with one out of six patients having a relatively rapid progression of more than 0.5 stages per year, and some patients progressing from no fibrosis to advanced fibrosis (F3-F4) on average in 12 years[23,24]. The determinants of fibrosis progression can be divided into genetic and clinical determinants.

Genetic determinants

Genetic factors are of major importance in the development[25] and the risk of fibrosis progression in NAFLD[26]. At least four genetic variants have been associated with fibrosis progression. The variant rs738409 in the human patatin-like phospholipase domain-containing 3 (PNPLA3) gene located in chromosome 22[25], is the best described and major genetic determinant of liver fibrosis development and progression in NAFLD[21,26-28]. The variant rs58542926, of the transmembrane 6 superfamily member 2 (*TM6SF2*) gene has also been implicated in de progression of fibrosis in NAFLD, however, the data is conflicting[28-30], probably due to the heterogeneity of the populations evaluated[27]. It is possible, however, that there is an additive effect of TM6SF2 and PNAPLA3 variants on the histological severity of NAFLD[27]. Finally, the rs641738 C>T genetic variant in Membrane-bound O-acyltransferase domain containing 7 (MBOAT7) and the variation in the glucokinase regulator have also been associated with higher severity of necroinflammation and fibrosis[31,32].

In a cohort of 515 patients with NAFLD, PCR-based assays were used to genotype the PNPLA3, TM6SF2, and MBOAT7 variants. The three variants were associated with increased liver injury. The TM6SF2 variant was associated predominantly with hepatic fat accumulation, whereas the MBOAT7 polymorphism was linked to fibrosis. The PNPLA3 polymorphism conferred a higher risk for both steatosis and fibrosis[33].

Clinical and environmental determinants

There are several clinical determinants of fibrosis progression in NAFLD and NASH, however, by far the presence of insulin resistance and T2DM are the major predictors of fibrosis progression[23]. Other clinical determinants of fibrosis progression rate are body mass index (BMI), sarcopenia, absence of treatment with renin-angiotensin system (RAS) inhibitors, non-obese NASH patients, alanine aminotransferase (ALT) levels above the upper limit of normal (ULN), and the severity of hepatic fat accumulation[22-24,34-36].

EVALUATION OF LIVER FIBROSIS IN NAFLD

Clinical evaluation

Most patients diagnosed with NAFLD are asymptomatic, with only a few of them complaining of mild upper quadrant pain related to fatty infiltration of the liver. Three general scenarios could arise the suspicion of NAFLD, including abnormalities on imaging performed for other reasons, abnormal liver enzymes, or based on high-risk features of NAFLD such as metabolic syndrome[37]. There are no specific signs or symptoms related to the early stages of NAFLD fibrosis, once the patient presents with

advanced fibrosis, portal hypertension or/and liver dysfunction they will develop specific symptoms of hepatic decompensation (ascites, splenomegaly, spider angiomas, palmar erythema, caput medusae, hepatic encephalopathy, and jaundice). Since most of the cases will present as NAFLD alone or mild fibrosis the physician should have a high suspicion index in patients with high-risk factors such as insulin resistance, T2DM, hypertension, obesity, and dyslipidemia. Some of the clinical hallmarks the clinician should pay attention to include acanthosis nigricans and skin tags, usually located in the lateral area around the neck and axillae, as well as hirsutism, polycystic ovary syndrome, and a high waist/hip ratio[38,39]. In the case of obstructive sleep apnea (OSA), clinical evaluation includes the presence of fatigue, sleepiness and snoring, and the use of the Epworth Sleepiness scale, measurement of neck circumference, and Mallampati scale evaluation[40]. Although these features are not specific of fibrosis, their presence should raise suspicion of a high-risk phenotype, rendering further assessment mandatory.

Blood tests and scores

Serologic tests for fibrosis detection can be divided into direct and indirect markers. Indirect markers of fibrosis aim to obtain information from the overall liver function, whereas direct serologic markers are molecules that are obtained directly from byproducts or products related to collagen deposition[37].

Indirect markers, such as routine laboratory tests are unreliable to accurately and promptly detect liver fibrosis in NAFLD unless advanced fibrosis and subsequent portal hypertension exist when thrombocytopenia and high levels of aspartate aminotransferase (AST) are observed. However, these variables provide a rather overt diagnosis, relying on the personal experience of their interpretation.

Several biomarkers have been proposed as direct markers of liver fibrosis, one of the most described is cytokeratin 18 (CK-18). Cytokeratins are proteins of keratin-containing intermediate filaments located in the intracytoplasmic cytoskeleton of epithelial tissue, being CK-18 the predominant in the liver and released as a consequence of increased apoptosis and associated with fibrosis in NASH[41]. CK-18 has been investigated as a potential biomarker of severity and liver fibrosis in different etiologies[42-44]. In NAFLD, CK-18 increased significantly with steatosis and fibrosis stages, however, it has a low sensitivity and specificity, ranging from 54% to 62% and 69% to 85%, respectively, limiting its use as a reliable diagnostic tool[43,45].

Other direct markers of liver fibrosis are collagens and their fragments since they represent the principal component of the fibrotic scars. The most validated biomarkers for the measurement of type III collagen formation are the amino-terminal propeptide of procollagen type III (PIIINP) and N-terminal pro-collagen III peptide (PRO-C3) biomarkers[46]. PRO-C3 which is a collagen fragment is significantly higher in NASH patients with advanced fibrosis than those without advanced fibrosis. PRO-C3 levels have a direct correlation with worsening of liver fibrosis, in the same manner, PRO-C3 levels decrease with fibrosis improvement, identifying patients with active fibrogenesis. It is noteworthy that patients with advanced fibrosis can have an inactive disease, implying lower production of collagen and therefore having normal levels of PRO-C3[47]. The European Liver Fibrosis project developed the enhanced liver fibrosis (ELF™) test, a blood-based score that was comprised of ELISA measurements of hyaluronic acid, PIIINP, and tissue inhibitor of matrix metalloproteinases; this score has a sensitivity and specificity for severe liver fibrosis of 78% and 76%, respectively[48].

None of the currently available biomarkers by itself has sufficient accuracy for diagnosing fibrosis which is why predictive scores play an important role in providing a cutoff able to discern between no fibrosis or the presence of advanced fibrosis. Among the predictive scores fibrosis-4 index (FIB-4) index, NAFLD fibrosis score (NFS), the BARD score, FibroTest, HepatoScore, hepamet fibrosis score (HFS), and AST to platelets ratio index (APRI) score, are the most widely used (Table 1)[49,50].

FIB-4 index: FIB-4 index is a complex marker, based on age, platelet count, AST, and ALT, it was developed in 2006 as a non-invasive panel to stage liver disease in subjects with human immunodeficiency virus and hepatitis C virus co-infection[51]. In NAFLD, a cutoff value < 1.45 has a negative predictive value (NPV) of 90% and a sensitivity of 84% to exclude advanced fibrosis. A cutoff > 3.25, had a positive predictive value (PPV) of 65% and a specificity of 68%[50,52]. This indicates that 84% of patients with suspected NAFLD-related advanced fibrosis would be identified by the FIB-4 index and avoid a liver biopsy. However, more than 30% of NAFLD patients diagnosed as non-advanced fibrosis by the FIB-4 index may have advanced fibrosis in liver biopsy. Given that about a third of patients could be misdiagnosed as non-advanced fibrosis, FIB-4 cannot replace liver biopsy[53,54].

Table 1 Diagnostic performance of blood tests and scores for fibrosis assessment methods from studies made in patients with non-alcoholic fatty liver disease

	Population (*n*)	Ref.	Cutoffs	Se	Sp	PPV	NPV	AUROC
FIB-4 (age, platelet count, AST and ALT)	541	[52]	≤ 1.3 NF	74%	71%	43%	90%	0.802
			≥ 2.67 AF	33%	98%	80%	83%	
	153	[53]	≥ 1.3 AF	87%	60%	NA	NA	0.895
	452	[56]	≥ 1.5 AF	75%	67%	58%	82%	0.780
	328	[57]	≤ 1.3 NF	56%	56%	22%	85%	0.540
			≥ 2.67 AF	22%	87%	27%	84%	
APRI (AST and platelet count)	153	[53]	> 1 AF	78%	82%	NA	NA	0.830
			> 2 AF	28%	92%	NA	NA	
	452	[56]	> 0.559 AF	62%	76%	61%	76%	0.754
NFS (age, glycaemia, BMI, platelet count, albumin, AST and ALT)	480	[55]	≤ -1.455 NAF	82%	77%	56%	93%	0.820
			≥ 0.676 AF	51%	98%	90%	85%	
	126	[58]	≤ -1.455 NAF; ≥ 0.676 AF	96%	84%	70%	98%	0.919
	138	[59]	≤ -1.455 NAF	22%	100%	100%	81%	0.680
			≥ 0.676 AF					
	452	[56]	> -1.036 AF	77%	60%	54%	81%	0.732
	328	[57]	≤ -1.455 NAF	53%	67%	26%	87%	0.640
	122	[61]	≥ 0.676 AF	9%	98%	50%	83%	0.840
				NA	NA	59%	89%	
BARD (BMI > 28 kg/m^2, AST/ALT ratio > 0.8 and diabetes)	126	[58]	0-1 NAF	89%	89%	69%	97%	0.919
			2-4 AF					
	138	[59]	0-1 NAF	51%	77%	45%	81%	0.670
			2-4 AF					
	160	[60]	0-1 NAF	NA	NA	27%	97%	0.780
			2-4 AF					
	452	[56]	2-4 AF	79%	51%	50%	80%	0.695
	122	[61]	2-4 AF	NA	NA	59%	77%	0.730
	328	[57]	2-4 AF	83%	37%	22%	91%	0.594
Fibrometer NAFLD	452	[56]	≥ 0.311 AF	80%	62%	56%	83%	0.817
Hepascore (age, sex, bilirubin, GGT, hyaluronic acid, and a2-macroglobulin)	452	[56]	≥ 0.322 AF	67%	76%	63%	79%	0.778
Fibrotest (α-2-macroglobulin, haptoglobin, apolipoprotein A1, GGT, and TB)	452	[56]	≥ 0.316 AF	81%	57%	54%	83%	0.736
HFS (sex, age, HOMA score, diabetes, AST, albumin, and platelets)	2452	[69]	< 0.12 NAF	73.9%	77.4%	46%	91.9%	0.848
			≥ 0.47 AF	35.2%	97.2%	76.3%	85.2%	
	49	[70]	≥ 0.47 AF	11%	100%	100%	83%	NA

Se: Sensitivity; Sp: Specificity; PPV: Positive predictive value; NPV: Negative predictive value; AUROC: Area under the curve; FIB-4: Fibrosis-4 index; APRI: Aspartate aminotransferase to platelet ratio index; NFS: Non-alcoholic fatty liver disease fibrosis score; HFS: Hepamet fibrosis score; AST: Aspartate aminotransferase; ALT: Alanine aminotransferase; BMI: Body mass index; GGT: Gamma-Glutamyltransferase; TB: Total bilirubin; HOMA: Homeostatic model assessment; NF: No fibrosis; AF: Advanced fibrosis; NAF: Non-advanced fibrosis; NA: Not available.

NFS score: NFS score includes age, glycemia, BMI, platelet count, albumin, AST, and ALT; unlike other prognostic scores in NAFLD which were created for other etiologies, NFS was developed in 733 patients with biopsy-proven NAFLD[55]. NFS uses two diagnostic cutoffs, the low cutoff score (-1.455) to exclude advanced fibrosis (NPV 88%-93%), and the high cutoff score (0.676) to diagnose advanced fibrosis (PPV 82%-90%)[55], leaving one-third of patients in a "grey zone" where liver biopsy is still required[56]. In further validations, NFS has remained with good NPV (81%-98%) for advanced fibrosis (F3-F4), however, PPV has had more fluctuation (50%-100%)[54,57-59].

The BARD score: BARD score is a simple index defined by the presence of three clinical and laboratory parameters, BMI (> 28 kg/m^2, 1 point), AST/ALT ratio (> 0.8, 2 points), and diabetes (1 point), ranging from 0 to 4. The BARD score was developed in 2008 in 827 patients with NAFLD. The result of the score is dichotomized as 0-1 and 2-4, for low and high risk of advanced fibrosis, respectively[60]. The PPV and NPV range from 26% to 68% and 81% to 96%, respectively[58-60]; while the sensitivity and specificity ranged from 51% to 88% and 66% to 88%, respectively[54,58,59]. The score can be easily derived from clinical data, however, as the BARD score takes into account the BMI, it may be less reliable for excluding the presence of advanced fibrosis in countries where subjects with NAFLD are not overweight or obese[61].

APRI score: This score is a simple ratio that takes into account the value of AST and platelets; it was developed in 2003 to predict liver fibrosis in patients with hepatitis C[62]. With an APRI threshold of 1.5, the sensitivity and specificity are 84.0% and 96.1%, respectively, for advanced fibrosis in NAFLD[63]. The score is a reliable tool to differentiate between patients with no fibrosis and patients with advanced fibrosis/cirrhosis, but it cannot reliably discriminate between intermediate stages of fibrosis. The area under the curve (AUROC) for the APRI score in patients with NADLF ranges from 0.8307 to 0.95[64,65].

FibroTest: FibroTest is a commercial algorithm that has shown good predictive values for diagnosing advanced fibrosis (AUROC = 0.81-0.88) in patients with NAFLD, however, its diagnostic accuracy may be affected by acute inflammation, sepsis or extrahepatic cholestasis[66,67]. This score integrates the value of five serum biomarkers (α-2-macroglobulin, haptoglobin, apolipoprotein A1, γ-glutamyltranspeptidase (GGT), and total bilirubin, adjusted for sex and age) for liver fibrosis (FibroTest), plus ALT for the necroinflammatory activity (ActiTest), into an equation-based algorithm, obtaining finally a result between 0 and 1, where higher values indicate a greater probability of liver fibrosis[68]. The AUROC to differentiate between fibrosis stages is lower, for intermediate stages, F1 *vs* F2 is 0.66 and for advanced fibrosis, F3 *vs* F4 is 0.69[67].

Hepascore: Hepascore is an algorithm to detect fibrosis in many chronic liver diseases, it combines clinical variables including age and sex with blood-based parameters such as bilirubin, gamma-glutamyl transferase, hyaluronic acid, and a-2-macroglobulin. In patients with NAFLD, a threshold of 0.37 helps to identify individuals with advanced fibrosis, with an AUROC of 0.778, NPV, and PPV of 79% and 63%, respectively[56].

Hepamet fibrosis scoring system: The HFS is the most recently developed score system, created from data of 2452 patients with biopsy proven-NAFLD at medical centers in Spain, Italy, France, Cuba, and China from the Hepamet registry. The HSF is calculated by a complex formula, using the following items: Patient sex, age, homeostatic model assessment score, presence of diabetes, AST levels, albumin, and platelet count; it is available online for public usage. HSF had an AUROC of 0.85 to discriminate between advanced fibrosis and no advanced fibrosis. In the validation cohort, a cut-off of 0.12 for low risk and 0.47 for high risk, identified patients with and without advanced fibrosis with 97.2% specificity, 74% sensitivity, a 92% NPV, and a 76.3% PPV. HFS is not affected by patient age, BMI, hypertransaminasemia, or the presence of T2DM. HFS was developed and validated in a large and heterogeneous population, giving it an advantage above other scores[69]. Recently, this score was evaluated in a cohort of 49 patients with morbid obesity undergoing bariatric surgery, a cut-off 0.47 for advanced fibrosis had a sensitivity of 11%, a specificity of 100%, a PPV of 100%, and an NPV of 83%[70].

After analyzing the data related to prediction scores, it is clear that overall, predictive scores for fibrosis have a good NPV for excluding advanced fibrosis with low PPV. Therefore, these scores may be confidently used for baseline risk stratification to exclude advanced fibrosis; however, due to their low specificity, a result of advanced fibrosis based in these scores should be further confirmed by other methods, such as imaging studies or liver biopsy depending upon availability[4].

Imaging studies

Conventional imaging studies such as ultrasonography (US), computed tomography (CT), and magnetic resonance imaging (MRI) are available techniques for the detection of fatty liver[71,72]. However, they have low to moderate accuracy to identify liver fibrosis[73,74].

Currently, elastography has become the non-invasive method of choice to quantify liver stiffness (elasticity). The basic principle is that fibrotic tissue is stiffer than normal tissue, therefore the waves spread faster in fibrotic tissue than in the normal liver. This technique uses a force to move the hepatic tissue, measuring this movement by US or MRI[75], giving the value of liver stiffness measurement (LSM) in kilopascal (kPa)[76]. The LSM obtained depends on the frequency of waves applied, therefore, it cannot be compared between different methods.

Transient elastography: One dimensional transient elastography (TE) is a non-invasive ultrasound-based method that uses shear wave velocity, providing LSM and controlled attenuation parameter (CAP) for the evaluation of steatosis. The benefit of TE compared with liver biopsy is that it measures a larger region, 100 times larger than the volume of the tissue obtained by biopsy[64]. The limitation is that occasionally measurements cannot be obtained in obese patients[49,77], reliable LSM measurements are obtained in about 80% to 90% of NASH/NAFLD patients[78,79]. It is noteworthy that at least three hours of fasting are necessary before evaluation with TE since a significant increase in LSM has been observed in patients with less than two hours of fasting[80]. In addition to this, there are quality standards that should be met to consider the result as adequate: At least 10 valid measurements (60% of success) and an IQR < 30%[81].

The cutoff value of CAP for differentiating hepatic steatosis is highly variable due to the heterogeneity of the populations evaluated, ranging from 214 to 289 dB/m, with moderate to high sensitivity and specificity (78%-91.9% and 79%-85.7%), as well as moderate to good predictive values (PPV of 77%-85.0% and NPV of 76%-92.3%)[78,82,83]. In one meta-analysis, in which 2735 patients were included, the optimal CAP cutoff was 248 dB/m, however, only 7% of the population had NAFLD diagnosis. Siddiqui *et al*[84], reported a prospective study of 393 patients with biopsy-proven NAFLD, in whom TE was performed, the median CAP scores for steatosis grades were 306 for S1 and, 340 for S2 and S3, the best cutoff, balancing sensitivity and specificity, to differentiate steatosis from no-steatosis was CAP of 285 dB/m, with a sensitivity of 80% and a specificity of 77%. It is noteworthy that the prevalence in the population, the etiology of liver disease, diabetes, and BMI deserve consideration when interpreting CAP, and perhaps lower thresholds should be applied to patients with high pretest probability, and higher thresholds in groups with low pretest probability[78].

For the detection of advanced fibrosis, TE has excellent accuracy (F3: Sensitivity 85%, specificity 82%, and F4: Sensitivity 92%, specificity 92%), whereas it has moderate accuracy for significant fibrosis (F2: Sensitivity 79%, specificity 75%)[61]. The diagnostic performance according to the AUROC values for the diagnosis of severe fibrosis and cirrhosis is good, ranging from 0.86 to 0.87; for the diagnosis of intermediate fibrosis (≥ F2), the AUROC is 0.82[85]. In general, the performance of TE is superior to prediction scores[63]. According to Siddiqui *et al*[84], a cutoff value of < 6.5 kPa excludes fibrosis with high accuracy (NPV 0.91), as well as a cutoff < 12.1 kPa excludes cirrhosis in NAFLD patients. Therefore we suggest that the cutoffs for the evaluation of steatosis and fibrosis should be the ones given by this work since the study evaluated only NAFLD patients with confirmed histology.

It is not clear if TE should be performed at defined intervals; recently a cohort of 611 patients with T2DM was followed with serial TE for 3.5 years, the majority of patients had NAFLD at baseline, and another 50% developed NAFLD during the period evaluated. Around 20% had advanced liver fibrosis at baseline, but only 4% developed advanced fibrosis in 3 years. Baseline BMI, ALT, and ΔALT independently predicted LSM increase[80]. Based on this data, we could advise performing TE every three years only in patients with risk factors such as T2DM, elevated BMI, and ALT above the UNL, otherwise, TE could be performed every 5 years.

Acoustic radiation force impulse: Acoustic radiation force impulse (ARFI) is an elastography technique that uses modified commercially available ultrasound machines, combining both elastography and conventional B-mode US. The liver is mechanically excited using short-duration acoustic pulses with a frequency of 2.67 MHz to generate localized tissue displacements in tissue[86]. Mean normal values range from 0.8 to 1.7 m/s and mean values indicating advanced fibrosis range from 1 to 3.4

m/s, with a clear overlap of values[87]. According to Fierbinteanu-Braticevici *et al*[88], the optimal cutoff value to identify advanced fibrosis is 1.54 m/s, with sensitivity and specificity of 97% and 100% respectively. In a meta-analysis of 13 studies, including 1163 patients, for detection of intermediate fibrosis (≥ F2), the summary sensitivity was 74% and the specificity was 83%, for the diagnosis of cirrhosis, the sensitivity was 87% and specificity was 87%. The diagnostic odds ratio of ARFI and TE did not differ significantly in the detection of significant fibrosis[89]. In NAFLD patients, several studies have investigated the best cutoff for the detection of advanced fibrosis, ranging from 1.15 m/s to 1.77 m/s with varying sensitivities (59%-90%) and specificities (63%-91%)[85,90-93].

Magnetic resonance elastography: Magnetic resonance elastography (MRE) is a phase contrast-based MRI technique[94] in which a passive drive generates vibrations at 60 Hz by varying acoustic pressure waves transmitted from an active driver device[95]. LSM is performed by drawing region of interest (ROI) on the elastograms, which cover regions of the liver with sufficient wave amplitude. The mean ROIs from 4 slices are averaged and reported as the mean LSM of the liver[96]. An advantage of MRE is that the area measured in the liver is larger than in TE or liver biopsy, which can avoid the sampling variability caused by the heterogeneity of advanced fibrosis[77]. The cutoff LSM for the detection of advanced fibrosis in NAFLD patients varies according to the population evaluated, ranging from 3.6 to 4.8 kPa with high sensitivity and specificity[63,77,97-99]. The diagnostic accuracy of MRE for liver fibrosis in NAFLD is higher than that of clinical scoring systems and TE[77]. A 15% increase in liver stiffness on repeated MRE may be associated with histologic fibrosis progression (≥ 1 stage) and progression from early fibrosis to advanced fibrosis[100]. Magnetic resonance also quantifies hepatic steatosis with high accuracy by measuring the proton density fat fraction which is the fraction of MRI-visible protons bound to fat divided by all protons in the liver[101].

Combined methods

Recently there have been reports of test combinations for better detection of liver fibrosis in NAFLD. The serial combination of NFS or FIB-4 with TE improves the performance of the tests when applying the second test only in patients in the uncertainty area of the first test. This algorithm is a low-cost alternative that can be applied in daily practice allowing the correct classification of a high proportion of NAFLD patients[102].

The FibroScan-AST (FAST) score, was recently proposed as a reliable algorithm to identify among patients with NAFLD, those with NASH, intermediate liver fibrosis (≥ F2), and elevated NAFLD activity score (NAS ≥ 4) (*i.e.*, those at high risk of progression of the disease). The results of the FAST score range from 0 to 1, and derive from a logarithm-based equation, considering 3 values, AST, CAP, and LSM, and are further divided into three zones, according to the value: Rule-out (≤ 0.35), gray (0.35-0.67) and rule-in (≥ 0.67). The performance of the test is good, with an AUROC of 0.85 (0.83-0.87), and a sensitivity, NPV, specificity, and PPV of 0.89, 0.94, 0.92, and 0.69, respectively[103].

Determining which method is best for the patient relies on several factors: The availability of the methods in a daily clinical care setting, the performance of the operator, the prevalence of the disease in the specific population, and the preference of the patient. As shown in some studies, a combination of non-invasive methods could help to improve the accuracy of the diagnosis.

Liver biopsy

Liver biopsy is the gold standard for the diagnosis and assessment of the severity of liver fibrosis in NAFLD[4]. In the context of NAFLD, liver biopsy is usually obtained *via* a percutaneous approach using ultrasound guidance. The use of a 16 gauge or wider needle is recommended for the biopsy. An adequate histology specimen should have at least 2 cm long and comprising 10 or more portal tracts, and the review of specimens should be carried out by two pathologists[104,105].

Specimens should be processed with hematoxylin and eosin staining and specifically with Masson's trichrome or Sirius red staining to assess fibrosis. Liver fibrosis has a singular pattern in NAFLD, frequently beginning in the pericentral zone 3 and eventually progressing to bridging fibrosis and cirrhosis[106]. There are several systems to evaluate NAFLD biopsies. The NAFLD activity score was developed as a tool to measure changes in NAFLD during therapeutic trials, the maximum score is 8, comprises steatosis (0-3), ballooning (0-2) and lobular inflammation (0-3), with a major

drawback as it does not take into account the amount of fibrosis[104]. For the evaluation of fibrosis in NAFLD, there are three scoring assessment systems, the Brunt system, the NASH Clinical Research Network (CRN) system, and the Steatosis, Activity, Fibrosis (SAF) system[107,108]. In the Brunt system, fibrosis stages are divided into four, stage 1, zone 3 perisinusoidal fibrosis; stage 2, portal fibrosis; stage 3, bridging fibrosis; and stage 4, liver cirrhosis[109]. The NASH CRN system is a modification of the Brunt system in which stage 1 is subdivided into three stages, to include a distinction between delicate (1a) and dense (1b) perisinusoidal fibrosis, and to detect portal-only fibrosis, without perisinusoidal fibrosis (stage 1c), showing reasonable interrater agreement among experienced pathologists[110]. The SAF system which includes the NASH CRN system was built from a cohort of morbidly obese patients undergoing bariatric surgery. This system separately assesses the grade of steatosis (S0 to S3), the grade of activity (A0 to A4) and the stage of fibrosis (F0 to F4), the latter according to the NASH-CRN staging system, with the single modification of pooling the three substages (1a, 1b, and 1c) into a single F1 score[111]. Some computerized techniques also have been developed for the quantification of fibrosis in NAFLD/NASH histology, representing promising and accurate methods for the evaluation of liver fibrosis in this group of patients[112,113].

Liver biopsy has some relevant inconveniences, including the fact that only 1/50000 of the whole liver tissue is sampled, therefore sampling error is a major concern. To prevent sampling error, it is important to collect a sufficient amount of tissue; the use of a thick needle and a collection of at least 2 samples are recommended[114]. Inter-observer variability of the pathologist is another important concern, for the diagnosis of liver fibrosis in NAFLD, pathologists have a moderate inter-observer agreement (κ scores of 0.52-0.56) for fibrosis stage[115], therefore, at least two pathologists should review the specimens. Finally, complications associated with percutaneous liver biopsy are rare, only 1% to 3% of patients require hospitalization and the mortality rate is extremely low, 1 in 10000 to 1 in 12000 liver biopsies[114].

Due to the high prevalence of steatosis, it is not practical to perform a liver biopsy in every patient with NAFLD. The European Association for the Study of the Liver (EASL) guidelines recommend that for the identification of advanced fibrosis or cirrhosis, serum biomarkers/scores and/or TE are less accurate, and it is important to confirm these advanced stages by liver biopsy. According to the clinical context and in selected patients at high risk of liver disease progression, monitoring should include a repeat liver biopsy after at least a 5-year follow-up[4]. The American Association for the Study of Liver Disease (AASLD) guidelines recommend performing a liver biopsy when the diagnosis is not clear (*i.e.*, there is a suspicion of another liver disease), or in those with a high probability of NASH/advanced fibrosis, especially in those considered for treatment with vitamin E or pioglitazone[116].

With the evidence above mentioned, it seems more practical to perform a liver biopsy in NAFLD only in patients with high suspicion of advanced fibrosis and/or rapid progression, when other causes of liver damage cannot be ruled out or for clinical trials exploring new-generation drugs.

Tables 1 and 2 summarize the diagnostic performance of the previously mentioned methods. It is of great importance to consider that some methods have different cutoff values, as can be seen in the table, and each cutoff holds different predictive values. This must be taken into account at the time of the patient's evaluation in the clinical practice and it is especially important to use the same cutoff if follow-up is to be done.

To further address this issue, we analyzed the diagnostic capabilities of several methods based on Fagan's nomogram, which considers the pre-test probability, or prevalence, of the disease we are looking to diagnose and, uses the likelihood ratio that derives from the sensitivity and specificity reported in published studies, to estimate a final post-test probability, which simply represents the probability of a patient truly having the condition of interest if the test is positive or truly not having the disease if the test is negative.

Figure 1A depicts the analysis of all TE studies presented in Table 2, and Figure 1B shows the MRE studies. As mentioned before, each study proposes different cutoffs, therefore it is of great importance to evaluate the behavior of each one by its post-test probability and not only by their sensitivity and specificity. In Figure 1A one can conclude that overall, the best cutoff to use is the one derived from the study by Imajo *et al*[77] where > 11.7 kPa has the highest probability to detect advance fibrosis if the patient actually has it, and the lowest probability of diagnosing it if the patient does not have advanced fibrosis. With respect to MRE studies in Figure 1B, two of the cutoffs have a great performance with a post-test probability > 80%; overall the best cutoff derives from the study of Kim *et al*[98] with a post-test probability of diagnosing advanced fibrosis of 84% in patients with the disease when the employed cutoff is >

Table 2 Diagnostic performance of imaging studies for fibrosis assessment methods from studies made in patients with non-alcoholic fatty liver disease

	Population	Ref.	Cutoffs	Se	Sp	PPV	NPV	AUROC
TE [LSM (kPA)]	*n* = 291	[85]	≥ 8.2 kPa AF	90%	61%	NA	NA	0.870
			≥ 12.5 kPa AF	57%	90%	NA	NA	NA
	452	[56]	≥ 8.7 kPa AF	88%	63%	59%	90%	0.831
	142	[77]	≥ 11.7 kPa AF	86%	84%	75%	92%	0.880
	79	[83]	≥ 9.5 kPa AF	92%	63%	54%	94%	NA
MRE [LSM (kPA)]	142	[77]	≥ 4.8 kPa AF	74%	87%	74%	81%	0.890
	628	[63]	≥ 3.6 kPa AF	86%	91%	71%	93%	NA
	117	[97]	≥ 3.63 kPa AF	81%	89%	68%	97%	NA
	142	[98]	≥ 4.15 kPa AF	85%	92%	NA	NA	0.954
	102	[99]	> 3.64 kPa AF	92%	90%	NA	NA	0.957
ARFI [SWV (m/s)]	291	[85]	≥ 1.15 AF	90%	63%	NA	NA	0.840
			≥ 1.53 AF	59%	90%	NA	NA	NA
	57	[90]	≥ 1.45 AF	76%	68%	NA	NA	0.910
	32	[91]	≥ 1.3 AF	85%	83%	NA	NA	NA
	23		≥ 1.47 AF	100%	75%	NA	NA	0.942
	NASH	[92]						
	54	[93]	≥ 1.77 AF	100%	91%	NA	NA	0.930

Se: Sensitivity; Sp: Specificity; PPV: Positive predictive value; NPV: Negative predictive value; AUROC: Area under the curve; TE: Transient elastography; MRE: Magnetic resonance elastography; ARFI: Acoustic radiation force impulse; LSM: Liver stiffness measurement; kPa: Kilopascal; SWV: Shear wave velocity; NASH: Non-alcoholic steatohepatitis; NF: No fibrosis; AF: Advanced fibrosis; NAF: Non-advanced fibrosis; NA: Not available.

4.15 kPa. Interestingly once we compare both methods in Figure 1 it is apparent that MRE has better diagnostic capabilities, hence we created a Fagan's nomogram using all the methods presented in Tables 1 and 2, to evaluate which one could diagnose or exclude AF better (Figure 2). Since the study by Boursier *et al*[56] evaluated most of the methods in their study we used those results to create the graph, for the remaining methods: MRE, HFS and AFRI, we selected the study by Xiao *et al*[63], Ampuero *et al*[69], and Cassinotto *et al*[85] respectively. The analysis of this graph shows that the best methods with higher post-test probability to detect advanced fibrosis in patients with the disease in order of detection are MRE, Hepamet fibrosis scoring system, NFS score, APRI, TE, fibrometer and FIB-4, the best methods to exclude advanced fibrosis in patients without the disease are, MRE, AFRI, Fibrometer and TE.

Finally, after a comprehensive evaluation we propose a stepwise assessment of fibrosis in NAFLD patients, according to the available data, which can be found in Figure 3.

MANAGEMENT OF LIVER FIBROSIS IN NAFLD

The appropriate management of patients with NAFLD and fibrosis should be a comprehensive treatment that takes into account three major components: The treatment of underlying metabolic diseases, weight loss (WL), and pharmacological therapy (Figure 4).

Treatment of underlying metabolic diseases

As referred before, the importance of liver fibrosis is beyond the liver prognosis[18,19]. Therefore, to improve the prognosis of patients with NAFLD and fibrosis the treatment of concomitant diseases must be a priority.

Nearly half of the patients with hypertension have concomitant NAFLD[117]. RAS seems to contribute to the development of liver fibrosis, interestingly, the

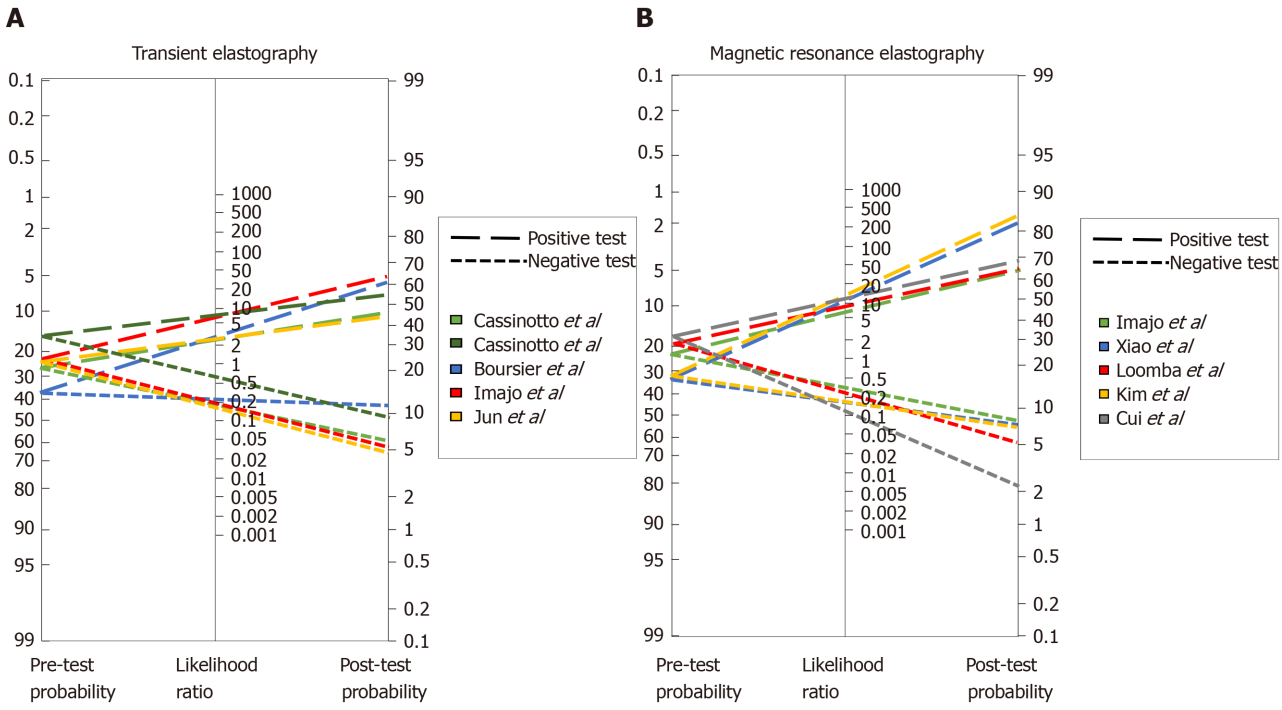

Figure 1 Fagan's nomogram for (A) transient elastography and (B) magnetic resonance elastography studies.

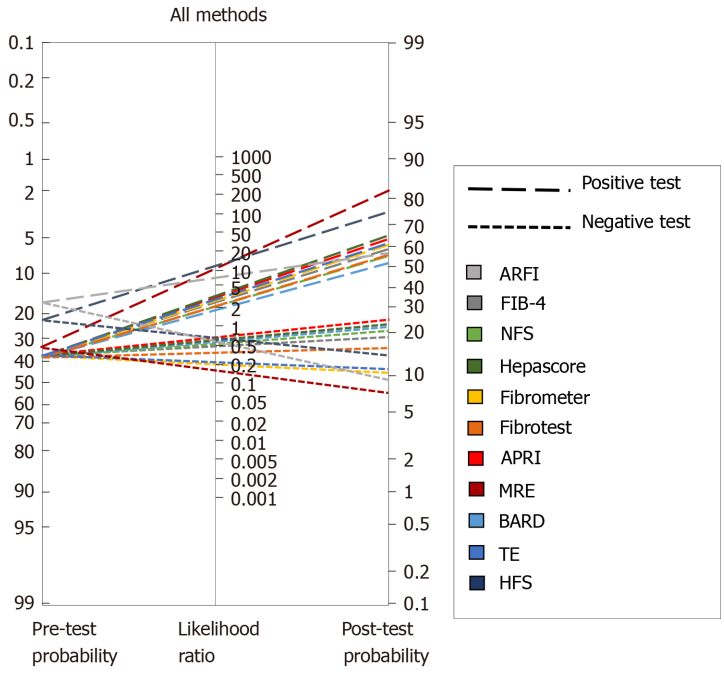

Figure 2 Fagan's nomogram for all diagnostic methods. ARFI: Acoustic radiation force impulse; FIB-4: Fibrosis-4 index; NFS: Non-alcoholic fatty liver disease fibrosis score; APRI: Aspartate aminotransferase to platelet ratio index; MRE: Magnetic resonance elastography; TE: Transient elastography; HFS: Hepamet fibrosis score.

administration of RAS inhibitors showed an improvement in liver histology and decrease in protein expression of alpha-smooth muscle actin and hepatic content of hydroxyproline in a murine model of NAFLD[118]. In a cross-sectional study in hypertensive patients with biopsy-proven NAFLD, the use of RAS blockers was associated with less advanced hepatic fibrosis suggesting a beneficial effect of RAS blockers in NAFLD[119]. A similar effect was found in a retrospective cohort of 118 NAFLD patients with paired liver biopsies, where the use of RAS inhibitors was associated with decreased fibrosis progression rate only in patients with T2DM[22]. Given these potential benefits, the high safety profile of the drugs, and the fact that

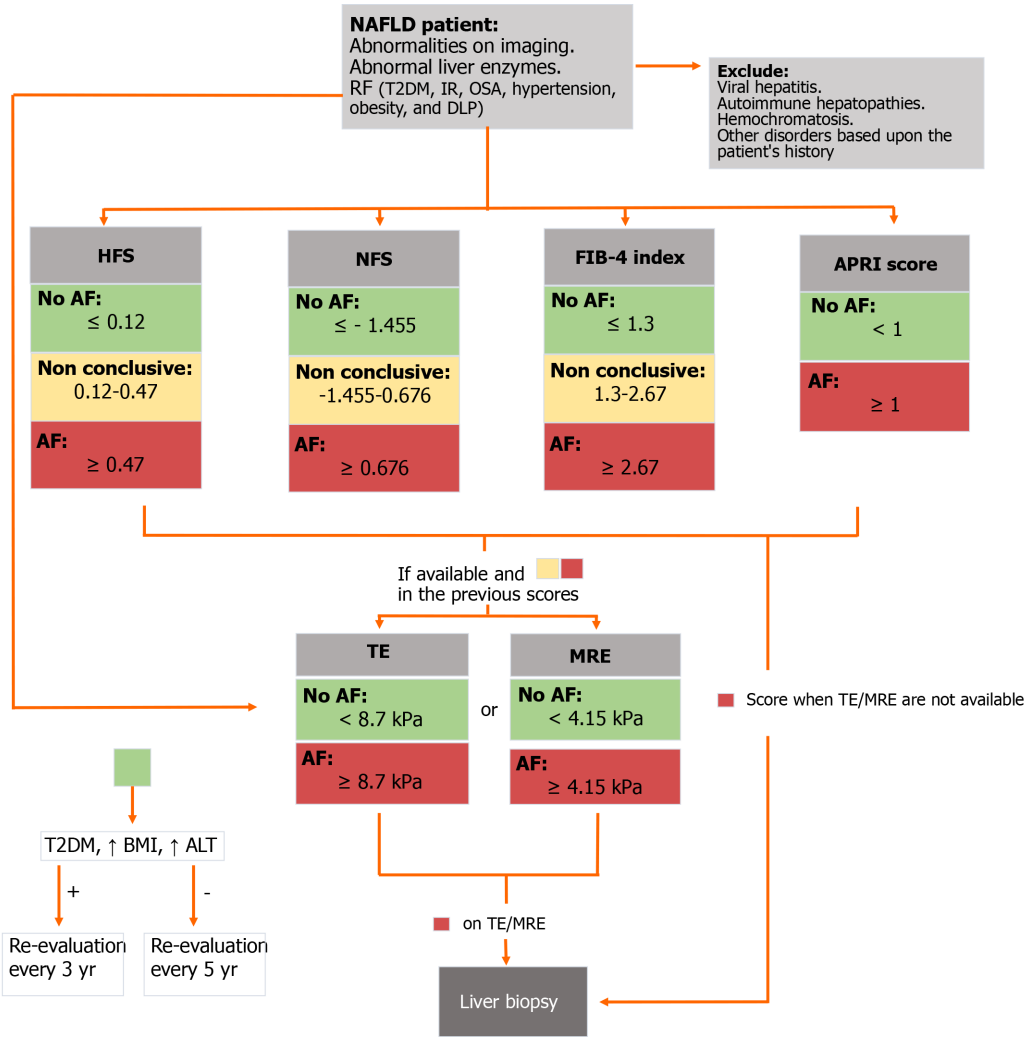

Figure 3 Diagnostic flow-chart to assess liver fibrosis in patients with non-alcoholic fatty liver disease. NAFLD: Non-alcoholic fatty liver disease; T2DM: Type 2 diabetes mellitus; IR: Insulin resistance; OSA: Obstructive sleep apnoea; DLP: Dyslipidemia; HFS: Hepamet fibrosis score; NFS: Non-alcoholic fatty liver disease fibrosis score; FIB-4: Fibrosis-4 index; APRI: Aspartate aminotransferase to platelet ratio index; AF: Advanced fibrosis; TE: Transient elastography; MRE: Magnetic resonance elastography; BMI: Body mass index; ALT: Alanine aminotransferase.

RAS blockers are one of the main classes of drugs recommended as initial therapy by hypertension guidelines[120,121], we suggest that RAS blockers should be considered as first-line therapy in patients with NAFLD and hypertension, after assessing the potential contraindications.

More than three-quarters of T2DM patients have coexistent NAFLD[9]; insulin resistance and hyperinsulinemia are the hallmarks of NAFLD and have an important role in stellate cell activation[122]. Therefore, treatment of patients with T2DM and NAFLD should be focused on improving insulin resistance. Even though metformin has not shown benefit in the histology of NAFLD, it remains the first-line drug for T2DM for its effects in the reduction of body weight, serum levels of lipids, and glucose[123,124]. Other benefits of metformin have been reported, such as the reduction in the risk of liver cancer[125,126]. Other insulin sensitizers such as dipeptidyl peptidase 4 inhibitors and glucagon-like peptide-1 analogs could also be good choices for the treatment of T2DM in patients with NAFLD[127]. Thiazolidinediones and Sodium-glucose co-transporter-2 (SGLT2) inhibitors are reviewed in the pharmacological management section[127]. Hence, insulin sensitizers should be the gold standard therapy for patients with T2DM and NAFLD.

OSA induces insulin resistance and systemic inflammation which as mentioned before are major features in NAFLD pathogenesis[128]. OSA patients should be screened for NAFLD and vice versa those with NAFLD for OSA[129]. The first-line treatment for OSA is continuous positive airway pressure (CPAP), which has several benefits, among which stand out the improvement of blood pressure and glucose resistance, and the reduction of overall and cardiovascular mortality[130-132]. The evidence of the benefit of CPAP on liver fibrosis in patients with NAFLD is scarce, at least three

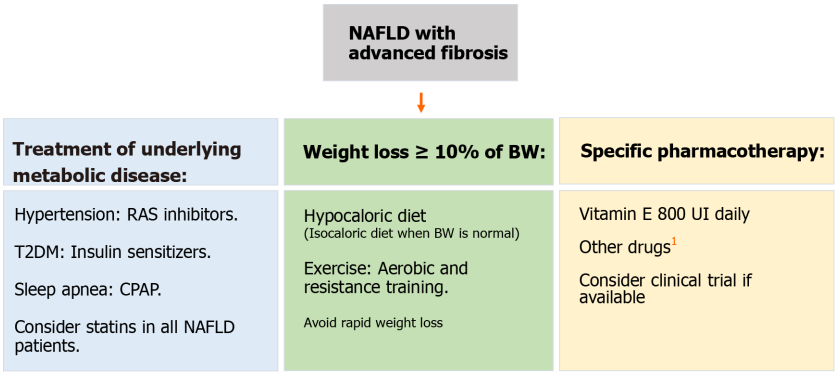

Figure 4 Management flow-chart for patients with non-alcoholic fatty liver disease advanced fibrosis. We suggest vitamin E as it has demonstrated higher transplant-free survival and lower rates of hepatic decompensation. [1]Other drugs such as cenicriviroc, obethicholic acid, dapagliflozin, and selonsertib have shown benefit in clinical trials and must be considered as well, especially as results continue to show beneficial results. NAFLD: Non-alcoholic fatty liver disease; RAS: Renin-angiotensin system; T2DM: Type 2 diabetes mellitus; CPAP: Continuous positive airway pressure; BW: Body weight.

studies have studied this, one showed improvement while the other two did not show this effect[132-134]. Longer trials may be needed to demonstrate a clear benefit. Although there is no clear evidence of a benefit to the liver in patients with OSA and NAFDL, CPAP should be encouraged in all patients with OSA.

Cardiovascular disease is one of the main causes of NAFLD-related deaths. Statins reduce NAFLD/NASH cardiovascular events, moreover, statins could reduce the risk of hepatocellular carcinoma related to NAFLD/NASH. Given these benefits and the fact that these medications have a high-security profile, they should be considered even in NAFLD patients without dyslipidemia[135,136].

Weight loss

To date, lifestyle modifications including diet and exercise are the first line and cornerstone of NAFLD/NASH treatment. Most studies have demonstrated a reduction of steatosis or/and steatohepatitis without improvement in liver fibrosis[137-143], nevertheless some have shown fibrosis regression, especially when a WL of 10% or more is achieved or when exercise therapy is included[144,145].

The Mediterranean diet (MD) with components such as fish, nuts, fruits, olive oil, whole grains, and vegetables is proposed by EASL guidelines for the treatment of NAFLD[4]. The MD has shown an inverse relationship with NAFLD prevalence and a reduction in liver steatosis[146-148]. In a non-randomized, open-label, 24-wk prospective study, 44 untreated NAFLD patients with non-significant fibrosis received nutritional counsel to increase adherence to MD with significant improvements in liver fibrosis at the end of the follow-up. It is noteworthy that the patients did not have significant fibrosis and that the technique for measurement was elastography ultrasound which could lead to unprecise data[149]. At the moment there is no evidence that diet *per se* could improve liver fibrosis, however, we must take into account that the diet that is going to have the maximum benefit is the one that will be followed by the patient in the long-term, therefore highly restrictive diets that induce a rapid WL should not be considered.

Regarding exercise, there is evidence that in selected patients with cirrhosis, moderate-intensity aerobic or resistance exercise, 4 d per week, 20 min, for at least 8 wk can have a positive physiological impact[150]. Moreover, it has been demonstrated that supervised exercise in cirrhotic patients can significantly lower the hepatic venous pressure gradient[151]. Exercise intervention studies in NAFLD are limited by low statistical power, and most have shown a reduction in intrahepatic triglyceride content without an improvement in liver fibrosis[152,153]. Few studies have shown a reduction in fibrosis, in particular, high-intensity interval training has recently been recognized as a novel exercise modality that demonstrated an improvement in liver stiffness (-16.8%), these benefits appeared to be independent of WL[154,155]. More evidence regarding the effect of exercise independently of the WL in fibrosis is required. As before concerning the diet, we consider that the exercise that is going to have the maximum impact is the one that can be maintained long-term, therefore the prescription of exercise should take into account the patients' preferences and capabilities.

Bariatric surgery could be another approach in the management of NAFLD fibrosis, possibly through improvement of insulin resistance and hyperinsulinemia, which are related to the development of fibrosis in NAFLD[122]. In this context, bariatric surgery

has proven to be an effective method for sustained WL in properly selected obese individuals[156-158], and importantly, in selected patients with T2DM, bariatric surgery is an effective therapy for glycemic control[159,160]. These changes have an additive effect considering that if 10% or more of WL is achieved with bariatric surgery, an improvement in fibrosis may be seen. There is some evidence of this benefit in retrospective and prospective cohorts with follow-up to 5 years[161-163]. Nevertheless, bariatric surgery should not be considered alone for the treatment of NAFLD fibrosis and the other indications of the procedure must be considered. The recommendation concerning this surgery in patients with advanced fibrosis must be individualized and evaluated by an experienced and interdisciplinary group[116].

Specific pharmacological management

Pharmacological management should be restricted to patients with NASH and/or advanced fibrosis. The current recommended drugs thus far in the guidelines are pioglitazone and vitamin E[4]. Although there are multiple treatments with different mechanisms of action under development for the treatment of NASH, and specifically aimed to reduce liver fibrosis, these drugs remain experimental and are considered for their use only in clinical trials.

Vitamin E is an antioxidant of polyunsaturated lipids and has a role in the treatment of NASH through antioxidant dependent and independent mechanisms[164]. In a NASH animal model, vitamin E supplementation decreased baseline levels of transforming growth factor beta 1 mRNA, suggesting a potential interference with both the initiation and progression of fibrosis[165]. Vitamin E improves transaminase activity, steatosis, inflammation, and ballooning in NASH patients[166-169]. Nevertheless, the data about its impact on liver fibrosis is controversial, several studies have shown an improvement in liver fibrosis[168-170], while others have not[124,169-172]. In the classical PIVENS study, 247 adults with NASH without T2DM were randomized to receive pioglitazone (30 mg/d), vitamin E (800 IU/d), or placebo, for 96 wk. Vitamin E therapy was associated with a significantly higher rate of improvement in NASH, with no reductions in fibrosis scores[167]. However, in a post hoc analysis, WL (≥ 2 kg) was associated with improvement on liver fibrosis scores, while weight gain (≥ 2 kg) was associated with worsening of fibrosis scores. These data reinforce the evidence-based recommendation for lifestyle modifications and WL as the basis of NASH/NAFLD treatment[116]. It is important to notice that since the PIVENS study did not include patients with T2DM[167], the evidence of Vitamin E in this group is not strong, and the few studies including T2DM have not shown benefit in liver fibrosis[173]. In a retrospective study, 90 patients with NASH and advanced fibrosis or cirrhosis consumed vitamin E (800 IU/d) for ≥ 2 years and were propensity-matched to 90 adults who did not take vitamin E, with a median follow-up was 5.6 years; vitamin E users had higher adjusted transplant-free survival, lower rates of hepatic decompensation than controls, and these benefits were evident in both, with and without T2DM patients[174]. There are some concerns with regard to the safety of vitamin E supplementation. A large long-term randomized trial (SELECT trial) showed a slight increase risk of prostate cancer in patients with vitamin E supplementation (Hazard ratio: 1.17; CI: 1.004-1.36)[175]. Furthermore, another large study associated vitamin E with an increased risk of hemorrhagic stroke, also with a marginal increment (Relative risk 1.22, 1.00-1.48)[176]. The significance of these side effects is not entirely clear since large-scale population studies tend to find statistical differences without clinical relevance, nevertheless, vitamin E must be prescribed with caution in high-risk groups.

Pioglitazone has a role in the treatment of NASH through modulation by an adiponectin-mediated effect on insulin sensitivity and hepatic fatty acid metabolism, as well as acting as a PPAR (gamma with Greek letter)[177]. Like vitamin E, pioglitazone has shown conflicting evidence regarding the reduction of fibrosis. The PIVENS study did not show an improvement[167], while two other randomized studies in diabetic and non-diabetic patients showed a reduction in liver fibrosis[171,172]. Cusi *et al*[172], studied 101 patients with prediabetes or T2DM and NASH, all patients were prescribed a hypocaloric diet and then randomly assigned to pioglitazone (45 mg/d), or placebo for 18 mo, followed by an 18-mo open-label phase with pioglitazone treatment. The pioglitazone group had improvement in the mean fibrosis score, however, this treatment was associated with significant weight gain, suggesting that pioglitazone could alter the natural history of the disease.

Cenicriviroc (CVC) is a dual antagonist of CCR2 and CCR5. CVC significantly reduced monocyte/macrophage recruitment and collagen deposition in animal models of fibrosis[178]. The CENTAUR study, a multicenter phase 2b clinical trial, randomized 289 patients to receive CVC (150 mg/d) or placebo for 12 mo, showed no

differences in NAS score between the CVC and placebo group, however, twice as many subjects on CVC achieved a reduction in the fibrosis stage (1 stage) with no worsening of steatohepatitis compared to those on placebo; this benefit was seen across all stages of fibrosis, particularly for stage 2 and 3[179]. Based on the prior results, a large phase 3 trial, the AURORA study, is currently recruiting patients with NASH and histopathological evidence of stage 2 or 3 liver fibrosis to evaluate the benefit of CVC on the improvement in fibrosis and determine long-term clinical outcomes[180].

Obeticholic acid (OCA), is a farnesoid-X receptor (FXR) agonist[181]. FXR is a nuclear hormone receptor that regulates glucose and lipid metabolism. In a double-blind, placebo-controlled, proof-of-concept study in patients with NAFLD and T2DM, OCA increased insulin sensitivity and decreased significantly markers of liver fibrosis, nevertheless, no histopathology was obtained[182]. The FLINT study, a multicenter, randomized, placebo-controlled trial in non-cirrhotic NASH patients to assess treatment with OCA (25 mg/d) or placebo for 72 wk. OCA improved fibrosis, hepatocellular ballooning, steatosis, and lobular inflammation when compared with placebo[183]. Finally, in a recent multicenter double-blind, placebo-controlled study, 1968 patients with stage F1-F3 fibrosis (931 with F2-F3) were randomized to receive oral placebo, OCA 10 mg, or OCA 25 mg daily for 18 mo; an improvement of at least 1 stage of liver fibrosis was observed in 18% of the 10 mg group, and 23% in the 25 mg group, however, mild to moderate pruritus was reported in half of the patients with 25 mg of OCA[184]. A baseline NAS > 5, baseline triglyceride level 154 mg/dL, baseline INR 1, baseline AST level 49 U/L, and decrease in ALT level at week 24, were significant predictors of histologic response in NASH patients treated with OCA[185]. Tropifexor is another FXR agonist[186]. In a murine model, tropifexor reversed established fibrosis and reduced the NAFLD activity score, hepatic triglycerides, and profibrogenic gene expression[187]. Currently, at least three clinical trials are evaluating the safety, tolerability, and efficacy of different doses of tropifexor in NASH patients[188-190].

Elafibranor is an agonist of the peroxisome proliferator-activated receptor-α and peroxisome proliferator-activated receptor-δ. In a randomized, double-blind placebo-controlled trial, including 276 patients for 52 wk, NASH resolved without fibrosis worsening in a higher proportion of patients in the Elafibranor group (120 mg/d), and NASH resolution was associated with a reduction in liver fibrosis stage[191].

SGLT2 inhibitors, a relatively novel class of oral antidiabetic drugs that reduce hyperglycemia by promoting the urinary excretion of glucose[192]. Dapagliflozin, an SGLT2 inhibitor, has proven beneficial effects other than lower glucose levels in T2DM, such as a significant reduction in total body weight, predominantly by reducing total body fat mass and visceral fat[193]. In an open-label trial, 57 patients with T2DM and NAFLD were randomized to dapagliflozin (5 mg/d) (n = 33) or standard treatment (n = 24) for 24 wk. In 14 patients from the dapagliflozin group who had significant fibrosis (≥ 8.0 kPa), LSM decreased significantly from 14.7 ± 5.7 to 11.0 ± 7.3 kPa[194]. Licoglicoflzin, a dual sodium-glucose co-transporter 1/2 inhibitor which has proven positive effects on body weight in obese patients[195,196], in combination with tropifexor is currently under recruitment to evaluate the efficacy, safety, and tolerability in patients with NASH and significant fibrosis (F2 and F3)[189].

Finally, selonsertib, an inhibitor of apoptosis signal-regulating kinase 1, a serine/threonine signaling kinase, that can lead to fibrosis was evaluated alone or in combination with simtuzumab, in NAFLD patients with stage 2 or 3 liver fibrosis for 24 wk. Reductions in LSM on MRE and collagen content and lobular inflammation on liver biopsy were observed[197].

It is expected that shortly evidence from these and new drugs will increase exponentially, however, given the complex physiopathology of NAFLD fibrosis, it is unlikely that one drug by itself will deliver significant clinical outcomes, and perhaps the combinations of drugs with different targets will be necessary to obtain better results. Additionally, it is important to mention that until now, there is no evidence showing a clear effect of the "hepatoprotectors" on liver fibrosis (ursodeoxycholic acid, pentoxifylline, antioxidants among others), and therefore should not be used indiscriminately.

CONCLUSION

The main concern in NAFLD/NASH patients is the presence and progression of liver fibrosis, therefore all the efforts should center on it. There are several available scores to predict and stratify the risk of advanced fibrosis although the accuracy is limited in

intermediate stages. To improve the accuracy of the diagnosis a combination of methods such as TE or US may be used, while MRE or liver biopsy alone are considered as the best options to accurately diagnose fibrosis. To select a diagnostic test or tests the prevalence of the disease in the specific center should be considered, as well as the experience of the center and the observers. The treatment should always take into account the presence of comorbidities such as the features of metabolic syndrome and should always include lifestyle modifications considering the preferences of the patient to ensure long-term adherence. The only approved pharmacological treatments so far are Vitamin E and pioglitazone, however, they have shown conflicting results on liver fibrosis improvement. Therefore, several new drugs and trials are being created and conducted aiming to improve both steatosis and liver fibrosis with very promising results thus far.

REFERENCES

1 **GBD 2017 Cirrhosis Collaborators**. The global, regional, and national burden of cirrhosis by cause in 195 countries and territories, 1990-2017: a systematic analysis for the Global Burden of Disease Study 2017. *Lancet Gastroenterol Hepatol* 2020; **5**: 245-266 [PMID: 31981519 DOI: 10.1016/S2468-1253(19)30349-8]

2 **Younossi ZM**, Koenig AB, Abdelatif D, Fazel Y, Henry L, Wymer M. Global epidemiology of nonalcoholic fatty liver disease-Meta-analytic assessment of prevalence, incidence, and outcomes. *Hepatology* 2016; **64**: 73-84 [PMID: 26707365 DOI: 10.1002/hep.28431]

3 **Younossi Z**, Anstee QM, Marietti M, Hardy T, Henry L, Eslam M, George J, Bugianesi E. Global burden of NAFLD and NASH: trends, predictions, risk factors and prevention. *Nat Rev Gastroenterol Hepatol* 2018; **15**: 11-20 [PMID: 28930295 DOI: 10.1038/nrgastro.2017.109]

4 **European Association for the Study of the Liver (EASL)**. ; European Association for the Study of Diabetes (EASD); European Association for the Study of Obesity (EASO). EASL-EASD-EASO Clinical Practice Guidelines for the management of non-alcoholic fatty liver disease. *J Hepatol* 2016; **64**: 1388-1402 [PMID: 27062661 DOI: 10.1016/j.jhep.2015.11.004]

5 **Brunt EM**, Wong VW, Nobili V, Day CP, Sookoian S, Maher JJ, Bugianesi E, Sirlin CB, Neuschwander-Tetri BA, Rinella ME. Nonalcoholic fatty liver disease. *Nat Rev Dis Primers* 2015; **1**: 15080 [PMID: 27188459 DOI: 10.1038/nrdp.2015.80]

6 **Zelber-Sagi S**, Nitzan-Kaluski D, Halpern Z, Oren R. Prevalence of primary non-alcoholic fatty liver disease in a population-based study and its association with biochemical and anthropometric measures. *Liver Int* 2006; **26**: 856-863 [PMID: 16911469 DOI: 10.1111/j.1478-3231.2006.01311.x]

7 **Browning JD**, Szczepaniak LS, Dobbins R, Nuremberg P, Horton JD, Cohen JC, Grundy SM, Hobbs HH. Prevalence of hepatic steatosis in an urban population in the United States: impact of ethnicity. *Hepatology* 2004; **40**: 1387-1395 [PMID: 15565570 DOI: 10.1002/hep.20466]

8 **Miyaaki H**, Nakao K. Significance of genetic polymorphisms in patients with nonalcoholic fatty liver disease. *Clin J Gastroenterol* 2017; **10**: 201-207 [PMID: 28290069 DOI: 10.1007/s12328-017-0732-5]

9 **Targher G**, Bertolini L, Padovani R, Rodella S, Tessari R, Zenari L, Day C, Arcaro G. Prevalence of nonalcoholic fatty liver disease and its association with cardiovascular disease among type 2 diabetic patients. *Diabetes Care* 2007; **30**: 1212-1218 [PMID: 17277038 DOI: 10.2337/dc06-2247]

10 **Oikonomou D**, Georgiopoulos G, Katsi V, Kourek C, Tsioufis C, Alexopoulou A, Koutli E, Tousoulis D. Non-alcoholic fatty liver disease and hypertension: coprevalent or correlated? *Eur J Gastroenterol Hepatol* 2018; **30**: 979-985 [PMID: 30048367 DOI: 10.1097/MEG.0000000000001191]

11 **Le MH**, Devaki P, Ha NB, Jun DW, Te HS, Cheung RC, Nguyen MH. Prevalence of non-alcoholic fatty liver disease and risk factors for advanced fibrosis and mortality in the United States. *PLoS One* 2017; **12**: e0173499 [PMID: 28346543 DOI: 10.1371/journal.pone.0173499]

12 **Angulo P**, Kleiner DE, Dam-Larsen S, Adams LA, Bjornsson ES, Charatcharoenwitthaya P, Mills PR, Keach JC, Lafferty HD, Stahler A, Haflidadottir S, Bendtsen F. Liver Fibrosis, but No Other Histologic Features, Is Associated With Long-term Outcomes of Patients With Nonalcoholic Fatty Liver Disease. *Gastroenterology* 2015; **149**: 389-397.e10 [PMID: 25935633 DOI: 10.1053/j.gastro.2015.04.043]

13 **Dulai PS**, Singh S, Patel J, Soni M, Prokop LJ, Younossi Z, Sebastiani G, Ekstedt M, Hagstrom H, Nasr P, Stal P, Wong VW, Kechagias S, Hultcrantz R, Loomba R. Increased risk of mortality by fibrosis stage in nonalcoholic fatty liver disease: Systematic review and meta-analysis. *Hepatology* 2017; **65**: 1557-1565 [PMID: 28130788 DOI: 10.1002/hep.29085]

14 **Hagström H**, Nasr P, Ekstedt M, Hammar U, Stål P, Hultcrantz R, Kechagias S. Fibrosis stage but not NASH predicts mortality and time to development of severe liver disease in biopsy-proven NAFLD. *J Hepatol* 2017; **67**: 1265-1273 [PMID: 28803953 DOI: 10.1016/j.jhep.2017.07.027]

15 **Shili-Masmoudi S**, Wong GL, Hiriart JB, Liu K, Chermak F, Shu SS, Foucher J, Tse YK, Bernard PH, Yip TC, Merrouche W, Chan HL, Wong VW, de Lédinghen V. Liver stiffness measurement predicts long-term survival and complications in non-alcoholic fatty liver disease. *Liver Int* 2020; **40**: 581-589 [PMID: 31749300 DOI: 10.1111/liv.14301]

16 **Kim SU**, Song D, Heo JH, Yoo J, Kim BK, Park JY, Kim DY, Ahn SH, Kim KJ, Han KH, Kim YD. Liver fibrosis assessed with transient elastography is an independent risk factor for ischemic stroke. *Atherosclerosis* 2017; **260**: 156-162 [PMID: 28222857 DOI: 10.1016/j.atherosclerosis.2017.02.005]

17 **Önnerhag K**, Hartman H, Nilsson PM, Lindgren S. Non-invasive fibrosis scoring systems can predict future metabolic complications and overall mortality in non-alcoholic fatty liver disease (NAFLD). *Scand J Gastroenterol* 2019; **54**: 328-334 [PMID: 30907181 DOI: 10.1080/00365521.2019.1583366]

18 **Baik M**, Kim SU, Kang S, Park HJ, Nam HS, Heo JH, Kim BK, Park JY, Kim DY, Ahn SH, Han KH, Lee

HS, Kim YD. Liver Fibrosis, Not Steatosis, Associates with Long-Term Outcomes in Ischaemic Stroke Patients. *Cerebrovasc Dis* 2019; **47**: 32-39 [PMID: 30763931 DOI: 10.1159/000497069]

19 **Mangla N**, Ajmera VH, Caussy C, Sirlin C, Brouha S, Bajwa-Dulai S, Madamba E, Bettencourt R, Richards L, Loomba R. Liver Stiffness Severity is Associated With Increased Cardiovascular Risk in Patients With Type 2 Diabetes. *Clin Gastroenterol Hepatol* 2020; **18**: 744-746.e1 [PMID: 31100460 DOI: 10.1016/j.cgh.2019.05.003]

20 **Matteoni CA**, Younossi ZM, Gramlich T, Boparai N, Liu YC, McCullough AJ. Nonalcoholic fatty liver disease: a spectrum of clinical and pathological severity. *Gastroenterology* 1999; **116**: 1413-1419 [PMID: 10348825 DOI: 10.1016/S0016-5085(99)70506-8]

21 **Pelusi S**, Cespiati A, Rametta R, Pennisi G, Mannisto V, Rosso C, Baselli G, Dongiovanni P, Fracanzani AL, Badiali S, Maggioni M, Craxi A, Fargion S, Prati D, Nobili V, Bugianesi E, Romeo S, Pihlajamaki J, Petta S, Valenti L. Prevalence and Risk Factors of Significant Fibrosis in Patients With Nonalcoholic Fatty Liver Without Steatohepatitis. *Clin Gastroenterol Hepatol* 2019; **17**: 2310-2319.e6 [PMID: 30708111 DOI: 10.1016/j.cgh.2019.01.027]

22 **Pelusi S**, Petta S, Rosso C, Borroni V, Fracanzani AL, Dongiovanni P, Craxi A, Bugianesi E, Fargion S, Valenti L. Renin-Angiotensin System Inhibitors, Type 2 Diabetes and Fibrosis Progression: An Observational Study in Patients with Nonalcoholic Fatty Liver Disease. *PLoS One* 2016; **11**: e0163069 [PMID: 27649410 DOI: 10.1371/journal.pone.0163069]

23 **McPherson S**, Hardy T, Henderson E, Burt AD, Day CP, Anstee QM. Evidence of NAFLD progression from steatosis to fibrosing-steatohepatitis using paired biopsies: implications for prognosis and clinical management. *J Hepatol* 2015; **62**: 1148-1155 [PMID: 25477264 DOI: 10.1016/j.jhep.2014.11.034]

24 **Adams LA**, Sanderson S, Lindor KD, Angulo P. The histological course of nonalcoholic fatty liver disease: a longitudinal study of 103 patients with sequential liver biopsies. *J Hepatol* 2005; **42**: 132-138 [PMID: 15629518 DOI: 10.1016/j.jhep.2004.09.012]

25 **Schwimmer JB**, Celedon MA, Lavine JE, Salem R, Campbell N, Schork NJ, Shiehmorteza M, Yokoo T, Chavez A, Middleton MS, Sirlin CB. Heritability of nonalcoholic fatty liver disease. *Gastroenterology* 2009; **136**: 1585-1592 [PMID: 19208353 DOI: 10.1053/j.gastro.2009.01.050]

26 **Eslam M**, Valenti L, Romeo S. Genetics and epigenetics of NAFLD and NASH: Clinical impact. *J Hepatol* 2018; **68**: 268-279 [PMID: 29122391 DOI: 10.1016/j.jhep.2017.09.003]

27 **Koo BK**, Joo SK, Kim D, Bae JM, Park JH, Kim JH, Kim W. Additive effects of PNPLA3 and TM6SF2 on the histological severity of non-alcoholic fatty liver disease. *J Gastroenterol Hepatol* 2018; **33**: 1277-1285 [PMID: 29193269 DOI: 10.1111/jgh.14056]

28 **Akuta N**, Kawamura Y, Arase Y, Suzuki F, Sezaki H, Hosaka T, Kobayashi M, Kobayashi M, Saitoh S, Suzuki Y, Ikeda K, Kumada H. Relationships between Genetic Variations of PNPLA3, TM6SF2 and Histological Features of Nonalcoholic Fatty Liver Disease in Japan. *Gut Liver* 2016; **10**: 437-445 [PMID: 26610348 DOI: 10.5009/gnl15163]

29 **Sookoian S**, Castaño GO, Scian R, Mallardi P, Fernández Gianotti T, Burgueño AL, San Martino J, Pirola CJ. Genetic variation in transmembrane 6 superfamily member 2 and the risk of nonalcoholic fatty liver disease and histological disease severity. *Hepatology* 2015; **61**: 515-525 [PMID: 25302781 DOI: 10.1002/hep.27556]

30 **Liu YL**, Reeves HL, Burt AD, Tiniakos D, McPherson S, Leathart JB, Allison ME, Alexander GJ, Piguet AC, Anty R, Donaldson P, Aithal GP, Francque S, Van Gaal L, Clement K, Ratziu V, Dufour JF, Day CP, Daly AK, Anstee QM. TM6SF2 rs58542926 influences hepatic fibrosis progression in patients with non-alcoholic fatty liver disease. *Nat Commun* 2014; **5**: 4309 [PMID: 24978903 DOI: 10.1038/ncomms5309]

31 **Mancina RM**, Dongiovanni P, Petta S, Pingitore P, Meroni M, Rametta R, Borén J, Montalcini T, Pujia A, Wiklund O, Hindy G, Spagnuolo R, Motta BM, Pipitone RM, Craxì A, Fargion S, Nobili V, Käkelä P, Kärjä V, Männistö V, Pihlajamäki J, Reilly DF, Castro-Perez J, Kozlitina J, Valenti L, Romeo S. The MBOAT7-TMC4 Variant rs641738 Increases Risk of Nonalcoholic Fatty Liver Disease in Individuals of European Descent. *Gastroenterology* 2016; **150**: 1219-1230.e6 [PMID: 26850495 DOI: 10.1053/j.gastro.2016.01.032]

32 **Petta S**, Miele L, Bugianesi E, Cammà C, Rosso C, Boccia S, Cabibi D, Di Marco V, Grimaudo S, Grieco A, Pipitone RM, Marchesini G, Craxì A. Glucokinase regulatory protein gene polymorphism affects liver fibrosis in non-alcoholic fatty liver disease. *PLoS One* 2014; **9**: e87523 [PMID: 24498332 DOI: 10.1371/journal.pone.0087523]

33 **Krawczyk M**, Rau M, Schattenberg JM, Bantel H, Pathil A, Demir M, Kluwe J, Boettler T, Lammert F, Geier A; NAFLD Clinical Study Group. Combined effects of the PNPLA3 rs738409, TM6SF2 rs58542926, and MBOAT7 rs641738 variants on NAFLD severity: a multicenter biopsy-based study. *J Lipid Res* 2017; **58**: 247-255 [PMID: 27836992 DOI: 10.1194/jlr.P067454]

34 **Wang Q**, You H, Ou X, Zhao X, Sun Y, Wang M, Wang P, Wang Y, Duan W, Wang X, Wu S, Kong Y, Saxena R, Gouw ASH, Jia J. Non-obese histologically confirmed NASH patients with abnormal liver biochemistry have more advanced fibrosis. *Hepatol Int* 2019; **13**: 766-776 [PMID: 31559605 DOI: 10.1007/s12072-019-09982-z]

35 **Petta S**, Ciminnisi S, Di Marco V, Cabibi D, Cammà C, Licata A, Marchesini G, Craxì A. Sarcopenia is associated with severe liver fibrosis in patients with non-alcoholic fatty liver disease. *Aliment Pharmacol Ther* 2017; **45**: 510-518 [PMID: 28028821 DOI: 10.1111/apt.13889]

36 **Koo BK**, Kim D, Joo SK, Kim JH, Chang MS, Kim BG, Lee KL, Kim W. Sarcopenia is an independent risk factor for non-alcoholic steatohepatitis and significant fibrosis. *J Hepatol* 2017; **66**: 123-131 [PMID: 27599824 DOI: 10.1016/j.jhep.2016.08.019]

37 **Patel V**, Sanyal AJ, Sterling R. Clinical Presentation and Patient Evaluation in Nonalcoholic Fatty Liver Disease. *Clin Liver Dis* 2016; **20**: 277-292 [PMID: 27063269 DOI: 10.1016/j.cld.2015.10.006]

38 **Pandey A**, Sonthalia S. Skin Tags. In: StatPearls [Internet]. Treasure Island (FL): StatPearls Publishing; 2020 Aug 8 [PMID: 31613504]

39 **Wu J**, Yao XY, Shi RX, Liu SF, Wang XY. A potential link between polycystic ovary syndrome and non-alcoholic fatty liver disease: an update meta-analysis. *Reprod Health* 2018; **15**: 77 [PMID: 29747678 DOI:

10.1186/s12978-018-0519-2]

40 **Benotti P**, Wood GC, Argyropoulos G, Pack A, Keenan BT, Gao X, Gerhard G, Still C. The impact of obstructive sleep apnea on nonalcoholic fatty liver disease in patients with severe obesity. *Obesity (Silver Spring)* 2016; **24**: 871-877 [PMID: 26880657 DOI: 10.1002/oby.21409]

41 **Feldstein AE**, Wieckowska A, Lopez AR, Liu YC, Zein NN, McCullough AJ. Cytokeratin-18 fragment levels as noninvasive biomarkers for nonalcoholic steatohepatitis: a multicenter validation study. *Hepatology* 2009; **50**: 1072-1078 [PMID: 19585618 DOI: 10.1002/hep.23050]

42 **Li J**, Verhaar AP, Pan Q, de Knegt RJ, Peppelenbosch MP. Serum levels of caspase-cleaved cytokeratin 18 (CK18-Asp396) predict severity of liver disease in chronic hepatitis B. *Clin Exp Gastroenterol* 2017; **10**: 203-209 [PMID: 28860836 DOI: 10.2147/CEG.S135526]

43 **Darweesh SK**, AbdElAziz RA, Abd-ElFatah DS, AbdElazim NA, Fathi SA, Attia D, AbdAllah M. Serum cytokeratin-18 and its relation to liver fibrosis and steatosis diagnosed by FibroScan and controlled attenuation parameter in nonalcoholic fatty liver disease and hepatitis C virus patients. *Eur J Gastroenterol Hepatol* 2019; **31**: 633-641 [PMID: 30839434 DOI: 10.1097/MEG.0000000000001385]

44 **Alt Y**, Grimm A, Schlegel L, Grambihler A, Kittner JM, Wiltink J, Galle PR, Wörns MA, Schattenberg JM. The Impact of Liver Cell Injury on Health-Related Quality of Life in Patients with Chronic Liver Disease. *PLoS One* 2016; **11**: e0151200 [PMID: 26990427 DOI: 10.1371/journal.pone.0151200]

45 **Cusi K**, Chang Z, Harrison S, Lomonaco R, Bril F, Orsak B, Ortiz-Lopez C, Hecht J, Feldstein AE, Webb A, Louden C, Goros M, Tio F. Limited value of plasma cytokeratin-18 as a biomarker for NASH and fibrosis in patients with non-alcoholic fatty liver disease. *J Hepatol* 2014; **60**: 167-174 [PMID: 23973932 DOI: 10.1016/j.jhep.2013.07.042]

46 **Karsdal MA**, Daniels SJ, Holm Nielsen S, Bager C, Rasmussen DGK, Loomba R, Surabattula R, Villesen IF, Luo Y, Shevell D, Gudmann NS, Nielsen MJ, George J, Christian R, Leeming DJ, Schuppan D. Collagen biology and non-invasive biomarkers of liver fibrosis. *Liver Int* 2020; **40**: 736-750 [PMID: 31997561 DOI: 10.1111/liv.14390]

47 **Luo Y**, Oseini A, Gagnon R, Charles ED, Sidik K, Vincent R, Collen R, Idowu M, Contos MJ, Mirshahi F, Daita K, Asgharpour A, Siddiqui MS, Jarai G, Rosen G, Christian R, Sanyal AJ. An Evaluation of the Collagen Fragments Related to Fibrogenesis and Fibrolysis in Nonalcoholic Steatohepatitis. *Sci Rep* 2018; **8**: 12414 [PMID: 30120271 DOI: 10.1038/s41598-018-30457-y]

48 **Xie Q**, Zhou X, Huang P, Wei J, Wang W, Zheng S. The performance of enhanced liver fibrosis (ELF) test for the staging of liver fibrosis: a meta-analysis. *PLoS One* 2014; **9**: e92772 [PMID: 24736610 DOI: 10.1371/journal.pone.0092772]

49 **Kwok R**, Tse YK, Wong GL, Ha Y, Lee AU, Ngu MC, Chan HL, Wong VW. Systematic review with meta-analysis: non-invasive assessment of non-alcoholic fatty liver disease -- the role of transient elastography and plasma cytokeratin-18 fragments. *Aliment Pharmacol Ther* 2014; **39**: 254-269 [PMID: 24308774 DOI: 10.1111/apt.12569]

50 **Kobayashi N**, Kumada T, Toyoda H, Tada T, Ito T, Kage M, Okanoue T, Kudo M. Ability of Cytokeratin-18 Fragments and FIB-4 Index to Diagnose Overall and Mild Fibrosis Nonalcoholic Steatohepatitis in Japanese Nonalcoholic Fatty Liver Disease Patients. *Dig Dis* 2017; **35**: 521-530 [PMID: 29040984 DOI: 10.1159/000480142]

51 **Sterling RK**, Lissen E, Clumeck N, Sola R, Correa MC, Montaner J, S Sulkowski M, Torriani FJ, Dieterich DT, Thomas DL, Messinger D, Nelson M; APRICOT Clinical Investigators. Development of a simple noninvasive index to predict significant fibrosis in patients with HIV/HCV coinfection. *Hepatology* 2006; **43**: 1317-1325 [PMID: 16729309 DOI: 10.1002/hep.21178]

52 **Shah AG**, Lydecker A, Murray K, Tetri BN, Contos MJ, Sanyal AJ; Nash Clinical Research Network. Comparison of noninvasive markers of fibrosis in patients with nonalcoholic fatty liver disease. *Clin Gastroenterol Hepatol* 2009; **7**: 1104-1112 [PMID: 19523535 DOI: 10.1016/j.cgh.2009.05.033]

53 **Peleg N**, Issachar A, Sneh-Arbib O, Shlomai A. AST to Platelet Ratio Index and fibrosis 4 calculator scores for non-invasive assessment of hepatic fibrosis in patients with non-alcoholic fatty liver disease. *Dig Liver Dis* 2017; **49**: 1133-1138 [PMID: 28572039 DOI: 10.1016/j.dld.2017.05.002]

54 **Sun W**, Cui H, Li N, Wei Y, Lai S, Yang Y, Yin X, Chen DF. Comparison of FIB-4 index, NAFLD fibrosis score and BARD score for prediction of advanced fibrosis in adult patients with non-alcoholic fatty liver disease: A meta-analysis study. *Hepatol Res* 2016; **46**: 862-870 [PMID: 26763834 DOI: 10.1111/hepr.12647]

55 **Angulo P**, Hui JM, Marchesini G, Bugianesi E, George J, Farrell GC, Enders F, Saksena S, Burt AD, Bida JP, Lindor K, Sanderson SO, Lenzi M, Adams LA, Kench J, Therneau TM, Day CP. The NAFLD fibrosis score: a noninvasive system that identifies liver fibrosis in patients with NAFLD. *Hepatology* 2007; **45**: 846-854 [PMID: 17393509 DOI: 10.1002/hep.21496]

56 **Boursier J**, Vergniol J, Guillet A, Hiriart JB, Lannes A, Le Bail B, Michalak S, Chermak F, Bertrais S, Foucher J, Oberti F, Charbonnier M, Fouchard-Hubert I, Rousselet MC, Calès P, de Lédinghen V. Diagnostic accuracy and prognostic significance of blood fibrosis tests and liver stiffness measurement by FibroScan in non-alcoholic fatty liver disease. *J Hepatol* 2016; **65**: 570-578 [PMID: 27151181 DOI: 10.1016/j.jhep.2016.04.023]

57 **Jun DW**, Kim SG, Park SH, Jin SY, Lee JS, Lee JW, Kim MY, Choi DH, Cho YK, Yeon JE, Sohn JH; Korean NAFLD study group (KNSG). External validation of the non-alcoholic fatty liver disease fibrosis score for assessing advanced fibrosis in Korean patients. *J Gastroenterol Hepatol* 2017; **32**: 1094-1099 [PMID: 27859583 DOI: 10.1111/jgh.13648]

58 **Cichoż-Lach H**, Celiński K, Prozorow-Król B, Swatek J, Słomka M, Lach T. The BARD score and the NAFLD fibrosis score in the assessment of advanced liver fibrosis in nonalcoholic fatty liver disease. *Med Sci Monit* 2012; **18**: CR735-CR740 [PMID: 23197236 DOI: 10.12659/msm.883601]

59 **Ruffillo G**, Fassio E, Alvarez E, Landeira G, Longo C, Domínguez N, Gualano G. Comparison of NAFLD fibrosis score and BARD score in predicting fibrosis in nonalcoholic fatty liver disease. *J Hepatol* 2011; **54**: 160-163 [PMID: 20934232 DOI: 10.1016/j.jhep.2010.06.028]

60 **Harrison SA**, Oliver D, Arnold HL, Gogia S, Neuschwander-Tetri BA. Development and validation of a simple NAFLD clinical scoring system for identifying patients without advanced disease. *Gut* 2008; **57**: 1441-1447 [PMID: 18390575 DOI: 10.1136/gut.2007.146019]

61 **Fujii H**, Enomoto M, Fukushima W, Tamori A, Sakaguchi H, Kawada N. Applicability of BARD score to Japanese patients with NAFLD. *Gut* 2009; **58**: 1566-1567 author reply 1567 [PMID: 19834122 DOI: 10.1136/gut.2009.182758]

62 **Wai CT**, Greenson JK, Fontana RJ, Kalbfleisch JD, Marrero JA, Conjeevaram HS, Lok AS. A simple noninvasive index can predict both significant fibrosis and cirrhosis in patients with chronic hepatitis C. *Hepatology* 2003; **38**: 518-526 [PMID: 12883497 DOI: 10.1053/jhep.2003.50346]

63 **Xiao G**, Zhu S, Xiao X, Yan L, Yang J, Wu G. Comparison of laboratory tests, ultrasound, or magnetic resonance elastography to detect fibrosis in patients with nonalcoholic fatty liver disease: A meta-analysis. *Hepatology* 2017; **66**: 1486-1501 [PMID: 28586172 DOI: 10.1002/hep.29302]

64 **Mikolasevic I**, Orlic L, Franjic N, Hauser G, Stimac D, Milic S. Transient elastography (FibroScan(®)) with controlled attenuation parameter in the assessment of liver steatosis and fibrosis in patients with nonalcoholic fatty liver disease - Where do we stand? *World J Gastroenterol* 2016; **22**: 7236-7251 [PMID: 27621571 DOI: 10.3748/wjg.v22.i32.7236]

65 **Kolhe KM**, Amarapurkar A, Parikh P, Chaubal A, Chauhan S, Khairnar H, Walke S, Ingle M, Pandey V, Shukla A. Aspartate transaminase to platelet ratio index (APRI) but not FIB-5 or FIB-4 is accurate in ruling out significant fibrosis in patients with non-alcoholic fatty liver disease (NAFLD) in an urban slum-dwelling population. *BMJ Open Gastroenterol* 2019; **6**: e000288 [PMID: 31275584 DOI: 10.1136/bmjgast-2019-000288]

66 **Vilar-Gomez E**, Chalasani N. Non-invasive assessment of non-alcoholic fatty liver disease: Clinical prediction rules and blood-based biomarkers. *J Hepatol* 2018; **68**: 305-315 [PMID: 29154965 DOI: 10.1016/j.jhep.2017.11.013]

67 **Poynard T**, Morra R, Halfon P, Castera L, Ratziu V, Imbert-Bismut F, Naveau S, Thabut D, Lebrec D, Zoulim F, Bourliere M, Cacoub P, Messous D, Munteanu M, de Ledinghen V. Meta-analyses of FibroTest diagnostic value in chronic liver disease. *BMC Gastroenterol* 2007; **7**: 40 [PMID: 17937811 DOI: 10.1186/1471-230X-7-40]

68 **Ratziu V**, Massard J, Charlotte F, Messous D, Imbert-Bismut F, Bonyhay L, Tahiri M, Munteanu M, Thabut D, Cadranel JF, Le Bail B, de Ledinghen V, Poynard T; LIDO Study Group; CYTOL study group. Diagnostic value of biochemical markers (FibroTest-FibroSURE) for the prediction of liver fibrosis in patients with non-alcoholic fatty liver disease. *BMC Gastroenterol* 2006; **6**: 6 [PMID: 16503961 DOI: 10.1186/1471-230X-6-6]

69 **Ampuero J**, Pais R, Aller R, Gallego-Durán R, Crespo J, García-Monzón C, Boursier J, Vilar E, Petta S, Zheng MH, Escudero D, Calleja JL, Aspichueta P, Diago M, Rosales JM, Caballería J, Gómez-Camarero J, Lo Iacono O, Benlloch S, Albillos A, Turnes J, Banales JM, Ratziu V, Romero-Gómez M; HEPAmet Registry. Development and Validation of Hepamet Fibrosis Scoring System-A Simple, Noninvasive Test to Identify Patients With Nonalcoholic Fatty Liver Disease With Advanced Fibrosis. *Clin Gastroenterol Hepatol* 2020; **18**: 216-225.e5 [PMID: 31195161 DOI: 10.1016/j.cgh.2019.05.051]

70 **Meneses D**, Olveira A, Corripio R, Del Carmen Méndez M, Romero M, Calvo-Viñuelas I, Herranz L, Vicent D, de-Cos-Blanco AI. Performance of Noninvasive Liver Fibrosis Scores in the Morbid Obese Patient, Same Scores but Different Thresholds. *Obes Surg* 2020; **30**: 2538-2546 [PMID: 32157523 DOI: 10.1007/s11695-020-04509-0]

71 **Gu J**, Liu S, Du S, Zhang Q, Xiao J, Dong Q, Xin Y. Diagnostic value of MRI-PDFF for hepatic steatosis in patients with non-alcoholic fatty liver disease: a meta-analysis. *Eur Radiol* 2019; **29**: 3564-3573 [PMID: 30899974 DOI: 10.1007/s00330-019-06072-4]

72 **Kim M**, Kang BK, Jun DW. Comparison of conventional sonographic signs and magnetic resonance imaging proton density fat fraction for assessment of hepatic steatosis. *Sci Rep* 2018; **8**: 7759 [PMID: 29773823 DOI: 10.1038/s41598-018-26019-x]

73 **Allan R**, Thoirs K, Phillips M. Accuracy of ultrasound to identify chronic liver disease. *World J Gastroenterol* 2010; **16**: 3510-3520 [PMID: 20653059 DOI: 10.3748/wjg.v16.i28.3510]

74 **Lo GC**, Besa C, King MJ, Kang M, Stueck A, Thung S, Wagner M, Smith AD, Taouli B. Feasibility and reproducibility of liver surface nodularity quantification for the assessment of liver cirrhosis using CT and MRI. *Eur J Radiol Open* 2017; **4**: 95-100 [PMID: 28761907 DOI: 10.1016/j.ejro.2017.07.001]

75 **Li Q**, Dhyani M, Grajo JR, Sirlin C, Samir AE. Current status of imaging in nonalcoholic fatty liver disease. *World J Hepatol* 2018; **10**: 530-542 [PMID: 30190781 DOI: 10.4254/wjh.v10.i8.530]

76 **Ozturk A**, Grajo JR, Dhyani M, Anthony BW, Samir AE. Principles of ultrasound elastography. *Abdom Radiol (NY)* 2018; **43**: 773-785 [PMID: 29487968 DOI: 10.1007/s00261-018-1475-6]

77 **Imajo K**, Kessoku T, Honda Y, Tomeno W, Ogawa Y, Mawatari H, Fujita K, Yoneda M, Taguri M, Hyogo H, Sumida Y, Ono M, Eguchi Y, Inoue T, Yamanaka T, Wada K, Saito S, Nakajima A. Magnetic Resonance Imaging More Accurately Classifies Steatosis and Fibrosis in Patients With Nonalcoholic Fatty Liver Disease Than Transient Elastography. *Gastroenterology* 2016; **150**: 626-637.e7 [PMID: 26677985 DOI: 10.1053/j.gastro.2015.11.048]

78 **Karlas T**, Petroff D, Sasso M, Fan JG, Mi YQ, de Lédinghen V, Kumar M, Lupsor-Platon M, Han KH, Cardoso AC, Ferraioli G, Chan WK, Wong VW, Myers RP, Chayama K, Friedrich-Rust M, Beaugrand M, Shen F, Hiriart JB, Sarin SK, Badea R, Jung KS, Marcellin P, Filice C, Mahadeva S, Wong GL, Crotty P, Masaki K, Bojunga J, Bedossa P, Keim V, Wiegand J. Individual patient data meta-analysis of controlled attenuation parameter (CAP) technology for assessing steatosis. *J Hepatol* 2017; **66**: 1022-1030 [PMID: 28039099 DOI: 10.1016/j.jhep.2016.12.022]

79 **Oeda S**, Takahashi H, Imajo K, Seko Y, Ogawa Y, Moriguchi M, Yoneda M, Anzai K, Aishima S, Kage M, Itoh Y, Nakajima A, Eguchi Y. Accuracy of liver stiffness measurement and controlled attenuation parameter using FibroScan® M/XL probes to diagnose liver fibrosis and steatosis in patients with nonalcoholic fatty liver disease: a multicenter prospective study. *J Gastroenterol* 2020; **55**: 428-440 [PMID: 31654131 DOI: 10.1007/s00535-019-01635-0]

80 **Lee HW**, Wong GL, Kwok R, Choi KC, Chan CK, Shu SS, Leung JK, Chim AM, Luk AO, Ma RC, Chan HL, Chan JC, Kong AP, Wong VW. Serial transient elastography examinations to monitor patients with type 2 diabetes: A prospective cohort study. *Hepatology* 2020 [PMID: 31991487 DOI: 10.1002/hep.31142]

81 **Boursier J**, Zarski JP, de Ledinghen V, Rousselet MC, Sturm N, Lebail B, Fouchard-Hubert I, Gallois Y, Oberti F, Bertrais S, Calès P; Multicentric Group from ANRS/HC/EP23 FIBROSTAR Studies. Determination of reliability criteria for liver stiffness evaluation by transient elastography. *Hepatology* 2013; **57**: 1182-1191 [PMID: 22899556 DOI: 10.1002/hep.25993]

82 **Shi KQ**, Tang JZ, Zhu XL, Ying L, Li DW, Gao J, Fang YX, Li GL, Song YJ, Deng ZJ, Wu JM, Tang KF. Controlled attenuation parameter for the detection of steatosis severity in chronic liver disease: a meta-analysis of diagnostic accuracy. *J Gastroenterol Hepatol* 2014; **29**: 1149-1158 [PMID: 24476011 DOI: 10.1111/jgh.12519]

83 **Jun BG**, Park WY, Park EJ, Jang JY, Jeong SW, Lee SH, Kim SG, Cha SW, Kim YS, Cho YD, Kim HS, Kim BS, Jin SY, Park S. A prospective comparative assessment of the accuracy of the FibroScan in evaluating liver steatosis. *PLoS One* 2017; **12**: e0182784 [PMID: 28813448 DOI: 10.1371/journal.pone.0182784]

84 **Siddiqui MS**, Vuppalanchi R, Van Natta ML, Hallinan E, Kowdley KV, Abdelmalek M, Neuschwander-Tetri BA, Loomba R, Dasarathy S, Brandman D, Doo E, Tonascia JA, Kleiner DE, Chalasani N, Sanyal AJ; NASH Clinical Research Network. Vibration-Controlled Transient Elastography to Assess Fibrosis and Steatosis in Patients With Nonalcoholic Fatty Liver Disease. *Clin Gastroenterol Hepatol* 2019; **17**: 156-163.e2 [PMID: 29705261 DOI: 10.1016/j.cgh.2018.04.043]

85 **Cassinotto C**, Boursier J, de Lédinghen V, Lebigot J, Lapuyade B, Cales P, Hiriart JB, Michalak S, Bail BL, Cartier V, Mouries A, Oberti F, Fouchard-Hubert I, Vergniol J, Aubé C. Liver stiffness in nonalcoholic fatty liver disease: A comparison of supersonic shear imaging, FibroScan, and ARFI with liver biopsy. *Hepatology* 2016; **63**: 1817-1827 [PMID: 26659452 DOI: 10.1002/hep.28394]

86 **Nightingale K**, Soo MS, Nightingale R, Trahey G. Acoustic radiation force impulse imaging: *in vivo* demonstration of clinical feasibility. *Ultrasound Med Biol* 2002; **28**: 227-235 [PMID: 11937286 DOI: 10.1016/S0301-5629(01)00499-9]

87 **D'Onofrio M**, Crosara S, De Robertis R, Canestrini S, Demozzi E, Gallotti A, Pozzi Mucelli R. Acoustic radiation force impulse of the liver. *World J Gastroenterol* 2013; **19**: 4841-4849 [PMID: 23946588 DOI: 10.3748/wjg.v19.i30.4841]

88 **Fierbinteanu-Braticevici C**, Andronescu D, Usvat R, Cretoiu D, Baicus C, Marinoschi G. Acoustic radiation force imaging sonoelastography for noninvasive staging of liver fibrosis. *World J Gastroenterol* 2009; **15**: 5525-5532 [PMID: 19938190 DOI: 10.3748/wjg.15.5525]

89 **Bota S**, Herkner H, Sporea I, Salzl P, Sirli R, Neghina AM, Peck-Radosavljevic M. Meta-analysis: ARFI elastography *versus* transient elastography for the evaluation of liver fibrosis. *Liver Int* 2013; **33**: 1138-1147 [PMID: 23859217 DOI: 10.1111/liv.12240]

90 **Friedrich-Rust M**, Romen D, Vermehren J, Kriener S, Sadet D, Herrmann E, Zeuzem S, Bojunga J. Acoustic radiation force impulse-imaging and transient elastography for non-invasive assessment of liver fibrosis and steatosis in NAFLD. *Eur J Radiol* 2012; **81**: e325-e331 [PMID: 22119555 DOI: 10.1016/j.ejrad.2011.10.029]

91 **Guzmán-Aroca F**, Frutos-Bernal MD, Bas A, Luján-Mompeán JA, Reus M, Berná-Serna Jde D, Parrilla P. Detection of non-alcoholic steatohepatitis in patients with morbid obesity before bariatric surgery: preliminary evaluation with acoustic radiation force impulse imaging. *Eur Radiol* 2012; **22**: 2525-2532 [PMID: 22648049 DOI: 10.1007/s00330-012-2505-3]

92 **Osaki A**, Kubota T, Suda T, Igarashi M, Nagasaki K, Tsuchiya A, Yano M, Tamura Y, Takamura M, Kawai H, Yamagiwa S, Kikuchi T, Nomoto M, Aoyagi Y. Shear wave velocity is a useful marker for managing nonalcoholic steatohepatitis. *World J Gastroenterol* 2010; **16**: 2918-2925 [PMID: 20556839 DOI: 10.3748/wjg.v16.i23.2918]

93 **Yoneda M**, Suzuki K, Kato S, Fujita K, Nozaki Y, Hosono K, Saito S, Nakajima A. Nonalcoholic fatty liver disease: US-based acoustic radiation force impulse elastography. *Radiology* 2010; **256**: 640-647 [PMID: 20529989 DOI: 10.1148/radiol.10091662]

94 **Venkatesh SK**, Ehman RL. Magnetic resonance elastography of liver. *Magn Reson Imaging Clin N Am* 2014; **22**: 433-446 [PMID: 25086938 DOI: 10.1016/j.mric.2014.05.001]

95 **Muthupillai R**, Lomas DJ, Rossman PJ, Greenleaf JF, Manduca A, Ehman RL. Magnetic resonance elastography by direct visualization of propagating acoustic strain waves. *Science* 1995; **269**: 1854-1857 [PMID: 7569924 DOI: 10.1126/science.7569924]

96 **Hoodeshenas S**, Yin M, Venkatesh SK. Magnetic Resonance Elastography of Liver: Current Update. *Top Magn Reson Imaging* 2018; **27**: 319-333 [PMID: 30289828 DOI: 10.1097/RMR.0000000000000177]

97 **Loomba R**, Wolfson T, Ang B, Hooker J, Behling C, Peterson M, Valasek M, Lin G, Brenner D, Gamst A, Ehman R, Sirlin C. Magnetic resonance elastography predicts advanced fibrosis in patients with nonalcoholic fatty liver disease: a prospective study. *Hepatology* 2014; **60**: 1920-1928 [PMID: 25103310 DOI: 10.1002/hep.27362]

98 **Kim D**, Kim WR, Talwalkar JA, Kim HJ, Ehman RL. Advanced fibrosis in nonalcoholic fatty liver disease: noninvasive assessment with MR elastography. *Radiology* 2013; **268**: 411-419 [PMID: 23564711 DOI: 10.1148/radiol.13121193]

99 **Cui J**, Ang B, Haufe W, Hernandez C, Verna EC, Sirlin CB, Loomba R. Comparative diagnostic accuracy of magnetic resonance elastography vs. eight clinical prediction rules for non-invasive diagnosis of advanced fibrosis in biopsy-proven non-alcoholic fatty liver disease: a prospective study. *Aliment Pharmacol Ther* 2015; **41**: 1271-1280 [PMID: 25873207 DOI: 10.1111/apt.13196]

100 **Ajmera VH**, Liu A, Singh S, Yachoa G, Ramey M, Bhargava M, Zamani A, Lopez S, Mangla N, Bettencourt R, Rizo E, Valasek M, Behling C, Richards L, Sirlin C, Loomba R. Clinical Utility of an Increase in Magnetic Resonance Elastography in Predicting Fibrosis Progression in Nonalcoholic Fatty Liver Disease. *Hepatology* 2020; **71**: 849-860 [PMID: 31556124 DOI: 10.1002/hep.30974]

101 **Dulai PS**, Sirlin CB, Loomba R. MRI and MRE for non-invasive quantitative assessment of hepatic

steatosis and fibrosis in NAFLD and NASH: Clinical trials to clinical practice. *J Hepatol* 2016; **65**: 1006-1016 [PMID: 27312947 DOI: 10.1016/j.jhep.2016.06.005]

102 **Petta S**, Wong VW, Cammà C, Hiriart JB, Wong GL, Vergniol J, Chan AW, Di Marco V, Merrouche W, Chan HL, Marra F, Le-Bail B, Arena U, Craxì A, de Ledinghen V. Serial combination of non-invasive tools improves the diagnostic accuracy of severe liver fibrosis in patients with NAFLD. *Aliment Pharmacol Ther* 2017; **46**: 617-627 [PMID: 28752524 DOI: 10.1111/apt.14219]

103 **Newsome PN**, Sasso M, Deeks JJ, Paredes A, Boursier J, Chan WK, Yilmaz Y, Czernichow S, Zheng MH, Wong VW, Allison M, Tsochatzis E, Anstee QM, Sheridan DA, Eddowes PJ, Guha IN, Cobbold JF, Paradis V, Bedossa P, Miette V, Fournier-Poizat C, Sandrin L, Harrison SA. FibroScan-AST (FAST) score for the non-invasive identification of patients with non-alcoholic steatohepatitis with significant activity and fibrosis: a prospective derivation and global validation study. *Lancet Gastroenterol Hepatol* 2020; **5**: 362-373 [PMID: 32027858 DOI: 10.1016/S2468-1253(19)30383-8]

104 **Boyd A**, Cain O, Chauhan A, Webb GJ. Medical liver biopsy: background, indications, procedure and histopathology. *Frontline Gastroenterol* 2020; **11**: 40-47 [PMID: 31885839 DOI: 10.1136/flgastro-2018-101139]

105 **Tublin ME**, Blair R, Martin J, Malik S, Ruppert K, Demetris A. Prospective Study of the Impact of Liver Biopsy Core Size on Specimen Adequacy and Procedural Complications. *AJR Am J Roentgenol* 2018; **210**: 183-188 [PMID: 29091001 DOI: 10.2214/AJR.17.17792]

106 **Gramlich T**, Kleiner DE, McCullough AJ, Matteoni CA, Boparai N, Younossi ZM. Pathologic features associated with fibrosis in nonalcoholic fatty liver disease. *Hum Pathol* 2004; **35**: 196-199 [PMID: 14991537 DOI: 10.1016/j.humpath.2003.09.018]

107 **Bedossa P**, Patel K, Castera L. Histologic and noninvasive estimates of liver fibrosis. *Clin Liver Dis (Hoboken)* 2015; **6**: 5-8 [PMID: 31040975 DOI: 10.1002/cld.481]

108 **Cheah MC**, McCullough AJ, Goh GB. Current Modalities of Fibrosis Assessment in Non-alcoholic Fatty Liver Disease. *J Clin Transl Hepatol* 2017; **5**: 261-271 [PMID: 28936407 DOI: 10.14218/JCTH.2017.00009]

109 **Brunt EM**, Janney CG, Di Bisceglie AM, Neuschwander-Tetri BA, Bacon BR. Nonalcoholic steatohepatitis: a proposal for grading and staging the histological lesions. *Am J Gastroenterol* 1999; **94**: 2467-2474 [PMID: 10484010 DOI: 10.1111/j.1572-0241.1999.01377.x]

110 **Kleiner DE**, Brunt EM, Van Natta M, Behling C, Contos MJ, Cummings OW, Ferrell LD, Liu YC, Torbenson MS, Unalp-Arida A, Yeh M, McCullough AJ, Sanyal AJ; Nonalcoholic Steatohepatitis Clinical Research Network. Design and validation of a histological scoring system for nonalcoholic fatty liver disease. *Hepatology* 2005; **41**: 1313-1321 [PMID: 15915461 DOI: 10.1002/hep.20701]

111 **Bedossa P**, Poitou C, Veyrie N, Bouillot JL, Basdevant A, Paradis V, Tordjman J, Clement K. Histopathological algorithm and scoring system for evaluation of liver lesions in morbidly obese patients. *Hepatology* 2012; **56**: 1751-1759 [PMID: 22707395 DOI: 10.1002/hep.25889]

112 **De Rudder M**, Bouzin C, Nachit M, Louvegny H, Vande Velde G, Julé Y, Leclercq IA. Automated computerized image analysis for the user-independent evaluation of disease severity in preclinical models of NAFLD/NASH. *Lab Invest* 2020; **100**: 147-160 [PMID: 31506634 DOI: 10.1038/s41374-019-0315-9]

113 **Masseroli M**, Caballero T, O'Valle F, Del Moral RM, Pérez-Milena A, Del Moral RG. Automatic quantification of liver fibrosis: design and validation of a new image analysis method: comparison with semi-quantitative indexes of fibrosis. *J Hepatol* 2000; **32**: 453-464 [PMID: 10735616 DOI: 10.1016/s0168-8278(00)80397-9]

114 **Bravo AA**, Sheth SG, Chopra S. Liver biopsy. *N Engl J Med* 2001; **344**: 495-500 [PMID: 11172192 DOI: 10.1056/NEJM200102153440706]

115 **Gawrieh S**, Knoedler DM, Saeian K, Wallace JR, Komorowski RA. Effects of interventions on intra- and interobserver agreement on interpretation of nonalcoholic fatty liver disease histology. *Ann Diagn Pathol* 2011; **15**: 19-24 [PMID: 21106424 DOI: 10.1016/j.anndiagpath.2010.08.001]

116 **Chalasani N**, Younossi Z, Lavine JE, Charlton M, Cusi K, Rinella M, Harrison SA, Brunt EM, Sanyal AJ. The diagnosis and management of nonalcoholic fatty liver disease: Practice guidance from the American Association for the Study of Liver Diseases. *Hepatology* 2018; **67**: 328-357 [PMID: 28714183 DOI: 10.1002/hep.29367]

117 **López-Suárez A**, Guerrero JM, Elvira-González J, Beltrán-Robles M, Cañas-Hormigo F, Bascuñana-Quirell A. Nonalcoholic fatty liver disease is associated with blood pressure in hypertensive and nonhypertensive individuals from the general population with normal levels of alanine aminotransferase. *Eur J Gastroenterol Hepatol* 2011; **23**: 1011-1017 [PMID: 21915061 DOI: 10.1097/MEG.0b013e32834b8d52]

118 **Saber S**, Mahmoud AAA, Helal NS, El-Ahwany E, Abdelghany RH. Renin-angiotensin system inhibition ameliorates CCl4-induced liver fibrosis in mice through the inactivation of nuclear transcription factor kappa B. *Can J Physiol Pharmacol* 2018; **96**: 569-576 [PMID: 29425464 DOI: 10.1139/cjpp-2017-0728]

119 **Goh GB**, Pagadala MR, Dasarathy J, Unalp-Arida A, Sargent R, Hawkins C, Sourianarayanane A, Khiyami A, Yerian L, Pai R, McCullough AJ, Dasarathy S. Renin-angiotensin system and fibrosis in non-alcoholic fatty liver disease. *Liver Int* 2015; **35**: 979-985 [PMID: 24905085 DOI: 10.1111/liv.12611]

120 **Unger T**, Borghi C, Charchar F, Khan NA, Poulter NR, Prabhakaran D, Ramirez A, Schlaich M, Stergiou GS, Tomaszewski M, Wainford RD, Williams B, Schutte AE. 2020 International Society of Hypertension Global Hypertension Practice Guidelines. *Hypertension* 2020; **75**: 1334-1357 [PMID: 32370572 DOI: 10.1161/HYPERTENSIONAHA.120.15026]

121 **Abraham HM**, White CM, White WB. The comparative efficacy and safety of the angiotensin receptor blockers in the management of hypertension and other cardiovascular diseases. *Drug Saf* 2015; **38**: 33-54 [PMID: 25416320 DOI: 10.1007/s40264-014-0239-7]

122 **Svegliati-Baroni G**, Ridolfi F, Di Sario A, Casini A, Marucci L, Gaggiotti G, Orlandoni P, Macarri G, Perego L, Benedetti A, Folli F. Insulin and insulin-like growth factor-1 stimulate proliferation and type I collagen accumulation by human hepatic stellate cells: differential effects on signal transduction pathways. *Hepatology* 1999; **29**: 1743-1751 [PMID: 10347117 DOI: 10.1002/hep.510290632]

123 **Haukeland JW**, Konopski Z, Eggesbø HB, von Volkmann HL, Raschpichler G, Bjøro K, Haaland T, Løberg EM, Birkeland K. Metformin in patients with non-alcoholic fatty liver disease: a randomized, controlled trial. *Scand J Gastroenterol* 2009; **44**: 853-860 [PMID: 19811343 DOI: 10.1080/00365520902845268]

124 **Lavine JE**, Schwimmer JB, Van Natta ML, Molleston JP, Murray KF, Rosenthal P, Abrams SH, Scheimann AO, Sanyal AJ, Chalasani N, Tonascia J, Ünalp A, Clark JM, Brunt EM, Kleiner DE, Hoofnagle JH, Robuck PR; Nonalcoholic Steatohepatitis Clinical Research Network. Effect of vitamin E or metformin for treatment of nonalcoholic fatty liver disease in children and adolescents: the TONIC randomized controlled trial. *JAMA* 2011; **305**: 1659-1668 [PMID: 21521847 DOI: 10.1001/jama.2011.520]

125 **Cunha V**, Cotrim HP, Rocha R, Carvalho K, Lins-Kusterer L. Metformin in the prevention of hepatocellular carcinoma in diabetic patients: A systematic review. *Ann Hepatol* 2020; **19**: 232-237 [PMID: 31836424 DOI: 10.1016/j.aohep.2019.10.005]

126 **Zhang ZJ**, Zheng ZJ, Shi R, Su Q, Jiang Q, Kip KE. Metformin for liver cancer prevention in patients with type 2 diabetes: a systematic review and meta-analysis. *J Clin Endocrinol Metab* 2012; **97**: 2347-2353 [PMID: 22523334 DOI: 10.1210/jc.2012-1267]

127 **Ozturk ZA**, Kadayifci A. Insulin sensitizers for the treatment of non-alcoholic fatty liver disease. *World J Hepatol* 2014; **6**: 199-206 [PMID: 24799988 DOI: 10.4254/wjh.v6.i4.199]

128 **Zhang L**, Zhang X, Meng H, Li Y, Han T, Wang C. Obstructive sleep apnea and liver injury in severely obese patients with nonalcoholic fatty liver disease. *Sleep Breath* 2020 [PMID: 32002742 DOI: 10.1007/s11325-020-02018-z]

129 **Aron-Wisnewsky J**, Clement K, Pépin JL. Nonalcoholic fatty liver disease and obstructive sleep apnea. *Metabolism* 2016; **65**: 1124-1135 [PMID: 27324067 DOI: 10.1016/j.metabol.2016.05.004]

130 **Salord N**, Fortuna AM, Monasterio C, Gasa M, Pérez A, Bonsignore MR, Vilarrasa N, Montserrat JM, Mayos M. A Randomized Controlled Trial of Continuous Positive Airway Pressure on Glucose Tolerance in Obese Patients with Obstructive Sleep Apnea. *Sleep* 2016; **39**: 35-41 [PMID: 26350474 DOI: 10.5665/sleep.5312]

131 **Fu Y**, Xia Y, Yi H, Xu H, Guan J, Yin S. Meta-analysis of all-cause and cardiovascular mortality in obstructive sleep apnea with or without continuous positive airway pressure treatment. *Sleep Breath* 2017; **21**: 181-189 [PMID: 27502205 DOI: 10.1007/s11325-016-1393-1]

132 **Jullian-Desayes I**, Tamisier R, Zarski JP, Aron-Wisnewsky J, Launois-Rollinat SH, Trocme C, Levy P, Joyeux-Faure M, Pepin JL. Impact of effective *versus* sham continuous positive airway pressure on liver injury in obstructive sleep apnoea: Data from randomized trials. *Respirology* 2016; **21**: 378-385 [PMID: 26567858 DOI: 10.1111/resp.12672]

133 **Kim D**, Ahmed A, Kushida C. Continuous Positive Airway Pressure Therapy on Nonalcoholic Fatty Liver Disease in Patients With Obstructive Sleep Apnea. *J Clin Sleep Med* 2018; **14**: 1315-1322 [PMID: 30092894 DOI: 10.5664/jcsm.7262]

134 **Buttacavoli M**, Gruttad'Auria CI, Olivo M, Virdone R, Castrogiovanni A, Mazzuca E, Marotta AM, Marrone O, Madonia S, Bonsignore MR. Liver Steatosis and Fibrosis in OSA patients After Long-term CPAP Treatment: A Preliminary Ultrasound Study. *Ultrasound Med Biol* 2016; **42**: 104-109 [PMID: 26385053 DOI: 10.1016/j.ultrasmedbio.2015.08.009]

135 **Athyros VG**, Boutari C, Stavropoulos K, Anagnostis P, Imprialos KP, Doumas M, Karagiannis A. Statins: An Under-Appreciated Asset for the Prevention and the Treatment of NAFLD or NASH and the Related Cardiovascular Risk. *Curr Vasc Pharmacol* 2018; **16**: 246-253 [PMID: 28676019 DOI: 10.2174/1570161115666170621082910]

136 **Doumas M**, Imprialos K, Dimakopoulou A, Stavropoulos K, Binas A, Athyros VG. The Role of Statins in the Management of Nonalcoholic Fatty Liver Disease. *Curr Pharm Des* 2018; **24**: 4587-4592 [PMID: 30652643 DOI: 10.2174/1381612825666190117114305]

137 **Sekiya M**, Yahagi N, Matsuzaka T, Najima Y, Nakakuki M, Nagai R, Ishibashi S, Osuga J, Yamada N, Shimano H. Polyunsaturated fatty acids ameliorate hepatic steatosis in obese mice by SREBP-1 suppression. *Hepatology* 2003; **38**: 1529-1539 [PMID: 14647064 DOI: 10.1016/j.hep.2003.09.028]

138 **Levy JR**, Clore JN, Stevens W. Dietary n-3 polyunsaturated fatty acids decrease hepatic triglycerides in Fischer 344 rats. *Hepatology* 2004; **39**: 608-616 [PMID: 14999679 DOI: 10.1002/hep.20093]

139 **Huang MA**, Greenson JK, Chao C, Anderson L, Peterman D, Jacobson J, Emick D, Lok AS, Conjeevaram HS. One-year intense nutritional counseling results in histological improvement in patients with non-alcoholic steatohepatitis: a pilot study. *Am J Gastroenterol* 2005; **100**: 1072-1081 [PMID: 15842581 DOI: 10.1111/j.1572-0241.2005.41334.x]

140 **Eckard C**, Cole R, Lockwood J, Torres DM, Williams CD, Shaw JC, Harrison SA. Prospective histopathologic evaluation of lifestyle modification in nonalcoholic fatty liver disease: a randomized trial. *Therap Adv Gastroenterol* 2013; **6**: 249-259 [PMID: 23814606 DOI: 10.1177/1756283X13484078]

141 **Ueno T**, Sugawara H, Sujaku K, Hashimoto O, Tsuji R, Tamaki S, Torimura T, Inuzuka S, Sata M, Tanikawa K. Therapeutic effects of restricted diet and exercise in obese patients with fatty liver. *J Hepatol* 1997; **27**: 103-107 [PMID: 9252081 DOI: 10.1016/S0168-8278(97)80287-5]

142 **Tendler D**, Lin S, Yancy WS Jr, Mavropoulos J, Sylvestre P, Rockey DC, Westman EC. The effect of a low-carbohydrate, ketogenic diet on nonalcoholic fatty liver disease: a pilot study. *Dig Dis Sci* 2007; **52**: 589-593 [PMID: 17219068 DOI: 10.1007/s10620-006-9433-5]

143 **Promrat K**, Kleiner DE, Niemeier HM, Jackvony E, Kearns M, Wands JR, Fava JL, Wing RR. Randomized controlled trial testing the effects of weight loss on nonalcoholic steatohepatitis. *Hepatology* 2010; **51**: 121-129 [PMID: 19827166 DOI: 10.1002/hep.23276]

144 **Vilar-Gomez E**, Martinez-Perez Y, Calzadilla-Bertot L, Torres-Gonzalez A, Gra-Oramas B, Gonzalez-Fabian L, Friedman SL, Diago M, Romero-Gomez M. Weight Loss Through Lifestyle Modification Significantly Reduces Features of Nonalcoholic Steatohepatitis. *Gastroenterology* 2015; **149**: 367-78.e5; quiz e14-5 [PMID: 25865049 DOI: 10.1053/j.gastro.2015.04.005]

145 **Glass LM**, Dickson RC, Anderson JC, Suriawinata AA, Putra J, Berk BS, Toor A. Total body weight loss

of ≥ 10 % is associated with improved hepatic fibrosis in patients with nonalcoholic steatohepatitis. *Dig Dis Sci* 2015; **60**: 1024-1030 [PMID: 25354830 DOI: 10.1007/s10620-014-3380-3]

146 **Zelber-Sagi S**, Salomone F, Mlynarsky L. The Mediterranean dietary pattern as the diet of choice for non-alcoholic fatty liver disease: Evidence and plausible mechanisms. *Liver Int* 2017; **37**: 936-949 [PMID: 28371239 DOI: 10.1111/liv.13435]

147 **Baratta F**, Pastori D, Polimeni L, Bucci T, Ceci F, Calabrese C, Ernesti I, Pannitteri G, Violi F, Angelico F, Del Ben M. Adherence to Mediterranean Diet and Non-Alcoholic Fatty Liver Disease: Effect on Insulin Resistance. *Am J Gastroenterol* 2017; **112**: 1832-1839 [PMID: 29063908 DOI: 10.1038/ajg.2017.371]

148 **Ryan MC**, Itsiopoulos C, Thodis T, Ward G, Trost N, Hofferberth S, O'Dea K, Desmond PV, Johnson NA, Wilson AM. The Mediterranean diet improves hepatic steatosis and insulin sensitivity in individuals with non-alcoholic fatty liver disease. *J Hepatol* 2013; **59**: 138-143 [PMID: 23485520 DOI: 10.1016/j.jhep.2013.02.012]

149 **Kaliora AC**, Gioxari A, Kalafati IP, Diolintzi A, Kokkinos A, Dedoussis GV. The Effectiveness of Mediterranean Diet in Nonalcoholic Fatty Liver Disease Clinical Course: An Intervention Study. *J Med Food* 2019; **22**: 729-740 [PMID: 31290733 DOI: 10.1089/jmf.2018.0020]

150 **Locklear CT**, Golabi P, Gerber L, Younossi ZM. Exercise as an intervention for patients with end-stage liver disease: Systematic review. *Medicine (Baltimore)* 2018; **97**: e12774 [PMID: 30334965 DOI: 10.1097/MD.0000000000012774]

151 **Macías-Rodríguez RU**, Ilarraza-Lomelí H, Ruiz-Margáin A, Ponce-de-León-Rosales S, Vargas-Vorácková F, García-Flores O, Torre A, Duarte-Rojo A. Changes in Hepatic Venous Pressure Gradient Induced by Physical Exercise in Cirrhosis: Results of a Pilot Randomized Open Clinical Trial. *Clin Transl Gastroenterol* 2016; **7**: e180 [PMID: 27415618 DOI: 10.1038/ctg.2016.38]

152 **Zhang HJ**, He J, Pan LL, Ma ZM, Han CK, Chen CS, Chen Z, Han HW, Chen S, Sun Q, Zhang JF, Li ZB, Yang SY, Li XJ, Li XY. Effects of Moderate and Vigorous Exercise on Nonalcoholic Fatty Liver Disease: A Randomized Clinical Trial. *JAMA Intern Med* 2016; **176**: 1074-1082 [PMID: 27379904 DOI: 10.1001/jamainternmed.2016.3202]

153 **Keating SE**, Hackett DA, George J, Johnson NA. Exercise and non-alcoholic fatty liver disease: a systematic review and meta-analysis. *J Hepatol* 2012; **57**: 157-166 [PMID: 22414768 DOI: 10.1016/j.jhep.2012.02.023]

154 **Hamasaki H**. Perspectives on Interval Exercise Interventions for Non-Alcoholic Fatty Liver Disease. *Medicines (Basel)* 2019; **6** [PMID: 31374827 DOI: 10.3390/medicines6030083]

155 **Oh S**, So R, Shida T, Matsuo T, Kim B, Akiyama K, Isobe T, Okamoto Y, Tanaka K, Shoda J. High-Intensity Aerobic Exercise Improves Both Hepatic Fat Content and Stiffness in Sedentary Obese Men with Nonalcoholic Fatty Liver Disease. *Sci Rep* 2017; **7**: 43029 [PMID: 28223710 DOI: 10.1038/srep43029]

156 **Pedroso FE**, Angriman F, Endo A, Dasenbrock H, Storino A, Castillo R, Watkins AA, Castillo-Angeles M, Goodman JE, Zitsman JL. Weight loss after bariatric surgery in obese adolescents: a systematic review and meta-analysis. *Surg Obes Relat Dis* 2018; **14**: 413-422 [PMID: 29248351 DOI: 10.1016/j.soard.2017.10.003]

157 **O'Brien PE**, Hindle A, Brennan L, Skinner S, Burton P, Smith A, Crosthwaite G, Brown W. Long-Term Outcomes After Bariatric Surgery: a Systematic Review and Meta-analysis of Weight Loss at 10 or More Years for All Bariatric Procedures and a Single-Centre Review of 20-Year Outcomes After Adjustable Gastric Banding. *Obes Surg* 2019; **29**: 3-14 [PMID: 30293134 DOI: 10.1007/s11695-018-3525-0]

158 **Sjöström L**, Lindroos AK, Peltonen M, Torgerson J, Bouchard C, Carlsson B, Dahlgren S, Larsson B, Narbro K, Sjöström CD, Sullivan M, Wedel H; Swedish Obese Subjects Study Scientific Group. Lifestyle, diabetes, and cardiovascular risk factors 10 years after bariatric surgery. *N Engl J Med* 2004; **351**: 2683-2693 [PMID: 15616203 DOI: 10.1056/NEJMoa035622]

159 **Schauer PR**, Bhatt DL, Kirwan JP, Wolski K, Aminian A, Brethauer SA, Navaneethan SD, Singh RP, Pothier CE, Nissen SE, Kashyap SR; STAMPEDE Investigators. Bariatric Surgery versus Intensive Medical Therapy for Diabetes - 5-Year Outcomes. *N Engl J Med* 2017; **376**: 641-651 [PMID: 28199805 DOI: 10.1056/NEJMoa1600869]

160 **Mingrone G**, Panunzi S, De Gaetano A, Guidone C, Iaconelli A, Nanni G, Castagneto M, Bornstein S, Rubino F. Bariatric-metabolic surgery versus conventional medical treatment in obese patients with type 2 diabetes: 5 year follow-up of an open-label, single-centre, randomised controlled trial. *Lancet* 2015; **386**: 964-973 [PMID: 26369473 DOI: 10.1016/S0140-6736(15)00075-6]

161 **Lassailly G**, Caiazzo R, Buob D, Pigeyre M, Verkindt H, Labreuche J, Raverdy V, Leteurtre E, Dharancy S, Louvet A, Romon M, Duhamel A, Pattou F, Mathurin P. Bariatric Surgery Reduces Features of Nonalcoholic Steatohepatitis in Morbidly Obese Patients. *Gastroenterology* 2015; **149**: 379-388; quiz e15-e16 [PMID: 25917783 DOI: 10.1053/j.gastro.2015.04.014]

162 **Caiazzo R**, Lassailly G, Leteurtre E, Baud G, Verkindt H, Raverdy V, Buob D, Pigeyre M, Mathurin P, Pattou F. Roux-en-Y gastric bypass versus adjustable gastric banding to reduce nonalcoholic fatty liver disease: a 5-year controlled longitudinal study. *Ann Surg* 2014; **260**: 893-899; discussion 898-899 [PMID: 25379859 DOI: 10.1097/SLA.0000000000000945]

163 **Moretto M**, Kupski C, da Silva VD, Padoin AV, Mottin CC. Effect of bariatric surgery on liver fibrosis. *Obes Surg* 2012; **22**: 1044-1049 [PMID: 22108808 DOI: 10.1007/s11695-011-0559-y]

164 **Galli F**, Azzi A, Birringer M, Cook-Mills JM, Eggersdorfer M, Frank J, Cruciani G, Lorkowski S, Özer NK. Vitamin E: Emerging aspects and new directions. *Free Radic Biol Med* 2017; **102**: 16-36 [PMID: 27816611 DOI: 10.1016/j.freeradbiomed.2016.09.017]

165 **Parola M**, Muraca R, Dianzani I, Barrera G, Leonarduzzi G, Bendinelli P, Piccoletti R, Poli G. Vitamin E dietary supplementation inhibits transforming growth factor beta 1 gene expression in the rat liver. *FEBS Lett* 1992; **308**: 267-270 [PMID: 1505665 DOI: 10.1016/0014-5793(92)81290-3]

166 **Sanyal AJ**, Mofrad PS, Contos MJ, Sargeant C, Luketic VA, Sterling RK, Stravitz RT, Shiffman ML, Clore J, Mills AS. A pilot study of vitamin E *versus* vitamin E and pioglitazone for the treatment of nonalcoholic steatohepatitis. *Clin Gastroenterol Hepatol* 2004; **2**: 1107-1115 [PMID: 15625656 DOI: 10.1016/S1542-3565(04)00457-4]

167 **Sanyal AJ**, Chalasani N, Kowdley KV, McCullough A, Diehl AM, Bass NM, Neuschwander-Tetri BA, Lavine JE, Tonascia J, Unalp A, Van Natta M, Clark J, Brunt EM, Kleiner DE, Hoofnagle JH, Robuck PR, NASH CRN. Pioglitazone, vitamin E, or placebo for nonalcoholic steatohepatitis. *N Engl J Med* 2010; **362**: 1675-1685 [PMID: 20427778 DOI: 10.1056/NEJMoa0907929]

168 **Sumida Y**, Naito Y, Tanaka S, Sakai K, Inada Y, Taketani H, Kanemasa K, Yasui K, Itoh Y, Okanoue T, Yoshikawa T. Long-term (>=2 yr) efficacy of vitamin E for non-alcoholic steatohepatitis. *Hepatogastroenterology* 2013; **60**: 1445-1450 [PMID: 23933938 DOI: 10.5754/hge11421]

169 **Xu R**, Tao A, Zhang S, Deng Y, Chen G. Association between vitamin E and non-alcoholic steatohepatitis: a meta-analysis. *Int J Clin Exp Med* 2015; **8**: 3924-3934 [PMID: 26064294]

170 **Harrison SA**, Torgerson S, Hayashi P, Ward J, Schenker S. Vitamin E and vitamin C treatment improves fibrosis in patients with nonalcoholic steatohepatitis. *Am J Gastroenterol* 2003; **98**: 2485-2490 [PMID: 14638353 DOI: 10.1111/j.1572-0241.2003.08699.x]

171 **Aithal GP**, Thomas JA, Kaye PV, Lawson A, Ryder SD, Spendlove I, Austin AS, Freeman JG, Morgan L, Webber J. Randomized, placebo-controlled trial of pioglitazone in nondiabetic subjects with nonalcoholic steatohepatitis. *Gastroenterology* 2008; **135**: 1176-1184 [PMID: 18718471 DOI: 10.1053/j.gastro.2008.06.047]

172 **Cusi K**, Orsak B, Bril F, Lomonaco R, Hecht J, Ortiz-Lopez C, Tio F, Hardies J, Darland C, Musi N, Webb A, Portillo-Sanchez P. Long-Term Pioglitazone Treatment for Patients With Nonalcoholic Steatohepatitis and Prediabetes or Type 2 Diabetes Mellitus: A Randomized Trial. *Ann Intern Med* 2016; **165**: 305-315 [PMID: 27322798 DOI: 10.7326/M15-1774]

173 **Bril F**, Biernacki DM, Kalavalapalli S, Lomonaco R, Subbarayan SK, Lai J, Tio F, Suman A, Orsak BK, Hecht J, Cusi K. Role of Vitamin E for Nonalcoholic Steatohepatitis in Patients With Type 2 Diabetes: A Randomized Controlled Trial. *Diabetes Care* 2019; **42**: 1481-1488 [PMID: 31332029 DOI: 10.2337/dc19-0167]

174 **Vilar-Gomez E**, Vuppalanchi R, Gawrieh S, Ghabril M, Saxena R, Cummings OW, Chalasani N. Vitamin E Improves Transplant-Free Survival and Hepatic Decompensation Among Patients With Nonalcoholic Steatohepatitis and Advanced Fibrosis. *Hepatology* 2020; **71**: 495-509 [PMID: 30506586 DOI: 10.1002/hep.30368]

175 **Klein EA**, Thompson IM Jr, Tangen CM, Crowley JJ, Lucia MS, Goodman PJ, Minasian LM, Ford LG, Parnes HL, Gaziano JM, Karp DD, Lieber MM, Walther PJ, Klotz L, Parsons JK, Chin JL, Darke AK, Lippman SM, Goodman GE, Meyskens FL Jr, Baker LH. Vitamin E and the risk of prostate cancer: the Selenium and Vitamin E Cancer Prevention Trial (SELECT). *JAMA* 2011; **306**: 1549-1556 [PMID: 21990298 DOI: 10.1001/jama.2011.1437]

176 **Schürks M**, Glynn RJ, Rist PM, Tzourio C, Kurth T. Effects of vitamin E on stroke subtypes: meta-analysis of randomised controlled trials. *BMJ* 2010; **341**: c5702 [PMID: 21051774 DOI: 10.1136/bmj.c5702]

177 **Lutchman G**, Promrat K, Kleiner DE, Heller T, Ghany MG, Yanovski JA, Liang TJ, Hoofnagle JH. Changes in serum adipokine levels during pioglitazone treatment for nonalcoholic steatohepatitis: relationship to histological improvement. *Clin Gastroenterol Hepatol* 2006; **4**: 1048-1052 [PMID: 16814613 DOI: 10.1016/j.cgh.2006.05.005]

178 **Lefebvre E**, Moyle G, Reshef R, Richman LP, Thompson M, Hong F, Chou HL, Hashiguchi T, Plato C, Poulin D, Richards T, Yoneyama H, Jenkins H, Wolfgang G, Friedman SL. Antifibrotic Effects of the Dual CCR2/CCR5 Antagonist Cenicriviroc in Animal Models of Liver and Kidney Fibrosis. *PLoS One* 2016; **11**: e0158156 [PMID: 27347680 DOI: 10.1371/journal.pone.0158156]

179 **Friedman SL**, Ratziu V, Harrison SA, Abdelmalek MF, Aithal GP, Caballeria J, Francque S, Farrell G, Kowdley KV, Craxi A, Simon K, Fischer L, Melchor-Khan L, Vest J, Wiens BL, Vig P, Seyedkazemi S, Goodman Z, Wong VW, Loomba R, Tacke F, Sanyal A, Lefebvre E. A randomized, placebo-controlled trial of cenicriviroc for treatment of nonalcoholic steatohepatitis with fibrosis. *Hepatology* 2018; **67**: 1754-1767 [PMID: 28833331 DOI: 10.1002/hep.29477]

180 **Mayo Clinic**. AURORA: Phase 3 Study for the Efficacy and Safety of CVC for the Treatment of Liver Fibrosis in Adults With NASH. Available from: www.mayo.edu/research/clinical-trials/cls-20425267

181 **Markham A**, Keam SJ. Obeticholic Acid: First Global Approval. *Drugs* 2016; **76**: 1221-1226 [PMID: 27406083 DOI: 10.1007/s40265-016-0616-x]

182 **Mudaliar S**, Henry RR, Sanyal AJ, Morrow L, Marschall HU, Kipnes M, Adorini L, Sciacca CI, Clopton P, Castelloe E, Dillon P, Pruzanski M, Shapiro D. Efficacy and safety of the farnesoid X receptor agonist obeticholic acid in patients with type 2 diabetes and nonalcoholic fatty liver disease. *Gastroenterology* 2013; **145**: 574-582.e1 [PMID: 23727264 DOI: 10.1053/j.gastro.2013.05.042]

183 **Neuschwander-Tetri BA**, Loomba R, Sanyal AJ, Lavine JE, Van Natta ML, Abdelmalek MF, Chalasani N, Dasarathy S, Diehl AM, Hameed B, Kowdley KV, McCullough A, Terrault N, Clark JM, Tonascia J, Brunt EM, Kleiner DE, Doo E; NASH Clinical Research Network. Farnesoid X nuclear receptor ligand obeticholic acid for non-cirrhotic, non-alcoholic steatohepatitis (FLINT): a multicentre, randomised, placebo-controlled trial. *Lancet* 2015; **385**: 956-965 [PMID: 25468160 DOI: 10.1016/S0140-6736(14)61933-4]

184 **Younossi ZM**, Ratziu V, Loomba R, Rinella M, Anstee QM, Goodman Z, Bedossa P, Geier A, Beckebaum S, Newsome PN, Sheridan D, Sheikh MY, Trotter J, Knapple W, Lawitz E, Abdelmalek MF, Kowdley KV, Montano-Loza AJ, Boursier J, Mathurin P, Bugianesi E, Mazzella G, Olveira A, Cortez-Pinto H, Graupera I, Orr D, Gluud LL, Dufour JF, Shapiro D, Campagna J, Zaru L, MacConell L, Shringarpure R, Harrison S, Sanyal AJ; REGENERATE Study Investigators. Obeticholic acid for the treatment of non-alcoholic steatohepatitis: interim analysis from a multicentre, randomised, placebo-controlled phase 3 trial. *Lancet* 2019; **394**: 2184-2196 [PMID: 31813633 DOI: 10.1016/S0140-6736(19)33041-7]

185 **Loomba R**, Sanyal AJ, Kowdley KV, Terrault N, Chalasani NP, Abdelmalek MF, McCullough AJ, Shringarpure R, Ferguson B, Lee L, Chen J, Liberman A, Shapiro D, Neuschwander-Tetri BA. Factors Associated With Histologic Response in Adult Patients With Nonalcoholic Steatohepatitis. *Gastroenterology* 2019; **156**: 88-95.e5 [PMID: 30222962 DOI: 10.1053/j.gastro.2018.09.021]

186 **Tully DC**, Rucker PV, Chianelli D, Williams J, Vidal A, Alper PB, Mutnick D, Bursulaya B, Schmeits J, Wu X, Bao D, Zoll J, Kim Y, Groessl T, McNamara P, Seidel HM, Molteni V, Liu B, Phimister A, Joseph SB, Laffitte B. Discovery of Tropifexor (LJN452), a Highly Potent Non-bile Acid FXR Agonist for the Treatment of Cholestatic Liver Diseases and Nonalcoholic Steatohepatitis (NASH). *J Med Chem* 2017; **60**: 9960-9973 [PMID: 29148806 DOI: 10.1021/acs.jmedchem.7b00907]

187 **Hernandez ED**, Zheng L, Kim Y, Fang B, Liu B, Valdez RA, Dietrich WF, Rucker PV, Chianelli D, Schmeits J, Bao D, Zoll J, Dubois C, Federe GC, Chen L, Joseph SB, Klickstein LB, Walker J, Molteni V, McNamara P, Meeusen S, Tully DC, Badman MK, Xu J, Laffitte B. Tropifexor-Mediated Abrogation of Steatohepatitis and Fibrosis Is Associated With the Antioxidative Gene Expression Profile in Rodents. *Hepatol Commun* 2019; **3**: 1085-1097 [PMID: 31388629 DOI: 10.1002/hep4.1368]

188 **Pedrosa M**, Seyedkazemi S, Francque S, Sanyal A, Rinella M, Charlton M, Loomba R, Ratziu V, Kochuparampil J, Fischer L, Vaidyanathan S, Anstee QM. A randomized, double-blind, multicenter, phase 2b study to evaluate the safety and efficacy of a combination of tropifexor and cenicriviroc in patients with nonalcoholic steatohepatitis and liver fibrosis: Study design of the TANDEM trial. *Contemp Clin Trials* 2020; **88**: 105889 [PMID: 31731005 DOI: 10.1016/j.cct.2019.105889]

189 Efficacy, Safety and Tolerability of the Combination of Tropifexor & Licogliflozin Compared to Each Monotherapy, in Adult Patients With NASH and Liver Fibrosis. In: ClinicalTrials.gov [Internet]. Bethesda (MD): U.S. National Library of Medicine. Available from: https://clinicaltrials.gov/ct2/show/NCT04065841 ClinicalTrials.gov Identifier: NCT04065841

190 Study of Safety and Efficacy of Tropifexor (LJN452) in Patients With Non-alcoholic Steatohepatitis (NASH). In: ClinicalTrials.gov [Internet]. Bethesda (MD): U.S. National Library of Medicine. Available from: https://clinicaltrials.gov/ct2/show/NCT02855164 ClinicalTrials.gov Identifier: NCT02855164

191 **Ratziu V**, Harrison SA, Francque S, Bedossa P, Lehert P, Serfaty L, Romero-Gomez M, Boursier J, Abdelmalek M, Caldwell S, Drenth J, Anstee QM, Hum D, Hanf R, Roudot A, Megnien S, Staels B, Sanyal A; GOLDEN-505 Investigator Study Group. Elafibranor, an Agonist of the Peroxisome Proliferator-Activated Receptor-α and -δ, Induces Resolution of Nonalcoholic Steatohepatitis Without Fibrosis Worsening. *Gastroenterology* 2016; **150**: 1147-1159.e5 [PMID: 26874076 DOI: 10.1053/j.gastro.2016.01.038]

192 **Idris I**, Donnelly R. Sodium-glucose co-transporter-2 inhibitors: an emerging new class of oral antidiabetic drug. *Diabetes Obes Metab* 2009; **11**: 79-88 [PMID: 19125776 DOI: 10.1111/j.1463-1326.2008.00982.x]

193 **Bolinder J**, Ljunggren Ö, Kullberg J, Johansson L, Wilding J, Langkilde AM, Sugg J, Parikh S. Effects of dapagliflozin on body weight, total fat mass, and regional adipose tissue distribution in patients with type 2 diabetes mellitus with inadequate glycemic control on metformin. *J Clin Endocrinol Metab* 2012; **97**: 1020-1031 [PMID: 22238392 DOI: 10.1210/jc.2011-2260]

194 **Shimizu M**, Suzuki K, Kato K, Jojima T, Iijima T, Murohisa T, Iijima M, Takekawa H, Usui I, Hiraishi H, Aso Y. Evaluation of the effects of dapagliflozin, a sodium-glucose co-transporter-2 inhibitor, on hepatic steatosis and fibrosis using transient elastography in patients with type 2 diabetes and non-alcoholic fatty liver disease. *Diabetes Obes Metab* 2019; **21**: 285-292 [PMID: 30178600 DOI: 10.1111/dom.13520]

195 **Yokote K**, Sano M, Tsumiyama I, Keefe D. Dose-dependent reduction in body weight with LIK066 (licogliflozin) treatment in Japanese patients with obesity. *Diabetes Obes Metab* 2020; **22**: 1102-1110 [PMID: 32072763 DOI: 10.1111/dom.14006]

196 **Bays HE**, Kozlovski P, Shao Q, Proot P, Keefe D. Licogliflozin, a Novel SGLT1 and 2 Inhibitor: Body Weight Effects in a Randomized Trial in Adults with Overweight or Obesity. *Obesity (Silver Spring)* 2020; **28**: 870-881 [PMID: 32187881 DOI: 10.1002/oby.22764]

197 **Loomba R**, Lawitz E, Mantry PS, Jayakumar S, Caldwell SH, Arnold H, Diehl AM, Djedjos CS, Han L, Myers RP, Subramanian GM, McHutchison JG, Goodman ZD, Afdhal NH, Charlton MR; GS-US-384-1497 Investigators. The ASK1 inhibitor selonsertib in patients with nonalcoholic steatohepatitis: A randomized, phase 2 trial. *Hepatology* 2018; **67**: 549-559 [PMID: 28892558 DOI: 10.1002/hep.29514]

World Journal of Gastroenterology

Submit a Manuscript: https://www.f6publishing.com

World J Gastroenterol 2020 October 21; 26(39): 5944-5958

DOI: 10.3748/wjg.v26.i39.5944

ISSN 1007-9327 (print) ISSN 2219-2840 (online)

MINIREVIEWS

Enteroscopy in children and adults with inflammatory bowel disease

Giovanni Di Nardo, Gianluca Esposito, Chiara Ziparo, Federica Micheli, Luigi Masoni, Maria Pia Villa, Pasquale Parisi, Maria Beatrice Manca, Flavia Baccini, Vito Domenico Corleto

ORCID number: Giovanni Di Nardo 0000-0002-9026-7758; Gianluca Esposito 0000-0002-2242-5048; Chiara Ziparo 0000-0002-4209-6958; Federica Micheli 0000-0001-5420-7005; Luigi Masoni 0000-0001-9866-4224; Maria Pia Villa 0000-0002-5859-0723; Pasquale Parisi 0000-0001-9042-8120; Maria Beatrice Manca 0000-0001-8993-5467; Flavia Baccini 0000-0002-3245-8329; Vito Domenico Corleto 0000-0001-6383-9581.

Author contributions: Di Nardo G, Villa MP and Parisi P wrote the pediatric section of the paper; Ziparo C and Manca MB collected and analyzed pediatric literature; Esposito G, Masoni L and Corleto VD wrote the adult section of the paper; Micheli F and Baccini F collected and analyzed adult literature.

Conflict-of-interest statement: Authors declare no conflict of interests for this article.

Giovanni Di Nardo, Chiara Ziparo, Maria Pia Villa, Pasquale Parisi, Chair of Pediatrics, Pediatric Gastroenterology and Endoscopy Unit, NESMOS Department, Faculty of Medicine and Psychology, Sapienza University of Rome, Sant' Andrea University Hospital, Rome 00189, Lazio, Italy

Gianluca Esposito, Department of Medical-Surgical Sciences and Translational Medicine, Sant' Andrea Hospital, Sapienza University of Rome, Rome 00189, Lazio, Italy

Federica Micheli, Flavia Baccini, Vito Domenico Corleto, Department of Medical-Surgical Sciences and Translational Medicine, Sant' Andrea University Hospital, Sapienza University of Rome, Rome 00189, Lazio, Italy

Luigi Masoni, Department of Surgery, Sapienza University of Rome, Sant' Andrea University Hospital, Rome 00189, Lazio, Italy

Maria Beatrice Manca, Department of Clinical and Surgical Translational Medicine, Anesthesia and Intensive Care Medicine, Sant'Andrea University Hospital, Sapienza University of Rome 00189, Lazio, Italy

Corresponding author: Giovanni Di Nardo, MD, PhD, Assistant Professor, Chair of Pediatrics, Pediatric Gastroenterology and Endoscopy Unit, NESMOS Department, Faculty of Medicine and Psychology, Sapienza University of Rome, Sant' Andrea University Hospital, Via di Grottarossa 1035-1039, Rome 00189, Lazio, Italy. giovanni.dinardo@uniroma1.it

Abstract

Inflammatory bowel disease (IBD) includes Crohn's disease (CD), ulcerative colitis and unclassified entities. CD commonly involves the terminal ileum and colon but at the time of diagnosis it can be confined to the small bowel (SB) in about 30% of the patients, especially in the young ones. Management of isolated SB-CD can be challenging and objective evaluation of the SB mucosa is essential in differentiating CD from other enteropathies to achieve therapeutic decisions and to plan the follow-up. The introduction of cross-sectional imaging techniques and capsule endoscopy (CE) have significantly expanded the ability to diagnose SB diseases providing a non-invasive test for the visualization of the entire SB mucosa. The main CE limitations are the low specificity, the lack of therapeutic capabilities and the impossibility to take biopsies. Device assisted enteroscopy (DAE) enables histological confirmation when traditional endoscopy, capsule endoscopy and cross-sectional imaging are inconclusive and also allows therapeutic interventions such as balloon stricture dilation, intralesional steroid injection, capsule retrieval and more recently stent insertion. In the current review

Manuscript source: Invited manuscript

Received: June 28, 2020
Peer-review started: June 28, 2020
First decision: July 28, 2020
Revised: August 8, 2020
Accepted: September 25, 2020
Article in press: September 25, 2020
Published online: October 21, 2020

P-Reviewer: Hijaz NM
S-Editor: Huang P
L-Editor: A
P-Editor: Ma YJ

we will discuss technical aspect, indications and safety profile of DAE in children and adults with IBD.

Key Words: Enteroscopy; Device assisted enteroscopy; Inflammatory bowel disease; Crohn's disease; Small bowel disease; Endoscopic balloon dilation

Core Tip: Evaluation of the small bowel (SB) mucosa is essential in differentiating Crohn's disease (CD) from other enteropathies to achieve therapeutic decisions and to plan follow-up. The introduction of cross-sectional imaging techniques and capsule endoscopy have significantly improved the diagnostic approach to SB disease providing a non-invasive diagnostic method for the visualization of the entire SB mucosa. However, Device assisted enteroscopy (DAE) has further revolutionized management of SB-CD enabling histological confirmation and allowing therapeutic interventions. In the current review we will discuss technical aspect, indications and safety profile of DAE in children and adults with inflammatory bowel disease.

Citation: Di Nardo G, Esposito G, Ziparo C, Micheli F, Masoni L, Villa MP, Parisi P, Manca MB, Baccini F, Corleto VD. Enteroscopy in children and adults with inflammatory bowel disease. *World J Gastroenterol* 2020; 26(39): 5944-5958
URL: https://www.wjgnet.com/1007-9327/full/v26/i39/5944.htm
DOI: https://dx.doi.org/10.3748/wjg.v26.i39.5944

INTRODUCTION

Inflammatory bowel disease (IBD) represents a group of chronic inflammatory disorders that involve the colon, small bowel (SB) and the entire gastrointestinal tract and include Crohn's disease (CD), ulcerative colitis (UC) and unclassified entities[1,2]. CD is a chronic immuno-mediated inflammation that most commonly involves the terminal ileum and colon, but at the time of diagnosis, it can be confined to the SB, as seen in approximately 30% of CD patients, especially young patients[2-8]. Isolated SB-CD can be challenging to diagnose and manage for several reasons. First, the SB is less easily accessible by endoscopy, making it easy to miss a SB-CD diagnosis with conventional endoscopy contributing to a delay in diagnosis as observed in many patients with CD[5]. Second, SB ulcerations induced by infection (such as tuberculosis) or drugs can sometimes be difficult to differentiate from CD[1,8]. Third, compared with the other phenotypes, SB-CD is associated with an increased risk of relapse and stricture development[1,3,6,7]. Fourth, SB cancer associated with CD is a rare but difficult problem because only a minority of these cases are diagnosed preoperatively and at an early stage[9]. Finally, in the paediatric population, SB-CD has particular clinical relevance for its negative impact on growth and pubertal development[2,7]. Thus, objective evaluation of the SB mucosa is essential in differentiating CD from other enteropathies to make therapeutic decisions and to plan follow-up.

For many years, investigation of the SB has been a challenge because of its anatomy, location, and relative tortuosity. The introduction of cross-sectional imaging techniques such as computed tomography (CT) and magnetic resonance imaging (MRI), enterography/enteroclysis and SB ultrasound, have enhanced SB assessment with great accuracy in evaluating transmural and extraluminal disease, but subtle mucosal changes can still be missed[8,10,11].

Capsule endoscopy (CE) and device-assisted enteroscopy (DAE) have significantly expanded the ability to diagnose SB diseases. CE provides a non-invasive test for the visualization of the entire SB mucosa, which can aid in the diagnosis of SB-CD and monitoring the therapeutic response. The main CE limitations in IBD patients are a low specificity, a lack of therapeutic capabilities and the inability to perform biopsies[12,13].

DAE enables histological confirmation when other modalities, such as traditional endoscopy, CE and cross-sectional imaging, are inconclusive and allows therapeutic interventions, such as balloon stricture dilation, intralesional steroid injection, capsule

retrieval and, more recently, stent insertion[12-14].

In the current review, we will discuss the technical aspects, indications and safety profiles of DAE in children and adults with IBD.

TECHNICAL ASPECTS

DAE is a generic term for any endoscopic technique that includes assisted progression (*i.e.*, balloons, overtubes or other devices) and includes double-balloon enteroscopy (DBE), single-balloon enteroscopy (SBE), balloon-guided endoscopy (BGE) and spiral enteroscopy (SE). Table 1 shows the main characteristics of the currently available DAE systems.

The DBE system was presented for the first time in Japan in 2001, and the first paediatric report was described in 2003. The DBE system is constituted of a high-resolution enteroscope with a latex balloon attached to the end of the enteroscope and a second balloon attached to the tip of a polyurethane overtube. Both balloons are inflated and deflated using an external pressure-controlled pump system. Currently, three DBE systems are available. The P type is the thinnest; however, the small diameter of its working channel (2.2 mm) limits the possibility of performing advanced therapeutic procedures. The T type has an outer diameter of 9.4 mm and a working channel diameter of 3.2 mm. The main advantage of the short type (working length of 152 cm) is the compatibility with all conventional devices; it can also be used for endoscopic retrograde cholangiopancreatography in patients with altered anatomy and difficult or failed colonoscopy[14-18].

SBE was introduced in 2007, and in contrast to DBE, there is no balloon at the tip of the enteroscope; therefore, handling of the balloon control unit is simplified. The enteroscope is a high-resolution video endoscope, the overtube and balloon are made of silicon, and a control unit with a safety pressure setting that controls the balloon inflation and deflation[14-18].

DBE and SBE use the push-and-pull method, however, the number of balloons makes a slight difference in the insertion technique between the two balloon assisted enteroscopy (BAE) systems.

Two operators are generally needed to perform DBE. For the antegrade approach, the endoscope and overtube are advanced to the duodenum beyond the major papilla, at which point the balloon located on the overtube is inflated to hold the small bowel tightly. The enteroscope is then advanced to the distal side of the SB, and its balloon is inflated to prevent slippage of the scope backward. The balloon on the overtube is then deflated, and the overtube is advanced towards the tip of the enteroscope. The balloon on the overtube is then reinflated. The enteroscope-overtube is then withdrawn to fold the SB along the overtube. This process can be repeated until the maximal insertion point or the target lesion is reached[16].

SBE is usually performed by two operators, but it may be easier than DBE to perform with a single-operator. The enteroscope and overtube are advanced similar to the DBE insertion technique. However, the enteroscope tip must be angled during advancement of the overtube and only after the angulation of the tip, the overtube is advanced towards the tip of the enteroscope, and the overtube balloon is then inflated. The enteroscope-overtube is then withdrawn to fold the SB along the overtube. The overtube balloon is left inflated and the enteroscope is advanced from the overtube tip. This cycle of forward advancement and withdrawal is repeated until the maximal insertion point or target lesion is reached[16].

Retrograde insertion is more difficult than antegrade insertion, even in experienced hands. For both techniques (DBE and SBE), the enteroscope and overtube are advanced to the caecum. After inflation of the overtube balloon, the enteroscope-overtube is withdrawn to decrease the ileo-colic angle. With the overtube balloon inflated, the enteroscope is then passed through the ileocecal valve, and endoscope balloon is inflated within the ileum to hold the position. The overtube is then advanced into the ileum with the balloon deflated. For SBE, although the insertion technique is the same, backward slippage of the tip of the enteroscope to the caecum during insertion of the overtube is frequent because of the lack of a balloon at the enteroscope tip, which would enable holding the position[16].

DBE and SBE have the same procedural technique in children and adults. BAE is suitable and safe for children aged > 3 years and weight > 14 kg. However, due to a smaller abdominal cavity, thinner intestinal walls and a narrower intestinal lumen, BAE requires a greater level of skill in younger children[18].

BGE is performed by using an on-demand through-the-scope (TTS) balloon inserted

Table 1 Technical characteristics of the currently available device-assisted endoscopes

Company	DAE system type	Endoscope model	Optical field of view	Optical depth of field	Endoscope distal outer diameter	Endoscope channel inner diameter	Endoscope working length	Overtube outer diameter	Image enhancement
Fujifilm Corporation (Tokyo, Japan)	DBE	EN-580T	140	2-100 mm	9, 4 mm	3, 2 mm	200 cm	13, 2 mm	FICE
	DBE	EN-580XP	140	2-100 mm	7, 5 mm	2, 2 mm	200 cm	11, 6 mm	FICE
	DBE	EI-580BT	140	2-100 mm	9, 4 mm	3, 2 mm	156 cm	13, 2 mm	FICE
Pentax Medical (Tokyo, Japan)	DBE on demand using BGE	G-EYE34-i10L/F	140	2-100 mm	11, 5 mm	3, 8 mm	170 cm	NA	i-scan OE
	DBE on demand using BGE	G-EYE38-i10L/F	140	2-100 mm	13, 2 mm	3, 8 mm	170 cm	NA	i-scan OE
	DBE on demand using BGE	G-EYE38-i10F2	140	2-100 mm	13, 2 mm	3, 8 mm	150 cm	NA	i-scan OE
Olympus (Tokyo, Japan)	SBE	SIF-Q180	140	3-100 mm	9, 2 mm	2, 8 mm	200 cm	13, 2 mm	NBI
	SBE	SIFH290S	140	3-100 mm	9, 2 mm	3, 2 mm	152 cm	13, 2 mm	NBI
	SE	SIF-Y0019 Motorized spiral overtube	140	2-100 mm	11, 3 mm	3, 2 mm	168 cm	31, 1 mm max[1];18, 1 mm distal[2]	NBI
NaviAid, Smart Medical Systems, (Ra'anana, Israel)	BGE	No specific scope required	NA	NA	NA	NA	NA	NA	NA
Spirus Medical (Stoughton, United States)	SE	No specific scope required	NA	NA	NA	NA	NA	14, 5 mm	NA

[1]Maximum outer diameter.
[2]Distal outer diameter. DAE: Device assisted enteroscopy; DBE: Double balloon enteroscopy; SBE: Single balloon enteroscopy; BGE: Balloon guided enterosopy; SE: Spiral enteroscopy; NA: Not applicable; NBI: Narrow band imaging; FICE: Flexible spectral imaging color enhancement; OE: Optical enhancement.

in the working channel of any endoscope. The balloon is then inflated, allowing anchoring in the SB, and progression is obtained with repeated push-and-pull maneuvres by sliding the endoscope over the catheter. The balloon catheter can be removed to perform therapeutic interventions. The main limitation of this technique is the low stability of the endoscope during the therapeutic procedure due to the lack of an anchoring balloon[14,15]. To overcome this drawback, a colonoscope with an integrated latex-free balloon at the bending section has recently been developed (see Table 1). These colonoscopes, combined with a disposable advancing balloon (AB) applied through the instrument channel, provide the assembly to perform deep SB double-balloon endoscopy. The balloon endoscopes as well as the AB devices are controlled simultaneously by the inflation system. The feasibility and safety of BGE using the NaviAid AB device has recently been evaluated in children with IBD[19].

SE involves the use of an overtube with a raised spiral ridge. The SB is pulled and pleated onto the overtube by continuous rotation of the spiral, and advancement into the SB is allowed by clockwise rotation of the overtube during insertion and anticlockwise rotation during withdrawal. SE overtubes have been replaced by a new motorized spiral enteroscopy (NMSE) system. NMSE system is composed of a reusable endoscope with an integrated motor permitting the rotation of a short spiral overtube placed on the insertion tube portion of the endoscope and a motor control

unit with a foot pedal and visual force gauge. The foot pedal activates the drive motor located in the endoscope handle, which controls the rotational direction and speed of a coupler located in the middle of the insertion tube of the endoscope. The bowel is pleated or unpleated on the insertion tube of the endoscope with clockwise or anticlockwise rotation, respectively. After reaching the required depth of insertion, the endoscope will be withdrawn using motorized anticlockwise spiral rotation[14,20]. Preliminary data shows that NMSE offers advantages over traditional methods, in particular concerning the duration of the procedure and the relative ease of use; otherwise, it has similar diagnostic and therapeutic yields as both SBE and DBE[20,21]. Nevertheless, data on SE in IBD patients are not yet available, and the large diameter of the SE overtube makes this technique unsuitable for children.

The approach (oral, anal or both) is determined on clinical judgement, cross-sectional imaging (CT/MRI - enterography) and CE. Usually, the oral approach is the first choice due to its lower technical difficulty[16,17,22]. Both oral and anal approaches are used if inspection of the whole intestine is clinically needed. An ink tattoo or clip is left at the deepest point of insertion achieved during the first approach.

Overnight fasting of 12 h for solid food and 4 h for clear liquids before starting the procedure is enough for the oral approach, the same bowel cleansing suggested for colonoscopy required for retrograde enteroscopy. General anaesthesia is recommended for long procedures or for patients in whom sedation is not appropriate (*i.e.*, paediatric and high-risk patients). Fluoroscopy is not always needed, except when adhesions or massive SB-CD involvement is expected and when enteroscopy is aimed to perform stricture dilation[16,17,22]. Insufflation of CO_2 is recommended due to its capability to allow deeper SB intubation of the scope and minimize postprocedural discomfort[22,23].

ENTEROSCOPY IN ADULT PATIENTS WITH SUSPECTED IBD

Five studies evaluated the impact of DAE on adults with suspected IBD (Table 2)[24-28].

In a retrospective German study, 16 adult patients with clinical suspicion of isolated SB-CD underwent DBE after negative gastroscopy and colonoscopy. Abnormal SB findings were detected in 7 patients (44%) but pathognomonic histological findings of CD were found in only one case (6%). However, a diagnosis of CD was confirmed in 11 out of 16 (69%) patients taking into account clinical, endoscopic and radiological features[24].

Navaneethan *et al*[25] retrospectively reviewed a BAE registry, which included DBE and SBE procedures performed on adult patients, to assess the diagnostic yield and clinical impact of BAE in suspected SB-CD. They identified 22 patients with suspected SB-CD and inconclusive results from conventional upper and lower gastrointestinal endoscopy, radiological cross-sectional imaging studies, and CE. These patients underwent BAE, which provided a histological diagnosis of CD in 6 patients (27.3%) and non-steroidal anti-inflammatory drug-induced enteropathy in 3 patients (13.6%), whereas no lesions were found in 13 patients (59.1%). One newly diagnosed CD patient underwent successful balloon dilation of a jejunal stricture without complications. The authors also evaluated the agreement rate between CT or MRI enterography and BAE findings which was quite low (36.4%).

In a multicenter retrospective study, 43 adult patients with suspected CD based on abnormal cross-sectional imaging or CE were evaluated by DBE. The diagnostic yield reached 79%. SB-CD diagnosis was confirmed in 17 patients, and DBE examination was normal in 12 cases. The remaining 5 patients received alternative diagnoses, such as NSAID ulceration, stricture/solitary ulcer, anastomotic ulcer, or Meckel's diverticulum. Another main outcome measure of this study was a comparison of DBE and CE findings. Overall, only 46% of lesions were confirmed on DBE. In 33 (77%) patients, BAE modified clinical management by the exclusion of CD in 11 patients, confirming CD in 17, diagnosing stenosis in 2, nonspecific ulcer in 2 and stopping the NSAID treatment in 1[26].

Tun *et al*[27] retrospectively evaluated the impact of DBE and histology on the diagnosis and management of 100 adult patients with suspected SB-CD for whom, based on clinical and laboratory data and after colonoscopy and radiological imaging studies or CE, a diagnosis of CD was not achieved. Abnormal macroscopic DBE findings were detected in 60 patients (ulcers, n = 47; stricture, n = 11; abnormal mucosa, n = 2), and biopsy samples was obtained. Twenty-three showed no histological abnormalities despite positive macroscopic appearances on DBE, whilst among the remaining 37 patients, according to histological examination, the diagnosis

Table 2 Available studies on diagnostic yield and impact on patient management of device assisted enteroscopy in adult Crohn's disease patients

Ref.	DAE system type	Study design	CD patients (*n*)		Diagnostic yield (%)		Impact on patient management (%)	
			Suspected	Known	Suspected	Known	Suspected	Known
Mensink *et al*[36], *J Gastroenterol* 2009	DBE	Retrospective	0	40	60		75	
Kondo *et al*[33], *J Gastroenterol* 2010	DBE	Retrospective	25	50	47		53	
Möschler *et al*[34], *Endoscopy* 2011	DBE	Prospective	193		47		NA	
Schulz *et al*[24], *Dig Endosc* 2014	DBE	Retrospective	16	0	69		NA	
Navaneethan *et al*[25], *Endosc Int Open* 2014	SBE or DBE	Retrospective	22	43	27	53	NA	53
Christian *et al*[35], *World J Gastrointest Endosc* 2016	Retrograde SBE	Retrospective	29		41.4		17	
Rahman *et al*[26], *Gastrointest Endosc* 2015	DBE	Retrospective	43	38	79	87	77	82
Tun *et al*[27], *Eur J Gastroenterol Hepatol* 2016	DBE	Retrospective	100	0	NA		45	
Holleran *et al*[28], *Scand J Gastroenterol* 2018	SBE	Retrospective	13	39	39	77	69	

DAE: Device-assisted enteroscopy; DBE: Double balloon enteroscopy; SBE: Single balloon enteroscopy; CD: Crohn's disease; NA: Not applicable.

of CD was confirmed in 8 patients (22%), and 15 (41%) had histology suggestive of CD.

Nevertheless, combining clinical, biochemical, endoscopic, and histological findings, 45% of all patients received treatment for CD. After a median follow-up period of 27 mo, the diagnosis of CD was confirmed in 38% of DBE-positive patients[27].

The diagnostic yield and the impact on clinical outcome of the use of SBE for suspected SB-CD were evaluated in an Italian retrospective study, which included 13 adult patients. The diagnostic yield was 39%, detecting four patients with active ileitis and one with ileal stricture. For the remaining eight patients, a new diagnosis of CD was reached in 4 patients (8%) and excluded in the other 4 patients (8%)[28].

ENTEROSCOPY IN CHILDREN WITH SUSPECTED IBD

Five studies, two on SBE, two on DBE and one on BGE, evaluated the impact of DAE on children with suspected IBD[19,29-32] (Table 3).

In a study previously published by our group, 16 paediatric patients with suspected CD and unspecific findings after extensive assessment with upper and lower GI endoscopy, MRE and CE were assessed by SBE. SBE provided a histological diagnosis of CD in 12 patients and eosinophilic enteropathy in 2 patients, no lesions were found in the remaining 2 patients. Moreover, SBE allowed dilation of SB strictures identified on MRI in 2 suspected CD patients[29].

de Ridder *et al*[30] evaluated the diagnostic yield of SBE for paediatric CD. In this study, patients were evaluated directly by two-route SBE, not preceded by conventional endoscopy or CE, and in 8 out of 14 patients with suspected CD, the diagnosis was confirmed after SBE.

Urs *et al*[31] performed DBE in 3 patients with suspected CD after CE examination indicating mucosal abnormalities. DBE led to a CD diagnosis in 2 out of 3 patients, and CD was excluded in the other child due to the lack of mucosal lesions and a normal histology.

The study from Uchida *et al*[32], evaluated the efficacy and safety of DBE in 8 children with suspected CD after inconclusive gastroscopy, colonoscopy and an SB-contrast study. DBE confirmed a CD diagnosis in 2 out of 8 patients, led to an alternative diagnosis in four patients and did not find mucosal lesions or histological abnormalities in the remaining 2 patients.

Recently, Broide *et al*[19] evaluated the feasibility and safety of BAE using a NaviAid AB device in children with suspected IBD. Technical success was achieved in 95.23%

Table 3 Available study on device assisted enteroscopy in pediatric inflammatory bowel disease

Ref.	DAE system type	Study design	Patients (*n*)	Previous diagnostic work-up	Impact on patient management (%)	Therapeutic procedure	Complications
Di Nardo *et al*[29], *Gastrointest Endosc* 2012	SBE	Prospective	Suspected CD = 16, known CD = 14	MRI and CE	Suspected CD = 87%, known CD = 64%	Balloon dilation = 5 pts	Not reported
de Ridder *et al*[30], *Gastrointest Endosc* 2012	SBE	Prospective	Suspected CD = 14, known CD = 6	MRI and US	Suspected CD = 57%, known CD = 83%	NA	Not reported
Uchida *et al*[32], *Pediatr Int* 2012	DBE	Prospective	Suspected CD = 8, known CD = 4	Upper GI endoscopy, colonoscopy and SB-contrast study	Suspected CD = 75%, known CD = 75%	Balloon dilation = 1 pt	Not reported
Urs *et al*[31], *J Pediatr Gastroenterol Nutr* 2014	DBE	Prospective	Suspected CD = 3, known CD = 5	CE	Suspected CD = 66%, known CD = 100%	NA	Not reported
Broide *et al*[19], *J Pediatr Gastroenterol Nutr* 2020	BGE	Prospective	Suspected IBD = 15, known IBD = 16	NA	NA	NA	Not reported

DAE: Device-assisted enteroscopy; DBE: Double balloon enteroscopy; SBE: Single balloon enteroscopy; BGE: Balloon guided enterosopy; CE: Capsule endoscopy; IBD: Inflammatory bowel disease; CD: Crohn's disease; NA: Not applicable; MRI: Magnetic resonance imaging; US: Ultrasonography; GI: Gastrointestinal; SB: Small bowel; CE: Capsule endoscopy.

and 85.7% of the anterograde and retrograde approaches, respectively. Moreover, the total procedure time was significantly shorter and the learning curve was faster than with BAE, as its operation is intuitive and simple. Unfortunately, the diagnostic yield of this technique was not assessed. In the 15 patients with suspected IBD, 3 patients were diagnosed with UC and 3 patients with CD; the remaining 9 patients showed no intestinal abnormalities.

According to the previously described literature and our previously published algorithm (Figure 1), in children with suspected IBD, we suggest the following approach. DAE is recommended when conventional endoscopy, imaging of the SB and CE are inconclusive and tissue sampling and/or therapeutic procedures would alter disease management. DAE should be the preferred primary endoscopic procedure only if a stricture or an easy-to-reach lesion (*i.e.*, proximal SB wall thickness) is suspected at imaging. This is reasonable due to DAE diagnostic and therapeutic possibilities and to the high capsule retention risk[6,18].

ENTEROSCOPY IN SUSPECTED AND ALREADY KNOWN IBD ADULT PATIENTS

Three studies evaluated the impact of DAE on both suspected and already known IBD adult patients (Table 2)[33-35].

Kondo *et al*[33] analyzed a total of 1444 cases of DBE performed for various indications collected in a multicenter database to investigate the efficacy of DBE for the diagnosis and treatment of CD on adult patient. A total of 50 known and 25 newly diagnosed patients with CD were included. Active inflammatory lesions (ulcer and erosion/redness) were found in 51.2% of the symptomatic patients, but they were also detected in 33.3% of the asymptomatic CD patients. Overall, the treatment was altered for 53.3% of the patients, resulting in introduction of anti-TNF antibody (20.4%) or other medication (17.5%), dose reduction (1.9%), endoscopic balloon dilation (EBD, 7.8%), and surgical treatment (5.8%).

In 2011, Möschler *et al*[34] published the results derived from a large prospective German database that reported data from 2245 DBE examinations carried out on 1765 adult patients over a 2-year period. Overall, 193 patients (11%) with known or suspected CD underwent endoscopic examination of the SB, showing pathological findings in 91 of them, with a diagnostic yield of 47%.

In a retrospective study, Christian *et al*[35] evaluated the diagnostic and therapeutic yields of SBE using solely a retrograde approach. Overall, 136 retrograde SBE procedures were considered. Twenty-nine (21.3%) were performed on adult patients

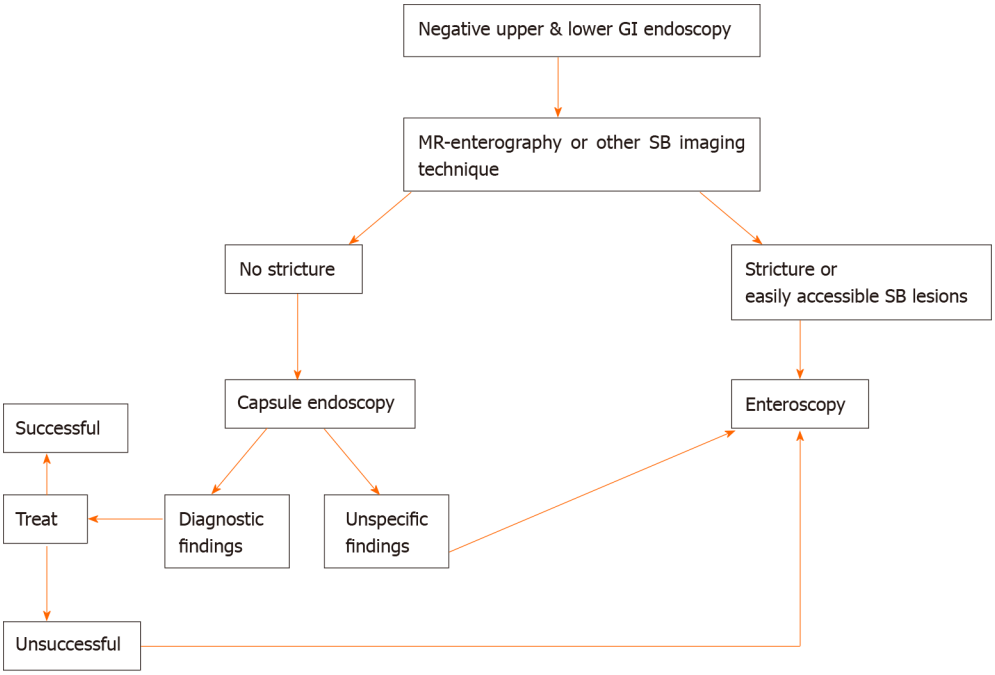

Figure 1 Suggested algorithm in children with suspected inflammatory bowel disease (adapted by reference 6). GI: Gastrointestinal; MR: Magnetic resonance; SB: Small bowel.

with suspected or known CD. Twelve new diagnoses of CD were established, with a diagnostic yield of 41.4%, and the therapeutic yield was 17.2%.

ENTEROSCOPY IN ADULT PATIENTS WITH KNOWN IBD

Four studies evaluated the impact of BAE on adults with known IBD (Table 2)[25,26,28,36].

Mensink *et al*[36] assessed the clinical impact of endoscopic evaluation of the SB by DBE for patients with known CD and clinical suspicion of SB activity. They retrospectively analyzed 52 DBE procedures performed in 40 adult patients. Twenty-four patients (60%) showed macroscopically active inflammation of the SB, and 18 of them (75%) had to switch therapy with persistent clinical improvement in 83% of patients after a mean follow-up of 13 mo. In particular, amongst the 18 patients, 11 introduced anti-TNF therapy, 2 switched from infliximab to adalimumab, 1 introduced steroid therapy, 2 underwent surgical resection, and 2 underwent balloon dilation.

In the study from Navaneethan *et al*[25], BAE was performed in 43 adult patients with an established diagnosis of CD whose main indications were disease activity and extent assessment in uninvestigated CD, anaemia or obscure gastrointestinal bleeding, confirmation and treatment of SB strictures diagnosed on radiological examination, and evaluation of activity and extent of CD in postoperative patients. BAE had impact on clinical management of 23 patients (53.4%): 18 patients (41.8%) had active inflammation with ulcers or strictures, which led to a switch of medical therapy or surgery, 5 (11.6%) with documented stenosis in the absence of active ulcers underwent EBD to treat obstructive symptoms. Overall, thirteen patients (30%) required surgery: Two due to lack of other therapeutic strategies, five as a result of medical treatment escalation failure, five based on patient's choice, and one due to bowel perforation after BAE. Finally, the authors found that the agreement rate between CT or MRI enterography and BAE findings were higher (75.6 %) in already diagnosed CD patients.

In the study by Rahman *et al*[26], the authors analyzed the diagnostic yield and the clinical impact of DBE on the management of 38 adult patients with known CD and clinical suspicion of SB disease activity. In this setting, the diagnostic yield was 87% (33/38 patients), revealing an active disease in 11 patients (29%), 5 with CD stricture (13%), 3 (8%) with functional obstruction due to fixed/angulated bowel, 3 (8%) with anastomotic ulcers, and 2 (5%) with nonspecific ulceration. DBE examination was normal in 9 cases (23.6%). Therefore, DBE resulted in a clinical management change for 82% of patients with known CD. Thirteen patients (34%) needed an increase or a

switch of therapy or surgery, and three patients (8%) underwent endoscopic dilation without any related complications. One patient (1.2%) underwent surgery due to perforation consequent to diagnostic DBE and directly related to an ulcer at an anastomosis site.

Holleran *et al*[28] evaluated the diagnostic yield and the impact on clinical outcome of the use of SBE for 39 patients with established SB-CD. In this setting, the diagnostic yield was significantly higher than for adult patients with suspected CD (77% *vs* 39%, $P < 0.01$). The most frequent findings were ileal or anastomotic strictures in 38% and 26%, respectively, and active ileitis in 21% of patients. SBE had an immediate clinical impact on 69% ($n = 33$) of patients, including stricture dilation in 27%, adjustment of medications in 48%, and referral for surgical resection in 6%. Long-term follow-up (mean duration of 11 mo, range of 3-22 mo), performed in 34 patients (65%) of the 52 patients, showed a significant change in the mean Harvey-Bradshaw index score from 6.6 to 4.2 after the procedure ($P < 0.0001$).

Regarding the therapeutic role of enteroscopy in adult patients with IBD complications, several studies evaluated the clinical impact of EBD using BAE for SB stricture in CD (Table 4)[25,28,33,37-45]. Among them, Hirai *et al*[45] conducted, to our knowledge, the largest multicenter study currently available, which prospectively enrolled 112 patients with symptomatic SB strictures related to CD to clarify the efficacy and safety of EBD. Ninety-five patients (85%) were included, and balloon dilation was successful in 89 (94%) of them. The primary endpoint related to short-term outcomes was an improvement of symptoms, which was achieved in 66 patients (70%). The dilation diameter was significantly larger (15.20 ± 1.70 mm *vs* 13.65 ± 2.59 mm, $P = 0.03$) in the short-term symptomatic improvement group than in the no improvement group. There were no other significant differences in the groups' baseline characteristics or stricture features.

The long-term outcomes of EBD for SB stricture in CD adult patients were extensively evaluated by two retrospective Japanese studies[43,44].

Hirai *et al*[43] evaluated 65 CD patients with obstructive symptoms caused by endoscopically manageable SB strictures (stricture length ≤ 5 cm, not associated with fistulae, abscesses or deep ulcers, and without severe curvature of the stricture) with clinical success in 80.0% of patients (52/65). During the observation period after the initial EBD (mean 41.8 ± 24.9 mo), seventeen patients (26.2%) underwent surgery. The cumulative surgery-free rate was 79% and 73% at 2 and 3 years, respectively, and it was significantly higher among successful EBD cases ($P < 0.0001$). Moreover, the cumulative re-dilation-free rate was 64% at 2 years and 47% at 3 years. No significant differences in terms of concomitant treatment or initial dilation method were detected between patients with and without the need for re-dilation.

More recently, Sunada *et al*[44] analyzed data regarding 85 patients who underwent DBE-assisted EBD for SB-CD strictures and were then followed-up for a mean period of 41.9 mo (range, 0-141). The surgery-free rate after the initial EBD was 87.3% at 1 year, 78.1% at 3 years, and 74.2% at 5 years. Univariate analysis showed that the presence of an internal fistula beside the refractory stricture was significantly associated with the need for surgical intervention (hazard ratio: 5.50; 95%CI: 2.16-14.0; $P = 0.01$).

ENTEROSCOPY IN CHILDREN WITH KNOWN IBD

Five studies, two on SBE, two on DBE and one on BGE evaluated the impact of BAE in children with established IBD (Table 3)[19,29-32].

In our study, the SBE findings of 14 patients with longstanding CD and symptoms unexplained by conventional endoscopy led to the introduction of or to a change in therapeutic approach in 11 patients. Moreover, SBE allowed successful and safe dilation of SB strictures identified on MRE in 3 patients[29].

In the study of de Ridder *et al*[30] SBE findings led to a change in therapy in five out of six patients with established CD.

In the paper from Urs *et al*[31], in the established CD group, 2 patients had adverse reactions to infliximab with poor response to adalimumab and 3 patients underwent DBE for disease evaluation and consideration of escalation of treatment. DBE led to a change of treatment in all 5 patients.

Uchida *et al*[32] evaluated the efficacy and safety of DBE in 4 children with established CD. After DBE, one patient underwent balloon dilatation and a change in medical therapy, and in two patients, surgical resection was planned. In one patient, DBE was performed for assessment of intestinal lesions due to persistent abdominal

Table 4 Available studies on endoscopic balloon dilation using balloon-assisted enteroscopy for small bowel stricture in adult Crohn's disease patients

Ref.	DAE system type	Study design	CD patients (*n*)	Dilation diameter (mm), mean (range)	Technical success (%)	Clinical efficacy (%)	Dilatations (*n*), mean per patient (range)	Perforation (%)	Observation period (mo), mean (range)	Symptom recurrence (%)
Fukumoto *et al*[37], *Gastrointest Endosc* 2007	DBE	Retrospective	23	NA	NA	74	35, (1.52; 1-6)	0	12, (1-40)	26
Pohl *et al*[38], *Eur J Gastroenterol Hepatol* 2007	Push enteroscopy	NA	10	17, (12-20)	80	60	15, (1.5; 1-3)	0	10, (4-16)	40
Ohmiya *et al*[39], *Gastrointest Endosc* 2009	DBE	Retrospective	16	NA, (8-20)	96	69	NA	0	16, (2-43)	31
Despott *et al*[40], *Gastrointest Endosc* 2009	DBE	Prospective	11	15.4, (12-20)	73	73	18, (2; 1-3)	9	20.5, (2-41)	25
Hirai *et al*[41], *Dig Endosc* 2010	DBE	Retrospective	25	NA, (12-18)	72	72	55, (2.2; 1-4)	0	11, (6-29)	22
Kondo *et al*[33], *J Gastroenterol* 2010	DBE	Retrospective	8	NA	100	87.5	18, 1.5 (1-2)	0	NA	NA
Gill *et al*[42], *Ther Adv Gastroenterol* 2014	DBE	Retrospective	10	13.5, (10-16.5)	80	70	17, (1.8; 1-4)	20	NA	14
Hirai *et al*[43], *Dig Endosc* 2014	DBE	Retrospective	65	NA, (12-18)	80	80	NA	1.5	NA	48
Navaneethan *et al*[25], *Endosc Int Open* 2014	BAE (SBE/DBE)	Retrospective	6	NA	100	100	7, (1.16; 1-2)	16	NA	NA
Sunada *et al*[44], *Inflamm Bowel Dis* 2016	DBE	Retrospective	85	12.4, (8–20)	NA	87	321, (3.8; 1–14)	5	41.9, (0–141)	78.5
Holleran *et al*[28], *Scand J Gastroenterol* 2018	SBE	Retrospective	13	13, (12-15)	100	80	14, (1; 1-2)	0	8, (2-16)	23
Hirai *et al*[45], *Journal of Crohn's and Colitis* 2018	SBE and DBE	Prospective	95	15, (8-20)	94	70	90, (1; 1-2)	0	24, (NA)	NA

BAE: Balloon-assisted enteroscopy; DBE: Double balloon enteroscopy; SBE: Single balloon enteroscopy; SB: Small bowel; CD: Crohn's disease; NA: Not available or not applicable; DAE: Device assisted enteroscopy.

pain, and only small erosion near the ileal stoma orifice was found; thus, therapy after DBE was not changed.

Recently, Broide *et al*[19] evaluated the feasibility and safety of BAE using a NaviAid AB device in 16 children with known IBD (undetermined colitis = 7; CD = 9). In this group, 6 patients with undetermined colitis at baseline were confirmed to have active UC, and 1 patient exhibited mucosal healing. Eight of the 9 patients with known CD were confirmed to have active CD, and 1 patient exhibited mucosal healing.

According to the previously described literature and our previously published

algorithm (Figure 2), we suggest the following approach for children with known IBD. DAE is recommended when endoscopic visualization and biopsies of the small intestine are needed to exclude an alternative diagnosis (lymphoma, tuberculosis or carcinoma) or to perform a therapeutic procedure including SB stricture dilation and removal of retained capsule. Endoscopists should keep in mind that in established CD adhesions may limit examination and that active stricturing CD significantly increases the perforation risk[6,18].

COMPLICATIONS

The most common complications related to DAE are perforation, bleeding, and pancreatitis, with an overall rate on adult patients of approximately 1%[34,46].

A large retrospective Japanese study identified 29068 patients who underwent diagnostic BAE, reporting 32 cases of perforation (0.11%). Nine hundred forty-two patients underwent a subsequent therapeutic BAE, but no perforations occurred in this group. Univariate logistic regression analysis showed that patients with IBD, irrespective of steroid therapy, had a significantly higher risk of perforation than patients without (8.6-fold and 2.5-fold, respectively)[47]. In most published studies, the perforation rate among CD patients who underwent EBD varied from 0% to 10% of subjects[25,28,33,37-41,44,45], although one small cohort reported a perforation rate of 20%[42] (Table 4). Bleeding after balloon dilation of CD strictures occurs in approximately 2.5% of patients, and it only often requires conservative management[25]. Finally, pancreatitis has been reported to occur in 0.3% of patients, especially after procedures with an anterograde approach[34,48,49]. Adverse event rates for the different types of DAE have been shown to be similar[50].

In paediatric literature, major complications have been reported only for therapeutic procedures. A large retrospective study on 257 DBE procedures in children reported an overall complication rate of 5.4% (10.4% in patients under 10 years)[51]. No major complications related to either diagnostic or therapeutic procedures have been reported in the paediatric IBD setting.

CONCLUSION

This review analyzed the use of enteroscopy in children and adults with IBD.

Regarding the use of DAE for diagnostic purposes in adult patients, recent ECCO-ESGAR guidelines recommend its use for: (1) Patients with negative endoscopy and suspicion of CD on MRI or CE, if endoscopic and histological diagnostic confirmation is needed; and (2) Patients who need endoscopic intervention in the SB[52].

According to the studies considered in this review, as shown in Table 2, the diagnostic yields of DAE in adult patients with suspected CD and with known CD is 27%-79% and 53%-87%, respectively, and are higher if the indication for DAE is based on previous SB investigations that may identify suspected lesions and guide the choice of insertion route[25,26,28]. Meanwhile, the diagnostic yield of DAE drops drastically when the indication is placed exclusively based on non-specific abdominal symptoms[34]. Similarly the agreement rate between imaging and DAE findings appears to be higher in already diagnosed CD patients than in suspected CD patients (75.6% *vs* 36.4% respectively)[25]. In published studies a significant impact of DAE on patient management, ranges from 17% to 82%, has been reported with a persistent clinical improvement reaching 83% after a mean follow-up of 13 mo in the study by Mensink *et al*[36] (Table 2)[25-28,33,35].

Endoscopic ballon dilation overall has a technical success rate from 72% to 100%, and a clinical success rate greater than 60%[25,28,33,37-45], although no standardized definitions of both these short-term outcomes has been clearly stated yet. The majority of studies evaluated clinical success basing on the obstructive symptoms reported by the patients often comparing the clinical improvement before and after dilation[40,45]. The most commonly used definition of technical success was a chance to get the successful inflation of a balloon catheter within the stenotic bowel segment and the subsequently endoscope passage through the dilated segment. Studies considered in this review showed that the mean stricture dilation diameter varied from 12.4 to 17 mm, up to a maximum of 20 mm, and the achievement of a larger dilation diameter seems to be related to a better short-term clinical improvement[45]. The recurrence of obstructive symptoms after EBD has been variously reported (14% to 78.5% of adult subjects) according to the time considered that in most cases was very short (less than

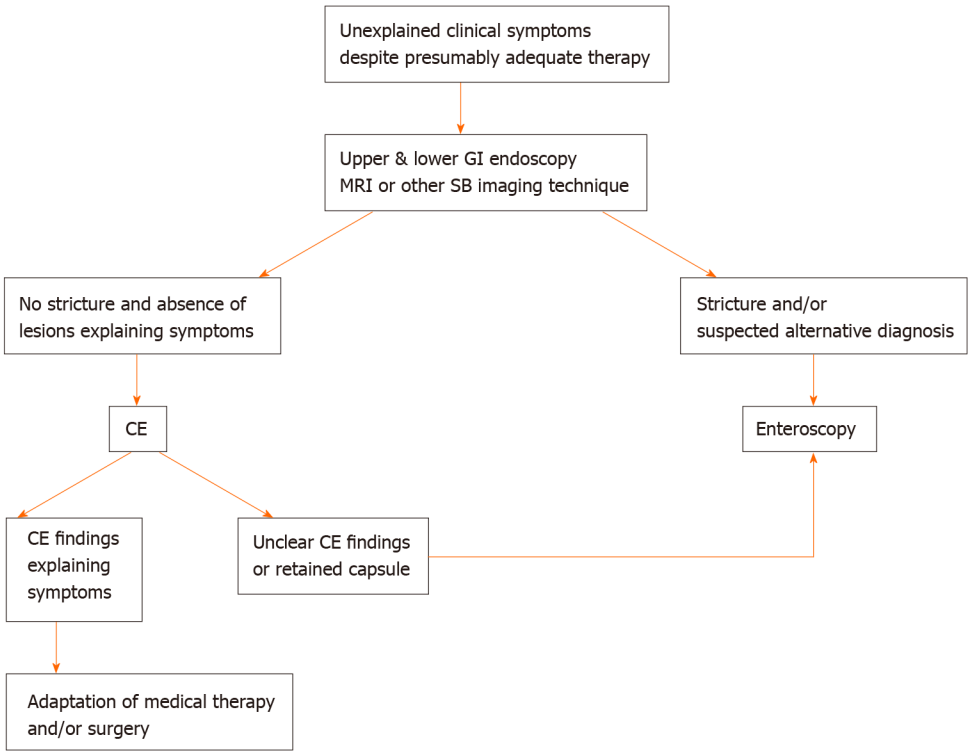

Figure 2 Suggested algorithm in children with known inflammatory bowel disease (adapted by reference 6). GI: Gastrointestinal; MRI: Magnetic resonance imaging; SB: Small bowel; CE: Capsule endoscopy.

fifteen months). However, in two studies the average duration of the observation period after initial EBD was greater than three years[43,44]. They showed the highest recurrence rates of obstructive symptoms (48% and 78.5%, respectively) but most patients underwent successful re-dilation with a high cumulative surgery-free rate (over 78% at three years). Although balloon dilation of CD strictures appears effective in the short term, it needs to take into consideration the high recurrence rate with the possibility of repeated endoscopic procedures and/or surgery. To our best knowledge, no RCT comparing surgery *vs* balloon dilation has been conducted. As suggested by the ECCO guidelines[53], EBD or surgery are both suitable treatment options for patients with short (< 5 cm) strictures of the terminal ileum in CD, and the choice of treatment depends on local expertise and patient choice (very low level of evidence). Overall, DAE is a relatively safe procedure if it is performed in expert hands. However, needs deep sedation with the presence of anesthesiologist, may require a bi-directional approach, and has a high complication rate, making this technique not very widespread. Moreover, in children with CD EBD it could delay or avoid invasive surgery to dilate the stenosis and potentially positively affect the natural history of chronic disease all the more important the more it is in childhood.

The present review underlines several limitations related to the studies currently available in the literature. First, most of them are retrospective and include a small number of patients. Second, the studies are often extremely heterogeneous in terms of patient selection, including IBD and non-IBD patients. Third, there are no standardized definitions of the principal outcome measures, such as technical success and clinical efficacy. Fourth, observational period after therapeutic endoscopic procedures, such as EBD, are often too short, not allowing a long-term evaluation. Fifth, into the manuscripts some results are not always clearly stated but have been calculated on the basis of results by the authors of the review.

In conclusion, enteroscopy seems a promising technique especially in patients with suspected isolated SB-CD and inconclusive results from conventional studies (including ileocolonoscopy and radiological cross-sectional imaging) in whom histological diagnosis would alter patient management. Moreover, DAE could have many roles in patients with known CD, in terms of adjustment of medical therapy to obtain more lasting and deep clinical improvement, concomitant diagnosis and treatment of stenosing complications and accurate localization of lesions to allow targeted surgical intervention. Because mucosal healing is increasingly becoming a

goal of therapy in CD, DBE may have a role in assessment response to therapy in the future in select cases. More standardized and wider studies are needed to confirm these evidences.

ACKNOWLEDGEMENTS

We thank Altobello Leo and Di Maio Adele for their tireless work to improve the care of pediatric patients.

REFERENCES

1 **Fong SC**, Irving PM. Distinct management issues with Crohn's disease of the small intestine. *Curr Opin Gastroenterol* 2015; **31**: 92-97 [PMID: 25594888 DOI: 10.1097/MOG.0000000000000149]
2 **Sauer CG**, Kugathasan S. Pediatric inflammatory bowel disease: highlighting pediatric differences in IBD. *Med Clin North Am* 2010; **94**: 35-52 [PMID: 19944797 DOI: 10.1016/j.mcna.2009.10.002]
3 **Hall B**, Holleran G, McNamara D. Small bowel Crohn's disease: an emerging disease phenotype? *Dig Dis* 2015; **33**: 42-51 [PMID: 25531496 DOI: 10.1159/000366047]
4 **Peyrin-Biroulet L**, Loftus EV Jr, Colombel JF, Sandborn WJ. The natural history of adult Crohn's disease in population-based cohorts. *Am J Gastroenterol* 2010; **105**: 289-297 [PMID: 19861953 DOI: 10.1038/ajg.2009.579]
5 **Pimentel M**, Chang M, Chow EJ, Tabibzadeh S, Kirit-Kiriak V, Targan SR, Lin HC. Identification of a prodromal period in Crohn's disease but not ulcerative colitis. *Am J Gastroenterol* 2000; **95**: 3458-3462 [PMID: 11151877 DOI: 10.1111/j.1572-0241.2000.03361.x]
6 **Di Nardo G**, de Ridder L, Oliva S, Casciani E, Escher JC, Cucchiara S. Enteroscopy in paediatric Crohn's disease. *Dig Liver Dis* 2013; **45**: 351-355 [PMID: 22947488 DOI: 10.1016/j.dld.2012.07.020]
7 **Chouraki V**, Savoye G, Dauchet L, Vernier-Massouille G, Dupas JL, Merle V, Laberenne JE, Salomez JL, Lerebours E, Turck D, Cortot A, Gower-Rousseau C, Colombel JF. The changing pattern of Crohn's disease incidence in northern France: a continuing increase in the 10- to 19-year-old age bracket (1988-2007). *Aliment Pharmacol Ther* 2011; **33**: 1133-1142 [PMID: 21488915 DOI: 10.1111/j.1365-2036.2011.04628.x]
8 **Leighton JA**, Pasha SF. Inflammatory Disorders of the Small Bowel. *Gastrointest Endosc Clin N Am* 2017; **27**: 63-77 [PMID: 27908519 DOI: 10.1016/j.giec.2016.08.004]
9 **Cuffari C**, Dubinsky M, Darbari A, Sena L, Baldassano R. Crohn's jejunoileitis: the pediatrician's perspective on diagnosis and management. *Inflamm Bowel Dis* 2005; **11**: 696-704 [PMID: 15973125 DOI: 10.1097/01.mib.0000166933.74477.69]
10 **Cullen G**, Donnellan F, Doherty GA, Smith M, Cheifetz AS. Evaluation of the small bowel in inflammatory bowel disease. *Expert Rev Gastroenterol Hepatol* 2013; **7**: 239-251 [PMID: 23445233 DOI: 10.1586/egh.13.11]
11 **Ou G**, Enns R. Capsule Endoscopy and Small Bowel Enteroscopy: Have They Rendered the Radiologist Obsolete? *Gastrointest Endosc Clin N Am* 2019; **29**: 471-485 [PMID: 31078248 DOI: 10.1016/j.giec.2019.02.007]
12 **Pennazio M**, Spada C, Eliakim R, Keuchel M, May A, Mulder CJ, Rondonotti E, Adler SN, Albert J, Baltes P, Barbaro F, Cellier C, Charton JP, Delvaux M, Despott EJ, Domagk D, Klein A, McAlindon M, Rosa B, Rowse G, Sanders DS, Saurin JC, Sidhu R, Dumonceau JM, Hassan C, Gralnek IM. Small-bowel capsule endoscopy and device-assisted enteroscopy for diagnosis and treatment of small-bowel disorders: European Society of Gastrointestinal Endoscopy (ESGE) Clinical Guideline. *Endoscopy* 2015; **47**: 352-376 [PMID: 25826168 DOI: 10.1055/s-0034-1391855]
13 **Di Nardo G**, Aloi M, Oliva S, Civitelli F, Casciani E, Cucchiara S. Investigation of small bowel in pediatric Crohn's disease. *Inflamm Bowel Dis* 2012; **18**: 1760-1776 [PMID: 22275336 DOI: 10.1002/ibd.22885]
14 **Pennazio M**, Venezia L, Cortegoso Valdivia P, Rondonotti E. Device-assisted enteroscopy: An update on techniques, clinical indications and safety. *Dig Liver Dis* 2019; **51**: 934-943 [PMID: 31138509 DOI: 10.1016/j.dld.2019.04.015]
15 **Schneider M**, Höllerich J, Beyna T. Device-assisted enteroscopy: A review of available techniques and upcoming new technologies. *World J Gastroenterol* 2019; **25**: 3538-3545 [PMID: 31367155 DOI: 10.3748/wjg.v25.i27.3538]
16 **Kim J**. Training in Endoscopy: Enteroscopy. *Clin Endosc* 2017; **50**: 328-333 [PMID: 28783921 DOI: 10.5946/ce.2017.089]
17 **ASGE Technology Committee**, Chauhan SS, Manfredi MA, Abu Dayyeh BK, Enestvedt BK, Fujii-Lau LL, Komanduri S, Konda V, Maple JT, Murad FM, Pannala R, Thosani NC, Banerjee S. Enteroscopy. *Gastrointest Endosc* 2015; **82**: 975-990 [PMID: 26388546 DOI: 10.1016/j.gie.2015.06.012]
18 **Di Nardo G**, Calabrese C, Conti Nibali R, De Matteis A, Casciani E, Martemucci L, Pagliaro G, Pagano N. Enteroscopy in children. *United European Gastroenterol J* 2018; **6**: 961-969 [PMID: 30228882 DOI: 10.1177/2050640618789853]
19 **Broide E**, Shalem T, Richter V, Matalon S, Shirin H. The Safety and Feasibility of a New Through-the-scope Balloon-assisted Enteroscopy in Children. *J Pediatr Gastroenterol Nutr* 2020; **71**: e6-e11 [PMID: 32187142 DOI: 10.1097/MPG.0000000000002706]
20 **Mans L**, Arvanitakis M, Neuhaus H, Devière J. Motorized Spiral Enteroscopy for Occult Bleeding. *Dig Dis* 2018; **36**: 325-327 [PMID: 29698967 DOI: 10.1159/000488479]
21 **Rahmi G**, Samaha E, Vahedi K, Ponchon T, Fumex F, Filoche B, Gay G, Delvaux M, Lorenceau-Savale C, Malamut G, Canard JM, Chatellier G, Cellier C. Multicenter comparison of double-balloon enteroscopy and

spiral enteroscopy. *J Gastroenterol Hepatol* 2013; **28**: 992-998 [PMID: 23488827 DOI: 10.1111/jgh.12188]
22 **Yamamoto H**, Ogata H, Matsumoto T, Ohmiya N, Ohtsuka K, Watanabe K, Yano T, Matsui T, Higuchi K, Nakamura T, Fujimoto K. Clinical Practice Guideline for Enteroscopy. *Dig Endosc* 2017; **29**: 519-546 [PMID: 28370422 DOI: 10.1111/den.12883]
23 **Li X**, Zhao YJ, Dai J, Li XB, Xue HB, Zhang Y, Xiong GS, Ohtsuka K, Gao YJ, Liu Q, Song Y, Fang JY, Ge ZZ. Carbon dioxide insufflation improves the intubation depth and total enteroscopy rate in single-balloon enteroscopy: a randomised, controlled, double-blind trial. *Gut* 2014; **63**: 1560-1565 [PMID: 24626435 DOI: 10.1136/gutjnl-2013-306069]
24 **Schulz C**, Mönkemüller K, Salheiser M, Bellutti M, Schütte K, Malfertheiner P. Double-balloon enteroscopy in the diagnosis of suspected isolated Crohn's disease of the small bowel. *Dig Endosc* 2014; **26**: 236-242 [PMID: 23855454 DOI: 10.1111/den.12142]
25 **Navaneethan U**, Vargo JJ, Menon KV, Sanaka MR, Tsai CJ. Impact of balloon-assisted enteroscopy on the diagnosis and management of suspected and established small-bowel Crohn's disease. *Endosc Int Open* 2014; **2**: E201-E206 [PMID: 26135093 DOI: 10.1055/s-0034-1377522]
26 **Rahman A**, Ross A, Leighton JA, Schembre D, Gerson L, Lo SK, Waxman I, Dye C, Semrad C. Double-balloon enteroscopy in Crohn's disease: findings and impact on management in a multicenter retrospective study. *Gastrointest Endosc* 2015; **82**: 102-107 [PMID: 25840927 DOI: 10.1016/j.gie.2014.12.039]
27 **Tun GS**, Rattehalli D, Sanders DS, McAlindon ME, Drew K, Sidhu R. Clinical utility of double-balloon enteroscopy in suspected Crohn's disease: a single-centre experience. *Eur J Gastroenterol Hepatol* 2016; **28**: 820-825 [PMID: 27010557 DOI: 10.1097/MEG.0000000000000629]
28 **Holleran G**, Valerii G, Tortora A, Scaldaferri F, Conti S, Amato A, Gasbarrini A, Costamagna G, Riccioni ME. The use of single balloon enteroscopy in Crohn's disease and its impact on clinical outcome. *Scand J Gastroenterol* 2018; **53**: 925-929 [PMID: 29966446 DOI: 10.1080/00365521.2018.1476914]
29 **Di Nardo G**, Oliva S, Aloi M, Rossi P, Casciani E, Masselli G, Ferrari F, Mallardo S, Stronati L, Cucchiara S. Usefulness of single-balloon enteroscopy in pediatric Crohn's disease. *Gastrointest Endosc* 2012; **75**: 80-86 [PMID: 21855873 DOI: 10.1016/j.gie.2011.06.021]
30 **de Ridder L**, Mensink PB, Lequin MH, Aktas H, de Krijger RR, van der Woude CJ, Escher JC. Single-balloon enteroscopy, magnetic resonance enterography, and abdominal US useful for evaluation of small-bowel disease in children with (suspected) Crohn's disease. *Gastrointest Endosc* 2012; **75**: 87-94 [PMID: 21963066 DOI: 10.1016/j.gie.2011.07.036]
31 **Urs AN**, Martinelli M, Rao P, Thomson MA. Diagnostic and therapeutic utility of double-balloon enteroscopy in children. *J Pediatr Gastroenterol Nutr* 2014; **58**: 204-212 [PMID: 24126830 DOI: 10.1097/MPG.0000000000000192]
32 **Uchida K**, Yoshiyama S, Inoue M, Koike Y, Yasuda H, Fujikawa H, Okita Y, Araki T, Tanaka K, Kusunoki M. Double balloon enteroscopy for pediatric inflammatory bowel disease. *Pediatr Int* 2012; **54**: 806-809 [PMID: 22564182 DOI: 10.1111/j.1442-200X.2012.03661.x]
33 **Kondo J**, Iijima H, Abe T, Komori M, Hiyama S, Ito T, Nakama A, Tominaga K, Kubo M, Suzuki K, Iwanaga Y, Ebara R, Takeda A, Tsuji S, Nishida T, Tsutsui S, Tsujii M, Hayashi N. Roles of double-balloon endoscopy in the diagnosis and treatment of Crohn's disease: a multicenter experience. *J Gastroenterol* 2010; **45**: 713-720 [PMID: 20174832 DOI: 10.1007/s00535-010-0216-6]
34 **Möschler O**, May A, Müller MK, Ell C; German DBE Study Group. Complications in and performance of double-balloon enteroscopy (DBE): results from a large prospective DBE database in Germany. *Endoscopy* 2011; **43**: 484-489 [PMID: 21370220 DOI: 10.1055/s-0030-1256249]
35 **Christian KE**, Kapoor K, Goldberg EM. Performance characteristics of retrograde single-balloon endoscopy: A single center experience. *World J Gastrointest Endosc* 2016; **8**: 501-507 [PMID: 27606042 DOI: 10.4253/wjge.v8.i15.501]
36 **Mensink PB**, Groenen MJ, van Buuren HR, Kuipers EJ, van der Woude CJ. Double-balloon enteroscopy in Crohn's disease patients suspected of small bowel activity: findings and clinical impact. *J Gastroenterol* 2009; **44**: 271-276 [PMID: 19271117 DOI: 10.1007/s00535-009-0011-4]
37 **Fukumoto A**, Tanaka S, Yamamoto H, Yao T, Matsui T, Iida M, Goto H, Sakamoto C, Chiba T, Sugano K. Diagnosis and treatment of small-bowel stricture by double balloon endoscopy. *Gastrointest Endosc* 2007; **66** Suppl 3: S108-S112 [PMID: 17709019 DOI: 10.1016/j.gie.2007.02.027]
38 **Pohl J**, May A, Nachbar L, Ell C. Diagnostic and therapeutic yield of push-and-pull enteroscopy for symptomatic small bowel Crohn's disease strictures. *Eur J Gastroenterol Hepatol* 2007; **19**: 529-534 [PMID: 17556897 DOI: 10.1097/MEG.0b013e328012b0d0]
39 **Ohmiya N**, Arakawa D, Nakamura M, Honda W, Shirai O, Taguchi A, Itoh A, Hirooka Y, Niwa Y, Maeda O, Ando T, Goto H. Small-bowel obstruction: diagnostic comparison between double-balloon endoscopy and fluoroscopic enteroclysis, and the outcome of enteroscopic treatment. *Gastrointest Endosc* 2009; **69**: 84-93 [PMID: 19111689 DOI: 10.1016/j.gie.2008.04.067]
40 **Despott EJ**, Gupta A, Burling D, Tripoli E, Konieczko K, Hart A, Fraser C. Effective dilation of small-bowel strictures by double-balloon enteroscopy in patients with symptomatic Crohn's disease (with video). *Gastrointest Endosc* 2009; **70**: 1030-1036 [PMID: 19640518 DOI: 10.1016/j.gie.2009.05.005]
41 **Hirai F**, Beppu T, Sou S, Seki T, Yao K, Matsui T. Endoscopic balloon dilatation using double-balloon endoscopy is a useful and safe treatment for small intestinal strictures in Crohn's disease. *Dig Endosc* 2010; **22**: 200-204 [PMID: 20642609 DOI: 10.1111/j.1443-1661.2010.00984.x]
42 **Gill RS**, Kaffes AJ. Small bowel stricture characterization and outcomes of dilatation by double-balloon enteroscopy: a single-centre experience. *Therap Adv Gastroenterol* 2014; **7**: 108-114 [PMID: 24790641 DOI: 10.1177/1756283X13513995]
43 **Hirai F**, Beppu T, Takatsu N, Yano Y, Ninomiya K, Ono Y, Hisabe T, Matsui T. Long-term outcome of endoscopic balloon dilation for small bowel strictures in patients with Crohn's disease. *Dig Endosc* 2014; **26**: 545-551 [PMID: 24528293 DOI: 10.1111/den.12236]
44 **Sunada K**, Shinozaki S, Nagayama M, Yano T, Takezawa T, Ino Y, Sakamoto H, Miura Y, Hayashi Y, Sato H, Lefor AK, Yamamoto H. Long-term Outcomes in Patients with Small Intestinal Strictures Secondary to

Crohn's Disease After Double-balloon Endoscopy-assisted Balloon Dilation. *Inflamm Bowel Dis* 2016; **22**: 380-386 [PMID: 26535767 DOI: 10.1097/MIB.0000000000000627]

45 **Hirai F**, Andoh A, Ueno F, Watanabe K, Ohmiya N, Nakase H, Kato S, Esaki M, Endo Y, Yamamoto H, Matsui T, Iida M, Hibi T, Watanabe M, Suzuki Y, Matsumoto T. Efficacy of Endoscopic Balloon Dilation for Small Bowel Strictures in Patients With Crohn's Disease: A Nationwide, Multi-centre, Open-label, Prospective Cohort Study. *J Crohns Colitis* 2018; **12**: 394-401 [PMID: 29194463 DOI: 10.1093/ecco-jcc/jjx159]

46 **Rondonotti E**, Sunada K, Yano T, Paggi S, Yamamoto H. Double-balloon endoscopy in clinical practice: where are we now? *Dig Endosc* 2012; **24**: 209-219 [PMID: 22725104 DOI: 10.1111/j.1443-1661.2012.01240.x]

47 **Odagiri H**, Matsui H, Fushimi K, Kaise M, Yasunaga H. Factors associated with perforation related to diagnostic balloon-assisted enteroscopy: analysis of a national inpatient database in Japan. *Endoscopy* 2015; **47**: 143-146 [PMID: 25412096 DOI: 10.1055/s-0034-1390891]

48 **Mensink PB**, Haringsma J, Kucharzik T, Cellier C, Pérez-Cuadrado E, Mönkemüller K, Gasbarrini A, Kaffes AJ, Nakamura K, Yen HH, Yamamoto H. Complications of double balloon enteroscopy: a multicenter survey. *Endoscopy* 2007; **39**: 613-615 [PMID: 17516287 DOI: 10.1055/s-2007-966444]

49 **Gerson LB**, Tokar J, Chiorean M, Lo S, Decker GA, Cave D, Bouhaidar D, Mishkin D, Dye C, Haluszka O, Leighton JA, Zfass A, Semrad C. Complications associated with double balloon enteroscopy at nine US centers. *Clin Gastroenterol Hepatol* 2009; **7**: 1177-1182, 1182.e1-1182. e3 [PMID: 19602453 DOI: 10.1016/j.cgh.2009.07.005]

50 **Rondonotti E**, Spada C, Adler S, May A, Despott EJ, Koulaouzidis A, Panter S, Domagk D, Fernandez-Urien I, Rahmi G, Riccioni ME, van Hooft JE, Hassan C, Pennazio M. Small-bowel capsule endoscopy and device-assisted enteroscopy for diagnosis and treatment of small-bowel disorders: European Society of Gastrointestinal Endoscopy (ESGE) Technical Review. *Endoscopy* 2018; **50**: 423-446 [PMID: 29539652 DOI: 10.1055/a-0576-0566]

51 **Yokoyama K**, Yano T, Kumagai H, Mizuta K, Ono S, Imagawa T, Yamamoto H, Yamagata T. Double-balloon Enteroscopy for Pediatric Patients: Evaluation of Safety and Efficacy in 257 Cases. *J Pediatr Gastroenterol Nutr* 2016; **63**: 34-40 [PMID: 26628449 DOI: 10.1097/MPG.0000000000001048]

52 **Maaser C**, Sturm A, Vavricka SR, Kucharzik T, Fiorino G, Annese V, Calabrese E, Baumgart DC, Bettenworth D, Borralho Nunes P, Burisch J, Castiglione F, Eliakim R, Ellul P, González-Lama Y, Gordon H, Halligan S, Katsanos K, Kopylov U, Kotze PG, Krustinš E, Laghi A, Limdi JK, Rieder F, Rimola J, Taylor SA, Tolan D, van Rheenen P, Verstockt B, Stoker J; European Crohn's and Colitis Organisation [ECCO] and the European Society of Gastrointestinal and Abdominal Radiology [ESGAR]. ECCO-ESGAR Guideline for Diagnostic Assessment in IBD Part 1: Initial diagnosis, monitoring of known IBD, detection of complications. *J Crohns Colitis* 2019; **13**: 144-164 [PMID: 30137275 DOI: 10.1093/ecco-jcc/jjy113]

53 **Adamina M**, Bonovas S, Raine T, Spinelli A, Warusavitarne J, Armuzzi A, Bachmann O, Bager P, Biancone L, Bokemeyer B, Bossuyt P, Burisch J, Collins P, Doherty G, El-Hussuna A, Ellul P, Fiorino G, Frei-Lanter C, Furfaro F, Gingert C, Gionchetti P, Gisbert JP, Gomollon F, González Lorenzo M, Gordon H, Hlavaty T, Juillerat P, Katsanos K, Kopylov U, Krustins E, Kucharzik T, Lytras T, Maaser C, Magro F, Marshall JK, Myrelid P, Pellino G, Rosa I, Sabino J, Savarino E, Stassen L, Torres J, Uzzan M, Vavricka S, Verstockt B, Zmora O. ECCO Guidelines on Therapeutics in Crohn's Disease: Surgical Treatment. *J Crohns Colitis* 2020; **14**: 155-168 [PMID: 31742338 DOI: 10.1093/ecco-jcc/jjz187]

World Journal of Gastroenterology

Submit a Manuscript: https://www.f6publishing.com

World J Gastroenterol 2020 October 21; 26(39): 5959-5969

DOI: 10.3748/wjg.v26.i39.5959

ISSN 1007-9327 (print) ISSN 2219-2840 (online)

MINIREVIEWS

Artificial intelligence technique in detection of early esophageal cancer

Lu-Ming Huang, Wen-Juan Yang, Zhi-Yin Huang, Cheng-Wei Tang, Jing Li

ORCID number: Lu-Ming Huang 0000-0002-3620-5767; Wen-Juan Yang 0000-0002-6163-1450; Zhi-Yin Huang 0000-0002-0639-4421; Cheng-Wei Tang 0000-0002-2289-8240; Jing Li 0000-0002-6929-409X.

Author contributions: Huang LM wrote the review; Li J and Tang CW designed and revised the manuscript; Huang LM, Yang WJ, and Huang ZY searched and collected the literature; all authors discussed the statement and conclusions and approved the final version to be published.

Supported by Key Research and Development Program of Science and Technology Department of Sichuan Province, No. 2018GZ0088; Science & Technology Bureau of Chengdu, China, No. 2017-CY02-00023-GX.

Conflict-of-interest statement: There is no conflict of interest associated with any of the senior author or other coauthors who contributed their efforts in this manuscript.

Lu-Ming Huang, Wen-Juan Yang, Zhi-Yin Huang, Cheng-Wei Tang, Jing Li, Department of Gastroenterology, West China Hospital Sichuan University, Chengdu 610041, Sichuan Province, China

Corresponding author: Jing Li, MD, PhD, Associate Professor, Department of Gastroenterology, West China Hospital Sichuan University, No. 37 Guoxue Lane, Chengdu 610041, Sichuan Province, China. melody224@163.com

Abstract

Due to the rapid progression and poor prognosis of esophageal cancer (EC), the early detection and diagnosis of early EC are of great value for the prognosis improvement of patients. However, the endoscopic detection of early EC, especially Barrett's dysplasia or squamous epithelial dysplasia, is difficult. Therefore, the requirement for more efficient methods of detection and characterization of early EC has led to intensive research in the field of artificial intelligence (AI). Deep learning (DL) has brought about breakthroughs in processing images, videos, and other aspects, whereas convolutional neural networks (CNNs) have shone lights on detection of endoscopic images and videos. Many studies on CNNs in endoscopic analysis of early EC demonstrate excellent performance including sensitivity and specificity and progress gradually from *in vitro* image analysis for classification to real-time detection of early esophageal neoplasia. When AI technique comes to the pathological diagnosis, borderline lesions that are difficult to determine may become easier than before. In gene diagnosis, due to the lack of tissue specificity of gene diagnostic markers, they can only be used as supplementary measures at present. In predicting the risk of cancer, there is still a lack of prospective clinical research to confirm the accuracy of the risk stratification model.

Key Words: Artificial intelligence; Early esophageal cancer; Barrett's esophagus; Esophageal squamous cell carcinoma; Endoscopic diagnosis; Pathological diagnosis

Core Tip: The requirement for more efficient methods of detection and characterization of early esophageal cancer (EC) has led to intensive research in the field of artificial

Manuscript source: Invited manuscript

Received: July 16, 2020
Peer-review started: July 16, 2020
First decision: August 8, 2020
Revised: August 22, 2020
Accepted: September 4, 2020
Article in press: September 4, 2020
Published online: October 21, 2020

P-Reviewer: Cabezuelo AS, Que J
S-Editor: Yan JP
L-Editor: Wang TQ
P-Editor: Li JH

intelligence (AI). Thus, application of AI technique in endoscopic detection of early EC is reviewed intensively. Furthermore, pathological and gene diagnosis for early EC as well as its risk stratification is also commented.

Citation: Huang LM, Yang WJ, Huang ZY, Tang CW, Li J. Artificial intelligence technique in detection of early esophageal cancer. *World J Gastroenterol* 2020; 26(39): 5959-5969
URL: https://www.wjgnet.com/1007-9327/full/v26/i39/5959.htm
DOI: https://dx.doi.org/10.3748/wjg.v26.i39.5959

INTRODUCTION

Esophageal cancer (EC) is the eighth most common cancer and the sixth leading cause of cancer death worldwide[1]. EC mainly consists of esophageal adenocarcinoma (EAC) and esophageal squamous cell carcinoma (ESCC). EAC is the most common pathological type in Western countries, more than 40% of patients with EAC are diagnosed after the disease has metastasized, and the 5-year survival rate is less than 20%[2,3]. Although the incidence of EAC has been increasing globally, ESCC remains the most common pathological type (80%) of all ECs with the highest incidence across a 'cancer belt' extending from East Africa and across the Middle East to Asia. Only 20% of patients with ESCC survive longer than 3 years, primarily due to late-stage diagnosis[4]. In low-resource settings, the 5-year survival is much lower at about 3.4%[5]. Early diagnosis may be associated with significantly improved outcomes for all ECs.

Barrett's esophagus (BE) is a premalignant condition characterized by the replacement of normal squamous esophageal epithelium by metaplastic intestinal epithelium containing goblet cells. It is a result of chronic inflammation of the esophagus, conferring a significantly increased risk of EAC. Endoscopic surveillance for BE patients to enable early detection of dysplasia or carcinoma was recommended by GI societies of Western countries[6,7]. The endoscopic surveillance in patients with BE is required with random 4-quadrant biopsy specimens obtained every 1 to 2 cm to detect dysplasia[8]. This method is invasive, time-consuming, and difficult to comply with[9].

Gastroscopy remains the major way to detection of early ESCC. However, endoscopic features of these early lesions are subtle and easily missed with conventional white-light endoscopy (WLE)[10]. Intrapapillary capillary loops (IPCLs) are microvessels, which have been considered a marker of ESCC, because their changes in morphology correlate with the invasion depth of ESCC. Advanced endoscopic-imaging modalities, such as narrow band imaging (NBI), in combination with magnification endoscopy, afford improved visualization of subtle microvascular patterns in the esophageal mucosa of patients with ESCC. Although NBI has showed a high sensitivity for the detection of ESCC, its performance in characterizing these lesions is still limited[11].

Therefore, the requirement for more efficient methods of detection and characterization of early EC has led to intensive research in the field of artificial intelligence (AI), which can be defined by an intelligence established by machines in contrast to the natural intelligence displayed by humans and other animals[12]. Machine learning (ML) and deep learning (DL) are important parts of AI. ML can be divided into supervised and unsupervised methods. Unsupervised learning is to identify groups within data according to commonalities, lack of knowledge of the number of groups or their significance. When the training packet contains input-output pairs, a supervised learning model is required to map new input to output. Conventional ML techniques are limited in their ability to process natural data in their raw form. During the early stage of research and development, the model training was mainly with ML by which researchers have to manually extract the possible disease features based on clinical knowledge. The power of this computer-aided diagnosis (CAD) system is weak and is not enough to be applied in clinical real-time diagnosis.

Convolutional neural networks (CNNs) are supervised ML models inspired by the visual cortex of the human brain processing and recognizing images. Each artificial neuron is a computing unit and all of them are connected to each other, forming a network. By the multiple network layers, CNNs may extract the key features from an

image with minimal preprocessing and then provide a final classification through the fully connected layers as the output. The competition of increasing performance has led to a progressive complexity of pooling layers resulting in the concept of DL[13]. The key aspect of DL is that these layers of features are not designed by human engineers. They are learned from data using a general-purpose learning procedure. DL has brought about breakthroughs in processing images, videos, and other aspects, whereas recurrent CNNs have shone lights on detection of endoscopic images and videos.

Application of AI technique in early EC detection has been over 15 years. Many studies on CNNs in endoscopic analysis of early EC demonstrate excellent performance including sensitivity and specificity and progress gradually from *in vitro* image analysis for classification to real-time detection of early esophageal neoplasia. In this manuscript, we will discuss the following: (1) Utility of AI technique in endoscopic detection of early EC; (2) Role of AI in pathological diagnosis of early EC; (3) AI in gene diagnosis of early EC; (4) AI in risk stratification of early EC; and (5) Conclusion and outlook.

AI IN ENDOSCOPIC DETECTION OF EARLY EC

Barrett's dysplasia and early EAC

AI based on WLE and NBI: There are some limitations to recognize BE-related early neoplastic lesions by WLE, a conventional technology. High-definition WLE (HD-WLE) and NBI were ever considered to enhance the accuracy of the diagnosis of BE-related early neoplastic lesions. But the improvement still not satisfied endoscopists. This situation stimulated development of CAD system for early neoplastic lesions in BE based on supervised ML[14,15]. However, it was still difficult for this system to locate BE-related early neoplastic lesions and to select biopsy sites. To solve those problems, Ebigbo *et al*[16] established a CAD system based on DL. The accuracy of the system using HD-WLE was better than that of general endoscopists. Moreover, the system displayed the ability to locate the lesion and the area coincidence rate between the lesions delineated by the system and by experts was up to 72%. Generally, the specificity of NBI was higher than that of conventional WLE[17]. Compared with the use of HD-WLE, the system showed no obvious advantage when using NBI[16]. However, there was a common problem in the above studies; that is, the same image dataset was used in both the training stage and validation stage. This obviously cannot reflect clinical practice, so it is very important to use different image datasets for training and validation. de Groof *et al*[18] used different HD-WLE images for training and testing, and the results showed that the sensitivity and specificity of the system were significantly higher than those of general endoscopists. The combinations of AI and HD-WLE/NBI, which are widely used in the clinic, perform well in the diagnosis of BE-related early tumor lesions and are superior to general endoscopists. However, in different studies, the precision of the CAD system in delineating lesions and the criteria for the evaluation of the ability of lesion location are quite inconsistent. More high-quality studies are needed in the future.

AI based on endoscopic optical coherence tomography and confocal laser endomicroscopy: In addition to WLE and NBI, endoscopic optical coherence tomography **(**EOCT) and confocal laser endomicroscopy **(**CLE) are also used to diagnose early EAC/BE-associated dysplasia. EOCT can identify BE-related early tumor lesions by analyzing esophageal mucosal and submucosal structures[19]. CLE can observe the mucosal tissue and cellular morphology to achieve optical biopsy[20]. However, the complexity of these two imaging technologies, the time-consuming reading of images, and the need for senior endoscopists limit their clinical use. To solve this problem, Qi *et al*[19,21] extracted multiple EOCT image features and combined one or multiple features to classify the lesions, but the results were not satisfactory. After that, Swager *et al*[22] used volumetric laser endomicroscopy (VLE, integrated with second-generation OCT) images for training and testing, and the results showed that the CAD system was superior to VLE experts. Veronese *et al*[20] used CLE images, and the results showed that the system could accurately distinguish gastric metaplasia (GM), intestinal metaplasia (IM), and neoplasia. Ghatwary *et al*[23] showed that the sensitivity of the system using CLE images to diagnose IM and neoplasia was significantly higher than that to diagnose GM. Similarly, the CAD system established by Hong failed to identify GM, the sensitivity of diagnosing IM was not significantly different from that of the above study, and the sensitivity of diagnosing neoplasia was slightly decreased[24]. This may be due to the limited number of images of GM and

neoplasia. At present, there are few clinical studies in this field, and the available images are limited. In the future, more research is needed to confirm the value of VLE/CLE combined with AI in the diagnosis of early EAC.

Real-time diagnosis by AI: Currently, research in this field is limited. Ebigbo *et al*[25] continued to optimize the CAD system based on previous research and applied it to clinical real-time detection for the first time. While 14 patients with Barrett's neoplasia were under endoscopic examination, 62 endoscopic images (36 early EAC and 26 BE without dysplasia) were captured using the CAD system for real-time classification, and the results showed that the sensitivity and specificity were 83.7% and 100%, respectively. There was no significant difference between the system and experienced endoscopists. However, there were still some shortcomings in this study. First, the numbers of patients and images were low. Second, the system still used images for diagnosis, not videos for real-time detection. Finally, the ability of AI to assist in the delineation of lesions and biopsy guidance was not verified. In addition, the CAD system built by Hashimoto *et al*[17] could meet the needs of clinical real-time detection; unfortunately, the researchers did not verify the performance of the system in real-time diagnosis.

Esophageal squamous dysplasia and early ESCC

AI based on WLE and NBI: Lugol's chromoendoscopy is the standard screening method for ESCC; however, in view of its low specificity and longtime consumption, it is necessary to adopt new endoscopic techniques. Although WLE has been proven to be unsuitable for screening early ESCC alone, considering its clinical popularity, some researchers still hope to introduce AI to improve the accuracy of WLE. Cai *et al*[26] built a CAD system based on DL and tested it with WLE images. The results showed that the accuracy of the system in the diagnosis of early EC was significantly higher than that of junior and mid-level endoscopists, and there was no significant difference between the system and senior endoscopists. The results of Ohmori *et al*[27] showed that the sensitivity of NBI was higher than that of WLE, but the specificity was lower, and there was no significant difference between the overall performance of the system and endoscopic experts[27]. The results of Horie *et al*[28] were similar to those of Ohmori *et al*[27].

In recent years, it has been found that esophageal intrapapillary capillary loop (IPCL) represents an endoscopically visible feature of esophageal squamous cell neoplasia, and its morphological changes are closely related to the depth of tumor invasion[29]. The classification of IPCL based on NBI proposed by the Japanese Endoscopic Society has been widely used in clinical practice because it is easy to understand[30]. Nevertheless, classifying IPCL still requires sufficient experience, and its interpretation is still subjective. Therefore, to classify the IPCL more objectively and help less experienced endoscopists make full use of NBI, combining NBI with AI will be the best solution. Zhao *et al*[31] analyzed magnifying NBI images and showed that the diagnostic accuracy of the CAD system was better than that of junior and mid-level endoscopists, and there was no significant difference between the system and senior endoscopists. However, this study focused on the classification of IPCL only and did not further verify the accuracy of the system to determine the depth of tumor invasion. For early ESCC, accurately determining the depth of tumor invasion is the premise of choosing the appropriate treatment. Nakagawa *et al*[32] used non-magnifying endoscopic images to test the CAD system and found that the sensitivity of the system to diagnose epithelial-submucosal cancers invading up to 200 μm (EP-SM1) was higher than that of endoscopic experts, but the specificity was lower. There was no significant difference between the system and endoscopic experts based on magnifying endoscopic images. Further analysis showed that the system performed well in the diagnosis of EP/lamina propria mucosa (LPM) and had no significant difference from endoscopic experts. However, the sensitivity of the system to diagnose muscularis mucosa (MM)/SM1 was poor, as was the performance of endoscopic experts. In the diagnosis of SM2/3, the sensitivity of this system was slightly higher than that of endoscopic experts. Tokai *et al*[33] also used non-magnifying endoscopic images for analysis and found that the sensitivity of NBI was slightly higher than that of WLE, and the diagnostic performance of the system was better than that of endoscopic experts. Further analysis showed that the accuracy of the CAD system in diagnosing EP/LPM and MM was more than 90%, which was significantly higher than that in diagnosing SM1 and SM2. The reasons may be that the training image set did not contain normal esophageal images, and the system mistook extramural compression and not fully extended esophageal wall for lesion features.

AI based on endocytoscopy and high-resolution microendoscopy: Endocytoscopy is a new technology that combines magnifying endoscopy with vital staining. Because of its excellent magnifying ability, endoscopists can clearly observe the epithelial cells of the esophageal mucosa to achieve a similar effect to pathological diagnosis[34]. However, if endoscopists want to use endocytoscopy to complete real-time detection independently, they need a solid foundation for pathology, which is obviously not practical. Therefore, AI may be the best option to assist endoscopic diagnosis. Kumagai *et al*[35] showed that the performance of the system using higher magnification images was better than that of lower magnification images. However, there was no stratified analysis of superficial EC and advanced EC in this study. The results could not accurately reflect the ability of endocytoscopy combined with AI in the diagnosis of early EC. High-resolution microendoscopy (HRME) can be used to observe the esophageal mucosal tissue and cellular morphology. Shin *et al*[36] tested the ability of different image features to distinguish tumors from non-tumor lesions, and the best features selected had an 84% sensitivity and 95% specificity. However, it took a long time to analyze a single image, and the sensitivity was not ideal. In the future, more high-quality studies are needed to confirm its role in the diagnosis of early EC.

Real-time diagnosis by AI: Quang *et al*[37] used the same HRME image data as Shin *et al*[36] for training and validation, and the results showed that the sensitivity was 95% and the specificity was 91%. Then, three patients with suspected EC underwent endoscopic examination with a 100% accuracy. However, there were some limitations in this study. First, the number of patients and images in real-time diagnosis was too small. Second, the system still used images for diagnosis, not videos for real-time detection. Everson *et al*[38] and Guo *et al*[39] established CAD systems based on DL with good diagnostic performance using NBI videos. Unfortunately, these systems have not been applied in real-time diagnosis. Endoscopic detection of early EC by various endoscopic techniques assisted by AI is summarized in Table 1.

AI IN PATHOLOGICAL DIAGNOSIS OF EARLY EC

Although AI combined with endoscopic diagnosis has made progress, endoscopic diagnosis is still unable to replace the gold standard of pathological diagnosis. However, there is a problem in the pathological diagnosis of early esophageal neoplasia; that is, the accuracy of diagnosing dysplasia is not ideal with considerable interobserver variability. To solve this problem, Sabo *et al*[40] established two models to distinguish no dysplasia (ND) from low grade dysplasia (LGD) and LGD from high grade dysplasia (HGD) by extracting the hematoxylin and eosin (HE) stained pathological section image features of BE patients. The results showed that the two models performed well in the diagnosis of indistinguishable borderline lesions. Baak *et al* combined HE stained pathological section image characteristics with p53/Ki67 immunohistochemical indicators and used pathological specimens of surgical resection[41] and endoscopic biopsy samples[42] of BE for testing. It was found that the system performed well in distinguishing ND from LGD and LGD from HGD; however, the accuracy of distinguishing HGD from intramucosal carcinoma needs to be improved. The performance of the system was better than that of the general pathologist and only slightly inferior to that of the experienced pathologist. In addition, there were still some studies using immunohistochemical indicators only[43] or the characteristics of nuclear DNA structure and organization combined with DNA ploidy analysis[44] to grade BE dysplasia, but the results were not satisfactory. Therefore, HE stained pathological image features supplemented by relevant immune indicators or other image enhancement techniques may be the main direction of AI-assisted pathological diagnosis in the future.

AI IN GENE DIAGNOSIS OF EARLY EC

As mentioned above, the invasiveness of endoscopic diagnosis and variability of pathological diagnosis, together with recent advances in the pathogenesis of EC and the development of various omics technologies, have made early EC gene diagnosis a hot topic of research. Zhang *et al*[45] and Yu *et al*[46] used microRNAs and long noncoding RNAs specifically expressed in patients with ESCC to establish diagnostic models, and the results showed that both of them can be used to effectively

Table 1 Application of artificial intelligence in endoscopic detection of early esophageal cancer

Ref.	Modality	AI technique	No. of images/cases in training dataset (positive/negative)	No. of images/cases in test dataset (positive/negative)	Results
van der Sommen *et al*[14], 2016	HD-WLE	SVM	100 (60 early BE neoplasia/40 BE)	100 (60 early BE neoplasia/40 BE)	Sensitivity 83%/specificity 83%
de Groof *et al*[15], 2019	HD-WLE	SVM	60 (40 early BE neoplasia/20 BE)	60 (40 early BE neoplasia/20 BE)	Sensitivity 95%/specificity 85%
Ebigbo *et al*[16], 2019	HD-WLE	CNN	100 (50 early BE neoplasia/50 BE)	100 (50 early BE neoplasia/50 BE)	Sensitivity 92%/specificity 100%
Ebigbo *et al*[16], 2019	HD-WLE/NBI	CNN	148 (early BE neoplasia/BE)	148 (early BE neoplasia/BE)	HD-WLE sensitivity 97%/specificity 88%; NBI sensitivity 94%/specificity 80%
Hashimoto *et al*[17], 2020	WLE/NBI	CNN	1374 (early BE neoplasia/BE)	253 WLE (146 early BE neoplasia/107 BE) 205 NBI (79 early BE neoplasia/126 BE)	WLE sensitivity 98.6%/specificity 88.8%; NBI sensitivity 92.4%/specificity 99.2%
de Groof *et al*[18], 2020	HD-WLE	ResNet-UNet	1247 WLE + 297 HD-WLE (early BE neoplasia/BE)	80 (40 early BE neoplasia/40 BE)	Sensitivity 90%/specificity 88%
Swager *et al*[22], 2017	VLE	SVM	60 (30 early BE neoplasia/30 BE)	60 (30 early BE neoplasia/30 BE)	Sensitivity 90%/specificity 93%
Veronese *et al*[20], 2013	CLE	SVM	337 (23 GM/263 IM/51 neoplasia)	337 (23 GM/263 IM/51 neoplasia)	Sensitivity 96%/95%/100%
Ghatwary *et al*[23], 2019	CLE	SVM	262 (GM/IM/neoplasia)	262 (GM/IM/neoplasia)	Sensitivity 70%/93%/93%
Hong *et al*[24], 2017	CLE	CNN	236 (26 GM/155 IM/55 neoplasia)	26 (4 GM/17 IM/5 neoplasia)	Sensitivity 0%/100%/80%
Ebigbo *et al*[25], 2020	HD-WLE	CNN	129 (early BE neoplasia/BE)	62 (36 early BE neoplasia/26 BE)	Sensitivity 83.7%/specificity 100%
Cai *et al*[26], 2019	WLE	CNN	2428 (1332 early ESCC/1096 healthy control)	187 (91 early ESCC/96 healthy control)	Sensitivity 97.8%/specificity 85.4%
Ohmori *et al*[27], 2020	WLE/NBI	Single Shot MultiBox Detector	22562 (17435 superficial ESCC/5127 control)	727 (255 WLE/268 non-magnifying NBI/204 magnifying NBI)	WLE sensitivity 90%/specificity 76%; non-magnifying NBI sensitivity 100%/specificity 63%; magnifying NBI sensitivity 98%/specificity 56%
Zhao *et al*[31], 2019	Magnifying NBI	Double-labeling fully convolutional network	1383 (207 type A IPCL/970 type B1 IPCL/206 type B2 IPCL)	1383 (207 type A IPCL/970 type B1 IPCL/206 type B2 IPCL)	Sensitivity 71.5%/91.1%/83.0%
Nakagawa *et al*[32], 2019	WLE/NBI	CNN	8660 non-magnifying (7230 EP-SM1/1430 SM2/3); 5678 magnifying (4916 EP-SM1/762 SM2/3)	914 (405 non-magnifying/509 magnifying)	Non-magnifying sensitivity 95.4%/specificity 79.2%; magnifying sensitivity 91.6%/specificity 79.2%
Tokai *et al*[33], 2020	WLE/NBI	CNN	1751 superficial ESCC	291 (201 EP-SM1/90 SM2)	Sensitivity 84.1%/specificity 73.3%
Shin *et al*[36], 2015	HRME	Two-class linear discriminant analysis	104 (15 early ESCC/89 control)	167 (19 early ESCC/148 control)	Sensitivity 84%/specificity 95%
Quang *et al*[37], 2016	HRME	Two-class linear discriminant analysis	104 (15 early ESCC/89 control)	3 (1 early ESCC/2 control)	Sensitivity 100%/specificity 100%
Everson *et al*[38], 2019	magnifying NBI	CNN	7046 sequential images (squamous cell	7046 sequential images (squamous cell	Sensitivity 89.7%/specificity 96.9%

			neoplasia/healthy control)	neoplasia/healthy control)	
Guo *et al*[39], 2020	NBI	SegNet	6473 (early ESCC/control)	47 (27 non-magnifying videos/20 magnifying videos)	Non-magnifying NBI sensitivity 60.8%; magnifying NBI sensitivity 96.1%

AI: Artificial intelligence; EC: Esophageal cancer; HD-WLE: High-definition white light endoscopy; SVM: Support vector machine; BE: Barrett's esophagus; CNN: Convolutional neural network; NBI: Narrow band imaging; VLE: Volumetric laser endomicroscopy; CLE: Confocal laser endomicroscopy; GM: Gastric metaplasia; IM: Intestinal metaplasia; ESCC: Esophageal squamous cell carcinoma; IPCL: Intrapapillary capillary loop; EP-SM1: Epithelium-submucosal cancers invading up to 200 μm; HRME: High-resolution microendoscopy.

distinguish early from advanced tumors. Xing *et al*[47] selected characteristic secretory proteins based on the RNA transcriptome data of ESCC patients to establish a diagnostic model with a high sensitivity but unsatisfactory specificity for early ESCC. It may be that the selection of characteristic secretory proteins in this study was based on genes up-regulated in tumor tissues and that the down-regulated genes were not fully utilized. In addition, Shen *et al*[48] and Zhai *et al*[49] used microRNA and protein markers specifically expressed in the plasma of ESCC patients to build diagnostic models and found that both of them could effectively distinguish esophageal squamous dysplasia (ESD) from healthy controls. However, compared with ESD or early ESCC, the AI-assisted gene diagnosis of BE-related dysplasia and early EAC is less studied. The results of Slaby *et al*[50] showed that characteristic microRNAs in BE tissues could be used to distinguish BE with or without dysplasia. These markers may not be specific for EC; therefore, gene diagnosis can only be used as an assistant measure for endoscopic and pathological diagnosis until specific markers of EC gene diagnosis are established.

AI IN RISK STRATIFICATION OF EARLY EC

Considering that only 0.12%-0.43% of BE patients may progress to EAC every year[51-53], it is particularly necessary to establish an effective model to predict the risk of EAC in BE patients. Previous risk stratification was mainly based on the presence of dysplasia, but its effect was not ideal. Critchley-Thorne *et al*[54] established a predictive model based on the characteristic differences of tissue immunofluorescence markers and histopathological images between patients with BE who developed EAC and those who did not. The results were not satisfactory, with more than 30% of BE patients who developed EAC classified as low-risk. Li *et al*[55] established a predictive model based on the differences in single nucleotide polymorphisms in the biopsy tissues of BE patients with good performance for predicting EC. Unlike EAC, ESCC has no recognized precancerous disease, and endoscopic screening for the general population is obviously impractical. Therefore, it will be the focus of clinical screening to establish an effective model to predict which individuals are more likely to develop ESD. Etemadi *et al*[56]'s model based on the epidemiological data of patients with ESD

and healthy controls showed that the performance of the model was not good. Moghtadaei *et al*[57]'s predictive model based on epidemiological data was better than Etemadi's. Unfortunately, there is a lack of prospective follow-up studies to verify the true accuracy of these models.

CONCLUSION

In conclusion, AI is trying to be used in the endoscopic detection, pathological diagnosis, gene diagnosis, and cancer risk prediction of early EC. It is helpful for endoscopists and pathologists to improve the accuracy of diagnosis and to assist clinicians for treatment and making follow-up strategies. The borderline lesions of EC pathology that remain difficult to determine may be the main direction of AI-assisted pathological diagnosis in the future. Gene diagnosis can only be used as an assistant measure for endoscopic and pathological diagnosis until specific markers of EC gene diagnosis are established. Higher precision of the CAD system in delineating lesions is necessary for improvement of the accuracy of diagnosis, and enhancement of accuracy for the risk stratification model may be of benefit for the prediction of EC risk.

REFERENCES

1 **Bray F**, Ferlay J, Soerjomataram I, Siegel RL, Torre LA, Jemal A. Global cancer statistics 2018: GLOBOCAN estimates of incidence and mortality worldwide for 36 cancers in 185 countries. *CA Cancer J Clin* 2018; **68**: 394-424 [PMID: 30207593 DOI: 10.3322/caac.21492]

2 **Hur C**, Miller M, Kong CY, Dowling EC, Nattinger KJ, Dunn M, Feuer EJ. Trends in esophageal adenocarcinoma incidence and mortality. *Cancer* 2013; **119**: 1149-1158 [PMID: 23303625 DOI: 10.1002/cncr.27834]

3 **Thrift AP**. The epidemic of oesophageal carcinoma: Where are we now? *Cancer Epidemiol* 2016; **41**: 88-95 [PMID: 26851752 DOI: 10.1016/j.canep.2016.01.013]

4 **Ferlay J**, Colombet M, Soerjomataram I, Mathers C, Parkin DM, Piñeros M, Znaor A, Bray F. Estimating the global cancer incidence and mortality in 2018: GLOBOCAN sources and methods. *Int J Cancer* 2019; **144**: 1941-1953 [PMID: 30350310 DOI: 10.1002/ijc.31937]

5 **Aghcheli K**, Marjani HA, Nasrollahzadeh D, Islami F, Shakeri R, Sotoudeh M, Abedi-Ardekani B, Ghavamnasiri MR, Razaei E, Khalilipour E, Mohtashami S, Makhdoomi Y, Rajabzadeh R, Merat S, Sotoudehmanesh R, Semnani S, Malekzadeh R. Prognostic factors for esophageal squamous cell carcinoma--a population-based study in Golestan Province, Iran, a high incidence area. *PLoS One* 2011; **6**: e22152 [PMID: 21811567 DOI: 10.1371/journal.pone.0022152]

6 **Shaheen NJ**, Falk GW, Iyer PG, Gerson LB; American College of Gastroenterology. ACG Clinical Guideline: Diagnosis and Management of Barrett's Esophagus. *Am J Gastroenterol* 2016; **111**: 30-50; quiz 51 [PMID: 26526079 DOI: 10.1038/ajg.2015.322]

7 **Fitzgerald RC**, di Pietro M, Ragunath K, Ang Y, Kang JY, Watson P, Trudgill N, Patel P, Kaye PV, Sanders S, O'Donovan M, Bird-Lieberman E, Bhandari P, Jankowski JA, Attwood S, Parsons SL, Loft D, Lagergren J, Moayyedi P, Lyratzopoulos G, de Caestecker J; British Society of Gastroenterology. British Society of Gastroenterology guidelines on the diagnosis and management of Barrett's oesophagus. *Gut* 2014; **63**: 7-42 [PMID: 24165758 DOI: 10.1136/gutjnl-2013-305372]

8 **Sharma P**, Savides TJ, Canto MI, Corley DA, Falk GW, Goldblum JR, Wang KK, Wallace MB, Wolfsen HC; ASGE Technology and Standards of Practice Committee. The American Society for Gastrointestinal Endoscopy PIVI (Preservation and Incorporation of Valuable Endoscopic Innovations) on imaging in Barrett's Esophagus. *Gastrointest Endosc* 2012; **76**: 252-254 [PMID: 22817781 DOI: 10.1016/j.gie.2012.05.007]

9 **Tavakkoli A**, Appelman HD, Beer DG, Madiyal C, Khodadost M, Nofz K, Metko V, Elta G, Wang T, Rubenstein JH. Use of Appropriate Surveillance for Patients With Nondysplastic Barrett's Esophagus. *Clin Gastroenterol Hepatol* 2018; **16**: 862-869.e3 [PMID: 29432922 DOI: 10.1016/j.cgh.2018.01.052]

10 **Menon S**, Trudgill N. How commonly is upper gastrointestinal cancer missed at endoscopy? A meta-analysis. *Endosc Int Open* 2014; **2**: E46-E50 [PMID: 26135259 DOI: 10.1055/s-0034-1365524]

11 **Nagami Y**, Tominaga K, Machida H, Nakatani M, Kameda N, Sugimori S, Okazaki H, Tanigawa T, Yamagami H, Kubo N, Shiba M, Watanabe K, Watanabe T, Iguchi H, Fujiwara Y, Ohira M, Hirakawa K, Arakawa T. Usefulness of non-magnifying narrow-band imaging in screening of early esophageal squamous cell carcinoma: a prospective comparative study using propensity score matching. *Am J Gastroenterol* 2014; **109**: 845-854 [PMID: 24751580 DOI: 10.1038/ajg.2014.94]

12 **Le Berre C**, Sandborn WJ, Aridhi S, Devignes MD, Fournier L, Smaïl-Tabbone M, Danese S, Peyrin-Biroulet L. Application of Artificial Intelligence to Gastroenterology and Hepatology. *Gastroenterology* 2020; **158**: 76-94.e2 [PMID: 31593701 DOI: 10.1053/j.gastro.2019.08.058]

13 **LeCun Y**, Bengio Y, Hinton G. Deep learning. *Nature* 2015; **521**: 436-444 [PMID: 26017442 DOI: 10.1038/nature14539]

14 **van der Sommen F**, Zinger S, Curvers WL, Bisschops R, Pech O, Weusten BL, Bergman JJ, de With PH, Schoon EJ. Computer-aided detection of early neoplastic lesions in Barrett's esophagus. *Endoscopy* 2016; **48**: 617-624 [PMID: 27100718 DOI: 10.1055/s-0042-105284]

15 **de Groof J**, van der Sommen F, van der Putten J, Struyvenberg MR, Zinger S, Curvers WL, Pech O,

Meining A, Neuhaus H, Bisschops R, Schoon EJ, de With PH, Bergman JJ. The Argos project: The development of a computer-aided detection system to improve detection of Barrett's neoplasia on white light endoscopy. *United European Gastroenterol J* 2019; **7**: 538-547 [PMID: 31065371 DOI: 10.1177/2050640619837443]

16 **Ebigbo A**, Mendel R, Probst A, Manzeneder J, Souza LA Jr, Papa JP, Palm C, Messmann H. Computer-aided diagnosis using deep learning in the evaluation of early oesophageal adenocarcinoma. *Gut* 2019; **68**: 1143-1145 [PMID: 30510110 DOI: 10.1136/gutjnl-2018-317573]

17 **Hashimoto R**, Requa J, Dao T, Ninh A, Tran E, Mai D, Lugo M, El-Hage Chehade N, Chang KJ, Karnes WE, Samarasena JB. Artificial intelligence using convolutional neural networks for real-time detection of early esophageal neoplasia in Barrett's esophagus (with video). *Gastrointest Endosc* 2020; **91**: 1264-1271.e1 [PMID: 31930967 DOI: 10.1016/j.gie.2019.12.049]

18 **de Groof AJ**, Struyvenberg MR, van der Putten J, van der Sommen F, Fockens KN, Curvers WL, Zinger S, Pouw RE, Coron E, Baldaque-Silva F, Pech O, Weusten B, Meining A, Neuhaus H, Bisschops R, Dent J, Schoon EJ, de With PH, Bergman JJ. Deep-Learning System Detects Neoplasia in Patients With Barrett's Esophagus With Higher Accuracy Than Endoscopists in a Multistep Training and Validation Study With Benchmarking. *Gastroenterology* 2020; **158**: 915-929.e4 [PMID: 31759929 DOI: 10.1053/j.gastro.2019.11.030]

19 **Qi X**, Sivak MV, Isenberg G, Willis JE, Rollins AM. Computer-aided diagnosis of dysplasia in Barrett's esophagus using endoscopic optical coherence tomography. *J Biomed Opt* 2006; **11**: 044010 [PMID: 16965167 DOI: 10.1117/1.2337314]

20 **Veronese E**, Grisan E, Diamantis G, Battaglia G, Crosta C, Trovato C. Hybrid patch-based and image-wide classification of confocal laser endomicroscopy images in Barrett's esophagus surveillance. IEEE International Symposium on Biomedical Imaging 2013 [DOI: 10.1109/ISBI.2013.6556487]

21 **Qi X**, Pan Y, Sivak MV, Willis JE, Isenberg G, Rollins AM. Image analysis for classification of dysplasia in Barrett's esophagus using endoscopic optical coherence tomography. *Biomed Opt Express* 2010; **1**: 825-847 [PMID: 21258512 DOI: 10.1364/BOE.1.000825]

22 **Swager AF**, van der Sommen F, Klomp SR, Zinger S, Meijer SL, Schoon EJ, Bergman JJGHM, de With PH, Curvers WL. Computer-aided detection of early Barrett's neoplasia using volumetric laser endomicroscopy. *Gastrointest Endosc* 2017; **86**: 839-846 [PMID: 28322771 DOI: 10.1016/j.gie.2017.03.011]

23 **Ghatwary N**, Ahmed A, Grisan E, Jalab H, Bidaut L, Ye X. *In-vivo* Barrett's esophagus digital pathology stage classification through feature enhancement of confocal laser endomicroscopy. *J Med Imaging (Bellingham)* 2019; **6**: 014502 [PMID: 30840732 DOI: 10.1117/1.JMI.6.1.014502]

24 **Jisu Hong**, Bo-Yong Park, Hyunjin Park. Convolutional neural network classifier for distinguishing Barrett's esophagus and neoplasia endomicroscopy images. *Conf Proc IEEE Eng Med Biol Soc* 2017; **2017**: 2892-2895 [PMID: 29060502 DOI: 10.1109/EMBC.2017.8037461]

25 **Ebigbo A**, Mendel R, Probst A, Manzeneder J, Prinz F, de Souza LA Jr, Papa J, Palm C, Messmann H. Real-time use of artificial intelligence in the evaluation of cancer in Barrett's oesophagus. *Gut* 2020; **69**: 615-616 [PMID: 31541004 DOI: 10.1136/gutjnl-2019-319460]

26 **Cai SL**, Li B, Tan WM, Niu XJ, Yu HH, Yao LQ, Zhou PH, Yan B, Zhong YS. Using a deep learning system in endoscopy for screening of early esophageal squamous cell carcinoma (with video). *Gastrointest Endosc* 2019; **90**: 745-753.e2 [PMID: 31302091 DOI: 10.1016/j.gie.2019.06.044]

27 **Ohmori M**, Ishihara R, Aoyama K, Nakagawa K, Iwagami H, Matsuura N, Shichijo S, Yamamoto K, Nagaike K, Nakahara M, Inoue T, Aoi K, Okada H, Tada T. Endoscopic detection and differentiation of esophageal lesions using a deep neural network. *Gastrointest Endosc* 2020; **91**: 301-309.e1 [PMID: 31585124 DOI: 10.1016/j.gie.2019.09.034]

28 **Horie Y**, Yoshio T, Aoyama K, Yoshimizu S, Horiuchi Y, Ishiyama A, Hirasawa T, Tsuchida T, Ozawa T, Ishihara S, Kumagai Y, Fujishiro M, Maetani I, Fujisaki J, Tada T. Diagnostic outcomes of esophageal cancer by artificial intelligence using convolutional neural networks. *Gastrointest Endosc* 2019; **89**: 25-32 [PMID: 30120958 DOI: 10.1016/j.gie.2018.07.037]

29 **Sato H**, Inoue H, Ikeda H, Sato C, Onimaru M, Hayee B, Phlanusi C, Santi EG, Kobayashi Y, Kudo SE. Utility of intrapapillary capillary loops seen on magnifying narrow-band imaging in estimating invasive depth of esophageal squamous cell carcinoma. *Endoscopy* 2015; **47**: 122-128 [PMID: 25590187 DOI: 10.1055/s-0034-1390858]

30 **Oyama T**, Inoue H, Arima M, Momma K, Omori T, Ishihara R, Hirasawa D, Takeuchi M, Tomori A, Goda K. Prediction of the invasion depth of superficial squamous cell carcinoma based on microvessel morphology: magnifying endoscopic classification of the Japan Esophageal Society. *Esophagus* 2017; **14**: 105-112 [PMID: 28386209 DOI: 10.1007/s10388-016-0527-7]

31 **Zhao YY**, Xue DX, Wang YL, Zhang R, Sun B, Cai YP, Feng H, Cai Y, Xu JM. Computer-assisted diagnosis of early esophageal squamous cell carcinoma using narrow-band imaging magnifying endoscopy. *Endoscopy* 2019; **51**: 333-341 [PMID: 30469155 DOI: 10.1055/a-0756-8754]

32 **Nakagawa K**, Ishihara R, Aoyama K, Ohmori M, Nakahira H, Matsuura N, Shichijo S, Nishida T, Yamada T, Yamaguchi S, Ogiyama H, Egawa S, Kishida O, Tada T. Classification for invasion depth of esophageal squamous cell carcinoma using a deep neural network compared with experienced endoscopists. *Gastrointest Endosc* 2019; **90**: 407-414 [PMID: 31077698 DOI: 10.1016/j.gie.2019.04.245]

33 **Tokai Y**, Yoshio T, Aoyama K, Horie Y, Yoshimizu S, Horiuchi Y, Ishiyama A, Tsuchida T, Hirasawa T, Sakakibara Y, Yamada T, Yamaguchi S, Fujisaki J, Tada T. Application of artificial intelligence using convolutional neural networks in determining the invasion depth of esophageal squamous cell carcinoma. *Esophagus* 2020; **17**: 250-256 [PMID: 31980977 DOI: 10.1007/s10388-020-00716-x]

34 **Kumagai Y**, Monma K, Kawada K. Magnifying chromoendoscopy of the esophagus: in-vivo pathological diagnosis using an endocytoscopy system. *Endoscopy* 2004; **36**: 590-594 [PMID: 15243880 DOI: 10.1055/s-2004-814533]

35 **Kumagai Y**, Takubo K, Kawada K, Aoyama K, Endo Y, Ozawa T, Hirasawa T, Yoshio T, Ishihara S, Fujishiro M, Tamaru JI, Mochiki E, Ishida H, Tada T. Diagnosis using deep-learning artificial intelligence

based on the endocytoscopic observation of the esophagus. *Esophagus* 2019; **16**: 180-187 [PMID: 30547352 DOI: 10.1007/s10388-018-0651-7]

36 **Shin D**, Protano MA, Polydorides AD, Dawsey SM, Pierce MC, Kim MK, Schwarz RA, Quang T, Parikh N, Bhutani MS, Zhang F, Wang G, Xue L, Wang X, Xu H, Anandasabapathy S, Richards-Kortum RR. Quantitative analysis of high-resolution microendoscopic images for diagnosis of esophageal squamous cell carcinoma. *Clin Gastroenterol Hepatol* 2015; **13**: 272-279.e2 [PMID: 25066838 DOI: 10.1016/j.cgh.2014.07.030]

37 **Quang T**, Schwarz RA, Dawsey SM, Tan MC, Patel K, Yu X, Wang G, Zhang F, Xu H, Anandasabapathy S, Richards-Kortum R. A tablet-interfaced high-resolution microendoscope with automated image interpretation for real-time evaluation of esophageal squamous cell neoplasia. *Gastrointest Endosc* 2016; **84**: 834-841 [PMID: 27036635 DOI: 10.1016/j.gie.2016.03.1472]

38 **Everson M**, Herrera L, Li W, Luengo IM, Ahmad O, Banks M, Magee C, Alzoubaidi D, Hsu HM, Graham D, Vercauteren T, Lovat L, Ourselin S, Kashin S, Wang HP, Wang WL, Haidry RJ. Artificial intelligence for the real-time classification of intrapapillary capillary loop patterns in the endoscopic diagnosis of early oesophageal squamous cell carcinoma: A proof-of-concept study. *United European Gastroenterol J* 2019; **7**: 297-306 [PMID: 31080614 DOI: 10.1177/2050640618821800]

39 **Guo L**, Xiao X, Wu C, Zeng X, Zhang Y, Du J, Bai S, Xie J, Zhang Z, Li Y, Wang X, Cheung O, Sharma M, Liu J, Hu B. Real-time automated diagnosis of precancerous lesions and early esophageal squamous cell carcinoma using a deep learning model (with videos). *Gastrointest Endosc* 2020; **91**: 41-51 [PMID: 31445040 DOI: 10.1016/j.gie.2019.08.018]

40 **Sabo E**, Beck AH, Montgomery EA, Bhattacharya B, Meitner P, Wang JY, Resnick MB. Computerized morphometry as an aid in determining the grade of dysplasia and progression to adenocarcinoma in Barrett's esophagus. *Lab Invest* 2006; **86**: 1261-1271 [PMID: 17075582 DOI: 10.1038/Labinvest.3700481]

41 **Polkowski W**, Baak JP, van Lanschot JJ, Meijer GA, Schuurmans LT, Ten Kate FJ, Obertop H, Offerhaus GJ. Clinical decision making in Barrett's oesophagus can be supported by computerized immunoquantitation and morphometry of features associated with proliferation and differentiation. *J Pathol* 1998; **184**: 161-168 [PMID: 9602707 DOI: 10.1002/(SICI)1096-9896(199802)184:2<161::AID-PATH971>3.0.CO;2-2]

42 **van Sandick JW**, Baak JP, van Lanschot JJ, Polkowski W, ten Kate FJ, Obertop H, Offerhaus GJ. Computerized quantitative pathology for the grading of dysplasia in surveillance biopsies of Barrett's oesophagus. *J Pathol* 2000; **190**: 177-183 [PMID: 10657016 DOI: 10.1002/(SICI)1096-9896(200002)190:2<177::AID-PATH508>3.0.CO;2-X]

43 **Karamchandani DM**, Lehman HL, Ohanessian SE, Massé J, Welsh PA, Odze RD, Goldblum JR, Berg AS, Stairs DB. Increasing diagnostic accuracy to grade dysplasia in Barrett's esophagus using an immunohistochemical panel for CDX2, p120ctn, c-Myc and Jagged1. *Diagn Pathol* 2016; **11**: 23 [PMID: 26926447 DOI: 10.1186/s13000-016-0473-7]

44 **Dunn JM**, Hveem T, Pretorius M, Oukrif D, Nielsen B, Albregtsen F, Lovat LB, Novelli MR, Danielsen HE. Comparison of nuclear texture analysis and image cytometric DNA analysis for the assessment of dysplasia in Barrett's oesophagus. *Br J Cancer* 2011; **105**: 1218-1223 [PMID: 21934680 DOI: 10.1038/bjc.2011.353]

45 **Zhang C**, Wang C, Chen X, Yang C, Li K, Wang J, Dai J, Hu Z, Zhou X, Chen L, Zhang Y, Li Y, Qiu H, Xing J, Liang Z, Ren B, Yang C, Zen K, Zhang CY. Expression profile of microRNAs in serum: a fingerprint for esophageal squamous cell carcinoma. *Clin Chem* 2010; **56**: 1871-1879 [PMID: 20943850 DOI: 10.1373/clinchem.2010.147553]

46 **Yu J**, Wu X, Huang K, Zhu M, Zhang X, Zhang Y, Chen S, Xu X, Zhang Q. Bioinformatics identification of lncRNA biomarkers associated with the progression of esophageal squamous cell carcinoma. *Mol Med Rep* 2019; **19**: 5309-5320 [PMID: 31059058 DOI: 10.3892/mmr.2019.10213]

47 **Xing S**, Zheng X, Wei LQ, Song SJ, Liu D, Xue N, Liu XM, Wu MT, Zhong Q, Huang CM, Zeng MS, Liu WL. Development and Validation of a Serum Biomarker Panel for the Detection of Esophageal Squamous Cell Carcinoma through RNA Transcriptome Sequencing. *J Cancer* 2017; **8**: 2346-2355 [PMID: 28819439 DOI: 10.7150/jca.19465]

48 **Shen Y**, Ding Y, Ma Q, Zhao L, Guo X, Shao Y, Niu C, He Y, Zhang F, Zheng D, Wei W, Liu F. Identification of Novel Circulating miRNA Biomarkers for the Diagnosis of Esophageal Squamous Cell Carcinoma and Squamous Dysplasia. *Cancer Epidemiol Biomarkers Prev* 2019; **28**: 1212-1220 [PMID: 30988139 DOI: 10.1158/1055-9965.EPI-18-1199]

49 **Zhai XH**, Yu JK, Lin C, Wang LD, Zheng S. Combining proteomics, serum biomarkers and bioinformatics to discriminate between esophageal squamous cell carcinoma and pre-cancerous lesion. *J Zhejiang Univ Sci B* 2012; **13**: 964-971 [PMID: 23225851 DOI: 10.1631/jzus.B1200066]

50 **Slaby O**, Srovnal J, Radova L, Gregar J, Juracek J, Luzna P, Svoboda M, Hajduch M, Ehrmann J. Dynamic changes in microRNA expression profiles reflect progression of Barrett's esophagus to esophageal adenocarcinoma. *Carcinogenesis* 2015; **36**: 521-527 [PMID: 25784377 DOI: 10.1093/carcin/bgv023]

51 **Bhat S**, Coleman HG, Yousef F, Johnston BT, McManus DT, Gavin AT, Murray LJ. Risk of malignant progression in Barrett's esophagus patients: results from a large population-based study. *J Natl Cancer Inst* 2011; **103**: 1049-1057 [PMID: 21680910 DOI: 10.1093/jnci/djr203]

52 **Hvid-Jensen F**, Pedersen L, Drewes AM, Sørensen HT, Funch-Jensen P. Incidence of adenocarcinoma among patients with Barrett's esophagus. *N Engl J Med* 2011; **365**: 1375-1383 [PMID: 21995385 DOI: 10.1056/NEJMoa1103042]

53 **de Jonge PJ**, van Blankenstein M, Looman CW, Casparie MK, Meijer GA, Kuipers EJ. Risk of malignant progression in patients with Barrett's oesophagus: a Dutch nationwide cohort study. *Gut* 2010; **59**: 1030-1036 [PMID: 20639249 DOI: 10.1136/gut.2009.176701]

54 **Critchley-Thorne RJ**, Duits LC, Prichard JW, Davison JM, Jobe BA, Campbell BB, Zhang Y, Repa KA, Reese LM, Li J, Diehl DL, Jhala NC, Ginsberg G, DeMarshall M, Foxwell T, Zaidi AH, Lansing Taylor D, Rustgi AK, Bergman JJ, Falk GW. A Tissue Systems Pathology Assay for High-Risk Barrett's Esophagus. *Cancer Epidemiol Biomarkers Prev* 2016; **25**: 958-968 [PMID: 27197290 DOI: 10.1158/1055-9965.EPI-15-1164]

55 **Li X**, Paulson TG, Galipeau PC, Sanchez CA, Liu K, Kuhner MK, Maley CC, Self SG, Vaughan TL, Reid BJ, Blount PL. Assessment of Esophageal Adenocarcinoma Risk Using Somatic Chromosome Alterations in Longitudinal Samples in Barrett's Esophagus. *Cancer Prev Res (Phila)* 2015; **8**: 845-856 [PMID: 26130253 DOI: 10.1158/1940-6207.CAPR-15-0130]

56 **Etemadi A**, Abnet CC, Golozar A, Malekzadeh R, Dawsey SM. Modeling the risk of esophageal squamous cell carcinoma and squamous dysplasia in a high risk area in Iran. *Arch Iran Med* 2012; **15**: 18-21 [PMID: 22208438]

57 **Moghtadaei M**, Hashemi Golpayegani MR, Malekzadeh R. A variable structure fuzzy neural network model of squamous dysplasia and esophageal squamous cell carcinoma based on a global chaotic optimization algorithm. *J Theor Biol* 2013; **318**: 164-172 [PMID: 23174279 DOI: 10.1016/j.jtbi.2012.11.013]

World Journal of Gastroenterology

Submit a Manuscript: https://www.f6publishing.com

World J Gastroenterol 2020 October 21; 26(39): 5970-5982

DOI: 10.3748/wjg.v26.i39.5970

ISSN 1007-9327 (print) ISSN 2219-2840 (online)

ORIGINAL ARTICLE

Basic Study

Polyethylene glycol 35 ameliorates pancreatic inflammatory response in cerulein-induced acute pancreatitis in rats

Ana Ferrero-Andrés, Arnau Panisello-Roselló, Joan Roselló-Catafau, Emma Folch-Puy

ORCID number: Ana Ferrero-Andrés 0000-0002-4874-7109; Arnau Panisello-Roselló 0000-0003-2062-6134; Joan Roselló-Catafau 0000-0001-7127-4883; Emma Folch-Puy 0000-0002-6277-9027.

Author contributions: Roselló-Catafau J and Folch-Puy E designed the study; Folch-Puy E coordinated the study; Ferrero-Andrés A and Panisello-Roselló A performed the experiments and acquired and analysed data; Ferrero-Andrés A and Folch-Puy E interpreted the data; Ferrero-Andrés A and Folch-Puy E wrote the original draft of the manuscript; Ferrero-Andrés A, Panisello-Roselló A, Roselló-Catafau J and Folch-Puy E reviewed and edited the manuscript; all authors approved the final version of the article.

Supported by the grant from Ministerio de Ciencia e Innovación, No. PID2019-104130RB-I00.

Institutional animal care and use committee statement: All experimental animals' procedures were conducted in accordance with European Union regulatory standards for animal experimentation (Directive 2010/63/EU on the protection of animals used for scientific

Ana Ferrero-Andrés, Arnau Panisello-Roselló, Experimental Pathology Department, Institut d'Investigacions Biomèdiques de Barcelona-Consejo Superior de Investigaciones científicas, Barcelona 08036, Catalonia, Spain

Joan Roselló-Catafau, Emma Folch-Puy, Experimental Pathology Department, Institut d'Investigacions Biomèdiques de Barcelona-Consejo Superior de Investigaciones científicas, Centro de Investigación Biomédica en Red de Enfermedades Hepáticas y Digestivas, Institut d'Investigacions Biomèdiques August Pi i Sunyer, Barcelona 08036, Catalonia, Spain

Corresponding author: Emma Folch-Puy, PhD, Senior Scientist, Experimental Pathology Department, Institut d'Investigacions Biomèdiques de Barcelona-Consejo Superior de Investigaciones científicas, Centro de Investigación Biomédica en Red de Enfermedades Hepáticas y Digestivas, Institut d'Investigacions Biomèdiques August Pi i Sunyer, C/Roselló 161, Barcelona 08036, Catalonia, Spain. emma.folch@iibb.csic.es

Abstract

BACKGROUND

Acute pancreatitis (AP) is a sudden inflammatory process of the pancreas that may also involve surrounding tissues and/or remote organs. Inflammation and parenchymal cell death are common pathological features of this condition and determinants of disease severity. Polyethylene glycols (PEGs) are non-immunogenic, non-toxic water-soluble polymers widely used in biological, chemical, clinical and pharmaceutical settings.

AIM

To evaluate the protective effect of a 35-kDa molecular weight PEG (PEG35) on the pancreatic damage associated to cerulein-induced acute pancreatitis *in vivo* and *in vitro*.

METHODS

Wistar rats were assigned at random to a control group, a cerulein–induced AP group and a PEG35 treatment group. AP was induced by five hourly intraperitoneal injections of cerulein (50 μg/kg/bw), while the control animals received saline solution. PEG35 was administered intraperitoneally 10 minutes before each cerulein injection in a dose of 10 mg/kg. After AP induction, samples of pancreatic tissue and blood were collected for analysis. AR42J pancreatic acinar cells were treated with increasing concentrations of PEG35 prior to exposure with tumor necrosis factor α (TNFα), staurosporine or cerulein. The severity of AP was

purposes). The Ethical Committee for Animal Experimentation (CEEA, ethic approval number: 211/18, University of Barcelona, 11/04/2018) approved the animal experiments.

Conflict-of-interest statement: The authors have disclosed that they do not have any conflict of interest.

Data sharing statement: No additional data are available.

ARRIVE guidelines statement: The authors have read the ARRIVE guidelines, and the manuscript was prepared and revised according to the ARRIVE guidelines.

Manuscript source: Unsolicited manuscript

Received: July 21, 2020
Peer-review started: July 21, 2020
First decision: August 8, 2020
Revised: August 12, 2020
Accepted: September 12, 2020
Article in press: September 12, 2020
Published online: October 21, 2020

P-Reviewer: Tian H
S-Editor: Zhang H
L-Editor: A
P-Editor: Ma YJ

determined on the basis of plasma levels of lipase, lactate dehydrogenase activity, pancreatic edema and histological changes. To evaluate the extent of the inflammatory response, the gene expression of inflammation-associated markers was determined in the pancreas and in AR42J-treated cells. Inflammation-induced cell death was also measured in models of *in vivo* and *in vitro* pancreatic damage.

RESULTS
Administration of PEG35 significantly improved pancreatic damage through reduction on lipase levels and tissue edema in cerulein-induced AP rats. The increased associated inflammatory response caused by cerulein administration was attenuated by a decrease in the gene expression of inflammation-related cytokines and inducible nitric oxide synthase enzyme in the pancreas. In contrast, pancreatic tissue mRNA expression of interleukin 10 was markedly increased. PEG35 treatment also protected against inflammation-induced cell death by attenuating lactate dehydrogenase activity and modulating the pancreatic levels of apoptosis regulator protein BCL-2 in cerulein hyperstimulated rats. Furthermore, the activation of pro-inflammatory markers and inflammation-induced cell death in pancreatic acinar cells treated with TNFα, cerulein or staurosporine was significantly reduced by PEG35 treatment, in a dose-dependent manner.

CONCLUSION
PEG35 ameliorates pancreatic damage in cerulein-induced AP and AR42J-treated cells through the attenuation of the inflammatory response and associated cell death. PEG35 may be a valuable option in the management of AP.

Key Words: Acute pancreatitis; Inflammation; Polyethylene glycols; Cytokines; AR42J cells; Cell death

Core Tip: Acute pancreatitis (AP) is a sudden inflammatory condition of the pancreas with variable involvement of peri-pancreatic tissues and/or remote organ systems. This disease is a major clinical challenge for which no specific pharmacological therapy currently exists. The manuscript describes the protective role of 35-kDa molecular weight polyethylene glycol (PEG35) on cerulein-induced AP. PEG35 treatment was able to lessen the inflammatory process in the pancreas and associated cell death in cerulein-induced AP and *in vitro* models of pancreatic damage.

Citation: Ferrero-Andrés A, Panisello-Roselló A, Roselló-Catafau J, Folch-Puy E. Polyethylene glycol 35 ameliorates pancreatic inflammatory response in cerulein-induced acute pancreatitis in rats. *World J Gastroenterol* 2020; 26(39): 5970-5982
URL: https://www.wjgnet.com/1007-9327/full/v26/i39/5970.htm
DOI: https://dx.doi.org/10.3748/wjg.v26.i39.5970

INTRODUCTION

Acute pancreatitis (AP) is an inflammatory disease of the exocrine pancreas characterized by abnormal intracellular activation of proteolytic enzymes. Parenchymal injury, pancreatic acinar cell death and an intense inflammatory reaction are common pathological features of this condition and determine the severity of the disease[1]. A majority of patients presenting with AP have the mild form of the disease, which is mostly self-limited and consists of the appearance of edema and inflammation of the pancreas[2]. In this group, organ failure and local complications are generally not observed, and the disease usually resolves in the first week. However, between 20% and 30% develop a severe form requiring intensive care unit admission, which is often associated with local and systemic complications and, in some occasions, leads to death[3]. To date, no drug is available to prevent or treat this condition, and any improved clinical outcomes have mostly been due to continuous

advancement of various supportive treatments.

Although pancreatic inflammation may be firstly caused by acinar events such as trypsinogen activation, it finally depends on the subsequent stimulation of components of the innate immune system. The initial acinar cell damage triggers the release of pro-inflammatory cytokines and chemokines, leading to increase of microvascular permeability and subsequent formation of interstitial edema[4]. Activation of inflammatory cells then provokes the production of additional cytokines and other mediators that initiate the inflammatory response. These mediators recruit different types of leukocytes (first neutrophils, followed by macrophages, monocytes and lymphocytes) to the pancreas. In parallel to the pro-inflammatory response, an anti-inflammatory response is also released[5]. If the anti-inflammatory response is adequate, the local inflammation resolves at this stage. However, in some cases, an overwhelming pro-inflammatory response drives the migration of inflammatory mediators into systemic circulation, leading to distant organ dysfunction[6].

Polyethylene glycols (PEGs) are hydrophilic polymers comprised of repeating ethylene glycol units[7]. PEGs have several physicochemical properties that make it advantageous in diverse biological, chemical and pharmaceutical settings, especially in view of its low toxicity. For instance, these polymers have been found to exert beneficial effects in several *in vivo* and *in vitro* models of cell and tissue injury[8-10].

There are very few studies linking PEGs of different molecular weight with an anti-inflammatory activity. In a model of traumatic inflammation, the intraperitoneal administration of 4-kDa molecular weight PEG prevented the formation of initial adhesions and reduced the leukocytes number in the peritoneal cavity as a consequence of an inflammatory peritoneal reaction[11]. Oral treatment with 4-kDa PEG in experimental colitis reinforced the epithelial barrier function and reduced the inflammation of the colon[12]. Likewise, in two different models of gut-derived sepsis, therapeutic administration of PEG reduced inflammatory cytokine expression and activation of neutrophils[13]. Our group has recently demonstrated an anti-inflammatory role for PEG35 in an experimental model of severe necrotizing AP. In this sense, the therapeutic administration of PEG35 notably alleviated the severity of AP and protected against the associated lung inflammatory response[14].

Based on the protective features of PEGs, we now have evaluated the effects of PEG35 in experimental models of pancreatic damage *in vivo* and *in vitro*.

MATERIALS AND METHODS

Experimental animals and model of cerulein-induced AP

All experimental animal proceedings were conducted according with European Union regulatory standards for experimentation with animals (Directive 2010/63/EU on the Protection of Animals Used for Scientific Purposes). The Ethical Committee for Animal Experimentation (CEEA, University of Barcelona, April 11, 2018, ethic approval number: 211/18) authorized all animal experimentation.

The protocol was designed to minimize pain and discomfort to animals. Adult male Wistar rats (n = 21) weighing 200-250 g were purchased from Charles River (Boston, MA, United States) and accommodated in a controlled environment with free access to standard laboratory pelleted formula (A04; Panlab, Barcelona, Spain) and tap water. Rats were kept in a climate-controlled environment with a 12-h light/12-h dark cycle for one week. For the 12 h prior to the experiment of AP induction, rats were fasted with free access to drinking water.

Rats were randomly selected and assigned to three equal groups: (1) Treated with saline, as controls (n = 7); and (2) Treated with cerulein, to induce AP (CerAP, n = 7) and (3) Treated with cerulein after a PEG35 pretreatment (PEG35 + CerAP, n = 7). Immediately before the first injection of PEG35 or saline, 0.05 mg/kg of buprenorphine was administered as an analgesic. Cerulein (Sigma-Aldrich, St. Louis, MO) was dissolved with phosphate-buffered saline (PBS) and administered intraperitoneally at a supramaximal stimulating concentration of 50 μg/kg/body weight (bw) at 1-h intervals (total of 5 injections); control animals received intraperitoneal saline solution with the same regime. The use of this supramaximal dosage of cerulein induce a transient form of interstitial edematous AP characterized by marked hyperamylasemia, pancreatic edema and neutrophil infiltration within the pancreas, as well as pancreatic acinar cell vacuolization and necrosis[15].

PEG35 was administered intraperitoneally at a dose of 10 mg/kg, 10 min prior to each cerulein injection. Immediately after the last injection of cerulein or saline, animals were euthanized by intraperitoneal injection of 40-60 mg/kg of sodium

pentobarbital, and blood was collected from the vena cava in heparinized syringes. Harvested blood was centrifuged and the obtained plasma was stored at −80 °C until analysis. Four tissue samples from each animal were taken from the head of the pancreas. One portion of each tissue sample was immediately weighed and oven-dried for the wet-to-dry weight ratio calculation. Another portion was fixed in 10% phosphate−buffered formalin for histological analysis. The third portion was frozen and stored at −80 °C for western blot analysis, and the last portion was saved in RNAlater solution for real-time qRT-PCR analysis.

Histopathological examination

Pancreas tissue was fixed in 10% phosphate-buffered formalin and then embedded in paraffin. 3-μm thickness sections were mounted on glass slides. Slides were dewaxed and rehydrated and stained with hematoxylin and eosin. Assessment of changes in the tissue was carried out by an experienced pathologist through the examination of different microscopic fields randomly chosen from each experimental group in a blinded manner. Pancreatic tissue sections were evaluated for the severity of pancreatitis based on edema, inflammatory infiltration, parenchymal necrosis, and vacuolation of acinar cells.

Cell lines and treatments

The rat pancreatic acinar AR42J cell line was purchased from Sigma (St. Louis, MI, United States). Cells were grown at 37 °C in RPMI medium supplemented with 100 mL/L fetal bovine serum, 100 U/ml penicillin and 100 μg/mL streptomycin in a humidified atmosphere of 50 mL/L CO_2. Acinar cells were plated at a density of 3 × 10^5/well in 12-well culture plates, or at a density of 2 × 10^4/well in 96-well plates, and allowed to attach for 24 h or 48 h. Cells were pretreated with PEG35 diluted in PBS, at a concentration of 0.5, 1, 2, 4, or 6% for 30 min prior to treatment with the appropriate stimuli: 2 μmol/L or 4 μmol/L staurosporine, 100 ng/mL TNFα or 10 nM cerulein. All three reagents were purchased from Sigma-Aldrich (St. Louis, MO, United States). Time points of 3 h were used for TNFα treatment, and of 24 h for the remaining stimuli.

Lipase activity

Plasma lipase activity levels were determined using a turbidimetric assay kit from Randox (County Antrim, Crumlin, United Kingdom), in accordance with the supplier's specifications. Briefly, the degradation of triolein by the pancreatic lipase results in lowered turbidity, which was determined in the sample at 340 nm using a microplate reader (iEMS Reader MF; Labsystems, Helsinki, Finland). The activity of the sample was obtained in U/L. All samples were run in duplicate.

Pancreas wet-to-dry weight ratio

Edema formation in the pancreas was evaluated by the determination of the wet-to-dry weight ratio. A portion of the pancreas was weighed. The content of water was measured by calculating the wet-to-dry weight ratio from the initial weight (wet weight) and its weight after incubation in an oven at 60 °C for 48 h (dry weight).

Lactate dehydrogenase activity

Lactate dehydrogenase (LDH) activity was measured in plasma samples and cell culture supernatants using the Lactate Dehydrogenase Assay Kit (Abcam; Cambridge, United Kingdom). Briefly, LDH reduces NAD to NADH, which interacts with a specific probe to produce colour. Changes in absorbance due to NADH formation were measured at 450 nm at 37 °C using an automated microplate reader (iEMS Reader MF; Labsystems, Helsinki, Finland). Sample activity was expressed in mU/mL. All samples were run in duplicate. The lower limit of detection for ELISA ranged from 14 to 36 mU/mL.

MTT cell proliferation assay

The cell proliferation was determined by measuring metabolic activity of the cells through the reduction of the tetrazolium dye MTT [3-(4,5-dimethylthiazol-2-yl)-2,5-diphenyltetrazolium bromide] to its insoluble formazan. AR42J cells were seeded in 96-well plates at a density of 2 × 10^4 cells/well in 100 μL of culture medium with or without the compounds to be tested for 24 h. MTT reagent was added and incubated for 2 h at 37 °C, and the formazan produced in the cells formed dark crystals at the bottom of the wells. Crystal-dissolving solution was added and the absorbance of each sample was quantified at 570 nm using an automated microplate reader (iEMS Reader

MF; Labsystems, Helsinki, Finland). All samples were run in duplicate. The absorbance intensity was proportional to the number of viable cells.

Real-time qRT-PCR

Total RNA from the pancreatic tissue and cultured cells was extracted with Nucleozol reagent (Macherey-Nagel, Dueren, Germany) in accordance with the manufacturer's protocol. RNA concentration and quality were measured with the OD A260/A280 ratio and the OD A260/A230 ratio, respectively. Reverse transcription was performed on a 1 μg RNA sample employing the iScript cDNA Synthesis Kit (Bio-Rad Laboratories, Hercules, CA, United States). PCR amplification was performed using SsoAdvanced™ Universal SYBR® Green Supermix (Bio-Rad Laboratories, Hercules, CA, United States) on a CFX Real-Time PCR Detection System (Bio-Rad Laboratories, Hercules, CA, United States) using 10 μL of amplification mixture containing 50 ng of reverse-transcribed RNA and 250 nmol/L of the corresponding forward and reverse primers.

PCR primers for the detection of interleukin (IL) 6, IL1β, IL10, inducible isoform of nitric oxide synthase (iNOS), or glyceraldehyde-3-phosphate dehydrogenase (GAPDH) were validated primers from BioRad (Hercules, CA, United States). PCR primers for tumor necrosis factor α (TNFα), designed with Primer3.0 plus[16], were: TNFα forward, 5'- ATGGGCTCCCTCTCATCAGT-3' and reverse, 5'-GCTTG GTGGTTTGCTACGAC-3'. The specificity of amplicon was determined by melting curve analysis. Threshold cycle values were normalized to GAPDH gene expression and the ratio of the relative expression of target genes to GAPDH was calculated by the DCt formula.

Western blot

Pancreatic tissue was homogenized in ice-cold RIPA buffer. Lysates were then centrifuged at 15000 *g* for 20 min at 4 °C, and the supernatants were collected. Supernatant protein concentrations were measured using the Bradford protein assay (Bio-Rad Laboratories, Hercules, CA, United States). SDS-PAGE was performed on a 10% gel and proteins were transferred to a polyvinylidene difluoride membrane for blotting.

The following antibodies were used for immunoblotting:rabbit polyclonal cleaved caspase-3 (Asp175) antibody (1:800 dilution, reference #9661) from Cell Signaling, rabbit polyclonal BCL-2 (1: 500 dilution, reference #59348) from Abcam (Cambridge, United Kingdom) and β-actin-HRP conjugated (1: 20000 dilution, reference A3854) from Sigma (Sigma-Aldrich, St. Louis, MO). Bound antibodies were detected using enhanced chemiluminescence (ECL) (Bio-Rad Laboratories, Hercules, CA, United States), and were analyzed using ChemiDoc™ Touch Imaging System (Bio-Rad Laboratories, Hercules, CA, United States). Protein expression of cleaved caspase-3 and BCL-2 were normalized to β-actin for quantification.

Statistical analysis

All data were exported into Graph Pad Prism 4 (GraphPad Software, Inc.) and presented as means ± SEM. Statistical analyses were carried out by one-way analysis of variance (ANOVA), followed by Tukey's multiple comparison test to determine the significance between pairs. The minimal level of statistical significance was considered to be < 0.05.

RESULTS

PEG35 reduced the release of lipase associated with cerulein-induced AP

Cerulein-induced AP in rats was associated with significant raised plasma levels of lipase, comparing with the control group, reflecting the degree of pancreatic injury (Figure 1A). Such increase was significantly reduced in rats pre-treated with intravenous PEG35 at 10 mg/kg.

PEG35 abrogated pancreatic edema following cerulein-induced AP

As cerulein-induced pancreatitis is characterized by a progressive interstitial edema development, we analyzed the pancreas wet-to-dry weight ratio (Figure 1B). A significant increase in the pancreas wet-to-dry weight ratio was observed in rats after AP induction with cerulein (7.865 ± 0.86) as compared to control rats (2.76 ± 0.28). However, this increase could be largely prevented by co-treatment with PEG35 in

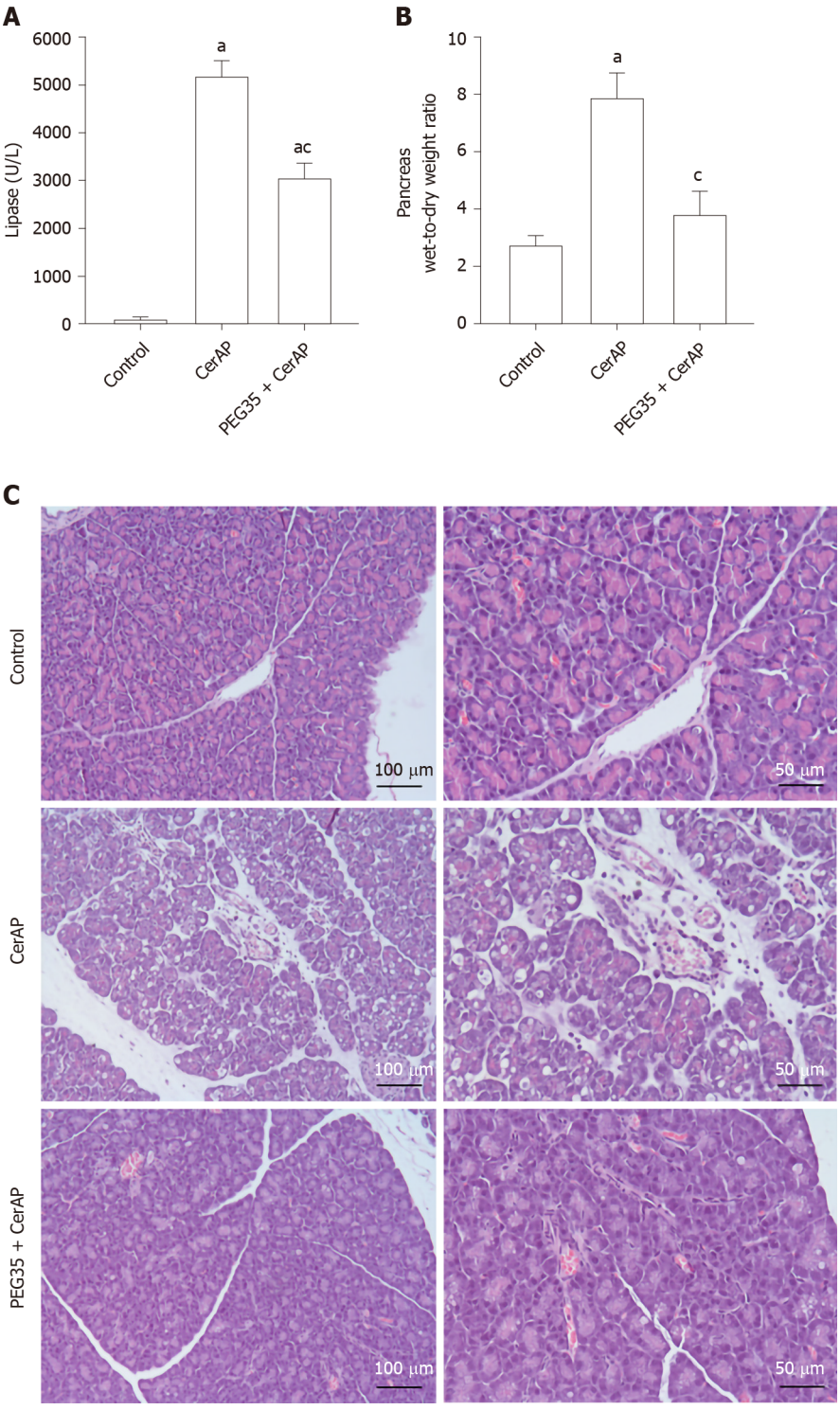

Figure 1 Effect of PEG35 treatment on plasma lipase activity, pancreatic edema and histological changes in experimental cerulein-induced acute pancreatitis. A: Plasma lipase levels in U/L; B: Pancreatic wet-to-dry weight ratio. Bars represent mean values of each group ± SEM. $^{a}P < 0.05$ *vs* control, $^{c}P < 0.05$ *vs* Cerulein-induced acute pancreatitis (CerAP). Each determination was carried out in triplicate; C: Representative images of hematoxylin and eosin-stained pancreatic sections for each experimental group. Control group showed normal pancreas structure. CerAP group presented areas of necrosis, infiltrated polymorphonuclear neutrophils, interstitial edema and vacuolation of the acinar cells. Administration of 35-kDa polyethylene glycol notably reduced these features. Scale bar, 100 and 50 μm. CerAP: Cerulein-induced acute pancreatitis; PEG35: 35-kDa polyethylene glycol.

cerulein-treated rats, with a wet-to-dry weight ratio of 3.8 ± 0.85.

PEG35 reduced local pancreatic tissue damage associated with cerulein-induced AP

Histopathological results showed that cerulein hyperstimulated rats caused an interstitial edematous acute pancreatitis with considerable areas of interstitial edema, local necrosis, infiltrated polymorphonuclear neutrophils and vacuolation of the acinar

cells. (Figure 1C). In the PEG35-treated group, there were consistent reductions in these characteristics.

PEG35 ameliorated the expression of inflammatory markers in cerulein-induced AP and AR42J-treated cells

Further, we explored whether PEG35 treatment improves the inflammatory response after cerulein hyperstimulation in rats, by measuring the gene expression of inflammatory mediators in the pancreas. Pancreatic tissue levels of IL6, IL1β, TNFα, IL10 and iNOS increased markedly in rats after AP induction as compared to that of control rats (Figure 2). Notably, PEG35 treatment significantly reduced the AP-induced increases in IL1β, IL6 and iNOS. While TNFα expression levels showed a tendency to decrease, this was not statistically significant. Finally, as expected based on its anti-inflammatory role, the gene expression of the IL10 cytokine was not reduced in PEG35-treated animals.

In addition to its *in vivo* effects, a direct anti-inflammatory effect of PEG35 was also observed in *in vitro* model. Specifically, in a model of cerulein-induced inflammation in the acinar cells using cultured AR42J cells, PEG35 attenuated the gene expression of the pro-inflammatory IL1β and TNFα in a dose-dependent manner (Figure 3A). Additionally, TNFα-treated cells induced the production of iNOS as well as of TNFα itself, both of which were markedly reduced after the treatment with increasing concentrations of PEG35 (Figure 3B).

PEG35 lessened inflammation-associated cell death in cerulein-induced AP

To investigate the potential protective effects of PEG35 on the pancreas, cell death was determined through LDH release and expression of the apoptosis-related proteins BCL-2 and cleaved-caspase-3 by Western blot. Indeed, a significant increment in LDH activity in plasma occurred in cerulein AP-induced animals (Figure 4A). Notably, rats that had PEG35 co-treatment had significantly reduced levels of the LDH necrotic marker.

The pancreatic levels of cleaved caspase-3 and BCL-2 were also markedly higher following cerulein-induced AP as compared to the control group, (Figure 4B and C). The administration of PEG35 promoted a further increase in the levels of anti-apoptotic BCL-2 as compared with cerulein hyperstimulated rats while the reduction in the pro-apoptotic cleaved caspase-3 was not statistically significant.

PEG35 reduced inflammation-associated cell death in models of pancreatic damage in vitro

The decreased LDH activity observed *in vivo* in PEG35-treated animals led us to examine cell death in *in vitro* models of inflammation. AR42J cells are a well-established cell model for studying intracellular mechanisms involved in the cell death and inflammatory responses of acute pancreatitis. We therefore analysed whether PEG35 affected the release of LDH in AR42J cells in the presence of the pro-inflammatory stimulus cerulein or TNFα (Figure 4D). Indeed, both cerulein and TNFα-induced cell death were significantly reduced by PEG35 in a dose-dependent manner. Likewise, PEG35 markedly prevented staurosporine-induced AR42J apoptotic cell death in a dose-dependent manner (Figure 4E). These results suggest that PEG35 exerts a protective role against inflammation-induced cell death *in vitro* and *in vivo*.

DISCUSSION

Acute pancreatitis (AP) is an inflammatory disease that can have a mild to severe course. We have recently reported an anti-inflammatory role for PEG35 in a severe necrotizing AP experimental model. To further investigate the effect of this polymer in a milder form of the disease, we used a model of cerulein-induced mild edematous pancreatitis that is mainly characterized by a dysregulation of the production and secretion of digestive enzymes, interstitial edema formation, infiltration of neutrophil and mononuclear cells within the pancreas, cytoplasmic vacuolization and the death of acinar cells[17]. We determined that PEG35 reduced the course of cerulein-induced AP by inhibiting the inflammatory response as well as inflammation-induced cell death. In our study, treating the animals with PEG35 significantly abrogated the severity of cerulein-induced AP, as indicated by the lessened activity of lipase in plasma and edema formation as well as histopathological features of AP in the PEG35-treated animals.

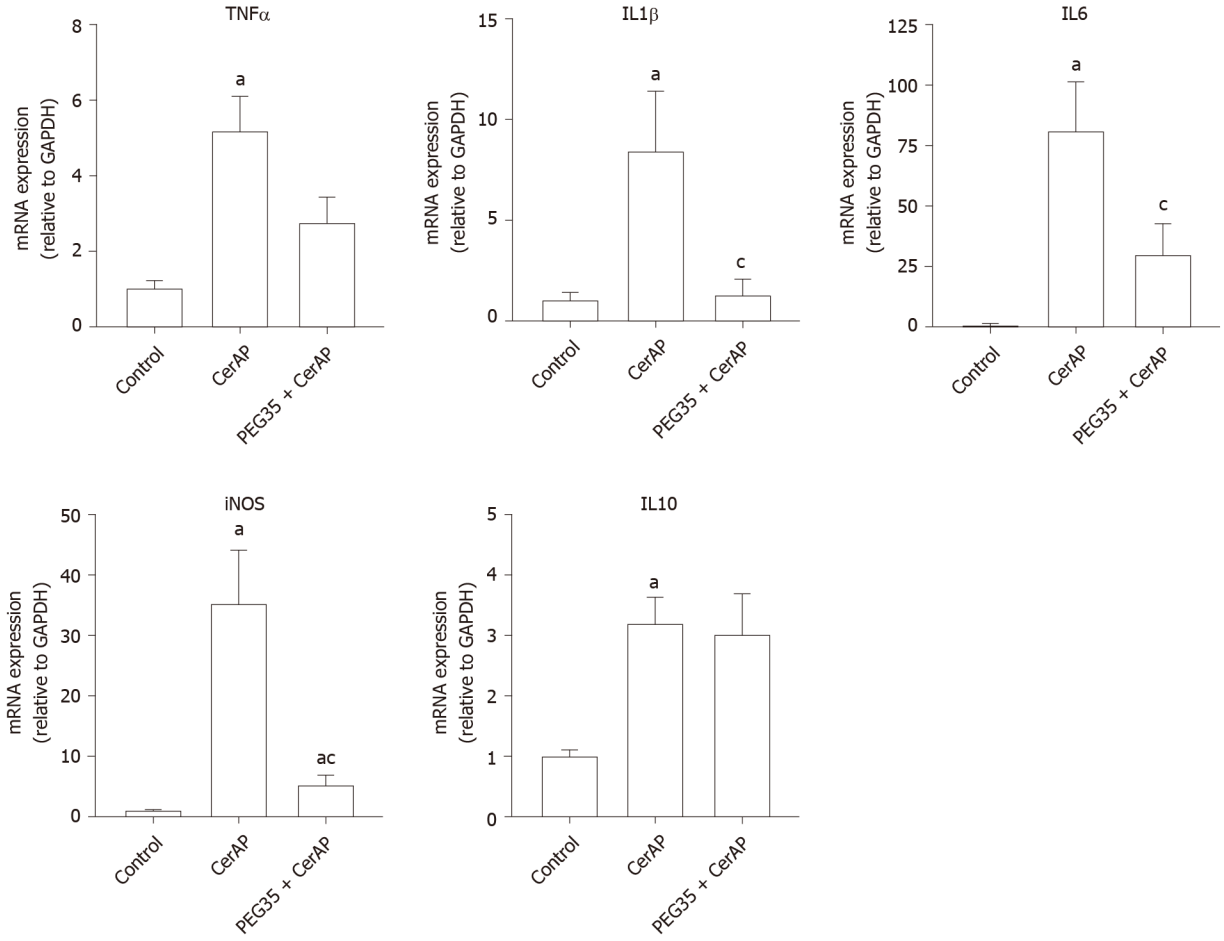

Figure 2 Role of PEG35 on the modulation of inflammation-associated cytokines and inducible nitric oxide synthase enzyme expression in cerulein-induced acute pancreatitis. Pancreatic tissue gene expression of tumor necrosis factor α, interleukin (IL) 1β, IL6, inducible nitric oxide synthase and IL10 by real-time qRT-PCR. Bars represent mean values of each group ± SEM. $^{a}P < 0.05$ *vs* control, $^{\circ}P < 0.05$ *vs* cerulein-induced acute pancreatitis. Each determination was carried out in triplicate. CerAP: Cerulein-induced acute pancreatitis; PEG35: 35-kDa polyethylene glycol.

A sudden inflammatory response in the pancreas contributes to the development of AP, primarily through the release of inflammatory cytokines. TNFα has long been considered as one of the initial triggers of the inflammatory cascade in experimental pancreatitis[18]. In this setting, stimulation of acinar cells of the pancreas by TNFα have been reported to cause a direct activation of pancreatic enzymes, contributing to premature protease activation and cell necrosis[19]. Increased accumulation of TNFα promotes the production of other inflammatory cytokines, including IL1β and IL6, which result in the activation of an inflammatory cascade that leads to widespread tissue damage in multiple tissues and organs. Indeed, the levels of TNFα, IL1β and IL6 have been correlated with the severity of AP[20-23]. In the current study, treatment with PEG35 was capable to significantly reduce the AP-induced raises in pro-inflammatory IL1β and IL6. However, no significant effect on TNFα was observed. This fact could be explained by the levels of IL10 found in rats co-treated with cerulein and PEG35, which were similar to those found in those only treated with cerulein. As IL10 plays a fundamental role in the attenuation of the cytokine response during acute inflammation, the significant increase of IL10 found in hyperstimulated rats may contribute to slow TNFα production, with an observed tendency towards a decrease in its expression. Indeed, in an experimental model of cerulein-induced AP, intraperitoneal IL10 administration attenuated TNFα production, which was associated with dramatically lessened pancreatitis severity and mortality[24].

Furthermore, a direct anti-inflammatory effect of PEG35 was observed in cultured AR42J cells. In an *in vitro* model of cerulein-induced inflammation, PEG35 was able to attenuate the gene expression of pro-inflammatory IL1β and TNFα in a dose-dependent manner. Moreover, PEG35 reduced the levels of TNFα in AR42J cells stimulated with TNFα.

Pro-inflammatory cytokines are known to activate the inducible iNOS and the subsequent production of nitric oxide, thus contributing to the pathophysiology of AP.

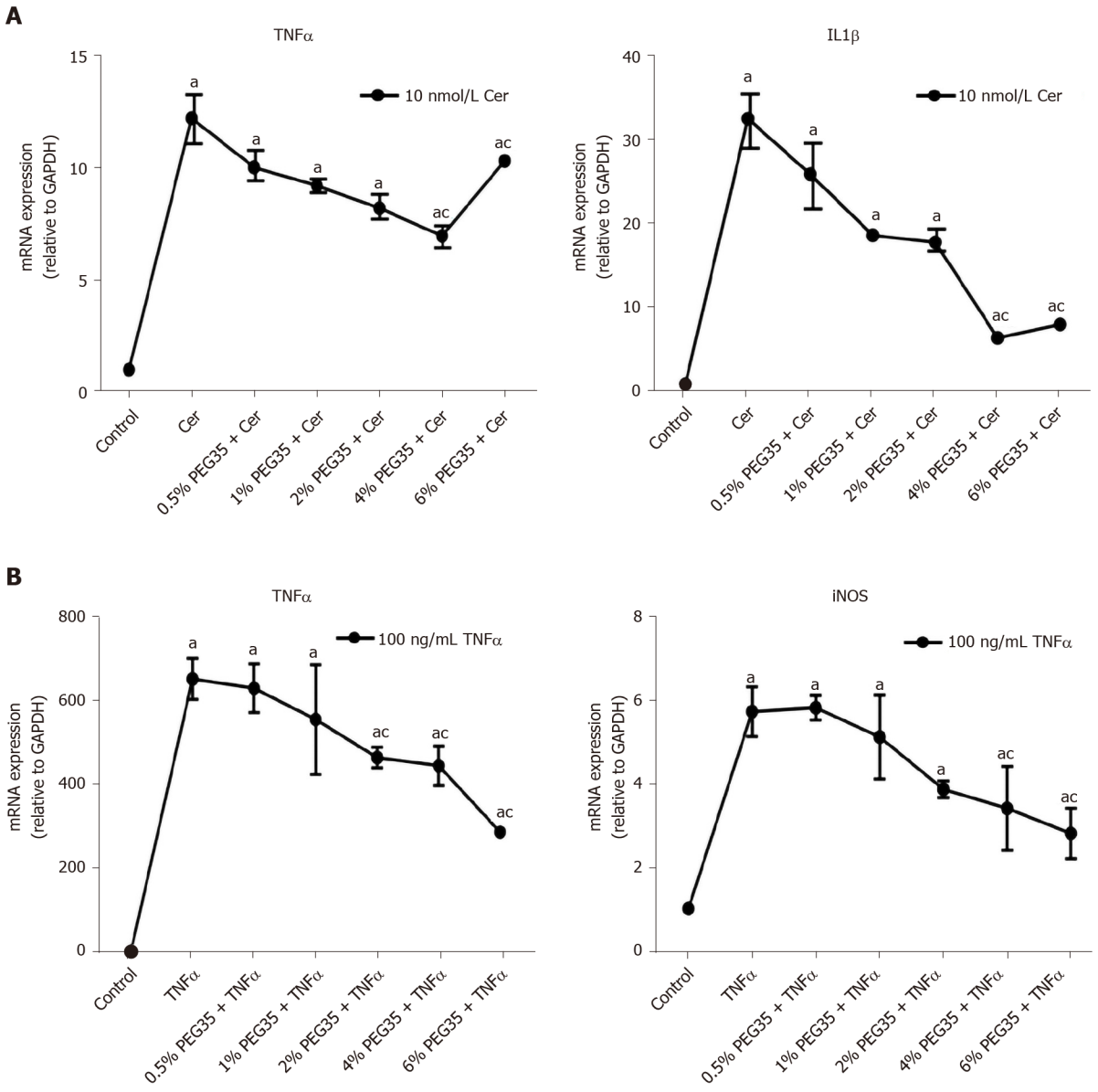

Figure 3 Gene expressions of inflammatory markers in AR42J-treated cells. A: Gene expression by real-time qRT-PCR of tumor necrosis factor α (TNFα) and IL1β in cerulein-treated AR42J cells subjected to increasing concentrations of 35-kDa polyethylene glycol (PEG35); B: Gene expression by real-time qRT-PCR of TNFα and inducible nitric oxide synthase in TNFα-treated AR42J cells subjected to increasing concentrations of PEG35. In both cases, mRNA induction levels were normalized to GAPDH mRNA expression. Bars represent mean values of each group ± SEM. $^{a}P < 0.05$ *vs* control, $^{c}P < 0.05$ *vs* cerulein or TNFα. Each determination was carried out in triplicate. Cer: Cerulein; PEG35: 35-kDa polyethylene glycol; TNFα: Tumor necrosis factor α.

In fact, the degree of pancreatic inflammation and tissue injury of cerulein-induced AP has been found to be markedly reduced in iNOS-deficient mice[25]. In our study, we observed an increased mRNA expression of iNOS following cerulein hyperstimulation in rats, which underwent a significant reduction after PEG35 treatment. Likewise, PEG35 abrogated TNFα-induced iNOS expression in acinar cells in a concentration-dependent manner. Altogether, these results suggest that PEG35 treatment reduced pancreatic inflammation in pancreatitis by suppressing the expression of pro-inflammatory mediators.

These changes in the inflammatory response brought about by PEG35 treatment were further emphasized by a reduction in pancreatic cell death. PEG35 treatment reduced cell death in cerulein-induced AP rats by lowering plasmatic LDH activity. In addition, the increased release of LDH observed in cerulein and TNFα-treated acinar cells *in vitro* was reverted upon incubation with increasing concentrations of PEG35.

In the pancreas, inflammation is associated with injured acinar cells that can go through necrosis or apoptosis. Thus, we measured the apoptosis index in pancreatic tissue following cerulein-induced AP. Injured pancreatic tissue induced a significant increase in cleaved caspase-3 and BCL-2 apoptotic proteins as compared to the

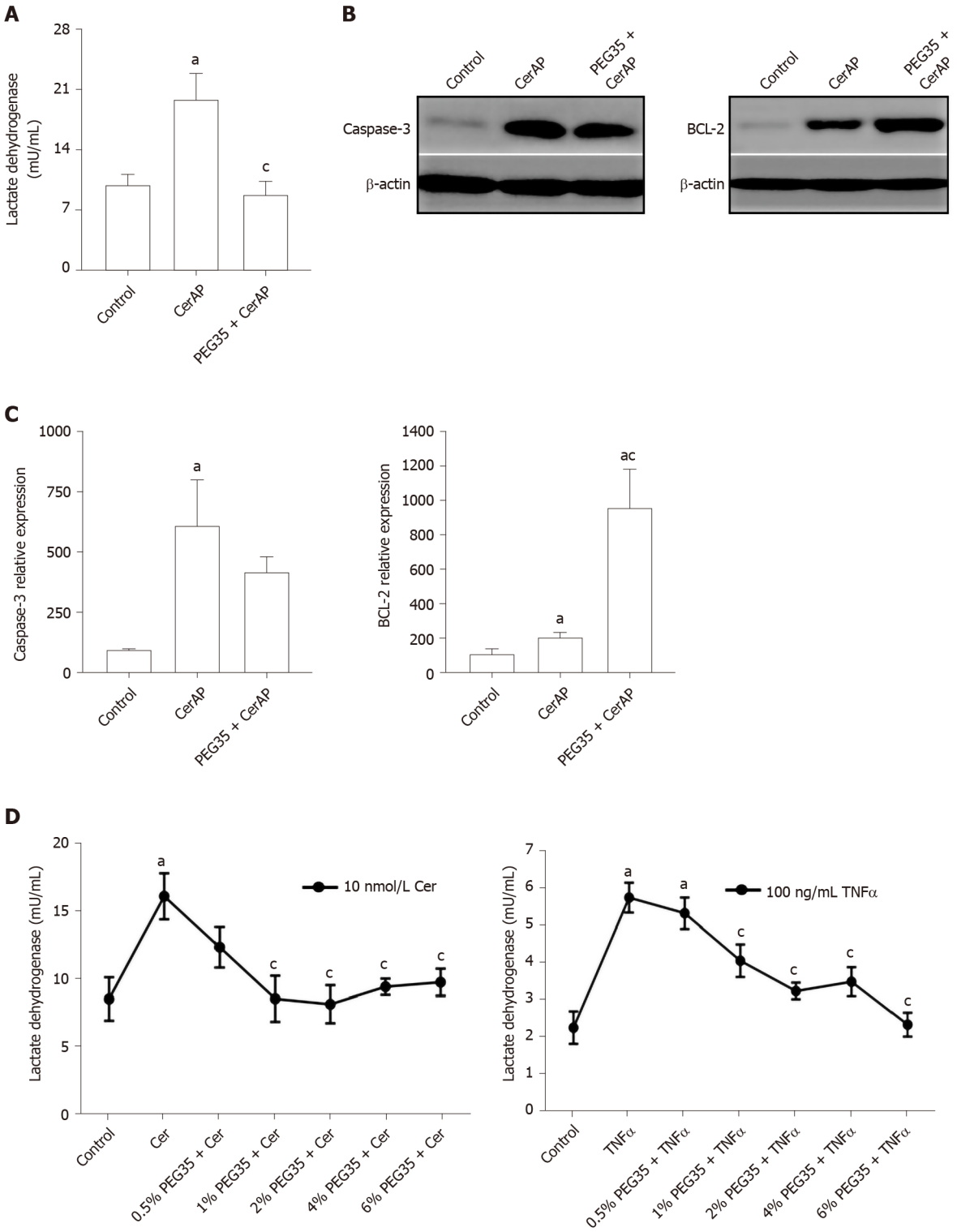
A
Lactate dehydrogenase (mU/mL)
28
21
14
7
0
a
c
Control
CerAP
PEG35 + CerAP
B
Control
CerAP
PEG35 + CerAP
Caspase-3
β-actin
BCL-2
β-actin
C
Caspase-3 relative expression
1000
750
500
250
0
a
Control
CerAP
PEG35 + CerAP
BCL-2 relative expression
1400
1200
1000
800
600
400
200
0
ac
a
D
Lactate dehydrogenase (mU/mL)
10 nmol/L Cer
Control
Cer
0.5% PEG35 + Cer
1% PEG35 + Cer
2% PEG35 + Cer
4% PEG35 + Cer
6% PEG35 + Cer
100 ng/mL TNFα
TNFα
0.5% PEG35 + TNFα
1% PEG35 + TNFα
2% PEG35 + TNFα
4% PEG35 + TNFα
6% PEG35 + TNFα

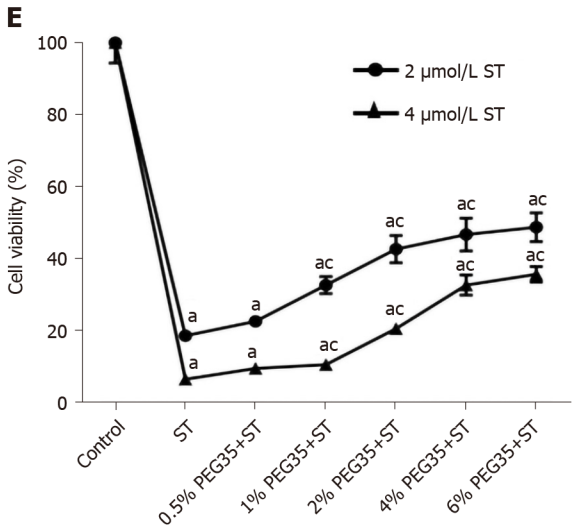

Figure 4 Effect of 35-kDa polyethylene glycol on inflammation-induced cell death in cerulein-induced acute pancreatitis and cultured pancreatic acinar AR42J cells. A: Plasma lactate dehydrogenase (LDH) activity after cerulein-induced acute pancreatitis expressed as mU/mL; B: Pancreatic protein expression of cleaved caspase-3 and BCL-2 assessed by western blot analysis. β-actin expression was used as loading control. Data shown are representative blots for each group; C: Densitometry quantification of western blot for cleaved caspase-3 and BCL-2 in pancreatic tissue; D: Cell death rate measured through LDH activity. AR42J cells pre-treated with increasing concentrations of PEG35 (0.5%, 1%, 2%, 4% or 6%) for 30 min and then co-incubated with 10nM cerulein for another 24 h or 100 ng/mL of tumor necrosis factor α (TNFα) for another 2.5 h; E: Cell viability rate determined by MTT assay. AR42J cells were pre-treated with increasing concentrations of PEG35, as indicated, for 30 min and then incubated with or without 2 μM or 4 μM staurosporine for another 24 h. The values shown represent the mean ± SEM. $^{a}P < 0.05$ *vs* control, $^{c}P < 0.05$ *vs* cerulein-induced acute pancreatitis, cerulein, TNFα or staurosporine. Each determination was carried out in triplicate. CerAP: Cerulein-induced acute pancreatitis; Cer: Cerulein; PEG35: 35-kDa polyethylene glycol; TNFα: Tumor necrosis factor α; ST: Staurosporine.

respective controls. Following treatment with PEG35, anti-apoptotic BCL-2 further increased as compared with cerulein-treated animals while cleaved caspase-3 levels were similar to that found in cerulein hyperstimulated animals. Collectively, these findings suggest that PEG35 has anti-apoptotic and anti-necrotic properties for cerulein-induced pancreatitis.

CONCLUSION

In conclusion, results from this study reveal a mechanism by which PEG35 exerts anti-inflammatory effects that alleviate experimental cerulein-induced AP, by inhibiting the inflammatory response as well as inflammation-induced cell death. Because of its low toxicity as well as its proven biocompatibility, PEG35 could be used as a new therapeutic tool to resolve the cellular damage associated to mild AP.

ARTICLE HIGHLIGHTS

Research background

Acute pancreatitis (AP) is a common gastrointestinal condition with an increasing incidence worldwide. The course of the disease ranges from a mild, self-limiting condition to a more severe acute illness with a high morbidity and mortality. Our group has previously demonstrated an anti-inflammatory role for a 35-kDa molecular weight polyethylene glycol (PEG35) in an experimental model of severe necrotizing AP. The therapeutic administration of PEG35 notably alleviated the severity of AP and protected against the associated lung inflammatory response, which is the main contributing factor to early death in patients with this condition.

Research motivation

To date, the treatment of AP continues to be supportive as there are no effective pharmacologic therapies available. Polyethylene glycols (PEGs) are neutral polymers widely used in biomedical applications due to its hydrophilic properties combined

with a low intrinsic toxicity. In this study, we demonstrated the protective role of PEG35 in a mild form of AP.

Research objectives

To evaluate the effect of PEG35 in experimental models of mild acute pancreatitis *in vivo* and *in vitro*.

Research methods

AP was induced by five hourly intraperitoneal injections of cerulein (50 μg/kg/bw). PEG35 was administered intraperitoneally 10 minutes before each cerulein injection in a dose of 10 mg/kg. After AP induction, samples of pancreatic tissue and blood were collected for analysis. AR42J pancreatic acinar cells were treated with increasing concentrations of PEG35 prior to exposure with tumor necrosis factor α, staurosporine or cerulein. The severity of AP was determined on the basis of plasma levels of lipase, lactate dehydrogenase activity, pancreatic edema and histological changes. To evaluate the extent of the inflammatory response, the gene expression of inflammation-associated markers was determined in the pancreas and in AR42J-treated cells. Inflammation-induced cell death was also measured in both *in vivo* and *in vitro* models of pancreatic damage through apoptosis and necrosis-related assays.

Research results

PEG35 treatment significantly improved pancreatic damage in cerulein-induced AP in rats through reduction on lipase levels and tissue edema. Furthermore, PEG35 ameliorated the inflammatory response and associated cell death *in vivo* and *in vitro*, in treated-acinar cells, by lowering inflammatory-related cytokines and iNOS gene expression, levels of apoptotic markers and the activity of lactate dehydrogenase.

Research conclusions

PEG35 ameliorated pancreatic damage in cerulein-induced AP and cultured acinar AR42J-treated cells through the attenuation of the inflammatory response and associated cell death.

Research perspectives

Our study provided evidence of a protective role of PEG35 in a mild form of AP suggesting that PEG35 may be a valuable option in the management of clinical AP.

ACKNOWLEDGEMENTS

This study was supported by grant from Ministerio de Ciencia e Innovación (PID2019-104130RB-I00) to Emma Folch-Puy. The authors thank Veronica Raker for revising the English text.

REFERENCES

1 **Gukovskaya AS**, Gukovsky I, Algül H, Habtezion A. Autophagy, Inflammation, and Immune Dysfunction in the Pathogenesis of Pancreatitis. *Gastroenterology* 2017; **153**: 1212-1226 [PMID: 28918190 DOI: 10.1053/j.gastro.2017.08.071]

2 **Banks PA**, Bollen TL, Dervenis C, Gooszen HG, Johnson CD, Sarr MG, Tsiotos GG, Vege SS; Acute Pancreatitis Classification Working Group. Classification of acute pancreatitis--2012: revision of the Atlanta classification and definitions by international consensus. *Gut* 2013; **62**: 102-111 [PMID: 23100216 DOI: 10.1136/gutjnl-2012-302779]

3 **van Santvoort HC**, Bakker OJ, Bollen TL, Besselink MG, Ahmed Ali U, Schrijver AM, Boermeester MA, van Goor H, Dejong CH, van Eijck CH, van Ramshorst B, Schaapherder AF, van der Harst E, Hofker S, Nieuwenhuijs VB, Brink MA, Kruyt PM, Manusama ER, van der Schelling GP, Karsten T, Hesselink EJ, van Laarhoven CJ, Rosman C, Bosscha K, de Wit RJ, Houdijk AP, Cuesta MA, Wahab PJ, Gooszen HG; Dutch Pancreatitis Study Group. A conservative and minimally invasive approach to necrotizing pancreatitis improves outcome. *Gastroenterology* 2011; **141**: 1254-1263 [PMID: 21741922 DOI: 10.1053/j.gastro.2011.06.073]

4 **Garber A**, Frakes C, Arora Z, Chahal P. Mechanisms and Management of Acute Pancreatitis. *Gastroenterol Res Pract* 2018; **2018**: 6218798 [PMID: 29736167 DOI: 10.1155/2018/6218798]

5 **Sendler M**, van den Brandt C, Glaubitz J, Wilden A, Golchert J, Weiss FU, Homuth G, De Freitas Chama LL, Mishra N, Mahajan UM, Bossaller L, Völker U, Bröker BM, Mayerle J, Lerch MM. NLRP3 Inflammasome Regulates Development of Systemic Inflammatory Response and Compensatory Anti-Inflammatory Response Syndromes in Mice With Acute Pancreatitis. *Gastroenterology* 2020; **158**: 253-

269.e14 [PMID: 31593700 DOI: 10.1053/j.gastro.2019.09.040]
6 **Kylänpää ML**, Repo H, Puolakkainen PA. Inflammation and immunosuppression in severe acute pancreatitis. *World J Gastroenterol* 2010; **16**: 2867-2872 [PMID: 20556831 DOI: 10.3748/wjg.v16.i23.2867]
7 **Pasut G**, Panisello A, Folch-Puy E, Lopez A, Castro-Benítez C, Calvo M, Carbonell T, García-Gil A, Adam R, Roselló-Catafau J. Polyethylene glycols: An effective strategy for limiting liver ischemia reperfusion injury. *World J Gastroenterol* 2016; **22**: 6501-6508 [PMID: 27605884 DOI: 10.3748/wjg.v22.i28.6501]
8 **Chen H**, Quick E, Leung G, Hamann K, Fu Y, Cheng JX, Shi R. Polyethylene glycol protects injured neuronal mitochondria. *Pathobiology* 2009; **76**: 117-128 [PMID: 19468251 DOI: 10.1159/000209389]
9 **Malhotra R**, Valuckaite V, Staron ML, Theccanat T, D'Souza KM, Alverdy JC, Akhter SA. High-molecular-weight polyethylene glycol protects cardiac myocytes from hypoxia- and reoxygenation-induced cell death and preserves ventricular function. *Am J Physiol Heart Circ Physiol* 2011; **300**: H1733-H1742 [PMID: 21335476 DOI: 10.1152/ajpheart.01054.2010]
10 **Chiang ET**, Camp SM, Dudek SM, Brown ME, Usatyuk PV, Zaborina O, Alverdy JC, Garcia JG. Protective effects of high-molecular weight polyethylene glycol (PEG) in human lung endothelial cell barrier regulation: role of actin cytoskeletal rearrangement. *Microvasc Res* 2009; **77**: 174-186 [PMID: 19121327 DOI: 10.1016/j.mvr.2008.11.007]
11 **Nagelschmidt M**, Minor T, Saad S. Polyethylene glycol 4000 attenuates adhesion formation in rats by suppression of peritoneal inflammation and collagen incorporation. *Am J Surg* 1998; **176**: 76-80 [PMID: 9683139 DOI: 10.1016/S0002-9610(98)00102-0]
12 **Videla S**, Lugea A, Vilaseca J, Guarner F, Treserra F, Salas A, Crespo E, Medina C, Malagelada JR. Polyethylene glycol enhances colonic barrier function and ameliorates experimental colitis in rats. *Int J Colorectal Dis* 2007; **22**: 571-580 [PMID: 17061105 DOI: 10.1007/s00384-006-0232-4]
13 **Ackland GL**, Gutierrez Del Arroyo A, Yao ST, Stephens RC, Dyson A, Klein NJ, Singer M, Gourine AV. Low-molecular-weight polyethylene glycol improves survival in experimental sepsis. *Crit Care Med* 2010; **38**: 629-636 [PMID: 20009757 DOI: 10.1097/CCM.0b013e3181c8fcd0]
14 **Ferrero-Andrés A**, Panisello-Roselló A, Serafín A, Roselló-Catafau J, Folch-Puy E. Polyethylene Glycol 35 (PEG35) Protects against Inflammation in Experimental Acute Necrotizing Pancreatitis and Associated Lung Injury. *Int J Mol Sci* 2020; **21**: 917 [PMID: 32019239 DOI: 10.3390/ijms21030917]
15 **Hyun JJ**, Lee HS. Experimental models of pancreatitis. *Clin Endosc* 2014; **47**: 212-216 [PMID: 24944983 DOI: 10.5946/ce.2014.47.3.212]
16 **Untergasser A**, Cutcutache I, Koressaar T, Ye J, Faircloth BC, Remm M, Rozen SG. Primer3--new capabilities and interfaces. *Nucleic Acids Res* 2012; **40**: e115 [PMID: 22730293 DOI: 10.1093/nar/gks596]
17 **Ding SP**, Li JC, Jin C. A mouse model of severe acute pancreatitis induced with caerulein and lipopolysaccharide. *World J Gastroenterol* 2003; **9**: 584-589 [PMID: 12632523 DOI: 10.3748/wjg.v9.i3.584]
18 **Surbatovic M**, Radakovic S. Tumor necrosis factor-α levels early in severe acute pancreatitis: is there predictive value regarding severity and outcome? *J Clin Gastroenterol* 2013; **47**: 637-643 [PMID: 23470643 DOI: 10.1097/MCG.0b013e31828a6cfc]
19 **Sendler M**, Dummer A, Weiss FU, Krüger B, Wartmann T, Scharffetter-Kochanek K, van Rooijen N, Malla SR, Aghdassi A, Halangk W, Lerch MM, Mayerle J. Tumour necrosis factor α secretion induces protease activation and acinar cell necrosis in acute experimental pancreatitis in mice. *Gut* 2013; **62**: 430-439 [PMID: 22490516 DOI: 10.1136/gutjnl-2011-300771]
20 **Sathyanarayan G**, Garg PK, Prasad H, Tandon RK. Elevated level of interleukin-6 predicts organ failure and severe disease in patients with acute pancreatitis. *J Gastroenterol Hepatol* 2007; **22**: 550-554 [PMID: 17376050 DOI: 10.1111/j.1440-1746.2006.04752.x]
21 **Pooran N**, Indaram A, Singh P, Bank S. Cytokines (IL-6, IL-8, TNF): early and reliable predictors of severe acute pancreatitis. *J Clin Gastroenterol* 2003; **37**: 263-266 [PMID: 12960727 DOI: 10.1097/00004836-200309000-00013]
22 **Silva-Vaz P**, Abrantes AM, Castelo-Branco M, Gouveia A, Botelho MF, Tralhão JG. Multifactorial Scores and Biomarkers of Prognosis of Acute Pancreatitis: Applications to Research and Practice. *Int J Mol Sci* 2020; **21**: 338 [PMID: 31947993 DOI: 10.3390/ijms21010338]
23 **Mayer J**, Rau B, Gansauge F, Beger HG. Inflammatory mediators in human acute pancreatitis: clinical and pathophysiological implications. *Gut* 2000; **47**: 546-552 [PMID: 10986216 DOI: 10.1136/gut.47.4.546]
24 **Rongione AJ**, Kusske AM, Kwan K, Ashley SW, Reber HA, McFadden DW. Interleukin 10 reduces the severity of acute pancreatitis in rats. *Gastroenterology* 1997; **112**: 960-967 [PMID: 9041259 DOI: 10.1053/gast.1997.v112.pm9041259]
25 **Cuzzocrea S**, Mazzon E, Dugo L, Serraino I, Centorrino T, Ciccolo A, Van de Loo FA, Britti D, Caputi AP, Thiemermann C. Inducible nitric oxide synthase-deficient mice exhibit resistance to the acute pancreatitis induced by cerulein. *Shock* 2002; **17**: 416-422 [PMID: 12022764 DOI: 10.1097/00024382-200205000-00013]

World Journal of Gastroenterology

Submit a Manuscript: https://www.f6publishing.com

World J Gastroenterol 2020 October 21; 26(39): 5983-5996

DOI: 10.3748/wjg.v26.i39.5983

ISSN 1007-9327 (print) ISSN 2219-2840 (online)

ORIGINAL ARTICLE

Basic Study

Identification of differentially expressed genes in ulcerative colitis and verification in a colitis mouse model by bioinformatics analyses

Lei Shi, Xiao Han, Jun-Xiang Li, Yu-Ting Liao, Fu-Shun Kou, Zhi-Bin Wang, Rui Shi, Xing-Jie Zhao, Zhong-Mei Sun, Yu Hao

ORCID number: Lei Shi 0000-0002-7925-5166; Xiao Han 0000-0003-1340-9692; Jun-Xiang Li 0000-0001-7590-9444; Yu-Ting Liao 0000-0003-1821-048X; Fu-Shun Kou 0000-0003-1841-3324; Zhi-Bin Wang 0000-0001-9274-635X; Rui Shi 0000-0002-9374-0897; Xing-Jie Zhao 0000-0002-7918-9576; Zhong-Mei Sun 0000-0001-8667-7300; Yu Hao 0000-0002-8544-5580.

Author contributions: Shi L wrote the article and Han X edited it; Liao YT, Kou FS and Sun ZM performed the animal experiments; Wang ZB, Shi R and Zhao XJ analyzed the bioinformatics data; Hao Y and Li JX conducted the study.

Supported by Chinese Medicine Inheritance and Innovation "One Hundred Million" Talent Project Qihuang Scholar (to Li JX); The National Key R&D Program of China during the 13th Five-Year Plan Period, No. 2018YFC1705405; and The 66th China Postdoctoral Science Foundation, No. 2019M660575.

Institutional review board statement: The data of ulcerative colitis we analyzed in this study were all from the National Center for Biotechnology Information-Gene Expression Omnibus

Lei Shi, Yu Hao, Department of Immunology and Microbiology, School of Life Sciences, Beijing University of Chinese Medicine, Beijing 100029, China

Xiao Han, Jun-Xiang Li, Fu-Shun Kou, Zhi-Bin Wang, Rui Shi, Xing-Jie Zhao, Zhong-Mei Sun, Gastroenterology Department, Dongfang Hospital, Beijing University of Chinese Medicine, Beijing 100078, China

Yu-Ting Liao, Department of Internal Medicine, Beijing Social Welfare Hospital, Beijing 100085, China

Corresponding author: Yu Hao, PhD, Professor, Department of Immunology and Microbiology, School of Life Sciences, Beijing University of Chinese Medicine, No. 11 North Third Ring East Road, Chaoyang District, Beijing 100029, China. yuhao64@sina.com

Abstract

BACKGROUND

Ulcerative colitis (UC) is an inflammatory bowel disease that is difficult to diagnose and treat. To date, the degree of inflammation in patients with UC has mainly been determined by measuring the levels of nonspecific indicators, such as C-reactive protein and the erythrocyte sedimentation rate, but these indicators have an unsatisfactory specificity. In this study, we performed bioinformatics analysis using data from the National Center for Biotechnology Information-Gene Expression Omnibus (NCBI-GEO) databases and verified the selected core genes in a mouse model of dextran sulfate sodium (DSS)-induced colitis.

AIM

To identify UC-related differentially expressed genes (DEGs) using a bioinformatics analysis and verify them *in vivo* and to identify novel biomarkers and the underlying mechanisms of UC.

METHODS

Two microarray datasets from the NCBI-GEO database were used, and DEGs between patients with UC and healthy controls were analyzed using GEO2R and Venn diagrams. We annotated these genes based on their functions and signaling pathways, and then protein-protein interactions (PPIs) were identified using the Search Tool for the Retrieval of Interacting Genes. The data were further analyzed with Cytoscape software and the Molecular Complex Detection (MCODE) app.

database. According to the guidelines approved by the National Center for Biotechnology Information-Gene Expression Omnibus, our study did not require the separate ethics committee approval.

Institutional animal care and use committee statement: We complied with the ethics standard for research activity established by the Animal Ethics Committee of Beijing University of Chinese Medicine in accordance with the guidelines issued by the Regulations of Beijing Laboratory Animal Management.

Conflict-of-interest statement: The authors declare that they have no conflicts of interest.

Data sharing statement: Database we used in this study can be shared from the National Center for Biotechnology Information-Gene Expression Omnibus databases.

ARRIVE guidelines statement: The authors have read the ARRIVE guidelines, and the manuscript was prepared and revised according to the ARRIVE guidelines.

Manuscript source: Unsolicited manuscript

Received: June 10, 2020
Peer-review started: June 10, 2020
First decision: August 22, 2020
Revised: August 30, 2020

The core genes were selected and a Kyoto Encyclopedia of Genes and Genomes pathway enrichment analysis was performed. Finally, colitis model mice were established by administering DSS, and the top three core genes were verified in colitis mice using real-time polymerase chain reaction (PCR).

RESULTS

One hundred and seventy-seven DEGs, 118 upregulated and 59 downregulated, were initially identified from the GEO2R analysis and predominantly participated in inflammation-related pathways. Seven clusters with close interactions in UC formed: Seventeen core genes were upregulated [*C-X-C motif chemokine ligand 13* (*CXCL13*), *C-X-C motif chemokine receptor 2* (*CXCR2*), *CXCL9*, *CXCL5*, *C-C motif chemokine ligand 18*, *interleukin 1 beta*, *matrix metallopeptidase 9*, *CXCL3*, *formyl peptide receptor 1*, *complement component 3*, *CXCL8*, *CXCL1*, *CXCL10*, *CXCL2*, *CXCL6*, *CXCL11 and hydroxycarboxylic acid receptor 3*] and one was downregulated [*neuropeptide Y receptor Y1* (*NYP1R*)] in the top cluster according to the PPI and MCODE analyses. These genes were substantially enriched in the cytokine-cytokine receptor interaction and chemokine signaling pathways. The top three core genes (*CXCL13*, *NYP1R*, and *CXCR2*) were selected and verified in a mouse model of colitis using real-time PCR Increased expression was observed compared with the control mice, but only CXCR2 expression was significantly different.

CONCLUSION

Core DEGs identified in UC are related to inflammation and immunity inflammation, indicating that these reactions are core features of the pathogenesis of UC. CXCR2 may reflect the degree of inflammation in patients with UC.

Key Words: Ulcerative colitis; Bioinformatics analysis; C-X-C motif chemokine ligand 13; Neuropeptide Y receptor Y1; C-X-C motif chemokine receptor 2; Colitis model mice

Core Tip: Two microarray datasets were used, and differentially expressed genes were analyzed. Seventeen core genes were upregulated, and one was downregulated. These genes were markedly enriched in the cytokine-cytokine receptor interaction and chemokine signaling pathways. The top three core genes [*C-X-C motif chemokine ligand 13*, *neuropeptide Y receptor Y1*, *C-X-C motif chemokine receptor 2* (*CXCR2*)] were verified in a dextran sulfate sodium-induced colitis model mice by real-time polymerase chain reaction and showed an increased expression, but only CXCR2 was statistically different. CXCR2 may represent a new biomarker to determine the degree of inflammation or a treatment target in ulcerative colitis.

Citation: Shi L, Han X, Li JX, Liao YT, Kou FS, Wang ZB, Shi R, Zhao XJ, Sun ZM, Hao Y. Identification of differentially expressed genes in ulcerative colitis and verification in a colitis mouse model by bioinformatics analyses. *World J Gastroenterol* 2020; 26(39): 5983-5996
URL: https://www.wjgnet.com/1007-9327/full/v26/i39/5983.htm
DOI: https://dx.doi.org/10.3748/wjg.v26.i39.5983

INTRODUCTION

Ulcerative colitis (UC), a nonspecific inflammatory disease that occurs in the colon or rectum, is the most common type of inflammatory bowel disease (IBD) and tends to occur in young and middle-aged people. Symptoms of UC, such as diarrhea, bloody stools with mucus-pus and abdominal pain, substantially affect quality of life[1,2]. Because UC is difficult to cure, readily relapses and has a high risk of cancer, UC has been classified as a refractory disease by the World Health Organization.

Epidemiological studies have confirmed that the annual incidence of UC worldwide is 10.5-14 cases per 100000 people, and the prevalence rate is approximately 246.7 cases

Accepted: September 16, 2020
Article in press: September 16, 2020
Published online: October 21, 2020

P-Reviewer: Ishizawa K, Li C
S-Editor: Huang P
L-Editor: Filipodia
P-Editor: Wang LL

per 100000 people[3]. Currently, the number of patients in Europe and the United States accounts for 0.5% of the global population, and the incidence and prevalence rates in urban areas have exceeded those in rural areas. Since the 1990s, the number of children who were initially treated for IBD in Western developed countries has gradually increased. In the past 20 years, the incidence and prevalence of IBD in developed countries have begun to stabilize and plateau, but in other countries an obvious increase in the incidence and prevalence still occurs, particularly in South America and East Asia[4,5]. Recently, a systematic review of 140 studies in 2018 showed that the incidence of IBD in children increased in both developed and developing countries[6].

The pathogenesis of UC is complex, and the interaction of multiple factors may lead to its occurrence. With contributions from the environment, mental factors and intestinal flora, the intestinal barrier of genetically susceptible people is destroyed, and the immune system is dysfunctional, resulting in excessively hyperactive immune reactions and inflammation[7,8]. The combination of C-reactive protein and fecal calprotectin levels may be beneficial for dynamically diagnosing and monitoring the progress of UC at present[9]. However, the limited number of significant and specific biomarkers for UC has become an increasingly prominent problem in its diagnosis and treatment.

Microarray technology reveals numerous genes that are activated in different tissues as well as their physiological and pathological statuses and has been regarded as a novel approach for clarifying the mechanisms underlying different diseases[10]. In recent years with the optimization of gene sequencing platforms, differentially expressed genes (DEGs) have been identified using bioinformatics analyses[11]. To date, several studies have reported the bioinformatics analysis of IBD using arrays or chips[12,13], but the analysis of UC is still lacking. Thus, bioinformatics methods may help us study and more clearly understand the underlying mechanisms of UC[14].

In this study, we applied two databases from Gene Expression Omnibus (GEO), GEO2R and online tools for constructing Venn diagrams to identify the DEGs, including upregulated and downregulated genes. Then, the Database for Annotation, Visualization and Integrated Discovery (DAVID) was used to analyze the DEGs based on the molecular function (MF), cellular component (CC), and biological process (BP) and different Kyoto Encyclopedia of Genes and Genomes (KEGG) pathways[11]. Third, we constructed a protein-protein interaction (PPI) network using Cytoscape and the Molecular Complex Detection (MCODE) app for further analysis. Using these methods, core genes were chosen, and the KEGG pathway enrichment analysis was repeated. Finally, we verified the top three core genes in the first cluster selected by MCODE in colon tissues from mice with dextran sulfate sodium (DSS)-induced colitis using real-time polymerase chain reaction (PCR).

MATERIALS AND METHODS

Microarray data

Microarray data were obtained from the National Center for Biotechnology Information-GEO, a free public database of microarray and gene profiles, and we obtained the gene expression profiles of GSE92415 and GSE87466 in colon mucosal tissues from patients with UC and healthy individuals. Microarray data included in GSE92415 and GSE87466 were obtained from GPL13158 Platforms (HT_HG-U133_Plus_PM] Affymetrix HT HG-U133+ PM Array Plate) and included 162 colonic mucosal tissues from patients with UC (who were treated with the anti-TNF agent golimumab and placebo) and 21 healthy colon mucosal tissues and 87 samples from patients with UC and 21 normal colon mucosal tissues, respectively.

DEG analysis

DEGs were identified between specimens from patients with UC and normal colonic mucosa using the GEO2R online tool with a $|\log FC| > 2$ and adjusted P value < 0.05. Then, the raw data in TXT format were imported into the online tool to construct a Venn diagram and identify the common DEGs among the two datasets. The DEGs with a $\log FC < 0$ were considered downregulated genes, while the DEGs with a $\log FC > 0$ were considered upregulated genes.

Gene Ontology and KEGG pathway enrichment analyses

Gene Ontology (GO) analysis is a commonly used method for identifying the biological properties of high-throughput transcriptome or genome data for genes and their RNA or protein products[15]. KEGG is a collection of databases for genomes,

diseases, biological pathways, drugs and chemical materials. DAVID is an online bioinformatics tool designed to identify a large number of gene or protein functions[10]. We used DAVID and performed a GO analysis to visualize the enrichment of DEGs in BP, MF, cellular components and KEGG pathways.

PPI network and module analysis

PPI information was evaluated using an online tool, the Search Tool for the Retrieval of Interacting Genes (STRING). A tab-separated file containing the values for the network from STRING was imported into Cytoscape (continuous mapping for columns depended on the frequency of genes; default size of the column = 30.0; upregulated genes were red and downregulated genes were blue), which was applied to detect the potential interactions between these DEGs[16]. In addition, the MCODE app in Cytoscape was used to assess the modules of the PPI network (cutoff = 2, max depth = 100, k-core = 2, node score cutoff = 0.2) and to identify the core genes in the top cluster in UC. Meanwhile, the KEGG pathway enrichment analysis of these core DEGs was repeated.

Establishment of the mouse model of colitis

We complied with the ethics standard for research activity established by the Animal Ethics Committee of Beijing University of Chinese Medicine in accordance with the guidelines issued by the Regulations of Beijing Laboratory Animal Management. Fourteen male specific-pathogen-free (SPF) C57BL/6 mice (weighing 20 ± 2 g) were procured from SPF Biological Technology Co., Ltd., Beijing, China (Certificate No. SCXK [jing] 2019-0010). They were housed in the SPF animal center of Beijing University of Chinese Medicine at a constant temperature of 20-26 °C and humidity of 50% to 60% in a light-controlled environment with a 12-h light/dark cycle. In addition, fodder and sterilized water were supplied. After adaptive feeding for 1 wk, these mice were divided into the control (n = 4) and model (n = 10) groups using the random number table method. Mice in the model group drank 3.5% (weight/volume) DSS (average molecular weight 36000-50000, MP Biomedicals) for 7 consecutive days[17].

Histological analysis of colon tissues from the colitis model mice

On the 7th d of the experiment, all the mice were fasted for 24 h. On the 8th d, mice were anesthetized by ether inhalation until the superficial reflex disappeared, and the mice were sacrificed by cervical spondylolisthesis. After disinfecting and preparing the skin, the abdomen was incised to separate the colon tissue. Specimens of colon tissues (three 1 cm pieces) from each mouse were fixed with a 10% neutral formaldehyde solution for at least 24 h. The lesion score was judged by the histological criterion after hematoxylin-eosin staining of 4 μm thick sections: 0, no signs of inflammation; 1, a low level of leukocyte infiltration (10-30 leukocytes per high-power field); 2, a moderate level of leukocyte infiltration (31-70 leukocytes per high-power field); 3, a high level of leukocyte infiltration (> 71 leukocytes per high-power field), high vascular density and thickening of the bowel wall; and 4, transmural infiltrations, loss of goblet cells, high vascular density, strong bowel wall thickening, ulcerations and cryptic abscesses[18].

Verification of top three core genes in the colitis model mice using real-time PCR

The other tissues were placed in cryotubes, frozen in liquid nitrogen overnight and stored at -80 °C. Total RNA was extracted from the colon tissues using TRIzol reagent (Invitrogen, United States). Specific primers were used to amplify the core genes (Table 1), and the expression of each gene was normalized to *β-actin* with the standard curve method. Reverse transcription was performed at 42 °C for 60 min, and reverse transcriptase was inactivated at 70 °C for 15 min. The relative quantitative analysis was performed using the $2^{-\Delta\Delta CT}$ approach.

Statistical analysis

The histological lesion score and relative expression levels obtained using real-time PCR were analyzed with SPSS (version 22.0, IBM, Corp., Armonk, NY, United States). Data were distributed normally, and the two groups were compared with an independent-sample t test. A P value < 0.05 indicated a statistically significant difference.

Table 1 Sequences of primers

Gene	Sequence, 5' to 3'
β-actin	Forward: GAGATTACTGCTCTGGCTCCTA
	Reverse: GGACTCATCGTACTCCTGCTTG
CXCL13	Forward: CCCAACCCACATCCTTGTTCCTT
	Reverse: CTGAAGTCCATCTCGCAAACCTCT
NPY1R	Forward: CCAGTGAGACCAAGCGAATCAACA
	Reverse: GCGGTGAGGTGACAGAGCAGAA
CXCR2	Forward: ATGGTGGAACTTGTGGCTCTAGC
	Reverse: CCATTCCTGGTCCTGGCATTCC

CXCL13: *C-X-C motif chemokine ligand 13*; *NPY1R*: *Neuropeptide Y receptor Y1*; *CXCR2*: *C-X-C motif chemokine receptor 2*.

RESULTS

Identification of DEGs

One hundred and ninety-six DEGs were identified in the GSE92415 database, including 130 upregulated and 66 downregulated genes. One hundred and eighty-four DEGs were identified in the GSE87466 database, including 122 upregulated and 62 downregulated genes. Among the two databases, 177 genes (118 upregulated and 59 downregulated) overlapped (Figure 1A and 1B).

Functional enrichment of DEGs in the GO analysis

Three categories of DEGs, MF, BP and CC, were classified by performing a GO analysis. Among these GO functions, extracellular region (GO: 0005576), defense response (GO: 0006952), extracellular region part (GO: 0044421), response to wounding (GO: 0009611), extracellular space (GO: 0005615) and inflammatory response (GO: 0006954) were the top six terms associated with UC with more than 30 genes identified in each category (Figure 1C). Upregulated genes were mainly enriched in defense response, inflammatory response, response to wounding, extracellular region, extracellular region part, extracellular space, cytokine activity, chemokine activity and chemokine receptor binding and were the top three enriched terms, depending on the P value of the respective categories (Table 2, $P < 0.05$). Downregulated genes were mainly enriched in transmembrane transport, carboxylic acid transport, organic acid transport, cell fraction, membrane fraction, insoluble fraction, symporter activity, xenobiotic-transporting ATPase activity and multidrug transporter activity and were the top three enriched terms, based on the P value of the respective categories (Table 3, $P < 0.05$). The KEGG pathway enrichment analysis suggested that DEGs predominantly participated in inflammation-related pathways, including the chemokine signaling pathway, cytokine-cytokine receptor interaction and complement and coagulation cascades (Table 4, $P < 0.05$).

Analysis of the PPI network using Cytoscape

One hundred and seventy-seven DEGs were entered into the PPI network using the Search Tool for the Retrieval of Interacting Genes, including 130 nodes and 639 edges. The thickness of the edges was adjusted based on the level of the combined score. The larger the area of a protein node, the more protein nodes that interacted with it. Upregulated genes were shown in red, and downregulated genes were shown in blue (Figure 2A). Then, we applied the MCODE app for further analysis and identified seven clusters with close interactions in patients with UC. Seventeen core genes were upregulated [*C-X-C motif chemokine ligand 13* (*CXCL13*), *C-X-C motif chemokine receptor 2* (*CXCR2*), *CXCL9*, *CXCL5*, *C-C motif chemokine ligand 18* (*CCL18*), *interleukin 1 beta* (*IL1B*), *matrix metallopeptidase 9* (*MMP9*), *CXCL3*, *formyl peptide receptor 1* (*FPR1*), *complement component 3* (*C3*), *CXCL8*, *CXCL1*, *CXCL10*, *CXCL2*, *CXCL6*, *CXCL11* and *hydroxycarboxylic acid receptor 3* (*HCAR3*)], and one gene was downregulated [*neuropeptide Y receptor Y1* (*NPY1R*)] in the first significant cluster (Figure 2B).

Table 2 Top three enriched terms in the respective categories of upregulated differentially expressed genes identified in ulcerative colitis ($P < 0.05$)

Category	Term	Count	Genes
BP	Defense response (GO: 0006952)	40	*CXCL1, KYNU, S100A8, FGR, C3, CXCL3, CXCL2, S100A9, CXCL9, CXCR2, CXCL6, DEFB4A, CXCL11, CXCL10, REG3A, SERPINA3, CSF3R, VNN1, IL1B, LTF, SERPINA1, CFI, SPP1, SELP, CR1, PDPN, CFB, IL1RN, C4BPB, IDO1, CCL18, S100A12, LILRB2, TNFAIP6, PROK2, DEFA6, CXCL13, DEFA5, PLA2G2D, DMBT1.*
BP	Inflammatory response (GO: 0006954)	31	*CXCL1, S100A8, C3, CXCL3, CXCL2, S100A9, CXCL9, CXCR2, CXCL6, CXCL11, CXCL10, REG3A, SERPINA3, VNN1, IL1B, SERPINA1, CFI, SPP1, SELP, CR1, PDPN, CFB, IL1RN, C4BPB, IDO1, CCL18, S100A12, TNFAIP6, PROK2, CXCL13, PLA2G2D.*
BP	Response to wounding (GO: 0009611)	33	*CXCL1, S100A8, C3, TNC, CXCL3, CXCL2, S100A9, CXCL9, CXCR2, CXCL6, CXCL11, CDH3, CXCL10, REG3A, SERPINA3, VNN1, IL1B, SERPINA1, CFI, SPP1, SELP, CR1, PDPN, CFB, IL1RN, C4BPB, IDO1, CCL18, S100A12, TNFAIP6, PROK2, CXCL13, PLA2G2D.*
CC	Extracellular region (GO: 0005576)	55	*REG4, MMP9, MMP7, CXCL11, MMP3, MMP1, CXCL10, REG3A, SERPINA3, CSF3R, IL1B, LTF, SERPINA1, KLK10, CFI, FCGR3B, CYR61, IL13RA2, EGFL6, IL24, TCN1, MMP12, MMP10, PROK2, GZMK, DEFA6, SERPINB5, DEFA5, STC1, PLA2G2D, CXCL1, CXCL5, C3, CXCL3, TNC, CXCL2, CXCL9, CXCL6, DEFB4A, GREM1, TIMP1, THBS2, OLFM1, SPP1, SELP, CFB, IL1RN, CHI3L1, CHI3L2, C4BPB, CCL18, LCN2, CXCL13, PI3, DMBT1.*
CC	Extracellular region part (GO: 0044421)	38	*CXCL1, CXCL5, C3, MMP9, TNC, CXCL3, CXCL2, MMP7, CXCL9, CXCL6, CXCL11, MMP3, GREM1, MMP1, CXCL10, TIMP1, REG3A, IL1B, SERPINA1, CFI, OLFM1, SPP1, IL13RA2, SELP, EGFL6, IL1RN, CHI3L1, CHI3L2, IL24, CCL18, MMP12, MMP10, SERPINB5, DEFA6, CXCL13, DEFA5, PI3, STC1.*
CC	Extracellular space (GO: 0005615)	33	*CXCL1, CXCL5, C3, MMP9, CXCL3, CXCL2, MMP7, CXCL9, CXCL6, GREM1, CXCL11, MMP3, CXCL10, REG3A, IL1B, SERPINA1, CFI, OLFM1, IL13RA2, SPP1, SELP, EGFL6, IL1RN, CHI3L1, CHI3L2, IL24, CCL18, MMP10, SERPINB5, DEFA6, CXCL13, DEFA5, STC1.*
MF	Cytokine activity (GO: 0005125)	16	*CXCL1, NAMPT, CXCL5, CXCL3, IL1RN, CXCL2, CXCL9, CXCL6, IL24, GREM1, CXCL11, CCL18, CXCL10, CXCL13, IL1B, SPP1.*
MF	Chemokine activity (GO: 0008009)	10	*CXCL1, CXCL5, CXCL13, CXCL3, CXCL2, CXCL9, CXCL6, CXCL11, CCL18, CXCL10.*
MF	Chemokine receptor binding (GO: 0042379)	10	*CXCL1, CXCL5, CXCL13, CXCL3, CXCL2, CXCL9, CXCL6, CXCL11, CCL18, CXCL10.*

MF: Molecular function; CC: Cellular component; BP: Biological process.

Repeated KEGG pathway enrichment analysis of 18 core genes

The KEGG pathway enrichment analysis was repeated using the DAVID GO analysis to identify the pathways in which these 18 core DEGs in the top cluster (18 nodes, 142 edges, and a score of 16.706) were involved ($P < 0.05$). These DEGs were markedly enriched in the cytokine-cytokine receptor interaction and chemokine signaling pathways (Table 5).

Verification of the top three genes in the colitis model mice

Finally, we verified the top three genes (*CXCL13*, *NPY1R* and *CXCR2*) among the 18 core DEGs in the colitis model mice. Four mice in the model group were sacrificed during the experimental period because of the severity of disease, and the colon tissues of all the remaining mice (control: $n = 4$; colitis model: $n = 6$) were observed under a microscope. The normal four-layer structure of intestinal tissues, goblet cells and crypts disappeared, and inflammatory cells had infiltrated the submucosa in the

Table 3 Top three enriched terms in the respective categories of downregulated differentially expressed genes identified in ulcerative colitis ($P < 0.05$)

Category	Term	Count	Genes
BP	Transmembrane transport (GO: 0055085)	9	*TRPM6, SLC23A1, SLC16A1, SLC25A34, SLC17A4, ABCB1, AQP7, SLC30A10, SLC26A2.*
BP	Carboxylic acid transport (GO: 0046942)	5	*SLC38A4, SLC23A1, SLC16A1, AQP8, SLC3A1.*
BP	Organic acid transport (GO: 0015849)	5	*SLC38A4, SLC23A1, SLC16A1, AQP8, SLC3A1.*
CC	Cell fraction (GO: 0000267)	12	*HSD3B2, SLC23A1, SLC16A1, AQP8, SLC17A4, CYP2B6, MEP1B, ABCB1, ANPEP, SLC3A1, SLC26A2, PCK1.*
CC	Membrane fraction (GO: 0005624)	10	*HSD3B2, SLC23A1, SLC16A1, AQP8, SLC17A4, CYP2B6, MEP1B, ABCB1, SLC3A1, SLC26A2.*
CC	Insoluble fraction (GO: 0005626)	10	*HSD3B2, SLC23A1, SLC16A1, AQP8, SLC17A4, CYP2B6, MEP1B, ABCB1, SLC3A1, SLC26A2.*
MF	Symporter activity (GO: 0015293)	4	*SLC38A4, SLC23A1, SLC16A1, SLC17A4.*
MF	Xenobiotic-transporting ATPase activity (GO: 0008559)	2	*ABCB1, ABCG2.*
MF	Multidrug transporter activity (GO: 0015239)	2	*ABCB1, ABCG2.*

MF: Molecular function; CC: Cellular component; BP: Biological process.

Table 4 Enriched terms in the Kyoto Encyclopedia of Genes and Genomes pathways for differentially expressed genes identified in ulcerative colitis ($P < 0.05$)

Pathway ID	Term	Genes
hsa04062	Chemokine signaling pathway	*CXCL1, FGR, CXCL5, CXCL3, CXCL2, CXCL9, CXCR2, CXCL6, CXCL11, CCL18, CXCL10, CXCL13, JAK3.*
hsa04060	Cytokine-cytokine receptor interaction	*CXCL1, CXCL5, CXCL3, CXCL2, CXCL9, CXCR2, CXCL6, IL24, CXCL11, CCL18, CXCL10, CXCL13, CSF3R, IL1B.*
hsa04610	Complement and coagulation cascades	*CR1, C3, CFB, C4BPB, SERPINA1, CFI.*
hsa04514	Cell adhesion molecules	*SELP, SELL, CD274, CTLA4, CLDN2, CDH3.*
hsa00830	Retinol metabolism	*CYP2B6, ADH1C, UGT2A3.*
hsa00980	Metabolism of xenobiotics by cytochrome P450	*CYP2B6, ADH1C, UGT2A3.*
hsa04620	Toll-like receptor signaling pathway	*CXCL9, IL1B, CXCL11, SPP1, CXCL10.*
hsa00982	Drug metabolism	*CYP2B6, ADH1C, UGT2A3.*
hsa03320	PPAR signaling pathway	*HMGCS2, AQP7, PCK1.*

PPAR: Peroxisome proliferator-activated receptor.

model group compared with the control group (Figure 3A-D). Histological lesions indicated the successful establishment of the colitis model (Figure 3E). The *CXCL13* and *CXCR2* mRNAs were expressed at higher levels in the colon tissues from the colitis model mice than in the mice from the control group (Figure 4), and the difference in CXCR2 expression was significant ($P < 0.01$). These manifestations were consistent with the results of the bioinformatics analysis in the present study. Interestingly, higher expression of the *NPY1R* mRNA was also observed in the colitis model mice (Figure 4), which differed from our bioinformatics results.

DISCUSSION

The incidence of UC in China and other Asian countries is gradually increasing[19], but due to the complicated pathogenesis, accurate molecular biomarkers for diagnosing UC are still lacking. In the past, biomarkers such as the C-reactive protein level and

Table 5 Repeated Kyoto Encyclopedia of Genes and Genomes pathway enrichment analysis of 18 core genes in the first cluster ($P < 0.05$)

Category	Term	Count, %	Genes
KEGG pathway	hsa04060, cytokine-cytokine receptor interaction.	12, 6.06	*CXCL1, CXCL5, CXCL13, CXCL3, CXCL2, CXCL9, IL1B, CXCR2, CXCL6, CXCL11, CCL18, CXCL10.*
KEGG pathway	hsa04062, chemokine signaling pathway.	11, 5.56	*CXCL1, CXCL5, CXCL13, CXCL3, CXCL2, CXCL9, CXCR2, CXCL6, CXCL11, CCL18, CXCL10.*
KEGG pathway	hsa04620, toll-like receptor signaling pathway.	4, 2.02	*CXCL9, IL1B, CXCL11, CXCL10.*
KEGG pathway	hsa04621, NOD-like receptor signaling pathway.	3, 1.52	*CXCL1, CXCL2, IL1B.*

KEGG: Kyoto Encyclopedia of Genes and Genomes.

erythrocyte sedimentation rate were used to judge the degree of inflammation in patients with UC but are generally nonspecific[20], which greatly complicated the determination of the clinical diagnosis, recurrence and prognosis. The lack of biomarkers has increased the medical burden and physical and psychological discomfort of patients and accelerated the waste of public social health resources. Therefore, the identification and excavation of relatively specific molecular biomarkers is a bottleneck problem that must be solved in the diagnosis of UC[21]. Focusing on methods to solve this problem, our study chose the GEO database for an in-depth analysis of biological information.

GEO is an international public repository for high-throughput microarray and next-generation sequencing functional genomic datasets submitted by the research community[22]. We selected two microarray datasets from the GEO database, combined GEO2R and Venn diagram analyses and initially identified 177 DEGs, including 118 upregulated and 59 downregulated genes. Next, we annotated these genes by function and signaling pathways and found that they were mainly related to inflammation, such as chemokines, cytokine receptors and complement proteins. The PPI analysis helped us identify 18 core genes based on their functional annotations, and cytokine-cytokine receptor interactions and chemokine signaling pathways were maximally enriched.

We established colitis model mice and verified the transcript levels of the top three genes in the first cluster in colon tissues using real-time PCR to clarify the expression of these core genes and their main pathophysiological functions. The expression of the *CXCL13* and *CXCR2* mRNAs, particularly the *CXCR2* mRNA, was increased in the colitis model mice, consistent with our bioinformatics analysis.

Chemokines and cytokines play pivotal roles in regulating mucosal inflammation and the immune system by promoting neutrophil migration to sites of inflammation, ultimately leading to tissue damage and destruction[23,24]. Carlsen *et al*[25] reported the expression of CXCL13 in both healthy individuals and patients with UC, in addition to reports in rodents from published studies; however, differences in the expression of CXCL13 between patients with UC and healthy individuals were unclear. Singh *et al*[23] reported significantly increased expression of CXCL13 in patients with IBD, including patients with UC and Crohn's disease, compared to healthy controls.

On the other hand, CXCR2 has been reported to regulate the migration and recruitment of neutrophils to the site of inflammation[26]. A review also suggested that in addition to calprotectin, CXCR2, a neutrophil-related protein, may have potential roles in diagnosis and treatment[27]. As shown in the study by Farooq *et al*[28], CXCR2-positive mice have more severe symptoms, such as the infiltration of polymorphonuclear neutrophils(PMNs), than CXCR2-deficient mice with DSS-induced colitis. The mechanism of increased CXCR2 expression in colitis has not been conclusively determined, as the infiltration of increased numbers of PMNs in the mucosa or submucosa is a feature of DSS-induced colitis. CXCR2 functions as a PMNchemokine receptor, which would lead to a significantly higher level in individuals with colitis. Our study verified this hypothesis by showing neutrophil infiltration and a high level of the *CXCR2* mRNA.

Notably, the expression of the *NPY1R* mRNA in the colitis model mice differed from our bioinformatics results. NPY is a 36-amino acid peptide with a wide distribution in the central and peripheral nervous system[29] that evokes numerous physiological

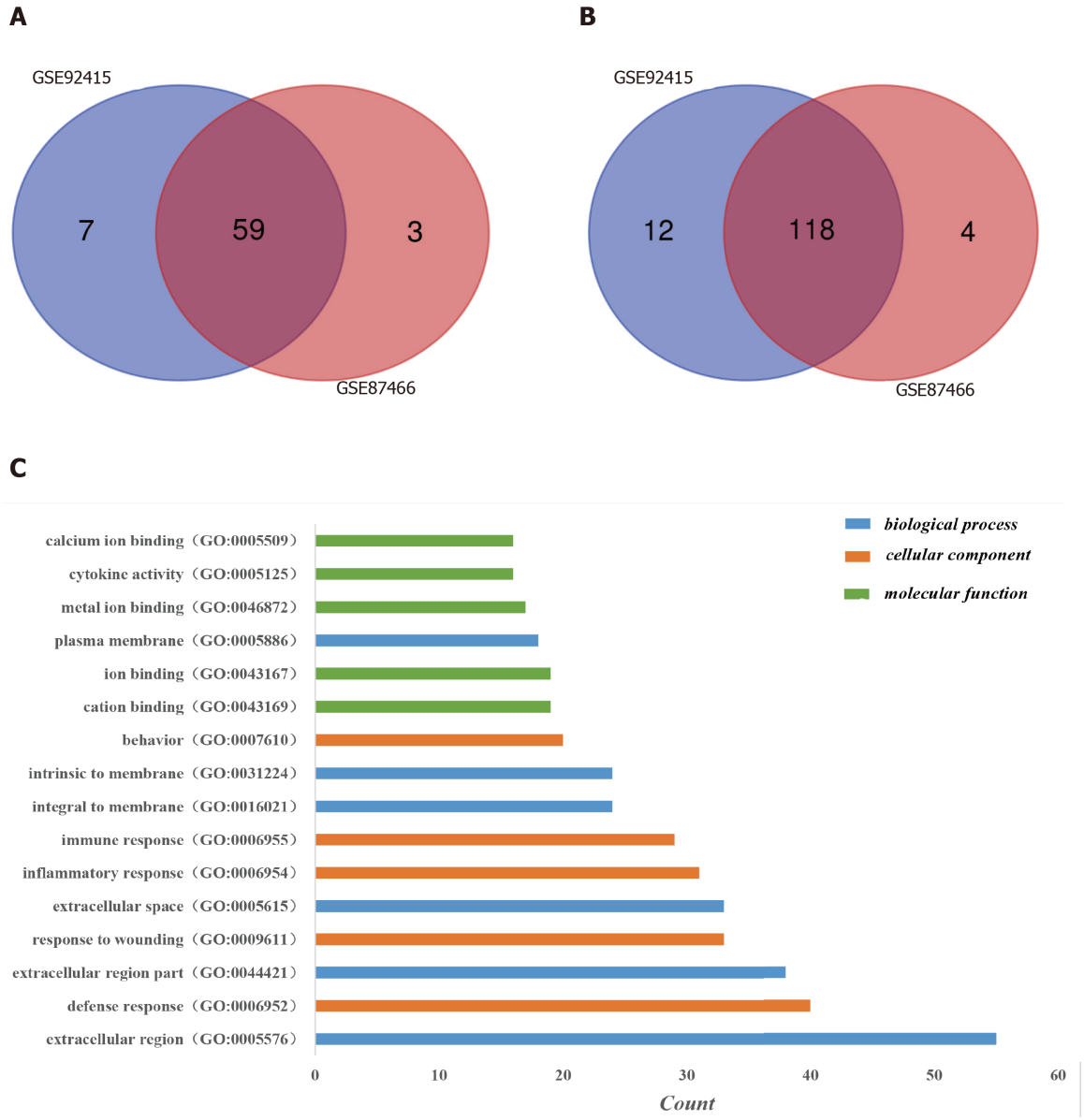

Figure 1 Identification of differentially expressed genes in the two databases (GSE92415 and GSE87466) and Gene Ontology analysis of differentially expressed genes in ulcerative colitis. A: Upregulated differentially expressed genes (DEGs); B: Downregulated DEGs. DEGs were identified with a *t*-test, and statistically significant DEGs were defined by the GEO2R online tool with a |logFC| > 2 and adjusted *P* value < 0.05; C: The Gene Ontology analysis classified the DEGs into three groups: Molecular function, biological process and cellular component. Terms were selected with > 15 genes and arrayed in ascending order from top to bottom according to the count. GO: Gene Ontology.

responses by activating different receptors (Y1, Y2, Y3)[30]. NPY is considered the most potent orexigenic neuropeptide and may be involved in the stress response, anxiety and mood-related disorders as well as the regulation of the immune system and cancer[31].

NPY1R expression was decreased in patients with UC based on the results of the bioinformatics analysis; however, its expression was increased in the colitis model mice as evidenced by real-time PCR, which might be related to the four aspects described below. First, our bioinformatics results were derived from human colon specimens, which were fundamentally heterologous compared to the mice. Second, microarray data were obtained from the human colonic mucosa, while RT-PCR was performed on mouse colon tissues, which contained the mucosa, submucosa, muscle layer and subserosa. Thus, differences in expression were observed between the bioinformatics results and *in vivo* analysis. Third, because of the current shortage of microarrays containing samples from patients with UC in the same platforms, we chose the GSE92415 microarray dataset, including patients with UC who were treated with a TNF-α inhibitor and placebos, and thus the result potentially did not accurately reflect the detailed scientific features of UC. Additionally, a 3.5% DSS solution was

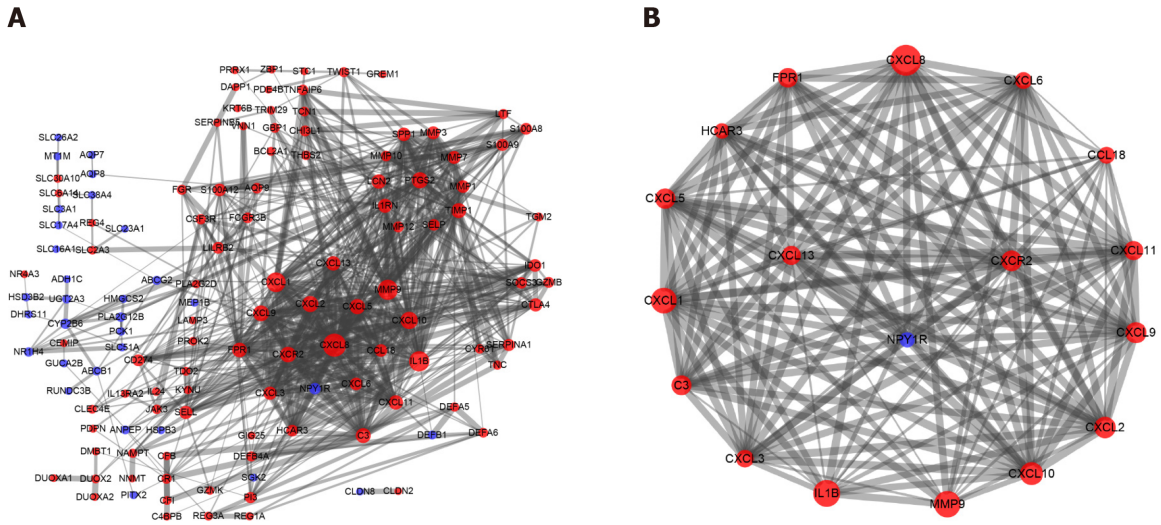

Figure 2 Protein-protein interactions of differentially expressed genes and the most significant module cluster identified by Molecular Complex Detection in the protein-protein interaction network of ulcerative colitis. A: Protein-protein interaction network of differentially expressed genes determined using Cytoscape. One hundred and seventy-seven differentially expressed genes from the Search Tool for the Retrieval of Interacting Genes online database were screened using Cytoscape, including 130 nodes and 639 edges. Upregulated genes were shown in red, and downregulated genes were shown in blue; B: The most significant cluster was analyzed with the Molecular Complex Detection app in Cytoscape. Seventeen core genes were upregulated, and one gene was downregulated; a larger node indicated more interactions with a gene or a protein.

used to establish the colitis model and combined with the histological lesions, the model was much more severe. Further studies are needed to confirm whether dysplasia of the intestinal epithelium occurred, and the NPY/NPY1R system was activated.

CONCLUSION

In conclusion, the core DEGs identified in patients with UC were *CXCL13*, *NPY1R*, *CXCR2*, *CXCL9*, *CXCL5*, *CCL18*, *IL1B*, *MMP9*, *CXCL3*, *formyl peptide receptor 1*, *C3*, *CXCL8*, *CXCL1*, *CXCL10*, *CXCL2*, *CXCL6*, *CXCL11* and *HCAR3*. These DEGs are related to inflammation and immune-inflammatory reactions, indicating that inflammation and abnormal activation of the immune system may represent the core features of the pathogenesis of UC. Based on the current data, we propose that CXCR2 may represent a new biomarker for the degree of inflammation or a treatment target, and our study may provide new insights into the diagnosis and treatment of UC.

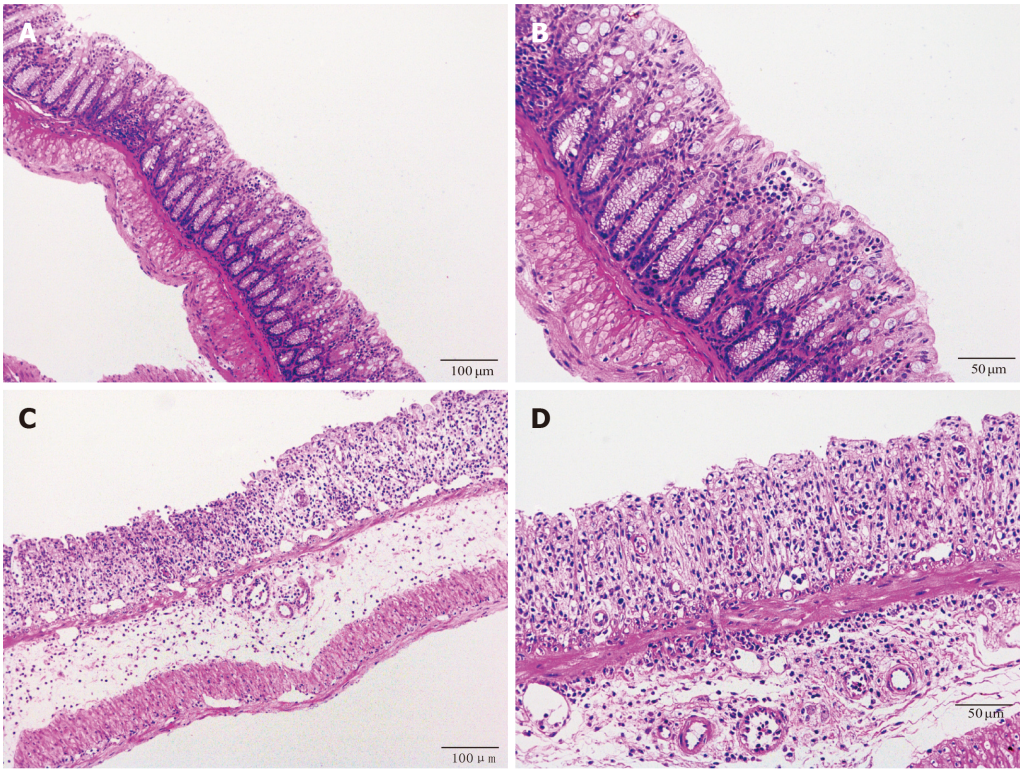

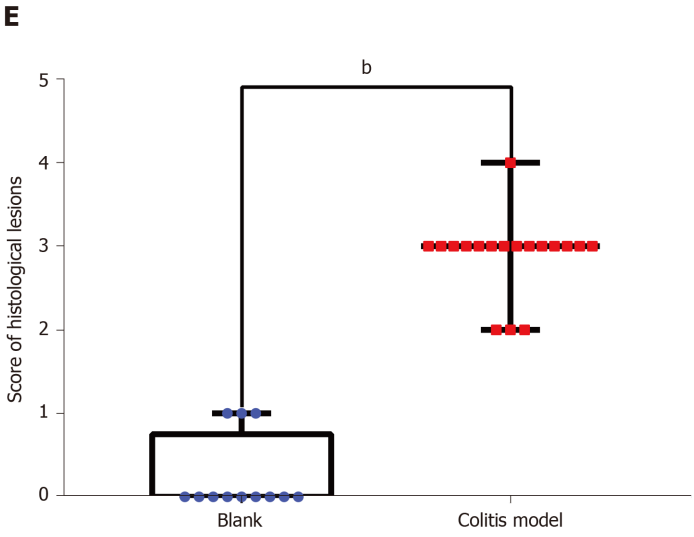

Figure 3 Hematoxylin-eosin staining and histological lesion score of colon tissues. Hematoxylin-eosin staining of colon tissues from the control and dextran sulfate sodium-induced colitis model mice. A: Control mice (× 100); B: Control mice (× 200); C: Colitis mice (× 100); D: Colitis mice (× 200); E: Histological lesion scores of colon tissues. Numerous neutrophils infiltrated and the crypts, goblet cells and normal four-layer structure of colon disappeared in the colitis model mice. Compared to the score of the control group (n = 4, 12 pieces), the score of the model group (n = 6, 18 pieces) increased significantly (P < 0.01).

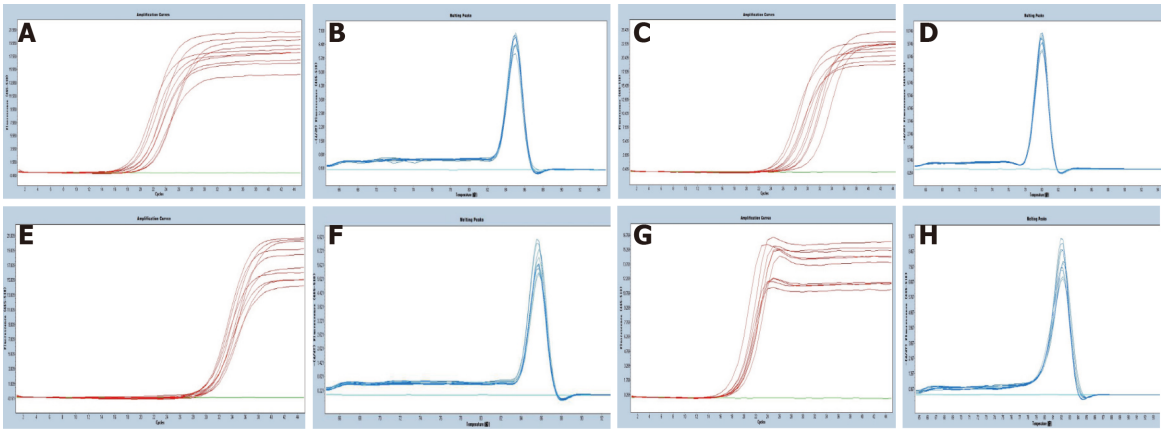

I

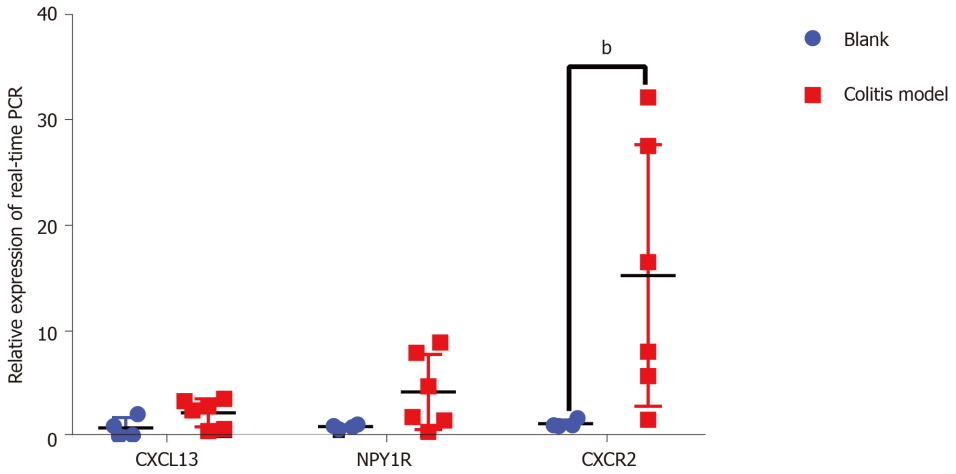

Figure 4 Real-time polymerase chain reaction of the top three core genes from the first cluster in colon tissues from the colitis model and control mice. A, C, E, and G: Amplification curves for *β-actin*, *C-X-C motif chemokine ligand 13*, *neuropeptide Y receptor Y1* and *C-X-C motif chemokine receptor 2* (*CXCR2*); B, D, F and H: Melting peaks for *β-actin*, *C-X-C motif chemokine ligand 13*, *neuropeptide Y receptor Y1* and *CXCR2*; I: Relative expression obtained using real-time polymerase chain reaction. *C-X-C motif chemokine ligand 13*, *neuropeptide Y receptor Y1* and *CXCR2* expression, particularly *CXCR2* expression ($P < 0.01$), increased in the colitis model mice. The other two genes were expressed at higher levels in the colitis mice than in the control mice, but the difference was not significant. CXCL13: *C-X-C motif chemokine ligand 13*; NPY1R: *Neuropeptide Y receptor Y1*; CXCR2: *C-X-C motif chemokine receptor 2*.

ARTICLE HIGHLIGHTS

Research background

Ulcerative colitis (UC) tends to occur in young and middle-aged people. It substantially affects the patient's quality of life because it is difficult to cure, readily relapses and poses a high risk of colon cancer. However, the pathogenesis of UC is complex and multifaceted, and specific biomarkers for UC are currently unavailable.

Research motivation

In recent years, with the optimization of gene sequencing platforms, differentially expressed genes (DEGs) have been identified through bioinformatics analyses by comparing microarrays. To date, several studies have reported the results of bioinformatics analyses of samples from patients with inflammatory bowel disease using arrays or chips, but the analysis of patients with UC is still lacking. The specific molecules or biomarkers of UC are insufficient. Thus, we will apply bioinformatics methods to more clearly elucidate the underlying biomarkers and mechanisms of UC.

Research objectives

To identify UC-related DEGs by performing a bioinformatics analysis and verify them *in vivo* and to identify novel biomarkers and the underlying mechanisms of UC.

Research methods

Two microarray datasets from the National Center for Biotechnology Information-Gene Expression Omnibus database were used, and DEGs were analyzed using GEO2R and Venn diagrams. We annotated these genes based on functions and signaling pathways. Then protein-protein interaction (PPI) were constructed using the Search Tool for the Retrieval of Interacting Genes. The data were further analyzed with Cytoscape software and the Molecular Complex Detection (MCODE) app. The core genes were selected, and the Kyoto Encyclopedia of Genes and Genomes pathway enrichment analysis was repeated. Finally, colitis model mice were established by administering dextran sulfate sodium, and the top three core genes were verified in colitis mice using real-time polymerase chain reaction.

Research results

One hundred and seventy-seven DEGs (118 upregulated genes and 59 downregulated genes) predominantly participated in inflammation-related pathways. Seventeen core genes were upregulated, and one gene was downregulated in the first cluster according to the PPI and MCODE analyses in Cytoscape. These genes were markedly enriched in the cytokine-cytokine receptor interaction and chemokine signaling pathways. The top three core genes showed increased expression compared with the control mice, but only the difference in C-X-C motif chemokine receptor 2 (CXCR2) expression was statistically significant. CXCR2 may reflect the degree of inflammation in patients with UC and serve as an underlying treatment target.

Research conclusions

Core DEGs identified in patients with UC are related to inflammation and immune inflammatory reactions, indicating that these reactions are core features of the pathogenesis of UC. CXCR2 may reflect the degree of inflammation in patients with UC.

Research perspectives

CXCR2 may represent a new biomarker to determine the degree of inflammation or a treatment target in UC. In the future, the combination of CXCR2 with other biomarkers will potentially improve the ability to diagnose and dynamically monitor UC.

REFERENCES

1 **da Silva BC**, Lyra AC, Rocha R, Santana GO. Epidemiology, demographic characteristics and prognostic predictors of ulcerative colitis. *World J Gastroenterol* 2014; **20**: 9458-9467 [PMID: 25071340 DOI: 10.3748/wjg.v20.i28.9458]

2 **Yu YR**, Rodriguez JR. Clinical presentation of Crohn's, ulcerative colitis, and indeterminate colitis: Symptoms, extraintestinal manifestations, and disease phenotypes. *Semin Pediatr Surg* 2017; **26**: 349-355 [PMID: 29126502 DOI: 10.1053/j.sempedsurg.2017.10.003]

3 **Shivashankar R**, Tremaine WJ, Harmsen WS, Loftus EV Jr. Incidence and Prevalence of Crohn's Disease and Ulcerative Colitis in Olmsted County, Minnesota From 1970 Through 2010. *Clin Gastroenterol Hepatol* 2017; **15**: 857-863 [PMID: 27856364 DOI: 10.1016/j.cgh.2016.10.039]

4 **Ng SC**, Shi HY, Hamidi N, Underwood FE, Tang W, Benchimol EI, Panaccione R, Ghosh S, Wu JCY, Chan FKL, Sung JJY, Kaplan GG. Worldwide incidence and prevalence of inflammatory bowel disease in the 21st century: a systematic review of population-based studies. *Lancet* 2018; **390**: 2769-2778 [PMID: 29050646 DOI: 10.1016/S0140-6736(17)32448-0]

5 **Torres J**, Mehandru S, Colombel JF, Peyrin-Biroulet L. Crohn's disease. *Lancet* 2017; **389**: 1741-1755 [PMID: 27914655 DOI: 10.1016/S0140-6736(16)31711-1]

6 **Sýkora J**, Pomahačová R, Kreslová M, Cvalínová D, Štych P, Schwarz J. Current global trends in the incidence of pediatric-onset inflammatory bowel disease. *World J Gastroenterol* 2018; **24**: 2741-2763 [PMID: 29991879 DOI: 10.3748/wjg.v24.i25.2741]

7 **Ungaro R**, Mehandru S, Allen PB, Peyrin-Biroulet L, Colombel JF. Ulcerative colitis. *Lancet* 2017; **389**: 1756-1770 [PMID: 27914657 DOI: 10.1016/S0140-6736(16)32126-2]

8 **Parikh K**, Antanaviciute A, Fawkner-Corbett D, Jagielowicz M, Aulicino A, Lagerholm C, Davis S, Kinchen J, Chen HH, Alham NK, Ashley N, Johnson E, Hublitz P, Bao L, Lukomska J, Andev RS, Björklund E, Kessler BM, Fischer R, Goldin R, Koohy H, Simmons A. Colonic epithelial cell diversity in health and inflammatory bowel disease. *Nature* 2019; **567**: 49-55 [PMID: 30814735 DOI: 10.1038/s41586-019-0992-y]

9 **Brookes MJ**, Whitehead S, Gaya DR, Hawthorne AB. Practical guidance on the use of faecal calprotectin. *Frontline Gastroenterol* 2018; **9**: 87-91 [PMID: 29588834 DOI: 10.1136/flgastro-2016-100762]

10 **Sobek J**, Bartscherer K, Jacob A, Hoheisel JD, Angenendt P. Microarray technology as a universal tool for high-throughput analysis of biological systems. *Comb Chem High Throughput Screen* 2006; **9**: 365-380

[PMID: 16787150 DOI: 10.2174/138620706777452429]
11 **Liang Y**, Zhang C, Dai DQ. Identification of differentially expressed genes regulated by methylation in colon cancer based on bioinformatics analysis. *World J Gastroenterol* 2019; **25**: 3392-3407 [PMID: 31341364 DOI: 10.3748/wjg.v25.i26.3392]
12 **Di Narzo AF**, Telesco SE, Brodmerkel C, Argmann C, Peters LA, Li K, Kidd B, Dudley J, Cho J, Schadt EE, Kasarskis A, Dobrin R, Hao K. High-Throughput Characterization of Blood Serum Proteomics of IBD Patients with Respect to Aging and Genetic Factors. *PLoS Genet* 2017; **13**: e1006565 [PMID: 28129359 DOI: 10.1371/journal.pgen.1006565]
13 **Lee HS**, Cleynen I. Molecular Profiling of Inflammatory Bowel Disease: Is It Ready for Use in Clinical Decision-Making? *Cells* 2019; **8** [PMID: 31167397 DOI: 10.3390/cells8060535]
14 **Feng H**, Gu ZY, Li Q, Liu QH, Yang XY, Zhang JJ. Identification of significant genes with poor prognosis in ovarian cancer *via* bioinformatical analysis. *J Ovarian Res* 2019; **12**: 35 [PMID: 31010415 DOI: 10.1186/s13048-019-0508-2]
15 **Dalmer TRA**, Clugston RD. Gene ontology enrichment analysis of congenital diaphragmatic hernia-associated genes. *Pediatr Res* 2019; **85**: 13-19 [PMID: 30287891 DOI: 10.1038/s41390-018-0192-8]
16 **Treister A**, Pico AR. Identifier Mapping in Cytoscape. *F1000Res* 2018; **7**: 725 [PMID: 30079244 DOI: 10.12688/f1000research.14807.2]
17 **Zhang X**, Wang Y, Ma Z, Liang Q, Tang X, Hu D, Tan H, Xiao C, Gao Y. Tanshinone IIA ameliorates dextran sulfate sodium-induced inflammatory bowel disease *via* the pregnane X receptor. *Drug Des Devel Ther* 2015; **9**: 6343-6362 [PMID: 26674743 DOI: 10.2147/DDDT.S79388]
18 **Kühl AA**, Pawlowski NN, Grollich K, Loddenkemper C, Zeitz M, Hoffmann JC. Aggravation of intestinal inflammation by depletion/deficiency of gammadelta T cells in different types of IBD animal models. *J Leukoc Biol* 2007; **81**: 168-175 [PMID: 17041003 DOI: 10.1189/jlb.1105696]
19 **Molodecky NA**, Soon IS, Rabi DM, Ghali WA, Ferris M, Chernoff G, Benchimol EI, Panaccione R, Ghosh S, Barkema HW, Kaplan GG. Increasing incidence and prevalence of the inflammatory bowel diseases with time, based on systematic review. *Gastroenterology* 2012; **142**: 46-54.e42; quiz e30 [PMID: 22001864 DOI: 10.1053/j.gastro.2011.10.001]
20 **Walsh AJ**, Bryant RV, Travis SP. Current best practice for disease activity assessment in IBD. *Nat Rev Gastroenterol Hepatol* 2016; **13**: 567-579 [PMID: 27580684 DOI: 10.1038/nrgastro.2016.128]
21 **Feigenbaum LZ**, Lee D, Ho J. Routine testing of folate levels in geriatric assessment for dementia. *J Am Geriatr Soc* 1988; **36**: 755 [PMID: 3136199 DOI: 10.1016/j.cca.2019.07.033]
22 **Barrett T**, Wilhite SE, Ledoux P, Evangelista C, Kim IF, Tomashevsky M, Marshall KA, Phillippy KH, Sherman PM, Holko M, Yefanov A, Lee H, Zhang N, Robertson CL, Serova N, Davis S, Soboleva A. NCBI GEO: archive for functional genomics data sets--update. *Nucleic Acids Res* 2013; **41**: D991-D995 [PMID: 23193258 DOI: 10.1093/nar/gks1193]
23 **Singh UP**, Singh NP, Murphy EA, Price RL, Fayad R, Nagarkatti M, Nagarkatti PS. Chemokine and cytokine levels in inflammatory bowel disease patients. *Cytokine* 2016; **77**: 44-49 [PMID: 26520877 DOI: 10.1016/j.cyto.2015.10.008]
24 **Trivedi PJ**, Adams DH. Chemokines and Chemokine Receptors as Therapeutic Targets in Inflammatory Bowel Disease; Pitfalls and Promise. *J Crohns Colitis* 2018; **12**: S641-S652 [PMID: 30137309 DOI: 10.1093/ecco-jcc/jjx145]
25 **Carlsen HS**, Baekkevold ES, Johansen FE, Haraldsen G, Brandtzaeg P. B cell attracting chemokine 1 (CXCL13) and its receptor CXCR5 are expressed in normal and aberrant gut associated lymphoid tissue. *Gut* 2002; **51**: 364-371 [PMID: 12171958 DOI: 10.1136/gut.51.3.364]
26 **Steele CW**, Karim SA, Leach JDG, Bailey P, Upstill-Goddard R, Rishi L, Foth M, Bryson S, McDaid K, Wilson Z, Eberlein C, Candido JB, Clarke M, Nixon C, Connelly J, Jamieson N, Carter CR, Balkwill F, Chang DK, Evans TRJ, Strathdee D, Biankin AV, Nibbs RJB, Barry ST, Sansom OJ, Morton JP. CXCR2 Inhibition Profoundly Suppresses Metastases and Augments Immunotherapy in Pancreatic Ductal Adenocarcinoma. *Cancer Cell* 2016; **29**: 832-845 [PMID: 27265504 DOI: 10.1016/j.ccell.2016.04.014]
27 **Muthas D**, Reznichenko A, Balendran CA, Böttcher G, Clausen IG, Kärrman Mårdh C, Ottosson T, Uddin M, MacDonald TT, Danese S, Berner Hansen M. Neutrophils in ulcerative colitis: a review of selected biomarkers and their potential therapeutic implications. *Scand J Gastroenterol* 2017; **52**: 125-135 [PMID: 27610713 DOI: 10.1080/00365521.2016.1235224]
28 **Farooq SM**, Stillie R, Svensson M, Svanborg C, Strieter RM, Stadnyk AW. Therapeutic effect of blocking CXCR2 on neutrophil recruitment and dextran sodium sulfate-induced colitis. *J Pharmacol Exp Ther* 2009; **329**: 123-129 [PMID: 19131582 DOI: 10.1124/jpet.108.145862]
29 **Duarte-Neves J**, Pereira de Almeida L, Cavadas C. Neuropeptide Y (NPY) as a therapeutic target for neurodegenerative diseases. *Neurobiol Dis* 2016; **95**: 210-224 [PMID: 27461050 DOI: 10.1016/j.nbd.2016.07.022]
30 **Wan CP**, Lau BH. Neuropeptide Y receptor subtypes. *Life Sci* 1995; **56**: 1055-1064 [PMID: 9001438 DOI: 10.1016/0024-3205(95)00041-4]
31 **Hofmann S**, Bellmann-Sickert K, Beck-Sickinger AG. Chemical modification of neuropeptide Y for human Y1 receptor targeting in health and disease. *Biol Chem* 2019; **400**: 299-311 [PMID: 30653463 DOI: 10.1515/hsz-2018-0364]

World Journal of Gastroenterology

Submit a Manuscript: https://www.f6publishing.com

World J Gastroenterol 2020 October 21; 26(39): 5997-6014

DOI: 10.3748/wjg.v26.i39.5997

ISSN 1007-9327 (print) ISSN 2219-2840 (online)

ORIGINAL ARTICLE

Basic Study

Herbal cake-partitioned moxibustion inhibits colonic autophagy in Crohn's disease *via* signaling involving distinct classes of phosphatidylinositol 3-kinases

Shi-Yuan Wang, Ji-Meng Zhao, Ci-Li Zhou, Han-Dan Zheng, Yan Huang, Min Zhao, Zhi-Ying Zhang, Lu-Yi Wu, Huan-Gan Wu, Hui-Rong Liu

ORCID number: Shi-Yuan Wang 0000-0002-6946-6947; Ji-Meng Zhao 0000-0001-9075-6036; Ci-Li Zhou 0000-0003-1636-4231; Han-Dan Zheng 0000-0002-8640-9194; Yan Huang 0000-0002-5588-0274; Min Zhao 0000-0001-9577-425X; Zhi-Ying Zhang 0000-0001-8959-763X; Lu-Yi Wu 0000-0002-7297-2509; Huan-Gan Wu 0000-0003-1725-6881; Hui-Rong Liu 0000-0002-9697-5085.

Author contributions: Wang SY, Huang Y, Wu HG, and Liu HR designed the research; Wang SY, Zhao JM, Zhou CL, and Zheng HD performed the experiments; Wang SY, Zhao M, Zhang ZY, and Wu LY collected and analyzed the data; Wang SY wrote the manuscript; all authors reviewed the manuscript prior to its submission, and read and approved the final manuscript.

Supported by the Program of Shanghai Academic Research Leader, No. 17XD1403400; National Natural Sciences Foundation of China, No. 81574079 and No. 81873374; Three-year Action Plan Project of Shanghai Traditional Chinese Medicine Development, No. ZY(2018-2020)-CCCX-2004-01; Chinese Medicine Inheritance and Innovation "100 Million" Talent Project, Qi Huang

Shi-Yuan Wang, Ji-Meng Zhao, Ci-Li Zhou, Han-Dan Zheng, Yan Huang, Min Zhao, Zhi-Ying Zhang, Lu-Yi Wu, Huan-Gan Wu, Hui-Rong Liu, Key Laboratory of Acupuncture-Moxibustion and Immunology, Shanghai University of Traditional Chinese Medicine, Shanghai 201203, China

Shi-Yuan Wang, Ji-Meng Zhao, Ci-Li Zhou, Han-Dan Zheng, Yan Huang, Min Zhao, Zhi-Ying Zhang, Huan-Gan Wu, Hui-Rong Liu, Shanghai Research Institute of Acupuncture and Meridian, Shanghai 200030, China

Corresponding author: Hui-Rong Liu, MD, PhD, Doctor, Professor, Research Fellow, Key Laboratory of Acupuncture-Moxibustion and Immunology, Shanghai University of Traditional Chinese Medicine, No. 650 South Wanping Road, Xuhui District, Shanghai 201203, China. lhr_tcm@139.com

Abstract

BACKGROUND

Autophagy is an evolutionarily conserved biological process in eukaryotic cells that involves lysosomal-mediated degradation and recycling of related cellular components. Recent studies have shown that autophagy plays an important role in the pathogenesis of Crohn's disease (CD). Herbal cake-partitioned moxibustion (HM) has been historically practiced to treat CD. However, the mechanism by which HM regulates colonic autophagy in CD remains unclear.

AIM

To observe whether HM can alleviate CD by regulating colonic autophagy and to elucidate the underlying mechanism.

METHODS

Rats were randomly divided into a normal control (NC) group, a CD group, an HM group, an insulin + CD (I + CD) group, an insulin + HM (I + HM) group, a rapamycin + CD (RA + CD) group, and a rapamycin + HM (RA + HM) group. 2,4,6-trinitrobenzenesulfonic acid was administered to establish a CD model. The morphology of the colonic mucosa was observed by hematoxylin-eosin staining, and the formation of autophagosomes was observed by electron microscopy. The expression of autophagy marker microtubule-associated protein 1 light chain 3

Scholar; and Shanghai Rising-Star Program, No. 16QA1403400.

Institutional review board statement: This study did not involve human subjects.

Institutional animal care and use committee statement: All animal experiments in this study were performed under guidelines approved by the Animal Ethics Committee of the Shanghai University of Traditional Chinese Medicine (No. PZSHUTCM200403009).

Conflict-of-interest statement: The authors declare no conflicts of interest.

Data sharing statement: No additional data are available.

ARRIVE guidelines statement: The authors have read the ARRIVE guidelines, and the manuscript was prepared and revised according to the ARRIVE guidelines.

Manuscript source: Unsolicited manuscript

Received: April 16, 2020
Peer-review started: April 16, 2020
First decision: May 1, 2020
Revised: July 14, 2020
Accepted: September 4, 2020
Article in press: September 4, 2020
Published online: October 21, 2020

P-Reviewer: Merigo F
S-Editor: Zhang H

beta (LC3B) was observed by immunofluorescence staining. Insulin and rapamycin were used to inhibit and activate colonic autophagy, respectively. The mRNA expression levels of phosphatidylinositol 3-kinase class I (*PI3KC1*), *Akt1*, *LC3B*, sequestosome 1 (*p62*), and mammalian target of rapamycin (*mTOR*) were evaluated by RT-qPCR. The protein expression levels of interleukin 18 (IL-18), tumor necrosis factor-α (TNF-α), nuclear factor κB/p65 (NF-κB p65), LC3B, p62, coiled-coil myosin-like BCL2-interacting protein (Beclin-1), p-mTOR, PI3KC1, class III phosphatidylinositol 3-kinase (PI3KC3/Vps34), and p-Akt were evaluated by Western blot analysis.

RESULTS

Compared with the NC group, the CD group showed severe damage to colon tissues and higher expression levels of IL-18 and NF-κB p65 in colon tissues (P < 0.01 for both). Compared with the CD group, the HM group showed significantly lower levels of these proteins ($P_{\text{IL-18}}$ < 0.01 and P_{p65} < 0.05). There were no significant differences in the expression of TNF-α protein in colon tissue among the rat groups. Typical autophagic vesicles were found in both the CD and HM groups. The expression of the autophagy proteins LC3B and Beclin-1 was upregulated (P < 0.01 for both) in the colon tissues of rats in the CD group compared with the NC group, while the protein expression of p62 and p-mTOR was downregulated (P < 0.01 for both). However, these expression trends were significantly reversed in the HM group compared with the CD group (P_{LC3B} < 0.01, $P_{\text{Beclin-1}}$ < 0.05, P_{p62} < 0.05, and $P_{\text{m-TOR}}$ < 0.05). Compared with those in the RA + CD group, the mRNA expression levels of *PI3KC1*, *Akt1*, *mTOR*, and *p62* in the RA + HM group were significantly higher (P_{PI3KC1} < 0.01 and $P_{\text{Akt1, mTOR, and p62}}$ < 0.05), while those of LC3B were significantly lower (P < 0.05). Compared with the RA + CD group, the RA + HM group exhibited significantly higher PI3KC1, p-Akt1, and p-mTOR protein levels (P_{PI3KC1} < 0.01, $P_{\text{p-Akt1}}$ < 0.05, and $P_{\text{p-mTOR}}$ < 0.01), a higher p62 protein level (P = 0.057), and significantly lower LC3B and Vps34 protein levels (P < 0.01 for both) in colon tissue.

CONCLUSION

HM can activate PI3KC1/Akt1/mTOR signaling while inhibiting the PI3KC3 (Vps34)-Beclin-1 protein complex in the colon tissues of CD rats, thereby inhibiting overactivated autophagy and thus exerting a therapeutic effect.

Key Words: Crohn's disease; Colon; Moxibustion; Macroautophagy; Immunity; Phosphatidylinositol 3-kinase signaling

Core Tip: Here, we demonstrated that overactivation of colonic autophagy can be observed in a 2,4,6-trinitrobenzenesulfonic acid (TNBS)-induced rat Crohn's Disease (CD) model. Herbal cake-partitioned moxibustion ameliorated TNBS-induced inflammation and colon damage, facilitated the repair of colonic epithelial cells, and inhibited colonic overactivated autophagy by activating the phosphatidylinositol 3-kinase class I/protein kinase B akt-1/mammalian target of rapamycin signaling pathway while inhibiting the class III phosphatidylinositol 3-kinase -coiled-coil myosin-like BCL2-interacting protein (Beclin-1) complex in CD rats.

Citation: Wang SY, Zhao JM, Zhou CL, Zheng HD, Huang Y, Zhao M, Zhang ZY, Wu LY, Wu HG, Liu HR. Herbal cake-partitioned moxibustion inhibits colonic autophagy in Crohn's disease *via* signaling involving distinct classes of phosphatidylinositol 3-kinases. *World J Gastroenterol* 2020; 26(39): 5997-6014
URL: https://www.wjgnet.com/1007-9327/full/v26/i39/5997.htm
DOI: https://dx.doi.org/10.3748/wjg.v26.i39.5997

L-Editor: Wang TQ
P-Editor: Li JH

INTRODUCTION

Crohn's disease (CD), a chronic inflammatory gastrointestinal disease, is a form of inflammatory bowel disease (IBD) characterized by abdominal pain, diarrhea, anal lesions, and systemic symptoms of varying degrees of severity. CD features recurrent and remitting changes that can affect all parts of the digestive tract, with the most common being the terminal ileum and colon[1]. A population-based cohort study of diagnosed IBD patients from 13 countries in the Asia-Pacific region (2011-2013) has revealed that the overall incidence of IBD in Asia is 1.4/100000[2]. A 2018 systematic review of the epidemiology of IBD in mainland China has shown that the current incidence of IBD is 1.80/1000000, of which CD accounts for 0.46/1000000 cases[3]. The pathogenesis of CD has not been fully elucidated. At present, it is believed that CD onset is caused by abnormal factors such as genetic susceptibility, environmental factors, and intestinal flora imbalance that result in an abnormal intestinal mucosal immune response and impaired epithelial barrier function[4].

Macroautophagy (commonly shortened to "autophagy") is an evolutionarily conserved biological process that occurs in eukaryotic cells and is mediated by lysosomal degradation and recycling of related cell components. Under normal conditions, autophagy occurs at a relatively low level, but it is activated when cells are stimulated by starvation, hypoxia, exposure to toxic molecules, or other stresses. Autophagy maintains intracellular homeostasis and promotes cell survival by decomposing related intracellular substrates[5]. Increasing evidence suggests that dysregulation of autophagy is inextricably linked to the onset of CD[6,11]. For example, autophagic dysfunction can reduce the restriction of intracellular replication of adherent-invasive *E. coli* (AIEC) and increase the secretion of proinflammatory factors such as tumor necrosis factor-α (TNF-α) and interleukin-6 (IL-6) in the intestine[12,13]. Autophagy in intestinal epithelial cells (IECs) may play a protective role in preventing TNF-induced apoptosis of IECs and thus play a role in limiting intestinal inflammation[14]. In-depth study of autophagy will help to further elucidate the pathogenesis of CD.

Mammalian target of rapamycin (mTOR) is a key mediator that regulates autophagy in response to cellular nutritional levels, hypoxia, and growth factors. As mTOR is a major regulator of autophagy, inhibiting mTOR is an important way to increase autophagy levels[15]. As a direct downstream target of phosphatidylinositol 3-kinase (PI3K) and Akt, mTOR can be activated by neurotrophic factors and growth factor receptors, thereby promoting cell growth, differentiation, and survival and simultaneously downregulating related apoptosis signals. Studies have shown that insulin, insulin-like growth factor (IGF), and epithelial growth factor (EGF) can activate PI3K[16-18], which promotes Akt (site 473) phosphorylation, and increases in Akt phosphorylation can directly or indirectly lead to increases in the phosphorylation of specific sites on mTOR downstream (such as Ser2448). Therefore, activation of the PI3K/AKT/mTOR pathway should in principle play a role in autophagy inhibition. In contrast, induction of autophagy (inhibition of mTOR) may impair cell survival by causing continuous activation of autophagy[19]. PI3K family members can be divided into 3 types; type I consists of regulatory and catalytic subunits (PI3Kα, β, γ, and δ), and its main pathway is the above mentioned PI3K/Akt/mTOR, whereas type III consists of only one member, the class III PI3K (PI3KC3/Vps34). Vps34 is also a major player in autophagy that mainly forms a complex with coiled-coil myosin-like BCL2-interacting protein (Beclin-1) to promote the formation of autophagosomes, and autophagy is inhibited when the formation of this complex is blocked. Therefore, the PI3K/Akt/mTOR pathway and the Vps34-Beclin-1 complex may play coregulatory roles in autophagy[20]. For example, administration of the mTOR-specific inhibitor rapamycin can lead to downregulation of mTOR phosphorylation and directly activate autophagy, and mTOR inhibition can directly lead to activation of the autophagy-related protein unc-51-like kinase 1 (ULK1). When ULK1 is activated, Beclin-1 is phosphorylated, which enhances the activity of the Vps34-Beclin-1 complex and further enhances autophagic activity[21].

Herbal cake-partitioned moxibustion (HM), an important type of moxibustion, has the characteristics and advantages of moxibustion combined with traditional Chinese medicine, and its clinical application scope has exceeded that of conventional moxibustion. Our previous research has shown that HM improves intestinal epithelial morphology and epithelial cell structure and increases the expression of tight junction proteins to repair damage to the intestinal epithelial barrier by upregulating tumor necrosis factor alpha-induced protein 3 (A20) expression[22,23], alleviates colon tissue ulcers and relieves intestinal inflammation by downregulating IL-17 and IL-23 mRNA and protein expression in the colonic mucosa in CD model rats[24], alleviates colonic

inflammation through regulation of Toll-like receptor 4 (TLR4), which induces nuclear factor κB (NF-κB) signal transduction[25], and ameliorates visceral pain and downregulates extracellular signal-regulated kinase, substance P, and neurokinin-1 protein and mRNA expression in the dorsal root ganglia in IBD[26]. However, there have been few studies on the regulation of autophagy in CD, and the related mechanism is unclear. Therefore, this study was conducted to explore the regulatory effects and mechanism of HM in CD rats from the perspective of colonic autophagy to provide a scientific basis for research on related signal transduction mechanisms and clinical applications of moxibustion in the treatment of CD.

MATERIALS AND METHODS

Chemicals and reagents

2,4,6-trinitrobenzenesulfonic acid (TNBS; P2297, Sigma), anti-IL-18 (ab191860, Abcam), anti-TNF-α (ab6671, Abcam), anti-NF-κB p65 (ab16502, Abcam), anti-microtubule-associated protein 1 Light chain 3 beta (LC3B; #3868, Cell Signaling Technology, CST), anti-sequestosome 1 (p62; #23214, CST), anti-Beclin-1 (#3738, CST), anti-phospho-mTOR (p-mTOR; #2971, CST), Cy3-AffiniPure goat anti-mouse IgG (H + L) (111-165-003, Jackson), HRP-labeled goat anti-rabbit IgG (H + L) (A0208, Beyotime), HRP-labeled goat anti-mouse IgG (H + L) (A0216, Beyotime), insulin (P3376, Beyotime), rapamycin (LC R-5000, LC Laboratories), anti-PI3K p85 (#4292, CST), anti-Akt (#9272, CST), anti-p-Akt (#9271, CST), anti-Vps34 (V9764, sigma), and Antifade mounting medium (Beyotime, P0126) were used in this study.

Animals

Sprague-Dawley (SD) rats (male, clean grade, 180 ± 20 g) were provided by the Experimental Animal Center of Shanghai University of Traditional Chinese Medicine. The rats were housed indoors in clean conditions under a 12-h light/dark cycle, a room temperature of 20 ± 2 °C, and a humidity of 50%-70%. After 1 wk of adaptive feeding, the formal experiments began. All animal experiments in this study were approved and performed under the guidelines of the Animal Ethics Committee of the Shanghai University of Traditional Chinese Medicine (No. PZSHUTCM200403009). Seventy rats were randomly divided into a normal control (NC) group, a CD group, an HM group, an insulin + CD (I + CD) group, an insulin + HM (I + HM) group, a rapamycin + CD (RA + CD) group, and a rapamycin + HM (RA + HM) group, with ten rats in each group. A CD rat model was established by using 2,4,6-TNBS enema (10 mg/100 g). To perform the enema, each rat was lifted upside down to expose the anus, and then a 1 mL syringe was connected to a gastric perfusion needle. The gastric perfusion needle was dipped in liquid paraffin and then slowly inserted into the anus of the rat to a depth of approximately 6-8 cm. After the injection was finished, the rats were kept in the head-down position for 5 min. The injection was repeated every 7 d for five times.

Intervention and HM treatment

Traditional Chinese medicines such as *Radix Aconiti Lateralis Preparata*, *Cortex Cinnamomi*, and *Radix Salviae Miltiorrhizae* were made into powder. Yellow rice wine was poured into the powder and blended to make a paste. The paste was then made into an herbal cake with a special cake mold (0.5 cm in diameter and 1.0 cm in height). After the CD rat model was confirmed to be successfully established, the rats in the I + CD and RA + CD groups were given intraperitoneal injections of insulin and rapamycin, respectively, once daily for 7 d. The CD rats in the HM group were treated with moxa cones. The cones were made of refined mugwort floss (90 mg) placed on an herbal cake and were placed on the abdominal acupoints [Tianshu (ST25) and Qihai (CV6)] of the rats before being ignited. Two moxa cones were used for each acupoint once daily for 7 d. The CD rats in the I + HM and RA + HM groups underwent the same procedures as those in the HM group and were given intraperitoneal injections of insulin and rapamycin, respectively, once daily at the same time for 7 d.

Immunofluorescence

Rat colon samples were fixed in 40 g/L formaldehyde for 24 h, embedded in paraffin, cut into 5 μm sections, and then heated at 60 °C for 20 min. The sections were collected and soaked in dimethylbenzene for 15 min twice; soaked in 100%, 95% and 70% alcohol for 5 min each; and washed with water. Antigen repair was conducted using

the microwave thermal repair method. Briefly, 0.01 mol/L citrate buffer (1000 mL with 3 g of trisodium citrate and 0.4 g of citric acid) was placed in a microwave oven and heated on a high setting. After the buffer began to boil, it was removed. Then, the sections were soaked in the buffer, put into the microwave oven, heated for 10 min, and cooled at room temperature for 1 h. The sections were then washed with phosphate buffer saline (PBS) for 5 min, blocked with goat serum for 30 min at room temperature, and incubated with a primary antibody (LC3B, 1:200) overnight at 4 °C. After the samples were incubated at 37 °C for 45 min and washed three times for 5 min with PBST, they were incubated with a secondary antibody (Cy3, 1:400) for 30 min at room temperature and then washed three times for 5 min with PBST. The samples were incubated with DAPI staining solution for 10 min and washed three times for 5 min with PBST. One drop of antifade mounting medium was added to each section, and laser confocal microscopy (Nikon, Japan) was used to detect the expression of LC3B.

Real-time qPCR

Total RNA was isolated using TRIzol reagent (Invitrogen), and cDNA was synthesized using a RevertAid First Strand cDNA Synthesis Kit (K1622, Invitrogen) according to the manufacturer's protocol. Detection of mRNA was performed using a QuantityNova SYBR Green Kit (208052, Qiagen) and a Roche480II Real-Time PCR System (Roche). The mRNA expression levels were normalized to those of GAPDH and were calculated using the $2^{-\Delta\Delta Ct}$ method. The primers used for PCR amplification are listed in Table 1.

Western blot analysis

Total proteins were extracted from colon tissues using RIPA buffer supplemented with protease and phosphatase inhibitors (P1046, Beyotime). Equal amounts of protein (50 μg) were separated by 8%-10% sodium dodecylsulphate polyacrylamide gel electrophoresis, and the separated proteins were transferred to polyvinylidene fluoride membranes. The membranes were blocked with 5% bovine serum albumin in Tris Buffered Saline with Tween-20 (TBST) and then incubated at 4 °C overnight with primary antibodies. Following several sequential washes, the membranes were incubated with secondary antibodies for 1 h at room temperature. The antibody concentrations/dilutions were prepared according to the instructions (IL-18 and p65, 0.5 μg/mL; Vps34, 2 μg/mL; TNF-α, LC3B, p62, Beclin-1, p-mTOR, p85, Akt, and p-Akt, 1:1000). The blots were then washed four times with TBST (10 min each time). The membranes were stained with enhanced chemiluminescence solution (Thermo) and visualized using an imager.

Transmission electron microscopy

Samples of the rat colonic mucosa were cut into 1 mm^3 strips and placed in glutaraldehyde fixation solution. The samples were washed for three times for 15 min each with 0.1 mol/L PBS, fixed with 2% glutaraldehyde fixative at 4 °C for at least 2 h, washed three times for 15 min each with 0.1 mol/L PBS, fixed with 2% osmium acid for 2 h, and again washed three times for 15 min each with 0.1 mol/L PBS. The samples were then dehydrated in 30%, 50%, and 70% ethanol solutions for 20 min each at 4 °C; incubated in uranyl acetate dihydrate overnight at 4 °C; placed sequentially into 80% and 90% ethanol solutions; soaked in 90% acetone: Embedding agent (1:1) for 20 min at 4 °C; soaked in 100% acetone three times for 20 min each at room temperature; Soaked in 100% acetone:embedding agent (1:1) for 2 h at room temperature; and Soaked in embedding agent two times for 1.5 h each at 37 °C. The samples were then heated in an oven at 37 °C for 12 h and at 60 °C for 48 h. For sectioning, the block of embedded sample was trimmed with a double-sided knife, and the top was cut into a pyramid shape. The top was flattened, and the tissue was exposed to facilitate slicing. A glass strip was fitted into an ultramicrotome knife-making machine to make the glass knife, which was fixed on the stage with sticking plaster. The block of sample in embedding agent was placed on the ultramicrotome and sliced at a thickness of 80 nm. The slices were removed and placed on a support membrane of copper mesh. Lead citrate staining solution was used to dye the slices for 15 min, after which the slices were washed with distilled water three times, dried naturally, and observed under a transmission electron microscope (Leica EMUC 7, Germany). The embedding agent consisted of 618 epoxy resin 40.5 g, dodeceny succinicanhydride 36 g, dibutyl phthalate 2.7 g, and 2,4,6-Tris(dimethylaminomethyl)phenol 0.675 mL.

Table 1 Primers used for PCR

NM	Length	Primer NM	Sequence (5'-3')
NM_017008.4	129 bp	Rat GAPDH F-primer	tgccactcagaagactgtgg
		Rat GAPDH R-primer	ttcagctctgggatgacctt
NM_175843.4	188 bp	Rat p62 F-primer	agaagtggacccatccacag
		Rat p62 R-primer	agaaacccatggacagcatc
NM_022867.2	114 bp	Rat Map1lc3b F-primer	ttcttcctcctggtgaatgg
		Rat Map1lc3b R-primer	ctgggaggcatagaccatgt
NM_019906.1	153 bp	Rat mTOR Forward primer	ggcttctgaagatgctgtcc
		Rat mTOR Reverse primer	gagttcgaagggcaagagtg
NM_013005.1	166 bp	Rat Pik3r1 F-primer	actactggggagaggggaga
		Rat Pik3r1 R-primer	caggaagggtcaacactggt
NM_033230.2	176 bp	Rat Akt1 F-primer	actcattccagacccacgac
		Rat Akt1 R-primer	ccggtacaccacgttcttct

GAPDH: Glyceraldehyde-3-phosphate dehydrogenase; p62: Sequestosome 1; Map1lc3b: Microtubule-associated protein 1 light chain 3 beta; mTOR: Mammalian target of rapamycin; Pik3r1: Phosphatidylinositol 3-kinase regulatory subunit alpha; Akt1: Protein kinase B akt-1.

Statistical analysis

SPSS 20.0 statistical software was used for statistical analyses. One-way ANOVA was used for data that met the assumptions of a normal distribution and homogeneity of variance. For data that did not meet the normal distribution or homogeneity of variance assumption, a nonparametric test was used. Continuous data are presented as the mean ± standard deviation or as medians (P25, P75) according to the distribution; $P < 0.05$ were considered to indicate statistical significance.

RESULTS

HM ameliorates TNBS-induced inflammation and colon damage in CD rats

We used the Morris method[27] to establish a rat model of CD. After TNBS induction, the colon was shortened and exhibited megacolon or intestinal obstruction. Upon cutting of the intestine, wall thickening, mucosal surface roughness, and cobblestone-like changes were observed, accompanied by scattered edema, congestion, and ulceration, suggesting that the rat model had been successfully established (Figure 1A). After confirming the success of the modeling, we selected the Qihai (CV6) and bilateral Tianshu (ST25) acupoints for HM and performed pathological observation. In the NC group, the colon tissues showed clear and intact colonic epithelial structures, complete and continuous mucosae, and neatly arranged glands. In the CD group, considerable inflammatory cell infiltration, destruction of mucosal structure, partial mucosal shedding, disappearance or deformation of glands, and fissure-like ulcers were observed. Compared with rats in the CD group, the colon tissue of rats in the HM group showed relatively complete mucosal epithelial coverage, ulcer repair, and partial amelioration of gland abnormalities and lymphocyte infiltration (Figure 1B). Our previous research has demonstrated that HM at the Qihai (CV6) and Tianshu (ST25) acupoints in CD rats can relieve intestinal inflammation by downregulating IL-17 and IL-23[24]. In the present study, we tested the expression levels of IL-18, TNF-α, and NF-κB in the colon tissues of the rats in each group. Compared with the NC group, the CD group exhibited significantly higher levels of IL-18 protein and NF-κB p65 in colon tissue ($P < 0.01$ for both). Compared with the CD group, the HM group exhibited significantly lower levels of these proteins ($P_{IL-18} < 0.01$ and $P_{p65} < 0.05$). There were no significant differences in the expression of TNF-α protein in colon tissue among the groups. However, compared with the NC group, the CD group exhibited a trend toward higher TNF-α protein expression, and compared with the CD group, the HM group exhibited a trend toward lower TNF-α protein expression (Figure 1C).

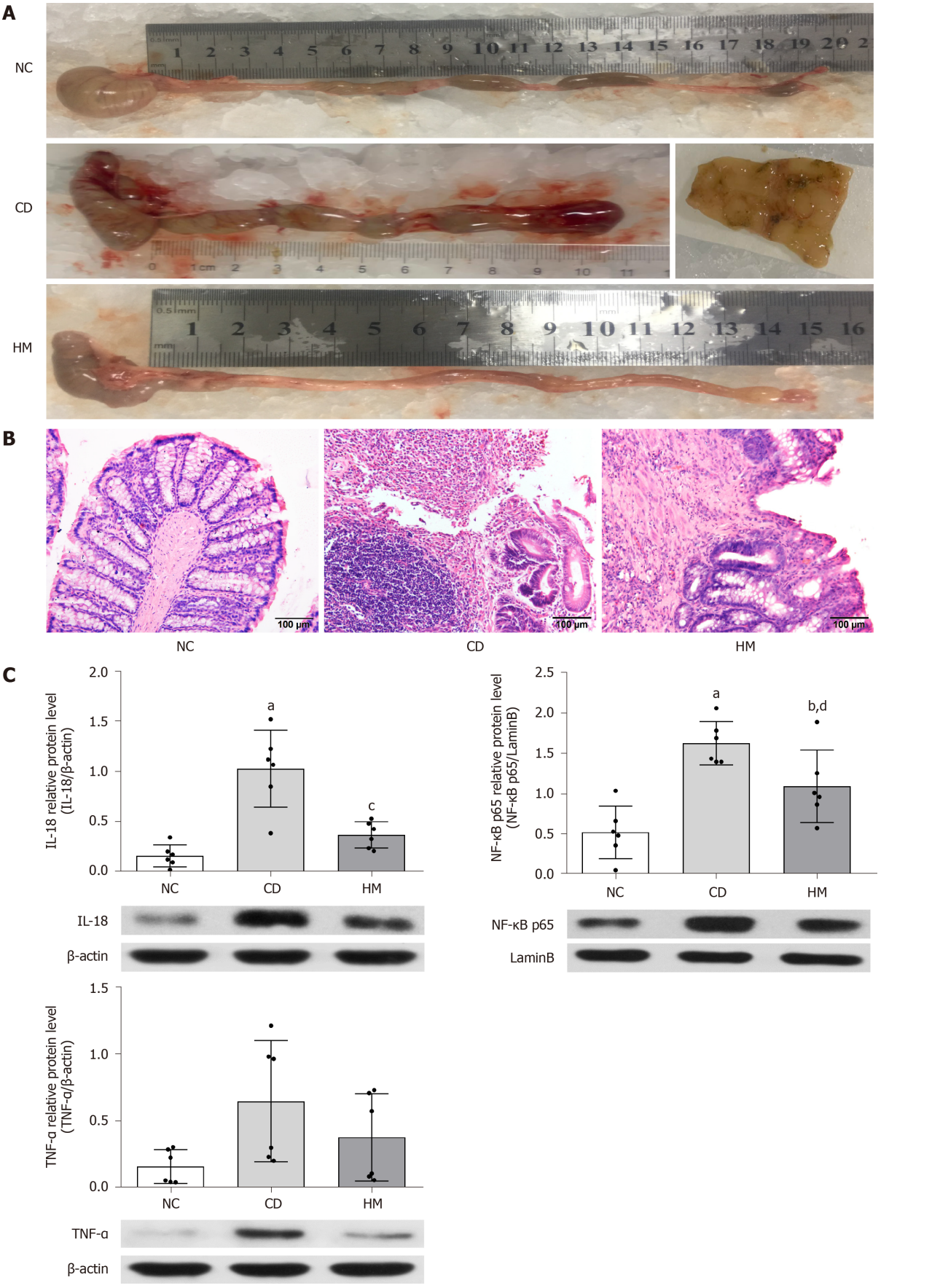

Figure 1 Herbal cake-partitioned moxibustion at the Qihai (CV6) and bilateral Tianshu (ST25) acupoints ameliorates colon damage and inflammation in Crohn's disease rats. A: Megacolon and cobblestone-like changes; B: Histopathological observations of colon tissue by hematoxylin and eosin staining. Scale bar: 100 μm; C: Expression of the colonic inflammatory factors interleukin-18 (IL-18), nuclear factor κB/p65 (NF-κB p65), and tumor necrosis

factor-α (TNF-α) proteins evaluated by Western blot. Six independent experiments were analyzed, and the data are presented as the mean ± SD. [a]*P* < 0.01, [b]*P* < 0.05 *vs* NC group; [c]*P* < 0.01, [d]*P* < 0.05 *vs* CD group. NC: Normal control; CD: Crohn's disease; HM: Herbal cake-partitioned moxibustion; IL-18: Interleukin 18; NF-κB p65: Nuclear factor κB p65; TNF-α: Tumor necrosis factor-α.

HM facilitates the repair of colonic epithelial cells

Since the intestinal mucosa is composed of a simple columnar epithelium that serves as a physical and chemical barrier and an absorptive surface[28], we next observed the damage, repair, and autophagosome formation of colon tissue epithelial cells in the rats in each group by electron microscopy (Figure 2). In the NC group, the colonic epithelial cell structure was intact, the organelles and microvilli were arranged neatly without damage, and no autophagosomes were present. In the CD group, injury, swelling, and deformation of organelles were observed. Typical autophagic vesicles were found that had double-layer membrane structures and contained damaged organelles. In the HM group, typical autophagic vesicles were still present, and organelle deformation and swelling could be observed, but these features were milder than those in the CD group, and repair of microvillus damage could be seen. These findings suggested that inflammation activated autophagy and that HM promoted the repair of colonic epithelial cells, but it remained unclear whether HM could regulate autophagy.

HM inhibits colonic autophagy in CD rats

Next, we observed the effect of HM on the colonic levels of autophagy proteins in each group of rats. As shown in Figure 3A, compared with the NC group, the CD group and the HM group exhibited significantly higher expression of LC3B protein in colon tissue ($P < 0.01$ for both). Compared with the CD group, the HM group exhibited significantly lower expression of LC3B protein in colon tissue ($P < 0.01$). Both p62 and LC3 are used to evaluate autophagy, and studies have shown that the expression levels of p62 decrease with increasing LC3 Levels[29]. Therefore, we tested the expression levels of p62 protein in colon tissues. As expected, compared with the NC group, the CD group and the HM group exhibited significantly lower expression of p62 protein in colon tissue ($P < 0.01$ for both). In addition, compared with the CD group, the HM group exhibited significantly higher expression of p62 protein in colon tissue ($P < 0.05$). Compared with the NC group, the CD group exhibited significantly higher expression of Beclin-1 protein in colon tissue ($P < 0.01$). Compared with the CD group, the HM group exhibited significantly lower expression of Beclin-1 protein in colon tissue ($P < 0.05$). Furthermore, compared with the NC group, the CD group and the HM group exhibited significantly lower expression of p-mTOR (ser 2448) protein in colon tissue ($P < 0.01$ and $P < 0.05$, respectively). Compared with the CD group, the HM group exhibited significantly higher expression of p-mTOR protein in colon tissue ($P < 0.05$). Immunofluorescence showed that LC3B was expressed in different layers of the colon, especially in the lamina propria and submucosa. Only a few positive puncta were observed in the NC group, while strong positive staining was observed in the CD group. Compared with the CD group, the HM group had obviously weaker positive staining (Figure 3B). The above results suggested that HM may have exerted a therapeutic effect by inhibiting autophagy in colon tissue in CD rats, but the mechanism was still unclear.

HM regulates autophagy through PI3K signaling

The activation of the PI3K/Akt/mTOR signaling pathway by insulin has been confirmed[30]. Specifically, insulin upregulates Akt phosphorylation and activates mTOR complex 1 (mTORC1), thereby inhibiting autophagy[31-33]. The protein mTOR is downstream of the PI3K and AKT pathway[19], and studies have shown that rapamycin can inhibit cyclophosphamide-induced activation of the PI3K/Akt/mTOR signaling pathway, thus activating autophagy[34,35]. In addition, rapamycin and its derivatives can not only inhibit mTORC1, but also inhibit the phosphorylation of Akt by inhibiting mTORC2 after long-term application[36,37]. Thus, we used insulin to activate the PI3KC1/Akt1/mTOR pathway to inhibit autophagy and used rapamycin to inhibit the PI3KC1/Akt1/mTOR pathway to activate autophagy, and subsequently observed the changes in the PI3K signaling pathway in the colon tissues of the rats in each group. The hematoxylin-eosin staining results showed that the colon tissue structure was severely damaged and that the glands had disappeared in both the CD and RA + CD groups. In addition, fissure-like ulcers and granulomas were found. In the other groups, healing ulcers, epithelial hyperplasia, partial loss of glands, and lymphocyte

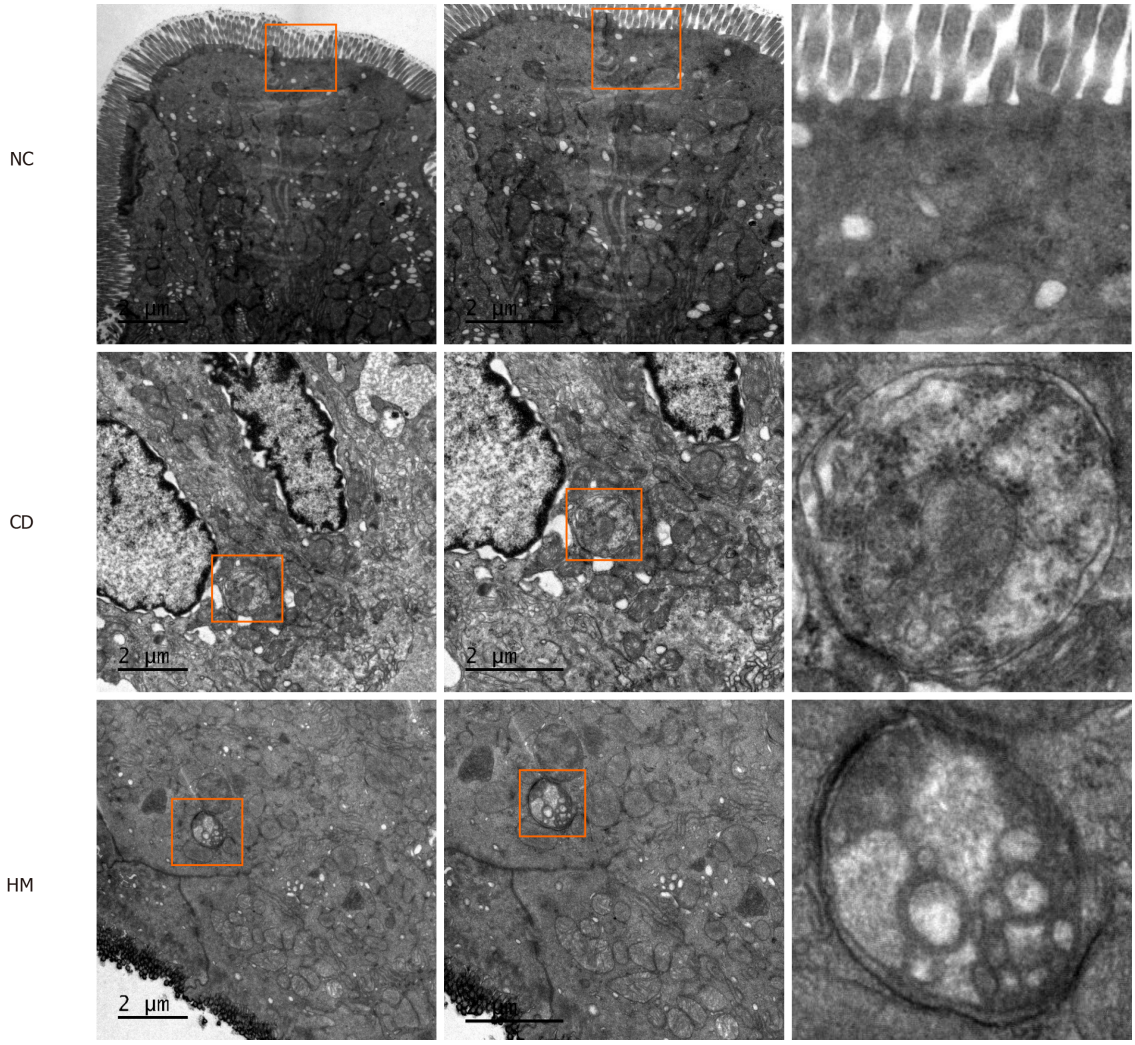

Figure 2 Ultrastructure of colonic epithelial tissue and autophagic vesicles in each group of rats. Scale bar: 2 μm. NC: Normal control; CD: Crohn's disease; HM: Herbal cake-partitioned moxibustion.

infiltration were observed (Figure 4). Immunofluorescence showed that compared with the CD and RA + CD groups, the I + CD, I + HM, and RA + HM groups exhibited lower expression of LC3B (Figure 5). In addition, compared with the RA + CD group, the RA + HM group exhibited significantly higher expression of *PI3KC1*, *Akt1*, *mTOR*, and *p62* mRNA ($P_{PI3KC1} < 0.01$ and $P_{Akt1,\ mTOR,\ and\ p62} < 0.05$) but significantly lower expression of *LC3B* mRNA ($P < 0.05$) (Figure 6A). Compared with the RA + CD group, colon tissue in the RA + HM group exhibited significantly higher expression of PI3KC1 protein ($P < 0.01$), significantly higher expression of p-Akt1 and p-mTOR proteins ($P < 0.05$ and $P < 0.01$, respectively), and higher expression of p62 protein ($P = 0.057$). LC3B protein expression was significantly downregulated in the RA + HM group ($P < 0.01$) (Figure 6B). Previous research has indicated that administration of the mTOR-specific inhibitor rapamycin can downregulate mTOR phosphorylation, directly activate autophagy, and cause phosphorylation of the autophagy-related protein Beclin-1, thus enhancing the activity of the Vps34-Beclin1 protein complex[21] and further enhancing autophagic activity. In addition, studies have shown that insulin can inhibit the autophagy-related gene *PI3KC3/Vps34*[38]. Since the expression of Beclin-1 could be inhibited by HM treatment (Figure 3A), thus, we observed the protein expression levels of Vps34 in the colon tissues of the rats in each group. The results showed that HM could significantly downregulate the expression of Vps34 protein in the colon tissues of CD rats. Compared with the CD group, the expression of Vps34 protein in RA + CD group was significantly upregulated ($P < 0.01$). Compared with the RA + CD group, Vps34 protein expression was significantly downregulated in the I + CD, I + HM, and RA + HM groups ($P < 0.01$ for all; Figure 6B).

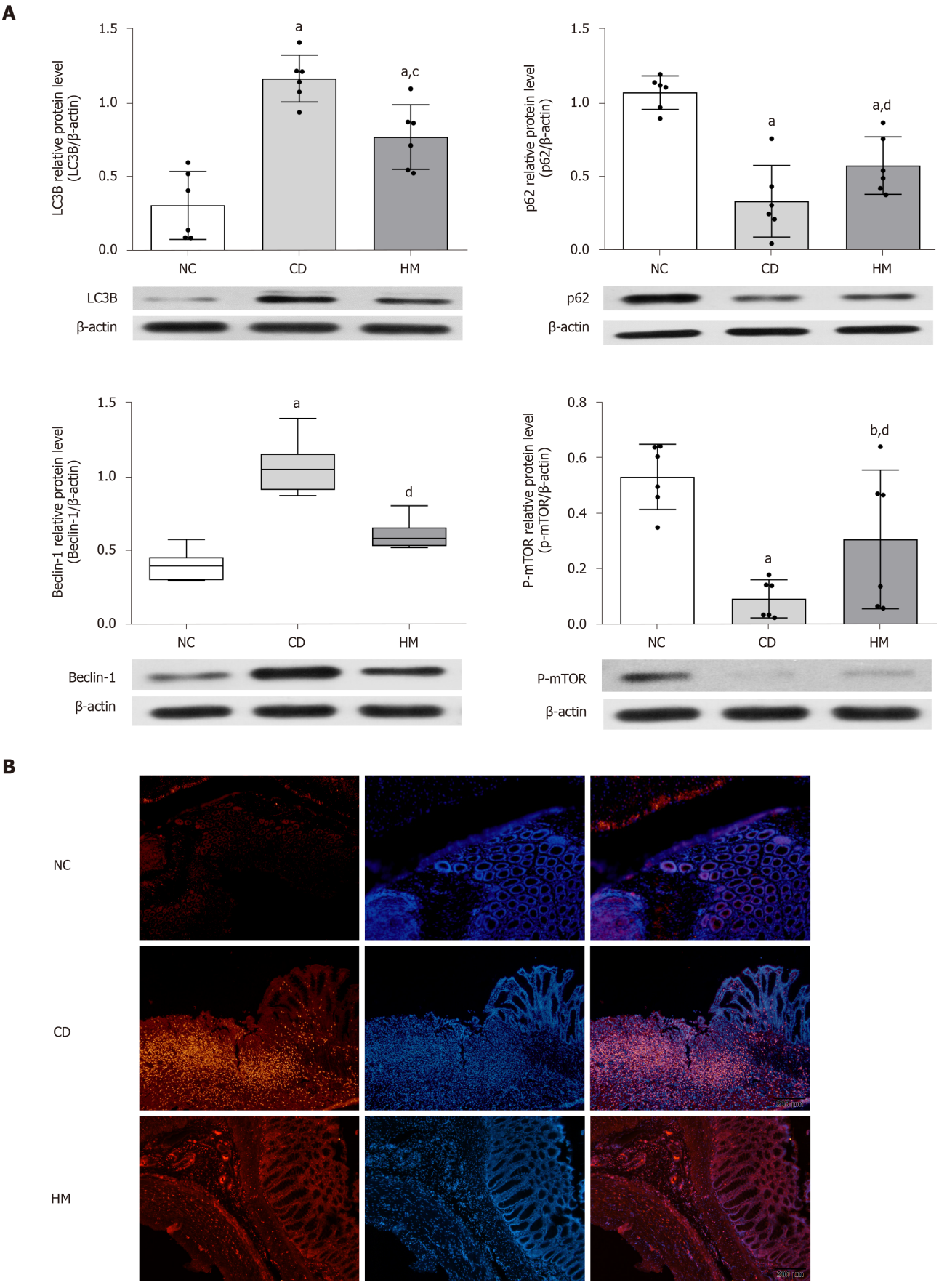

Figure 3 Herbal cake-partitioned moxibustion at the Qihai (CV6) and bilateral Tianshu (ST25) acupoints regulates the expression of autophagy proteins in the colon tissues of Crohn's disease rats. A: Expression changes of the microtubule-associated protein 1 light chain 3 beta, sequestosome 1, coiled-coil myosin-like BCL2-interacting protein, and phospho-mammalian target of rapamycin proteins evaluated by Western blot. Six independent

experiments were analyzed, and the data are presented as the mean ± SD or medians (P25, P75). [a]*P* < 0.01, [b]*P* < 0.05 *vs* NC group; [c]*P* < 0.01, [d]*P* < 0.05 *vs* CD group; B: Immunofluorescence images for LC3B (Red) in each group. Scale bar: 200 μm. NC: Normal control; CD: Crohn's disease; HM: Herbal cake-partitioned moxibustion; LC3B: Microtubule-associated protein 1 light chain 3 beta; p62: Sequestosome 1; Beclin-1: Coiled-coil myosin-like BCL2-interacting protein; p-mTOR: Phospho-mammalian target of rapamycin.

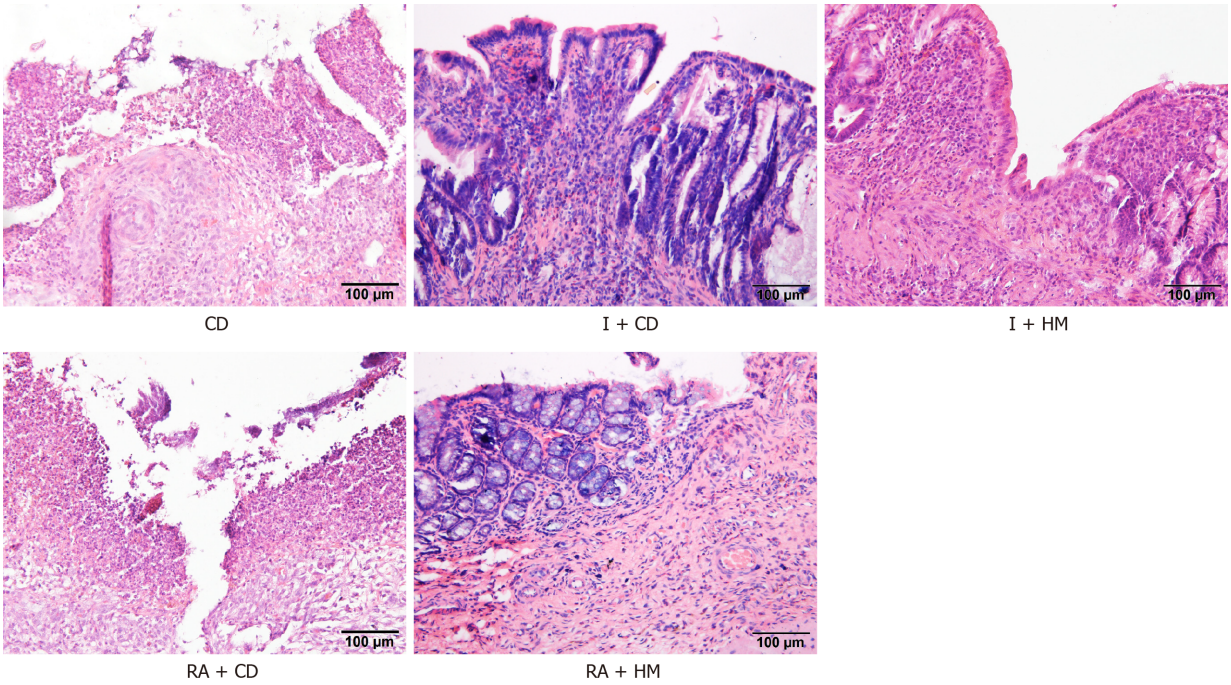

Figure 4 Histopathological observations of colon tissue from each group by hematoxylin and eosin staining. Scale bar: 100 μm. CD: Crohn's disease; I + CD: Insulin + Crohn's disease; I + HM: Insulin + herbal cake-partitioned moxibustion; RA + CD: Rapamycin + Crohn's disease; RA + HM: Rapamycin + herbal cake-partitioned moxibustion.

DISCUSSION

At present, autophagy is broadly divided into three types: Macroautophagy, microautophagy, and molecular chaperone-mediated autophagy[39]. Among them, macroautophagy (commonly shortened to "autophagy") has received the most attention in research. This type of autophagy can be triggered by different stimuli, such as starvation, inflammation, oxidative stress, hypoxia, and toxic molecules. Studies have shown that dysregulation of autophagy is inextricably linked to the occurrence and development of CD[6,7]. Thus, in the present study, we used the Morris method to establish a rat model of CD and observed the effects of TNBS on colonic autophagy in rats. The results showed that after TNBS stimulation, the colons of the rats showed severe inflammation and damage; they also showed significant activation of autophagy, as indicated by the upregulated protein expression of LC3B and Beclin-1 and the downregulated protein expression of p62 and p-mTOR and as further validated by transmission electron microscopy. In addition, treatment with rapamycin (a widely used autophagy activator) did not attenuate the pathological damage in the colon; however, HM and/or insulin treatment not only greatly ameliorated colon damage but also inhibited colonic autophagy, suggesting that under inflammatory conditions, overactivation of autophagy is harmful to colon tissues. This finding is consistent with the findings of previous studies[40,41].

Among the autophagy-related proteins, the kinase mTOR is a major regulator of autophagy. It can receive input from different signaling pathways and become inactivated under stress conditions, thereby activating ATG1 kinases (mammalian homologs of unc-51-like autophagy-activating kinases 1 and 2) and initiating autophagosome formation, thus activating autophagy[39]. Our results showed that the expression of p-mTOR protein in colon tissues was significantly downregulated in the CD group but that HM treatment reversed this downregulation, suggesting that TNBS may activate autophagy through the mTOR pathway and that mTOR may be one of the targets of HM therapy.

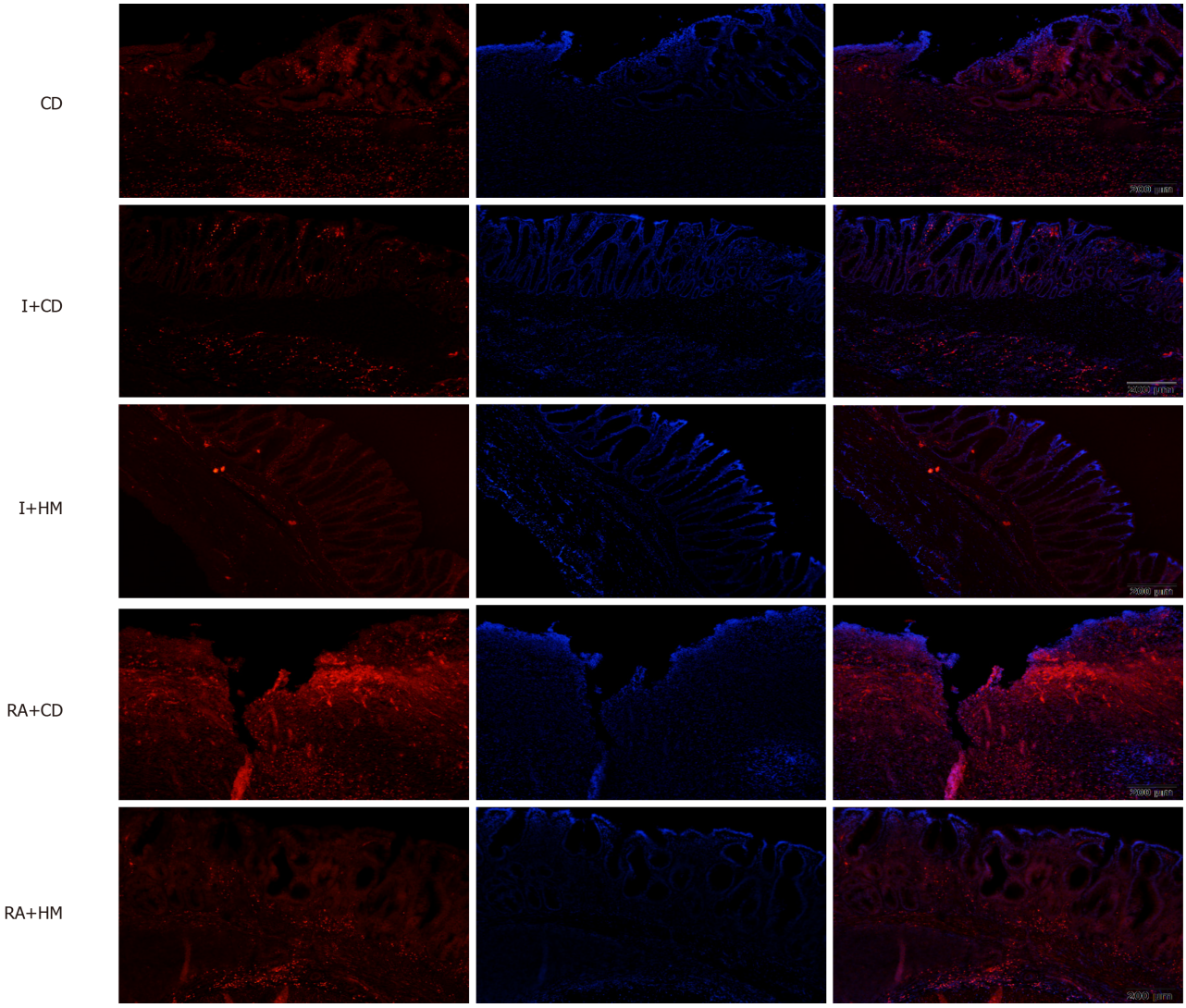

Figure 5 Immunofluorescence images for microtubule-associated protein 1 light chain 3 beta (Red) in each group. Scale bar: 200 μm. CD: Crohn's disease; I + CD: Insulin + Crohn's disease; I + HM: Insulin + herbal cake-partitioned moxibustion; RA+CD: Rapamycin + Crohn's disease; RA + HM: Rapamycin + herbal cake-partitioned moxibustion; LC3B: Microtubule-associated protein 1 light chain 3 beta.

mTOR is downstream of PI3K/Akt signaling[42], and studies have shown that inhibiting the PI3K/Akt/mTOR pathway enhances autophagy and induces apoptosis[31,43], while activation of the PI3K/Akt/mTOR pathway inhibits autophagy[44]. PI3K is an enzyme that catalyzes the phosphorylation of inositol phospholipids at position 3 of the inositol ring. Its function is to generate specific molecular messengers on the cell membrane. There are eight types of PI3Ks in mammalian cells that are divided into three classes: Class I, which includes four isomers (PI3KC1α, β, γ, and δ); Class II, which includes three isomers (PI3KC2α, β, and γ); and Class III, which includes a single isomer (PI3KC3)[45,46]. PI3KC1 is the main type involved in the PI3K/Akt signaling pathway, and phosphorylation and activation of the serine kinase PKB (also known as AKT) appears to be a general response to class I PI3K activation[47]. Activation of the PI3K/Akt/mTOR pathway is initiated by interactions between PI3K and transmembrane G protein-coupled receptors or receptor tyrosine kinases such as IGF and fibroblast growth factor that lead to Akt phosphorylation; Akt phosphorylation then leads to activation of downstream mTOR[42]. Therefore, activation of the PI3K/Akt pathway can promote mTOR activation and inhibit autophagy, which in turn may lead to upregulation of autophagy. Based on the relationship between the PI3K/Akt/mTOR signaling pathway and autophagy mentioned above, we used insulin to inhibit autophagy and used rapamycin to activate autophagy. The results showed that after administration of rapamycin to CD rats, the mRNA expression of *PI3K*, *Akt*, *mTOR*, and *p62* and the protein expression of PI3K, p-Akt, p-mTOR, and p62 in colon tissues were further downregulated, while the mRNA and protein expression of LC3B was further

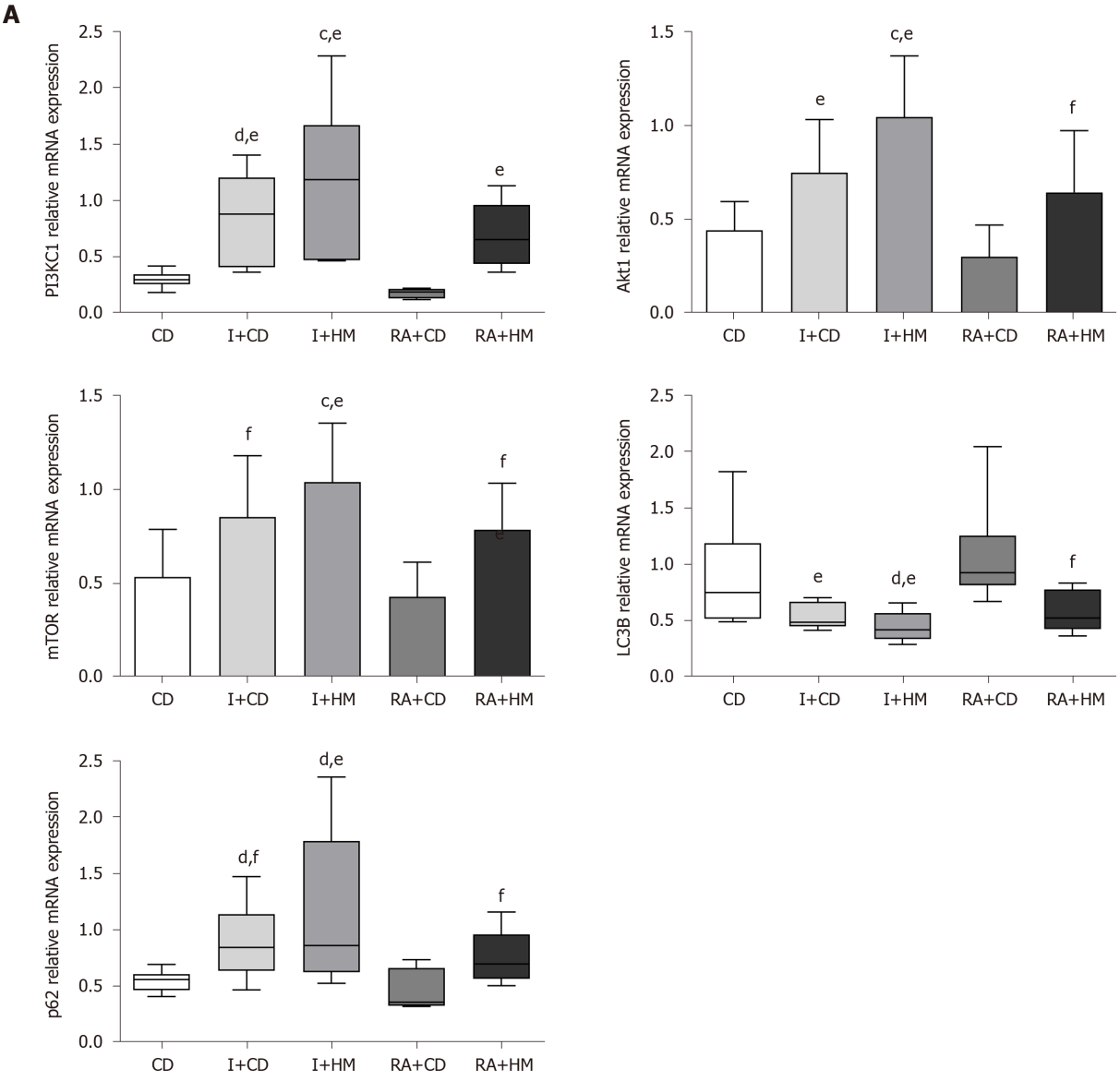
A
PI3KC1 relative mRNA expression
2.5
2.0
1.5
1.0
0.5
0.0
c,e
d,e
e
CD
I+CD
I+HM
RA+CD
RA+HM
Akt1 relative mRNA expression
1.5
1.0
0.5
0.0
c,e
e
f
CD
I+CD
I+HM
RA+CD
RA+HM
mTOR relative mRNA expression
1.5
1.0
0.5
0.0
c,e
f
f
CD
I+CD
I+HM
RA+CD
RA+HM
LC3B relative mRNA expression
2.5
2.0
1.5
1.0
0.5
0.0
e
d,e
f
CD
I+CD
I+HM
RA+CD
RA+HM
p62 relative mRNA expression
2.5
2.0
1.5
1.0
0.5
0.0
d,e
d,f
f
CD
I+CD
I+HM
RA+CD
RA+HM

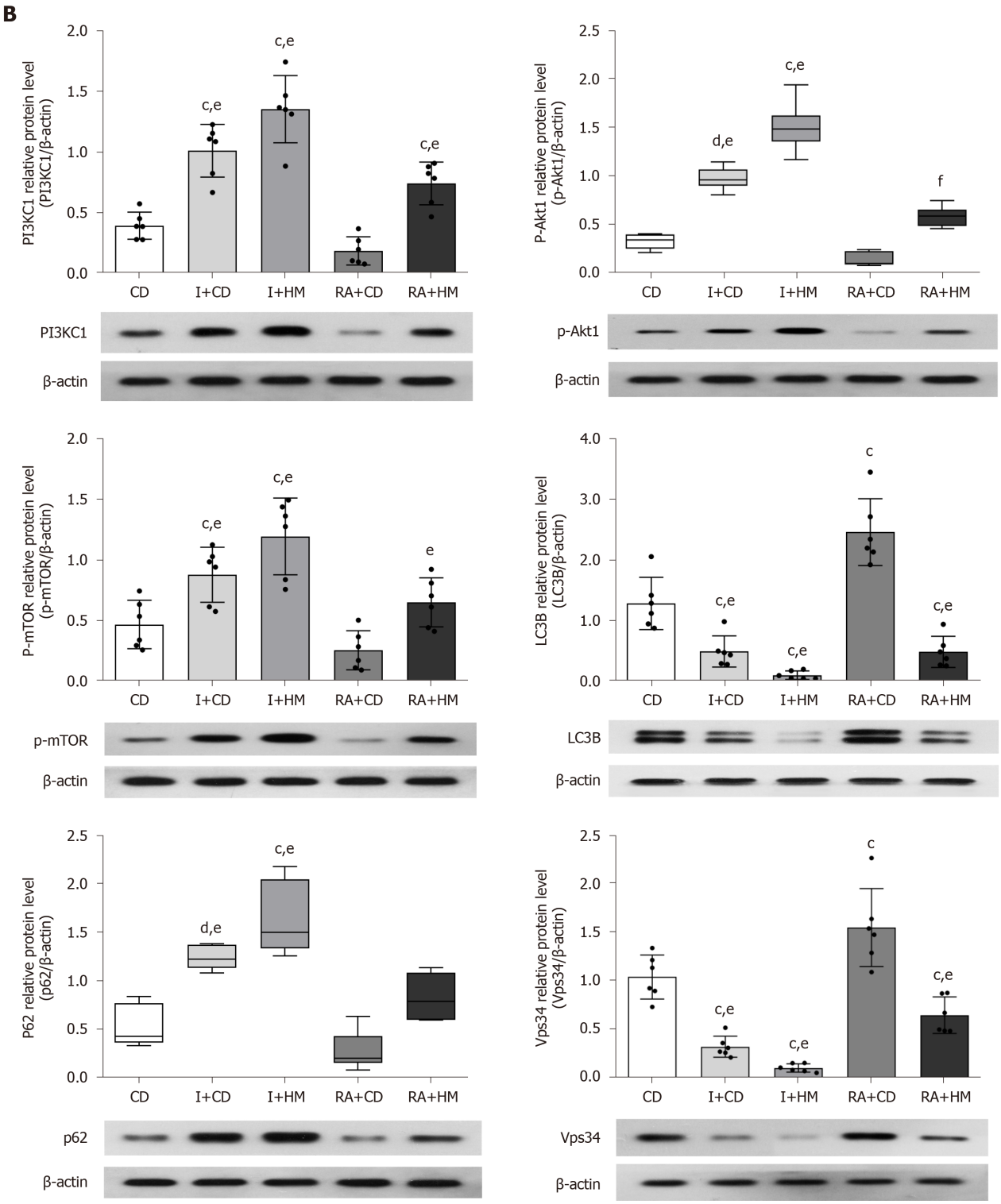

Figure 6 Herbal cake-partitioned moxibustion at the Qihai (CV6) and bilateral Tianshu (ST25) acupoints regulates the mRNA and protein expression of PI3KC signaling-related molecules in the colon tissues of Crohn's disease rats. A: The mRNA levels of phosphatidylinositol 3-kinase class I (*PI3KC1*), *Akt1*, mammalian target of rapamycin (*mTOR*), microtubule-associated protein 1 light chain 3 beta (*LC3B*), and sequestosome 1 (*p62*) were determined by real-time PCR; B: Expression changes of the PI3KC1, p-Akt1, mTOR, LC3B, p62, and class III phosphatidylinositol 3-kinase proteins evaluated by Western blot. Six independent experiments were analyzed, and the data are presented as the mean ± SD or medians (P25, P75). $^{c}P < 0.01$, $^{d}P < 0.05$ *vs* CD group; $^{e}P < 0.01$, $^{f}P < 0.05$ *vs* RA+CD group. CD: Crohn's disease; I + CD: Insulin + Crohn's disease; I + HM: Insulin + herbal cake-partitioned moxibustion; RA+CD: Rapamycin + Crohn's disease; RA + HM: Rapamycin + herbal cake-partitioned moxibustion; PI3KC1: Phosphatidylinositol 3-kinase class I; Akt1: Protein kinase B akt-1; p-Akt1: Phospho-protein kinase B akt-1; mTOR: Mammalian target of rapamycin; p-mTOR: Phospho-mammalian target of rapamycin; LC3B: Microtubule-associated protein 1 light chain 3 beta; p62: Sequestosome 1; Vps34: Class III phosphatidylinositol 3-kinase.

upregulated. These changes indicated that autophagy in colon tissue was further upregulated. Notably, the changes in these indicators were reversed by HM or/and insulin treatment. These results suggest that HM can inhibit excessively activated

autophagy during CD by activating the PI3K/Akt/mTOR signaling pathway.

PI3K class III currently contains only one member, PI3KC3, also known as Vps34[48], which is one of the main participants in autophagy[49]. Vps34 complexes with Beclin-1 (an autophagy-related protein 6 homolog) and provides a PI3P-rich domain that mediates autophagosome membrane formation[20,39]. Vps34-Beclin-1 complexes have been identified in mammals to play an important role in regulating autophagy[50]. For example, acetylation of Vps34 can inhibit the formation of the Vps34-Beclin 1 complex, thereby suppressing autophagy[51]. In contrast, phosphorylation of Beclin-1 can enhance the activity of the Vps34-Beclin1-ATG14L complex, thereby enhancing autophagy[52]. Studies have shown that insulin has an inhibitory effect on Vps34[38] and that inactivation of Vps34 enhances insulin-related effects[53]. Rapamycin can directly activate ULK1 by inhibiting mTOR; after activation of ULK1, rapamycin phosphorylates Beclin-1 at the Ser14 site, thereby strengthening Vps34-Beclin1-ATG14 complex activity, which is essential for autophagic vesicle formation and initiation of autophagy[21,54]. Based on the above findings, we observed the effect of HM on the Vps34-Beclin-1 complex core protein Vps34 in colon tissues. As expected, compared with the CD group, the CD + RA group exhibited further upregulation of VPS34 protein expression, and the Vps34 protein expression level was significantly downregulated after HM and/or insulin treatment. These results suggest that HM can inhibit overactivated autophagy by inhibiting the PI3KC3 (Vps34)-Beclin-1 protein complex.

CONCLUSION

In summary, our results suggest that HM can inhibit TNBS induced excessive autophagy in colon tissues of CD rats by activating PI3KC1/Akt1/mTOR signaling while inhibiting the PI3KC3 (Vps34)-Beclin-1 protein complex. Additionally, our findings raise the question of whether insulin has dual therapeutic effects on diabetic patients with CD. However, since the PI3KC signaling pathway may have different mechanisms between the two diseases, further clinical observations are needed to answer this question.

ARTICLE HIGHLIGHTS

Research background

Recent studies have shown that autophagy dysfunction plays an important role in the pathogenesis of Crohn's disease (CD). Our previous studies have indicated that herbal cake-partitioned moxibustion (HM) can attenuate inflammation and ameliorate pathological changes in colon tissue in CD. However, it is unclear whether HM can regulate colonic autophagy in CD.

Research motivation

The mechanism of HM in the treatment of CD has remained unclear. We sought to elucidate the relevant mechanism by which HM alleviates CD from the perspective of autophagy.

Research objectives

To observe the effect of HM on colonic autophagy in CD rats and further explore the underlying mechanism.

Research methods

2,4,6-trinitrobenzene sulfonic acid (TNBS) was used to establish a rat CD model. The morphology of the colonic mucosa, formation of autophagosomes, and expression of microtubule-associated protein 1 Light chain 3 beta (LC3B) were observed by hematoxylin-eosin staining, electron microscopy, and immunofluorescence staining, respectively. Insulin and rapamycin were used to inhibit and activate colonic autophagy, respectively. The mRNA expression levels of phosphatidylinositol 3-kinase class I (*PI3KC1*), *Akt1*, *LC3B*, sequestosome 1 (*p62*), and mammalian target of rapamycin (*mTOR*) and the protein expression levels of interleukin-18 (IL-18), tumor necrosis factor-α (TNF-α), nuclear factor κB/p65 (NF-κB p65), LC3B, p62, coiled-coil myosin-like BCL2-interacting protein (Beclin-1), p-mTOR, PI3KC1, class III

phosphatidylinositol 3-kinase (PI3KC3/Vps34), and p-Akt1 were evaluated by RT-qPCR and Western blot analysis, respectively.

Research results

Our experiments revealed that TNBS-induced inflammation activated autophagy in rat colon tissues. HM at the Qihai (CV6) and bilateral Tianshu (ST25) acupoints reversed the expression changes in the autophagy proteins LC3B, p62, Beclin-1, and p-mTOR in colon tissues while ameliorating colonic inflammation (indicated by IL-18, TNF-α, and NF-κB p65 levels) and damage. Furthermore, HM facilitated the repair of colonic epithelial cells. We hypothesized that the mechanisms by which HM alleviates CD may involve the PI3KC1/Akt1/mTOR pathway and the PI3KC3 (VPS34)-Beclin-1 protein complex and confirmed this hypothesis through our experiments.

Research conclusions

HM can activate the PI3KC1/Akt1/mTOR signaling pathway while inhibiting the PI3KC3 (VPS34)-Beclin-1 protein complex, thereby inhibiting overactivated colonic autophagy in CD rats.

Research perspectives

Our findings provide insights into the molecular mechanism of HM and shed new light on a cost-effective and safe therapy for CD.

REFERENCES

1 **Torres J**, Mehandru S, Colombel JF, Peyrin-Biroulet L. Crohn's disease. *Lancet* 2017; **389**: 1741-1755 [PMID: 27914655 DOI: 10.1016/S0140-6736(16)31711-1]

2 **Ng SC**, Tang W, Ching JY, Wong M, Chow CM, Hui AJ, Wong TC, Leung VK, Tsang SW, Yu HH, Li MF, Ng KK, Kamm MA, Studd C, Bell S, Leong R, de Silva HJ, Kasturiratne A, Mufeena MNF, Ling KL, Ooi CJ, Tan PS, Ong D, Goh KL, Hilmi I, Pisespongsa P, Manatsathit S, Rerknimitr R, Aniwan S, Wang YF, Ouyang Q, Zeng Z, Zhu Z, Chen MH, Hu PJ, Wu K, Wang X, Simadibrata M, Abdullah M, Wu JC, Sung JJY, Chan FKL; Asia–Pacific Crohn's and Colitis Epidemiologic Study (ACCESS) Study Group. Incidence and phenotype of inflammatory bowel disease based on results from the Asia-pacific Crohn's and colitis epidemiology study. *Gastroenterology* 2013; **145**: 158-165.e2 [PMID: 23583432 DOI: 10.1053/j.gastro.2013.04.007]

3 **Cui G**, Yuan A. A Systematic Review of Epidemiology and Risk Factors Associated With Chinese Inflammatory Bowel Disease. *Front Med (Lausanne)* 2018; **5**: 183 [PMID: 29971235 DOI: 10.3389/fmed.2018.00183]

4 **Abraham C**, Cho JH. Inflammatory bowel disease. *N Engl J Med* 2009; **361**: 2066-2078 [PMID: 19923578 DOI: 10.1056/NEJMra0804647]

5 **Bento CF**, Renna M, Ghislat G, Puri C, Ashkenazi A, Vicinanza M, Menzies FM, Rubinsztein DC. Mammalian Autophagy: How Does It Work? *Annu Rev Biochem* 2016; **85**: 685-713 [PMID: 26865532 DOI: 10.1146/annurev-biochem-060815-014556]

6 **Kim S**, Eun HS, Jo EK. Roles of Autophagy-Related Genes in the Pathogenesis of Inflammatory Bowel Disease. *Cells* 2019; **8** [PMID: 30669622 DOI: 10.3390/cells8010077]

7 **Iida T**, Yokoyama Y, Wagatsuma K, Hirayama D, Nakase H. Impact of Autophagy of Innate Immune Cells on Inflammatory Bowel Disease. *Cells* 2018; **8** [PMID: 30583538 DOI: 10.3390/cells8010007]

8 **Haq S**, Grondin J, Banskota S, Khan WI. Autophagy: roles in intestinal mucosal homeostasis and inflammation. *J Biomed Sci* 2019; **26**: 19 [PMID: 30764829 DOI: 10.1186/s12929-019-0512-2]

9 **Tschurtschenthaler M**, Adolph TE. The Selective Autophagy Receptor Optineurin in Crohn's Disease. *Front Immunol* 2018; **9**: 766 [PMID: 29692785 DOI: 10.3389/fimmu.2018.00766]

10 **Baxt LA**, Xavier RJ. Role of Autophagy in the Maintenance of Intestinal Homeostasis. *Gastroenterology* 2015; **149**: 553-562 [PMID: 26170139 DOI: 10.1053/j.gastro.2015.06.046]

11 **Plantinga TS**, Joosten LA, van der Meer JW, Netea MG. Modulation of inflammation by autophagy: consequences for Crohn's disease. *Curr Opin Pharmacol* 2012; **12**: 497-502 [PMID: 22342166 DOI: 10.1016/j.coph.2012.01.017]

12 **Lapaquette P**, Bringer MA, Darfeuille-Michaud A. Defects in autophagy favour adherent-invasive Escherichia coli persistence within macrophages leading to increased pro-inflammatory response. *Cell Microbiol* 2012; **14**: 791-807 [PMID: 22309232 DOI: 10.1111/j.1462-5822.2012.01768.x]

13 **Lapaquette P**, Glasser AL, Huett A, Xavier RJ, Darfeuille-Michaud A. Crohn's disease-associated adherent-invasive E. coli are selectively favoured by impaired autophagy to replicate intracellularly. *Cell Microbiol* 2010; **12**: 99-113 [PMID: 19747213 DOI: 10.1111/j.1462-5822.2009.01381.x]

14 **Pott J**, Maloy KJ. Epithelial autophagy controls chronic colitis by reducing TNF-induced apoptosis. *Autophagy* 2018; **14**: 1460-1461 [PMID: 29799774 DOI: 10.1080/15548627.2018.1450021]

15 **Lai SL**, Mustafa MR, Wong PF. Panduratin A induces protective autophagy in melanoma *via* the AMPK and mTOR pathway. *Phytomedicine* 2018; **42**: 144-151 [PMID: 29655680 DOI: 10.1016/j.phymed.2018.03.027]

16 **Lee JH**, Liu R, Li J, Wang Y, Tan L, Li XJ, Qian X, Zhang C, Xia Y, Xu D, Guo W, Ding Z, Du L, Zheng Y, Chen Q, Lorenzi PL, Mills GB, Jiang T, Lu Z. EGFR-Phosphorylated Platelet Isoform of Phosphofructokinase 1 Promotes PI3K Activation. *Mol Cell* 2018; **70**: 197-210.e7 [PMID: 29677490 DOI:

10.1016/j.molcel.2018.03.018]
17 **Zhu C**, Yin Z, Tan B, Guo W. Insulin regulates titin pre-mRNA splicing through the PI3K-Akt-mTOR kinase axis in a RBM20-dependent manner. *Biochim Biophys Acta Mol Basis Dis* 2017; **1863**: 2363-2371 [PMID: 28676430 DOI: 10.1016/j.bbadis.2017.06.023]
18 **Wang G**, Lu M, Yao Y, Wang J, Li J. Esculetin exerts antitumor effect on human gastric cancer cells through IGF-1/PI3K/Akt signaling pathway. *Eur J Pharmacol* 2017; **814**: 207-215 [PMID: 28847482 DOI: 10.1016/j.ejphar.2017.08.025]
19 **Heras-Sandoval D**, Pérez-Rojas JM, Hernández-Damián J, Pedraza-Chaverri J. The role of PI3K/AKT/mTOR pathway in the modulation of autophagy and the clearance of protein aggregates in neurodegeneration. *Cell Signal* 2014; **26**: 2694-2701 [PMID: 25173700 DOI: 10.1016/j.cellsig.2014.08.019]
20 **Wang S**, Li J, Du Y, Xu Y, Wang Y, Zhang Z, Xu Z, Zeng Y, Mao X, Cao B. The Class I PI3K inhibitor S14161 induces autophagy in malignant blood cells by modulating the Beclin 1/Vps34 complex. *J Pharmacol Sci* 2017; **134**: 197-202 [PMID: 28779993 DOI: 10.1016/j.jphs.2017.07.001]
21 **Russell RC**, Tian Y, Yuan H, Park HW, Chang YY, Kim J, Kim H, Neufeld TP, Dillin A, Guan KL. ULK1 induces autophagy by phosphorylating Beclin-1 and activating VPS34 lipid kinase. *Nat Cell Biol* 2013; **15**: 741-750 [PMID: 23685627 DOI: 10.1038/ncb2757]
22 **Shi Y**, Guo Y, Zhou J, Wu L, Chen L, Sun Y, Li T, Zhao J, Bao C, Wu H. Herbs-partitioned moxibustion improves intestinal epithelial tight junctions by upregulating A20 expression in a mouse model of Crohn's disease. *Biomed Pharmacother* 2019; **118**: 109149 [PMID: 31302421 DOI: 10.1016/j.biopha.2019.109149]
23 **Zhou J**, Wu LY, Chen L, Guo YJ, Sun Y, Li T, Zhao JM, Bao CH, Wu HG, Shi Y. Herbs-partitioned moxibustion alleviates aberrant intestinal epithelial cell apoptosis by upregulating A20 expression in a mouse model of Crohn's disease. *World J Gastroenterol* 2019; **25**: 2071-2085 [PMID: 31114134 DOI: 10.3748/wjg.v25.i17.2071]
24 **Weng ZJ**, Wu LY, Lü TT, Zhang F, Xie HR, Sun TA, Liu HR, Wu HG. Regulatory effects of herbal cake-partitioned moxibustion on the expressions of IL-17, IL-23 and their mRNAs in the colon of rats with Crohn's disease. *J Acupunct Tuina Sci* 2016; **14**: 156-163 [DOI: 10.1007/s11726-016-0917-3]
25 **Zhang D**, Ma X, Wu H, Hong J, Zhang C, Wu L, Liu J, Zhu Y, Yang L, Wei K, Yan H. Efficacy of herb-partitioned moxibustion at Qihai (CV 6) and bilateral Tianshu (ST 25) on colonic damage and the TLR4/NF-κB signaling pathway in rats with Crohn's disease. *J Tradit Chin Med* 2018; **38**: 218-226 [PMID: 32186061 DOI: 10.1016/j.jtcm.2018.04.004]
26 **Li ZY**, Yang YT, Hong J, Zhang D, Huang XF, Wu LJ, Wu HG, Shi Z, Liu J, Zhu Y, Ma XP. Extracellular signal-regulated kinase, substance P and neurokinin-1 are involved in the analgesic mechanism of herb-partitioned moxibustion. *Neural Regen Res* 2017; **12**: 1472-1478 [PMID: 29089993 DOI: 10.4103/1673-5374.215259]
27 **Morris GP**, Beck PL, Herridge MS, Depew WT, Szewczuk MR, Wallace JL. Hapten-induced model of chronic inflammation and ulceration in the rat colon. *Gastroenterology* 1989; **96**: 795-803 [PMID: 2914642]
28 **Wosen JE**, Mukhopadhyay D, Macaubas C, Mellins ED. Epithelial MHC Class II Expression and Its Role in Antigen Presentation in the Gastrointestinal and Respiratory Tracts. *Front Immunol* 2018; **9**: 2144 [PMID: 30319613 DOI: 10.3389/fimmu.2018.02144]
29 **Rodríguez-Arribas M**, Yakhine-Diop SM, González-Polo RA, Niso-Santano M, Fuentes JM. Turnover of Lipidated LC3 and Autophagic Cargoes in Mammalian Cells. *Methods Enzymol* 2017; **587**: 55-70 [PMID: 28253976 DOI: 10.1016/bs.mie.2016.09.053]
30 **Yao H**, Han X, Han X. The cardioprotection of the insulin-mediated PI3K/Akt/mTOR signaling pathway. *Am J Cardiovasc Drugs* 2014; **14**: 433-442 [PMID: 25160498 DOI: 10.1007/s40256-014-0089-9]
31 **Saiki S**, Sasazawa Y, Imamichi Y, Kawajiri S, Fujimaki T, Tanida I, Kobayashi H, Sato F, Sato S, Ishikawa K, Imoto M, Hattori N. Caffeine induces apoptosis by enhancement of autophagy *via* PI3K/Akt/mTOR/p70S6K inhibition. *Autophagy* 2011; **7**: 176-187 [PMID: 21081844 DOI: 10.4161/auto.7.2.14074]
32 **Sancak Y**, Thoreen CC, Peterson TR, Lindquist RA, Kang SA, Spooner E, Carr SA, Sabatini DM. PRAS40 is an insulin-regulated inhibitor of the mTORC1 protein kinase. *Mol Cell* 2007; **25**: 903-915 [PMID: 17386266 DOI: 10.1016/j.molcel.2007.03.003]
33 **Lee CC**, Huang CC, Hsu KS. Insulin promotes dendritic spine and synapse formation by the PI3K/Akt/mTOR and Rac1 signaling pathways. *Neuropharmacology* 2011; **61**: 867-879 [PMID: 21683721 DOI: 10.1016/j.neuropharm.2011.06.003]
34 **Wang LQ**, Cheng XS, Huang CH, Huang B, Liang Q. Rapamycin protects cardiomyocytes against anoxia/reoxygenation injury by inducing autophagy through the PI3k/Akt pathway. *J Huazhong Univ Sci Technolog Med Sci* 2015; **35**: 10-15 [PMID: 25673186 DOI: 10.1007/s11596-015-1381-x]
35 **Zhou L**, Xie Y, Li S, Liang Y, Qiu Q, Lin H, Zhang Q. Rapamycin Prevents cyclophosphamide-induced Over-activation of Primordial Follicle pool through PI3K/Akt/mTOR Signaling Pathway in vivo. *J Ovarian Res* 2017; **10**: 56 [PMID: 28814333 DOI: 10.1186/s13048-017-0350-3]
36 **Zeng Z**, Sarbassov dos D, Samudio IJ, Yee KW, Munsell MF, Ellen Jackson C, Giles FJ, Sabatini DM, Andreeff M, Konopleva M. Rapamycin derivatives reduce mTORC2 signaling and inhibit AKT activation in AML. *Blood* 2007; **109**: 3509-3512 [PMID: 17179228 DOI: 10.1182/blood-2006-06-030833]
37 **Sarbassov DD**, Ali SM, Sengupta S, Sheen JH, Hsu PP, Bagley AF, Markhard AL, Sabatini DM. Prolonged rapamycin treatment inhibits mTORC2 assembly and Akt/PKB. *Mol Cell* 2006; **22**: 159-168 [PMID: 16603397 DOI: 10.1016/j.molcel.2006.03.029]
38 **Liu HY**, Han J, Cao SY, Hong T, Zhuo D, Shi J, Liu Z, Cao W. Hepatic autophagy is suppressed in the presence of insulin resistance and hyperinsulinemia: inhibition of FoxO1-dependent expression of key autophagy genes by insulin. *J Biol Chem* 2009; **284**: 31484-31492 [PMID: 19758991 DOI: 10.1074/jbc.M109.033936]
39 **Saha S**, Panigrahi DP, Patil S, Bhutia SK. Autophagy in health and disease: A comprehensive review. *Biomed Pharmacother* 2018; **104**: 485-495 [PMID: 29800913 DOI: 10.1016/j.biopha.2018.05.007]
40 **Zhang F**, Wang W, Niu J, Yang G, Luo J, Lan D, Wu J, Li M, Sun Y, Wang K, Miao Y. Heat-shock

transcription factor 2 promotes sodium butyrate-induced autophagy by inhibiting mTOR in ulcerative colitis. *Exp Cell Res* 2020; **388**: 111820 [PMID: 31923427 DOI: 10.1016/j.yexcr.2020.111820]

41 **Talero E**, Alcaide A, Ávila-Román J, García-Mauriño S, Vendramini-Costa D, Motilva V. Expression patterns of sirtuin 1-AMPK-autophagy pathway in chronic colitis and inflammation-associated colon neoplasia in IL-10-deficient mice. *Int Immunopharmacol* 2016; **35**: 248-256 [PMID: 27085036 DOI: 10.1016/j.intimp.2016.03.046]

42 **McKenna M**, McGarrigle S, Pidgeon GP. The next generation of PI3K-Akt-mTOR pathway inhibitors in breast cancer cohorts. *Biochim Biophys Acta Rev Cancer* 2018; **1870**: 185-197 [PMID: 30318472 DOI: 10.1016/j.bbcan.2018.08.001]

43 **Singh BN**, Kumar D, Shankar S, Srivastava RK. Rottlerin induces autophagy which leads to apoptotic cell death through inhibition of PI3K/Akt/mTOR pathway in human pancreatic cancer stem cells. *Biochem Pharmacol* 2012; **84**: 1154-1163 [PMID: 22902833 DOI: 10.1016/j.bcp.2012.08.007]

44 **Wu YT**, Tan HL, Huang Q, Ong CN, Shen HM. Activation of the PI3K-Akt-mTOR signaling pathway promotes necrotic cell death *via* suppression of autophagy. *Autophagy* 2009; **5**: 824-834 [PMID: 19556857 DOI: 10.4161/auto.9099]

45 **Hawkins PT**, Stephens LR. PI3K signalling in inflammation. *Biochim Biophys Acta* 2015; **1851**: 882-897 [PMID: 25514767 DOI: 10.1016/j.bbalip.2014.12.006]

46 **Vanhaesebroeck B**, Guillermet-Guibert J, Graupera M, Bilanges B. The emerging mechanisms of isoform-specific PI3K signalling. *Nat Rev Mol Cell Biol* 2010; **11**: 329-341 [PMID: 20379207 DOI: 10.1038/nrm2882]

47 **Manning BD**, Cantley LC. AKT/PKB signaling: navigating downstream. *Cell* 2007; **129**: 1261-1274 [PMID: 17604717 DOI: 10.1016/j.cell.2007.06.009]

48 **Backer JM**. The regulation and function of Class III PI3Ks: novel roles for Vps34. *Biochem J* 2008; **410**: 1-17 [PMID: 18215151 DOI: 10.1042/BJ20071427]

49 **Xie Z**, Klionsky DJ. Autophagosome formation: core machinery and adaptations. *Nat Cell Biol* 2007; **9**: 1102-1109 [PMID: 17909521 DOI: 10.1038/ncb1007-1102]

50 **Funderburk SF**, Wang QJ, Yue Z. The Beclin 1-VPS34 complex--at the crossroads of autophagy and beyond. *Trends Cell Biol* 2010; **20**: 355-362 [PMID: 20356743 DOI: 10.1016/j.tcb.2010.03.002]

51 **Su H**, Yang F, Wang Q, Shen Q, Huang J, Peng C, Zhang Y, Wan W, Wong CCL, Sun Q, Wang F, Zhou T, Liu W. VPS34 Acetylation Controls Its Lipid Kinase Activity and the Initiation of Canonical and Non-canonical Autophagy. *Mol Cell* 2017; **67**: 907-921.e7 [PMID: 28844862 DOI: 10.1016/j.molcel.2017.07.024]

52 **Qian X**, Li X, Cai Q, Zhang C, Yu Q, Jiang Y, Lee JH, Hawke D, Wang Y, Xia Y, Zheng Y, Jiang BH, Liu DX, Jiang T, Lu Z. Phosphoglycerate Kinase 1 Phosphorylates Beclin1 to Induce Autophagy. *Mol Cell* 2017; **65**: 917-931.e6 [PMID: 28238651 DOI: 10.1016/j.molcel.2017.01.027]

53 **Bilanges B**, Alliouachene S, Pearce W, Morelli D, Szabadkai G, Chung YL, Chicanne G, Valet C, Hill JM, Voshol PJ, Collinson L, Peddie C, Ali K, Ghazaly E, Rajeeve V, Trichas G, Srinivas S, Chaussade C, Salamon RS, Backer JM, Scudamore CL, Whitehead MA, Keaney EP, Murphy LO, Semple RK, Payrastre B, Tooze SA, Vanhaesebroeck B. Vps34 PI 3-kinase inactivation enhances insulin sensitivity through reprogramming of mitochondrial metabolism. *Nat Commun* 2017; **8**: 1804 [PMID: 29180704 DOI: 10.1038/s41467-017-01969-4]

54 **Pyo KE**, Kim CR, Lee M, Kim JS, Kim KI, Baek SH. ULK1 O-GlcNAcylation Is Crucial for Activating VPS34 *via* ATG14L during Autophagy Initiation. *Cell Rep* 2018; **25**: 2878-2890.e4 [PMID: 30517873 DOI: 10.1016/j.celrep.2018.11.042]

World Journal of Gastroenterology

Submit a Manuscript: https://www.f6publishing.com

World J Gastroenterol 2020 October 21; 26(39): 6015-6026

DOI: 10.3748/wjg.v26.i39.6015

ISSN 1007-9327 (print) ISSN 2219-2840 (online)

ORIGINAL ARTICLE

Case Control Study

Single access laparoscopic total colectomy for severe refractory ulcerative colitis

John Burke, Des Toomey, Frank Reilly, Ronan Cahill

ORCID number: John Burke 0000-0002-9519-3890; Des Toomey 0000-0003-1788-778X; Frank Reilly 0000-0002-7938-6780; Ronan Cahill 0000-0002-1270-4000.

Author contributions: All authors contributed substantially to this work; Cahill R was involved in study concept and design; Burke J, Toomey D and Reilly F were involved in data collection; all authors contributed to data analysis, manuscript drafting and approval.

Institutional review board statement: The study was reviewed and approved by the Institutional Review Board at the Mater Misericordiae University Hospital Clinical Audit and Effectiveness Committee.

Conflict-of-interest statement: No author has a conflict of interest with regard to the subject of this work.

Data sharing statement: Data will be made available *via* the UCD data registry and also on request.

John Burke, Des Toomey, Frank Reilly, Department of Colorectal Surgery, Beaumont Hospital, Dublin D09, Ireland

Ronan Cahill, Department of Surgery, Mater Misericordiae University Hospital, Dublin D07, Ireland

Corresponding author: Ronan Cahill, FRCS, MBBAOBCh, MD, Professor, Department of Surgery, Mater Misericordiae University Hospital, 47 Eccles Street, Dublin D01, Ireland. ronan.cahill@ucd.ie

Abstract

BACKGROUND

Single port laparoscopic surgery allows total colectomy and end ileostomy for medically uncontrolled ulcerative colitis solely *via* the stoma site incision. While intuitively appealing, there is sparse evidence for its use beyond feasibility.

AIM

To examine the usefulness of single access laparoscopy (SAL) in a general series experience of patients sick with ulcerative colitis.

METHODS

All patients presenting electively, urgently or emergently over a three-year period under a colorectal specialist team were studied. SAL was performed *via* the stoma site on a near-consecutive basis by one surgical team using a "surgical glove port" allowing group-comparative and case-control analysis with a contemporary cohort undergoing conventional multiport surgery. Standard, straight rigid laparoscopic instrumentation were used without additional resource.

RESULTS

Of 46 consecutive patients requiring surgery, 39 (85%) had their procedure begun laparoscopically. 27 (69%) of these were commenced by single port access with an 89% completion rate thereafter (three were concluded by multi-trocar laparoscopy). SAL proved effective in comparison to multiport access regardless of disease severity providing significantly reduced operative access costs (> 100€case) and postoperative hospital stay (median 5 d *vs* 7.5 d, $P = 0.045$) without increasing operative time. It proved especially efficient in those with preoperative albumin > 30 g/dL ($n = 20$). Its comparative advantages were further confirmed in ten pairs case-matched for gender, body mass index and preoperative albumin.

Manuscript source: Invited manuscript

Received: December 31, 2019
Peer-review started: December 31, 2019
First decision: February 19, 2020
Revised: June 15, 2020
Accepted: October 12, 2020
Article in press: October 12, 2020
Published online: October 21, 2020

P-Reviewer: Bandyopadhyay SK, Weiss H, Yang MS
S-Editor: Zhang L
L-Editor: A
P-Editor: Ma YJ

SAL outcomes proved durable in the intermediate term (median follow-up = 20 mo).

CONCLUSION
Single port total colectomy proved useful in planned and acute settings for patients with medically refractory colitis. Assumptions regarding duration and cost should not be barriers to its implementation.

Key Words: Single incision laparoscopy; Minimal access surgery; Inflammatory bowel disease; Ulcerative colitis; Total colectomy and end ileostomy; Case match analysis

Core Tip: Single access laparoscopy performed *via* the stoma site for patient's sick with ulcerative colitis and needing total colectomy with ileostomy is shown to be appropriate and with some advantages over its multiport equivalent. Operative costs and total hospital stay were significantly reduced with the Single access laparoscopy approach (using a "glove port") and outcomes were sustained in the intermediate term.

Citation: Burke J, Toomey D, Reilly F, Cahill R. Single access laparoscopic total colectomy for severe refractory ulcerative colitis. *World J Gastroenterol* 2020; 26(39): 6015-6026
URL: https://www.wjgnet.com/1007-9327/full/v26/i39/6015.htm
DOI: https://dx.doi.org/10.3748/wjg.v26.i39.6015

INTRODUCTION

The acceptance of the clear advantages of laparoscopy over open surgery for patients with inflammatory bowel disease[1], particularly in the acute setting[2-4], has been relatively recent[5]. For patients undergoing a total abdominal colectomy for ulcerative colitis (UC), a laparoscopic approach is associated with lower overall complication and mortality rates[6]. However, surgical technique and technology continues to undergo evolutionary change.

Single access laparoscopic (SAL) surgery is a recent modified access technique that allows grouping of laparoscopic instrumentation at a single confined site in the abdomen in order to further minimize the degree of parietal wounding associated with intraperitoneal surgery. Meta-analyses demonstrate that overall, SAL for segmental colorectal resection compared to standard multiport approaches has no difference in conversion to open laparotomy, morbidity or operation time but a significantly shorter total skin incision and a shorter post-operative length of stay is observed[7]. As the size of an ileostomy approximates that of a single port access site, total colectomy with end ileostomy should be ideally suited to this access modality. Early reports demonstrated that with judicious patient selection and considered operative technique, SAL total colectomy for medically UC can be safely performed[8]. To date however, experience analyses have predominantly focused on feasibility and technical adequacy in small series predominantly in the elective setting and mostly without a concurrent comparative cohort[8-12].

Here we analyze, including case-matching, our experience of SAL in a consecutive series of patients requiring planned, urgent or emergency total colectomy for refractory UC in comparison with contemporaneous others in the same departments undergoing multiport access colectomy. The purpose of this study is to examine the role of this access in an all-comers experience reflective of general practice in patients with UC including those with acute severe colitis and those with severe disease and systemic toxicaemia in debilitated condition as indicated by symptoms, endoscopy and biochemistry including albumin and inflammatory markers. This a retrospective study of a clinical experience whose details were recorded prospectively.

MATERIALS AND METHODS

All patients presenting for total colectomy with end ileostomy for medically refractory severe UC to a tertiary referral centre over a 36-mo period were considered for inclusion regardless of urgency of presentation. Patients requiring surgery for dysplasia or neoplasia were excluded. Laparoscopic surgery is the standard approach for all colorectal resections in the departments although only one surgeon has trained in SAL. All procedures were performed either solely by a Senior Resident alongside the scrubbed consultant or shared between the two depending on procedure circumstance, difficulty and duration as would be our typical practice within a teaching hospital.

Preoperative preparation

Those patients already in the hospital and those who were referred as out-patients for planned resections were prepared for surgery similarly with the latter routinely being admitted on the morning of surgery. Preoperative mechanical bowel preparation for bowel cleansing was not utilized. All patients were marked for optimal stoma site by a specialist nurse practitioner or senior member of the Surgical Team. A formal Enhanced Recovery Programme with a dedicated nurse specialist was in place over the duration of the study period and implemented uniformly across all surgical teams. All patients received standard anti-thrombosis and antimicrobial prophylaxis and underwent general anesthesia without epidural/spinal anesthesia. The anaesthetized patient was placed in a Trendelenburg position on an anti-slip beanbag and painted and draped in the standard fashion.

Single port access device

The single port access device of preference was the "Surgical Glove Port"[13]. Constructed table-side, in short, this comprises a standard surgical glove into which laparoscopic trocar sleeves (one 10 mm and two 5 mm) are inserted without needing obturators into three fingers cut at their tips (Figure 1). The ports are tied in position using strips cut from the other glove in the pair and the cuff of the "Glove port" stretched onto the outer ring of a wound protector-retractor (ALEXIS™ XS, Applied Medical) sited in the operative access wound.

Single port procedure

A local anesthetic block (bupivicaine) was infiltrated around the intended incision site in the right iliac fossa at the site planned ultimately for stoma maturation. A 3 cm skin and fascial incision was measured and made in the appropriate site. On securing safe entry into the peritoneum, a wound protector-retractor was placed into the wound and its outer ring adjusted down to the abdominal wall. The "Glove Port" was then stretched onto the outer ring. The operation was performed using standard rigid laparoscopic instruments, a 10 mm 30° high definition laparoscope (where possible using the Endoeye™, Olympus Corporation, which has sterilized in-line optical cabling) along with an atraumatic grasper and an energy sealer-divider (Ligasure, Covidien). Total colectomy with end ileostomy for colitis recalcitrant to medical therapy was performed as previously described[14]. In brief, early rectosigmoid transection was achieved by laparoscopic stapling at the level of the sacral promonitory. Thereafter the operation was performed progressively quadrant by quadrant, working in a close pericolic plane and proceeding distal to proximal until the caecum was reached. After intracorporeal stapling across the distal ileum, the entire colon was then withdrawn "caecum first" *via* the stoma site. Relaparoscopy was performed *via* the stoma site and the rectal stump checked in addition to peritoneal lavage and haemostasis control. The end ileostomy was then matured at the single port access site (Figure 2).

Multiport procedure

The multiport procedure was performed in a conventional fashion typically beginning with an open induction of the pneumoperitoneum in a subumbilical site and thereafter typically employing four additional trocars of between 5 and 10 mm diameter (two on the left side and two on the right). The specimen was extracted either *via* the stoma site incision or *via* a separate incision (most commonly a dedicated Pfanniestiel, suprapubic or subumbilical incision). Local anaesthetic was infiltrated at all wounds on completion of the procedure.

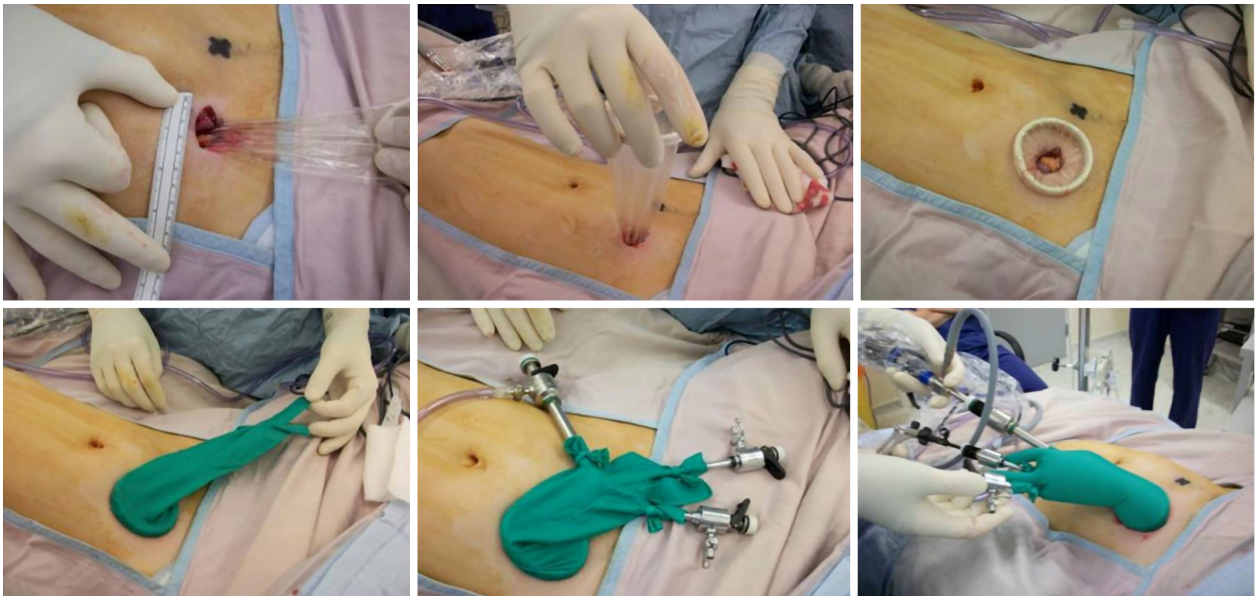

Figure 1 Photographs detailing the surgical glove port set-up for single port total colectomy with end ileostomy.

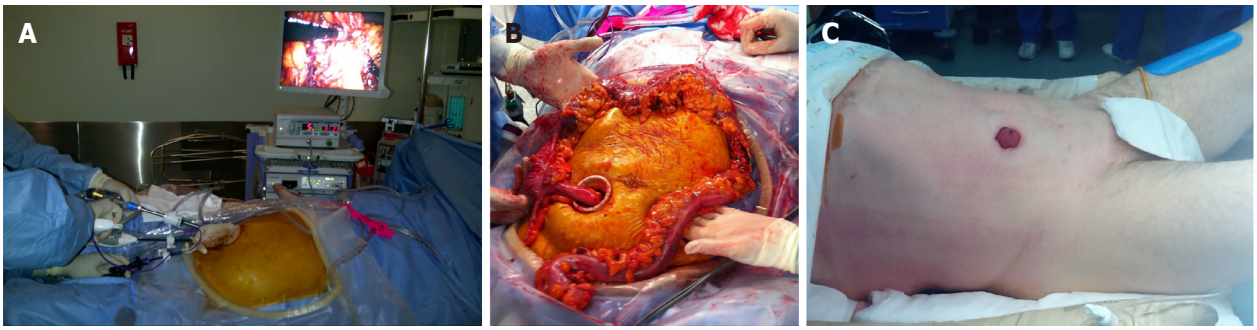

Figure 2 The end ileostomy was then matured at the single port access site. Intraoperative photographs showing (A) operating *via* the stoma site port during the procedure (B) the colonic specimen after extraction *via* the stoma site incision (C) The end ileostomy fashioned at the site of the single port as the only operative incision.

Access selection

SAL was the preferred commencement access of RAC in patients considered potentially suitable (precluding exceptional cases) and so this approach required this surgeon be available. As many patients with UC can undergo planned surgery rather than needing immediate operation this allowed the majority of patients be considered for this approach. There was no especial referral to any particular surgeon for the patients who tended to be seen by the surgeon taking acute referrals at the time of surgical need.

Postoperative management

All patients were managed postoperatively using an enhanced recovery protocol. Analgesia was by means of patient-controlled analgesia transitioning to oral medicines once oral diet commenced. Patient with extraction site or laparotomy wounds had local an aesthetic infusion catheters placed at time of wound closure. Nasogastric tubes were routinely removed at procedure completion and the patients are mobilized within the first 6-12 h of surgery. Oral intake was commenced on demand commencing within six hours of surgery and built up steadily as tolerated thereafter. Urinary catheters were removed on the first postoperative day. Intra-abdominal drains and transanal decompressive catheters were placed by surgeon judgment and were removed on or before the third postoperative day.

Ethical considerations

Departmental approval was agreed in advance of this experience. The technique of

SAL was not itself considered experimental as it is a variation of standard multiport laparoscopy that has been already proved valid and feasible and is in common use for other resectional procedures in the department. All patients were fully consented regarding the approach and informed of alternatives. As the intention in treatment was always to ensure safe, effective and efficient surgery, all patients were assured a low threshold for conversion if any deviation from operative plan was encountered. The authors have no conflicts of interest or relevant disclosures to declare with respect to this report.

Data collection and analysis

Patient demographics along with their clinical, haematological, biochemical and radiological profiles and disease characteristics were recorded prospectively on a dedicated database in addition to operative and postoperative details. Access equipment and length of stay costs were determined by the directorate business manager. Postoperative classifications were categorized as by Clavien-Dindo[15]. Unless otherwise stated, data is represented as median (range) and *n* represents the number of patients included in the analysis. Differences in categorical variables were evaluated using a Pearson's chi-squared test and differences in continuous variables were evaluated using Mann–Whitney *U* and Student's *t*-testing where appropriate (the latter for comparison between paired patients). All calculations were done using SPSS version 12.0 (SPSS, Inc., Chicago, IL, United States).

RESULTS

Over the thirty-six month study period, 46 patients with confirmed UC required scheduled, urgent or emergency total colectomy with end ileostomy by a colorectal specialist consultant for medically uncontrolled severe disease alone. Overall, the median age (range) was 38 (19-73) years and median (range) body mass index was 22.8 (17.3-38.9) kg/m^2. Twenty-six patients were male. Nine patients had acutely severe disease resulting in clinical deteriorating conditions with toxaemia and low preoperative albumin (< 30 g/dL). Thirteen patients had their surgery performed on scheduled lists while the others were done either urgently (n = 25) or emergently (n = 8). Overall, co-morbidity was low (one patient had multiple sclerosis while two had asthma). Only five patients had had prior abdominal surgery (only one had a prior midline laparotomy and another was a renal transplant recipient).

All patients were considered for a laparoscopic approach ab initio with 39 (85%) having their procedure commenced in such fashion at the attending surgeon's discretion. 29 of these patients were already inpatient in the hospital under the care of the gastroenterology service for an acute exacerbative episode. The other ten patients were admitted specifically for surgery. 27 patients (59% of total cohort, 69% of those having laparoscopic surgery) had their procedure begun *via* a single port approach (three on scheduled lists) with a completion rate thereafter of 89% (Table 1). The SAL approach patients were begun consecutively on a non-selected basis with the exception of two patients (7% of this cohort) over the time period who had their operation commenced by multiport laparoscopic access due to exceptional co-morbidity (one had concurrent acute bilateral ileofemoral deep venous thrombosis and steroid psychosis while the other had congenital micrognathia and oesphageotracheal atresia with long-term feeding jejeunostomy) and both were in fact converted to open operations due to extreme friability of the colon. The three "converted" SAL patients had between 1 (n = 2) and three additional trocars inserted for reasons of difficult splenic flexure mobilization, intra-operative evidence of colitis-related perforation and extensive adhesiolysis (related to prior open nephrectomy for trauma) respectively. All patients in the SAL group had their specimens removed *via* the stoma site incision. Ten other patients had their operation performed by a multiport approach (no conversions) while the remaining seven patients had their operations commenced *via* laparotomy by other surgeons in the department (Table 2).

The characteristics of the patients undergoing surgery are shown by access (both at start and by completion) in Table 1 and postoperative complications for patients undergoing laparoscopic surgery are shown in Table 3. Overall there was no significant difference between the groups in terms of age, gender, Body mass index (BMI) or preoperative disease suppressant medications and the postoperative morbidity was predominantly reflective of the severity of the disease process rather than of operative access route. One patient in the single port group (4%), required an early return to theatre for a fascial release for an oedematous stoma while, after a

Table 1 Characteristics of patients undergoing total colectomy and end ileostomy for medically refractory colitis by laparoscopic access including how commenced and completed and by patient preoperative albumin

	Single port started (*n* = 27)	Single port completed (*n* = 24)	Single port completed, preop Alb > 30 (*n* = 18)	Single port completed, preop Alb < 30 (*n* = 6)	Multiport started (*n* = 12)	Multiport completed (*n* = 13)	Multiport completed, Alb > 30 (*n* = 12)
Median age (yr)	37	36	39	34.4	36.6	37.6	41
Range	19-59	19-59	19-59	29-45	18-70	31-70	33-69
Median BMI (kg/m^2)	23.3	23	23.5	21.4	22.2	25.8	25.9
Range	18.9-31.8	18.9-31.8	18.9-31.8	20.1-24.7	17.3-38	17.3-38.9	17.3-38.9
Males	16 (59%)	14 (58%)	9 (50%)	4 (66%)	4 (33%)	4 (31%)	4 (33%)
Anti-TNF agents	16 (59%)	14 (58%)	9 (50%)	5 (83%)	7 (58%)	9 (69%)	8 (66%)
Median preop Alb	36	37	39	24.5	38	38	38
Range	17-44	17-44	30-44	17-28	15-43	27-44	32-44
Median preop Hb	12.9	12.6	13.1	10.4	11.6	11.9	12
Range	7.9-17.2	7.9-17.2	7.9-17.2	8.4-13.2	8.2-13.5	8.2-14.6	8.2-14.6
Median preop CRP	29	25	10	51	9	9	18.7
Range	1-221	1-221	1-53	21-221	1-7	1-71	1-71
Total OT time (min)	290	285	285	275	300	302	301
Range	100-395	100-380	100-380	250-363	200-423	200-420	200-420
Operative time (min)	182	180	180	177.5	205	235	230
Range	90-270	90-270	90-270	150-240	120-345	120-345	120-345
Postop length of stay	5	5	5	7.5	7.5	8	7
Range	3-21	3-21	3-9	3-12	4-31	4-23	4-23

Alb: Albumin; BMI: Body mass index; CRP: C-reactive protein; Hb: Haemoglobin; Min: Minutes; OT: Operating theatre; Preop: Preoperative.

median follow-up of 20 mo (range 5-40 mo), two patients (7%) who had single port surgery have had parastomal hernia requiring repair (one done at the same time as completion proctectomy). One patient in the multiport group has complained of a parastomal hernia after an overall mean follow-up of 19 mo (range 1-25 mo).

As compared to other patients with preoperative albumin > 30 g/dL, those having laparoscopic surgery with preoperative albumin < 30 g/dL (n = 9, 7 of whom had their procedure started by SAL with one in this group being converted to multiport access) were significantly more likely to be anaemic (median preoperative haemoglobin 10.4 *vs* 12.25, P = 0.002) and have elevated preoperative (median 10 *vs* 51, P = 0.03) and postoperative C-Reactive Protein (CRP) levels (Figure 3). They were also more likely to have an urgent or emergent operation and to be converted from their initial access approach whether started by multi-port or single-port.

As a group overall, patients having their surgery by single port access had a significantly shorter postoperative hospital stay (5 d *vs* 7.5 d, P = 0.045) being especially evident in those who were non-toxic (P = 0.034) and who also had their surgery completed by this access (P = 0.005). Furthermore, these patients were also significantly more often discharged on or before day 5 as compared with patients undergoing multiport surgery (P = 0.04, Pearson Chi-square). While as an overall group the single port patients had trends towards reduced operative time (P = 0.46) and total theatre occupancy (P = 0.85), these did not reach statistical significance. There

Table 2 Characteristics of patients undergoing total colectomy and end ileostomy for medically refractory colitis by laparotomy (either at commencement or by completion)

	Laparotomy commenced (*n* = 7)	Laparotomy completed (*n* = 9)
Age (yr)	49	45
Range	26-73	22-73
Males	6 (85%)	8 (88%)
Preop Alb	30	27
Range	15-42	(15-42)
Median length of stay	11	16
Range	7-56	7-56

Alb: Albumin.

was also no significance difference overall in terms of resumption of bowel function, postoperative pain scores, analgesia requirements, daily CRP levels or complications. Interestingly, although patients who were toxic and underwent single port surgery had a significantly longer hospital stay (median 9 d, $P = 0.03$) as well as CRP levels on each day before and after their surgery than those non-toxic patients having the same operation by the same access approach, there was no significant difference in terms of operating length of time or indeed with postoperative length of stay between these patients and those having multiport access (whether as a group overall or those with preoperative albumin > 30 g/dL) with a median hospital stay of 7.5 and 7 d respectively.

Case-matching for gender, albumin > 30 g/dL and BMI (+/-3 kg/m^2) in addition to commencement and completion by method of laparoscopic access, surgery type and indication, presented 10 pairs for analysis. Comparison between the groups again shows significant difference in favour for single port surgery for postoperative length of stay, both by group medians ($P = 0.02$ Student's *t*-test) as well as day of discharge on or before day 5 ($P = 0.02$ Pearson Chi-square) with no significant difference in either operative time or total theatre occupancy. While there was no significant difference in terms of opiate requirement or pain score, the trend was in favour of single port access for opiate requirement (day 3, $P = 0.07$).

Economically, the cost of the glove port per case is €63.80 (comprising wound protector with three trocar sleeves). Assuming the use of disposable trocars, as compared to a four port trocar technique (comprising a balloon Hassan Port, a 12 mm port with obturator for stapling as well as one 5 mm trocar with obturator and another one without) there is a cost saving of €101.10 per case (a wound protector is also used in the latter cases while both techniques require two staplers fires, an energy sealer and suction/irrigation). The cost of a 24-h stay in our unit has been averaged at €950. Therefore, the total cost saving when a SPLS total colectomy is compared to case matched multiport equivalent is €2476.10.

DISCUSSION

Aside from isolated cases and small series describing elective colectomy for colitis, the effectiveness and appropriateness of SAL for severe colitis has only recently begun to be specifically reflected in the literature. Its practitioners view SAL as particularly useful for these individuals who are often slim and young and without previous laparotomy and who value body image[16,17]. Psychologically, a minimally invasive approach may also seem less traumatic. Many in addition will need their surgery performed urgently at a time when they are physically and immunologically debilitated and so have an impaired capacity for wound healing. Furthermore, such patients have to come to terms with managing a stoma in the early postoperative period and an ability to concentrate on this alone rather than any additional abdominal wall wounds may be advantageous. Many in this group will also need further surgery in the future for proctectomy with or without restorative ileal pouch-anal reconstruction. Preservation of the majority of the abdominal wall to facilitate future surgery along with the minimization of peritoneal adhesions could therefore be

Table 3 Postoperative complications after laparoscopic total colectomy and end ileostomy presented for groups by how operation was commenced as per Clavian-Dindo (contracted form)

Complication grade	Definition by Clavien-Dindo	Single port group (*n* = 27)		Multiport group (*n* = 12)	
First 30 d		*n*	Comment	*n*	Comment
I	Any deviation from postop course without intervention	3	Serous discharge from around stoma site (all patients albumin < 30)	3	Persistent pneumoperitoneum with pain; Non-cardiac chest pain, high output stoma
II	Pharmacological treatment	2	Parastomal wound infection; Portal vein thrombosis treated by anticoagulation diagnoses after discharge	2	Parastomal wound infection; Umbilical port infection (pt started single port, converted due to adhesions); Portal vein thrombosis treated by anticoagulation (CT diagnosis on day 2 postop in patient begun multiport and converted to open due to extreme colonic friability)
III	Surgical, endoscopic or radiological intervention	1	Return to theatre on day 4 postop for fascial release for oedematous stoma (pt with preop Alb < 30)	2	Radiological drain of intrabdominal collection in one patient started by single port but converted to multiport laparoscopy and in another started by multiport but converted to open (retroperitoneal colon perforations found at surgery)
IV/V	Life-threatening complication/Death	0	-	0	-
After 30 d			Median follow-up 12.3 mo		Median follow-up 10.5 mo
I		0	-	1	Parastomal hernia
III		2	Both parastomal hernia requiring repair. (One performed at time of complection proctectomy, other requiring urgent laparoscopic repair)		

Alb: Albumin; Preop: Preoperative; CT: Computed tomography; pt: Pharmacological treatment.

advantageous. SAL may therefore be particularly relevant to this patient cohort.

While prior series have compared patients undergoing SAL and multiport total colectomy[18] or total proctocolectomy and ileal pouch anal anastomosis[19], these have predominantly been performed solely with respect to the elective setting. The current data represents an all comers' experience, including both planned and urgent total colectomies for ulcerative colitis whether or not the procedure could be included on a scheduled list. Importantly no patient in this cohort is purely elective in that all suffered a debilitating disease requiring operative intervention and indeed most were already inpatients under the gastroenterology service or urgent transfers from outside institutions and were therapeutically immunosuppressed. This is why these patients were chosen to undergo total colectomy and end ileostomy while of course patients presenting purely electively for surgical relief of ulcerative colitis can undergo panproctocolectomy with ileo-anal pouch formation as part of a two stage procedure towards gastrointestinal reconstitution (rather than three stage as is our practice with the sicker medically refractory group). The current data demonstrates that both overall and when matched for gender, preoperative albumin, BMI and method of completion, SAL was directly applicable to this patient group and provided shorter postoperative

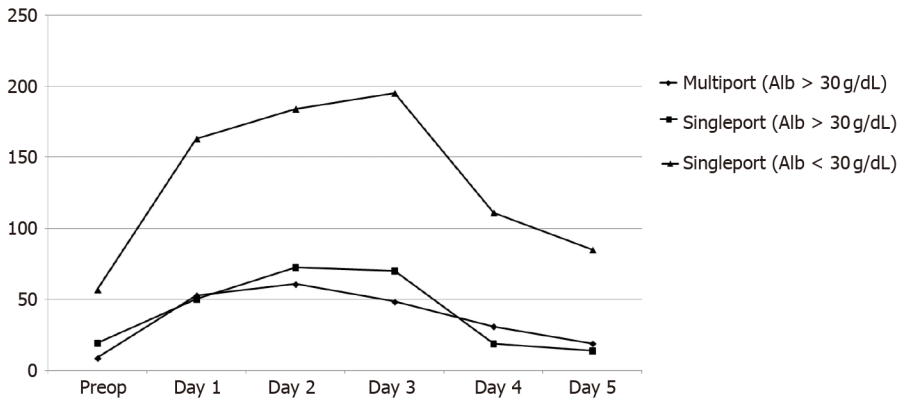

Figure 3 Daily median C-reactive protein level following surgery by access (multiport versus single port) including by the patients preoperative albumin (< or > 30 g/dL).

length of stays without increased operative time then patients undergoing the same operation for the same disease by a multiport access approach.

Preoperative albumin level is a reasonable indicator of preoperative clinical deterioration upon which to case match disease severity[20] as, in general, pre-operative hypoalbuminaemia is associated with increased surgical site infection following gastrointestinal surgery[21] and, specifically for patients undergoing laparoscopic total abdominal colectomy for ulcerative colitis, is associated with reoperation[22]. Furthermore, prior series have shown a higher pre-operative serum albumin is associated with performance of a laparoscopic approach[23]. This study shows that, while the advantages of the single port access are particularly evident in those undergoing their surgery when in a less toxic state, single port access can also be implemented in sicker patients without significantly compromise of theatre or hospital efficiency as compared to patients undergoing multiport total colectomy although the numbers are too limited to define specific comparative advantage in relation to wound healing in this cohort.

Therefore the current experience has shown that SAL allows completion of surgery *via* the stoma site alone as the only point of transabdominal access, thereby obviating any additional port sites, in the majority of cases. While not the same magnitude of advance that laparoscopy represents over laparotomy (prior to introduction of laparoscopy as access of preference in 2010, the median length of stay for this category of operation overall was ten days in our unit), there are nonetheless advantages for both the patient and healthcare provider. Although the morbidity associated with 5 mm internal diameter trocars is considered minimal, colorectal surgery typically requires a stapler and/or clip applicator and so mandates at least one extra 12 mm port, a diameter more likely to be associated with postoperative complications including discomfort, infection and fascial herniation[24]. Furthermore, the sole site of abdominal wounding is confined to one small area of the parietal wall, a factor likely to favor effective local postoperative analgesic techniques reducing opiate requirements although the current data show did not show a statistically significant difference in this parameter compared between the groups (indeed it is difficult from this data to be specific regarding why exactly the confined access route translated into significantly shortened postoperative hospital stays).

Although demonstrated feasible for colorectal surgery in general[7], some experts continue to feel SAL is undermined by the current expense of the commercially available devices[25]. Our choice of access port obviates this issue proving in fact cheaper than the multi-port equivalent as the surgical glove port needs only trocar sleeves rather than the otherwise necessary obturators. In addition, because these ports are placed into the glove space (and so are in fact extracorporeal) rather than into the patient means that the risk visceral or vascular injury at the time of trocar placement is reduced. However the main advantage of this innovative access modality is its performance which is, in our experience, better than the commercial equivalent by virtue of its elasticity and lack of fulcrum point (permitting enhanced horizontal, vertical and rotational maneuverability as well as augmented instrument tip ab/adduction and triangulation) while being equally stable and durable during a case. Furthermore, the device is always available (without needing prepurchasing), applicable to every patient regardless of body wall depth (due to the adaptable wound protector-retractor component) and is associated with no financial penalty if

conversion to a multiport or open operation is required due to the specifics of the patient or case. Also there were no costs accrued due to loss of theatre efficiency, in fact the operative time of a SAL total colectomy tended to be shorter than its multiport equivalent (although interestingly any potential gain in this aspect is noticeably offset by the fact overall theatre occupancy was the same reflecting a need for engagement and focus of the entire perioperative team in order to maximize any potential gain associated with innovation in operative access). One of the primary delays following colorectal resection is patient education in ostomy care. The shortened hospital stay associated with a laparoscopic approach, particularly SAL, can increase demands on the stoma education service that traditionally has had several days to get to know the patient and provide appropriate training. However, the dedicated nurse practitioners in our unit have responded to this issue by providing additional visits, commencing preoperatively. The reduced period of ileus facilitates early eating and increased opportunity to gain experience in ostomy management.

While the relatively small numbers of patients in this study period is a limitation of the study, this experience does still represent the largest reported experience of single port total colectomy with end ileostomy for recalcitrant ulcerative colitis to date. The published experience even regarding multiport total colectomy is also relatively small as these cases present relatively infrequently even in large centres with most groups tending to publish figures that at most approximate 20 cases annually. There is in addition a possible bias in that choice of surgical approach reflected surgeon experience. We have tried to control for this aspect by including case match analysis rather than crude group analysis overall. Furthermore, the operations presented here were never solely done by one operator alone but included resident performance of the majority of the procedure in most cases as is routine for all cases in our university teaching hospital. The postoperative care pathways are shared for all patients also including common postoperative care pathways and protocols in addition to common ward rounds and allied health professional input in all cases. Certainly, further experience with larger patient numbers is required to understand why exactly patients are significantly more likely to be discharged earlier when having their surgery by single access *vs* the conventional, standard multiport approach. Lastly, single port access itself can impose technical limitations on surgeons performing this aspect and its usefulness of course relates to experience across the discipline and our practice incudes its employment in elective surgery for neoplasia either for part or the entirety of the operation in addition to its employment for such multiquadrant operating as for this indication. We have found empirically however that its need for only two experienced surgeons and very limited instrument set-up does seem positive in the case of urgent operations which often in our institution take place at inconvenient times and in general, non-specialist and emergency operating theatres.

In conclusion, SAL represents an adapted laparoscopic access technique that can safely and effectively allow total colectomy with end ileostomy in the majority of patients with medically uncontrolled ulcerative colitis in both scheduled and acute settings. Not only does it not need to be associated with increased costs either in terms of access devices or theatre efficiency, it can in fact be an economically favorable option that enables earlier discharge from hospital.

CONCLUSION

SAL was confirmed as a therapeutic option for surgical approach for patients with UC and should be considered more often where the skillsets and technology exist.

ARTICLE HIGHLIGHTS

Research background

Single access laparoscopy (SAL) is a modification of standard laparoscopy that has not be studied in detail for the operation of total colectomy in patients sick with ulcerative colitis (UC). Here we examine its impact in this patient cohort.

Research motivation

Clinical outcomes were examined along with measure of operative efficiency to define the comparative advantages of the SAL approach for this surgery.

Research objectives
SAL was safely and efficiently applied meaning this approach can be considered in future for this patient group.

Research methods
Clinical data along with patient demographics and outcomes including complications.

Research results
SAL was associated with satisfactory outcomes in patients sick with UC and compared favourably to standard surgery in terms of cost and operative time.

Research conclusions
SAL was confirmed as a therapeutic option for surgical approach for patients with UC and should be considered more often where the skillsets and technology exist.

Research perspectives
Further work can expand on this series in particular to show the generalisability of these findings and also define better the relative merits of the different operative approaches now available.

REFERENCES

1 **Holder-Murray J**, Zoccali M, Hurst RD, Umanskiy K, Rubin M, Fichera A. Totally laparoscopic total proctocolectomy: a safe alternative to open surgery in inflammatory bowel disease. *Inflamm Bowel Dis* 2012; **18**: 863-868 [PMID: 21761510 DOI: 10.1002/ibd.21808]
2 **Fowkes L**, Krishna K, Menon A, Greenslade GL, Dixon AR. Laparoscopic emergency and elective surgery for ulcerative colitis. *Colorectal Dis* 2008; **10**: 373-378 [PMID: 17714533 DOI: 10.1111/j.1463-1318.2007.01321.x]
3 **Champagne B**, Stulberg JJ, Fan Z, Delaney CP. The feasibility of laparoscopic colectomy in urgent and emergent settings. *Surg Endosc* 2009; **23**: 1791-1796 [PMID: 19067063 DOI: 10.1007/s00464-008-0227-z]
4 **Nash GM**, Bleier J, Milsom JW, Trencheva K, Sonoda T, Lee SW. Minimally invasive surgery is safe and effective for urgent and emergent colectomy. *Colorectal Dis* 2010; **12**: 480-484 [PMID: 19508540 DOI: 10.1111/j.1463-1318.2009.01843.x]
5 **Telem DA**, Vine AJ, Swain G, Divino CM, Salky B, Greenstein AJ, Harris M, Katz LB. Laparoscopic subtotal colectomy for medically refractory ulcerative colitis: the time has come. *Surg Endosc* 2010; **24**: 1616-1620 [PMID: 20204417 DOI: 10.1007/s00464-009-0819-2]
6 **Causey MW**, Stoddard D, Johnson EK, Maykel JA, Martin MJ, Rivadeneira D, Steele SR. Laparoscopy impacts outcomes favorably following colectomy for ulcerative colitis: a critical analysis of the ACS-NSQIP database. *Surg Endosc* 2013; **27**: 603-609 [PMID: 22955999 DOI: 10.1007/s00464-012-2498-7]
7 **Maggiori L**, Gaujoux S, Tribillon E, Bretagnol F, Panis Y. Single-incision laparoscopy for colorectal resection: a systematic review and meta-analysis of more than a thousand procedures. *Colorectal Dis* 2012; **14**: e643-e654 [PMID: 22632808 DOI: 10.1111/j.1463-1318.2012.03105.x]
8 **Cahill RA**, Lindsey I, Jones O, Guy R, Mortensen N, Cunningham C. Single-port laparoscopic total colectomy for medically uncontrolled colitis. *Dis Colon Rectum* 2010; **53**: 1143-1147 [PMID: 20628277 DOI: 10.1007/DCR.0b013e3181dd062f]
9 **Leblanc F**, Makhija R, Champagne BJ, Delaney CP. Single incision laparoscopic total colectomy and proctocolectomy for benign disease: initial experience. *Colorectal Dis* 2011; **13**: 1290-1293 [PMID: 20955513 DOI: 10.1111/j.1463-1318.2010.02448.x]
10 **Geisler DP**, Kirat HT, Remzi FH. Single-port laparoscopic total proctocolectomy with ileal pouch-anal anastomosis: initial operative experience. *Surg Endosc* 2011; **25**: 2175-2178 [PMID: 21197548 DOI: 10.1007/s00464-010-1518-8]
11 **Gash KJ**, Goede AC, Kaldowski B, Vestweber B, Dixon AR. Single incision laparoscopic (SILS) restorative proctocolectomy with ileal pouch-anal anastomosis. *Surg Endosc* 2011; **25**: 3877-3880 [PMID: 21761270 DOI: 10.1007/s00464-011-1814-y]
12 **Fichera A**, Zoccali M, Gullo R. Single incision ("scarless") laparoscopic total abdominal colectomy with end ileostomy for ulcerative colitis. *J Gastrointest Surg* 2011; **15**: 1247-1251 [PMID: 21336500 DOI: 10.1007/s11605-011-1440-y]
13 **Hompes R**, Lindsey I, Jones OM, Guy R, Cunningham C, Mortensen NJ, Cahill RA. Step-wise integration of single-port laparoscopic surgery into routine colorectal surgical practice by use of a surgical glove port. *Tech Coloproctol* 2011; **15**: 165-171 [PMID: 21528438 DOI: 10.1007/s10151-011-0686-4]
14 **Moftah M**, Sehgal R, Cahill RA. Single port laparoscopic colorectal surgery in debilitated patients and in the urgent setting. *Minerva Gastroenterol Dietol* 2012; **58**: 213-225 [PMID: 22971632]
15 **Dindo D**, Demartines N, Clavien PA. Classification of surgical complications: a new proposal with evaluation in a cohort of 6336 patients and results of a survey. *Ann Surg* 2004; **240**: 205-213 [PMID: 15273542 DOI: 10.1097/01.sla.0000133083.54934.ae]
16 **Polle SW**, Bemelman WA. Surgery insight: minimally invasive surgery for IBD. *Nat Clin Pract Gastroenterol Hepatol* 2007; **4**: 324-335 [PMID: 17541446 DOI: 10.1038/ncpgasthep0839]
17 **Muller KR**, Prosser R, Bampton P, Mountifield R, Andrews JM. Female gender and surgery impair

relationships, body image, and sexuality in inflammatory bowel disease: patient perceptions. *Inflamm Bowel Dis* 2010; **16**: 657-663 [PMID: 19714755 DOI: 10.1002/ibd.21090]

18 **Fichera A**, Zoccali M, Felice C, Rubin DT. Total abdominal colectomy for refractory ulcerative colitis. Surgical treatment in evolution. *J Gastrointest Surg* 2011; **15**: 1909-1916 [PMID: 21909842 DOI: 10.1007/s11605-011-1666-8]

19 **Costedio MM**, Aytac E, Gorgun E, Kiran RP, Remzi FH. Reduced port *vs* conventional laparoscopic total proctocolectomy and ileal J pouch-anal anastomosis. *Surg Endosc* 2012; **26**: 3495-3499 [PMID: 22707112 DOI: 10.1007/s00464-012-2372-7]

20 **Wang C**, He L, Zhang J, Ouyang C, Wu X, Lu F, Liu X. Clinical, laboratory, endoscopical and histological characteristics predict severe ulcerative colitis. *Hepatogastroenterology* 2013; **60**: 318-323 [PMID: 23353708 DOI: 10.5754/hge12607]

21 **Hennessey DB**, Burke JP, Ni-Dhonochu T, Shields C, Winter DC, Mealy K. Preoperative hypoalbuminemia is an independent risk factor for the development of surgical site infection following gastrointestinal surgery: a multi-institutional study. *Ann Surg* 2010; **252**: 325-329 [PMID: 20647925 DOI: 10.1097/SLA.0b013e3181e9819a]

22 **Gu J**, Stocchi L, Remzi F, Kiran RP. Factors associated with postoperative morbidity, reoperation and readmission rates after laparoscopic total abdominal colectomy for ulcerative colitis. *Colorectal Dis* 2013; **15**: 1123-1129 [PMID: 23627886 DOI: 10.1111/codi.12267]

23 **Chung TP**, Fleshman JW, Birnbaum EH, Hunt SR, Dietz DW, Read TE, Mutch MG. Laparoscopic vs. open total abdominal colectomy for severe colitis: impact on recovery and subsequent completion restorative proctectomy. *Dis Colon Rectum* 2009; **52**: 4-10 [PMID: 19273949 DOI: 10.1007/DCR.0b013e3181975701]

24 **Vilos GA**, Ternamian A, Dempster J, Laberge PY; Clinical Practice Gynaecology Committee. Laparoscopic entry: a review of techniques, technologies, and complications. *J Obstet Gynaecol Can* 2007; **29**: 433-447 [PMID: 17493376 DOI: 10.1016/S1701-2163(16)35496-2]

25 **Champagne BJ**, Lee EC, Leblanc F, Stein SL, Delaney CP. Single-incision *vs* straight laparoscopic segmental colectomy: a case-controlled study. *Dis Colon Rectum* 2011; **54**: 183-186 [PMID: 21228666 DOI: 10.1007/DCR.0b013e3181fd48af]

World Journal of Gastroenterology

Submit a Manuscript: https://www.f6publishing.com

World J Gastroenterol 2020 October 21; 26(39): 6027-6036

DOI: 10.3748/wjg.v26.i39.6027

ISSN 1007-9327 (print) ISSN 2219-2840 (online)

ORIGINAL ARTICLE

Retrospective Study

Real-world treatment attrition rates in advanced esophagogastric cancer

Erica S Tsang, Howard J Lim, Daniel J Renouf, Janine M Davies, Jonathan M Loree, Sharlene Gill

ORCID number: Erica S Tsang 0000-0003-2317-2721; Howard J Lim 0000-0002-5814-714X; Daniel J Renouf 0000-0002-7597-6089; Janine M Davies 0000-0003-3834-6835; Jonathan M Loree 0000-0001-8189-2132; Sharlene Gill 0000-0003-3306-3617.

Author contributions: Tsang ES and Gill S were responsible for conception and design, collection and assembly of data, and data analysis and interpretation; all authors contributed to manuscript writing and provided final approval of the manuscript.

Institutional review board statement: This study was reviewed and approved by Systemic Therapy - Vancouver (BC Cancer), REB number H19-01865.

Conflict-of-interest statement: All authors have no any conflicts of interest.

Data sharing statement: No additional data.

Erica S Tsang, Howard J Lim, Daniel J Renouf, Janine M Davies, Jonathan M Loree, Sharlene Gill, Department of Medicine, BC Cancer, Vancouver V5Z 4E6, Canada

Erica S Tsang, Howard J Lim, Daniel J Renouf, Janine M Davies, Jonathan M Loree, Sharlene Gill, Division of Medical Oncology, University of British Columbia, Vancouver V5Z 4E6, Canada

Corresponding author: Sharlene Gill, MD, Professor, Department of Medicine, BC Cancer, 600 West 10th Avenue, Vancouver V5Z 4E6, Canada. sgill@bccancer.bc.ca

Abstract

BACKGROUND

Over the last decade, multiple agents have demonstrated efficacy for advanced esophagogastric cancer (EGC). Despite the availability of later lines of therapy, there remains limited real-world data about the treatment attrition rates between lines of therapy.

AIM

To characterize the use and attrition rates between lines of therapy for patients with advanced EGC.

METHODS

We identified patients who received at least one cycle of chemotherapy for advanced EGC between July 1, 2017 and July 31, 2018 across six regional centers in British Columbia (BC), Canada. Clinicopathologic, treatment, and outcomes data were extracted.

RESULTS

Of 245 patients who received at least one line of therapy, median age was 66 years (IQR 58.2-72.3) and 186 (76%) were male, Eastern Cooperative Oncology Group (ECOG) performance status 0/1 (80%), gastric *vs* GEJ (36% *vs* 64%). Histologies included adenocarcinoma (78%), squamous cell carcinoma (8%), and signet ring (14%), with 31% HER2 positive. 72% presented with de novo disease, and 25% had received previous chemoradiation. There was a high level of treatment attrition, with patients receiving only one line of therapy n = 122, 50%), two lines n = 83, 34%), three lines n = 34, 14%), and four lines n = 6, 2%). Kaplan-Meier analysis demonstrated improved survival with increasing lines of therapy (median overall survival 7.7 *vs* 16.6 *vs* 22.8 *vs* 40.4 mo, $P < 0.05$). On multivariable Cox regression, improved survival was associated with better baseline ECOG and

Manuscript source: Unsolicited manuscript

Received: May 10, 2020
Peer-review started: May 10, 2020
First decision: June 13, 2020
Revised: June 24, 2020
Accepted: September 25, 2020
Article in press: September 25, 2020
Published online: October 21, 2020

P-Reviewer: D'Ugo DM, Zhe MM
S-Editor: Ma YJ
L-Editor: A
P-Editor: Zhang YL

increased lines of therapy ($P < 0.05$).

CONCLUSION
The steep attrition rates between therapies highlight the unmet need for more efficacious early-line treatment options for patients with advanced EGC.

Key Words: Esophagogastric cancer; Gastric cancer; Treatment attrition; Systemic therapy; Treatment outcomes; Real-world evidence

Core Tip: Despite the availability of later lines of therapy for esophagogastric cancer (EGC), there remains limited real-world data about the treatment attrition rates between lines of therapy. In this population-based analysis, we characterize the use and treatment attrition rates for patients with advanced EGC. Among 245 patients, there was a high level of treatment attrition, with 50% receiving one line of therapy, 34% receiving two lines, and 14% receiving three-lines. Improved survival was associated with better baseline Eastern Cooperative Oncology Group and increased lines of therapy. This real-world analysis demonstrating such steep attrition rates highlights the unmet need for more efficacious early-line treatment options.

Citation: Tsang ES, Lim HJ, Renouf DJ, Davies JM, Loree JM, Gill S. Real-world treatment attrition rates in advanced esophagogastric cancer. *World J Gastroenterol* 2020; 26(39): 6027-6036
URL: https://www.wjgnet.com/1007-9327/full/v26/i39/6027.htm
DOI: https://dx.doi.org/10.3748/wjg.v26.i39.6027

INTRODUCTION

Gastric cancer is the fourth most common type of cancer, while esophageal cancer remains the eight most common type of cancer[1]. Locally advanced unresectable and metastatic disease in both sites have dismal outcomes, with 5-year survival rates measuring less than 4%[2,3]. The current standard of care for advanced esophagogastric cancer is systemic chemotherapy with a first-line platinum and fluoropyrimidine combination[4]. Rates of second-line treatment have been reported to be between 14% and 75%[5,6]. A retrospective Italian study early in the ramucirumab era examined rates of second-line treatment and reported a range of 7%-41%; however, this was limited by a small number of patients who received ramucirumab, which has now been established as a standard second-line regimen[7].

Over the last decade, multiple agents have also been tried in later line settings, including ramucirumab, irinotecan, trifluridine/tipiracil, and immunotherapy[8-11]. Current trials such as the CCTG GA.3 trial focus on examining the role of regorafenib in the later line setting (NCT02773524). It is important to gauge the real-world use of multiple lines of therapy for patients with metastatic esophagogastric cancer, beyond a clinical trial population.

The objectives of this study were to characterize the attrition rates between lines of therapy for patients with unresectable locally advanced or metastatic esophagogastric cancer (EGC), and to identify prognostic factors for improved survival.

MATERIALS AND METHODS

In British Columbia (BC), Canada, BC Cancer is the provincial institution responsible for overseeing cancer-related care for 4.4 million residents, including the development of cancer therapy guidelines, provision of radiation therapy, and funding for all approved systemic therapies. The BC Cancer Provincial Pharmacy Database provides and holds records for all provincially funded systemic therapies across six cancer centres in BC.

We sought to characterize the use and attrition rates between lines of therapy for

patients with advanced EGC, defined as either esophageal, gastroesophageal junction, or gastric cancer. We identified patients who received at least one cycle of systemic therapy for advanced histology-confirmed EGC between July 1, 2017 and July 31, 2018 from the BC Cancer Provincial Pharmacy Database. These dates were chosen based on the funding and availability of ramucirumab and paclitaxel after May 2017, and to allow for sufficient follow-up. Clinicopathologic data, treatment details, and survival outcomes were extracted by chart review. Patients who continued on treatment were censored at the date of last contact. Given the focus on systemic therapy, data regarding radiotherapy for palliative purposes was not explicitly included. This study was approved by the BC Cancer Research Ethics Board.

Statistical analysis

Baseline clinicopathologic characteristics and delivery of multiple lines of therapies were reported using descriptive statistics, with differences in variables analyzed using the chi-square or Wilcoxon rank-sum tests where appropriate. Overall survival (OS) was calculated from the date of diagnosis of advanced disease to date of death or date of last follow-up. Univariable and multivariable logistic regression analyses exploring factors associated with improved survival were performed with the Cox proportional hazards model. Variables included in the Cox proportional hazards models were selected based on known prognostic factors and those significant on univariable analysis ($P < 0.05$). OS was estimated using the Kaplan-Meier method, with the log-rank test used to compare differences. All tests were two-sided, and a P value of < 0.05 was considered statistically significant. Stata version 15.1 was used for all statistical analyses (Stata, College Station, TX, United States).

RESULTS

Of 245 patients who received at least one line of therapy, median age was 66 years (IQR 58.2-72.3) and 186 (76%) were male. Baseline Eastern Cooperative Oncology Group (ECOG) performance status was 0-1 in 80%, and site of primary was gastric *vs* GEJ (36% *vs* 64%). Histologies included adenocarcinoma (78%), squamous cell carcinoma (8%), and signet ring (14%), with 31% HER2 positive. 72% presented with de novo disease, and 25% had received previous chemoradiation. Further clinicopathologic characteristics are detailed in Table 1.

There was a high level of treatment attrition, with 50% of patients (n = 122) receiving only one line of therapy. Distribution across subsequent lines was: two lines (n = 83, 34%), three lines (n = 34, 14%), and four lines (n = 6, 2%). Patients who received at least two lines of therapy were younger (median age 62.2 *vs* 67.6 years, $P < 0.05$) and demonstrated a longer and improved response to first-line systemic therapy compared to those who only received one line of treatment (median duration 5.0 *vs* 2.7 mo, $P < 0.05$; 50% complete or partial response (40% *vs* 32%, $P < 0.05$).

In terms of systemic therapy regimens, ramucirumab and paclitaxel was the most common second line treatment (62%), with an objective response (complete or partial response) observed in only 16% of patients (Table 2). In the third-line setting, 5-fluorouracil and irinotecan was the most common regimen (35%). Fourth-line regimens were largely 5-fluorouracil based, with one of six patients receiving nivolumab.

Kaplan-Meier survival analysis demonstrated improved survival with increasing lines of therapy (median OS 7.7 *vs* 16.6 *vs* 22.8 *vs* 40.4 mo, $P < 0.05$; Figure 1). On multivariable Cox regression, improved survival was associated with better baseline ECOG and increased lines of therapy ($P < 0.05$; Table 3).

DISCUSSION

In this population-based analysis, we demonstrate high treatment attrition rates among patients with advanced EGC, with only half of patients proceeding to receive two or more systemic therapy regimens. Survival improved with the application of multiple lines of therapy and a good baseline ECOG performance status.

Our findings of high levels of attrition are consistent with other retrospective studies reported in the literature, with a number of these employing electronic health record (EHR) data. Le *et al*[12] examined EHR data from the Flatiron Health database, and found a 75% rate of first-line, 32% rate of second-line, 14% rate of third-line, and

Table 1 Baseline characteristics of 245 patients with advanced esophagogastric cancer who received at least one line of systemic therapy

	Only one line of therapy (*n* = 122)	At least two lines of therapy (*n* = 123)	*P* value
Median age (IQR)	68 (61.7-73.7)	62 (56.1-70.6)	< 0.05
Gender, *n* (%)			0.37
Male	96 (79)	90 (73)	
Female	26 (21)	33 (27)	
Ethnicity, *n* (%)			0.59
Caucasian	101 (83)	95 (77)	
Asian	15 (12)	21 (17)	
East Asian	6 (5)	6 (5)	
Other	0	1 (1)	
Histology, *n* (%)			0.92
Adenocarcinoma	96 (79)	95 (77)	
Squamous cell carcinoma	9 (7)	11 (9)	
Signet ring cell	17 (14)	17 (14)	
HER2 status, *n* (%)			0.41
Positive	27 (22)	37 (30)	
Negative	70 (57)	72 (59)	
Unknown	25 (20)	14 (11)	
MMR status by IHC, *n* (%)			1.0
Deficient MMR	1 (1)	1 (1)	
Proficient MMR	34 (28)	55 (45)	
Unknown	87 (71)	67 (54)	
Grade, *n* (%)			0.14
Well	3 (2)	5 (4)	
Moderate	30 (25)	42 (34)	
Poor	58 (48)	45 (37)	
Unknown	31 (25)	31 (25)	
Site of primary, *n* (%)			0.44
Gastric	44 (36)	46 (37)	
GEJ/esophagus	78 (64)	77 (63)	
Location of metastases, *n* (%)			
Lymph node	64 (52)	54 (44)	0.20
Lung	29 (24)	28 (67)	0.88
Liver	39 (32)	50 (41)	0.18
Peritoneum	31 (25)	23 (19)	0.22
Other	28 (23)	16 (13)	0.05
Disease presentation, *n* (%)			0.89
De novo disease	87 (71)	89 (72)	
Recurrent disease	35 (29)	34 (28)	
Previous chemoradiation, *n* (%)	32 (26)	29 (24)	0.66
Previous resection, *n* (%)	27 (22)	24 (20)	0.64

ECOG at baseline, *n* (%)			0.14
0	11 (9)	20 (16)	
1	83 (68)	84 (68)	
2	28 (23)	19 (15)	
Best response to first-line treatment, *n* (%)			< 0.05
Complete response	6 (5)	4 (3)	
Partial response	33 (27)	46 (37)	
Stable disease	20 (16)	38 (31)	
Progressive disease	58 (48)	33 (27)	
Unknown	5 (4)	2 (2)	
Median duration of first-line treatment	2.7 (0.9-6.1)	5.00 (3.5-9.8)	< 0.05
Reason for discontinuation of first-line treatment, *n* (%)			0.02
Progression	82 (67)	101 (82)	
Toxicity	15 (12)	4 (3)	
Other	23 (19)	17 (14)	
Unknown	2 (2)	1 (1)	

IQR: Interquartile range; HER2: Human epidermal growth factor receptor 2; MMR: Mismatch repair; IHC: Immunohistochemistry; GEJ: Gastroesophageal junction.

6% rate of fourth-line therapies. We note that this was primarily in a United States community-based practice setting, compared to our Canadian single-payer system. In a similar EHR-based analysis, Barzi *et al*[13] described a 60% rate of second-line therapy use. Previous retrospective EHR-based studies have reported an approximately 50% rate of second-line therapies[14,15]. In a Japanese single institution study, Ueno *et al*[16] reported a 26% rate of third-line systemic therapy.

Similarly, improved survival outcomes have been associated with an increasing number of lines of therapy and improved baseline performance status[12,17]. Fanotto *et al*[18] described additional prognostic factors, including lower LDH levels and a lower neutrophil/Lymphocyte ratio at the initiation of second-line therapy. There was insufficient LDH data to examine this, and we did not find a similar association with the neutrophil/Lymphocyte ratio.

The survival outcomes and high level of treatment attrition highlight the lethality of EGC. Screening can play a role in detecting these cancers at an earlier stage. While this is feasible in countries with a high incidence rate such as South Korea and Japan, this is not readily available in Canada[19-21]. For patients already diagnosed with advanced disease, better risk stratification and more effective frontline therapies are urgently needed. The combined positive score is now used to identify patients who are more likely to benefit from immunotherapy, after the findings from KEYNOTE-181[22]. Improved biomarkers for risk stratification and treatment selection are also being investigated. Despite the work done in molecular subtyping of gastric cancer, there are few actionable targets and significant intratumoral heterogeneity; thus, limiting the role for precision medicine in the upfront treatment setting[23,24]. Some markers, such as *MET* overexpression, have been associated with poor prognosis and this continues to be studied as a potential actionable target[25,26]. In recent years, there has been a shift towards immunotherapy-based combinations, such as in the MORPHEUS umbrella trial[27]. It remains to be seen whether this can play an effective earlier-line strategy in patients with advanced EGC.

Limitations of our study include the retrospective nature, which limits causal inference regarding prognostic factors for improved survival. The limited sample size in a Canadian single-payer health system may limit generalizability. However, while our sample size of 245 patients is smaller than the United States nationwide EHR database, our data are manually curated and provide more granularity as a result. There is also selection bias and practitioner variability in defining ECOG performance status, and in offering a subsequent line of therapy. Finally, this study was done prior to the approval and availability of oral trifluridine/tipiracil in the third-line setting, which may influence treatment practices in this population.

Table 2 Treatment details for patients who received at least two lines of systemic therapy

Second-line chemotherapy backbone [*n* = 123, *n* (%)]	
5-FU/oxaliplatin	9 (7)
5-FU/irinotecan	21 (17)
5-FU/cisplatin	3 (2)
Ramucirumab/paclitaxel	76 (62)
Docetaxel	8 (7)
Capecitabine	2 (2)
Irinotecan	3 (2)
Trastuzumab alone	1 (1)
Best response to second-line treatment, *n* (%)	
Complete response	2 (2)
Partial response	17 (14)
Stable disease	27 (22)
Progressive disease	73 (59)
Unknown	4 (3)
Median duration of second-line treatment (mo)	2.8 (1.4-5.7)
Reason for discontinuation of second-line treatment, *n* (%)	
Progression	100 (81)
Toxicity	7 (6)
Other	12 (10)
Unknown	11 (9)
Third-line chemotherapy backbone [*n* = 40, *n* (%)]	
5-FU	1 (2.5)
5-FU/irinotecan	14 (35)
5-FU/oxaliplatin	1 (2.5)
Docetaxel	2 (5)
Irinotecan	8 (20)
Ramucirumab/paclitaxel	11 (28)
Pembrolizumab	1 (2.5)
Nivolumab	1 (2.5)
Durvalumab/Tremelimumab	1 (2.5)
Best response to third-line treatment, *n* (%)	
Complete response	1 (2.5)
Partial response	7 (18)
Stable disease	6 (15)
Progressive disease	25 (63)
Unknown	1 (2.5)
Median duration of third-line treatment (mo)	1.9 (0.9-4.4)
Reason for discontinuation of third-line treatment, *n* (%)	
Progression	34 (85)
Toxicity	0
Other	3 (8)

Unknown	3 (8)
Fourth-line chemotherapy backbone [*n* = 6, *n* (%)]	
5-FU	1 (17)
5-FU/oxaliplatin	2 (33)
5-FU/irinotecan	1 (17)
5-FU/cisplatin	1 (17)
Nivolumab	1 (17)
Best response to fourth-line treatment, *n* (%)	
Complete response	0
Partial response	0
Stable disease	1 (17)
Progressive disease	5 (83)
Median duration of fourth-line treatment (mo)	2.57 (2.08-3.75)
Reason for discontinuation of fourth-line treatment, *n* (%)	
Progression	6 (100)
Toxicity	0
Other	0
Unknown	0

5-FU: 5-fluorouracil.

Table 3 Multivariable Cox regression analysis for overall survival

	Hazard ratio (95%CI)	*P* value
Gender (male *vs* female)	1.07 (0.77-1.48)	0.69
Baseline ECOG (continuous)	1.33 (1.02-1.73)	**0.04**
Recurrent disease (*vs de novo*)	0.86 (0.62-1.19)	0.37
Duration of first-line treatment	1.00 (1.00-1.002)	0.09
Lines of treatment	0.61 (0.50-0.74)	**< 0.01**

ECOG: Eastern Cooperative Oncology Group.

CONCLUSION

We present a population-based analysis of real-world use of later-line therapy in patients with advanced EGC. The steep attrition rates between therapies highlight the high symptom burden in this setting and the unmet need for more efficacious early-line treatment options for patients with advanced EGC. Improved biomarkers may provide informed risk stratification in selecting later lines of treatment, and identifying patients who would derive greater benefit from multiple lines of therapy.

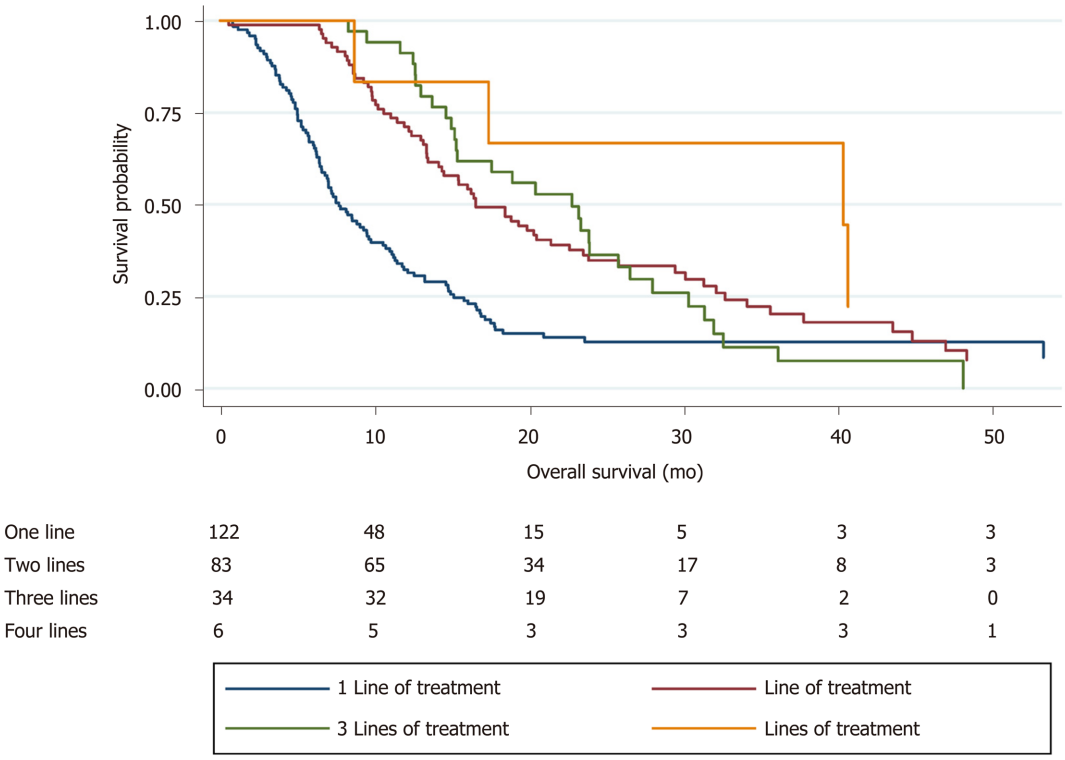

Figure 1 Overall survival by number of lines of treatment.

ARTICLE HIGHLIGHTS

Research background

Over the last decade, multiple agents have demonstrated efficacy for advanced esophagogastric cancer (EGC).

Research motivation

Despite the availability of later lines of therapy, there remains limited real-world data about the treatment attrition rates between lines of therapy.

Research objectives

We aimed to characterize the use and attrition rates between lines of therapy for patients with advanced EGC.

Research methods

We identified patients who received at least one cycle of chemotherapy for advanced EGC between July 1, 2017 and July 31, 2018 across six regional centers in British Columbia, Canada. Clinicopathologic, treatment, and outcomes data were extracted.

Research results

Of 245 patients who received at least one line of therapy, median age was 66 years (IQR 58.2-72.3) and 186 (76%) were male, Eastern Cooperative Oncology Group (ECOG) performance status 0/1 (80%), gastric *vs* GEJ (36% *vs* 64%). Histologies included adenocarcinoma (78%), squamous cell carcinoma (8%), and signet ring (14%), with 31% HER2 positive. Seventy-two percent presented with de novo disease, and 25% had received previous chemoradiation. There was a high level of treatment attrition, with patients receiving only one line of therapy (n = 122, 50%), two lines (n = 83, 34%), three lines (n = 34, 14%), and four lines (n = 6, 2%). Kaplan-Meier analysis demonstrated improved survival with increasing lines of therapy (median overall survival 7.7 *vs* 16.6 *vs* 22.8 *vs* 40.4 mo, $P < 0.05$). On multivariable Cox regression, improved survival was associated with better baseline ECOG and increased lines of therapy ($P < 0.05$).

Research conclusions

The steep attrition rates between therapies highlight the unmet need for more efficacious early-line treatment options for patients with advanced EGC.

Research perspectives

This real-world analysis demonstrating such steep attrition rates highlights the unmet need for more efficacious early-line treatment options.

REFERENCES

1 **Siegel RL**, Miller KD, Jemal A. Cancer statistics, 2018. *CA Cancer J Clin* 2018; **68**: 7-30 [PMID: 29313949 DOI: 10.3322/caac.21442]

2 **Van Cutsem E**, Sagaert X, Topal B, Haustermans K, Prenen H. Gastric cancer. *Lancet* 2016; **388**: 2654-2664 [PMID: 27156933 DOI: 10.1016/S0140-6736(16)30354-3]

3 **Napier KJ**, Scheerer M, Misra S. Esophageal cancer: A Review of epidemiology, pathogenesis, staging workup and treatment modalities. *World J Gastrointest Oncol* 2014; **6**: 112-120 [PMID: 24834141 DOI: 10.4251/wjgo.v6.i5.112]

4 **Ilson DH**. Advances in the treatment of gastric cancer. *Curr Opin Gastroenterol* 2018; **34**: 465-468 [PMID: 30303856 DOI: 10.1097/MOG.0000000000000475]

5 **Cunningham D**, Starling N, Rao S, Iveson T, Nicolson M, Coxon F, Middleton G, Daniel F, Oates J, Norman AR; Upper Gastrointestinal Clinical Studies Group of the National Cancer Research Institute of the United Kingdom. Capecitabine and oxaliplatin for advanced esophagogastric cancer. *N Engl J Med* 2008; **358**: 36-46 [PMID: 18172173 DOI: 10.1056/NEJMoa073149]

6 **Koizumi W**, Narahara H, Hara T, Takagane A, Akiya T, Takagi M, Miyashita K, Nishizaki T, Kobayashi O, Takiyama W, Toh Y, Nagaie T, Takagi S, Yamamura Y, Yanaoka K, Orita H, Takeuchi M. S-1 plus cisplatin versus S-1 alone for first-line treatment of advanced gastric cancer (SPIRITS trial): a phase III trial. *Lancet Oncol* 2008; **9**: 215-221 [PMID: 18282805 DOI: 10.1016/S1470-2045(08)70035-4]

7 **Fanotto V**, Uccello M, Pecora I, Rimassa L, Leone F, Rosati G, Santini D, Giampieri R, Di Donato S, Tomasello G, Silvestris N, Pietrantonio F, Battaglin F, Avallone A, Scartozzi M, Lutrino ES, Melisi D, Antonuzzo L, Pellegrino A, Ferrari L, Bordonaro R, Vivaldi C, Gerratana L, Bozzarelli S, Filippi R, Bilancia D, Russano M, Aprile G. Outcomes of Advanced Gastric Cancer Patients Treated with at Least Three Lines of Systemic Chemotherapy. *Oncologist* 2017; **22**: 1463-1469 [PMID: 28860412 DOI: 10.1634/theoncologist.2017-0158]

8 **Fuchs CS**, Tomasek J, Yong CJ, Dumitru F, Passalacqua R, Goswami C, Safran H, Dos Santos LV, Aprile G, Ferry DR, Melichar B, Tehfe M, Topuzov E, Zalcberg JR, Chau I, Campbell W, Sivanandan C, Pikiel J, Koshiji M, Hsu Y, Liepa AM, Gao L, Schwartz JD, Tabernero J; REGARD Trial Investigators. Ramucirumab monotherapy for previously treated advanced gastric or gastro-oesophageal junction adenocarcinoma (REGARD): an international, randomised, multicentre, placebo-controlled, phase 3 trial. *Lancet* 2014; **383**: 31-39 [PMID: 24094768 DOI: 10.1016/S0140-6736(13)61719-5]

9 **Shitara K**, Özgüroğlu M, Bang YJ, Di Bartolomeo M, Mandalà M, Ryu MH, Fornaro L, Olesiński T, Caglevic C, Chung HC, Muro K, Goekkurt E, Mansoor W, McDermott RS, Shacham-Shmueli E, Chen X, Mayo C, Kang SP, Ohtsu A, Fuchs CS; KEYNOTE-061 investigators. Pembrolizumab versus paclitaxel for previously treated, advanced gastric or gastro-oesophageal junction cancer (KEYNOTE-061): a randomised, open-label, controlled, phase 3 trial. *Lancet* 2018; **392**: 123-133 [PMID: 29880231 DOI: 10.1016/S0140-6736(18)31257-1]

10 **Shitara K**, Doi T, Dvorkin M, Mansoor W, Arkenau HT, Prokharau A, Alsina M, Ghidini M, Faustino C, Gorbunova V, Zhavrid E, Nishikawa K, Hosokawa A, Yalçın Ş, Fujitani K, Beretta GD, Cutsem EV, Winkler RE, Makris L, Ilson DH, Tabernero J. Trifluridine/tipiracil versus placebo in patients with heavily pretreated metastatic gastric cancer (TAGS): a randomised, double-blind, placebo-controlled, phase 3 trial. *Lancet Oncol* 2018; **19**: 1437-1448 [PMID: 30355453 DOI: 10.1016/S1470-2045(18)30739-3]

11 **Wilke H**, Muro K, Van Cutsem E, Oh SC, Bodoky G, Shimada Y, Hironaka S, Sugimoto N, Lipatov O, Kim TY, Cunningham D, Rougier P, Komatsu Y, Ajani J, Emig M, Carlesi R, Ferry D, Chandrawansa K, Schwartz JD, Ohtsu A; RAINBOW Study Group. Ramucirumab plus paclitaxel versus placebo plus paclitaxel in patients with previously treated advanced gastric or gastro-oesophageal junction adenocarcinoma (RAINBOW): a double-blind, randomised phase 3 trial. *Lancet Oncol* 2014; **15**: 1224-1235 [PMID: 25240821 DOI: 10.1016/S1470-2045(14)70420-6]

12 **Le DT**, Ott PA, Korytowsky B, Le H, Le TK, Zhang Y, Maglinte GA, Abraham P, Patel D, Shangguan T, Chau I. Real-world Treatment Patterns and Clinical Outcomes Across Lines of Therapy in Patients With Advanced/Metastatic Gastric or Gastroesophageal Junction Cancer. *Clin Colorectal Cancer* 2020; **19**: 32-38.e3 [PMID: 31813769 DOI: 10.1016/j.clcc.2019.09.001]

13 **Barzi A**, Hess LM, Zhu YE, Liepa AM, Sugihara T, Beyrer J, Chao J. Real-World Outcomes and Factors Associated With the Second-Line Treatment of Patients With Gastric, Gastroesophageal Junction, or Esophageal Adenocarcinoma. *Cancer Control* 2019; **26**: 1073274819847642 [PMID: 31056940 DOI: 10.1177/1073274819847642]

14 **Hess LM**, Michael D, Mytelka DS, Beyrer J, Liepa AM, Nicol S. Chemotherapy treatment patterns, costs, and outcomes of patients with gastric cancer in the United States: a retrospective analysis of electronic medical record (EMR) and administrative claims data. *Gastric Cancer* 2016; **19**: 607-615 [PMID: 25792290 DOI: 10.1007/s10120-015-0486-z]

15 **Karve S**, Lorenzo M, Liepa AM, Hess LM, Kaye JA, Calingaert B. Treatment Patterns, Costs, and Survival among Medicare-Enrolled Elderly Patients Diagnosed with Advanced Stage Gastric Cancer: Analysis of a

Linked Population-Based Cancer Registry and Administrative Claims Database. *J Gastric Cancer* 2015; **15**: 87-104 [PMID: 26161282 DOI: 10.5230/jgc.2015.15.2.87]

16 **Ueno M**, Doi A, Sunami T, Takayama H, Mouri H, Mizuno M. Delivery rate of patients with advanced gastric cancer to third-line chemotherapy and those patients' characteristics: an analysis in real-world setting. *J Gastrointest Oncol* 2019; **10**: 957-964 [PMID: 31602334 DOI: 10.21037/jgo.2019.05.07]

17 **Davidson M**, Cafferkey C, Goode EF, Kouvelakis K, Hughes D, Reguera P, Kalaitzaki E, Peckitt C, Rao S, Watkins D, Chau I, Cunningham D, Starling N. Survival in Advanced Esophagogastric Adenocarcinoma Improves With Use of Multiple Lines of Therapy: Results From an Analysis of More Than 500 Patients. *Clin Colorectal Cancer* 2018; **17**: 223-230 [PMID: 29980492 DOI: 10.1016/j.clcc.2018.05.014]

18 **Fanotto V**, Cordio S, Pasquini G, Fontanella C, Rimassa L, Leone F, Rosati G, Santini D, Giampieri R, Di Donato S, Tomasello G, Silvestris N, Pietrantonio F, Battaglin F, Avallone A, Scartozzi M, Lutrino ES, Melisi D, Antonuzzo L, Pellegrino A, Torri V, Aprile G. Prognostic factors in 868 advanced gastric cancer patients treated with second-line chemotherapy in the real world. *Gastric Cancer* 2017; **20**: 825-833 [PMID: 28028664 DOI: 10.1007/s10120-016-0681-6]

19 **Choi IJ**. Endoscopic gastric cancer screening and surveillance in high-risk groups. *Clin Endosc* 2014; **47**: 497-503 [PMID: 25505714 DOI: 10.5946/ce.2014.47.6.497]

20 **Yoo KY**. Cancer control activities in the Republic of Korea. *Jpn J Clin Oncol* 2008; **38**: 327-333 [PMID: 18407932 DOI: 10.1093/jjco/hyn026]

21 **Mulder KE**, Ahmed S, Davies JD, Doll CM, Dowden S, Gill S, Gordon V, Hebbard P, Lim H, McFadden A, McGhie JP, Park J, Wong R. Report from the 17th Annual Western Canadian Gastrointestinal Cancer Consensus Conference; Edmonton, Alberta; 11-12 September 2015. *Curr Oncol* 2016; **23**: 425-434 [PMID: 28050139 DOI: 10.3747/co.23.3384]

22 **Kojima T**, Muro K, Francois E, Hsu C, Moriwaki T, Kim S, Lee S, Bennouna J, Kato K, Lin S, Qin S, Ferreira P, Doi T, Adenis A, Enzinger PC, Shah MA, Wang R, Bhagia P, Kang SP, Metges J. Pembrolizumab vs chemotherapy as second-line therapy for advanced esophageal cancer: Phase III KEYNOTE-181 study. *J Clin Oncol* 2019; **37**: 2-2 [DOI: 10.1200/JCO.2019.37.4_suppl.2]

23 **Röcken C**. Molecular classification of gastric cancer. *Expert Rev Mol Diagn* 2017; **17**: 293-301 [PMID: 28118758 DOI: 10.1080/14737159.2017.1286985]

24 **Cancer Genome Atlas Research Network**. Comprehensive molecular characterization of gastric adenocarcinoma. *Nature* 2014; **513**: 202-209 [PMID: 25079317 DOI: 10.1038/nature13480]

25 **Nakajima M**, Sawada H, Yamada Y, Watanabe A, Tatsumi M, Yamashita J, Matsuda M, Sakaguchi T, Hirao T, Nakano H. The prognostic significance of amplification and overexpression of c-met and c-erb B-2 in human gastric carcinomas. *Cancer* 1999; **85**: 1894-1902 [PMID: 10223227 DOI: 10.1002/(SICI)1097-0142(19990501)85:93.0.CO;2-J]

26 **Van Cutsem E**, Karaszewska B, Kang YK, Chung HC, Shankaran V, Siena S, Go NF, Yang H, Schupp M, Cunningham D. A Multicenter Phase II Study of AMG 337 in Patients with *MET*-Amplified Gastric/Gastroesophageal Junction/Esophageal Adenocarcinoma and Other *MET*-Amplified Solid Tumors. *Clin Cancer Res* 2019; **25**: 2414-2423 [PMID: 30366938 DOI: 10.1158/1078-0432.CCR-18-1337]

27 **Desai J**, Kortmansky JS, Segal NH, Fakih M, Oh D, Kim K, Rahma OE, Ko AH, Chung HC, Alsina M, Yeh K, Li S, Al-Sakaff N, Patel J, Barak H, Wang J, Zhang X, Bleul C, Cha E, Lee J. MORPHEUS: A phase Ib/II study platform evaluating the safety and clinical efficacy of cancer immunotherapy (CIT)–based combinations in gastrointestinal (GI) cancers. *J Clin Oncol* 2019; **37**: TPS467-TPS467 [DOI: 10.1200/JCO.2019.37.4_suppl.TPS467]

World Journal of Gastroenterology

Submit a Manuscript: https://www.f6publishing.com

World J Gastroenterol 2020 October 21; 26(39): 6037-6046

DOI: 10.3748/wjg.v26.i39.6037

ISSN 1007-9327 (print) ISSN 2219-2840 (online)

ORIGINAL ARTICLE

Retrospective Study

Metastatic pattern in esophageal and gastric cancer: Influenced by site and histology

Moniek HP Verstegen, Mitchell Harker, Carlijn van de Water, Jolanda van Dieren, Niek Hugen, Iris D Nagtegaal, Camiel Rosman, Rachel S van der Post

ORCID number: Moniek HP Verstegen 0000-0002-8371-509X; Mitchell Harker 0000-0002-4084-5468; Carlijn van de Water 0000-0002-2587-5407; Jolanda van Dieren 0000-0003-3958-4990; Niek Hugen 0000-0002-2157-1561; Iris D Nagtegaal 0000-0003-0887-4127; Camiel Rosman 0000-0002-9152-3987; Rachel S van der Post 0000-0002-7531-9599.

Author contributions: Verstegen MHP, Rosman C, Nagtegaal ID and van der Post RS designed the research; Verstegen MHP, Harker M and van der Post RS analyzed the data; Verstegen MHP and van der Post RS drafted the manuscript; van de Water C prepared the figures; All authors contributed and critically revised the manuscript for important intellectual content; all authors have approved the final version of this manuscript.

Institutional review board statement: This type of study does not require approval from an ethics committee under Dutch law. Please also see the attached document.

Conflict-of-interest statement: None to declare.

Data sharing statement: Technical appendix, statistical code, and

Moniek HP Verstegen, Mitchell Harker, Niek Hugen, Camiel Rosman, Department of Surgery, Radboud Institute for Health Sciences, Radboud University Medical Center, Radboud University Medical Center, Nijmegen 6525 GA, Netherlands

Carlijn van de Water, Iris D Nagtegaal, Rachel S van der Post, Department of Pathology, Radboud Institute for Molecular Life Sciences, Radboud University Medical Center, Radboud University Medical Center, Nijmegen 6525 GA, Netherlands

Jolanda van Dieren, Department of Gastroenterology Oncology, Netherlands Cancer Institute, Amsterdam 1066 CX, Netherlands

Corresponding author: Moniek HP Verstegen, MD, Research Fellow, Department of Surgery, Radboud Institute of Health Sciences, Radboud University Medical Center, Radboud University Medical Center, Geert Grooteplein Zuid 10, Nijmegen 6525 GA, Netherlands. moniek.verstegen@radboudumc.nl

Abstract

BACKGROUND

Detailed information on metastatic patterns in of patients with esophageal and gastric cancer is limited. Early recognition of metastases is important to avoid futile locoregional treatments. Furthermore, knowledge on metastatic patterns is necessary for further development of personalized treatment modalities.

AIM

To gain insight into the metastatic pattern of gastroesophageal cancer.

METHODS

A nationwide retrospective autopsy study of 3876 patients with adenocarcinoma (AC) or squamous cell carcinoma (SCC) of the esophagus or stomach between 1990 and 2017 was performed. Only patient with metastases were included for analysis. The metastatic pattern was analyzed according to the primary tumor location and histological subtype.

RESULTS

Metastatic disease was found in 268 esophageal and 331 gastric cancer patients. In esophageal cancer, the most common metastatic locations were liver (56%), distant lymph nodes (53%) and lung (50%). Esophageal AC showed more

dataset available from the corresponding author at [chella.vanderpost@radboudumc.nl]. Consent was not obtained but the presented data are anonymized and risk of identification is low.

Manuscript source: Unsolicited manuscript

Received: May 28, 2020
Peer-review started: May 28, 2020
First decision: June 18, 2020
Revised: August 28, 2020
Accepted: September 5, 2020
Article in press: September 5, 2020
Published online: October 21, 2020

P-Reviewer: Ilson DH
S-Editor: Wang DM
L-Editor: A
P-Editor: Zhang YL

frequently metastases to the peritoneum and bone compared with esophageal SCC. In gastric cancer, the most common metastatic locations were distant lymph nodes (56%), liver (53%) and peritoneum (51%). Intestinal-type AC of the stomach showed metastases to the liver more frequently, whereas metastases to the bone, female reproductive organs and colorectum were observed more frequently in diffuse-type gastric AC.

CONCLUSION
This study showed differences in metastatic patterns of patients with esophageal and gastric cancer according to the primary tumor location and histological subtype.

Key Words: Esophageal cancer; Gastric cancer; Metastases; Histology; Gastroesophageal junction; Adenocarcinoma; Carcinoma; Squamous cell

Core tip: In this nationwide retrospective autopsy study, the metastatic pattern of 599 patients with metastases of primary adenocarcinoma or squamous cell carcinoma of the esophagus or stomach were evaluated. Differences in metastatic patterns of these patients were found according both to the primary tumor location as well as the histological subtype. This study provides robust data regarding metastatic patterns in esophageal and gastric cancer patients. Knowledge of metastatic patterns is helpful during preoperative staging, follow-up and in future research.

Citation: Verstegen MHP, Harker M, van de Water C, van Dieren J, Hugen N, Nagtegaal ID, Rosman C, van der Post RS. Metastatic pattern in esophageal and gastric cancer: Influenced by site and histology. *World J Gastroenterol* 2020; 26(39): 6037-6046
URL: https://www.wjgnet.com/1007-9327/full/v26/i39/6037.htm
DOI: https://dx.doi.org/10.3748/wjg.v26.i39.6037

INTRODUCTION

In 2018, over 570000 esophageal cancer and over 1000000 gastric cancer cases occurred globally, respectively the 6th and 3rd leading cause of cancer related death[1,2]. Over the last decade, peri-operative treatment modalities for patients with potentially curable esophageal or gastric cancer have improved. In the Netherlands, most patients with locally advanced esophageal cancer are treated with neo-adjuvant chemoradiotherapy, followed by resection[3]. Patients with potentially curable gastric cancer are treated with peri-operative chemotherapy and resection[4,5]. Despite the fact that these treatment modalities resulted in improved overall survival, the prognosis of patients with gastric or esophageal cancer is still dismal mainly due to the high incidence of locoregional recurrence and distant metastases. Moreover, up to 50% of gastro-esophageal cancer patients present with metastatic disease at time of diagnosis[6,7]. Early recognition of metastases is important to avoid futile locoregional treatments. There is a wide variability in the timing, location and extent of metastatic disease. In order to optimize pretreatment evaluation of patients and to ensure adequate surveillance, it is essential to know more about the metastatic pattern occurring in this patient group.

Metastases of esophageal cancer are most frequently seen in the liver, lung and distant lymph nodes[8-10]. The most common metastatic sites of gastric cancer are the liver, peritoneum and distant lymph nodes[11,12]. There are limited studies reporting on differences of the metastatic spreading according to the primary tumor location, for example, upper esophageal *vs* distal esophageal cancer or cardia *vs* non-cardia gastric cancer[9,12]. Few studies reported data on differences in metastatic site according to histological subtype[8,9,11,12].

As upper gastrointestinal tract tumors are a heterogenous group, further improvement of survival probably lies within a more personalized treatment strategy. Therefore, it is important to attain deeper knowledge on the different patterns of

metastatic spreading and the factors that are instrumental in the determination of these patterns. The aim of this study is to gain insight into the location of metastases and the metastatic pattern according to the primary tumor site and the histology of the primary tumor.

MATERIALS AND METHODS

Study design

A nationwide retrospective review was conducted of pathological records of patients diagnosed with esophageal or gastric cancer who underwent autopsy between 1990 and 2017. Patients were selected from the nationwide network and registry of histopathology and cytopathology in the Netherlands (PALGA)[13]. In the Netherlands, post-mortem examination is performed at the request of the family or treating physician with consent of the family and is carried out by a pathologist. All autopsies included in this study were performed in order to obtain information on the medical status of the deceased or to determine the exact cause of death. This type of study does not require approval from an ethics committee under Dutch law.

Inclusion and exclusion criteria

Patients with a history of esophageal or gastric cancer who underwent autopsy were selected from the Dutch pathology registry (PALGA). Only patients with a history of esophageal or gastric cancer with metastases, or those who were diagnosed with metastatic esophageal or gastric cancer during autopsy, were included. Patients with a primary diagnosis of a premalignant lesion, (*i.e.* dysplasia and in-situ carcinoma), neuroendocrine neoplasm, mesenchymal tumor, lymphoma or metastases from elsewhere to the esophagus or stomach were excluded. Incomplete autopsies were excluded. Patients were excluded if the location of the metastases could not be retrieved from the records.

Study characteristics and outcome parameters

Gender, date of autopsy, age at autopsy, type of autopsy (body or body and brain), location of primary cancer (proximal esophagus, mid esophagus, distal esophagus [incl. gastro-esophageal junction (GEJ)], proximal stomach (*i.e.* cardia and fundus), stomach corpus, distal stomach (*i.e.* antrum, pylorus and linitis plastica), number of metastases and location of metastases were recorded. The histological type of carcinoma was recorded according to the World Health Organization and Laurén classification. In case of adenocarcinoma not otherwise specified, the carcinoma was assigned to the intestinal-type adenocarcinoma group. In case of metastases to the abdominal organs, records where thoroughly screened whether it was a peritoneal metastasis rather than an organ specific metastasis.

Statistical analysis

Statistical analyses were performed with the statistical software package IBM SPSS Statistics for Windows, version 22.0 (IBM Corp., Armonk, NY, United States). For dichotomous data, frequencies are presented. Continuous data are presented as mean and range. Values are compared by the chi^2-squared test. All tests of significance were two-tailed: P values of < 0.05 were considered to be significant.

RESULTS

A total of 3876 autopsy records were initially retrieved in this study: Esophageal cancer was diagnosed in 1686 cases, gastric cancer in 2190 cases. We excluded 3277 patients from further analysis, since they did not have metastatic disease (n = 2919), tumor type was not specified (n = 7) or patients did not have a primary gastroesophageal carcinoma (n = 351). The remaining 599 patients were included in our analysis; 268 (45%) patients had primary esophageal and 331 (55%) gastric carcinoma. Two hundred four patients (34.1%) underwent a resection. The mean age of patients at diagnosis was 66 years (range 25-94 years) and age of patients at death was 67 years (range 25-94 years). In only 28 (5%) cases the neurocranium was examined. The mean number of metastatic locations per patient was 3 (SD 1.86) and 21% of the patients had only one metastasis at the time of death.

Of the 268 esophageal cancer patients with metastatic disease, 62% had AC (167

cases) and 38% SCC (101 cases). AC was subdivided into intestinal-type (144 cases, 86%) and diffuse-type AC (23 cases, 14%). The 331 gastric adenocarcinoma patients were categorized as diffuse-type (including signet-ring cell carcinoma) in 37% (122 cases) or intestinal-type AC in 63% (209 cases). Clinicopathological data of metastatic esophageal and gastric cancer patients are presented in Table 1.

Pattern of metastases in 268 esophageal cancer patients

Of the 268 esophageal cancer patients, 54.5% had multiple (3 or more) metastases, 23.9% had 2 metastases and 21.6% had only one metastasis. Overall, esophageal cancer patients presented most frequently with liver, distant lymph node and lung metastases (56.0%, 52.6%, and 50.0% respectively) (Figure 1). Metastases to the liver were most common in AC (59.9%), whereas metastases to the lungs were most frequently seen in SCC (57.4%). There were three major differences in metastatic pattern between histological subtypes (Figure 2A and B). AC more frequently had metastases to the peritoneum and bone compared with SCC, 34.7% *vs* 15.8% ($P < 0.01$) and 29.9% *vs* 17.8% ($P < 0.05$), respectively. Lung metastases were observed more frequently in SCC (57.4%) compared with AC (45.5%, $P = 0.059$). Patients with a single metastatic location predominantly seem to have a liver metastasis in AC and a liver or lung metastasis in SCC esophageal cancer (Figure 2A and B).

Pattern of metastases in 331 gastric cancer patients

Of the gastric cancer patients, 54.1% had multiple (3 or more) metastases, 26.3% had 2 metastases and 19.6% had only one metastasis. Overall, gastric cancer patients presented most frequently with distant lymph node, liver and peritoneal metastases (55.9%, 52.9%, and 51.4% respectively) (Figure 3). Intestinal-type AC showed predominantly metastases to the liver (67.5%), whereas diffuse-type AC more likely present with metastases to the peritoneum (57.4%). Significant differences were found in the occurrence of metastases to the liver (67.5% in intestinal-type *vs* 27.9% in diffuse-type, $P < 0.0001$), bone (15.3% in intestinal-type *vs* 29.5% in diffuse-type, $P < 0.01$), female reproductive organs (5.7% in intestinal-type *vs* 16.4% in diffuse-type, $P < 0.01$) and colorectum (1.0% in intestinal-type *vs* 5.7% in diffuse-type, $P < 0.05$). In diffuse-type gastric cancer, patients with metastases to the female productive organs often were simultaneously diagnosed with metastases to the peritoneal cavity (Figure 2C and D).

Pattern of metastases according to primary tumor location

Esophageal *vs* gastric carcinomas: For both esophageal (including GEJ) and gastric cancer (all histological types), the liver was the most frequent metastatic site (56.0% and 52.9%, respectively). Esophageal cancer was more likely to show metastases to the lung (50.0% *vs* 35.3%, $P < 0.0001$) and heart (13.4% *vs* 7.0%, $P < 0.01$). Metastases to the peritoneum (*e.g.* peritoneum, mesentery, omentum, abdominal cavity not further specified) (27.6% *vs* 51.4%, $P < 0.0001$), female reproductive organs (1.1% *vs* 9.7%, $P < 0.0001$) and the urinary bladder (0.4% *vs* 2.4%, $P < 0.05$) were seen more often in gastric cancer.

Proximal and mid esophageal carcinomas *vs* distal esophageal and GEJ carcinomas: A sub-analysis for the metastatic site of proximal and mid *vs* distal esophageal cancer (including GEJ carcinoma) was impeded due to the small number of upper esophageal carcinomas ($n = 25$). Upper esophageal carcinomas tend to show metastases to the spleen more often (3 out of 25 patients (12%) *vs* 2 out of 174 patients (1.1%), $P < 0.01$), while distal esophageal carcinomas more often showed metastases to the peritoneum (3 out of 25 patients (12%) *vs* 57 *vs* 174 patients (32.8%), $P < 0.05$).

Distal esophageal, GEJ and cardia carcinomas: Comparing distal esophageal, GEJ and cardia adenocarcinomas (intestinal- and diffuse-type) *vs* non-cardia gastric adenocarcinomas showed differences in the metastatic pattern. Metastases to the peritoneum and female reproductive organs were seen more frequently in non-cardia gastric cancer (56.3% *vs* 37.6%, $P < 0.001$ and 12.2% *vs* 2.1%, $P < 0.001$, respectively). Distal esophageal, GEJ and cardia carcinomas more often showed metastases to the liver (61.5% *vs* 47.2%, $P < 0.05$), pleura (27.8% *vs* 17.9%, $P < 0.05$) and heart (12.0% *vs* 6.1%, $P < 0.05$) compared with non-cardia gastric carcinomas. Lung metastases were more frequently found when comparing only distal esophageal and GEJ carcinomas with cardia adenocarcinomas (49.2% *vs* 36.2%, $P < 0.05$).

Table 1 Clinicopathological data of esophageal and gastric cancer patients with metastatic disease

	Esophageal carcinoma		Gastric adenocarcinoma	
	AC	SCC	Intestinal-type AC	Diffuse-type AC
	n = 167	*n* = 101	*n* = 209	*n* = 122
Sex				
Female	31 (18.6%)	32 (31.7%)	54 (25.8%)	50 (41.0%)
Men	136 (81.4%)	69 (68.3%)	155 (74.2%)	72 (59.0%)
Year of diagnosis				
1987-1993	24 (14.4%)	20 (19.8%)	40 (19.1%)	22 (18.0%)
1994-1999	38 (22.8%)	30 (29.7%)	69 (33.0%)	28 (23.0%)
2000-2005	28 (16.8%)	19 (18.8%)	41 (19.6%)	23 (18.9%)
2006-2011	34 (20.4%)	17 (16.8%)	30 (14.4%)	20 (16.4%)
2011-2017	43 (25.7%)	15 (14.9%)	29 (13.9%)	29 (23.8%)
Mean age at diagnosis (years)	66	64	69	64
Mean age at death (years)	67	65	70	65
Location of primary tumor				
Proximal	1 (0.6%)	12 (11.9%)	73 (34.9%)	29 (23.8%)
Mid	2 (1.2%)	10 (9.9%)	25 (12.0%)	20 (16.4%)
Distal	132 (79.0%)	42 (41.6%)	43 (20.6%)	18 (14.8%)
NOS	32 (19.2%)	37 (36.6%)	68 (32.5%)	44 (36.1%)
Linitis plastica	-	-	-	11 (9.0%)

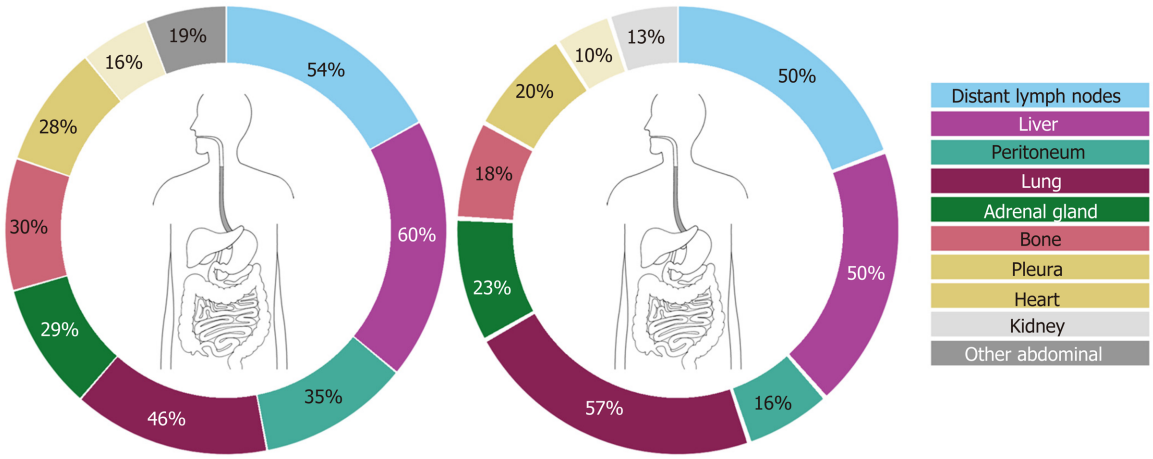

A. Esophageal AC B. Esophageal SCC

Figure 1 Metastatic sites of patients with esophageal cancer. Other metastases of esophageal cancer (all types) with proportion ≥ 2%: pancreas (6%), brain (4%), mediastinum (3%), skin/subcutis (3%), thyroid gland (3%), spleen (3%), gallbladder (2%). AC: Adenocarcinoma; SSC: Squamous cell carcinoma.

DISCUSSION

This nationwide autopsy study provides insight into the metastatic patterns in patients with esophageal or gastric cancer (n = 599). The two most common metastatic sites for esophageal and gastric cancer are liver and distant lymph nodes. Lung metastases are more frequently observed in patients with esophageal cancer while peritoneal metastases are more common in gastric cancer patients. Furthermore, differences in metastatic pattern according to primary tumor location and histological subtype were

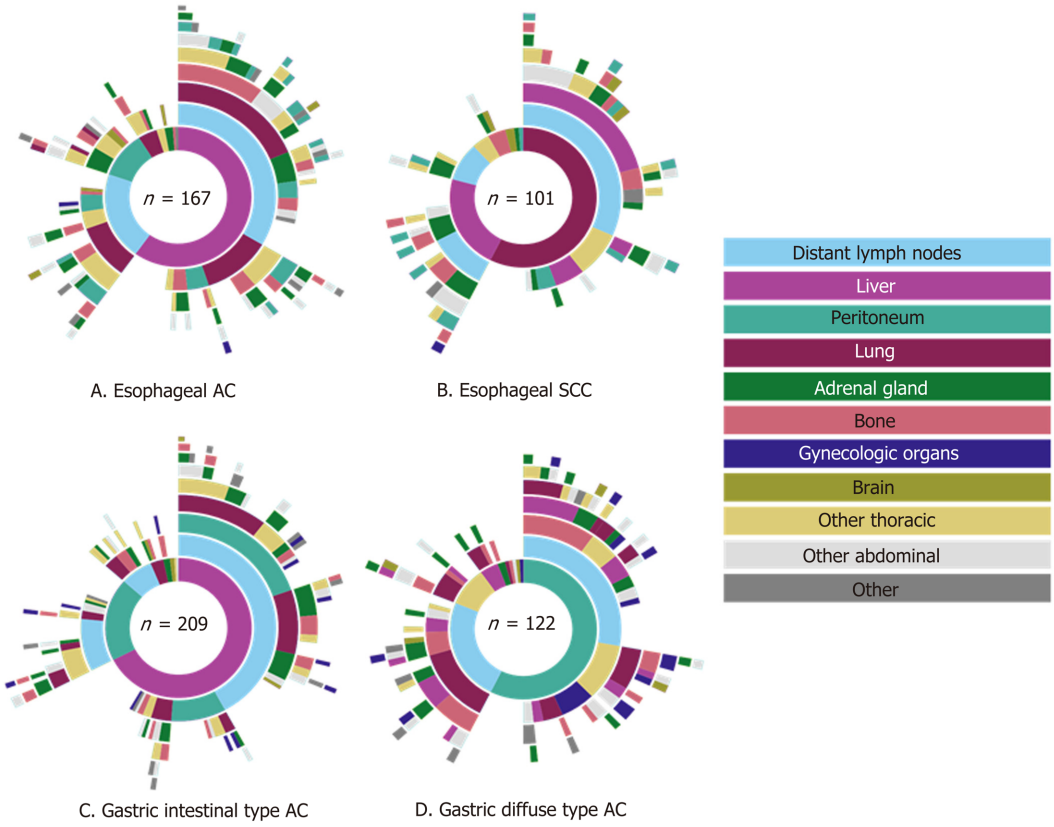

Figure 2 Metastatic pattern of esophageal and gastric cancer by histological subtype. AC: Adenocarcinoma; SSC: Squamous cell carcinoma.

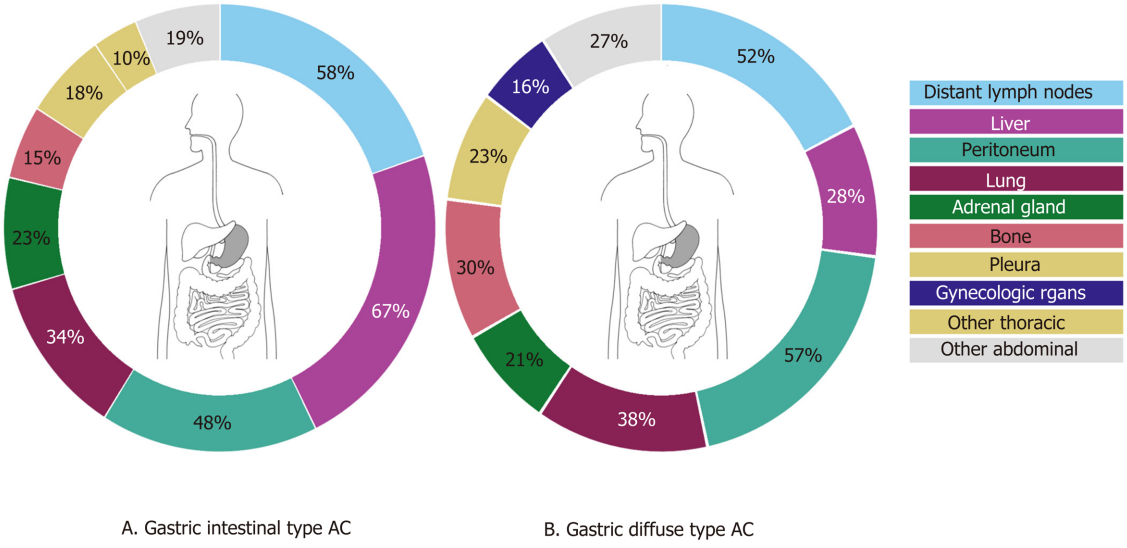

Figure 3 Metastatic sites of patients with gastric cancer. Other metastases of gastric cancer (all types) with proportion ≥ 2%: heart (7%), kidney (6%), pancreas (5%), thyroid gland (4%), brain (3%), large intestine (3%), small intestine (2%), mediastinum (2%), skin/subcutis (2%), urine bladder (2%). AC: Adenocarcinoma.

observed.

Overall, the most common metastatic sites of esophageal and gastric cancer found in this study are comparable to the literature[8-12]. Metastases to the liver are frequently observed in both esophageal and gastric cancer. The venous drainage of the distal esophagus is partly provided by the left gastric vein and by the gastroepiploic veins for the stomach which both drain directly into the portal vein. This may explain a high frequency of liver metastases in both groups. The other part of the venous drainage of

the distal esophagus, as well as the mid and proximal part of the esophagus, is provided by the azygos vein which directly drains to the superior vena cava which probably explains the high frequency of lung metastases[14]. In addition to anatomical factors which promote specific spreading, organ specific tropism of circulating tumor cells as suggested by the seed and soil hypothesis[15] may also account for frequent metastases to the liver and lung. In esophageal and gastric cancer patients with metastatic disease, we surprisingly also observed frequent metastases in the adrenal gland (27% and 23%), heart (13% and 7%) and kidney (10% and 7%). In literature, metastases to the adrenal gland, heart and kidney are sparsely described. This can probably be explained by the fact that our study is based on autopsy cases, and these distant metastases might be later occurrences, that are also part of a more widespread disease[9,16-18]. Major differences in metastatic sites between histological subtypes were found. While esophageal AC had a predilection for peritoneal and bone metastases, SCC more often spread to the lungs, as is in line with previous findings[8,9]. Underlying mechanisms for differences in metastatic patterns between histological esophageal cancer subtypes are not clear, although the tumor location can be a confounding factor as ACs are generally located in the distal esophagus and SCC generally represent the more proximal tumors. For gastric intestinal adenocarcinoma, more metastases were found in the liver while diffuse-type gastric cancer spreads more often to bone, colorectum, peritoneum and female reproductive organs. The preference of signet-ring cell carcinoma for metastases to the female reproductive organs and peritoneum has been described before in colorectal cancer and may be organ specific tropism of circulating signet-ring cells[19]. Furthermore, previous research reported on the affinity of diffuse-type gastric cancer for peritoneal seeding[12,20]. However, subclassifying of adenocarcinomas into intestinal- and diffuse-type cancers may vary between pathologists since the subclassification of these carcinomas was ill-defined until very recently[21].

This study has limitations due to the retrospective nature of the study. Post-mortem studies offer a unique opportunity to examine the extent and location of metastases and can been seen as the gold standard in the study of cancer metastatic pattern. An autopsy study can lead to a biased population in which patients are included who have died postoperatively, had an unexpected clinical course, or died of other causes than esophageal or gastric cancer. However, previous studies confirmed the validity of data from autopsy studies in other cancer types where independent clinical trial and population-based cohorts showed identical patterns[19,22], illustrating that the bias is indeed limited. Unfortunately, the PALGA database does not include a broad spectrum of patient characteristics regarding, for example, comorbidities and demographics and therefore the exact external validity of this study is unclear. Another limitation is the problem of classifying cardia cancers, since the cardia is an ill-defined region of the stomach[23]. This may explain the differences in the metastatic pattern of proximal stomach (cardia) carcinomas in our cohort compared to literature[12].

Over the last decades, considerable improvements of diagnostic techniques in preoperative staging have been made[24]. Still, early recognition of metastases is necessary to avoid futile locoregional treatments. For example, diffuse-type gastric cancer has the tendency to spread to the peritoneal cavity, and therefore a diagnostic laparoscopy for the detection of peritoneal metastases is now common practice in the staging of gastric cancer[25]. Interestingly, this study shows that peritoneal metastases are also frequently observed in patients with metastatic distal esophageal and GEJ AC (38%). Few clinical studies do show the added value of a diagnostic laparoscopy for occult metastatic disease in distal esophageal and GEJ adenocarcinoma patients, whilst other studies report a relatively low rate of positive findings for routine laparoscopy in these patients. Further clinical studies are warranted to investigate if a pre-treatment diagnostic laparoscopy could also be of value for these patients[26,27]. Furthermore, knowledge of the preference location of metastases may help to develop individualized treatment strategies in case of metastatic disease such as Selective liver Internal Radiation therapy (SIRT) for liver metastases or adjuvant pressurized intraperitoneal aerosol chemotherapy or hyperthermic intraperitoneal chemotherapy for peritoneal metastases[28].

CONCLUSION

In conclusion, this autopsy study shows differences in the spread of distant metastases based on the primary tumor location and their histological subtypes in a large national

cohort. These results should be taken into account during preoperative staging, during follow-up and in future research.

ARTICLE HIGHLIGHTS

Research background

Patients with gastric or esophageal cancer have a high incidence of locoregional recurrence and distant metastases and therefore have limited survival. There are limited studies reporting on differences of the metastatic spreading according to the primary tumor location and histological subtype.

Research motivation

As upper gastrointestinal tract tumors are a heterogenous group, further improvement of survival probably lies within a more personalized treatment strategy. Also, early recognition of metastases is important to avoid futile locoregional treatments. Therefore, it is important to attain deeper knowledge on the different patterns of metastatic spreading and the factors that are instrumental in the determination of these patterns.

Research objectives

The aim of this study is to gain insight into the metastatic pattern of gastroesophageal cancer.

Research methods

A nationwide retrospective autopsy study of patients with adenocarcinoma or squamous cell carcinoma (SCC) of the esophagus or stomach with metastases between 1990 and 2017 was performed. The metastatic pattern was analyzed according to the primary tumor location and histological subtype.

Research results

Metastatic disease was found in 268 esophageal and 331 gastric cancer patients that underwent an autopsy. In esophageal cancer, the most common metastatic locations were liver (56%), distant lymph nodes (53%) and lung (50%). Esophageal adenocarcinoma showed more frequently metastases to the peritoneum and bone compared with esophageal SCC. In gastric cancer, the most common metastatic locations were distant lymph nodes (56%), liver (53%) and peritoneum (51%). Intestinal-type adenocarcinoma of the stomach showed metastases to the liver more frequently, whereas metastases to the bone, female reproductive organs and colorectum were observed more frequently in diffuse-type gastric adenocarcinoma.

Research conclusions

This autopsy study provides novel data on differences in the spread of distant metastases based on the primary tumor location and their histological subtypes in a large national autopsy cohort.

Research perspectives

These results should be taken into account during preoperative staging, during follow-up and in future research.

REFERENCES

1 **Torre LA**, Siegel RL, Ward EM, Jemal A. Global Cancer Incidence and Mortality Rates and Trends--An Update. *Cancer Epidemiol Biomarkers Prev* 2016; **25**: 16-27 [PMID: 26667886 DOI: 10.1158/1055-9965.EPI-15-0578]

2 **Bray F**, Ferlay J, Soerjomataram I, Siegel RL, Torre LA, Jemal A. Global cancer statistics 2018: GLOBOCAN estimates of incidence and mortality worldwide for 36 cancers in 185 countries. *CA Cancer J Clin* 2018; **68**: 394-424 [PMID: 30207593 DOI: 10.3322/caac.21492]

3 **van Hagen P**, Hulshof MC, van Lanschot JJ, Steyerberg EW, van Berge Henegouwen MI, Wijnhoven BP, Richel DJ, Nieuwenhuijzen GA, Hospers GA, Bonenkamp JJ, Cuesta MA, Blaisse RJ, Busch OR, ten Kate FJ, Creemers GJ, Punt CJ, Plukker JT, Verheul HM, Spillenaar Bilgen EJ, van Dekken H, van der Sangen MJ, Rozema T, Biermann K, Beukema JC, Piet AH, van Rij CM, Reinders JG, Tilanus HW, van der Gaast A; CROSS Group. Preoperative chemoradiotherapy for esophageal or junctional cancer. *N Engl J Med* 2012;

366: 2074-2084 [PMID: 22646630 DOI: 10.1056/NEJMoa1112088]

4 **Cats A**, Jansen EPM, van Grieken NCT, Sikorska K, Lind P, Nordsmark M, Meershoek-Klein Kranenbarg E, Boot H, Trip AK, Swellengrebel HAM, van Laarhoven HWM, Putter H, van Sandick JW, van Berge Henegouwen MI, Hartgrink HH, van Tinteren H, van de Velde CJH, Verheij M; CRITICS investigators. Chemotherapy *vs* chemoradiotherapy after surgery and preoperative chemotherapy for resectable gastric cancer (CRITICS): an international, open-label, randomised phase 3 trial. *Lancet Oncol* 2018; **19**: 616-628 [PMID: 29650363 DOI: 10.1016/S1470-2045(18)30132-3]

5 **Al-Batran SE**, Homann N, Pauligk C, Goetze TO, Meiler J, Kasper S, Kopp HG, Mayer F, Haag GM, Luley K, Lindig U, Schmiegel W, Pohl M, Stoehlmacher J, Folprecht G, Probst S, Prasnikar N, Fischbach W, Mahlberg R, Trojan J, Koenigsmann M, Martens UM, Thuss-Patience P, Egger M, Block A, Heinemann V, Illerhaus G, Moehler M, Schenk M, Kullmann F, Behringer DM, Heike M, Pink D, Teschendorf C, Löhr C, Bernhard H, Schuch G, Rethwisch V, von Weikersthal LF, Hartmann JT, Kneba M, Daum S, Schulmann K, Weniger J, Belle S, Gaiser T, Oduncu FS, Güntner M, Hozaeel W, Reichart A, Jäger E, Kraus T, Mönig S, Bechstein WO, Schuler M, Schmalenberg H, Hofheinz RD; FLOT4-AIO Investigators. Perioperative chemotherapy with fluorouracil plus leucovorin, oxaliplatin, and docetaxel *vs* fluorouracil or capecitabine plus cisplatin and epirubicin for locally advanced, resectable gastric or gastro-oesophageal junction adenocarcinoma (FLOT4): a randomised, phase 2/3 trial. *Lancet* 2019; **393**: 1948-1957 [PMID: 30982686 DOI: 10.1016/S0140-6736(18)32557-1]

6 **Dikken JL**, Lemmens VE, Wouters MW, Wijnhoven BP, Siersema PD, Nieuwenhuijzen GA, van Sandick JW, Cats A, Verheij M, Coebergh JW, van de Velde CJ. Increased incidence and survival for oesophageal cancer but not for gastric cardia cancer in the Netherlands. *Eur J Cancer* 2012; **48**: 1624-1632 [PMID: 22317953 DOI: 10.1016/j.ejca.2012.01.009]

7 **Pennathur A**, Gibson MK, Jobe BA, Luketich JD. Oesophageal carcinoma. *Lancet* 2013; **381**: 400-412 [PMID: 23374478 DOI: 10.1016/S0140-6736(12)60643-6]

8 **Ai D**, Zhu H, Ren W, Chen Y, Liu Q, Deng J, Ye J, Fan J, Zhao K. Patterns of distant organ metastases in esophageal cancer: a population-based study. *J Thorac Dis* 2017; **9**: 3023-3030 [PMID: 29221275 DOI: 10.21037/jtd.2017.08.72]

9 **Quint LE**, Hepburn LM, Francis IR, Whyte RI, Orringer MB. Incidence and distribution of distant metastases from newly diagnosed esophageal carcinoma. *Cancer* 1995; **76**: 1120-1125 [PMID: 8630886]

10 **Shiozaki H**, Sudo K, Xiao L, Wadhwa R, Elimova E, Hofstetter WL, Skinner HD, Lee JH, Weston B, Bhutani MS, Blum MA, Maru DM, Ajani JA. Distribution and timing of distant metastasis after local therapy in a large cohort of patients with esophageal and esophagogastric junction cancer. *Oncology* 2014; **86**: 336-339 [PMID: 24925190 DOI: 10.1159/000360703]

11 **Mori M**, Sakaguchi H, Akazawa K, Tsuneyoshi M, Sueishi K, Sugimachi K. Correlation between metastatic site, histological type, and serum tumor markers of gastric carcinoma. *Hum Pathol* 1995; **26**: 504-508 [PMID: 7750934]

12 **Riihimäki M**, Hemminki A, Sundquist K, Sundquist J, Hemminki K. Metastatic spread in patients with gastric cancer. *Oncotarget* 2016; **7**: 52307-52316 [PMID: 27447571 DOI: 10.18632/oncotarget.10740]

13 **Casparie M**, Tiebosch AT, Burger G, Blauwgeers H, van de Pol A, van Krieken JH, Meijer GA. Pathology databanking and biobanking in The Netherlands, a central role for PALGA, the nationwide histopathology and cytopathology data network and archive. *Cell Oncol* 2007; **29**: 19-24 [PMID: 17429138]

14 **Viadana E**, Bross ID, Pickren JW. The metastatic spread of cancers of the digestive system in man. *Oncology* 1978; **35**: 114-126 [PMID: 673317 DOI: 10.1159/000225269]

15 **Paget S**. The distribution of secondary growths in cancer of the breast. 1889. *Cancer Metastasis Rev* 1989; **8**: 98-101 [PMID: 2673568]

16 **Grise P**, Botto H, Camey M. Esophageal cancer metastatic to kidney: report of 2 cases. *J Urol* 1987; **137**: 274-276 [PMID: 3806818]

17 **Nakahashi C**, Kinoshita T, Konishi M, Nakagohri T, Inoue K, Oda T, Yoshida J, Hasebe T, Ochiai A. Long-term survival achieved by repeated resections of metachronous pulmonary and adrenal metastases of alpha-fetoprotein-producing gastric cancer: report of a case. *Surg Today* 2004; **34**: 784-787 [PMID: 15338356 DOI: 10.1007/s00595-004-2796-3]

18 **Shaheen O**, Ghibour A, Alsaid B. Esophageal Cancer Metastases to Unexpected Sites: A Systematic Review. *Gastroenterol Res Pract* 2017; **2017**: 1657310 [PMID: 28659974 DOI: 10.1155/2017/1657310]

19 **Hugen N**, van de Velde CJH, de Wilt JHW, Nagtegaal ID. Metastatic pattern in colorectal cancer is strongly influenced by histological subtype. *Ann Oncol* 2014; **25**: 651-657 [PMID: 24504447 DOI: 10.1093/annonc/mdt591]

20 **Honoré C**, Goéré D, Messager M, Souadka A, Dumont F, Piessen G, Elias D, Mariette C; FREGAT Working Group – FRENCH. Risk factors of peritoneal recurrence in eso-gastric signet ring cell adenocarcinoma: results of a multicentre retrospective study. *Eur J Surg Oncol* 2013; **39**: 235-241 [PMID: 23313257 DOI: 10.1016/j.ejso.2012.12.013]

21 **Mariette C**, Carneiro F, Grabsch HI, van der Post RS, Allum W, de Manzoni G; European Chapter of International Gastric Cancer Association. Consensus on the pathological definition and classification of poorly cohesive gastric carcinoma. *Gastric Cancer* 2019; **22**: 1-9 [PMID: 30167905 DOI: 10.1007/s10120-018-0868-0]

22 **Knijn N**, van Erning FN, Overbeek LI, Punt CJ, Lemmens VE, Hugen N, Nagtegaal ID. Limited effect of lymph node status on the metastatic pattern in colorectal cancer. *Oncotarget* 2016; **7**: 31699-31707 [PMID: 27145371 DOI: 10.18632/oncotarget.9064]

23 **von Rahden BH**, Feith M, Stein HJ. Carcinoma of the cardia: classification as esophageal or gastric cancer? *Int J Colorectal Dis* 2005; **20**: 89-93 [PMID: 15688098 DOI: 10.1007/s00384-004-0646-9]

24 **Rubenstein JH**, Shaheen NJ. Epidemiology, Diagnosis, and Management of Esophageal Adenocarcinoma. *Gastroenterology* 2015; **149**: 302-17. e1 [PMID: 25957861 DOI: 10.1053/j.gastro.2015.04.053]

25 **Hori Y**; SAGES Guidelines Committee. Diagnostic laparoscopy guidelines : This guideline was prepared by the SAGES Guidelines Committee and reviewed and approved by the Board of Governors of the Society of

American Gastrointestinal and Endoscopic Surgeons (SAGES), November 2007. *Surg Endosc* 2008; **22**: 1353-1383 [PMID: 18389320 DOI: 10.1007/s00464-008-9759-5]

26 **Yoon HH**, Lowe VJ, Cassivi SD, Romero Y. The role of FDG-PET and staging laparoscopy in the management of patients with cancer of the esophagus or gastroesophageal junction. *Gastroenterol Clin North Am* 2009; **38**: 105-120, ix [PMID: 19327570 DOI: 10.1016/j.gtc.2009.01.007]

27 **Mehta K**, Bianco V, Awais O, Luketich JD, Pennathur A. Minimally invasive staging of esophageal cancer. *Ann Cardiothorac Surg* 2017; **6**: 110-118 [PMID: 28446999 DOI: 10.21037/acs.2017.03.18]

28 **Koemans WJ**, van der Kaaij RT, Boot H, Buffart T, Veenhof AAFA, Hartemink KJ, Grootscholten C, Snaebjornsson P, Retel VP, van Tinteren H, Vanhoutvin S, van der Noort V, Houwink A, Hahn C, Huitema ADR, Lahaye M, Los M, van den Barselaar P, Imhof O, Aalbers A, van Dam GM, van Etten B, Wijnhoven BPL, Luyer MDP, Boerma D, van Sandick JW. Cytoreductive surgery and hyperthermic intraperitoneal chemotherapy *vs* palliative systemic chemotherapy in stomach cancer patients with peritoneal dissemination, the study protocol of a multicentre randomised controlled trial (PERISCOPE II). *BMC Cancer* 2019; **19**: 420 [PMID: 31060544 DOI: 10.1186/s12885-019-5640-2]

World Journal of Gastroenterology

Submit a Manuscript: https://www.f6publishing.com

World J Gastroenterol 2020 October 21; 26(39): 6047-6056

DOI: 10.3748/wjg.v26.i39.6047

ISSN 1007-9327 (print) ISSN 2219-2840 (online)

ORIGINAL ARTICLE

Retrospective Study

Relationships of early esophageal cancer with human papillomavirus and alcohol metabolism

Masaki Inoue, Yuichi Shimizu, Marin Ishikawa, Satoshi Abiko, Yoshihiko Shimoda, Ikko Tanaka, Sayoko Kinowaki, Masayoshi Ono, Keiko Yamamoto, Shoko Ono, Naoya Sakamoto

ORCID number: Masaki Inoue 0000-0002-2912-9305; Yuichi Shimizu 0000-0001-5367-4832; Marin Ishikawa 0000-0001-8221-8385; Satoshi Abiko 0000-0002-0962-8342; Yoshihiko Shimoda 0000-0001-7532-7903; Ikko Tanaka 0000-0002-1186-6884; Sayoko Kinowaki 0000-0003-4299-2477; Masayoshi Ono 0000-0002-3116-1638; Keiko Yamamoto 0000-0001-6548-0840; Shoko Ono orcid.org/0000-0002-4485-6367; Naoya Sakamoto 0000-0003-0061-059X.

Author contributions: Inoue M and Shimizu Y contributed equally to this work; Shimizu Y designed the research study; Inoue M, Shimoda Y, Tanaka I, Kinowaki S performed the research; Shimizu Y, Ono M, Yamamoto K, Ono S and Sakamoto N supervised the research; Inoue M, Shimizu Y and Abiko S analyzed data; Ishikawa M pathologically supervised the reseach; Inoue M and Shimizu Y wrote the manuscript; All authors have read and approve the final manuscript.

Institutional review board statement: This study was reviewed and approved by Hokkaido University Hospital Division of Clinical Research Administration.

Masaki Inoue, Yoshihiko Shimoda, Ikko Tanaka, Sayoko Kinowaki, Naoya Sakamoto, Department of Gastroenterology and Hepatology, Graduate School of Medicine and Faculty of Medicine, Hokkaido University, Sapporo, Hokkaido 060-0808, Japan

Yuichi Shimizu, Masayoshi Ono, Keiko Yamamoto, Division of Endoscopy, Hokkaido University Hospital, Sapporo, Hokkaido 060-8648, Japan

Marin Ishikawa, Department of Cancer Pathology, Hokkaido University Graduate School of Medicine, Sapporo, Hokkaido 060-0808, Japan

Marin Ishikawa, Shoko Ono, Department of Gastroenterology, Hokkaido University Hospital, Sapporo, Hokkaido 060-8648, Japan

Satoshi Abiko, Department of Gastroenterology and Hepatology, Hakodate Municipal Hospital, Hakodate, Hokkaido 041-8680, Japan

Corresponding author: Yuichi Shimizu, MD, PhD, Associate Professor, Division of Endoscopy, Hokkaido University Hospital, kita 14 jo, nishi 5 chome, kita-ku, Sapporo, Hokkaido 060-8648, Japan. yshimizu@med.hokudai.ac.jp

Abstract

BACKGROUND

It is well known that an alcohol consumption habit together with inactive heterozygous aldehyde dehydrogenase-2 (ALDH2) is an important risk factor for the development of esophageal squamous cell carcinoma (ESCC). It remains controversial whether human papillomavirus (HPV) infection contributes to the occurrence/development of ESCC. There has been no study in which the relationship between ESCC and HPV in addition to alcohol dehydrogenase-1B (ADH1B) and ALDH2 genotypes was evaluated.

AIM

To evaluate relationships between HPV infection and development of esophageal cancer, particularly early esophageal cancer, based on ADH1B/ALDH2 polymorphisms.

METHODS

We conducted an exploratory retrospective study using new specimens, and we

Informed consent statement: Patients were not required to give informed consent to the study because the analysis used anonymous clinical data that were obtained after each patient agreed to treatment by written consent. For full disclosure, the details of the study are published on the home page of Hokkaido University.

Conflict-of-interest statement: We have no financial relationships to disclose.

Data sharing statement: No additional data are available.

Manuscript source: Unsolicited manuscript

Received: July 1, 2020
Peer-review started: July 1, 2020
First decision: July 28, 2020
Revised: August 13, 2020
Accepted: September 25, 2020
Article in press: September 25, 2020
Published online: October 21, 2020

P-Reviewer: Xu YW
S-Editor: Zhang H
L-Editor: A
P-Editor: Li JH

enrolled 145 patients who underwent endoscopic resection for superficial ESCC and had been observed for more than two years by both physical examination and endoscopic examination in Hokkaido University Hospital. Saliva was collected to analyze genetic polymorphisms of ADH1B/ALDH2. We performed in situ hybridization for resected specimens to detect HPV by using an HPV type 16/18 probe.

RESULTS

HPV was detected in 15 (10.3%) of the 145 patients with ESCC. HPV-positive rates in inactive ALDH2*1/*2 and ALDH2*1/*1 + *2/*2 were 10.8% and 9.8%, respectively (P = 1.00). HPV-positive rates in slow-metabolizing ADH1B*1/*1 and ADH1B*1/*2 + *2/*2 were 12.0% and 10.0%, respectively (P = 0.72). HPV-positive rates in the heavy or moderate alcohol consumption group and the light or rare consumption group were 11.1% and 8.7%, respectively (P = 0.68). HPV-positive rates in the heavy smoking group and the light or no smoking group were 11.8% and 8.3%, respectively (P = 0.59). The 3-year incidence rates of secondary ESCC or head and neck cancer after initial treatment in the HPV-positive and HPV-negative groups were 14.4% and 21.4% (P = 0.22), respectively.

CONCLUSION

In the present situation, HPV status is considered to be less important than other risk factors, such as alcohol consumption, smoking habit, ADH1B/ALDH2 polymorphisms, and HPV status would therefore have no effect on ESCC risk management.

Key Words: Human papillomavirus; Esophageal squamous cell carcinoma; Early esophageal cancer; Alcohol dehydrogenase-1B; Aldehyde dehydrogenase-2; Endoscopic resection

Core Tip: We examined esophageal squamous cell carcinoma (ESCC) tissues obtained by endoscopic mucosal resection or endoscopic submucosal dissection for human papillomavirus (HPV) infection. Genotyping of alcohol dehydrogenase-1B (ADH1B)/aldehyde dehydrogenase-2 (ALDH2) by using saliva sampling was performed. As a result, significant differences were not found between HPV infection and ADH1B/ALDH2. However, results of investigations including investigation of genetic polymorphisms in alcohol metabolism were shown for the first time, and there has so far been study on only early ESCC. We therefore consider the results of our study to be important.

Citation: Inoue M, Shimizu Y, Ishikawa M, Abiko S, Shimoda Y, Tanaka I, Kinowaki S, Ono M, Yamamoto K, Ono S, Sakamoto N. Relationships of early esophageal cancer with human papillomavirus and alcohol metabolism. *World J Gastroenterol* 2020; 26(39): 6047-6056
URL: https://www.wjgnet.com/1007-9327/full/v26/i39/6047.htm
DOI: https://dx.doi.org/10.3748/wjg.v26.i39.6047

INTRODUCTION

Esophageal cancer is a prevalent cancer and has a high mortality rate with a 5-year relative survival rate of only about 20% despite recent technological advances in surgery and chemoradiotherapy[1]. It is well known that smoking and alcohol consumption are risk factors for esophageal squamous cell carcinoma (ESCC). However, some ESCC patients have had no smoking or alcohol consumption habit until they are diagnosed with ESCC. This indicates that there might be other risk factors for the development of ESCC including polycyclic aromatic hydrocarbons, high-temperature foods, diet, oral health, and microbiome and human papillomavirus (HPV) infection[2]. The hypothesis of a relationship between HPV infection and development of ESCC was first proposed in 1982[3]. After that, various studies were

performed, and the results of some studies supported the hypothesis, while the results of other studies did not support the hypothesis[4-13]. It remains controversial whether HPV contributes to the development of ESCC. In head and neck squamous cell carcinoma (HNSCC), which is the same squamous cell carcinoma as ESCC is, it has been shown that HPV infection promotes the development of cancer, and HPV has been recognized as a carcinogenic agent[14]. Moreover, it has been reported that HPV infection in oropharyngeal squamous cell carcinoma is a significant prognostic factor for good survival. Notably, it has been reported that the incidence of second primary tumors is significantly lower in patients with HPV-positive oropharyngeal squamous cell carcinoma[15]. Subsequent investigations revealed that not only the prognosis of oropharyngeal squamous cell carcinoma (SCC) but also that of other head and neck cancers such as hypopharyngeal, laryngeal, oral cavity cancer is related to HPV status[16].

Alcohol consumption is known to be the most important risk factor for ESCC. Ethanol, which is one type of alcohol, itself does not cause the occurrence of ESCC, but acetaldehyde produced by alcohol has been reported to have carcinogenicity[17,18]. Ethanol is broken down by an enzyme called alcohol dehydrogenase 1B (ADH1B), resulting in the formation of acetaldehyde. Acetaldehyde is mostly metabolized in the liver by an enzyme called aldehyde dehydrogenase 2 (ALDH2), resulting in the formation of harmless acetic acid[19]. ADH1B and ALDH2 have active and inactive forms in the metabolism to acetaldehyde, and the combination of these forms is associated with not only advanced ESCC but also early stage ESCC[20,21]. Many studies have shown an association between ADH1B/ALDH2 and incidence of ESCC[21,22]. As for metachronous ESCC, Abiko *et al*[23] demonstrated that superficial ESCC patients with inactive ALDH2 have a high incidence of secondary ESCC.

There has been no study in which the risk of ESCC depending on the HPV status and the genetic polymorphisms of ADH1B/ALDH2 was investigated. In this study, we therefore investigated the relationship between HPV infection and development of esophageal cancer, particularly early esophageal cancer, based on ADH1B/ALDH2 polymorphisms.

MATERIALS AND METHODS

Patients

The subjects for this study were registered during the period from July 2016 to August 2017. The subjects were patients who underwent endoscopic mucosal dissection (ESD) or endoscopic mucosal resection (EMR) for ESCC at Hokkaido University Hospital and received follow-up endoscopic examinations for 2 years or more. Endoscopic examinations were performed in all patients using iodine staining at 3 mo, 6 mo, and 1 year after the EMR/ESD and every 6 mo to 1 year thereafter. All of the patients underwent annual physical examinations including laryngoscopy conducted by otolaryngologists. Inclusion criteria for this study were (1) pathological diagnosis of ESCC in resected specimens; (2) complete endoscopic resection by EMR or ESD; (3) written informed consent obtained from the patient; and (4) possibility of collecting saliva samples. Exclusion criteria were (1) surgical resection after EMR/ESD; (2) unsuitability as subjects; (3) age < 20 years; and (4) current pregnancy. After exclusion, 158 patients were included in the study. No patients had lymph node metastasis. This study was a retrospective study in which newly obtained specimens were used. Written informed consent was obtained from the study subjects.

Information on alcohol consumption and smoking before and after EMR/ESD was obtained by using a questionnaire. Information on past treatment for esophageal cancer or head and neck cancer by EMR/ESD and histological diagnosis was obtained from electronic health records. Before the endoscopic examination, approximately 1 mL of saliva was obtained by using a pipette or a cotton swab to examine two single nucleotide polymorphisms (SNPs) in ADH1B and ALDH2 genotyping.

This study was approved by the Medical Ethics and Human Clinical Trial Committee of Hokkaido University Hospital.

Alcohol consumption and smoking habits

Subjects whose alcohol consumption was less than 1 unit/wk were classified as rare drinkers, those whose alcohol consumption was 1 to 8.9 units/wk were classified as light drinkers, those whose alcohol consumption was 9 to 17.9 units/wk were classified as moderate drinkers, and those whose alcohol consumption was 18 or more units/wk were classified as heavy drinkers. We defined 1 unit of alcohol as 22 g of

ethanol, which is contained in 500 mL of beer or 1/4 bottle of wine. Subjects who did not smoke or smoked rarely were classified as rare smokers (nonsmokers). Current smokers with a smoking history of 30 pack years were classified as light smokers, while subjects who had a smoking history of ≥ 30 pack years were classified as heavy smokers. Thirty pack years = one package of cigarettes (20 cigarettes) daily for 30 years[24,25].

HPV in situ hybridization

We conducted in situ hybridization to detect HPV using the ENZO PATHO-GENE HPV type 16/18 probe according to the protocol of manufacturer (Morpho Technology Co., Ltd, Sapporo, Japan). Fixed specimens were deparaffinized and rehydrated through a graded ethanol series and then washed with phosphate buffered saline. The deparaffinized tissue sections were incubated with pronase, rinsed in deionized water, immersed in 0.3% H_2O_2 in methanol for 20 min, and rinsed in deionized water again. A drop of HPV probe was added to the air-dried sections. After heart denaturation at 90 °C, hybridization was done in a pre-warmed humid chamber at 37 °C for 16 to 18 h. The slides were washed in Tris-buffered saline with Tween 20 (TBST). Hybridized probes were detected by streptavidin. HPV-positive cervical cancer was used as a positive control. All pathological diagnoses including whether HPV is positive or negative were made by a pathologist.

ADH1B/ALDH2 polymorphisms

SNPs of ADH1B and ALDH2 genes were genotyped using the TaqMan assay on an ABI 7300 Real-Time polymerase chain reaction (PCR) System (Applied Biosystems)[26]. The ADH1B*1 allele encodes the slow-metabolizing form of ADH1B, while the ALDH2*2 allele encodes the inactive form of ALDH2. The ADH1B and ALDH2 genotype combinations were classified into five categories according to the classification proposed by Yokoyama *et al*[27]: A group, ADH1B*1/*1 + ALDH2*1/*1; B group, ADH1B*2 carrier + ALDH2*1/*1; C group, ADH1B*1/*1 + ALDH2*1/*2; D group, ADH1B*2 carrier + ALDH2*1/*2; E group, ADH1B any + ALDH2*2/*2.

Statistical analysis

Analyses of data were performed by using JMP® Pro 14.0.1 (SAS Institute, Inc., Cary, NC, United States). Age is expressed as mean ± SD values. Differences in frequency distributions were tested using Fisher's exact test, and quantitative data were examined with Student's *t*-test. Differences were considered statistically significant at $P < 0.05$. The time to development of metachronous ESCC/HNSCC was defined as the period from the day of EMR/ESD to the day of endoscopic diagnosis of metachronous ESCC/HNSCC. The Kaplan–Meier method and log-rank test were used for analysis of the development of metachronous ESCC as well as HNSCC.

RESULTS

Among the 158 patients, 13 patients were excluded because their primary lesions were not large enough to assess HPV. Finally, 145 patients were assessed. Characteristics of the patients and lesions are shown in Table 1. Specimens from 15 (10.3%) of the 145 patients were HPV-positive. There was no significant difference between HPV-positive patients and HPV-negative patients in sex, age or tumor location. The main macroscopic types were 0-Is in 1 patient (0.7%), 0-IIa in 16 patients (15.2%), 0-IIb in 43 patients (29.7%), and 0-IIc in 85 patients (58.6%). The main macroscopic type was related to HPV infection, and the number of 0-IIa cases was significantly larger in HPV-positive ESCC cases ($P = 0.045$). The mean tumor size was 22.4 ± 10.6 mm. There was no difference between the HPV-positive and the HPV-negative groups in depth of invasion or vascular invasion.

The relationships of HPV status with risk factors for ESCC are summarized in Table 2. HPV-positive rates in inactive ALDH2*1/*2 and ALDH2*1/*1 + *2/*2 were 10.8% and 9.6%, respectively ($P = 1.00$). HPV-positive rates in slow-metabolizing ADH1B*1/*1 and ADH1B*1/*2 + *2/*2 were 12.0% and 10.0%, respectively ($P = 0.72$). HPV-positive rates in the heavy or moderate alcohol consumption group and the light or rare consumption group were 11.1% and 8.7%, respectively ($P = 0.68$). HPV-positive rates in the heavy smoking group and the light or no smoking group were 11.8% and 8.3%, respectively ($P = 0.59$). Genotype combinations did not show significant differences in HPV-positive rates (group A, 0%; group B, 10.9%; group C, 15.0%; group D, 9.6%; group E, 0.0%; $P = 0.87$). There were no significant differences in HPV-

Table 1 Clinicopathological findings according to the human papillomavirus positive or negative, *n* (%)

	Total (*n* = 145)	HPV positive (*n* = 15)	HPV negative (*n* = 130)	*P* value
Sex				
Male	119 (82.1)	12 (80.0)	107 (82.3)	0.73
Female	26 (17.9)	3 (20.0)	23 (17.7)	
Age (yr), mean ± SD	66.3 ± 7.8	63.9 ± 9.3	66.6 ± 7.6	0.21
Tumor location				
Cervical	1 (0.7)	1 (6.7)	0 (0)	0.059
Upper	22 (15.2)	0 (0)	22 (16.9)	
Middle	85 (58.6)	11 (73.3)	74 (56.9)	
Lower	36 (24.8)	3 (20.0)	33 (25.4)	
Abdominal	1 (0.7)	0 (0)	1 (0.8)	
Main macroscopic type				
0-Is	1 (0.7)	0 (0)	1 (0.8)	0.045
0-IIa	16 (11.0)	5 (33.3)	11 (8.5)	
0-IIb	43 (29.7)	4 (26.7)	39 (30.0)	
0-IIc	85 (58.6)	6 (40.0)	79 (60.8)	
Tumor size (mm), mean (SD)	22.4 (10.6)	26.5 (12.7)	21.9 (10.3)	0.11
Depth of invasion				
EP	53 (36.6)	5 (33.3)	48 (36.9)	0.74
LPM	66 (45.5)	7 (46.7)	59 (45.4)	
MM	19 (13.1)	2 (13.3)	17 (13.1)	
SM1	4 (2.8)	1 (6.7)	3 (2.3)	
SM2	3 (2.1)	0 (0)	3 (2.3)	
Vascular invasion				
Yes	6 (4.1)	2 (13.3)	4 (3.1)	0.12
No	139 (95.9)	13 (86.7)	126 (96.9)	

EP: Epithelium; LPM: Lamina propria mucosae; MM: Muscularis mucosae; HPV: Human papillomavirus; SM1: ≤ 200 μm from MM; SM2: > 200 μm from MM.

positive rates according to either ADH1B/ALDH2 genotype or smoking and alcohol consumption histories. The median follow-up period was 73 mo (range, 24-244 mo). The 3-year incidence rates of secondary ESCC or HNSCC after initial treatment in the HPV-positive and HPV-negative groups were 14.4% and 21.4% (P = 0.22), respectively (Figure 1).

DISCUSSION

This study is the first study that focused on HPV infection in cases of early ESCC based on ADH1B/ALDH2 polymorphisms. Many studies have been carried out to determine whether the hypothesis that HPV contributes to the occurrence of ESCC is true, but the results have not been consistent[4-13]. Even in a recent meta-analysis and systematic review, the conclusions are still confusing. Petrick *et al*[13] conducted a meta-analysis including 124 studies with a total of 13832 ESCC cases and reported that the highest HPV prevalence was found in Africa and Asia, notably among Chinese studies from provinces with high ESCC incidence rates. Halec *et al*[10] conducted a study on HPV-transformation of ESCC by using tissues from high-incidence ESCC regions and a meta-analysis of 14 other similar studies. They concluded that the results of the

Table 2 Relationships of human papillomavirus status according to ISH with risk factors for esophageal squamous cell carcinoma, *n* (%)

HPV	*ALDH2* genotype					*P* value
	*1/*2 (*n* = 93)			*1/*1 + *2/*2 (*n* = 52)		
Positive (*n* = 15)	10 (10.8)			5 (9.6)		1.00
Negative (*n* = 130)	83 (89.3)			47 (90.4)		
	***ADH1B* genotype**					
	*1/*1 (*n* = 25)			*2 carrier (*n* = 120)		
Positive (*n* = 15)	3 (12.0)			12 (10.0)		0.72
Negative (*n* = 130)	22 (88.0)			108 (90.0)		
	Alcohol consumption					
	Light – Rare (*n* = 46)			Heavy – Moderate (*n* = 99)		
Positive (*n* = 15)	4 (8.7)			11 (11.1)		0.68
Negative (*n* = 130)	42 (91.3)			88 (88.9)		
	Smoking habits					
	Light – Rare (*n* = 60)			Heavy (*n* = 85)		
Positive (*n* = 15)	5 (8.3)			10 (11.8)		0.59
Negative (*n* = 130)	55 (91.7)			75 (88.2)		
	Genotype combinations					
	A	B	C	D	E	
Positive (*n* = 15)	0 (0.0)	5 (10.9)	3 (15.0)	7 (9.6)	0 (0.0)	0.87
Negative (*n* = 130)	5 (100.0)	41 (89.1)	17 (85.0)	66 (90.4)	1 (100.0)	

A: *ADH1B* genotype (*1/*1), *ALDH2* genotype (*1/*1); B: *ADH1B* genotype (*2 carrier), *ALDH2* genotype (*1/*1); C: *ADH1B* genotype (*1/*1), *ALDH2* genotype (*1/*2); D: *ADH1B* genotype (*2 carrier), *ALDH2* genotype (*1/*2); E: *ADH1B* genotype (Any), *ALDH2* genotype (*2/*2).

studies did not support an etiological role of HPV in ESCC carcinogenesis. Although the effects of HPV infection on the occurrence of ESCC with consideration of smoking and drinking habits were examined in many previous studies, there has been no study focusing on ADH1B/ALDH2. Assuming that HPV infection is involved in the development of ESCC, we thought that patients who do not have ESCC risk factors, particularly inactive ALDH2, would tend to show high HPV-positive rates. However, we could not find any significant difference between HPV infection and any of the ESCC risk factors. From another point of view, early ESCC after endoscopic resection often causes metachronous recurrence. After examining the possibility that HPV infection contributes to less prevalence of metachronous recurrence of ESCC, no significant difference was found between HPV-positive and HPV-negative groups in the incidence of secondary SCC. As for the characteristics of HPV-positive ESCC, in our analyses, type IIa lesions, which have mild protrusion up to about 1 mm, tended to be detected in HPV-positive lesions. In many previous studies, significant clinicopathological differences between HPV-positive ESCC and HPV-negative ESCC were not revealed[28-33]. Since the relationship between HPV infection and development of ESCC is not clear, it is debatable whether HPV infection contributes to upward growth. The influence of HPV infection on tumor growth and morphology in the esophagus remains unknown.

In a past review, it was shown that HPV-positive rates in patients with ESCC range from 11.7% to 38.9%[9]. Some differences in HPV-positive rates have been observed in previous studies, and the HPV-positive rate of 10.3% in our study is slightly lower than the rates in previous studies. There are various possible reasons for the differences, but geographic variation has been reported to be the main reason for the differences in HPV-positive rates[34]. Studies showing high HPV prevalence rates were studies conducted in Asia, while studies showing low HPV prevalence rates were studies conducted in North America and Europe[8,34,35]. Previous studies including meta-analyses in which the relationship between HPV infection and esophageal cancer

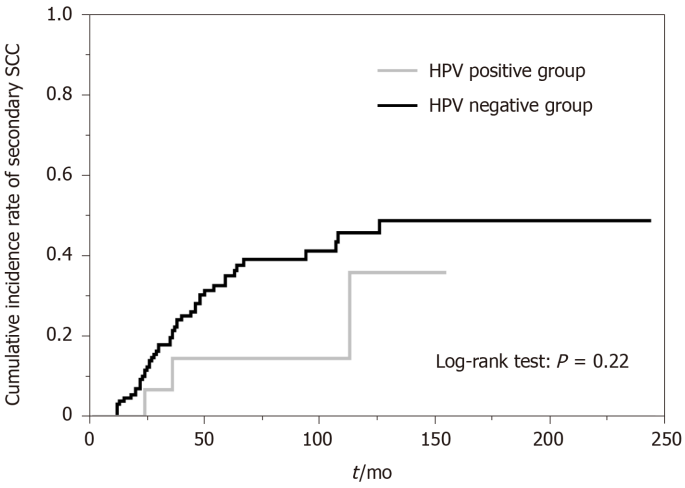

Figure 1 Metachronous development of esophageal squamous cell carcinoma or head and neck squamous cell carcinoma after endoscopic mucosal dissection/endoscopic mucosal resection. The median follow-up period was 73 mo (range, 24-244 mo). The 3-year incidence rates of secondary esophageal squamous cell carcinoma or head and neck squamous cell carcinoma after initial treatment in the human papillomavirus (HPV)-positive and HPV-negative groups were 14.4% and 21.4% (P = 0.22), respectively. SCC: Squamous cell carcinoma; HPV: Human papillomavirus.

was investigated included many studies conducted in Asia, which is considered to be a region with a high incidence of HPV. Such publication bias has been an issue of discussion[9]. For example, Syrjänen conducted a meta-analysis including 10234 ESCC cases and reported that the overall HPV prevalence was 30.6%. However, when regions were limited to North America, which is a region with a low incidence of HPV, the rate fell to 10.1%[36]. Japan is a country in Asia, but considering HPV prevalence regions, it is not clear whether Japan, like other Asian countries, can be regarded as a region with a high incidence of HPV. There have been only a few reports about the prevalence of HPV in Japan. Goto *et al*[37] reported that the HPV-positive rate in patients with esophageal carcinoma in Asia including Japan was 9.4%, and they also showed that HPV-positive rates varied depending on the location in Japan. These regional differences might be caused by environmental risk factors, genetic background, and histological types. We therefore cannot simply compare HPV-positive rates in our region with HPV-positive rates in previous reports. However, there would not be large differences. Moreover, even if HPV infection rate varies depending on the region, the role HPV in ESCC would not change. HPV-positive rates are also affected by the quality of patient samples and the methods used for evaluating HPV status. Sampling by endoscopic biopsies might result in inadequate or incorrect tissue samples[38]. EMR/ESD for ESCC can provide precise tissue samples of almost exclusively ESCC without the problem of excessive or insufficient tissue samples. We analyzed early ESCC specimens, all of which were endoscopically resected. In the most past studies, the association of HPV with ESCC was investigated using samples derived from endoscopic biopsy or parts of surgical specimens. There is no information about HPV-positive rates only in early ESCC specimens derived from EMR/ESD. The use of specimens obtained from EMR/ESD would reduce sampling errors such errors caused by inaccurate endoscopic biopsy and would enable accurate evaluation of ESCC cases of the same stage. We therefore consider that HPV-ESCC prevalence was evaluated with a high level of accuracy and under the most possible uniform condition in our study. With regard to methodological issues, another concern is the method used for inspection of tissue samples. In most recent studies, ISH or PCR was used for detecting HPV infection. It has been reported that HPV infection rate varied depending on the method used for detecting HPV[34,36,39,40]. In general, ISH has higher specificity but lower sensitivity than those of PCR for detection of HPV[41]. In our study, lower HPV prevalence might have resulted from the characteristics of ISH.

This study has some limitations. First, participants in this study were all Japanese patients, and the study was conducted in a single institution. Therefore, geographic bias, especially for HPV prevalence, could not be completely excluded. Second, methodological bias must be considered for accurate estimation of HPV-positive rates. HPV-positive rate would differ depending on the sensitivity and accuracy of the method used for detecting HPV infection. However, in our study conducted with EMR/ESD samples and using ISH for detection of HPV, it is thought that bias was reduced as much as possible. Third, this study was conducted with a restricted sample

size. To improve statistical reliability, further studies with large sample sizes are required.

CONCLUSION

In conclusion, our study in which genetic polymorphisms of ADH1B/ALDH2 were considered suggested that HPV did not have an association with ESCC. In the present situation, HPV status is considered to be less important than other risk factors, such as alcohol consumption, smoking habit, and ADH1B/ALDH2 polymorphisms, and HPV status would therefore have no effect on ESCC risk management.

ARTICLE HIGHLIGHTS

Research background

There has been no study in which the relationship between superficial esophageal squamous cell carcinoma (ESCC) and human papillomavirus (HPV) in addition to alcohol metabolism was evaluated.

Research motivation

We aimed to clarify whether HPV infection together with alcohol metabolism genes affects the carcinogenesis of ESCC.

Research objectives

We enrolled 145 patients who underwent endoscopic submucosal dissection (ESD) or endoscopic mucosal resection (EMR) for ESCC.

Research methods

We analyzed patients' genetic polymorphisms of alcohol dehydrogenase-1B (ADH1B)/ aldehyde dehydrogenase-2 (ALDH2) and performed in situ hybridization for resected specimens to detect HPV by using an HPV type 16/18 probe.

Research results

There were no significant differences in HPV-positive rates according to either ADH1B/ALDH2 genotype or smoking and alcohol consumption histories.

Research conclusions

HPV status is considered to be less important than other risk factors, such as alcohol consumption, smoking habit, ADH1B/ALDH2 polymorphisms and HPV status would therefore have no effect on ESCC risk management.

Research perspectives

We are planning a multicenter study of patients with superficial pharyngeal cancer evaluating ADH1B/ALDH2 and HPV status.

REFERENCES

1 **Allemani C**, Weir HK, Carreira H, Harewood R, Spika D, Wang XS, Bannon F, Ahn JV, Johnson CJ, Bonaventure A, Marcos-Gragera R, Stiller C, Azevedo e Silva G, Chen WQ, Ogunbiyi OJ, Rachet B, Soeberg MJ, You H, Matsuda T, Bielska-Lasota M, Storm H, Tucker TC, Coleman MP; CONCORD Working Group. Global surveillance of cancer survival 1995-2009: analysis of individual data for 25,676,887 patients from 279 population-based registries in 67 countries (CONCORD-2). *Lancet* 2015; **385**: 977-1010 [PMID: 25467588 DOI: 10.1016/S0140-6736(14)62038-9]

2 **Abnet CC**, Arnold M, Wei WQ. Epidemiology of Esophageal Squamous Cell Carcinoma. *Gastroenterology* 2018; **154**: 360-373 [PMID: 28823862 DOI: 10.1053/j.gastro.2017.08.023]

3 **Syrjänen KJ**. Histological changes identical to those of condylomatous lesions found in esophageal squamous cell carcinomas. *Arch Geschwulstforsch* 1982; **52**: 283-292 [PMID: 7138240]

4 **Dong HC**, Cui XB, Wang LH, Li M, Shen YY, Zhu JB, Li CF, Hu JM, Li SG, Yang L, Zhang WJ, Chen YZ, Li F. Type-specific detection of human papillomaviruses in Kazakh esophageal squamous cell carcinoma by genotyping both E6 and L1 genes with MALDI-TOF mass spectrometry. *Int J Clin Exp Pathol* 2015; **8**: 13156-13165 [PMID: 26722514]

5 **Türkay DÖ**, Vural Ç, Sayan M, Gürbüz Y. Detection of human papillomavirus in esophageal and

gastroesophageal junction tumors: A retrospective study by real-time polymerase chain reaction in an instutional experience from Turkey and review of literature. *Pathol Res Pract* 2016; **212**: 77-82 [PMID: 26608416 DOI: 10.1016/j.prp.2015.10.007]

6 **Li X**, Gao C, Yang Y, Zhou F, Li M, Jin Q, Gao L. Systematic review with meta-analysis: the association between human papillomavirus infection and oesophageal cancer. *Aliment Pharmacol Ther* 2014; **39**: 270-281 [PMID: 24308856 DOI: 10.1111/apt.12574]

7 **Liyanage SS**, Rahman B, Ridda I, Newall AT, Tabrizi SN, Garland SM, Segelov E, Seale H, Crowe PJ, Moa A, Macintyre CR. The aetiological role of human papillomavirus in oesophageal squamous cell carcinoma: a meta-analysis. *PLoS One* 2013; **8**: e69238 [PMID: 23894436 DOI: 10.1371/journal.pone.0069238]

8 **Yong F**, Xudong N, Lijie T. Human papillomavirus types 16 and 18 in esophagus squamous cell carcinoma: a meta-analysis. *Ann Epidemiol* 2013; **23**: 726-734 [PMID: 23916383 DOI: 10.1016/j.annepidem.2013.07.002]

9 **Ludmir EB**, Stephens SJ, Palta M, Willett CG, Czito BG. Human papillomavirus tumor infection in esophageal squamous cell carcinoma. *J Gastrointest Oncol* 2015; **6**: 287-295 [PMID: 26029456 DOI: 10.3978/j.issn.2078-6891.2015.001]

10 **Halec G**, Schmitt M, Egger S, Abnet CC, Babb C, Dawsey SM, Flechtenmacher C, Gheit T, Hale M, Holzinger D, Malekzadeh R, Taylor PR, Tommasino M, Urban MI, Waterboer T, Pawlita M, Sitas F; InterSCOPE Collaboration. Mucosal alpha-papillomaviruses are not associated with esophageal squamous cell carcinomas: Lack of mechanistic evidence from South Africa, China and Iran and from a world-wide meta-analysis. *Int J Cancer* 2016; **139**: 85-98 [PMID: 26529033 DOI: 10.1002/ijc.29911]

11 **Gao GF**, Roth MJ, Wei WQ, Abnet CC, Chen F, Lu N, Zhao FH, Li XQ, Wang GQ, Taylor PR, Pan QJ, Chen W, Dawsey SM, Qiao YL. No association between HPV infection and the neoplastic progression of esophageal squamous cell carcinoma: result from a cross-sectional study in a high-risk region of China. *Int J Cancer* 2006; **119**: 1354-1359 [PMID: 16615110 DOI: 10.1002/ijc.21980]

12 **Koshiol J**, Wei WQ, Kreimer AR, Chen W, Gravitt P, Ren JS, Abnet CC, Wang JB, Kamangar F, Lin DM, von Knebel-Doeberitz M, Zhang Y, Viscidi R, Wang GQ, Gillison ML, Roth MJ, Dong ZW, Kim E, Taylor PR, Qiao YL, Dawsey SM. No role for human papillomavirus in esophageal squamous cell carcinoma in China. *Int J Cancer* 2010; **127**: 93-100 [PMID: 19918949 DOI: 10.1002/ijc.25023]

13 **Petrick JL**, Wyss AB, Butler AM, Cummings C, Sun X, Poole C, Smith JS, Olshan AF. Prevalence of human papillomavirus among oesophageal squamous cell carcinoma cases: systematic review and meta-analysis. *Br J Cancer* 2014; **110**: 2369-2377 [PMID: 24619077 DOI: 10.1038/bjc.2014.96]

14 **D'Souza G**, Kreimer AR, Viscidi R, Pawlita M, Fakhry C, Koch WM, Westra WH, Gillison ML. Case-control study of human papillomavirus and oropharyngeal cancer. *N Engl J Med* 2007; **356**: 1944-1956 [PMID: 17494927 DOI: 10.1056/NEJMoa065497]

15 **Ang KK**, Harris J, Wheeler R, Weber R, Rosenthal DI, Nguyen-Tân PF, Westra WH, Chung CH, Jordan RC, Lu C, Kim H, Axelrod R, Silverman CC, Redmond KP, Gillison ML. Human papillomavirus and survival of patients with oropharyngeal cancer. *N Engl J Med* 2010; **363**: 24-35 [PMID: 20530316 DOI: 10.1056/NEJMoa0912217]

16 **Bryant AK**, Sojourner EJ, Vitzthum LK, Zakeri K, Shen H, Nguyen C, Murphy JD, Califano JA, Cohen EEW, Mell LK. Prognostic Role of p16 in Nonoropharyngeal Head and Neck Cancer. *J Natl Cancer Inst* 2018; **110**: 1393-1399 [PMID: 29878161 DOI: 10.1093/jnci/djy072]

17 **Seitz HK**, Stickel F. Molecular mechanisms of alcohol-mediated carcinogenesis. *Nat Rev Cancer* 2007; **7**: 599-612 [PMID: 17646865 DOI: 10.1038/nrc2191]

18 **Brooks PJ**, Zakhari S. Acetaldehyde and the genome: beyond nuclear DNA adducts and carcinogenesis. *Environ Mol Mutagen* 2014; **55**: 77-91 [PMID: 24282063 DOI: 10.1002/em.21824]

19 **Zakhari S**. Overview: how is alcohol metabolized by the body? *Alcohol Res Health* 2006; **29**: 245-254 [PMID: 17718403]

20 **Matejcic M**, Gunter MJ, Ferrari P. Alcohol metabolism and oesophageal cancer: a systematic review of the evidence. *Carcinogenesis* 2017; **38**: 859-872 [PMID: 28645180 DOI: 10.1093/carcin/bgx067]

21 **Cui R**, Kamatani Y, Takahashi A, Usami M, Hosono N, Kawaguchi T, Tsunoda T, Kamatani N, Kubo M, Nakamura Y, Matsuda K. Functional variants in ADH1B and ALDH2 coupled with alcohol and smoking synergistically enhance esophageal cancer risk. *Gastroenterology* 2009; **137**: 1768-1775 [PMID: 19698717 DOI: 10.1053/j.gastro.2009.07.070]

22 **Tanaka F**, Yamamoto K, Suzuki S, Inoue H, Tsurumaru M, Kajiyama Y, Kato H, Igaki H, Furuta K, Fujita H, Tanaka T, Tanaka Y, Kawashima Y, Natsugoe S, Setoyama T, Tokudome S, Mimori K, Haraguchi N, Ishii H, Mori M. Strong interaction between the effects of alcohol consumption and smoking on oesophageal squamous cell carcinoma among individuals with ADH1B and/or ALDH2 risk alleles. *Gut* 2010; **59**: 1457-1464 [PMID: 20833657 DOI: 10.1136/gut.2009.205724]

23 **Abiko S**, Shimizu Y, Miyamoto S, Ishikawa M, Matsuda K, Tsuda M, Mizushima T, Yamamoto K, Ono S, Kudo T, Ono K, Sakamoto N. Risk assessment of metachronous squamous cell carcinoma after endoscopic resection for esophageal carcinoma based on the genetic polymorphisms of alcoholdehydrogense-1B aldehyde dehydrogenase-2: temperance reduces the risk. *J Gastroenterol* 2018; **53**: 1120-1130 [PMID: 29423536 DOI: 10.1007/s00535-018-1441-7]

24 **Yokoyama A**, Katada C, Yokoyama T, Yano T, Kaneko K, Oda I, Shimizu Y, Doyama H, Koike T, Takizawa K, Hirao M, Okada H, Yoshii T, Konishi K, Yamanouchi T, Tsuda T, Omori T, Kobayashi N, Suzuki H, Tanabe S, Hori K, Nakayama N, Kawakubo H, Ishikawa H, Muto M. Alcohol abstinence and risk assessment for second esophageal cancer in Japanese men after mucosectomy for early esophageal cancer. *PLoS One* 2017; **12**: e0175182 [PMID: 28384229 DOI: 10.1371/journal.pone.0175182]

25 **Yokoyama T**, Yokoyama A, Kato H, Tsujinaka T, Muto M, Omori T, Haneda T, Kumagai Y, Igaki H, Yokoyama M, Watanabe H, Yoshimizu H. Alcohol flushing, alcohol and aldehyde dehydrogenase genotypes, and risk for esophageal squamous cell carcinoma in Japanese men. *Cancer Epidemiol Biomarkers Prev* 2003; **12**: 1227-1233 [PMID: 14652286]

26 **Hayashida M**, Ota T, Ishii M, Iwao-Koizumi K, Murata S, Kinoshita K. Direct detection of single nucleotide

polymorphism (SNP) by the TaqMan PCR assay using dried saliva on water-soluble paper and hair-roots, without DNA extraction. *Anal Sci* 2014; **30**: 427-429 [PMID: 24614740]

27 **Yokoyama A**, Brooks PJ, Yokoyama T, Mizukami T, Shiba S, Nakamoto N, Maruyama K. Recovery from anemia and leukocytopenia after abstinence in Japanese alcoholic men and their genetic polymorphisms of alcohol dehydrogenase-1B and aldehyde dehydrogenase-2. *Jpn J Clin Oncol* 2017; **47**: 306-312 [PMID: 28158658 DOI: 10.1093/jjco/hyw208]

28 **Abdirad A**, Eram N, Behzadi AH, Koriyama C, Parvaneh N, Akiba S, Kato T, Kahn N, Ghofrani M, Sadigh N. Human papillomavirus detected in esophageal squamous cell carcinoma in Iran. *Eur J Intern Med* 2012; **23**: e59-e62 [PMID: 22284258 DOI: 10.1016/j.ejim.2011.06.011]

29 **Herrera-Goepfert R**, Lizano M, Akiba S, Carrillo-García A, Becker-D'Acosta M. Human papilloma virus and esophageal carcinoma in a Latin-American region. *World J Gastroenterol* 2009; **15**: 3142-3147 [PMID: 19575494 DOI: 10.3748/wjg.15.3142]

30 **Castillo A**, Aguayo F, Koriyama C, Torres M, Carrascal E, Corvalan A, Roblero JP, Naquira C, Palma M, Backhouse C, Argandona J, Itoh T, Shuyama K, Eizuru Y, Akiba S. Human papillomavirus in esophageal squamous cell carcinoma in Colombia and Chile. *World J Gastroenterol* 2006; **12**: 6188-6192 [PMID: 17036393 DOI: 10.3748/wjg.v12.i38.6188]

31 **Yao PF**, Li GC, Li J, Xia HS, Yang XL, Huang HY, Fu YG, Wang RQ, Wang XY, Sha JW. Evidence of human papilloma virus infection and its epidemiology in esophageal squamous cell carcinoma. *World J Gastroenterol* 2006; **12**: 1352-1355 [PMID: 16552800 DOI: 10.3748/wjg.v12.i9.1352]

32 **Antonsson A**, Nancarrow DJ, Brown IS, Green AC, Drew PA, Watson DI, Hayward NK, Whiteman DC; Australian Cancer Study. High-risk human papillomavirus in esophageal squamous cell carcinoma. *Cancer Epidemiol Biomarkers Prev* 2010; **19**: 2080-2087 [PMID: 20696664 DOI: 10.1158/1055-9965.EPI-10-0033]

33 **Shuyama K**, Castillo A, Aguayo F, Sun Q, Khan N, Koriyama C, Akiba S. Human papillomavirus in high- and low-risk areas of oesophageal squamous cell carcinoma in China. *Br J Cancer* 2007; **96**: 1554-1559 [PMID: 17453003 DOI: 10.1038/sj.bjc.6603765]

34 **Syrjänen KJ**. HPV infections and oesophageal cancer. *J Clin Pathol* 2002; **55**: 721-728 [PMID: 12354793 DOI: 10.1136/jcp.55.10.721]

35 **Hardefeldt HA**, Cox MR, Eslick GD. Association between human papillomavirus (HPV) and oesophageal squamous cell carcinoma: a meta-analysis. *Epidemiol Infect* 2014; **142**: 1119-1137 [PMID: 24721187 DOI: 10.1017/S0950268814000016]

36 **Syrjänen K**. Geographic origin is a significant determinant of human papillomavirus prevalence in oesophageal squamous cell carcinoma: systematic review and meta-analysis. *Scand J Infect Dis* 2013; **45**: 1-18 [PMID: 22830571 DOI: 10.3109/00365548.2012.702281]

37 **Goto A**, Li CP, Ota S, Niki T, Ohtsuki Y, Kitajima S, Yonezawa S, Koriyama C, Akiba S, Uchima H, Lin YM, Yeh KT, Koh JS, Kim CW, Kwon KY, Nga ME, Fukayama M. Human papillomavirus infection in lung and esophageal cancers: analysis of 485 Asian cases. *J Med Virol* 2011; **83**: 1383-1390 [PMID: 21678442 DOI: 10.1002/jmv.22150]

38 **Löfdahl HE**, Du J, Näsman A, Andersson E, Rubio CA, Lu Y, Ramqvist T, Dalianis T, Lagergren J, Dahlstrand H. Prevalence of human papillomavirus (HPV) in oesophageal squamous cell carcinoma in relation to anatomical site of the tumour. *PLoS One* 2012; **7**: e46538 [PMID: 23077513 DOI: 10.1371/journal.pone.0046538]

39 **Poljak M**, Cerar A, Seme K. Human papillomavirus infection in esophageal carcinomas: a study of 121 lesions using multiple broad-spectrum polymerase chain reactions and literature review. *Hum Pathol* 1998; **29**: 266-271 [PMID: 9496830 DOI: 10.1016/s0046-8177(98)90046-6]

40 **Matsha T**, Erasmus R, Kafuko AB, Mugwanya D, Stepien A, Parker MI; CANSA/MRC Oesophageal Cancer Research Group. Human papillomavirus associated with oesophageal cancer. *J Clin Pathol* 2002; **55**: 587-590 [PMID: 12147651 DOI: 10.1136/jcp.55.8.587]

41 **Kimple AJ**, Torres AD, Yang RZ, Kimple RJ. HPV-associated head and neck cancer: molecular and nano-scale markers for prognosis and therapeutic stratification. *Sensors (Basel)* 2012; **12**: 5159-5169 [PMID: 22666080 DOI: 10.3390/s120405159]

World Journal of Gastroenterology

Submit a Manuscript: https://www.f6publishing.com

World J Gastroenterol 2020 October 21; 26(39): 6057-6073

DOI: 10.3748/wjg.v26.i39.6057

ISSN 1007-9327 (print) ISSN 2219-2840 (online)

ORIGINAL ARTICLE

Retrospective Study

Dynamic contrast-enhanced magnetic resonance imaging and diffusion-weighted imaging in the activity staging of terminal ileum Crohn's disease

Yin-Chen Wu, Ze-Bin Xiao, Xue-Hua Lin, Xian-Ying Zheng, Dai-Rong Cao, Zhong-Shuai Zhang

ORCID number: Yin-Chen Wu 0000-0001-7353-6605; Ze-Bin Xiao 0000-0002-3311-7403; Xue-Hua Lin 0000-0002-7305-0223; Xian-Ying Zheng 0000-0001-7261-9177; Dai-Rong Cao 0000-0002-0051-3143; Zhong-Shuai Zhang 0000-0002-1594-0906.

Author contributions: Wu YC made substantial contributions to the conception and design of the study, performing the study, acquisition of data and drafting the manuscript; Xiao ZB carried out the statistical analyses and image post-processing; Lin XH performed the scanning sequences; Zhang ZS was responsible for sequence optimization; Cao DR participated in the design and helped in drafting the manuscript; Zheng XY conceived the study idea, participated in its design, and helped in drafting the manuscript; all authors have read and approved the final manuscript.

Supported by Medical Innovation Program of Fujian Province, No. 2018-CX-30; and Startup Fund for Scientific Research of Fujian Medical University, No. 2018QH1054.

Institutional review board statement: The study was reviewed and approved by the

Yin-Chen Wu, Xue-Hua Lin, Xian-Ying Zheng, Dai-Rong Cao, Department of Radiology, The First Affiliated Hospital of Fujian Medical University, Fuzhou 350005, Fujian Province, China

Ze-Bin Xiao, Department of Biomedical Sciences, University of Pennsylvania, Philadelphia, PA 19104, United States

Zhong-Shuai Zhang, Department of Diagnosis Imaging, Siemens Healthcare Ltd, Shanghai 201318, China

Corresponding author: Xian-Ying Zheng, MD, Professor, Department of Radiology, The First Affiliated Hospital of Fujian Medical University, No. 20 Chazhong Road, Fuzhou 350005, Fujian Province, China. fyzhengxianying@163.com

Abstract

BACKGROUND

The activity staging of Crohn's disease (CD) in the terminal ileum is critical in developing an accurate clinical treatment plan. The activity of terminal ileum CD is associated with the microcirculation of involved bowel walls. Dynamic contrast-enhanced magnetic resonance imaging (DCE-MRI) and diffusion-weighted imaging (DWI) can reflect perfusion and permeability of bowel walls by providing microcirculation information. As such, we hypothesize that DCE-MRI and DWI parameters can assess terminal ileum CD, thereby providing an opportunity to stage CD activity.

AIM

To evaluate the value of DCE-MRI and DWI in assessing activity of terminal ileum CD.

METHODS

Forty-eight patients with CD who underwent DCE-MRI and DWI were enrolled. The patients' activity was graded as remission, mild and moderate-severe. The transfer constant (K^{trans}), wash-out constant (K_{ep}), and extravascular extracellular volume fraction (V_e) were calculated from DCE-MRI and the apparent diffusion coefficient (ADC) was obtained from DWI. Magnetic Resonance Index of Activity (MaRIA) was calculated from magnetic resonance enterography. Differences in these quantitative parameters were compared between normal ileal loop (NIL)

Branch for Medical Research and Clinical Technology Application, Ethics Committee of First Affiliated Hospital of Fujian Medical University.

Informed consent statement: All study participants, or their legal guardian, provided informed written consent prior to study enrollment.

Conflict-of-interest statement: The authors declare that they have no conflict of interest.

Data sharing statement: No additional data are available.

Manuscript source: Unsolicited manuscript

Received: June 19, 2020
Peer-review started: June 19, 2020
First decision: July 28, 2020
Revised: August 6, 2020
Accepted: September 12, 2020
Article in press: September 12, 2020
Published online: October 21, 2020

P-Reviewer: Hayano K
S-Editor: Gao CC
L-Editor: Webster JR
P-Editor: Wang LL

and inflamed terminal ileum (ITI) and among different activity grades. The correlations between these parameters, MaRIA, the Crohn's Disease Activity Index (CDAI), and Crohn's Disease Endoscopic Index of Severity (CDEIS) were examined. Receiver operating characteristic curve analyses were used to determine the diagnostic performance of these parameters in differentiating between CD activity levels.

RESULTS

Higher K^{trans} (0.07 ± 0.04 *vs* 0.01 ± 0.01), K_{ep} (0.24 ± 0.11 *vs* 0.15 ± 0.05) and V_e (0.27 ± 0.07 *vs* 0.08 ± 0.03), but lower ADC (1.41 ± 0.26 *vs* 2.41 ± 0.30) values were found in ITI than in NIL (all $P < 0.001$). The K^{trans}, K_{ep}, V_e and MaRIA increased with disease activity, whereas the ADC decreased (all $P < 0.001$). The K^{trans}, K_{ep}, V_e and MaRIA showed positive correlations with the CDAI ($r = 0.866$ for K^{trans}, 0.870 for K_{ep}, 0.858 for V_e, 0.890 for MaRIA, all $P < 0.001$) and CDEIS ($r = 0.563$ for K^{trans}, 0.567 for K_{ep}, 0.571 for V_e, 0.842 for MaRIA, all $P < 0.001$), while the ADC showed negative correlations with the CDAI ($r = -0.857$, $P < 0.001$) and CDEIS ($r = -0.536$, $P < 0.001$). The areas under the curve (AUC) for the K^{trans}, K_{ep}, V_e, ADC and MaRIA values ranged from 0.68 to 0.91 for differentiating inactive CD (CD remission) from active CD (mild to severe CD). The AUC when combining the K^{trans}, K_{ep} and V_e was 0.80, while combining DCE-MRI parameters and ADC values yielded the highest AUC of 0.95.

CONCLUSION

DCE-MRI and DWI parameters all serve as measures to stage CD activity. When they are combined, the assessment performance is improved and better than MaRIA.

Key Words: Crohn's disease; Ileum; Magnetic resonance imaging; Diffusion-weighted imaging; Perfusion imaging

Core Tip: Dynamic contrast-enhanced magnetic resonance imaging (DCE-MRI) and diffusion-weighted imaging (DWI) can reflect quantitative changes in perfusion and permeability information on the microcirculation of bowel walls due to variable degrees of inflammation. This study investigated the performances of DCE-MRI and DWI for assessing the activity of Crohn's disease (CD). The results showed that DCE-MRI and DWI parameters were correlated with CD inflammation indices and were valuable in noninvasively staging CD activity. Furthermore, the diagnostic performance of the transfer constant (K^{trans}), wash-out constant (K_{ep}), extravascular extracellular volume fraction (V_e) and ADC was better than the Magnetic Resonance Index of Activity, which can assist clinical diagnosis and monitoring.

Citation: Wu YC, Xiao ZB, Lin XH, Zheng XY, Cao DR, Zhang ZS. Dynamic contrast-enhanced magnetic resonance imaging and diffusion-weighted imaging in the activity staging of terminal ileum Crohn's disease. *World J Gastroenterol* 2020; 26(39): 6057-6073
URL: https://www.wjgnet.com/1007-9327/full/v26/i39/6057.htm
DOI: https://dx.doi.org/10.3748/wjg.v26.i39.6057

INTRODUCTION

Crohn's disease (CD) is a chronic relapsing inflammatory disease of the whole gastrointestinal tract that commonly involves the terminal ileum with a complicated and unclear pathogenesis[1]. This disease has a high morbidity and disability rate among young adults along with a poor curative rate, and the prognosis leads to a low quality of life[2]. The diagnosis and activity staging of CD located in the terminal ileum are usually difficult due to occult onset, which often leads to delayed clinical treatment. However, this type of CD deserves more attention, because it is more likely

to have complications requiring surgery than other types[3,4]. Therefore, an accurate evaluation of the activity of this condition is highly necessary for gastroenterologists to develop a reasonable treatment plan. Currently, the activity of CD is diagnosed according to clinical symptoms and staged by the subjective Crohn's Disease Activity Index (CDAI) based on symptoms, or the objective Crohn's Disease Endoscopic Index of Severity (CDEIS) on the basis of endoscopy findings[5]. However, the patients' symptoms are sometimes nonspecific, and the related evaluation also suffers from the clinicians' subjectivity. Even endoscopy has some inherent disadvantages, such as the inadequate evaluation of large parts of the small bowel, the risk of procedure-related complications and the low patient acceptance rate due to discomfort during the procedure[6,7].

In contrast, magnetic resonance enterography (MRE), as a non-invasive, non-traumatic and non-ionizing method with high soft-tissue resolution, has been increasingly used for the detection of bowel abnormalities[8,9]. However, this method contributes little to assessing the activity of CD. Conventional Magnetic Resonance Index of Activity (MaRIA) is calculated by multiple embedded formulas by wall thickness, relative contrast enhancement (RCE) and two qualitative variables, edema and ulceration, to identify inactive and active disease[10]. Dynamic contrast-enhanced magnetic resonance imaging (DCE-MRI) has been widely accepted as a tool to monitor disease progression in other organs[11-13] and can provide quantitative perfusion and permeability information on the bowel wall to accurately localize lesions, monitor disease activity and evaluate treatment responses[14-17]. Menys *et al*[18] proposed grading CD with MRE on the basis of magnetic resonance (MR) contrast enhancement, indicating that DCE-MRI may be useful in grading CD. Diffusion-weighted imaging (DWI), which characterizes the random motion of water molecules within the tissue, has been utilized to detect abnormal small bowel segments in CD[19,20]. Oto *et al*[21] pointed out that DCE-MRI and DWI could differentiate actively inflamed small bowel segments from normal small bowel segments in CD. Thus, DCE-MRI and DWI are both potentially available methods for evaluating the activity of CD. However, few studies have compared correlations of DCE-MRI and DWI with endoscopic findings and CD inflammatory indices to analyze the value of accurate staging CD using these two methods. Moreover, to the best of our knowledge, comprehensive comparisons of the diagnostic performance obtained from single or combined use of DCE-MRI and DWI and these two methods with MaRIA in assessing CD activity staging has not been reported.

Therefore, the purpose of this study was to investigate the diagnostic performance of quantitative parameters derived from DCE-MRI and DWI, the combination of both and MaRIA in staging CD using comprehensive assessment of CDAI and CDEIS by gastroenterologist as the reference standard.

MATERIALS AND METHODS

Patients and preparation

The institutional review board of our hospital approved this retrospective study, and the requirement for patient informed consent was waived because of the retrospective nature of this study. From September 2018 to July 2019, 48 patients (32 males and 16 females, mean age 33.8 ± 14.6 years) were included in this study. The inclusion criteria were as follows: (1) Clinically proven CD involving the terminal ileum (confirmed uniformly by clinical characteristics, medical history and endoscopic histopathology performed within 1 wk before MRE); (2) No treatment between MRE and endoscopy; and (3) Availability of CDAI and CDEIS evaluations (CDAI and CDEIS scores were provided by the gastroenterologists with at least 7 years of experience). The exclusion criteria were as follows: (1) Insufficient MR image quality and (2) Affected bowel walls in the colon segments. On endoscopy, CD appeared as patchy segmental inflammation, cobblestone appearance, worsening friability and ulceration, erosion, edema, and pseudopolyp formation. The sampling sites for endoscopic histopathological examination were the tissue around ulceration and erosion and some normal tissue as a comparison. According to the CDAI and CDEIS values, the enrolled patients were divided into three groups: Remission group (CDAI < 151, CDEIS < 3), mild group (CDAI 151-219, CDEIS 3-8), and moderate-severe group (CDAI > 219, CDEIS > 8).

The magnetic resonance imaging (MRI) examinations were performed after the patients fasted for 8 h. Twenty-four hours before the examination, the patients orally took 10 g Senna leaf mixed with 2000 mL water to clean the bowel. Approximately 1 h

and 30 min before the examination, 1500 mL of 137.5 mOsm/L mannitol solution mixed with water was ingested to distend the bowels (150 mL per time in 5-min intervals). Ten minutes before the examination, 20 mg of raceanisodamine hydrochloride was slowly injected to prevent intestinal peristalsis.

MRI protocols

The MRI examinations were performed in a 3T MRI scanner (Magnetom Skyra; Siemens) with the patient in a supine position using a multichannel phased-array body coil covering the whole abdomen and pelvis. Before the scan, a bellyband was wrapped around the patient's abdomen to reduce the motion artefacts. The MRI protocol included conventional static MRE sequences and DCE-MRI sequences. First, static MRE was applied: Coronal and axial 2D fat-suppressed T2-weighted half-Fourier acquisition single-shot turbo spin echo, two axial T2-weighted True FISP (Trufi) sequences with and without fat saturation, DWI (b = 50/800), and unenhanced 3D fat-suppressed T1-weighted volumetric interpolated breath hold examination (3D-VIBE). After the intravenous administration of a gadolinium-based contrast medium (0.1 mL/kg bodyweight of gadobenate dimeglumine, MultiHance, Bracco Diagnostics) at an injection rate of 2 mL/s followed by a subsequent injection of the same amount of normal saline, the Twist VIBE-based DCE sequence was continuously applied followed by the coronal and axial T1-weighted Dixon sequence 3 min after administration. The detailed parameters of the MRI protocol are given in Table 1.

Image analyses

The conventional MRE was independently reviewed by two radiologists with 7 years and 10 years of experience in abdominal imaging, respectively. For each patient, the two radiologists identified the inflammatory and normal small bowel. The standards of CD were as follows: (1) Mural segmental thickening (> 3 mm); (2) Distinct abnormal mural hyperenhancement; (3) High signal in the wall on T2-weighted and DWI scans; (4) Adjacent fat stranding and enlarged lymph nodes (> 5 mm in shortest diameter); (5) Penetrating disease (sinus tract, fistula or abscess); and (6) The comb sign (prominent vasa recta)[22]. Based on the conventional MRE and subsequent postcontrast images, the normal-appearing and abnormal segments and locations were defined for further analysis by another gastrointestinal radiologist with 28 years of experience.

MaRIA was calculated for the terminal ileum segment using the following formula[10]: MaRIA = 1.5 × wall thickness (mm) + 0.02 × RCE + 5 × edema + 10 × ulceration (1); RCE was calculated according to: $RCE = (WSI_{post\text{-}enhancement} - WSI_{pre\text{-}enhancement}) / WSI_{pre\text{-}enhancement} \times 100 \times SD_{noise\ pre\text{-}enhancement} / SD_{noise\ post\text{-}enhancement}$ (2); where $SD_{noise\ pre\text{-}enhancement}$ is the average of three standard deviations (SDs) of the signal intensity measured outside of the body before enhancement, and $SD_{noise\ post\text{-}enhancement}$ is the same result after enhancement.

The DCE-MRI data were processed using commercially available software (Tissue 4D, Syngo.via; Siemens Healthcare, Erlangen, Germany) to calculate the corresponding parameters using the Tofts model. Specifically, first, a volume of interest (VOI) that contained both normal tissue and the lesion in the terminal ileum was selected on the DCE-MRI. Then, the concentration curve of the VOI was calculated according to the two-compartment Tofts model. This post-processing perfusion model describes the distribution of gadodiamide after injection and predicts a change in the contrast concentration in the tissue as a function of time, $C(t)$, as follows[23]: $dC(t)/dt = K^{trans} \times (C_p(t) - C(t)/v_e)$ (3); where K^{trans} (min^{-1}) is the transfer constant from the intravascular to extravascular extracellular space (EES), V_e is the EES volume, and $C_p(t)$ is the arterial input function (AIF). K_{ep}, the wash-out constant, is equal to the K^{trans} divided by V_e.

Three concentration curves with different AIF and the value of Chi2 of each were provided by the software. The AIF with the minimum of Chi2 was chosen for the subsequent operation. As for the analysis of DCE-MRI parameters, the two radiologists independently and manually delineated two regions of interest (ROIs) (range 39-177 mm^2) among the VOI on the normal ileal loop (NIL) and two ROIs (range 15-47 mm^2) on the inflamed terminal ileum (ITI) with caution to avoid the image artifacts. All radiologists were blinded to the CDEIS and CDAI score. Then, the K^{trans}, K_{ep} and V_e were calculated and the measurements from two radiologists was averaged as the final results for the NIL and ITI. The ADCs were also calculated from the walls of the NIL and ITI. ADC measurements were performed by the same two observers on the same workstation with diffusion analysis software. ITI results were obtained from the area with the brightest signal on the DWI image. Because two DCE-MRI and ADC values were calculated for the NIL and ITI in each patient, the mean values were defined as the final results for each patient.

Table 1 Magnetic resonance enterography acquisition parameters

Parameter	HASTE	Trufi	DWI	Dixon	Twist	Dixon
Imaging plane (s)	Coronal/axial	Axial	Axial	Axial	Axial	Axial/coronal
TR (ms)	1800/1600	382.48/398.94	8300	3.93	4.5	3.93/4.21
TE (ms)	88/95	1.68/1.72	54	1.26 2.49	1.23 2.46	1.26 2.49/1.34 2.57
Flip angle (°)	180/160	50/52	-	9	6.1	9
FOV (mm^2)	360 × 360/380 × 380	380 × 380	400 × 400	400 × 400	380 × 380	400 × 400/450 × 450
Slices	30/50	55	48	96	96	96/72
Slice thickness (mm)	5	5	5	3	3	3/1.5
Slice gap (%)	20	20	20	20	20	20
Fat saturation	Yes	No/Yes	-	-	-	-
TA (min : s)	0:54/1:32	0:21/0:22	3:03	0:16	2:05	0:16/0:12

HASTE: Half-Fourier acquisition single-shot turbo spin echo; DWI: Diffusion-weighted imaging; TR: Repetition time; TE: Echo time; TA: Acquisition time; FOV: Field of view.

Statistical analysis

Statistical analysis was performed with SPSS software (version 19.0, IBM). The quantitative DCE-MRI parameters, the K^{trans}, K_{ep} and V_e, the ADC and MaRIA were tested with the Kolmogorov-Smirnov test for normality and then with the Levene test for variance homogeneity. The quantitative parameters were compared between the terminal ileum and normal ileal loop using the paired *t*-test. If the data followed a normal distribution, the parameters were tested by the LSD-test (data obey homogeneity of variance) or Dunnett's T3-test (data do not obey homogeneity of variance) for differences between groups; otherwise, the Kruskal-Wallis test was used. The Spearman test was used to analyze correlations among MaRIA and the parameters and the CDAI and CDEIS scores. Binary logistic regression was used to calculate predicted probability of the K^{trans}, K_{ep}, V_e, and ADC. For multi-factors, K^{trans} + K_{ep} + V_e and K^{trans} + K_{ep} + V_e + ADC, the beta coefficients were calculated through logistic regression analysis. The scores of both were calculated according to: K^{trans} + K_{ep} + V_e score = -16.123 -191.557 × K^{trans} + 55.077 × K_{ep} + 66.178 × V_e (4); K^{trans} + K_{ep} + V_e + ADC score = -27.228 -106.268 × K^{trans} + 34.849 × K_{ep} + 37.763 × V_e + 27.749 × ADC (5).

Finally, receiver operating characteristic (ROC) curves of the K^{trans}, K_{ep}, V_e, ADC, MaRIA, K^{trans} + K_{ep} + V_e score, and K^{trans} + K_{ep} + V_e + ADC score, including the area under the curve (AUC), were analyzed to evaluate the ability to differentiate inactive CD (CD remission) from active CD (mild to severe CD). The threshold was determined by calculating the ROC curves followed by Youden's index [1- (sensitivity + specificity)]. Statistical significance was defined as $P < 0.05$. The AUCs were compared using the DeLong test.

Intra- and interclass agreement for the K^{trans}, K_{ep}, V_e, ADC and MaRIA in ROI-related measurements was evaluated by Bland-Altman analysis. Statistical significance was defined as $P < 0.05$.

RESULTS

Forty-eight patients underwent conventional MRE and DCE-MRI, and forty-eight groups of processible images were acquired. Of these, 27.08% were in the remission group (13/48), 41.67% were in the mild activity group (20/48), and 31.25% were in the moderate-severe activity group (15/48).

On DCE-MRI, the K^{trans}, K_{ep} and V_e in the ITI were higher than those in the NIL (all $P < 0.001$), and the ADC derived from DWI in the ITI was lower than that in the NIL (all $P < 0.001$). The differences in the K^{trans}, K_{ep}, V_e and ADC in the ITI between the groups were statistically significant (all $P < 0.001$). The K^{trans}, K_{ep}, V_e and MaRIA were lower in the CD remission group than those in the active CD group, and the ADC was higher in the CD remission group. As the activity increased, the K^{trans}, K_{ep}, V_e and MaRIA also increased, and the K^{trans} increased most among the three groups in three DCE-MRI

parameters (Table 2, Figure 1-3).

As shown in Table 3 and Figure 4, the K_{ep} showed the strongest positive correlations with the CDAI (r = 0.870, P < 0.001), followed by the K^{trans} (r = 0.866, P < 0.001) and V_e (r = 0.858, P < 0.001) in DCE-MRI parameters. The ADC showed a strong negative correlation with the CDAI (r = -0.857, P < 0.001). The V_e, K_{ep}, and K^{trans} showed moderate positive correlations with the CDEIS (r = 0.571, 0.567, and 0.563, P < 0.001, respectively). The ADC showed a moderate negative correlation with the CDEIS (r = -0.536, P < 0.001). MaRIA showed strong positive correlations with both CDAI (r = 0.890, P < 0.001) and CDEIS (r = 0.842, P < 0.001).

The ROC analysis results of the ability of MaRIA, these parameters and combined parameters, including K^{trans} + K_{ep} + V_e and K^{trans} + K_{ep} + V_e + ADC, to differentiate inactive CD from active CD are shown in Table 4. The ROC analysis showed that MaRIA had higher accuracy for differentiating inactive CD from active CD than the individual parameters. The ADC had the highest accuracy for differentiation among the individual parameters, with an AUC of 0.89, and the threshold value was 1.6 × 10^{-3} mm^2/s. With only DCE-MRI parameters, when the threshold V_e value was 0.29, differentiation with a sensitivity of 0.83 and a specificity of 0.85 was achieved. By combining the K^{trans}, K_{ep} and V_e, the diagnostic performance for detecting remission was improved, with an AUC of 0.80, while the highest AUC was observed when DCE-MRI and DWI parameters were combined (K^{trans} + K_{ep} + V_e + ADC), with an observed AUC of 0.95 (Figure 5). This combination of parameters had the highest AUC among the combination of DCE-MRI parameters, the ADC and MaRIA alone (all P < 0.05).

The intraclass correlation coefficient was 0.957 for the K^{trans}, 0.855 for the K_{ep}, 0.973 for the V_e, 0.941 for the ADC and 0.971 for MaRIA between the two observers (all P < 0.001). The interclass correlation coefficient between observer 1's first and second measurements was 0.902 for the K^{trans}, 0.740 for the K_{ep}, 0.961 for the V_e, and 0.913 for the ADC (all P < 0.001). The interclass correlation coefficient between observer 2's first and second measurements was 0.922 for the K^{trans}, 0.772 for the K_{ep}, 0.957 for the V_e, and 0.900 for the ADC (all P < 0.001). The results of the Bland-Altman analysis for the intraclass and interclass coefficients are shown in Figure 6.

DISCUSSION

Our study demonstrated that the ITI was able to be differentiated from the NIL in patients with CD in the terminal ileum, and that the inflammatory activity could be graded quantitively based on both DCE-MRI and DWI parameters. When the ADC and DCE-MRI parameters were combined, the assessment performance was improved and better than MaRIA.

The ITI had restricted diffusion compared with the NIL as indicated by lower ADC values, which is supported by previous studies, and one of the other important and well-known findings of CD is increased small intestinal wall enhancement[24-26]. As a direct method to evaluate enhancement, the DCE-MRI parameters were derived from a two-compartment general kinetic model to describe the contrast agent distribution after a bolus injection[23]. K^{trans} and K_{ep}, the transfer constant and the wash-out constant, are proportional to the capillary permeability and blood flow, and V_e, the plasma volume fraction, is proportional to the leakage space. We found that the ITI had higher K^{trans}, K_{ep} and V_e values than those of the NIL, indicating that an inflamed bowel wall could be detected by visual assessments of gadolinium enhancement and abnormal angiogenesis as a feature of the pathogenesis of CD, which manifested as increased blood perfusion and permeability reflected by higher parameters[27-29]. Although this finding is similar to that of previous studies, some results have striking magnitude differences. In Oto's study[15], the K^{trans} values of the NIL and the ITI were 0.18 to 0.36 min^{-1} and 0.31 to 0.92 min^{-1}, respectively, while the K^{trans} values in this study were 0.07 min^{-1} and 0.12 min^{-1}, respectively. One reason for this discrepancy may be patient preparation before the examination. In Oto's study[15], a total volume of 1350 mL was administered orally over the course of 45 min before scanning, which may lead to nonuniform and incomplete distension of the bowel segments due to inhomogeneous drinking. This may have an impact on the perfusion measurements as it can lead to an oversized ROI or lower signal in the collapsed small bowel loops[30,31]. Another possible reason for the discrepancy between the two studies lies in the different sample sizes. A total of two ROIs were selected for each segment in the perfusion images of Oto's study[15], and the mean value was defined, which may lead to a smaller simple size and a higher K^{trans}.

Compared to previous studies, our study focused on the correlations of DCE-MRI

Table 2 Parameters in the normal ileal loop and the inflamed terminal ileum in different staging of Crohn's disease

Parameter	Total			Remission CD			Mild CD			Moderate-severe CD		
	NIL	ITI	*P* value	NIL	ITI	*P* value	NIL	ITI	*P* value	NIL	ITI	*P* value
K^{trans} (min^{-1})	0.01 ± 0.01	0.07 ± 0.04	< 0.001	0.01 ± 0.01	0.03 ± 0.01	< 0.001	0.01 ± 0.00	0.05 ± 0.01	< 0.001	0.01 ± 0.00	0.12 ± 0.04	< 0.001
K_{ep} (min^{-1})	0.15 ± 0.05	0.24 ± 0.11	< 0.001	0.11 ± 0.03	0.16 ± 0.05	< 0.001	0.18 ± 0.05	0.21 ± 0.05	< 0.001	0.15 ± 0.05	0.35 ± 0.11	< 0.001
V_e	0.08 ± 0.03	0.27 ± 0.07	< 0.001	0.10 ± 0.04	0.18 ± 0.03	< 0.001	0.07 ± 0.02	0.26 ± 0.03	< 0.001	0.08 ± 0.03	0.35 ± 0.05	< 0.001
ADC ($\times 10^{-3}$ mm^2/s)	2.41 ± 0.30	1.41 ± 0.26	< 0.001	2.33 ± 0.26	1.72 ± 0.12	< 0.001	2.45 ± 0.31	1.42 ± 0.12	< 0.001	2.42 ± 0.30	1.12 ± 1.12	< 0.001
MaRIA		14.10 ± 10.09			6.39 ± 1.07			9.34 ± 1.30			27.12 ± 8.23	

NIL: Normal ileal loop; ITI: Inflamed terminal ileum; CD: Crohn's disease; ADC: Apparent diffusion coefficient; MaRIA: Magnetic Resonance Index of Activity.

and DWI parameters with CD activity estimated by more objective indices to grade CD-the CDAI, CDEIS and K_{ep}, the latter of which is a new parameter. We found that the K^{trans}, K_{ep} and V_e all showed positive correlations with the CDAI and CDEIS, while the ADC decreased when the CDAI and CDEIS increased. The major determinants of the K^{trans} and K_{ep} are blood flow and the capillary permeability surface area[32]. The high K^{trans} and K_{ep} in the ITI are likely related to an increase in blood flow but also the vascularity supplying the inflamed tissue[33]. Microvessel density and the vascular endothelial growth factor levels are increased in the mucosal extracts of patients with inflammatory bowel disease compared with those in the normal mucosa[34,35]. Increased vascularity and edema correlating with the level of inflammation in the bowel was shown *in vitro* by angiography of the resected bowel specimens of patients with inflammatory bowel disease[15]. The basement membrane of the neovasculature is incomplete, which causes a wide endothelial cell gap. The contrast agent molecules can easily pass through and wash out[7]. We believe that both the microvessel density and imperfections increase with disease chronicity, which leads to increased K^{trans} and K_{ep} values in the inflamed bowel wall. The positive correlations of K^{trans} and K_{ep} with CDAI and CDEIS also confirm this. V_e represents the volume of extracted contrast agent. Microvascular alterations and continuous epithelial damage to the mucosa have a pathogenic role in initiation and maintenance throughout the whole course of CD. In the advanced stage of inflammation, increases in vascular perfusion, vasospasm, and incomplete neovasculature lead to increased EES contrast agent leakage[21]. This applies to V_e, which has a positive association with CDAI and CDEIS. The negative correlation of ADC and CDAI as well as CDEIS was also observed in this study. The reduced water diffusion is likely related to infiltration of inflammatory cells, dilated lymphatic channels and granuloma development during the CD process[15] and is also associated with fibrosis in the bowel wall[36]. Although, the histologic degrees of bowel fibrosis and inflammation cannot be accurately detected by DWI during the disease

Table 3 Correlations of parameters of inflamed terminal ileum with Crohn's Disease Activity Index and Crohn's Disease Endoscopic Index of Severity in different staging of Crohn's disease

Parameter	CDAI		CDEIS	
	r	*P* value	*r*	*P* value
K^{trans} (min^{-1})	0.866	< 0.001	0.563	< 0.001
K_{ep} (min^{-1})	0.870	< 0.001	0.567	< 0.001
V_e	0.858	< 0.001	0.571	< 0.001
ADC ($\times 10^{-3}$ mm^2/s)	-0.857	< 0.001	-0.536	< 0.001
MaRIA	0.890	< 0.001	0.842	< 0.001

CDAI: Crohn's Disease Activity Index; CDEIS: Crohn's Disease Endoscopic Index of Severity; ADC: Apparent diffusion coefficient; MaRIA: Magnetic Resonance Index of Activity.

Table 4 Receiver operating characteristic analysis results for the parameters for differentiating inactive Crohn's disease from active Crohn's disease

Parameter	AUC (CI)	Threshold	Sensitivity (CI)	Specificity (CI)	PPV (CI)	NPV (CI)	LR+ (CI)	LR- (CI)
K^{trans} (min^{-1})	0.76 (0.61-0.91)	0.03	0.83 (0.66-0.93)	0.69 (0.39-0.90)	0.88 (0.71-0.96)	0.6 (0.33-0.83)	2.69 (1.18-6.17)	0.25 (0.11-0.55)
K_{ep} (min^{-1})	0.68 (0.50-0.85)	0.19	0.69 (0.51-0.83)	0.69 (0.39-0.90)	0.86 (0.66-0.95)	0.45 (0.24-0.68)	2.23 (0.96-5.19)	0.45 (0.26-0.79)
V_e	0.78 (0.60-0.96)	0.29	0.83 (0.66-0.93)	0.85 (0.54-0.97)	0.94 (0.77-0.99)	0.65 (0.39-0.85)	5.39 (1.49-19.44)	0.20 (0.10-0.43)
ADC ($\times 10^{-3}$ mm^2/s)	0.89 (0.78-1.00)	1.6	0.91 (0.76-0.98)	0.77 (0.46-0.94)	0.91 (0.76-0.98)	0.77 (0.46-0.94)	3.96 (1.46-10.74)	0.11 (0.04-0.34)
MaRIA	0.91 (0.82-1.00)	7.2	0.89 (0.72-0.96)	0.85 (0.54-0.97)	0.94 (0.78-0.99)	0.73 (0.45-0.91)	5.76 (1.60-20.71)	0.14 (0.05-0.35)
K^{trans} + K_{ep} + V_e	0.80 (0.62-0.98)	-	0.89 (0.72-0.96)	0.85 (0.54-0.97)	0.94 (0.78-0.99)	0.73 (0.45-0.91)	5.76 (1.60-20.71)	0.14 (0.05-0.35)
K^{trans} + K_{ep} + V_e + ADC	0.95 (0.85-1.00)	-	0.97 (0.83-1.00)	0.92 (0.62-1.00)	0.97 (0.83-1.00)	0.92 (0.62-1.00)	12.63 (1.92-83.09)	0.03 (0.00-0.22)

AUC: Area under the curve; CI: 95% confidence interval; NPV: Negative predictive value; PPV: Positive predictive value; LR+: Positive likelihood ratios; LR-: Negative likelihood ratios; ADC: Apparent diffusion coefficient; MaRIA: Magnetic Resonance Index of Activity.

course, it is certain that water diffusion restriction develops progressively with the increased activity of CD[36]. These results indicate the potential clinical utility of these quantitative parameters for non-invasive assessment of CD severity. We noted that the correlations between these parameters and CDAI were slightly stronger than those with CDEIS, which may be related to the objectivity of the indicators. CDAI is a subjective assessment of the patients and may overestimate the severity of CD.

MaRIA, an external validation of conventional MRE was used to predict the disease activity of CD due to different clinical treatment plans for inactive CD and active CD in previous studies[10]. This conclusion was verified in our study. However, it is worth noting that the calculation is complicated and inconvenient due to multiple embedded formulas, especially the RCE formula. Moreover, MaRIA included two qualitative parameters, edema and ulceration. Therefore, our study focused on the improved performance of quantitative techniques to differentiate inactive CD from active CD, and further refine its staging. The combination of DCE-MRI and DWI parameters, K^{trans} + K_{ep} + V_e + ADC, exhibited a higher AUC for differentiation between inactive CD and active CD compared to individual parameters and MaRIA. It is suggested that the combination of parameters enhances contrast between inactive and active segments, which indicates the potential value of combined DCE-MRI and DWI parameters for grading CD. Even though a variety of clinical scoring tools have been used to monitor the disease activity, there is no established gold standard to provide pathologic information of inactive or active CD[37]. The main advantage of DCE-MRI and DWI in

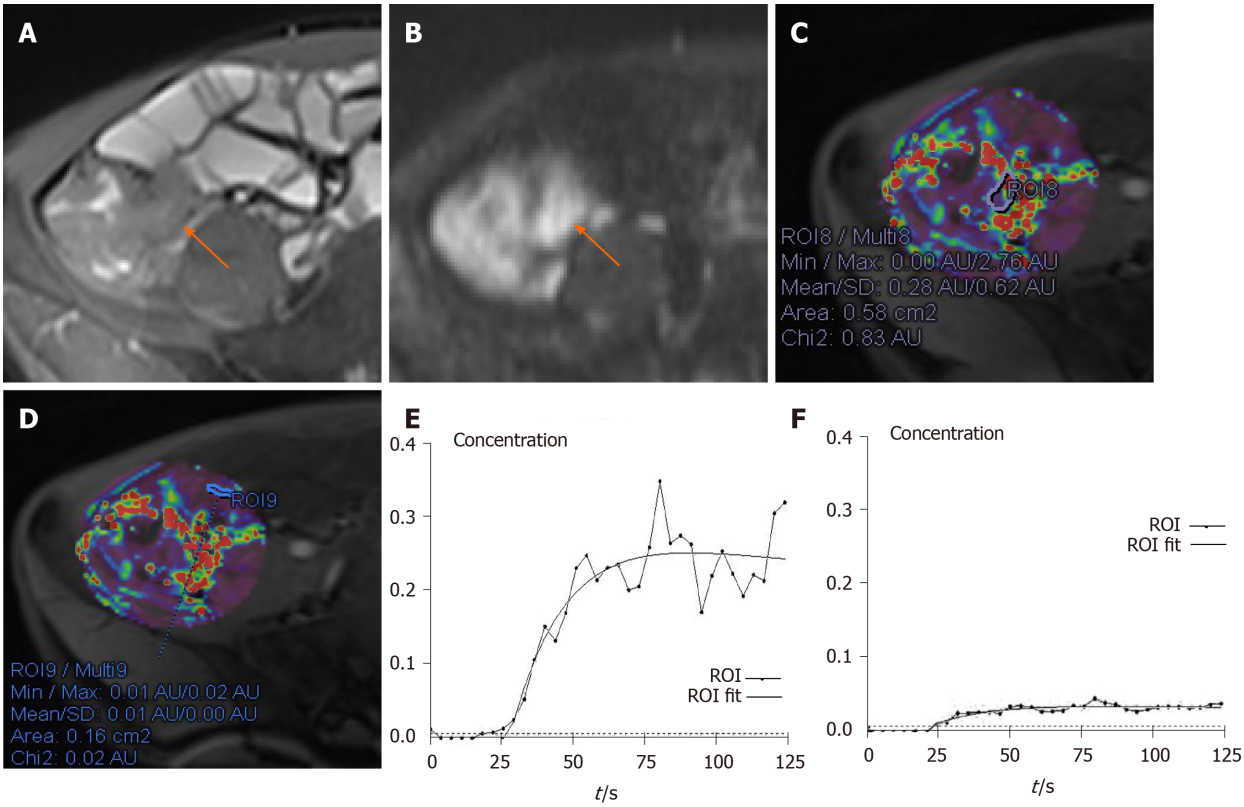

Figure 1 A 41-year-old male with moderate active Crohn's disease in the terminal ileum and a Crohn's Disease Activity Index of 267 and Crohn's Disease Endoscopic Index of Severity of 12. A: Terminal ileum demonstrates wall thickening and increased signal on axial T2-weighted image; B: Terminal ileum wall has a high signal. Axial diffusion-weighted imaging image (b = 800 s/mm^2) demonstrates high signal (arrow) in the same bowel segment. Region of interest (ROI) for the inflammatory bowel wall shows that apparent diffusion coefficient = 1.11×10^{-3} mm^2/s; C: ROI for the inflammatory bowel wall shows that K^{trans} = 0.10 min^{-1} (K_{ep} = 0.87 min^{-1}, V_e = 0.11); D: In contrast, ROI of the normal appearing ileal loop shows that K^{trans} = 0.01 min^{-1} (K_{ep} = 0.80 min^{-1}, V_e = 0.02); E: The contrast concentration curve of inflammatory bowel is plotted as ROI (line with circle) and fitted with the model (line); F: The contrast concentration curve of normal loop is plotted as ROI (line with circle) and fitted with the model (line). ROI: Region of interest.

addition to conventional MRE is the ability to provide quantitative, spatially encoded information on entire small bowel segments, which provides more possibility for the objective assessment of CD activity to determine therapies.

Our study has several limitations. First, motion artefacts (*e.g.*, respiration, peristalsis) and compromised signal-to-noise ratios are inevitable. Expansion of the lumen with oral contrast and antiperistaltic agents before the examination helped reduce the motion artefacts. However, the errors due to motion in the estimation of these parameters were not investigated in this study. In addition, the ROI was manually delineated. We cannot completely exclude the possibility of a partial volume of alvine gas or perienteric tissues, especially in the normal bowel walls. However, the use of the mean parameter values reduces the influence of this partial volume effect to some degree.

CONCLUSION

In conclusion, the ITI in CD patients exhibits increased perfusion and restricted diffusion with activity progression. DCE-MRI and DWI parameters, particularly when used in combination, are promising for assessing CD activity. Such data may provide further insight into therapeutic monitoring of the disease.

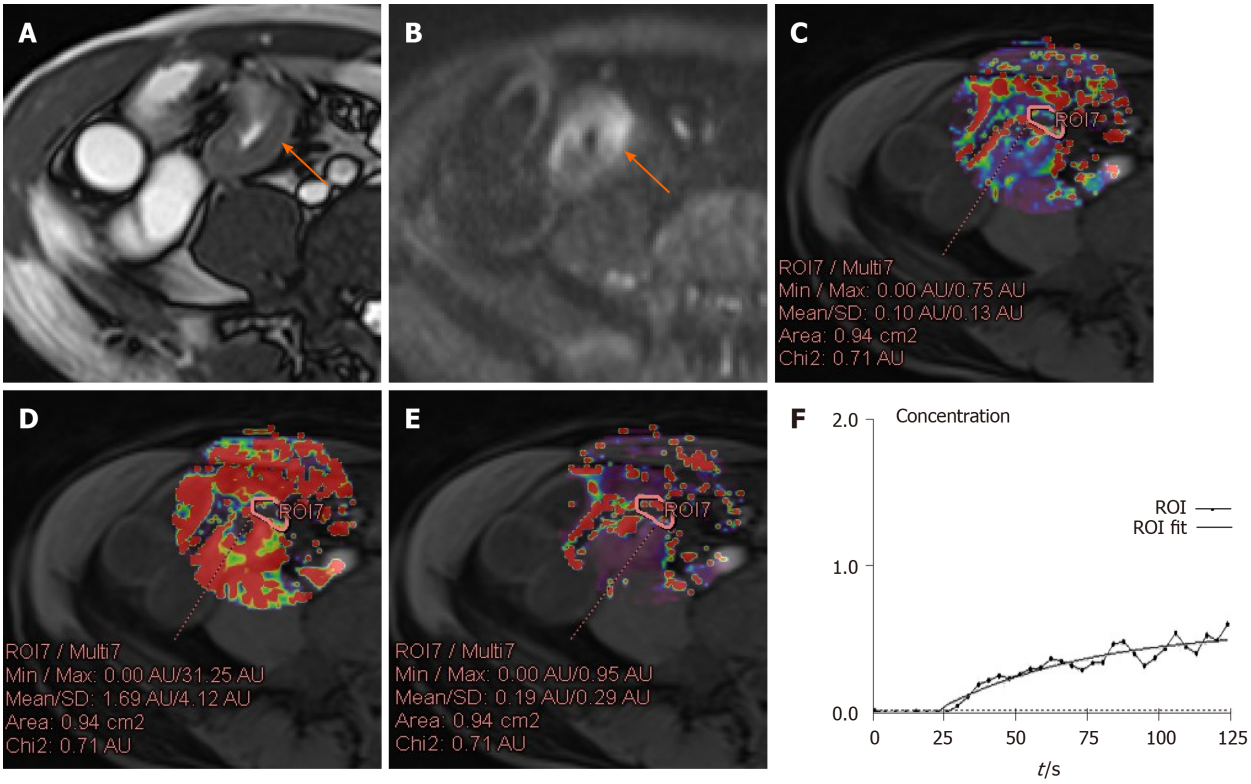

Figure 2 A 42-year-old male with remission of Crohn's disease in the terminal ileum and a Crohn's Disease Activity Index of 108 and Crohn's Disease Endoscopic Index of Severity of 2. A: Axial T2-weighted image shows mural thickening and hyperintensity in the terminal ileum (arrow); B: Axial diffusion-weighted imaging image (b = 800 s/mm^2) demonstrates high signal (arrow) in the same bowel segment. Regions of interest (ROI) for the inflammatory bowel wall shows that apparent diffusion coefficient = 1.89×10^{-3} mm^2/s; C: K^{trans} map is obtained through the relevant phase. The perfusion parameters of the ROI placed in the terminal ileum is calculated by TCM (K^{trans} = 0.18 min^{-1}); D: K_{ep} map is obtained through the relevant phase. The K_{ep} of the ROI placed is 0.98 min^{-1}; E: V_e map is obtained through the relevant phase. The V_e of the ROI placed is 0.19; F: The contrast concentration curve is plotted as ROI (line with circle) and fitted with the model (line). ROI: Region of interest.

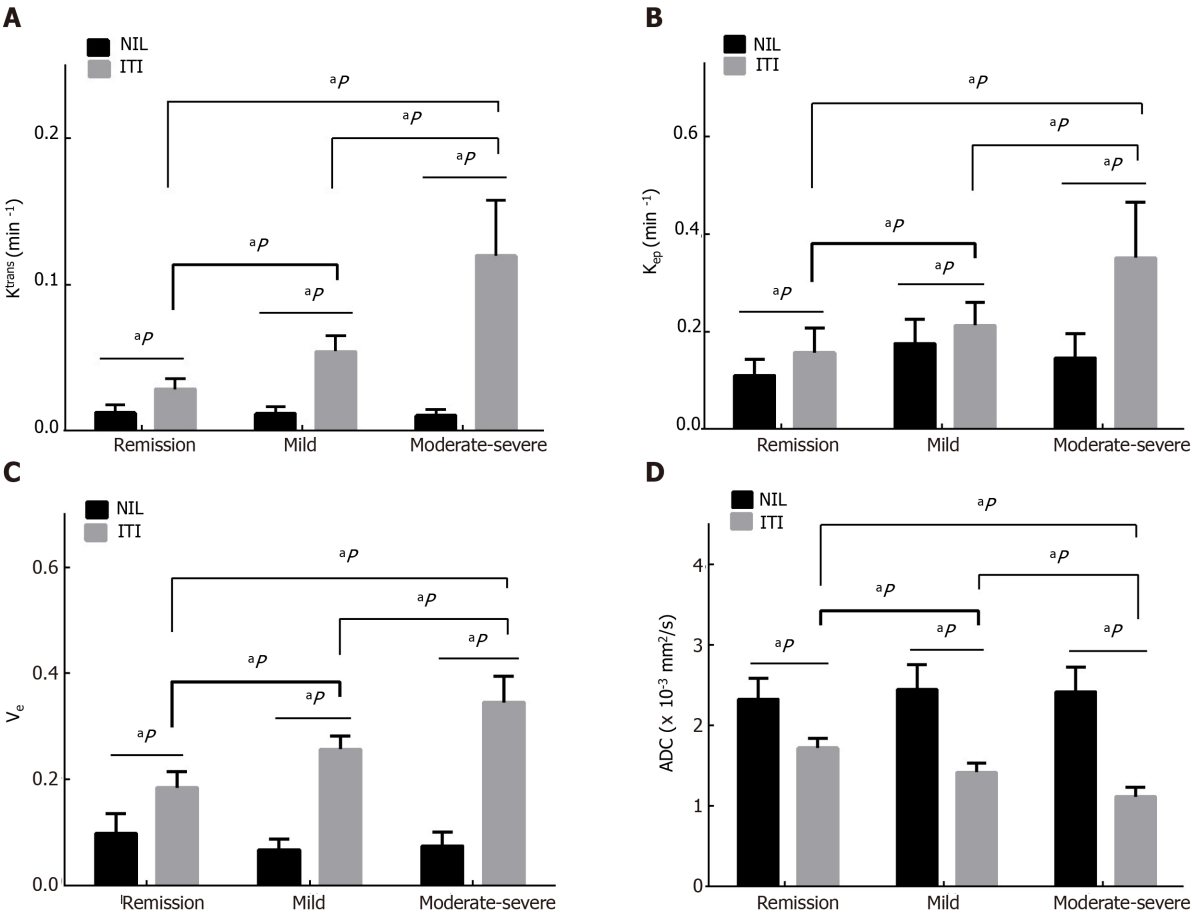

Figure 3 The K^{trans}, K_{ep}, V_e and apparent diffusion coefficient among the three groups. A: Bar charts show increasing K^{trans}, between the normal ileal loop (NIL) and the inflamed terminal ileum (ITI) and pairwise comparisons of them is different (all $P < 0.001$); B: K_{ep} between the NIL and the ITI is different (all $P < 0.001$); C: V_e between the NIL and the ITI is different (all $P < 0.001$); D: Apparent diffusion coefficient between the NIL and the ITI is different (all $P < 0.001$). Furthermore, increasing K^{trans}, K_{ep} and V_e are shown with activity of CD in remission, mild and moderate-severe CD while decreasing apparent diffusion coefficients are shown (all $P < 0.001$). ^aP indicate difference with $P < 0.001$. NIL: Normal ileal loop; ITI: Inflamed terminal ileum.

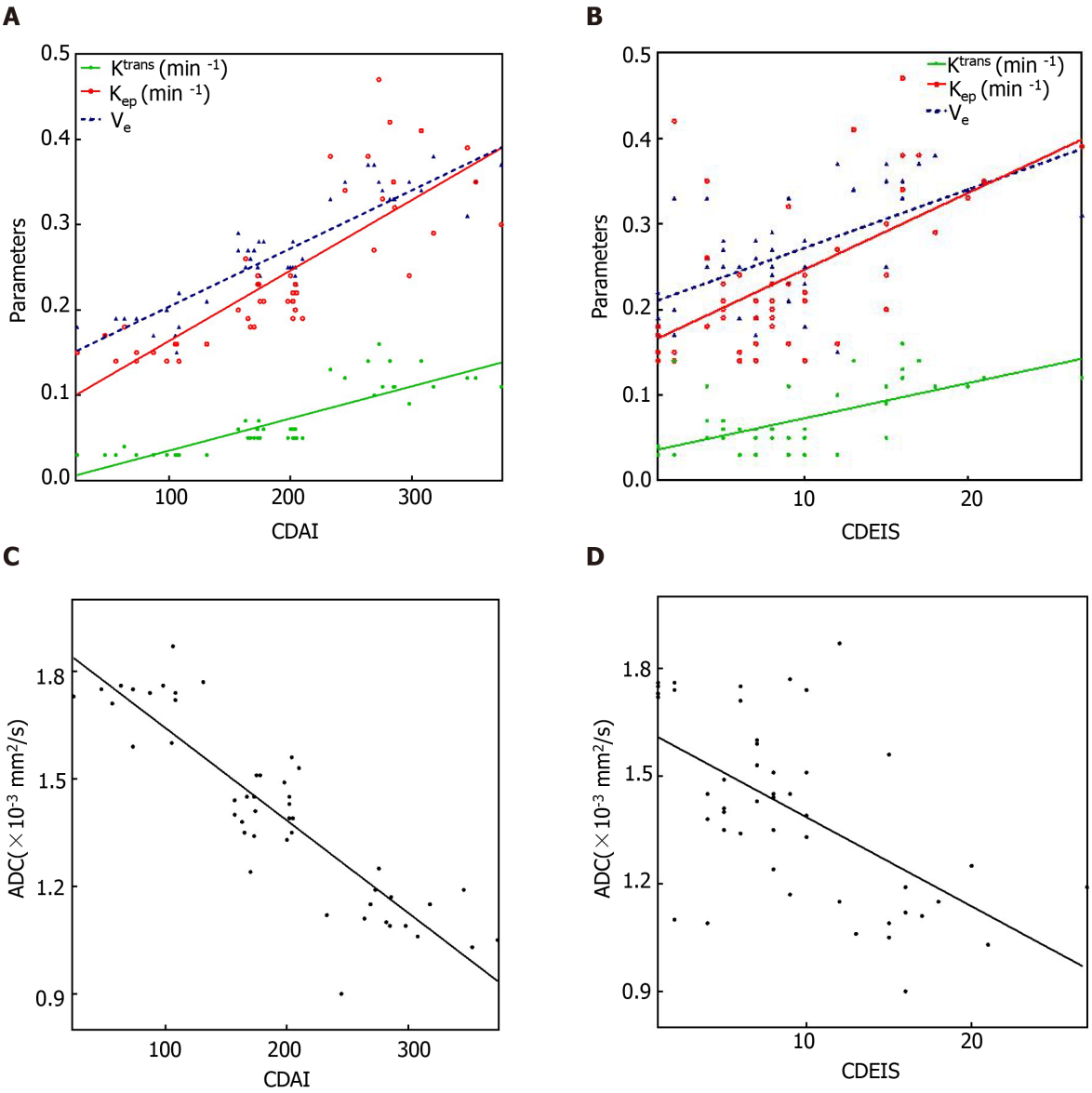

Figure 4 Correlations of inflamed terminal ileum with Crohn's Disease Activity Index and Crohn's Disease Endoscopic Index of Severity in Crohn's disease. A and C: Scatterplots show positive correlation of K^{trans}, K_{ep} and V_e and negative correlation of apparent diffusion coefficient in inflamed terminal ileum of Crohn's disease patients with Crohn's Disease Activity Index score; B and D: Positive correlation of K^{trans}, K_{ep} and V_e and negative correlation of apparent diffusion coefficient in inflamed terminal ileum of Crohn's disease patients with Crohn's Disease Endoscopic Index of Severity score. CDAI: Crohn's Disease Activity Index; CDEIS: Crohn's Disease Endoscopic Index of Severity; ADC: Apparent diffusion coefficient.

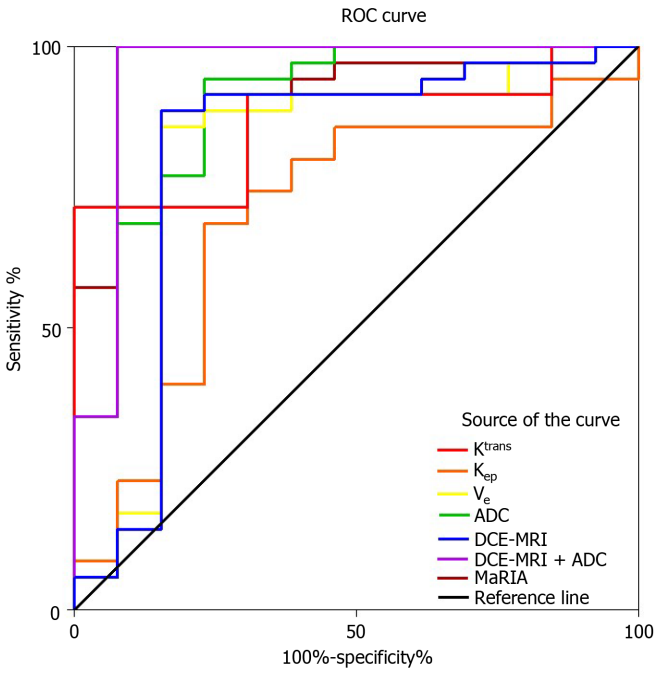

Figure 5 Receiver operating characteristic curve analysis. Receiver operating characteristic curve analysis shows high accuracy of K^{trans} (areas under the curve [AUC] = 0.76), V_e (AUC = 0.78), K_{ep} (AUC = 0.68), apparent diffusion coefficient (AUC = 0.89) and Magnetic Resonance Index of Activity (AUC = 0.91) for differentiating inactive from active Crohn's disease. Accuracy of combining the K^{trans}, K_{ep} and V_e (AUC = 0.80) is higher than the individual dynamic contrast-enhanced magnetic resonance imaging parameters. The highest AUC is observed when combining dynamic contrast-enhanced magnetic resonance imaging and diffusion-weighted imaging parameters (AUC = 0.95). ROC: Receiver operating characteristic; ADC: Apparent diffusion coefficient; DCE-MRI: Dynamic contrast-enhanced magnetic resonance imaging; MaRIA: Magnetic Resonance Index of Activity.

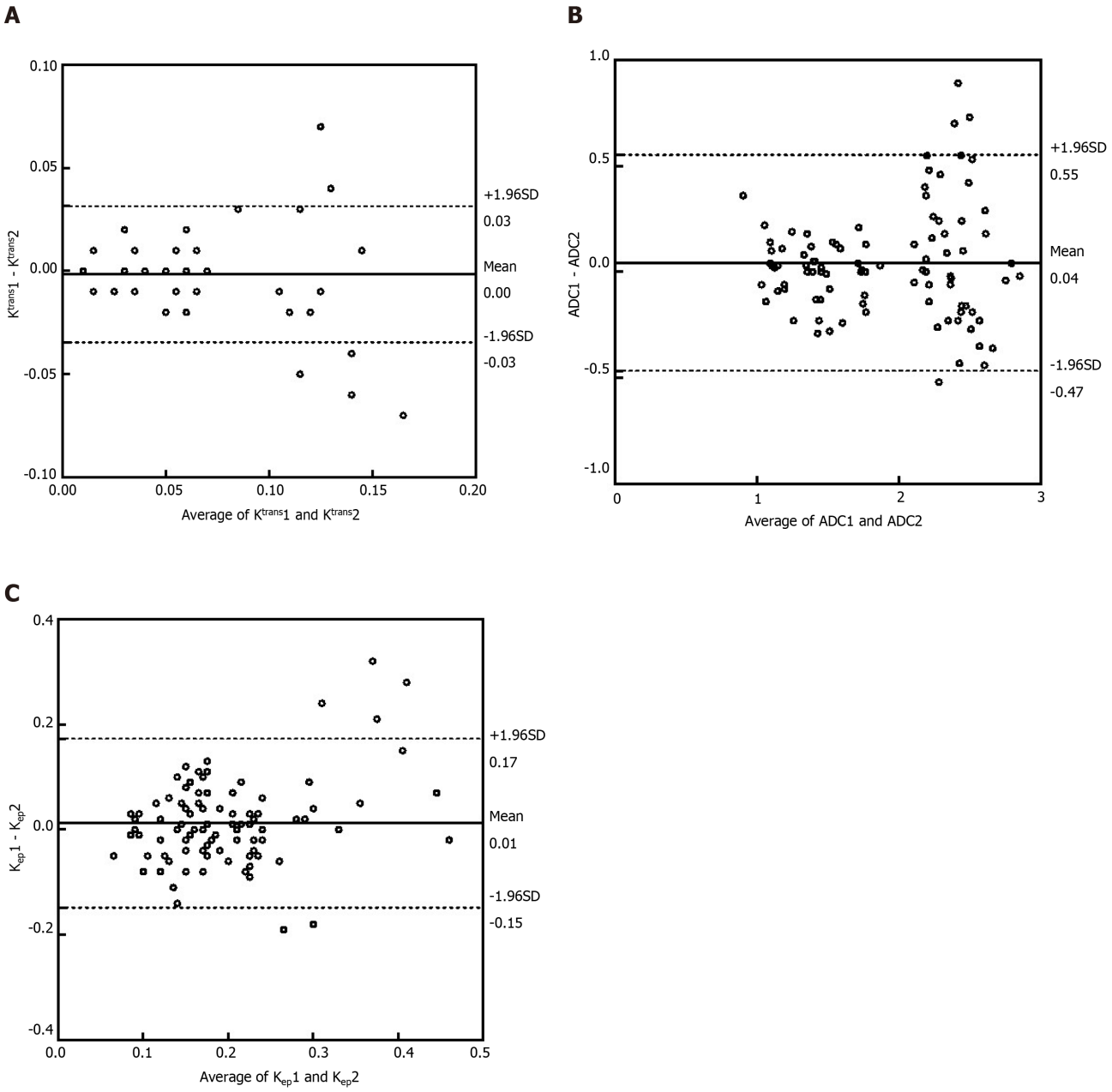

Figure 6 Bland-Altman analysis for the intraclass and interclass coefficients. A: Bland-Altman analysis of the difference between the two observers' average results for K^{trans}; B: Bland-Altman analysis of the difference between the two observers' average results for apparent diffusion coefficient; C: Bland-Altman analysis of the difference between the two observers' average results for K_{ep}. ADC: Apparent diffusion coefficient; SD: Standard deviation.

ARTICLE HIGHLIGHTS

Research background

Crohn's disease (CD) is a chronic inflammatory bowel disease which usually involves the terminal ileum. Clinically, it is important to evaluate accurately and noninvasively the activity of terminal ileum CD in order to make a precise treatment plan. However, current evaluation methods have their inherent disadvantages. Specifically, the Crohn's Disease Activity Index (CDAI) is subjective, Crohn's Disease Endoscopic Index of Severity (CDEIS) is invasive, and Magnetic Resonance Index of Activity (MaRIA) is complex.

The activity of terminal ileum CD is associated with the microcirculation of involved bowel walls. During the process of CD, blood perfusion and permeability increase and water diffusion will be restricted. Dynamic contrast-enhanced magnetic resonance imaging (DCE-MRI) and diffusion-weighted imaging (DWI) can reflect perfusion and permeability of bowel walls by providing microcirculation information. As such, we hypothesize that DCE-MRI and DWI parameters can assess terminal

ileum CD, thereby providing an opportunity to stage CD activity.

Research motivation

The parameters of DCE-MRI, based on the two-compartment Tofts model (TCM), and apparent diffusion coefficient (ADC), based on DWI, allow for the evaluation of perfusion and permeability in bowel walls. Few studies have analyzed the diagnostic performance of the combination of DCE-MRI and DWI in staging CD activity.

Research objectives

The purpose of this study was to investigate the performance of DCE-MRI and DWI as non-invasive methods in staging CD activity with CDAI and CDEIS as references.

Research methods

Forty-eight patients with CD were analyzed retrospectively. According to the CDAI and CDEIS values, the patients were divided into the remission group (CDAI < 151, CDEIS < 3), mild group (CDAI 151-219, CDEIS 3-8), and moderate-severe group (CDAI > 219, CDEIS > 8). K^{trans}, K_{ep}, and V_e were calculated from DCE-MRI and ADC was obtained from DWI. MaRIA was calculated from magnetic resonance enterography. The parameters were compared between normal ileal loop (NIL) and inflamed terminal ileum (ITI). Correlations between these parameters, MaRIA with CDAI, CDEIS were examined. Receiver operating characteristic curve analyses were used to evaluate the performance of these parameters in staging CD activity.

Research results

In the present study, the results showed that higher K^{trans} (0.07 ± 0.04 *vs* 0.01 ± 0.01), K_{ep} (0.24 ± 0.11 *vs* 0.15 ± 0.05) and V_e (0.27 ± 0.07 *vs* 0.08 ± 0.03) but lower ADC (1.41 ± 0.26 *vs* 2.41 ± 0.30) values were displayed in the ITI than in the NIL (all $P < 0.001$). The parameters of DCE-MRI and MaRIA increased in CD progression, whereas the ADC decreased. The K^{trans}, K_{ep}, V_e and MaRIA showed positive correlations with the CDAI ($r = 0.866$ for K^{trans}, 0.870 for K_{ep}, 0.858 for V_e, 0.890 for MaRIA, all $P < 0.001$) and CDEIS ($r = 0.563$ for K^{trans}, 0.567 for K_{ep}, 0.571 for V_e, 0.842 for MaRIA, all $P < 0.001$), while the ADC showed negative correlations with the CDAI ($r = -0.857$, $P < 0.001$) and CDEIS ($r = -0.536$, $P < 0.001$). The areas under the curve (AUC) for the individual values ranged from 0.68 to 0.91 for differentiating inactive CD (CD remission) from active CD (mild to severe CD) and MaRIA had the higher AUC of 0.91. The AUC when combining the K^{trans}, K_{ep} and V_e was 0.80, while the AUC when combining DCE-MRI parameters and ADC was the highest (AUC = 0.95).

Research conclusions

DCE-MRI and DWI are non-invasive methods with good performances in staging the activity of terminal ileum CD. When they were used in combination, the value was greater, which can supplement clinical diagnosis and monitoring.

Research perspectives

DCE-MRI and DWI are valuable tools in staging CD with CDAI and CDEIS as the references. The correlation of the DCE-MRI and DWI parameters between pathological activity status of CD, and the performance of DCE-MRI and DWI in monitoring the treatment effect of CD should be explored in the future.

REFERENCES

1 **Peyrin-Biroulet L**, Loftus EV Jr, Colombel JF, Sandborn WJ. The natural history of adult Crohn's disease in population-based cohorts. *Am J Gastroenterol* 2010; **105**: 289-297 [PMID: 19861953 DOI: 10.1038/ajg.2009.579]

2 **Kwak MS**, Kim DH, Park SJ, Kim TI, Hong SP, Kim WH, Cheon JH. Efficacy of early immunomodulator therapy on the outcomes of Crohn's disease. *BMC Gastroenterol* 2014; **14**: 85 [PMID: 24886458 DOI: 10.1186/1471-230X-14-85]

3 **Silverberg MS**, Satsangi J, Ahmad T, Arnott ID, Bernstein CN, Brant SR, Caprilli R, Colombel JF, Gasche C, Geboes K, Jewell DP, Karban A, Loftus EV Jr, Peña AS, Riddell RH, Sachar DB, Schreiber S, Steinhart AH, Targan SR, Vermeire S, Warren BF. Toward an integrated clinical, molecular and serological classification of inflammatory bowel disease: report of a Working Party of the 2005 Montreal World Congress of Gastroenterology. *Can J Gastroenterol* 2005; **19** Suppl A: 5A-36A [PMID: 16151544 DOI: 10.1155/2005/269076]

4 **Magro F**, Portela F, Lago P, Ramos de Deus J, Vieira A, Peixe P, Cremers I, Cotter J, Cravo M, Tavares L, Reis J, Gonçalves R, Lopes H, Caldeira P, Ministro P, Carvalho L, Azevedo L, da Costa-Pereira A; GEDII.

Crohn's disease in a southern European country: Montreal classification and clinical activity. *Inflamm Bowel Dis* 2009; **15**: 1343-1350 [PMID: 19235885 DOI: 10.1002/ibd.20901]

5 **Hart L**, Bessissow T. Endoscopic scoring systems for the evaluation and monitoring of disease activity in Crohn's disease. *Best Pract Res Clin Gastroenterol* 2019; **38-39**: 101616 [PMID: 31327405 DOI: 10.1016/j.bpg.2019.05.003]

6 **Best WR**, Becktel JM, Singleton JW, Kern F Jr. Development of a Crohn's disease activity index. National Cooperative Crohn's Disease Study. *Gastroenterology* 1976; **70**: 439-444 [PMID: 1248701 DOI: 10.1016/S0016-5085(76)80163-1]

7 **Niv Y**, Gal E, Gabovitz V, Hershkovitz M, Lichtenstein L, Avni I. Capsule Endoscopy Crohn's Disease Activity Index (CECDAIic or Niv Score) for the Small Bowel and Colon. *J Clin Gastroenterol* 2018; **52**: 45-49 [PMID: 27753700 DOI: 10.1097/MCG.0000000000000720]

8 **Bhatnagar G**, Von Stempel C, Halligan S, Taylor SA. Utility of MR enterography and ultrasound for the investigation of small bowel Crohn's disease. *J Magn Reson Imaging* 2017; **45**: 1573-1588 [PMID: 27943484 DOI: 10.1002/jmri.25569]

9 **Coimbra AJ**, Rimola J, O'Byrne S, Lu TT, Bengtsson T, de Crespigny A, Luca D, Rutgeerts P, Bruining DH, Fidler JL, Sandborn WJ, Santillan CS, Higgins PD, Al-Hawary MM, Vermeire S, Vanbeckevoort D, Vanslembrouck R, Peyrin-Biroulet L, Laurent V, Herrmann KA, Panes J. Magnetic resonance enterography is feasible and reliable in multicenter clinical trials in patients with Crohn's disease, and may help select subjects with active inflammation. *Aliment Pharmacol Ther* 2016; **43**: 61-72 [PMID: 26548868 DOI: 10.1111/apt.13453]

10 **Rimola J**, Ordás I, Rodriguez S, García-Bosch O, Aceituno M, Llach J, Ayuso C, Ricart E, Panés J. Magnetic resonance imaging for evaluation of Crohn's disease: validation of parameters of severity and quantitative index of activity. *Inflamm Bowel Dis* 2011; **17**: 1759-1768 [PMID: 21744431 DOI: 10.1002/ibd.21551]

11 **Karahaliou A**, Vassiou K, Arikidis NS, Skiadopoulos S, Kanavou T, Costaridou L. Assessing heterogeneity of lesion enhancement kinetics in dynamic contrast-enhanced MRI for breast cancer diagnosis. *Br J Radiol* 2010; **83**: 296-309 [PMID: 20335440 DOI: 10.1259/bjr/50743919]

12 **Barrett T**, Brechbiel M, Bernardo M, Choyke PL. MRI of tumor angiogenesis. *J Magn Reson Imaging* 2007; **26**: 235-249 [PMID: 17623889 DOI: 10.1002/jmri.20991]

13 **Yeo DM**, Oh SN, Jung CK, Lee MA, Oh ST, Rha SE, Jung SE, Byun JY, Gall P, Son Y. Correlation of dynamic contrast-enhanced MRI perfusion parameters with angiogenesis and biologic aggressiveness of rectal cancer: Preliminary results. *J Magn Reson Imaging* 2015; **41**: 474-480 [PMID: 24375840 DOI: 10.1002/jmri.24541]

14 **Florie J**, Wasser MN, Arts-Cieslik K, Akkerman EM, Siersema PD, Stoker J. Dynamic contrast-enhanced MRI of the bowel wall for assessment of disease activity in Crohn's disease. *AJR Am J Roentgenol* 2006; **186**: 1384-1392 [PMID: 16632735 DOI: 10.2214/AJR.04.1454]

15 **Oto A**, Kayhan A, Williams JT, Fan X, Yun L, Arkani S, Rubin DT. Active Crohn's disease in the small bowel: evaluation by diffusion weighted imaging and quantitative dynamic contrast enhanced MR imaging. *J Magn Reson Imaging* 2011; **33**: 615-624 [PMID: 21563245 DOI: 10.1002/jmri.22435]

16 **Tielbeek JA**, Ziech ML, Li Z, Lavini C, Bipat S, Bemelman WA, Roelofs JJ, Ponsioen CY, Vos FM, Stoker J. Evaluation of conventional, dynamic contrast enhanced and diffusion weighted MRI for quantitative Crohn's disease assessment with histopathology of surgical specimens. *Eur Radiol* 2014; **24**: 619-629 [PMID: 24037299 DOI: 10.1007/s00330-013-3015-7]

17 **Zhu J**, Zhang F, Luan Y, Cao P, Liu F, He W, Wang D. Can Dynamic Contrast-Enhanced MRI (DCE-MRI) and Diffusion-Weighted MRI (DW-MRI) Evaluate Inflammation Disease: A Preliminary Study of Crohn's Disease. *Medicine (Baltimore)* 2016; **95**: e3239 [PMID: 27057860 DOI: 10.1097/MD.0000000000003239]

18 **Menys A**, Atkinson D, Odille F, Ahmed A, Novelli M, Rodriguez-Justo M, Proctor I, Punwani S, Halligan S, Taylor SA. Quantified terminal ileal motility during MR enterography as a potential biomarker of Crohn's disease activity: a preliminary study. *Eur Radiol* 2012; **22**: 2494-2501 [PMID: 22661057 DOI: 10.1007/s00330-012-2514-2]

19 **Oto A**, Zhu F, Kulkarni K, Karczmar GS, Turner JR, Rubin D. Evaluation of diffusion-weighted MR imaging for detection of bowel inflammation in patients with Crohn's disease. *Acad Radiol* 2009; **16**: 597-603 [PMID: 19282206 DOI: 10.1016/j.acra.2008.11.009]

20 **Kiryu S**, Dodanuki K, Takao H, Watanabe M, Inoue Y, Takazoe M, Sahara R, Unuma K, Ohtomo K. Free-breathing diffusion-weighted imaging for the assessment of inflammatory activity in Crohn's disease. *J Magn Reson Imaging* 2009; **29**: 880-886 [PMID: 19306416 DOI: 10.1002/jmri.21725]

21 **Oto A**, Fan X, Mustafi D, Jansen SA, Karczmar GS, Rubin DT, Kayhan A. Quantitative analysis of dynamic contrast enhanced MRI for assessment of bowel inflammation in Crohn's disease pilot study. *Acad Radiol* 2009; **16**: 1223-1230 [PMID: 19524458 DOI: 10.1016/j.acra.2009.04.010]

22 **Khatri G**, Coleman J, Leyendecker JR. Magnetic Resonance Enterography for Inflammatory and Noninflammatory Conditions of the Small Bowel. *Radiol Clin North Am* 2018; **56**: 671-689 [PMID: 30119767 DOI: 10.1016/j.rcl.2018.04.003]

23 **Tofts PS**. Modeling tracer kinetics in dynamic Gd-DTPA MR imaging. *J Magn Reson Imaging* 1997; **7**: 91-101 [PMID: 9039598 DOI: 10.1002/jmri.1880070113]

24 **Low RN**, Sebrechts CP, Politoske DA, Bennett MT, Flores S, Snyder RJ, Pressman JH. Crohn disease with endoscopic correlation: single-shot fast spin-echo and gadolinium-enhanced fat-suppressed spoiled gradient-echo MR imaging. *Radiology* 2002; **222**: 652-660 [PMID: 11867781 DOI: 10.1148/radiol.2223010811]

25 **Maccioni F**, Bruni A, Viscido A, Colaiacomo MC, Cocco A, Montesani C, Caprilli R, Marini M. MR imaging in patients with Crohn disease: value of T2- *vs* T1-weighted gadolinium-enhanced MR sequences with use of an oral superparamagnetic contrast agent. *Radiology* 2006; **238**: 517-530 [PMID: 16371574 DOI: 10.1148/radiol.2381040244]

26 **Maccioni F**, Bencardino D, Buonocore V, Mazzamurro F, Viola F, Oliva S, Vernia P, Merli M, Vestri AR, Catalano C, Cucchiara S. MRI reveals different Crohn's disease phenotypes in children and adults. *Eur Radiol* 2019; **29**: 5082-5092 [PMID: 30729332 DOI: 10.1007/s00330-019-6006-5]

27 **Maccioni F**, Viscido A, Broglia L, Marrollo M, Masciangelo R, Caprilli R, Rossi P. Evaluation of Crohn disease activity with magnetic resonance imaging. *Abdom Imaging* 2000; **25**: 219-228 [PMID: 10823437 DOI: 10.1007/s002610000004]

28 **Laghi A**, Borrelli O, Paolantonio P, Dito L, Buena de Mesquita M, Falconieri P, Passariello R, Cucchiara S. Contrast enhanced magnetic resonance imaging of the terminal ileum in children with Crohn's disease. *Gut* 2003; **52**: 393-397 [PMID: 12584222 DOI: 10.1136/gut.52.3.393]

29 **Gourtsoyiannis N**, Papanikolaou N, Grammatikakis J, Papamastorakis G, Prassopoulos P, Roussomoustakaki M. Assessment of Crohn's disease activity in the small bowel with MR and conventional enteroclysis: preliminary results. *Eur Radiol* 2004; **14**: 1017-1024 [PMID: 15057562 DOI: 10.1007/s00330-004-2302-8]

30 **Taylor SA**, Punwani S, Rodriguez-Justo M, Bainbridge A, Greenhalgh R, De Vita E, Forbes A, Cohen R, Windsor A, Obichere A, Hansmann A, Rajan J, Novelli M, Halligan S. Mural Crohn disease: correlation of dynamic contrast-enhanced MR imaging findings with angiogenesis and inflammation at histologic examination--pilot study. *Radiology* 2009; **251**: 369-379 [PMID: 19276323 DOI: 10.1148/radiol.2512081292]

31 **Bickelhaupt S**, Wurnig M, Boss A, Patak MA. Correlation between morphological expansion and impairment of intra- and prelesionary motility in inflammatory small bowel lesions in patients with Crohn's disease - preliminary data. *Eur J Radiol* 2014; **83**: 1044-1050 [PMID: 24794863 DOI: 10.1016/j.ejrad.2014.03.009]

32 **Walker-Samuel S**, Leach MO, Collins DJ. Evaluation of response to treatment using DCE-MRI: the relationship between initial area under the gadolinium curve (IAUGC) and quantitative pharmacokinetic analysis. *Phys Med Biol* 2006; **51**: 3593-3602 [PMID: 16825751 DOI: 10.1088/0031-9155/51/14/021]

33 **Hectors SJ**, Gordic S, Semaan S, Bane O, Hirten R, Jia X, Colombel JF, Taouli B. Diffusion and perfusion MRI quantification in ileal Crohn's disease. *Eur Radiol* 2019; **29**: 993-1002 [PMID: 30019143 DOI: 10.1007/s00330-018-5627-4]

34 **Deban L**, Correale C, Vetrano S, Malesci A, Danese S. Multiple pathogenic roles of microvasculature in inflammatory bowel disease: a Jack of all trades. *Am J Pathol* 2008; **172**: 1457-1466 [PMID: 18458096 DOI: 10.2353/ajpath.2008.070593]

35 **Knod JL**, Crawford K, Dusing M, Collins MH, Chernoguz A, Frischer JS. Angiogenesis and Vascular Endothelial Growth Factor-A Expression Associated with Inflammation in Pediatric Crohn's Disease. *J Gastrointest Surg* 2016; **20**: 624-630 [PMID: 26530519 DOI: 10.1007/s11605-015-3002-1]

36 **Li XH**, Mao R, Huang SY, Fang ZN, Lu BL, Lin JJ, Xiong SS, Chen MH, Li ZP, Sun CH, Feng ST. Ability of DWI to characterize bowel fibrosis depends on the degree of bowel inflammation. *Eur Radiol* 2019; **29**: 2465-2473 [PMID: 30635756 DOI: 10.1007/s00330-018-5860-x]

37 **Cibor D**, Domagala-Rodacka R, Rodacki T, Jurczyszyn A, Mach T, Owczarek D. Endothelial dysfunction in inflammatory bowel diseases: Pathogenesis, assessment and implications. *World J Gastroenterol* 2016; **22**: 1067-1077 [PMID: 26811647 DOI: 10.3748/wjg.v22.i3.1067]

World Journal of Gastroenterology

Submit a Manuscript: https://www.f6publishing.com

World J Gastroenterol 2020 October 21; 26(39): 6074-6086

DOI: 10.3748/wjg.v26.i39.6074

ISSN 1007-9327 (print) ISSN 2219-2840 (online)

ORIGINAL ARTICLE

Observational Study

Relationship of meteorological factors and air pollutants with medical care utilization for gastroesophageal reflux disease in urban area

Ho Seok Seo, Jinwook Hong, Jaehun Jung

ORCID number: Ho Seok Seo 0000-0002-3606-6074; Jinwook Hong 0000-0003-1855-9649; Jaehun Jung 0000-0002-4856-3668.

Author contributions: Jung J designed the study and participated in the data acquisition; Hong J did data analysis and interpretation; Seo HS drafted the manuscript; all approved final manuscript.

Supported by Gachon University Gil Medical Center, No. FRD2018-17 and No. FRD2019-11.

Institutional review board statement: This study was approved by the Institutional Review Board of the Gachon University Gil Medical Center, which waived the need for informed consent, No. GCIRB2019-039.

Informed consent statement: Owing to the retrospective nature of this study, patients and the public were not involved in the study design, data collection, analysis, or interpretation of data.

Conflict-of-interest statement: Authors have no conflicts of interest or financial ties to disclose.

Ho Seok Seo, Division of Gastrointestinal Surgery, Department of Surgery, Seoul St. Mary's Hospital, College of Medicine, The Catholic University of Korea, Seoul 06591, South Korea

Jinwook Hong, Jaehun Jung, Artificial Intelligence and Big-Data Convergence Center, Gil Medical Center, Gachon University College of Medicine and Science, Incheon 21565, South Korea

Jaehun Jung, Department of Preventive Medicine, Gachon University College of Medicine, Incheon 21565, South Korea

Corresponding author: Jaehun Jung, MD, PhD, Assistant Professor, Department of Preventive Medicine, Gachon University College of Medicine, 38-13, Dokjeom-ro, Incheon 21565, South Korea. eastside1st@gmail.com

Abstract

BACKGROUND

Gastroesophageal reflux disease (GERD) is a highly prevalent disease of the upper gastrointestinal tract, and it is associated with environmental and lifestyle habits. Due to an increasing interest in the environment, several groups are studying the effects of meteorological factors and air pollutants (MFAPs) on disease development.

AIM

To identify MFAPs effect on GERD-related medical utilization.

METHODS

Data on GERD-related medical utilization from 2002 to 2017 were obtained from the National Health Insurance Service of Korea, while those on MFAPs were obtained from eight metropolitan areas and merged. In total, 20071900 instances of GERD-related medical utilizations were identified, and 200000 MFAPs were randomly selected from the eight metropolitan areas. Data were analyzed using a multivariable generalized additive Poisson regression model to control for time trends, seasonality, and day of the week.

RESULTS

Five MFAPs were selected for the prediction model. GERD-related medical

Data sharing statement: The datasets generated for and/or analyzed in the current study are available from the corresponding author upon reasonable request.

STROBE statement: The authors have read the STROBE Statement-checklist of items, and the manuscript was prepared and revised according to the STROBE Statement-checklist of items.

Manuscript source: Unsolicited manuscript

Received: July 19, 2020
Peer-review started: July 19, 2020
First decision: August 8, 2020
Revised: August 19, 2020
Accepted: September 16, 2020
Article in press: September 16, 2020
Published online: October 21, 2020

P-Reviewer: Morozov S
S-Editor: Gao CC
L-Editor: A
P-Editor: Ma YJ

utilization increased with the levels of particulate matter with a diameter ≤ 2.5 μm ($PM_{2.5}$) and carbon monoxide (CO). S-shaped and inverted U-shaped changes were observed in average temperature and air pollutants, respectively. The time lag of each variable was significant around nine days after exposure.

CONCLUSION
Using five MFAPs, the final model significantly predicted GERD-related medical utilization. In particular, $PM_{2.5}$ and CO were identified as risk or aggravating factors for GERD.

Key Words: Gastroesophageal reflux disease; Air pollution; Meteorological factor; Particulate matter; Carbon monoxide

Core Tip: The model showed correlation between five meteorological factors and air pollutants and gastroesophageal reflux disease (GERD)-related medical utilization. S- and inverted U-shaped changes were noted in average temperature and air pollutants. Average temperature, sunshine duration, wind speed, $PM_{2.5}$, and carbon monoxide are risk factors of GERD. GERD occurrence is reduced using environmental management and national alarm systems.

Citation: Seo HS, Hong J, Jung J. Relationship of meteorological factors and air pollutants with medical care utilization for gastroesophageal reflux disease in urban area. *World J Gastroenterol* 2020; 26(39): 6074-6086
URL: https://www.wjgnet.com/1007-9327/full/v26/i39/6074.htm
DOI: https://dx.doi.org/10.3748/wjg.v26.i39.6074

INTRODUCTION

Technological advancements have made possible to measure various meteorological factors and air pollutants (MFAPs). Additionally, multiple studies focusing on the relationship of weather and air pollutants with disease are being conducted[1-4]. However, the majority of previous studies on the topic focused only on acute-phase medical diseases[5-7], while others performed analyses without including various MFAPs as potential confounding factors[3-5,7]. Since the relationship among MFAPs is highly complex, it is not possible to analyze each factor separately[8,9]. Therefore, it is essential to perform the analyses after appropriate correction, considering correlations among these factors.

Gastroesophageal reflux disease (GERD) is among the most commonly occurring benign diseases of the upper gastrointestinal tract[10,11]. The incidence of GERD is rapidly increasing owing to changes in people's lifestyle and eating habits[12]. GERD can be treated with proton pump inhibitors (PPIs), while surgery may be necessary in severe cases[13]. To date, only one study investigated the relationship between humidity and monthly GERD occurrence[14]. However, it was limited by the exclusive inclusion of patients in Taiwan, where there is a hot and humid weather, and a lack of data on air pollutants.

This study aimed to identify the factors affecting GERD-related medical utilization through complex MFAPs data analyses in the Republic of Korea, in combination with the analyses of reliable meteorological and national health insurance data.

MATERIALS AND METHODS

Study population and MFAPs

Data on GERD-related medical utilizations from 2002 to 2017 were obtained from the National Health Insurance Services (NHIS). All inpatient and outpatient data on Korea's population can be identified using NHIS data, due to a single-payer healthcare

insurance system in the country. GERD was identified by the International Classification of Disease, 10th Revision, Clinical Modification (ICD-10-CM) codes and pharmaceutical codes, as well as procedure or operation codes. Only patients with a clear GERD as defined by the presence of an ICD-10 K21 code, an operation code corresponding to fundoplication, and a procedure code related to esophagogastroduodenoscopy, esophagography, esophageal manometry, or pH monitoring of the esophagus, as well as the pharmaceutical code for PPIs were included in the study. The date of GERD-related medical utilization was defined as the first date of PPI administration.

Data on meteorological factors were obtained from the National Climate Data Center of the Korea Meteorological Administration (http://data.kma.go.kr) and included the following factors: Average temperature (AT) (°C), high temperature (°C), low temperature (°C), diurnal temperature range (°C), vapor pressure (hPa), solar radiation (MJ/m^2), sunshine duration (SD) (hr), wind speed (WS) (m/s), daily rain (mm), dew point temperature (°C), humidity (%), daily snow (cm), and presence of clouds (1/10). Each factor was measured hourly using automated equipment at 77 manned stations located on high mountains or in central cities; these factors were merged as a daily average with the GERD-related medical utilization. Additionally, data on air pollutants, including atmospheric particulate matter of diameter ≤ 2.5 μm ($PM_{2.5}$) (μg/m^3), PM_{10} (μg/m^3), ozone (O_3) (parts-per-billion [ppb]), nitrogen dioxide (NO_2) (ppb), sulphur dioxide (SO_2) (ppb), and carbon monoxide (CO) (parts-per-million [ppm]) were obtained from the AirKorea database (http://airkorea.or.kr), operated by the Korea Environment Corporation[15]. Levels of the following gases were measured as follows: $PM_{2.5}$ and PM_{10} levels were determined using the beta-ray absorption method, SO_2 levels using ultraviolet pulse fluorescence, CO levels using the non-dispersive infrared method, NO_2 levels using chemiluminescence, and O_3 levels using ultraviolet photometry. We also calculated the 8-hour maximum level per time period. An observation center was selected in the eight largest cities in the country (Seoul, Incheon, Daejeon, Gwangju, Daegu, Ulsan, Busan, and Jeju) (Supplementary Figure 1). In these eight metropolitan areas, the distance between the MFAP observation center and medical utilization point is very short. In the case of non-metropolitan areas, the distance may be longer. We used random sampling to identify the 2007190 instances of medical utilization due to GERD in Korea from 2002 to 2017 for inclusion in this study. These represented 10% of all instances of medical utilization; and corresponded to only those pertaining to the chosen eight metropolitan areas. There were 799537 GERD-related medical utilizations in the eight urban areas after merging with meteorological factors. Due to the possibility of operating the generalized additive model with cubic splines through the degree of freedom parameter in limited computing power, we chose a random sample from the urban dataset. In the end, 200000 out of 799537 cases from the eight metropolitan areas were randomly selected for inclusion (Supplementary Figure 2). This study was approved by the Institutional Review Board of the Gachon University Gil Medical Center, which waived the need for informed consent, No. GCIRB2019-039.

Modelling approach

A Granger causality (GC) test was performed to identify the MFAPs showing the strongest correlation with the daily number of GERD-related medical utilizations for GERD[16] and to identify causality between the two time-series variables. In this study, the GC test showed the direct and indirect relationships between MFAPs and GERD-related medical utilization and was used to determine the MFAPs that influenced each other intricately.

In the time-series analysis, we created a generalized additive Poisson regression model (GAM) to control for time trends, seasonality, and day of the week. The GAM provided tool optimization of nonparametric smooth functions for the management of potential nonlinear weather variables and flexibility pertaining to the logarithm of the number of GERD-related medical utilizations. Since the GAM model produces unstable estimates as an autocorrelation between meteorological factors, we accounted for time lags using the Durbin-Watson test. Lag detection was performed until the autocorrelation was considered to be white noise. The sum of autocorrelation terms was included as covariate in GAM, after which we validated our dataset for over-dispersion and multicollinearity problems (Supplementary Table 1).

Additionally, we accounted for the daily number of GERD-related medical utilizations in the eight metropolitan areas using the logged variable as the offset variable for control of regional variations in the GAM. Among the meteorological factors, we compared both the Akaike Information Criterion (AIC) and the Bayesian Information Criterion (BIC) for each candidate model using backward elimination for

a better fit. AT, WS, SD, $PM_{2.5}$, and CO were selected in the model, as they had the lowest AIC values (Supplementary Table 2)[17,18]. Our final multivariable model was as follows: Log[E(Y)] = a_0 + *S* (AT, *df* = 4) + *S* (WS, *df* = 20) + *S* (SD, *df* = 18) + *S* ($PM_{2.5}$, *df* = 14) + *S* (CO, *df* = 1) + *offset* [log (province population)] + γ (Day of Week) + γ (Year) + $\sum_{1\leq 0\leq j}AR_j$. Where Log[E(Y)] was the logged expected number of GERD-related medical utilizations, the intercept, *S* the smooth function of meteorological factors as obtained using natural cubic splines, *offset* denoted province population; γ indicator variable for day of the week and year, and overall autocorrelation effect as AR_1 +… + AR_j.

Statistical analyses

Statistical analyses were conducted using SAS version 9.4 for Windows (SAS Institute, Cary, NC, United States). The results are presented as relative risk ratios with 95% confidence intervals. *P* values < 0.05 were considered to indicate statistical significance.

RESULTS

Of the 200000 included patients, 59.2% (*n* = 118313) were female, and the peak age at GERD-related medical utilization was between 60 and 69 years (24.6%, *n* = 49190) (Table 1).

The GC test revealed the presence of an intricate correlation between various MFAPs and GERD-related medical utilizations (Figure 1). Each factor was directly or indirectly associated with GERD-related medical utilization (Figure 1A). Figure 1B shows the findings of the GC test representing the relationship between the selected MFAPs and GERD-related medical utilization. Based on these correlations, the BIC and AIC values of each model for GED-related medical utilization were analyzed. The most valid and effective combination for the predictive model, with the lowest BIC and AIC values (8.33 and 14.0, respectively), included AT, WS, SD, $PM_{2.5}$, and CO (Supplementary Table 1).

The prediction model for the number of GERD-related medical utilizations, developed using the univariate GAM for the three major MFAPs, is shown in Figure 2. The trend between GERD-related medical utilizations and AT indicated that GERD is less likely to develop within an AT of 5-7 °C. However, a gradual S-shape curve between 5.4 °C and 22.4 °C, corresponding to the IQR of AT could be observed. For AT > 23 °C, GERD-related medical utilizations tended to decrease; this may be attributed to people's tendency not to go out in extreme weather conditions (Figure 2A).

Interestingly, at 3-26 μg/m^3, the IQR for $PM_{2.5}$, a higher number of GERD-related medical utilizations were observed. Medical utilization began to decrease when $PM_{2.5}$ levels exceeded 40 μg/m^3. This pattern was similar to that observed for fine dust related diseases (Figure 2B). The positive relative risk for GERD-related medical utilizations was between 0.4 and 0.6 ppm (IQR of CO). Within this range, the number of GERD-related medical utilizations increased rapidly according to CO concentration in a similar fashion as $PM_{2.5}$ (Figure 2C).

For the five selected variables (AT, WS, SD, $PM_{2.5}$, and CO), lags were analyzed using GAM with cubic spline analysis to identify the manner in which prolonged exposure to each variable affects GERD-related medical utilization (Supplementary Table 3). All five selected MFAPs showed a maximum lag period of 9 d; no further effect was observed beyond this time point in multivariate cubic spline analysis (Figure 3). The effects were relatively stable up to 7 d and then declined over time. Results were consistent for the five MFAPs in the multivariate analyses. Box-plot models of estimated risk for GERD-related medical utilization concerning the five MFAPs are shown in Figure 3.

Figure 4 shows the three-dimensional graphs of the prediction models for GERD-related medical utilization using the five selected MFAPs. The estimated risk according to the values and time lags of each variable was included. In univariate GAM, a nonlinear relationship between medical utilizations due to GERD and MFAP was observed, and in multivariable GAM, a consistent relationship up to 9 days of MFAP and medical utilizations was found.

DISCUSSION

In this study we developed a model using five MFAPs, which showed a significant

Table 1 Summary statistics of the relationship of gastroesophageal reflux disease-related medical utilizations with meteorological factors and air pollutants

	mean ± SD	Quantiles				
		Min	25%	50%	75%	Max
Sex, *n* (%)						
Male	81687 (40.8)					
Female	118313 (59.2)					
Age group, yr, *n* (%)						
< 10	341 (0.17)					
10-19	2402 (1.20)					
20-29	6863 (3.43)					
30-39	12477 (6.24)					
40-49	23564 (11.78)					
50-59	46228 (23.11)					
60-69	49190 (24.60)					
70-79	43077 (21.54)					
≥ 80	15858 (7.93)					
Meteorological factors						
Average temperature (°C)	13.8 ± 9.8	-13.7	5.4	15.2	22.4	33.1
High temperature (°C)	18.4 ± 10.0	-10.7	10.1	20.2	27.0	38.8
Low temperature (°C)	10.0 ± 10.0	-17.1	1.0	10.9	18.9	28.8
Diurnal temperature Range (°C)	8.4 ± 3.3	0.0	6.3	8.3	10.5	23.4
Vapor pressure (hPa)	12.2 ± 8.5	0.0	4.7	10.4	18.7	38.3
Solar radiation (MJ/m^2)	12.6 ± 7.3	0.0	7.2	12.2	18.3	33.0
Sunshine duration (hr)	12.0 ± 2.3	9.7	10.5	12.2	13.9	14.8
Wind speed (m/s)	2.5 ± 1.1	0.0	1.8	2.4	3.1	10.1
Daily rain (mm)	3.2 ± 12.5	0.0	0.0	0.0	0.3	310.0
Dew point temperature (°C)	6.3 ± 11.6	-25.9	-3.0	7.3	16.4	28.2
Humidity (%)	62.1 ± 18.6	0.0	49.9	63.3	75.5	100.0
Daily snow (cm)	0.1 ± 0.9	0.0	0.0	0.0	0.0	29.2
Cloud (1/10)	4.5 ± 3.2	0.0	1.6	4.5	7.4	10.0
Air pollutants						
$PM_{2.5}$ (μg/m^3)	15.9 ± 16.1	0.0	3.0	14.0	26.0	99.0
PM_{10} (μg/m^3)	46.6 ± 25.9	0.0	31.2	42.6	57.0	1025.4
[1]O_3 (ppb)	23.7 ± 11.6	0.0	15.4	23.0	31.3	83.8
NO_2 (ppb)	28.2 ± 12.6	0.0	18.9	26.4	35.5	94.9
SO_2 (ppb)	5.1 ± 2.1	0.0	3.8	4.9	6.2	25.8
CO (ppm)	0.5 ± 0.2	0.0	0.4	0.5	0.6	2.2

[1]An 8 h maximum was used for O_3. SD: Standard deviation; $PM_{2.5}$: Particulate matter with a diameter ≤ 2.5 μm; PM_{10}: Particulate matter with a diameter ≤ 10 μm; NO_2: Nitrogen dioxide; SO_2: Sulphur dioxide; CO: Carbon monoxide; ppb: Parts-per-billion; ppm: Parts-per-million.

correlation between these five (MFAPs) and GERD-related medical utilization. Furthermore, two MFAPs, $PM_{2.5}$ and CO, were identified as risk factors for GERD.

Various recent studies have focused on the relationship between meteorological factors and disease. Several commonly occurring diseases have been shown to be associated with meteorological factors; for example, pneumonia was found to be related to AT and the range of diurnal temperature[2,6,19]. Out-of-hospital cardiac arrest is related to temperature, humidity, vapor pressure, and wind speed, and also season-dependent[3,5,20,21]. In this same context, many studies have reported on infectious diseases, strokes, and even fractures[1,4,7,22,23]. However, most of them focused on acute-phase medical diseases, which are considered appropriate targets for meteorological research owing to rapid disease progression, precise diagnosis, and clear medical course.

GERD has a high prevalence and can be treated with medication, even though surgery is required in some cases[13]. GERD usually can become chronic, and patients usually visit the hospital when the symptoms are severe. In general, PPIs are administered only to patients with clinical symptoms without special diagnostic examinations; when symptoms are severe or drug therapy ineffective, examinations such as endoscopy are also performed[13]. Several methods, such as observation after administering PPI based on symptoms, esophagogastroduodenoscopy, or pH monitoring, are used to diagnose GERD. Manometry and esophagogram can be performed for differential diagnosis. In this study, patients who had more than one of the diagnostic examination codes (*i.e.*, codes for esophagogastroduodenoscopy, esophagogram, manometry, and pH monitoring) were defined as an occurrence in order to improve the accuracy of diagnosis, excluding empirical PPI administration or PPI administration for the treatment of other diseases. Besides, in the case of chronic and non-life-threatening medical conditions such as GERD, the national medical environment, insurance coverage, and access to medical care might have a significant impact on medical care utilization. In Korea, the entire national medical insurance system is implemented, medical accessibility is high, and when GERD is suspected, PPI administration, various examinations, and fundoplication are all covered by national insurance. In particular, in the case of urban areas, the race of the population and medical insurance coverage is very homogenous, and medical accessibility is very high due to the high population density. Notably, the use of endoscopy is widespread, owing to its low cost and easy accessibility; thus, it is unlikely that many patients were excluded based on this examination[24]. Therefore, the national medical environment is thought to affect similarly to the entire study group. Additionally, to confirm the time at which GERD symptoms became severe, the day of PPI first administration was defined as the date of GERD occurrence. Therefore, the cohort included in the present study comprised patients who received PPIs after a correct GERD diagnosis.

A study from Taiwan (China) reported that humidity correlates to GERD monthly incidence[14]. However, Taiwan is a tropical region with extremely high temperature and humidity levels throughout the year, leading to difficulties in observing seasonal variation[25,26]. In contrast, the Republic of Korea has four distinct seasons and difference in MFAPs types among seasons is significant. Moreover, the Korea Meteorological Administration conducts detailed measurements by region, while the National Health Insurance provides extensive data on the total population. Thus, the Republic of Korea was a suitable area for this study. However, numerous meteorological studies have been limited to partial analyses or univariate analyses of meteorological variables without consideration of their complexity[3-5,7]. However, MFAPs are closely related to each other. For example, $PM_{2.5}$ is known to be negatively correlated with WS, SD, and daily rainfall, and positively correlated with humidity and vapor pressure[8,9,27]. Therefore, it is necessary to consider these complex correlations in MFAPs analysis. To compensate for this complexity, we investigated the correlation of GERD-related medical utilization with all MFAPs using a GC test, and then selected the appropriate model based on BIC and AIC values. Afterwards, we run the GC test once again to determine the adequacy of the selected model.

The analysis of the correlation between MFAPs and GERD-related medical utilization showed that a model combining AT, SD, WS, $PM_{2.5}$, and CO, was the most suitable for prediction. The number of GERD-related medical utilizations increased as AT dropped to sub-zero values or when AT was > 10 °C. There is no direct evidence that an increase in AT is a risk factor for GERD. However, as AT increases, the number of outdoor activities that individuals partake in also increases. Additionally, eating habits may change, increasing the intake of fatty foods. Fatty food and soda intake are well-known GERD risk factors; thus, dietary changes as a result of climate variations could explain the increase in GERD-related medical utilization[28].

Some studies have shown that cold temperatures are associated with the

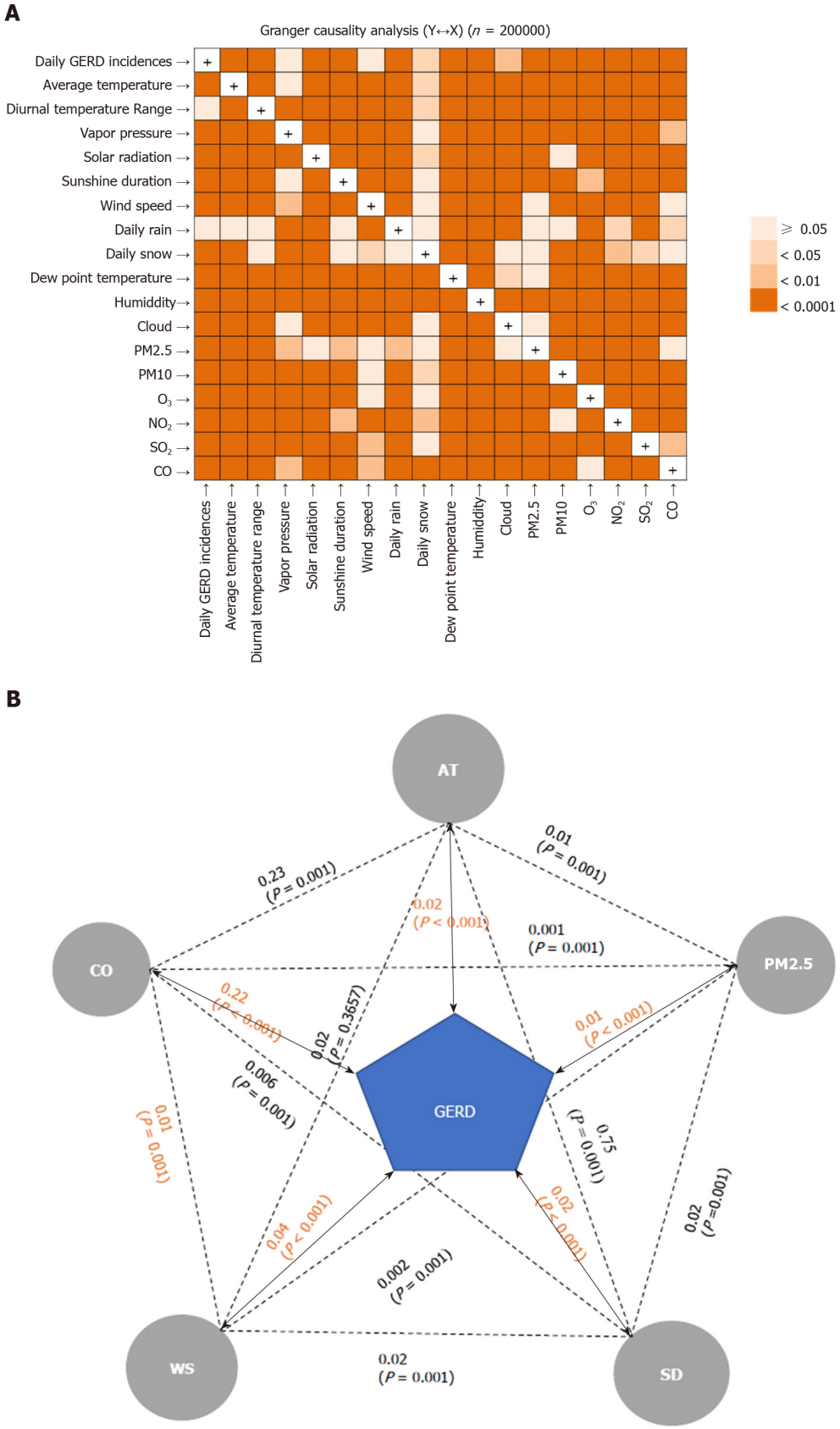

Figure 1 Granger causality test of the relationship between meteorological factors and air pollutants and GERD-related medical utilization. A: Various meteorological factors and air pollutants (MFAPs) show a direct or indirect association with GERD-related medical utilization; B: Relationship between the five selected MFAPs and GERD-related medical utilization. All variables were significantly correlated except AT and WS. The five selected MFAPs were significantly correlated to GERD-related medical utilization. MFAPs: Meteorological factors and air pollutants; GERD: Gastroesophageal reflux disease; WS: Wind speed; SD: Sunshine duration; AT: Average temperature; CO: Carbon monoxide; $PM_{2.5}$: Particulate matter with a diameter ≤ 2.5 μm.

development of respiratory diseases[6,29]. Coughing, the most commonly reported symptom of respiratory disease, leads to increased abdominal pressure, which may result in GERD development or a worsening of its symptoms. Coughing has been associated with $PM_{2.5}$ levels as well as cold temperatures[30,31], while higher $PM_{2.5}$ concentrations can cause a cough, which can likewise cause or worsen GERD symptoms.

$PM_{2.5}$ enters the circulatory system directly through the alveoli, and causes cardiac and respiratory diseases through vascular inflammation[32]. In mice, particulate matter was found to cause oxidative stress or inflammatory changes through its influence on the microbiome in the gastrointestinal tract[33,34]. No study to date has focused on the direct mechanism through which $PM_{2.5}$ leads to GERD; thus, further research is needed to identify how these inflammatory and metabolic changes of the vascular or gastrointestinal tract affect the lower esophageal sphincter and surrounding structures. In terms of WS, GERD-related medical utilization increased with low WS (2-4 m/s), and decreased as WS increased to values > 4 m/s. Previous studies have reported that $PM_{2.5}$ concentration is negatively correlated to WS[8,9,27]. This may be due to the fact that strong winds result in decreasing $PM_{2.5}$ levels, which in turn maintains GERD-related medical utilizations at a low level.

Chronic CO intoxication has been known to cause headache, confusion, nausea, vomiting, seizure, and muscle weakness[35,36]. In the present study, GERD-related medical utilizations increased with CO concentrations of 0.4-0.6 ppm. It is unknown how long-term exposure to low CO concentrations affects GERD occurrence or worsening of its symptoms. However, CO can bind to myoglobin with high affinity, resulting in muscle weakness, which may lead to lower esophageal sphincter pressure weakness[37]. Additionally, continued and repeated exposure may cause nausea or vomiting, which could increase the abdominal pressure and worsen GERD symptoms.

For all five variables selected for modelling, we observed that GERD-related medical utilizations rapidly decreased at values above the extreme or national weather MFAP alarm values. GERD-related medical utilizations decreased in hot weather conditions, when AT was > 23 °C or on very windy days. Of note, in terms of $PM_{2.5}$, GERD-related medical utilizations decreased rapidly when the concentration exceeded 40 μg/m^3. In Korea, a national alarm is issued when $PM_{2.5}$ concentration exceeds 40 μg/m^3. Therefore, people pay more attention to personal protection, such as wearing a mask, and refrain from going out as much as possible. As GERD is not a life-threatening disease, the decrease in GERD-related medical utilizations as a result of national alarm, high temperatures, or strong winds is likely due to people's behavioral changes. Furthermore, the time lag for the prediction model in this study was approximately 7 d. This finding suggests that GERD may occur or be aggravated by various MFAPs through different mechanisms, and it may take up to 7 d for patients to visit the hospital. As GERD is a relatively chronic disease with limited severity, this time lag appears reasonable.

This study was subject to several limitations. First, although GERD is greatly affected by lifestyle, individual factors such as dietary habits, smoking status, or body mass index were not investigated. More, the first visit date of the outpatient clinic, the duration for observation or medication, the first date for PPI, the dose of medication, the duration of hospitalization, and compliance for medication are important related factors for GERD-related medical utilization. Besides, the first date of PPI administration could be affected by other conditions of the patient or the physicians, such as interest in health or preference of medication. However, this study is a big-data study using NHIS data, and the detailed information about the patient's situation, symptoms, compliance, preferences, or the physician's preference is difficult to be identified. Therefore, in order to minimize the bias, the authors defined the first date of PPI administration, the most clearly definable, as the occurrence of GERD. Second, an inaccurate GERD diagnosis could result in bias, since PPI is commonly used for patients with only clinical symptoms but without a definite diagnostic GERD examination. However, this bias was reduced through the use of diagnostic examination codes (*i.e.*, codes for esophagogastroduodenoscopy, pH monitoring, manometry, or esophagogram). Third, individual MFAP exposure levels were not evaluated. This was an ecological study; thus, the ecological fallacy that people living in the same city are exposed to the same environment could not be ruled out. Finally, the mechanisms underlying the effect of each MFAP on GERD-related medical utilizations could not be identified. Further well-designed animal studies are needed to reveal the underlying mechanisms.

To the best of our knowledge, this study is the first to identify the relationship between MFAPs and GERD-related medical utilization. Additionally, it involved a large sample size, with the 200000 cases being selected from areas with significant

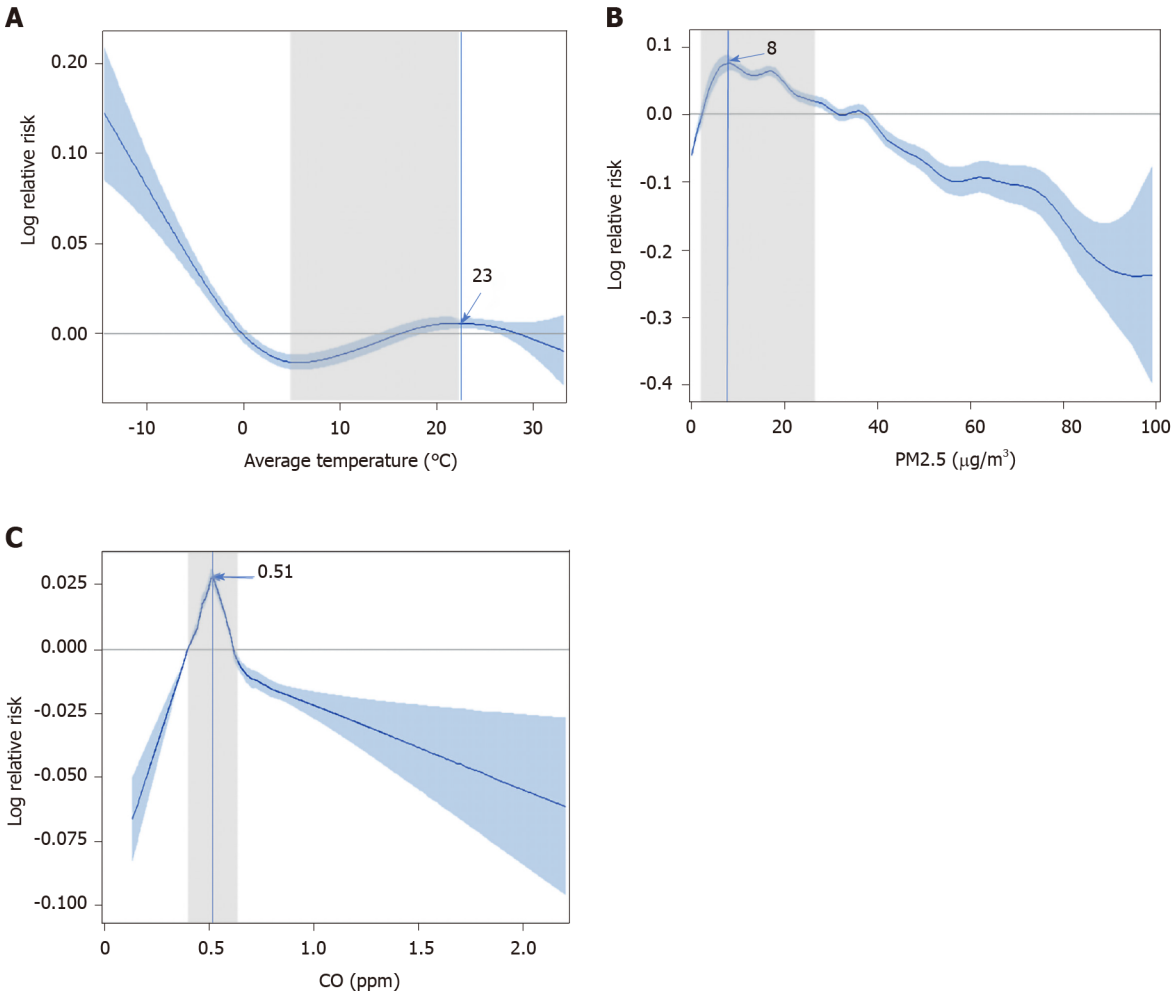

Figure 2 Prediction model of gastroesophageal reflux disease -related medical utilization using a univariate generalized additive Poisson regression model. A: Gastroesophageal reflux disease (GERD)-related medical utilizations with AT; B: GERD-related medical utilizations as with particulate matter with a diameter ≤ 2.5 μm levels ≤ 40 μg/m^3; C: GERD-related medical utilizations in the range of the IQR for carbon monoxide. CO: Carbon monoxide; $PM_{2.5}$: Particulate matter with a diameter ≤ 2.5 μm; ppm: Parts-per-million.

season-related variations in MFAPs levels. Finally, bias was reduced by sampling only in large cities with similar races, cultures, eating habits, economic levels, and accessibility to hospitals. Thus, the data analyzed in this study took into consideration the complexity of all MFAPs.

CONCLUSION

In conclusion, our results suggest that a model using AT, SD, WS, $PM_{2.5}$, and CO has significant power for the prediction of GERD-related medical utilizations. Additionally, the aforementioned variables were found to be risk factors for GERD. The time-lag to disease progression was 7 d. Therefore, to reduce GERD occurrence and aggravation, environmental management and national alarm systems for each factor should be established.

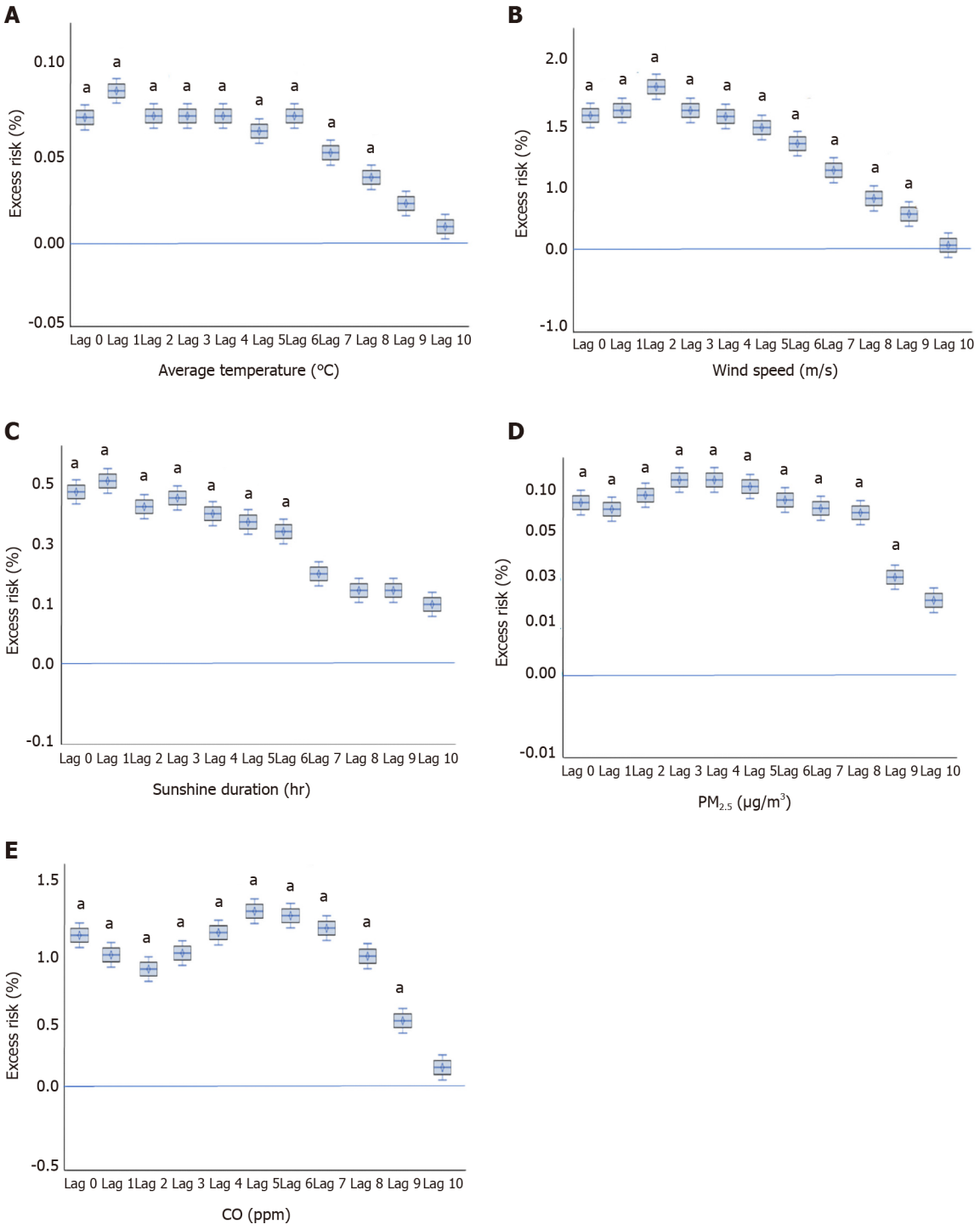

Figure 3 Time lag for exposure in multivariate analyses. A: Excess risk was significant after exposure up until 8 d for average temperature; B: Excess risk was significant after exposure up until 9 d for wind speed; C: Excess risk was significant after exposure up until 6 d for sunshine duration; D: Excess risk was significant after exposure up until 9 d for particulate matter with a diameter ≤ 2.5 μm; E: Excess risk was significant after exposure up until 9 d for carbon monoxide. [a] $P < 0.05$. CO: Carbon monoxide; $PM_{2.5}$: Particulate matter with a diameter ≤ 2.5 μm; ppm: Parts-per-million.

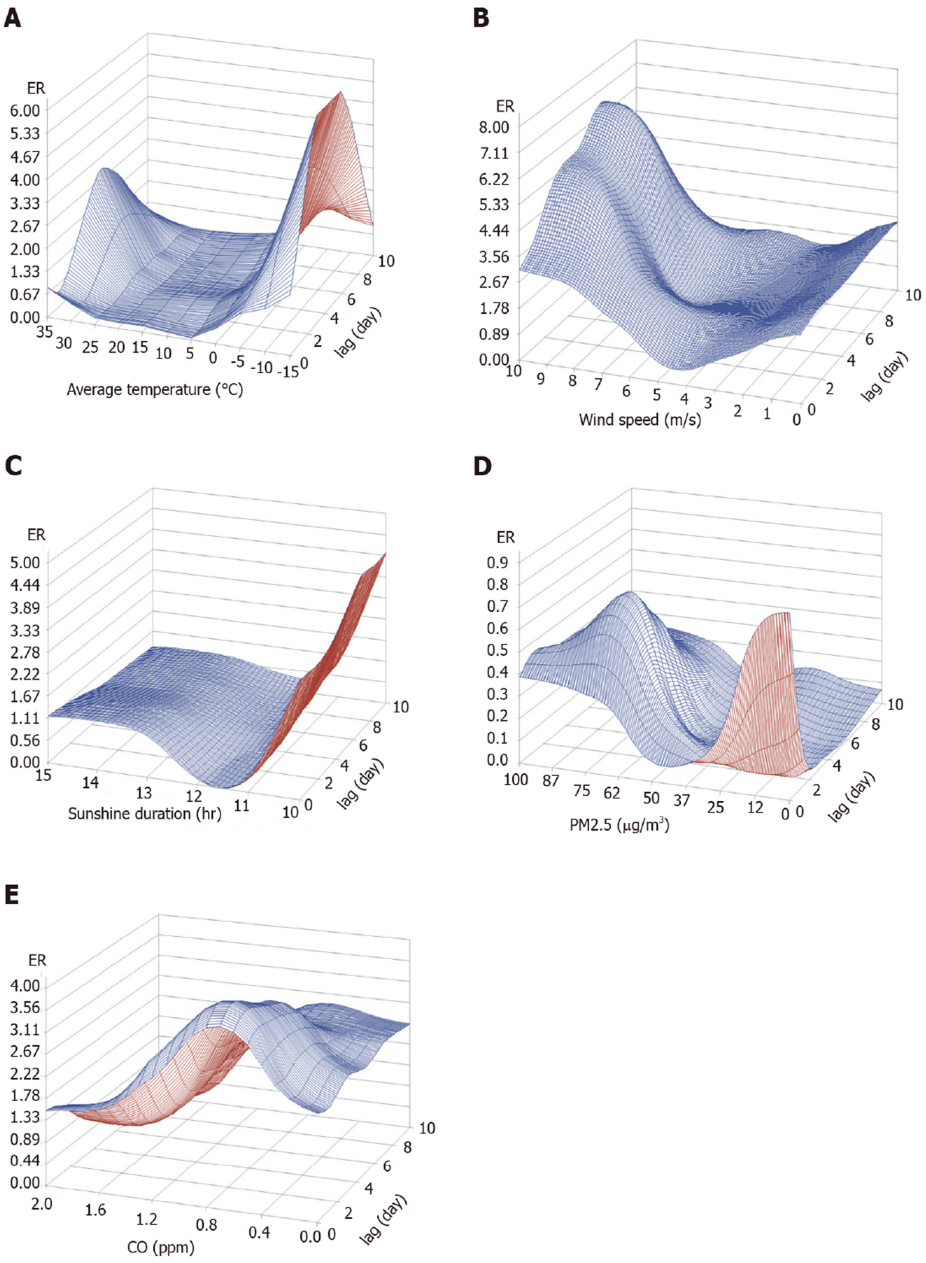

Figure 4 Three-dimensional graph of the prediction model. Each graph shows excess risk according to factor and time lag. A: Average temperature; B: Wind speed; C: Sunshine duration; D: Particulate matter with a diameter ≤ 2.5 μm; E: Carbon monoxide. CO: Carbon monoxide; $PM_{2.5}$: Particulate matter with a diameter ≤ 2.5 μm; ppm: Parts-per-million.

ARTICLE HIGHLIGHTS

Research background

The incidence of gastroesophageal reflux disease (GERD) is rapidly increasing owing to changes in people's lifestyle and eating habits. It is essential to perform the analyses after considering correlations among meteorological factors and air pollutants (MFAPs).

Research motivation

To date, only one study investigated the relationship between humidity and monthly GERD occurrence. However, it was limited by the exclusive inclusion of patients in study population.

Research objectives

This work aims to identify MFAPs effect on GERD-related medical utilization.

Research methods

Data on GERD-related medical utilizations were obtained from the National Health Insurance Services. Data on meteorological factors were obtained from the National Climate Data Center of the Korea Meteorological Administration. A Granger causality test was performed to identify the MFAPs showing the strongest correlation with the daily number of GERD-related medical utilizations for GERD and to identify causality between the two time-series variables.

Research results

GERD-related medical utilization increased with the levels of particulate matter with a diameter ≤ 2.5 μm ($PM_{2.5}$) and carbon monoxide (CO). S-shaped and inverted U-shaped changes were observed in average temperature and air pollutants, respectively. The time lag of each variable was significant around nine days after exposure.

Research conclusions

Current study suggests that a model using average temperature, sunshine duration, wind speed, $PM_{2.5}$, and CO has significant power for the prediction of GERD-related medical utilizations.

Research perspectives

To reduce GERD occurrence and aggravation, environmental management and national alarm systems for each factor should be established.

REFERENCES

1 **Mazzucchelli R**, Crespí-Villarías N, Pérez-Fernández E, Durbán Reguera ML, Guzón Illescas O, Quirós J, García-Vadillo A, Carmona L, Rodriguez-Caravaca G, Gil de Miguel A. Weather conditions and their effect on seasonality of incident osteoporotic hip fracture. *Arch Osteoporos* 2018; **13**: 28 [PMID: 29546463 DOI: 10.1007/s11657-018-0438-4]

2 **Sohn S**, Cho W, Kim JA, Altaluoni A, Hong K, Chun BC. 'Pneumonia Weather': Short-term Effects of Meteorological Factors on Emergency Room Visits Due to Pneumonia in Seoul, Korea. *J Prev Med Public Health* 2019; **52**: 82-91 [PMID: 30971074 DOI: 10.3961/jpmph.18.232]

3 **Stratil P**, Wallmueller C, Schober A, Stoeckl M, Hoerburger D, Weiser C, Testori C, Krizanac D, Spiel A, Uray T, Sterz F, Haugk M. Seasonal variability and influence of outdoor temperature on body temperature of cardiac arrest victims. *Resuscitation* 2013; **84**: 630-634 [PMID: 23022435 DOI: 10.1016/j.resuscitation.2012.09.027]

4 **Tarnoki AD**, Turker A, Tarnoki DL, Iyisoy MS, Szilagyi BK, Duong H, Miskolczi L. Relationship between weather conditions and admissions for ischemic stroke and subarachnoid hemorrhage. *Croat Med J* 2017; **58**: 56-62 [PMID: 28252876 DOI: 10.3325/cmj.2017.58.56]

5 **Hensel M**, Geppert D, Kersten JF, Stuhr M, Lorenz J, Wirtz S, Kerner T. Association between Weather-Related Factors and Cardiac Arrest of Presumed Cardiac Etiology: A Prospective Observational Study Based on Out-of-Hospital Care Data. *Prehosp Emerg Care* 2018; **22**: 345-352 [PMID: 29345516 DOI: 10.1080/10903127.2017.1381790]

6 **Liu Y**, Kan H, Xu J, Rogers D, Peng L, Ye X, Chen R, Zhang Y, Wang W. Temporal relationship between hospital admissions for pneumonia and weather conditions in Shanghai, China: a time-series analysis. *BMJ Open* 2014; **4**: e004961 [PMID: 24989619 DOI: 10.1136/bmjopen-2014-004961]

7 **Simmering JE**, Polgreen LA, Hornick DB, Sewell DK, Polgreen PM. Weather-Dependent Risk for Legionnaires' Disease, United States. *Emerg Infect Dis* 2017; **23**: 1843-1851 [PMID: 29048279 DOI: 10.3201/eid2311.170137]

8 **Huang F**, Li X, Wang C, Xu Q, Wang W, Luo Y, Tao L, Gao Q, Guo J, Chen S, Cao K, Liu L, Gao N, Liu X, Yang K, Yan A, Guo X. PM2.5 Spatiotemporal Variations and the Relationship with Meteorological Factors during 2013-2014 in Beijing, China. *PLoS One* 2015; **10**: e0141642 [PMID: 26528542 DOI: 10.1371/journal.pone.0141642]

9 **Zhang H**, Wang Z, Zhang W. Exploring spatiotemporal patterns of PM2.5 in China based on ground-level observations for 190 cities. *Environ Pollut* 2016; **216**: 559-567 [PMID: 27318543 DOI: 10.1016/j.envpol.2016.06.009]

10 **Jung HK**. Epidemiology of gastroesophageal reflux disease in Asia: a systematic review. *J Neurogastroenterol Motil* 2011; **17**: 14-27 [PMID: 21369488 DOI: 10.5056/jnm.2011.17.1.14]

11 **Ronkainen J**, Agréus L. Epidemiology of reflux symptoms and GORD. *Best Pract Res Clin Gastroenterol* 2013; **27**: 325-337 [PMID: 23998972 DOI: 10.1016/j.bpg.2013.06.008]

12 **Savarino E**, de Bortoli N, De Cassan C, Della Coletta M, Bartolo O, Furnari M, Ottonello A, Marabotto E, Bodini G, Savarino V. The natural history of gastro-esophageal reflux disease: a comprehensive review. *Dis Esophagus* 2017; **30**: 1-9 [PMID: 27862680 DOI: 10.1111/dote.12511]

13 **Seo HS**, Choi M, Son SY, Kim MG, Han DS, Lee HH. Evidence-Based Practice Guideline for Surgical Treatment of Gastroesophageal Reflux Disease 2018. *J Gastric Cancer* 2018; **18**: 313-327 [PMID: 30607295 DOI: 10.5230/jgc.2018.18.e41]

14 **Chen KY**, Lou HY, Lin HC, Lee SH. Seasonal variation in the incidence of gastroesophageal reflux disease.

Am J Med Sci 2009; **338**: 453-458 [PMID: 19826247 DOI: 10.1097/MAJ.0b013e3181b51fbd]
15 **Raheem OA**, Khandwala YS, Sur RL, Ghani KR, Denstedt JD. Burden of Urolithiasis: Trends in Prevalence, Treatments, and Costs. *Eur Urol Focus* 2017; **3**: 18-26 [PMID: 28720363 DOI: 10.1016/j.euf.2017.04.001]
16 **Granger CWJ**. Investigating Causal Relations by Econometric Models and Cross-spectral Methods. *Econometrica* 1969; **37**: 424-438 [DOI: 10.2307/1912791]
17 **Akaike H**. A new look at the statistical model identification. *IEEE Transactions on Automatic Control* 1974; **19**: 716-723 [DOI: 10.1109/TAC.1974.1100705]
18 **Schwarz G**. Estimating the Dimension of a Model. *Ann Stat* 1978; **6**: 461-464
19 **Hossain MZ**, Tong S, Bambrick H, Khan AF, Hore SK, Hu W. Weather factors, PCV intervention and childhood pneumonia in rural Bangladesh. *Int J Biometeorol* 2020; **64**: 561-569 [PMID: 31848699 DOI: 10.1007/s00484-019-01842-7]
20 **Mohammad MA**, Koul S, Rylance R, Fröbert O, Alfredsson J, Sahlén A, Witt N, Jernberg T, Muller J, Erlinge D. Association of Weather With Day-to-Day Incidence of Myocardial Infarction: A SWEDEHEART Nationwide Observational Study. *JAMA Cardiol* 2018; **3**: 1081-1089 [PMID: 30422202 DOI: 10.1001/jamacardio.2018.3466]
21 **Shiue I**, Perkins DR, Bearman N. Hospital admissions of hypertension, angina, myocardial infarction and ischemic heart disease peaked at physiologically equivalent temperature 0°C in Germany in 2009-2011. *Environ Sci Pollut Res Int* 2016; **23**: 298-306 [PMID: 26286805 DOI: 10.1007/s11356-015-5224-x]
22 **Gleason JA**, Kratz NR, Greeley RD, Fagliano JA. Under the Weather: Legionellosis and Meteorological Factors. *Ecohealth* 2016; **13**: 293-302 [PMID: 26993637 DOI: 10.1007/s10393-016-1115-y]
23 **Hu W**, Li Y, Han W, Xue L, Zhang W, Ma W, Bi P. Meteorological factors and the incidence of mumps in Fujian Province, China, 2005-2013: Non-linear effects. *Sci Total Environ* 2018; **619-620**: 1286-1298 [PMID: 29734606 DOI: 10.1016/j.scitotenv.2017.11.108]
24 **Cha JM**, Moon JS, Chung IK, Kim JO, Im JP, Cho YK, Kim HG, Lee SK, Lee HL, Jang JY, Kim ES, Jung Y, Moon CM, Kim Y, Park BY. National Endoscopy Quality Improvement Program Remains Suboptimal in Korea. *Gut Liver* 2016; **10**: 699-705 [PMID: 27282270 DOI: 10.5009/gnl15623]
25 **Beck HE**, Zimmermann NE, McVicar TR, Vergopolan N, Berg A, Wood EF. Present and future Köppen-Geiger climate classification maps at 1-km resolution. *Sci Data* 2018; **5**: 180214 [PMID: 30375988 DOI: 10.1038/sdata.2018.214]
26 **Geiger R Überarbeitete**, Neuausgabe von Geiger, R Köppen-Geiger/Klima der Erde. (Wandkarte 1: 16 Mill.)-Klett-Perthes, Gotha 1961
27 **Wang J**, Ogawa S. Effects of Meteorological Conditions on PM2.5 Concentrations in Nagasaki, Japan. *Int J Environ Res Public Health* 2015; **12**: 9089-9101 [PMID: 26247953 DOI: 10.3390/ijerph120809089]
28 **Surdea-Blaga T**, Negrutiu DE, Palage M, Dumitrascu DL. Food and Gastroesophageal Reflux Disease. *Curr Med Chem* 2019; **26**: 3497-3511 [PMID: 28521699 DOI: 10.2174/0929867324666170515123807]
29 **Zhao Q**, Zhao Y, Li S, Zhang Y, Wang Q, Zhang H, Qiao H, Li W, Huxley R, Williams G, Zhang Y, Guo Y. Impact of ambient temperature on clinical visits for cardio-respiratory diseases in rural villages in northwest China. *Sci Total Environ* 2018; **612**: 379-385 [PMID: 28858748 DOI: 10.1016/j.scitotenv.2017.08.244]
30 **Abramson MJ**, Blackman J, Carroll M, Gao CX, Del Monaco A, Brown D, Dimitriadis C, Johnson A, Guo Y, Sim MR, Walker J. Chronic cough is related to cumulative PM2.5 exposure from a coal mine fire. *European Respiratory Journal* 2019; **54** Suppl 63: PA4455 [DOI: 10.1183/13993003.congress-2019.PA4455]
31 **Xing YF**, Xu YH, Shi MH, Lian YX. The impact of PM2.5 on the human respiratory system. *J Thorac Dis* 2016; **8**: E69-E74 [PMID: 26904255 DOI: 10.3978/j.issn.2072-1439.2016.01.19]
32 **Mar TF**, Koenig JQ, Jansen K, Sullivan J, Kaufman J, Trenga CA, Siahpush SH, Liu LJ, Neas L. Fine particulate air pollution and cardiorespiratory effects in the elderly. *Epidemiology* 2005; **16**: 681-687 [PMID: 16135945 DOI: 10.1097/01.ede.0000173037.83211.d6]
33 **Mutlu EA**, Comba IY, Cho T, Engen PA, Yazıcı C, Soberanes S, Hamanaka RB, Niğdelioğlu R, Meliton AY, Ghio AJ, Budinger GRS, Mutlu GM. Inhalational exposure to particulate matter air pollution alters the composition of the gut microbiome. *Environ Pollut* 2018; **240**: 817-830 [PMID: 29783199 DOI: 10.1016/j.envpol.2018.04.130]
34 **Zhang Y**, Li Y, Shi Z, Wu J, Yang X, Feng L, Ren L, Duan J, Sun Z. Metabolic impact induced by total, water soluble and insoluble components of $PM_{2.5}$ acute exposure in mice. *Chemosphere* 2018; **207**: 337-346 [PMID: 29803883 DOI: 10.1016/j.chemosphere.2018.05.098]
35 **Fawcett TA**, Moon RE, Fracica PJ, Mebane GY, Theil DR, Piantadosi CA. Warehouse workers' headache. Carbon monoxide poisoning from propane-fueled forklifts. *J Occup Med* 1992; **34**: 12-15 [PMID: 1552375]
36 **Johnson AC**, Morata TC. The Nordic Expert Group for criteria documentation of health risks from chemicals: 142, Göteborg: University of Gothenburg, 2009
37 **Bateman DN**. Carbon Monoxide. *Medicine* 2003; **31**: 41-42 [DOI: 10.1383/medc.31.10.41.27810]

World Journal of Gastroenterology

Submit a Manuscript: https://www.f6publishing.com

World J Gastroenterol 2020 October 21; 26(39): 6087-6097

DOI: 10.3748/wjg.v26.i39.6087

ISSN 1007-9327 (print) ISSN 2219-2840 (online)

ORIGINAL ARTICLE

Observational Study

Acute gastrointestinal injury in critically ill patients with COVID-19 in Wuhan, China

Jia-Kui Sun, Ying Liu, Lei Zou, Wen-Hao Zhang, Jing-Jing Li, Yu Wang, Xiao-Hua Kan, Jiu-Dong Chen, Qian-Kun Shi, Shou-Tao Yuan

ORCID number: Jia-Kui Sun 0000-0002-1248-7974; Ying Liu 0000-0002-0811-514X; Lei Zou 0000-0001-8738-848X; Wen-Hao Zhang 0000-0003-2708-2221; Jing-Jing Li 0000-0003-0028-857X; Yu Wang 0000-0002-9179-2124; Xiao-Hua Kan 0000-0003-2794-723X; Jiu-Dong Chen 0000-0001-5142-3124; Qian-Kun Shi 0000-0003-4193-9754; Shou-Tao Yuan 0000-0002-0228-0152.

Author contributions: Sun JK and Liu Y contributed equally to this study; Sun JK, Shi QK and Yuan ST designed the research; Sun JK, Liu Y, Zou L, Zhang WH, Li JJ, Wang Y, Kan XH and Chen JD performed the research; Sun JK, Liu Y and Zou L analyzed the data; Sun JK and Zou L wrote the paper; Shi QK and Yuan ST are both corresponding authors.

Supported by National Natural Science Foundation of China, No. 81701881; and Nanjing Medical Science and Technology Development Foundation, No. YKK17102.

Institutional review board statement: The study was reviewed and approved by the institutional review board of Nanjing First Hospital and Tongji Hospital. Written informed consent was waived as this was a

Jia-Kui Sun, Ying Liu, Lei Zou, Wen-Hao Zhang, Yu Wang, Xiao-Hua Kan, Jiu-Dong Chen, Qian-Kun Shi, Shou-Tao Yuan, Department of Intensive Care Unit, Nanjing First Hospital, Nanjing Medical University, Nanjing 210006, Jiangsu Province, China

Jia-Kui Sun, Ying Liu, Lei Zou, Wen-Hao Zhang, Jing-Jing Li, Yu Wang, Xiao-Hua Kan, Qian-Kun Shi, Shou-Tao Yuan, Department of Isolation Units, Tongji Hospital, Huazhong University of Science and Technology, Wuhan 430030, Hubei Province, China

Jing-Jing Li, Department of Intensive Care Unit, Lishui People's Hospital, Nanjing 211200, Jiangsu Province, China

Corresponding author: Qian-Kun Shi, MD, Doctor, Department of Intensive Care Unit, Nanjing First Hospital, Nanjing Medical University, No. 68 Changle Road, Nanjing 210006, Jiangsu Province, China. njdrsqw2019@163.com

Abstract

BACKGROUND

The coronavirus disease 2019 (COVID-19) is spreading rapidly around the world. Most critically ill patients have organ injury, including acute respiratory distress syndrome, acute kidney injury, cardiac injury, or liver dysfunction. However, few studies on acute gastrointestinal injury (AGI) have been reported in critically ill patients with COVID-19.

AIM

To investigate the prevalence and outcomes of AGI in critically ill patients with COVID-19.

METHODS

In this retrospective study, demographic data, laboratory parameters, AGI grades, clinical severity and outcomes were collected. The primary endpoints were AGI incidence and 28-d mortality.

RESULTS

From February 10 to March 10 2020, 83 critically ill patients out of 1314 patients with COVID-19 were enrolled. Seventy-two (86.7%) patients had AGI during hospital stay, of these patients, 30 had AGI grade I, 35 had AGI grade II, 5 had AGI grade III, and 2 had AGI grade IV. The incidence of AGI grade II and above

retrospective study.

Informed consent statement: All study participants, or their legal guardian, provided informed written consent prior to study enrollment.

Conflict-of-interest statement: The authors declare no conflicts of interest.

Data sharing statement: No additional data are available.

STROBE statement: The authors have read the STROBE Statement-checklist of items, and the manuscript was prepared and revised according to the STROBE Statement-checklist of items.

Manuscript source: Unsolicited manuscript

Received: June 2, 2020
Peer-review started: June 2, 2020
First decision: July 29, 2020
Revised: August 6, 2020
Accepted: September 16, 2020
Article in press: September 16, 2020
Published online: October 21, 2020

P-Reviewer: Nesek-Adam V, Vunnam SR
S-Editor: Gao CC
L-Editor: Webster JR
P-Editor: Ma YJ

was 50.6%. Forty (48.2%) patients died within 28 days of admission. Multiple organ dysfunction syndrome developed in 58 (69.9%) patients, and septic shock in 16 (19.3%) patients. Patients with worse AGI grades had worse clinical variables, a higher incidence of septic shock and 28-d mortality. Sequential organ failure assessment (SOFA) scores (95%CI: 1.374-2.860; $P < 0.001$), white blood cell (WBC) counts (95%CI: 1.037-1.379; $P = 0.014$), and duration of mechanical ventilation (MV) (95%CI: 1.020-1.340; $P = 0.025$) were risk factors for the development of AGI grade II and above.

CONCLUSION

The incidence of AGI was 86.7%, and hospital mortality was 48.2% in critically ill patients with COVID-19. SOFA scores, WBC counts, and duration of MV were risk factors for the development of AGI grade II and above. Patients with worse AGI grades had a higher incidence of septic shock and 28-d mortality.

Key Words: Gastrointestinal injury; Organ dysfunction; Septic shock; Critically ill; COVID-19

Core Tip: This is the first study to investigate acute gastrointestinal injury (AGI) in critically ill patients with coronavirus disease 2019. The incidence of AGI was 86.7%, and hospital mortality was 48.2% in critically ill patients. Sequential organ failure assessment scores, white blood cell counts, and duration of mechanical ventilation were risk factors for the development of AGI grade II and above. Patients with worse AGI grades had worse clinical severity variables, a higher incidence of septic shock, and higher hospital mortality.

Citation: Sun JK, Liu Y, Zou L, Zhang WH, Li JJ, Wang Y, Kan XH, Chen JD, Shi QK, Yuan ST. Acute gastrointestinal injury in critically ill patients with COVID-19 in Wuhan, China. *World J Gastroenterol* 2020; 26(39): 6087-6097
URL: https://www.wjgnet.com/1007-9327/full/v26/i39/6087.htm
DOI: https://dx.doi.org/10.3748/wjg.v26.i39.6087

INTRODUCTION

In December 2019, clusters of acute pneumonia cases of unclear etiology were identified in Wuhan, the capital of Hubei province in China[1-3]. The pathogen was reported to be a novel coronavirus that was named severe acute respiratory syndrome coronavirus 2 (SARS-CoV-2). Coronavirus disease 2019 (COVID-19) was characterized by the World Health Organization (WHO) as a pandemic due to the rapid spread of the disease around the world[4]. As of May 16, 2020, a total of 82947 cases (4634 deaths) were confirmed in China, including 50339 cases (3869 deaths) in Wuhan city[5].

The National Health Commission of China issued a series of diagnosis and treatment recommendations and suggested classifying the disease into four grades: Mild, moderate, severe and critical[5]. Recent studies have reported the clinical characteristics and prognosis of COVID-19 with varied severity[1,2,6-8]. Most critically ill patients had organ injury, including acute respiratory distress syndrome (ARDS), acute kidney injury (AKI), cardiac injury, or liver dysfunction[9]. During our clinical work against the epidemic of COVID-19 in Wuhan, we observed that numerous patients had gastrointestinal symptoms during the course of disease development. It is known that gastrointestinal dysfunction is closely related to adverse outcomes in critically ill patients. However, few studies on acute gastrointestinal injury (AGI) have been reported in critically ill patients with COVID-19. In this study, we investigated the prevalence and outcomes of AGI in critically ill patients with COVID-19 who were admitted to Guanggu District of Wuhan Tongji Hospital.

MATERIALS AND METHODS

Patients

From February 10 to March 10 2020, adult patients (age ≥ 18 years) with confirmed critical COVID-19 admitted to our specialized isolation units and intensive care unit (ICU), Guanggu district of Wuhan Tongji Hospital were enrolled in this retrospective study. Patients with chronic organ dysfunction (*e.g.*, hepatic or renal dysfunction), immunodeficiency, terminal cancer, and patients with a history of long-term use of corticosteroids were excluded. Written informed consent was waived by our institutional review board as this was a retrospective study for emerging infectious disease. The diagnosis of COVID-19 was according to the WHO interim guidance and recommendations of the National Health Commission of China[4,5], and identified by the detection of SARS-CoV-2 RNA in the clinical laboratory of Tongji Hospital.

Definitions

An identified case of COVID-19 was defined as a positive finding on real-time reverse-transcriptase–polymerase-chain-reaction (RT-PCR) assay of nasal and pharyngeal swab specimens[4,5,7]. Only laboratory-confirmed cases were enrolled in the analysis. The diagnosis of critical COVID-19 was in accordance with the Chinese recommendations[5]: Meeting any of the following: I, respiratory failure with mechanical ventilation (MV); II, shock; III, multiple organ failure requiring ICU treatment. AGI was defined as a malfunction of the gastrointestinal tract due to acute illness and was categorized into four grades according to its severity[10]. This AGI grading system was based mainly on gastrointestinal symptoms, intra-abdominal pressure, and the presence/absence of feeding tolerance. AGI grade I was defined as an increased risk of developing gastrointestinal dysfunction or failure (a self-limiting condition); AGI grade II was defined as gastrointestinal dysfunction (a condition that requires interventions); AGI grade III was defined as gastrointestinal failure (GI function cannot be restored with interventions); AGI grade IV was defined as marked gastrointestinal failure (a condition that is immediately life-threatening)[10]. Sepsis was defined as life-threatening organ dysfunction caused by a dysregulated host response to infection, septic shock was defined as a subset of sepsis with circulatory and cellular/metabolic dysfunction associated with a higher risk of mortality[11]. The diagnostic criteria for ARDS were in accordance with the Berlin definitions[12]. The definition of AKI was based on the 2012 Kidney Disease: Improving Global Outcomes guidelines[13]. Cardiac injury was defined as serum levels of cardiac biomarkers (*e.g.*, troponin I) above the 99th percentile reference upper limit or new abnormalities on electrocardiography and echocardiography[2]. Liver injury was defined as serum levels of hepatic biomarkers (*e.g.*, alanine aminotransferase) more than twice the reference upper limit or a disproportionate elevation of alanine aminotransferase and aspartate aminotransferase levels compared with alkaline phosphatase levels[14]. Multiple organ dysfunction syndrome (MODS) was defined as the combined dysfunction of two or more organs.

Data collection

The baseline clinical characteristics, including sex, age, days from onset to admission, initial symptoms or signs, and body mass index (BMI) were collected from electronic medical and nursing records, and all laboratory tests were performed according to the clinical needs of patients. The acute physiology and chronic health evaluation (APACHE) II score, sequential organ failure assessment (SOFA) score, serum levels of C-reactive protein (CRP), D-dimer, white blood cell (WBC) count, lymphocyte count, procalcitonin (PCT), and blood lactate within 24 h of admission were recorded. The RT-PCR assay of viral RNA was performed using a commercial kit (Tianlong, Xi'an, China) according to the manufacturer's instructions. All laboratory parameters were detected by the clinical laboratory of Tongji Hospital. Moreover, the numbers of patients with AGI (grades), ARDS, AKI, cardiac injury, liver injury, septic shock, MODS, and patients receiving MV or continuous renal replacement therapy (CRRT) during hospital stay were also recorded. The primary endpoints were the incidence of AGI and 28-d mortality. The secondary endpoints were the incidence of MODS and septic shock.

Statistical analysis

The Kolmogorov-Smirnov test was first performed to test the normal distribution of the data. Normally distributed data were expressed as the means ± standard deviation and were compared by *t* tests. Non-normally distributed data were expressed as the

medians (interquartile ranges, IQR) and were compared by the Mann-Whitney *U* test or the Kruskal-Wallis test. Categorical variables were presented as absolute numbers or percentages and were analyzed using the χ^2 test or Fisher's exact test. To take into account the repeated nature of the variables, analysis of variance (ANOVA) for repeated measurements of the general linear model was implemented. Pearson's test was used to analyze the correlation between two variables. To determine the risk factors associated with AGI grade II and above, we performed a series of several univariate logistic regression analyses using the above-mentioned variables. Variables with $P < 0.1$ in univariate analyses were tested in further multivariate logistic regression analyses. Receiver operating characteristic (ROC) curves were used to evaluate the associations between AGI and MODS, septic shock, and 28-d mortality. Survival curves for up to 28 d after admission and 60 d from disease onset were generated using the Kaplan–Meier method and were compared by the log-rank test. IBM Statistical Package for the Social Sciences (SPSS, version 22.0, NY, United States) software was used for statistical analysis, and two-sided $P < 0.05$ was considered statistically significant. The statistical methods used in this study were reviewed by Liu Q, a biostatistician from the Center for Disease Control and Prevention of Jiangsu Province in China.

RESULTS

As shown in Figure 1, a total of 83 critically ill patients with confirmed COVID-19 were enrolled in this retrospective study. The median age was 70 (IQR, 60-79) years, and most patients were male 59 (71.1%). Fever (33/83, 39.8%) and cough (18/83, 21.7%) were the main initial symptoms. Seventy-two (86.7%) patients had AGI during hospital stay, of them, 30 had AGI grade I, 35 had AGI grade II, 5 had AGI grade III, and 2 had AGI grade IV. The incidence of AGI grade II and above was 50.6% (42/83). The detailed clinical data of the patients are presented in Table 1. Forty (48.2%) patients died within 28 d of admission, their median hospital stay was 12.0 (IQR, 8.0-17.8) d, ranging from 3 d to 27 d. The median duration from disease onset to death was 22.0 (IQR, 15.3-33.0) d, ranging from 8 d to 44 d. ARDS developed in most patients (77/83, 92.8%), and 5 patients received extracorporeal membrane oxygenation. MODS developed in 58 (69.9%) patients, and septic shock in 16 (19.3%) patients.

AGI grades and clinical variables

We divided the patients into four groups based on the AGI grades: No AGI ($n = 11$), AGI grade I ($n = 30$), AGI grade II ($n = 35$), and AGI grade III to IV ($n = 7$). As shown in Table 2, significant differences in APACHEII scores, SOFA scores, WBC counts, and D-dimer levels were found among the four groups ($P < 0.05$). Statistical differences in CRP ($P = 0.024$) and PCT ($P = 0.033$) were only found between group AGI grade I and grade III to IV. Significant differences in lactate levels were found between group no AGI and AGI grade II ($P = 0.027$) or grade III to IV ($P = 0.009$). Statistical differences in lymphocyte counts were found between group no AGI and AGI grade I ($P = 0.028$) or grade II ($P = 0.007$). No differences in BMI were found among the four groups ($P > 0.05$).

Patients without AGI had longer hospital stay than those with AGI grade I ($P = 0.002$), II ($P = 0.022$), and III to IV ($P = 0.012$). Patients with AGI grade III to IV had longer days of MV and CRRT than those without AGI ($P = 0.011$, 0.013) and with AGI grade I ($P = 0.009$, 0.007). No differences in days from onset to admission were found among the four groups ($P > 0.05$).

Correlation analysis showed that the AGI grades were positively correlated with MV days ($r = 0.377$, $P < 0.001$), APACHEII ($r = 0.590$, $P < 0.001$) and SOFA scores ($r = 0.662$, $P < 0.001$), WBC counts ($r = 0.433$, $P < 0.001$), CRP ($r = 0.261$, $P = 0.017$) and D-dimer levels ($r = 0.425$, $P < 0.001$).

AGI grades and clinical outcomes

As shown in Table 2, patients with AGI grade III to IV had a higher incidence of septic shock than those without AGI ($P = 0.002$) and with AGI grade I ($P = 0.001$) and II ($P = 0.031$). Significant differences in 28-d mortality were found among the four groups ($P < 0.05$) except for group AGI grade I and II ($P = 0.540$). No differences in the incidence of MODS were found among the four groups ($P > 0.05$). Non-survivors were accompanied by a higher incidence of AGI grade III to IV than survivors (17.5% *vs* 0.0%, $P = 0.004$) (Table 3), whereas survivors had a higher incidence of no AGI than non-survivors (25.6% *vs* 0.0%, $P < 0.001$) (Table 3).

Table 1 Demographic data and clinical parameters

Variable	Value
Age (yr)	70 (60-79)
Sex (male: female)	59:24
Days from onset to admission	10 (7-15)
BMI (kg/m^2)	23.8 (22.1-25.1)
APACHEII scores	14.0 (12.0-17.0)
SOFA scores	6.0 (4.0-7.0)
Initial symptoms or signs, *n* (%)	
Fever	33 (39.8)
Cough	18 (21.7)
Chest tightness or pain	8 (9.6)
Dyspnea	7 (8.4)
Fatigue	6 (7.2)
Diarrhea	3 (3.6)
Nausea or vomiting	3 (3.6)
Pharyngalgia/myalgia	3 (3.6)
Abdominal pain	2 (2.4)
Laboratory parameters	
CRP (mg/L)	85.9 (49.9-136.0)
WBC (10^9/L)	10.30 (7.44-14.0)
Lymphocyte (10^9/L)	0.60 (0.43-0.83)
PCT (ng/mL)	0.27 (0.14-0.50)
D-dimer (μg/mL)	8.29 (2.00-14.19)
Lactate (mmol/L)	2.22 (1.68-2.73)
Organ injury, *n* (%)	
ARDS	77 (92.8)
Liver injury	15 (18.1)
AKI	30 (36.1)
Cardiac injury	37 (44.6)
MODS, *n* (%)	58 (69.9)
Septic shock, *n* (%)	16 (19.3)
Duration of MV (d)	9.0 (6.0-13.0)
Duration of CRRT (d)	0.0 (0.0-5.0)
Hospital stay (d)	18.0 (11.0-29.0)
Death, *n* (%)	40 (48.2)

BMI: Body mass index; APACHEII: Acute physiology and chronic health evaluation II; SOFA: Sequential organ failure assessment; CRP: C-reactive protein; WBC: White blood cell; PCT: Procalcitonin; ARDS: Acute respiratory distress syndrome; AKI: Acute kidney injury; MODS: Multiple organ dysfunction syndrome; MV: Mechanical ventilation; CRRT: Continuous renal replacement therapy.

To determine the risk factors associated with AGI grade II and above, univariate logistic regression was performed using the above-mentioned variables (sex, age, days from onset to admission, BMI, APACHEII scores, SOFA scores, CRP, D-dimer, WBC counts, lymphocyte counts, PCT, blood lactate, MV days, CRRT days, and hospital stay). Variables with $P < 0.1$ in univariate analyses were tested in further multivariate

Table 2 Acute gastrointestinal injury grades and clinical variables

Variables	No AGI (*n* = 11)	AGI I (*n* = 30)	AGI II (*n* = 35)	AGI III-IV (*n* = 7)	*P* value
BMI (kg/m^2)	23.9 (22.5-24.9)	23.8 (21.5-26.1)	23.8 (22.1-24.9)	22.4 (21.6-23.1)	0.426
APACHEII scores	11.0 (9.0-12.0)	13.0 (10.0-14.3)	15.0 (13.0-18.0)	18.0 (16.0-21.0)	< 0.001
SOFA scores	3.0 (3.0-4.0)	5.0 (4.0-6.0)	6.0 (5.0-9.0)	10.0 (7.0-12.0)	< 0.001
CRP (mg/L)	82.7 (46.1-136.0)	72.3 (47.3-113.2)	99.8 (54.6-145.2)	130.4 (87.3-221.0)	0.155
WBC (10^9/L)	7.9 (6.4-11.3)	8.7 (7.2-11.8)	11.9 (8.1-15.1)	16.6 (12.9-25.5)	0.001
Lymphocyte (10^9/L)	0.85 (0.62-1.12)	0.66 (0.43-0.82)	0.51 (0.38-0.76)	0.59 (0.37-0.85)	0.044
PCT (ng/mL)	0.17 (0.08-0.49)	0.19 (0.13-0.41)	0.29 (0.16-0.50)	0.41 (0.31-0.97)	0.079
D-dimer (μg/mL)	2.65 (0.97-7.06)	4.60 (1.72-12.30)	11.90 (4.64-22.00)	15.51 (3.76-22.00)	0.001
Lactate (mmol/L)	1.17 (1.09-1.88)	2.09 (1.68-2.44)	2.25 (1.94-2.99)	2.55 (1.92-3.84)	0.038
MV days	6.0 (4.0-11.0)	7.0 (5.8-10.5)	10.0 (6.0-14.0)	14.0 (11.0-19.0)	0.029
CRRT days	0.0 (0.0-4.0)	0.0 (0.0-3.0)	0.0 (0.0-7.0)	6.0 (5.0-8.0)	0.045
Days from onset to admission	10.0 (7.0-15.0)	10.0 (6.0-14.3)	10.0 (7.0-15.0)	15.0 (10.0-21.0)	0.263
Hospital stay (d)	30.0 (28.0-34.0)	13.5 (9.0-24.0)	18.0 (11.0-31.0)	19.0 (13.0-28.0)	0.020
MODS, *n* (%)	6 (54.5)	18 (60.0)	27 (77.1)	7 (100.0)	0.089
Septic shock, *n* (%)	0 (0)	2 (6.7)	9 (25.7)	5 (71.4)	0.001
Death, *n* (%)	0 (0)	14 (46.7)	19 (54.3)	7 (100.0)	0.037

AGI: Acute gastrointestinal injury; BMI: Body mass index; APACHEII: Acute physiology and chronic health evaluation II; SOFA: Sequential organ failure assessment; CRP: C-reactive protein; WBC: White blood cell; PCT: Procalcitonin; ARDS: Acute respiratory distress syndrome; AKI: Acute kidney injury; MV: Mechanical ventilation; CRRT: Continuous renal replacement therapy; MODS: Multiple organ dysfunction syndrome.

Table 3 The incidence of different acute gastrointestinal injury grades in non-survivors and survivors, *n* (%)

AGI grades	Non-survivors (*n* = 40)	Survivors (*n* = 43)	*P* value
No AGI	0 (0)	11 (25.6)	< 0.001
AGI I	14 (35.0)	16 (37.2)	0.834
AGI II	19 (47.5)	16 (37.2)	0.343
AGI III-IV	7 (17.5)	0 (0)	0.004

AGI: Acute gastrointestinal injury.

logistic regression analyses. As shown in Table 4, three variables (SOFA scores, WBC counts, MV days) were established as independent risk factors for the development of AGI grade II and above.

ROC curves were performed to evaluate the associations between AGI and clinical outcome variables. As shown in Figure 2, the area under the curves of MODS (Figure 2A), septic shock (Figure 2B), and 28-d mortality (Figure 2C) were 0.659 (P = 0.022), 0.793 (P < 0.001), and 0.716 (P = 0.001), respectively. Significant differences in 28-d mortality after admission (P = 0.002) and 60-day mortality after disease onset (P = 0.003) were found between group no AGI (n = 11) and AGI (n = 72). As shown in Figure 3, statistical differences in 28-d mortality (P = 0.037) (Figure 3A) and 60-d mortality (P = 0.049) (Figure 3B) were also found between group AGI grade I/no AGI (n = 41) and AGI grade II to IV (n = 42).

DISCUSSION

This retrospective study investigated the prevalence and outcomes of AGI in critically ill patients with COVID-19. 86.7% of the patients had AGI, and 50.6% had AGI grade II

Table 4 Independent factors associated with acute gastrointestinal injury grade II and above in multivariate logistic regression analysis

Variable	OR	95%CI	*P* value
SOFA scores	1.982	1.374-2.860	< 0.001
WBC counts	1.196	1.037-1.379	0.014
MV days	1.169	1.020-1.340	0.025

OR: Odds ratio; CI: Confidence interval; SOFA: Sequential organ failure assessment; WBC: White blood cell; MV: Mechanical ventilation.

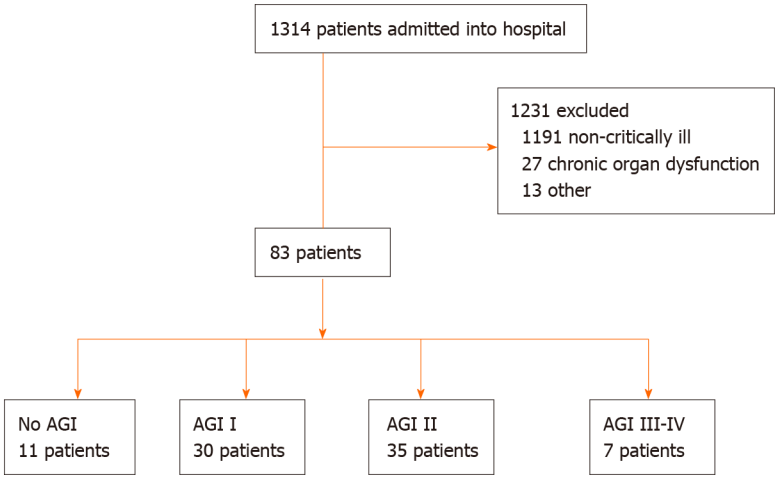

Figure 1 The flow diagram of participants. AGI: Acute gastrointestinal injury.

and above during hospital stay. We found that patients with worse AGI grades had worse clinical severity variables, a higher incidence of septic shock, higher 28-d mortality after admission and 60-d mortality after disease onset. SOFA scores, WBC counts, and duration of MV were risk factors for the development of AGI grade II and above. The 28-d mortality and incidence of MODS and septic shock in critically ill patients were 48.2%, 69.9%, and 19.3%, respectively. Non-survivors had a higher incidence of AGI grade III to IV than survivors.

Most of critically ill patients with COVID-19 had organ injury, including ARDS and AKI[9]. However, few studies on gastrointestinal injury have been reported in patients with COVID-19. Gastrointestinal dysfunction is common and closely related to adverse outcomes in critically ill patients[10,15-17]. In 2012, the Working Group on Abdominal Problems of the European Society of Intensive Care Medicine developed the definitions and a grading system for AGI in intensive care patients[10]. This expert opinion-based AGI grading system had been proven to be a predictor of all-cause mortality[16]. To our knowledge, this is the first study to investigate AGI in critically ill patients infected by SARS-CoV-2. Our results showed that the incidence of AGI was very high in critically ill patients with COVID-19. AGI was also correlated with clinical severity and outcomes of this novel disease. A recent meta-analysis showed that the incidence of AGI was about 40% and mortality was 33% in critically ill patients[15]. The corresponding data in this study were higher than those in previous reports. This indicated that SARS-CoV-2 was also very virulent in the gastrointestinal tract. However, the underlying mechanisms of SARS-CoV-2 causing organ dysfunction are unknown.

Gastrointestinal injury is often caused by an inflammatory reaction, infection or sepsis, severe trauma, shock, pancreatitis, and other critical diseases[10,15,16]. The receptor for SARS-CoV, which is angiotensin-converting enzyme 2 (ACE2) has also been suggested to be the receptor for SARS-CoV-2[18]. ACE2 is expressed in endothelial cells and smooth muscle cells of almost all organs, especially in lung alveolar cells[18]. That is why COVID-19 patients are susceptible to ARDS and even MODS. Our findings also showed that the incidence of ARDS was very high (92.8%), and AGI grades were significantly positively correlated with MV days. Liang *et al*[19] reported that ACE2 is highly expressed in the small intestine, especially in proximal and distal enterocytes. ACE2 expression in epithelial cells is required for maintaining antimicrobial peptide

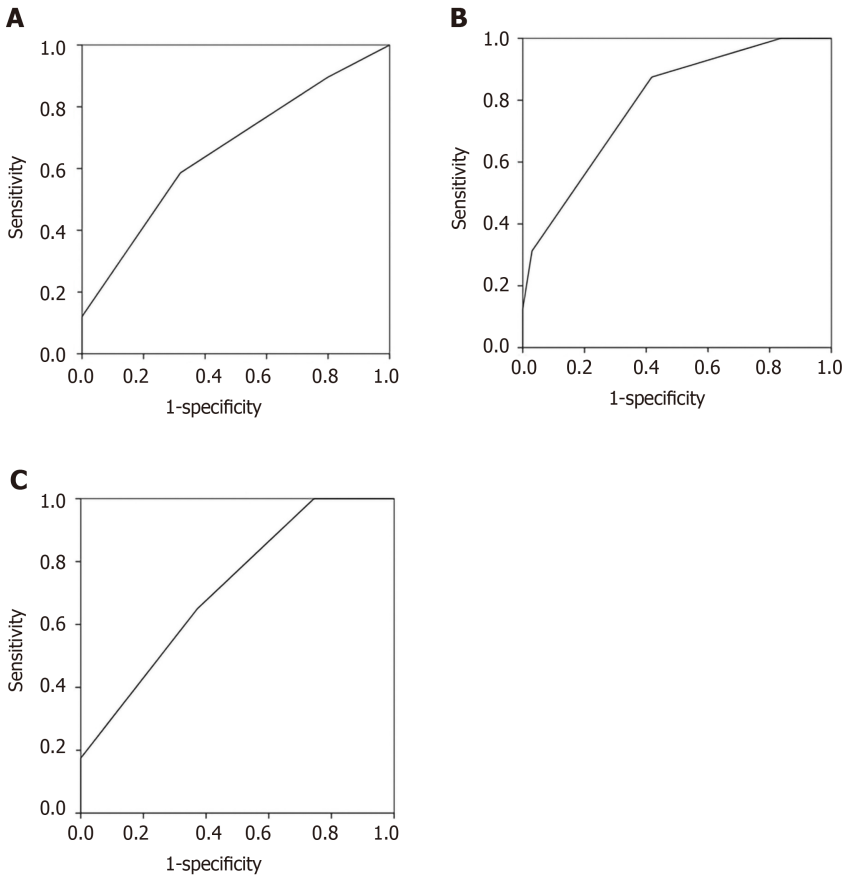

Figure 2 The areas under the receiver operating characteristic curves. A: Multiple organ dysfunction syndrome (0.659, P = 0.022); B: Septic shock (0.793, P < 0.001); C: 28-d mortality (0.716, P = 0.001).

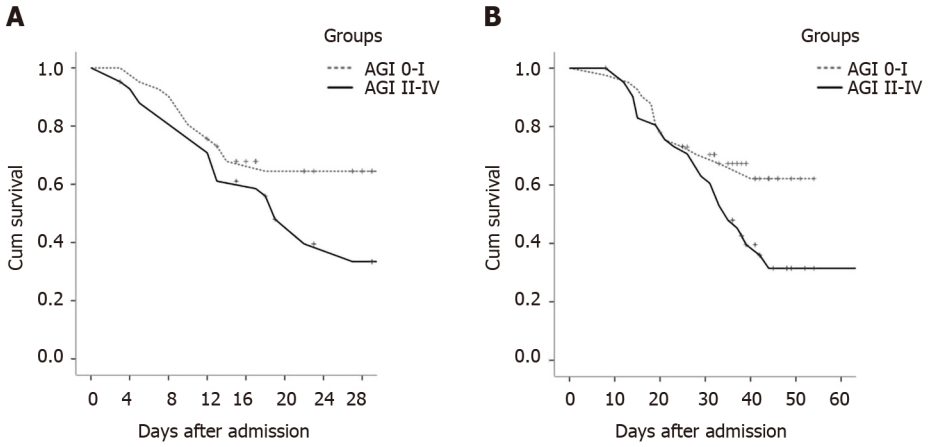

Figure 3 Cumulative survival. Significant differences in 28-d mortality after admission and 60-d mortality after disease onset were found between the group with acute gastrointestinal injury (AGI) grade I/no AGI (n = 41) and the group with acute gastrointestinal injury grade II to IV (n = 42). A: 28-d mortality after admission (P = 0.037); B: 60-d mortality after disease onset (P = 0.049). AGI: Acute gastrointestinal injury.

expression, amino acid homeostasis, and the ecology of gut microbiome in the intestine[20]. Therefore, gastrointestinal symptoms were also reported in previous studies on COVID-19[7,8]. We believe that these gastrointestinal symptoms were the early manifestations of AGI and should be taken seriously in clinical treatment.

In this study, we found that AGI grades were correlated with APACHEII and SOFA scores, WBC counts, CRP and D-dimer levels. Moreover, SOFA scores, WBC counts, and duration of MV were risk factors for the development of AGI grade II and above. These results indicated that patients with worse AGI grades had a more serious virus infection and severe inflammatory response, which may lead to a vicious circle

between systemic infection and intestinal barrier damage. D-dimer, a fibrin degradation product, is also considered to be associated with adverse outcomes in COVID-19 patients[21]. The abnormal elevation of D-dimer indicated microcirculation disturbance, including microthrombosis formation in intestinal mucosa[21]. During our clinical work against the epidemic of COVID-19 in Wuhan, we observed that gastrointestinal hemorrhage developed in several severe patients. We speculated that stress ulcer and intestinal microcirculation disturbance may be causes of the disorder.

Yang *et al*[9] reported that ARDS developed in 67%, AKI in 29%, cardiac injury in 23%, and liver dysfunction in 29% of critically ill patients with SARS-CoV-2 pneumonia. The study by Zhou *et al*[21] showed that septic shock developed in 20%, ARDS in 31%, AKI in 15%, and cardiac injury in 17% of the total number of patients with COVID-19. Our results showed that ARDS developed in 92.8%, AKI in 36.1%, cardiac injury in 44.6%, and liver injury in 18.1% of critically ill patients with COVID-19. The incidence of organ injury in this study was higher than that in previous studies, which may suggest that patients with AGI have worse clinical outcomes. The high incidence of MODS (69.9%) and hospital mortality (48.2%) in critically ill patients in this study also confirmed this conclusion. Moreover, we found that hospital duration in patients without AGI was significantly longer than that in patients with AGI. This could be explained by the high 28-d mortality in patients with AGI, as the median hospital stay of non-survivors was only 12.0 (IQR, 8.0-17.8) days, ranging from 3 d to 27 d.

This study had some limitations. Due to the single-center retrospective design and small sample size, the results might be inconclusive, and the accuracy should be confirmed by large-scale clinical prospective studies. Moreover, because the study was not based on pathophysiological models, the results were hypothesis generating, the exact mechanisms of AGI in COVID-19 should be tested by more basic experiments. In addition, patients were sometimes transferred to our hospital late in their illness. Lack of effective antivirals and inadequate adherence to standard supportive therapy may have contributed to the poor clinical outcomes in some patients.

CONCLUSION

To our knowledge, this is the first study to investigate AGI in critically ill patients with COVID-19. The incidence of AGI was 86.7%, and hospital mortality was 48.2% in critically ill patients. SOFA scores, WBC counts, and duration of MV were risk factors for the development of AGI grade II and above. Patients with worse AGI grades had worse clinical severity variables, a higher incidence of septic shock, and higher hospital mortality.

ARTICLE HIGHLIGHTS

Research background

Few studies on acute gastrointestinal injury have been reported in critically ill patients with coronavirus disease 2019 (COVID-19).

Research motivation

This was the first study to investigate acute gastrointestinal injury (AGI) in critically ill patients with COVID-19.

Research objectives

To investigate the prevalence and outcomes of AGI in critically ill patients with COVID-19.

Research methods

In this retrospective study, the primary endpoints were the incidence of AGI and 28-d mortality.

Research results

The incidence of AGI was 86.7%, and hospital mortality was 48.2% in critically ill patients. Sequential organ failure assessment scores, white blood cell (WBC) counts, and duration of mechanical ventilation were risk factors for the development of AGI

grade II and above.

Research conclusions

Patients with worse AGI grades had worse clinical severity variables, a higher incidence of septic shock, and higher hospital mortality.

Research perspectives

To our knowledge, this is the first study to investigate AGI in critically ill patients with COVID-19. The incidence of AGI was 86.7%, and hospital mortality was 48.2% in critically ill patients. Sequential organ failure assessment scores, WBC counts, and duration of mechanical ventilation were risk factors for the development of AGI grade II and above. Patients with worse AGI grades had worse clinical severity variables, a higher incidence of septic shock, and higher hospital mortality.

ACKNOWLEDGEMENTS

The authors thank Liu Q for her assistance in the statistical analysis of this study. The authors also thank Li H, Zou J, Dong K, and Jin CC of Tongji Hospital for their contributions to this study. In addition, Sun JK and his family especially thank Sun XP for her meticulous care and support during the past ten years.

REFERENCES

1 **Zhu N**, Zhang D, Wang W, Li X, Yang B, Song J, Zhao X, Huang B, Shi W, Lu R, Niu P, Zhan F, Ma X, Wang D, Xu W, Wu G, Gao GF, Tan W; China Novel Coronavirus Investigating and Research Team. A Novel Coronavirus from Patients with Pneumonia in China, 2019. *N Engl J Med* 2020; **382**: 727-733 [PMID: 31978945 DOI: 10.1056/NEJMoa2001017]

2 **Wang D**, Hu B, Hu C, Zhu F, Liu X, Zhang J, Wang B, Xiang H, Cheng Z, Xiong Y, Zhao Y, Li Y, Wang X, Peng Z. Clinical Characteristics of 138 Hospitalized Patients With 2019 Novel Coronavirus-Infected Pneumonia in Wuhan, China. *JAMA* 2020; **323**: 1061-1069 [PMID: 32031570 DOI: 10.1001/jama.2020.1585]

3 **Li Q**, Guan X, Wu P, Wang X, Zhou L, Tong Y, Ren R, Leung KSM, Lau EHY, Wong JY, Xing X, Xiang N, Wu Y, Li C, Chen Q, Li D, Liu T, Zhao J, Liu M, Tu W, Chen C, Jin L, Yang R, Wang Q, Zhou S, Wang R, Liu H, Luo Y, Liu Y, Shao G, Li H, Tao Z, Yang Y, Deng Z, Liu B, Ma Z, Zhang Y, Shi G, Lam TTY, Wu JT, Gao GF, Cowling BJ, Yang B, Leung GM, Feng Z. Early Transmission Dynamics in Wuhan, China, of Novel Coronavirus-Infected Pneumonia. *N Engl J Med* 2020; **382**: 1199-1207 [PMID: 31995857 DOI: 10.1056/NEJMoa2001316]

4 **World Health Organization**. Coronavirus disease (COVID-19) outbreak. Available from: URL: https://www.who.int

5 National Health Commission of the People's Republic of China home page. Available from: URL: http://www.nhc.gov.cn

6 **Xu XW**, Wu XX, Jiang XG, Xu KJ, Ying LJ, Ma CL, Li SB, Wang HY, Zhang S, Gao HN, Sheng JF, Cai HL, Qiu YQ, Li LJ. Clinical findings in a group of patients infected with the 2019 novel coronavirus (SARS-Cov-2) outside of Wuhan, China: retrospective case series. *BMJ* 2020; **368**: m606 [PMID: 32075786 DOI: 10.1136/bmj.m606]

7 **Guan WJ**, Ni ZY, Hu Y, Liang WH, Ou CQ, He JX, Liu L, Shan H, Lei CL, Hui DSC, Du B, Li LJ, Zeng G, Yuen KY, Chen RC, Tang CL, Wang T, Chen PY, Xiang J, Li SY, Wang JL, Liang ZJ, Peng YX, Wei L, Liu Y, Hu YH, Peng P, Wang JM, Liu JY, Chen Z, Li G, Zheng ZJ, Qiu SQ, Luo J, Ye CJ, Zhu SY, Zhong NS; China Medical Treatment Expert Group for Covid-19. Clinical Characteristics of Coronavirus Disease 2019 in China. *N Engl J Med* 2020; **382**: 1708-1720 [PMID: 32109013 DOI: 10.1056/NEJMoa2002032]

8 **Huang C**, Wang Y, Li X, Ren L, Zhao J, Hu Y, Zhang L, Fan G, Xu J, Gu X, Cheng Z, Yu T, Xia J, Wei Y, Wu W, Xie X, Yin W, Li H, Liu M, Xiao Y, Gao H, Guo L, Xie J, Wang G, Jiang R, Gao Z, Jin Q, Wang J, Cao B. Clinical features of patients infected with 2019 novel coronavirus in Wuhan, China. *Lancet* 2020; **395**: 497-506 [PMID: 31986264 DOI: 10.1016/S0140-6736(20)30183-5]

9 **Yang X**, Yu Y, Xu J, Shu H, Xia J, Liu H, Wu Y, Zhang L, Yu Z, Fang M, Yu T, Wang Y, Pan S, Zou X, Yuan S, Shang Y. Clinical course and outcomes of critically ill patients with SARS-CoV-2 pneumonia in Wuhan, China: a single-centered, retrospective, observational study. *Lancet Respir Med* 2020; **8**: 475-481 [PMID: 32105632 DOI: 10.1016/S2213-2600(20)30079-5]

10 **Reintam Blaser A**, Malbrain ML, Starkopf J, Fruhwald S, Jakob SM, De Waele J, Braun JP, Poeze M, Spies C. Gastrointestinal function in intensive care patients: terminology, definitions and management. Recommendations of the ESICM Working Group on Abdominal Problems. *Intensive Care Med* 2012; **38**: 384-394 [PMID: 22310869 DOI: 10.1007/s00134-011-2459-y]

11 **Rhodes A**, Evans LE, Alhazzani W, Levy MM, Antonelli M, Ferrer R, Kumar A, Sevransky JE, Sprung CL, Nunnally ME, Rochwerg B, Rubenfeld GD, Angus DC, Annane D, Beale RJ, Bellinghan GJ, Bernard GR, Chiche JD, Coopersmith C, De Backer DP, French CJ, Fujishima S, Gerlach H, Hidalgo JL, Hollenberg SM, Jones AE, Karnad DR, Kleinpell RM, Koh Y, Lisboa TC, Machado FR, Marini JJ, Marshall JC, Mazuski JE, McIntyre LA, McLean AS, Mehta S, Moreno RP, Myburgh J, Navalesi P, Nishida O, Osborn TM, Perner A,

Plunkett CM, Ranieri M, Schorr CA, Seckel MA, Seymour CW, Shieh L, Shukri KA, Simpson SQ, Singer M, Thompson BT, Townsend SR, Van der Poll T, Vincent JL, Wiersinga WJ, Zimmerman JL, Dellinger RP. Surviving Sepsis Campaign: International Guidelines for Management of Sepsis and Septic Shock: 2016. *Crit Care Med* 2017; **45**: 486-552 [PMID: 28098591 DOI: 10.1097/CCM.0000000000002255]

12 **ARDS Definition Task Force**, Ranieri VM, Rubenfeld GD, Thompson BT, Ferguson ND, Caldwell E, Fan E, Camporota L, Slutsky AS. Acute respiratory distress syndrome: the Berlin Definition. *JAMA* 2012; **307**: 2526-2533 [PMID: 22797452 DOI: 10.1001/jama.2012.5669]

13 **Ostermann M**, Bellomo R, Burdmann EA, Doi K, Endre ZH, Goldstein SL, Kane-Gill SL, Liu KD, Prowle JR, Shaw AD, Srisawat N, Cheung M, Jadoul M, Winkelmayer WC, Kellum JA; Conference Participants. Controversies in acute kidney injury: conclusions from a Kidney Disease: Improving Global Outcomes (KDIGO) Conference. *Kidney Int* 2020; **98**: 294-309 [PMID: 32709292 DOI: 10.1016/j.kint.2020.04.020]

14 **Kwo PY**, Cohen SM, Lim JK. ACG Clinical Guideline: Evaluation of Abnormal Liver Chemistries. *Am J Gastroenterol* 2017; **112**: 18-35 [PMID: 27995906 DOI: 10.1038/ajg.2016.517]

15 **Zhang D**, Li Y, Ding L, Fu Y, Dong X, Li H. Prevalence and outcome of acute gastrointestinal injury in critically ill patients: A systematic review and meta-analysis. *Medicine (Baltimore)* 2018; **97**: e12970 [PMID: 30412121 DOI: 10.1097/MD.0000000000012970]

16 **Hu B**, Sun R, Wu A, Ni Y, Liu J, Guo F, Ying L, Ge G, Ding A, Shi Y, Liu C, Xu L, Jiang R, Lu J, Lin R, Zhu Y, Wu W, Xie B. Severity of acute gastrointestinal injury grade is a predictor of all-cause mortality in critically ill patients: a multicenter, prospective, observational study. *Crit Care* 2017; **21**: 188 [PMID: 28709443 DOI: 10.1186/s13054-017-1780-4]

17 **Li H**, Zhang D, Wang Y, Zhao S. Association between acute gastrointestinal injury grading system and disease severity and prognosis in critically ill patients: A multicenter, prospective, observational study in China. *J Crit Care* 2016; **36**: 24-28 [PMID: 27546743 DOI: 10.1016/j.jcrc.2016.05.001]

18 **Chan JF**, Kok KH, Zhu Z, Chu H, To KK, Yuan S, Yuen KY. Genomic characterization of the 2019 novel human-pathogenic coronavirus isolated from a patient with atypical pneumonia after visiting Wuhan. *Emerg Microbes Infect* 2020; **9**: 221-236 [PMID: 31987001 DOI: 10.1080/22221751.2020.1719902]

19 **Liang W**, Feng Z, Rao S, Xiao C, Xue X, Lin Z, Zhang Q, Qi W. Diarrhoea may be underestimated: a missing link in 2019 novel coronavirus. *Gut* 2020; **69**: 1141-1143 [PMID: 32102928 DOI: 10.1136/gutjnl-2020-320832]

20 **Hashimoto T**, Perlot T, Rehman A, Trichereau J, Ishiguro H, Paolino M, Sigl V, Hanada T, Hanada R, Lipinski S, Wild B, Camargo SM, Singer D, Richter A, Kuba K, Fukamizu A, Schreiber S, Clevers H, Verrey F, Rosenstiel P, Penninger JM. ACE2 Links amino acid malnutrition to microbial ecology and intestinal inflammation. *Nature* 2012; **487**: 477-481 [PMID: 22837003 DOI: 10.1038/nature11228]

21 **Zhou F**, Yu T, Du R, Fan G, Liu Y, Liu Z, Xiang J, Wang Y, Song B, Gu X, Guan L, Wei Y, Li H, Wu X, Xu J, Tu S, Zhang Y, Chen H, Cao B. Clinical course and risk factors for mortality of adult inpatients with COVID-19 in Wuhan, China: a retrospective cohort study. *Lancet* 2020; **395**: 1054-1062 [PMID: 32171076 DOI: 10.1016/S0140-6736(20)30566-3]

World Journal of Gastroenterology

Submit a Manuscript: https://www.f6publishing.com

World J Gastroenterol 2020 October 21; 26(39): 6098-6110

DOI: 10.3748/wjg.v26.i39.6098

ISSN 1007-9327 (print) ISSN 2219-2840 (online)

ORIGINAL ARTICLE

Randomized Controlled Trial

Impact of cap-assisted colonoscopy during transendoscopic enteral tubing: A randomized controlled trial

Quan Wen, Kang-Jian Liu, Bo-Ta Cui, Pan Li, Xia Wu, Min Zhong, Lu Wei, Hua Tu, Yu Yuan, Da Lin, Wen-Hung Hsu, Deng-Chyang Wu, Hong Yin, Fa-Ming Zhang

ORCID number: Quan Wen 0000-0001-5178-3226; Kang-Jian Liu 0000-0001-7205-0013; Bo-Ta Cui 0000-0002-9238-7788; Pan Li 0000-0002-4383-8191; Xia Wu 0000-0002-0959-308X; Min Zhong 0000-0002-4560-5324; Lu Wei 0000-0003-4529-8157; Hua Tu 0000-0003-3013-8855; Yu Yuan 0000-0002-9536-3167; Da Lin 0000-0003-3758-3628; Wen-Hung Hsu 0000-0002-9539-5281; Deng-Chyang Wu 0000-0003-3742-0634; Hong Yin 0000-0002-5266-9385; Fa-Ming Zhang 0000-0003-4157-1144.

Author contributions: Wen Q and Liu KJ equally contributed to this work; Zhang FM contributed to the design of the research; Wen Q, Liu KJ, Cui BT, Li P, Wu X, Zhong M, Wei L, Tu H, Yuan Y, Lin D, Hsu WH, Wu DC, Yin H, and Zhang FM performed the research; Wen Q and Liu KJ analyzed the data; Wen Q drafted the manuscript; All authors read and approved the final manuscript.

Supported by the public donated Intestine Initiative Foundation; Jiangsu Province Creation Team and Leading Talents Project; National Natural Science Foundation of China, No. 81670495, No. 81600417; and Top-notch Talent Research Projects, No. LGY2017080.

Quan Wen, Kang-Jian Liu, Bo-Ta Cui, Pan Li, Xia Wu, Min Zhong, Lu Wei, Fa-Ming Zhang, Medical Center for Digestive Diseases, The Second Affiliated Hospital of Nanjing Medical University, Nanjing 210011, Jiangsu Province, China

Hua Tu, Department of Spleen and Stomach Diseases, Hubei Provincial Hospital of Traditional Chinese Medicine, Wuhan 430061, Hubei Province, China

Yu Yuan, Da Lin, Department of Gastroenterology, The First Affiliated Hospital of Guangdong Pharmaceutical University, Guangzhou 510080, Guangdong Province, China

Wen-Hung Hsu, Deng-Chyang Wu, Division of Gastroenterology, Department of Internal Medicine, Kaohsiung Medical University Hospital, Kaohsiung 807, Taiwan

Hong Yin, Department of Gastroenterology, Zigong Fourth People's Hospital, Zigong 643000, Sichuan Province, China

Corresponding author: Fa-Ming Zhang, MD, PhD, Doctor, Professor, Medical Center for Digestive Diseases, The Second Affiliated Hospital of Nanjing Medical University, No. 121 Jiangjiayuan, Nanjing 210011, Jiangsu Province, China. fzhang@njmu.edu.cn

Abstract

BACKGROUND

Colonic transendoscopic enteral tubing (TET) requires double cecal intubation, raising a common concern of how to save cecal intubation time and make the tube stable. We hypothesized that cap-assisted colonoscopy (CC) might reduce the second cecal intubation time and bring potential benefits during the TET procedure.

AIM

To investigate if CC can decrease the second cecal intubation time compared with regular colonoscopy (RC).

METHODS

This prospective multicenter, randomized controlled trial was performed at four centers. Subjects ≥ 7 years needing colonic TET were recruited from August 2018 to January 2020. All subjects were randomly assigned to two groups. The primary outcome was the second cecal intubation time. Secondary outcomes included

Institutional review board statement: The study was reviewed and approved by the Second Affiliated Hospital of Nanjing Medical University Institutional Review Board on October 10, 2017, and subsequently by all the other participating centers.

Clinical trial registration statement: This study is registered at ClinicalTrials.gov. The registration identification number is NCT03621033.

Informed consent statement: All study participants, or their legal guardians, provided informed written consent prior to study enrollment.

Conflict-of-interest statement: Zhang FM conceived the concept of transendoscopic enteral tubing and the related device. Other authors declare that they have no competing interests.

Data sharing statement: No additional data are available.

CONSORT 2010 statement: We have read the CONSORT 2010 Statement, and the manuscript was prepared and revised according to the CONSORT 2010 Statement.

Manuscript source: Unsolicited manuscript

Received: May 20, 2020
Peer-review started: May 19, 2020
First decision: May 29, 2020

success rate, insertion pain score, single clip fixation time, purpose and retention time of TET tube, length of TET tube inserted into the colon, and all procedure-related (serious) adverse events.

RESULTS

A total of 331 subjects were randomized to the RC (n = 165) or CC (n = 166) group. The median time of the second cecal intubation was significantly shorter for CC than RC (2.2 min *vs* 2.8 min, $P < 0.001$). In patients with constipation, the median time of second cecal intubation in the CC group (n = 50) was shorter than that in the RC group (n = 43) (2.6 min *vs* 3.8 min, $P = 0.004$). However, no difference was observed in the CC (n = 42) and RC (n = 46) groups of ulcerative colitis patients (2.0 min *vs* 2.5 min, $P = 0.152$). The insertion pain score during the procedure in CC (n = 14) was lower than that in RC (n = 19) in unsedated colonoscopy (3.8 ± 1.7 *vs* 5.4 ± 1.9; $P = 0.015$). Multivariate analysis revealed that only CC (odds ratio [OR]: 2.250, 95% confidence interval [CI]: 1.161-4.360; $P = 0.016$) was an independent factor affecting the second cecal intubation time in difficult colonoscopy. CC did not affect the colonic TET tube's retention time and length of the tube inserted into the colon. Moreover, multivariate analysis found that only endoscopic clip number (OR: 2.201, 95%CI: 1.541-3.143; $P < 0.001$) was an independent factor affecting the retention time. Multiple regression analysis showed that height (OR: 1.144, 95%CI: 1.027-1.275; $P = 0.014$) was the only independent factor influencing the length of TET tube inserted into the colon in adults.

CONCLUSION

CC for colonic TET procedure is a safe and less painful technique, which can reduce cecal intubation time.

Key Words: Transendoscopic enteral tube; Endoscopy; Colonoscopy; Fecal microbiota transplant; Washed microbiota transplant; Colon

Core Tip: The design of colonic transendoscopic enteral tubing (TET) requires repeated colonoscopies, which increase procedure time and potential procedure-related risk. This multicenter, prospective, randomized controlled trial explored whether cap-assisted colonoscopy (CC) can decrease the second cecal intubation time and has potential benefits compared with regular colonoscopy during the TET procedure. Our findings show that CC can decrease the second cecal intubation time during the TET procedure, especially for difficult colonoscopy. Moreover, CC for colonic TET can reduce the insertion pain score in unsedated colonoscopy and does not affect the safety and stability of the TET tube.

Citation: Wen Q, Liu KJ, Cui BT, Li P, Wu X, Zhong M, Wei L, Tu H, Yuan Y, Lin D, Hsu WH, Wu DC, Yin H, Zhang FM. Impact of cap-assisted colonoscopy during transendoscopic enteral tubing: A randomized controlled trial. *World J Gastroenterol* 2020; 26(39): 6098-6110
URL: https://www.wjgnet.com/1007-9327/full/v26/i39/6098.htm
DOI: https://dx.doi.org/10.3748/wjg.v26.i39.6098

INTRODUCTION

Fecal microbiota transplantation (FMT) as a promising novel therapeutic approach has shown superior effectiveness in many microbiota-related diseases such as *Clostridium difficile* infection (CDI) and inflammatory bowel disease (IBD)[1-4]. As reported in most studies, multiple fecal infusions are often necessary to obtain a higher remission rate. Ianiro *et al*[5] proved that multiple infusions of FMT were significantly more effective than a single infusion in curing severe refractory CDI *via* colonoscopy. Several randomized controlled trials have also confirmed the outstanding benefit of FMT in

Revised: June 2, 2020
Accepted: September 1, 2020
Article in press: September 1, 2020
Published online: October 21, 2020

P-Reviewer: Lohsiriwat V
S-Editor: Zhang H
L-Editor: Filipodia
P-Editor: Wang LL

treating ulcerative colitis (UC) using the protocol of multiple fecal infusions by colonoscopy or enema[6,7]. Furthermore, previous studies have suggested that FMT *via* lower gut delivery is more effective than upper gut delivery[8,9]. The higher efficacy of FMT in CDI treatment *via* colonoscopy than duodenal delivery has also been proven by a meta-analysis[10]. However, delivering multiple FMTs by colonoscopy needs repeated bowel preparation over a short period of time, and it is challenging to retain the infused fecal suspensions on account of the residual effect of laxatives. Importantly, we have to consider the higher risk of complications in severe colitis *via* repeated colonoscopies. Although enema can meet the needs of multiple FMT treatments, the bacteria can only cover the rectum and sigmoid colon, which limits the input bacteria volume and is not suitable for patients who have difficulty in retaining the bacterial fluid. Thus, since 2014, our team have been exploring the placement of a tube through the anus into the cecum, a method called colonic transendoscopic enteral tubing (TET), capable of meeting the needs of patients receiving multiple fresh FMT treatments or whole-colon administration of drugs during a period of time[11-13]. The TET device (FMT Medical, Nanjing, China) has been approved by the China Food and Drug Agency for endoscopic use since 2017. At present, the colonic TET as a sought-after technique has been successfully used in many hospitals in Asia[3,11,14-17]. Allegretti *et al*[18] commented in the Lancet review that colonic TET is a promising method of FMT delivery. Recently, the consensus on the methodology of washed microbiota transplantation released a statement that washed microbiota suspensions can be delivered *via* colonic TET[19].

We first reported a colonic endoscopic procedure for TET in 2016 that requires cecal intubation twice, the first inserting the TET tube through the endoscopic channel, and the second affixing the TET tube to the intestinal wall using clips[11]. Generally, it is easier to insert the colonoscope for the second time with the TET tube's guidance. However, for some patients, the intestinal lumen is difficult to find during the second insertion of colonoscope into the cecum because intestinal mucosa wrinkles and sharp corners could be caused by the TET tube pulling. This increases the difficulty of cecal intubation (Figure 1A). Thus, the TET technique raises a common concern on longer procedure time, increased medical cost and potential procedure-related risk. Cap-assisted colonoscopy (CC) is a well-known simple technique of attaching a transparent plastic cap to the tip of the colonoscope. In our early experience, we found that CC was beneficial to the decrease of cecal intubation time and difficulty of colonoscopy (Figure 1B). Cap method is a simple, practical, and inexpensive technique that serves several useful purposes in enhancing colonoscopy performance[20]. A Cochrane review indicated that CC had a faster cecal intubation time than the regular colonoscopy (RC)[21]. Reviewing studies individually would also seem to favor CC for cecal intubation rate and pain during the procedure[21]. Lee and colleagues found that CC shortened the cecal intubation time and performed better as a rescue method when the first attempt failed[22]. Kim *et al*[23] reported that CC had advantages in overcoming the problems associated with angulated and/or narrowed sigmoid and redundant colon. However, it is uncertain whether CC would facilitate the technical performance after the TET tube is inserted into the intestinal lumen during the TET procedure.

Therefore, this prospective randomized controlled trial compared CC with RC regarding second cecal intubation time among subjects undergoing colonic TET. We tested the hypothesis that CC might reduce the second cecal intubation time and bring potential benefits during the TET procedure.

MATERIALS AND METHODS

Subjects

This multicenter, prospective, subject-blinded, and randomized controlled trial was conducted at four tertiary hospitals from August 2018 to January 2020. The study protocol was approved by the Second Affiliated Hospital of Nanjing Medical University Institutional Review Board on October 10, 2017, and subsequently in all other participating centers. Written informed consent was obtained from all adult subjects or parents in pediatric cases. The study was registered at ClinicalTrials.gov (NCT03621033).

Inclusion criteria: Subjects aged ≥ 7 years who had suitability for endoscopy and needed colonic TET. Exclusion criteria were: (1) Severe bowel lesions with stenosis, fistula, or the risk of perforation; (2) Complex perianal lesions or serious lesions in the ileocecal junction or ascending colon; (3) No proper site for endoscopic clip fixation; (4) The distal of TET tube not placed in the cecum; (5) Use of the cap-assisted method in

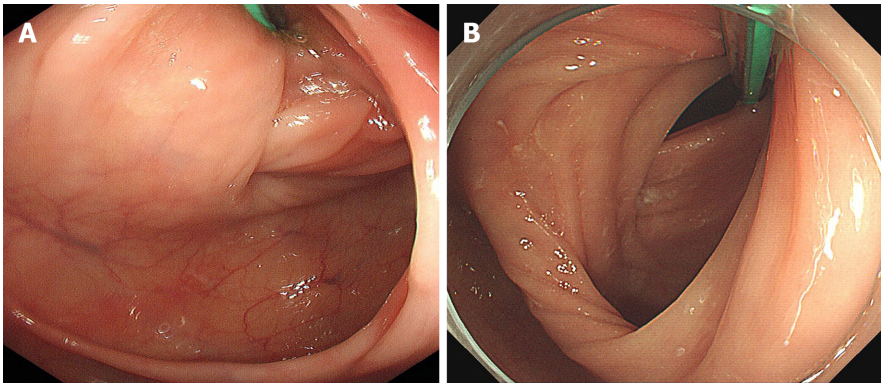

Figure 1 Procedure-related colonic transendoscopic enteral tubing. A: It is difficult to find the lumen after the tube is inserted in some subjects because of the gathering of colonic folds and acute angle of colonic lumen caused by the transendoscopic enteral tube pulling; B: Cap-assisted colonoscopy uses a transparent plastic cap attached to the tip of the colonoscope to flatten the semilunar folds and improve mucosal exposure.

the first insertion of colonoscope; (6) Changed endoscopists during colonoscopy; (7) Poor bowel preparation affecting cecal intubation; (8) Allergy to TET tube material; and (9) Being unable to give informed consent.

Randomization

Subjects were randomized (1:1) to CC and RC groups by computer-generated random numbers. Randomization was stratified by individual colonoscopists using permuted blocks of random sizes six. Each colonoscopist had his own set of randomization envelopes throughout the study at each center. The sealed opaque envelopes containing the codes were prepared by the clinical research coordinator who kept the randomization key under lock until the data collection was completed.

Subject blinding involved colonoscopists not informing the subjects of the methods and the equipment setup was the same for both groups. The endoscopic display screen was placed over the head of the subjects so they could not see the images. All data were collected by one investigator at each center who did not participate in data analysis.

All TET endoscopic procedures were performed by six colonoscopists with the experience of at least 500 colonoscopies and 10 colonic TET procedures before joining the study. All endoscopists were required to perform procedures with the same workflow.

Endoscopic procedure

The variable-stiffness colonoscope (CF-H260AI or CF-HQ290I; Olympus, Tokyo, Japan) was used. Some of the subjects received intravenous sedation with propofol and/or sufentanil and/or dezocine by anesthesiologists. Spasmolytic agents were not used before or during the procedure. The concept of colonic TET is to insert a tiny and soft tube into the deep colon and fix it onto the intestinal wall through the anus under endoscopy with endoscopic clips[11,24]. The endoscopic procedure of colonic TET was in accordance with our previous study[11,24].

During the first cecal intubation, when the scope reached the cecum, the TET tube (outer diameter of 2.7 mm and the inner diameter of 1.8 mm, FMT-DT-F-27/1350, FMT medical, Nanjing, China) was inserted into the endoscopic channel. Then, as the TET tube reached the cecum, the colonoscope was removed. For CC, before re-insertion of the colonoscope (the second cecal intubation), a transparent plastic cap (D-201-14304; Olympus) was attached to the tip of the colonoscope (diameter 15 mm). The edge of the cap protruded for approximately 4 mm beyond the tip of the colonoscope. For RC, the colonoscope was directly re-inserted until it reached the cecum. Then the disposable endoscopic clip (ROCC-D-26-195-C, 2.6 mm × 1950 mm; Nanjing Microtech Co., Ltd, Nanjing, China) was inserted through the endoscopic channel and the loop of the TET tube was fixed to the intestinal wall. The biopsy and polypectomy were performed after the TET procedure.

Data collection and outcome measurement

Baseline characteristics including age, sex, body mass index, previous abdominal or pelvic surgery, and disease category were collected before colonic TET. The diagnosis of constipation was based on Rome IV criteria[25]. The primary outcome was the second

cecal intubation time which was recorded from the beginning of the second insertion (after inserting the TET tube) to reaching the cecum. The secondary outcomes included TET success rate, maximum insertion pain score, single clip fixation time, purpose and retaining time of TET tube, length of TET tube inserted into the colon, and all procedure-related (serious) adverse events (AEs). The first cecal intubation time was also recorded (from the anus to cecum). The cecal intubation time, maximum pain score and other outcomes of TET were recorded by one investigator at each center who was not involved in colonoscopy. Successful colonic TET was defined as inserting the TET tube into the cecum and closing the last clip to fix the tube onto the intestinal wall. The maximum real-time insertion pain in subjects undergoing unsedated colonoscopy was evaluated by visual rating scale. The assistant explained the pain scores (degree of abdominal pain) to the subjects. At the second insertion phase, the subjects were asked by the assistant to report the pain score by using an 11-point visual analog scale (0 no pain and 10 most severe pain imaginable) at regular intervals. Clip fixation time was defined as the time of insertion of the first clip into the endoscopic channel to the last clip closed. The number of endoscopic clips used was also recorded. The purposes of TET tube insertion included microbiota transplantation treatment, administration of medications, and collection of intestinal fluid samples to analyze the dynamic changes of healthy human intestinal microbiome at the ileocecal interface. The friction between the cap and the TET tube may potentially affect the safety and reliability of the procedure of TET. Thus, the retaining time and the length of TET tube inserted into the colon were recorded. The retaining time of TET tube was defined as the time from the implantation of the TET tube to its falling out naturally. The length of TET tube inserted into the colon was defined as the length of the tube from the distal of TET tube (close to mouth direction) to the anus. AEs with a potential relation to colonic TET during and after TET were also investigated.

Statistical analysis

Sample size calculation was carried out using Stata software system (version 14.0; Stata Corp., College Station, TX, United States). We assumed that the time of the second cecal intubation is 3.5 min by regular colonoscopic tube placement based on our previous experience and can be accelerated 0.4 min by the cap-assisted method. To detect the difference with a significance level (a) of 0.05 and a power of 90% with a two-tailed test, we calculated that at least 132 subjects in each group were needed. Considering possible dropout rate of 10% (unsuccessful intubation and inspection due to technical difficulty), 146 subjects were planned to be enrolled in each group.

Quantitative data were summarized as mean ± standard deviation or median (interquartile range [IQR]), and categorical variables were reported as percentages. Differences in continuous variables between both arms were tested using the *t*-test or Mann–Whitney nonparametric test, depending on which assumption was met. Categorical variables were analyzed using the χ^2 test or Fisher's exact test. The Kruskal-Wallis test was used to compare the relationship between the number of endoscopic clips and retention time of TET tube. Subjects were divided into two groups according to the median of the first cecal intubation time, and those with longer time than the median were defined as difficult colonoscopy. Univariate and multivariate logistic regression analyses were performed, and multivariate analysis was done using variables with P value < 0.20 in the univariate analysis. Analyses were performed with the SPSS software V.25.0 (IBM Corp., Armonk, NY, United States). A two-tailed P value < 0.05 was considered statistically significant.

RESULTS

Enrollment and baseline characteristics

Between August 2018 and January 2020, 413 subjects referred to the four centers were considered for enrollment, with a total of 82 subjects excluded. Four subjects switched to the cap method successfully achieved cecal intubation. The tubes of six subjects were fixed at the terminal ileum for enteral administration, including two Crohn's disease (CD) patients with terminal ileum lesions (RC *vs* CC, 0 *vs* 2; P = 0.498) and four UC patients with extensive colitis (RC *vs* CC, 2 *vs* 2; P = 1.000), who had no proper site for endoscopic clip fixation. Moreover, the tubes were fixed at ascending colon or transverse colon in nine UC patients with left-side colitis for better coverage of intestinal lesions with medication (RC *vs* CC, 5 *vs* 4; P = 0.750). Finally, 152 subjects in the RC group and 151 in the CC group underwent analysis. The study flow is detailed in Figure 2. Baseline characteristics were well balanced between the two groups as

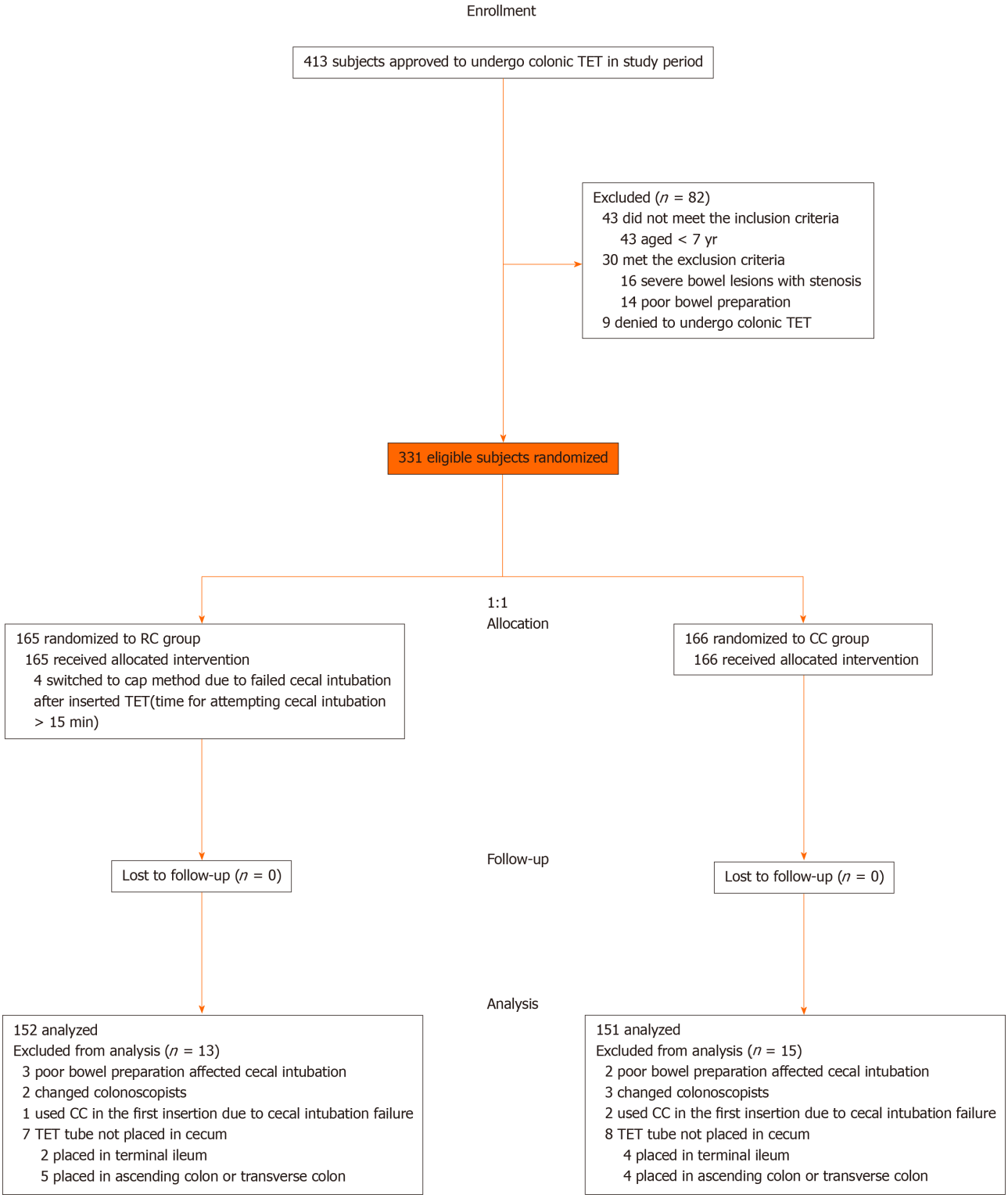

Figure 2 Study flowchart. TET: Transendoscopic enteral tubing; CC: Cap-assisted colonoscopy; RC: Regular colonoscopy.

shown in Table 1.

Procedure-related outcomes

The study outcomes related to TET procedure are summarized in Table 2. The median second cecal intubation time in RC and CC groups was 2.8 (1.8-4.0) and 2.2 (1.6-3.2) min, respectively ($P < 0.001$). A subgroup analysis was done in the constipation patients, and the median time of the second cecal intubation in RC ($n = 43$) and CC ($n = 50$) groups was 3.8 (2.2-5.6) and 2.6 (1.9-3.7) min, respectively ($P = 0.004$). However, no statistical difference was observed in patients with UC, the median time of the second cecal intubation in RC ($n = 46$) and CC ($n = 42$) groups being 2.5 (1.6-3.5) and

Table 1 Baseline characteristics of the study subjects

	RC group, *n* = 152	CC group, *n* = 151	*P* value
Age in yr, mean ± SD	44.4 ± 17.6	46.7 ± 17.0	0.248
Children[1],*n* (%)	4 (2.6)	4 (2.6)	1.000
Male, *n* (%)	76 (50.0)	79 (52.3)	0.687
Body mass index in kg/m^2, mean ± SD	21.1 ± 3.8	21.6 ± 3.3	0.243
Disease category, *n* (%)			
Ulcerative colitis	46 (30.3)	42 (27.8)	0.639
Constipation	43 (28.3)	50 (33.1)	0.363
Irritable bowel syndrome	14 (9.2)	18 (11.9)	0.443
Crohn's disease	6 (3.9)	3 (2.0)	0.501
Healthy volunteers	3 (2.0)	3 (2.0)	1.000
Others[2]	40 (26.3)	35 (23.2)	0.527
Previous surgery, abdominal or pelvic, *n* (%)	38 (25.0)	33 (21.9)	0.518

[1]Aged ≤ 15 years.
[2]Other disease categories include antibiotic-associated diarrhea, diabetes, Parkinson's disease, Tourette's syndrome, autism, epilepsy, cirrhosis, *etc*. RC: Regular colonoscopy; CC: Cap-assisted colonoscopy.

Table 2 Outcomes related to transendoscopic enteral tubing procedure

	RC group,*n* = 152	CC group,*n* = 151	*P* value
Cecal intubation rate after inserting TET tube, *n* (%) (%)	148 (97.4)	151 (100)	-
The first cecal intubation time in min, median (IQR)	5.9 (4.3-8.5)	6.2 (4.1-8.3)	0.921
The second cecal intubation time in min, median (IQR)	2.8 (1.8-4.0)	2.2 (1.6-3.2)	0.000
The second cecal intubation time of constipation patients	3.8 (2.2-5.6)	2.6 (1.9-3.7)	0.004
The second cecal intubation time of ulcerative colitis patients	2.5 (1.6-3.5)	2.0 (1.5-3.0)	0.152
Average fixation time per endoscopic clip in min, mean ± SD	1.1 ± 0.4	1.2 ± 0.6	0.238
Number of endoscopic clips, mean ± SD	2.7 ± 1.1	2.6 ± 1.1	0.339
Colonoscopy type, *n* (%)			
Sedated	133 (87.5)	137 (90.7)	0.367
Unsedated	19 (12.5)	14 (9.3)	0.367
Maximum pain score, mean ± SD	5.4 ± 1.9	3.8 ± 1.7	0.015
TET success rate, *n* (%)	152 (100)	151 (100)	-
Serious adverse event, *n* (%)	0	0	-
Adverse events, *n* (%)	4 (2.6)	5 (3.3)	0.750
Anal pain	2 (1.3)	1 (0.7)	1.000
Mild anal discomfort	1 (0.7)	3 (2.0)	0.371
Transient anal bleeding	1 (0.7)	1 (0.7)	1.000

TET: Transendoscopic enteral tubing; RC: Regular colonoscopy; CC: Cap-assisted colonoscopy; IQR: Interquartile range; SD: Standard deviation.

2.0 (1.5-3.0) min, respectively (P = 0.152).

In total, 296 (97.7%) subjects used TET for single or multiple microbiota transplantations, 75 (24.8%) for intracolonic medication administrations, and 6 (2.0%) healthy volunteers for sampling. After the treatment was completed, 85 subjects (28.1%) actively pulled out the TET tube. The TET tube spontaneously fell out in 218

subjects (71.9%), and the median retention time was 8.0 (6.0-10.0) d. We analyzed possible factors contributing to the retention time of TET tube. These subjects were divided into the short retention time group (< 8 d) and the long retention time group (≥ 8 d). As shown in Table 3, multivariate analysis showed that only endoscopic clip number (OR = 2.201, 95%CI: 1.541-3.143, P < 0.001) was an independent factor affecting the retention time.

The maximum retention time of the TET tube was 28 d. As shown in Figure 3, the retention time of 1 (n = 37), 2 (n = 74), 3 (n = 78), and 4 (n = 29) clips used by the TET was 6.0 (4.5-7.0) d, 7.0 (6.0-10.0) d, 8.0 (7.0-11.0) d, and 10.0 (7.0-11.5) d, respectively.

Factors associated with the second cecal intubation time in difficult colonoscopy

The median of the first cecal intubation time was 6.1 min. The median of the second cecal intubation time was 3.1 min in the subjects with difficult colonoscopy. The subjects were divided into the fast cecal intubation group (< 3.1 min) and the slow cecal intubation group (≥ 3.1 min). As shown in Table 4, according to multivariate analysis, only CC (OR = 2.250, 95%CI: 1.161-4.360; P = 0.016) was an independent factor affecting the second cecal intubation time in subjects with difficult colonoscopy.

Factors associated with the length of TET tube inserted into the colon

During the late stage of the current procedure, we recorded the length of the tube at the anus in 63 adult subjects (aged ≥ 18). The mean length of TET tube inserted into the colon was 85.9 ± 10.0 cm. As shown in Table 5, in multiple regression analysis, height (OR = 1.144, 95%CI: 1.027-1.275; P = 0.014) was the only independent factor influencing the length of TET tube inserted into the colon in adults.

Safety

There was no cap displacement during the TET procedure. No serious AE was observed during and after the procedure of TET in either group. Among all subjects with TET, merely 3.0% (9/303) complained of mild AEs as shown in Table 2. The anal pain in three cases was considered to be related to hemorrhoids. Four subjects reported abdominal discomfort during the TET tube retention period, and the abdominal discomfort disappeared after TET tube was removed.

DISCUSSION

In this randomized controlled study, we showed that CC shortened the second cecal intubation time during the TET procedure. Multiple studies have reported a significant decrease in cecal intubation time in CC compared with RC. The use of cap decreased the cecal intubation time by an average of 0.63 and 0.88 min, respectively, in two meta-analyses[26,27]. Among meta-analyses of randomized controlled trials, no study has shown a longer intubation time by the cap method[21]. Short cecal intubation time is vital for several reasons: Less anesthetic drug and sufficient withdrawal time for accurate examination and endoscopic treatment. A previous study reported that a longer cecal insertion time was associated with a decreased detection of adenomas and advanced adenomas[28]. Moreover, in the stratified subgroup analysis, the effect of cecal intubation time with a transparent cap was strong in the subgroups of constipation patients. However, the cap failed to show significant benefit in UC patients, probably because it is easier to cecal intubation due to chronic inflammation that results in the shortening of colon length, stiff colon and loss of haustral pattern. Most of the constipation patients with redundant colon, twisted colon, and mucosal prolapse receive typical difficult colonoscopy. As proven by multiple studies[22,23] the cap method showed significantly higher performance under challenging cases. Kim *et al*[23] found that CC helped shorten the cecal intubation time in difficult cases by an average of 1.43 min. An earlier study by Lee and colleagues also found that CC was effective as a back-up procedure in difficult cases[22]. Consistent with these previous results, we further demonstrated that CC was an independent factor affecting the insertion time in difficult cases during TET procedure. If the time of the endoscopy is prolonged during the procedure of TET, patients potentially have the risk of complications, including abdominal pain, respiratory depression, low oxygen saturation, hypotension, cardiac arrhythmia, aspiration, *etc*. Besides, rare serious complications related to barotraumas, such as mucosal tears, intestinal perforation and air embolism, might be observed[29]. Therefore, use of CC is recommended in TET procedure for difficult colonoscopy, except for UC patients, who may have more mucosal traumas, particularly in severe cases of colitis[30].

Table 3 Univariate and multivariate analyses of factors associated with the retention time of transendoscopic enteral tube < 8 d

	Univariate analysis		Multivariate analysis	
	OR (95%CI)	*P* value	OR (95%CI)	*P* value
Age in yr	1.008 (0.992-1.025)	0.343	-	-
Sex, male *vs* female	1.517 (0.804-2.862)	0.198	1.930 (0.966-3.858)	0.063
Disease type, IBD *vs* others	0.589 (0.339-1.025)	0.061	0.960 (0.499-1.846)	0.903
Number of endoscopic clips	2.137 (1.546-2.954)	0.000	2.201 (1.541-3.143)	0.000
Grouping, RC *vs* CC	0.775 (0.455-1.320)	0.348	-	-

IBD: Inflammatory bowel disease; RC: Regular colonoscopy; CC: Cap-assisted colonoscopy.

Table 4 Univariate and multivariate analyses of factors associated with the second cecal intubation time of < 3.1 min in difficult colonoscopy

	Univariate analysis		Multivariate analysis	
	OR (95%CI)	*P* value	OR (95%CI)	*P* value
Age in yr	1.002 (0.477-2.102)	0.996	-	-
Sex, male *vs* female	0.930 (0.487-1.774)	0.825	-	-
Body mass index, < 21 *vs* ≥ 21 kg/m^2	0.855 (0.452-1.616)	0.629	-	-
Previous surgery, abdominal or pelvic[1]	0.868 (0.414-1.822)	0.709	-	-
Colonoscopy, sedated *vs* unsedated	1.062 (0.406-2.781)	0.902	-	-
Constipation[1]	0.559 (0.291-1.073)	0.080	0.514 (0.263-1.005)	0.052
Grouping, RC *vs* CC	2.103 (1.101-4.017)	0.024	2.250 (1.161-4.360)	0.016

[1]Without *vs* with each factor. RC: Regular colonoscopy; CC: Cap-assisted colonoscopy.

Table 5 Univariate and multivariate analyses of factors associated with the length of transendoscopic enteral tube inserted into the colon ≥ 86 cm

	Univariate analysis		Multivariate analysis	
	OR (95%CI)	*P* value	OR (95%CI)	*P* value
Age in yr	0.996 (0.967-1.025)	0.774	-	-
Height, < 165 *vs* ≥ 165 cm)	9.750 (2.523-37.675)	0.001	1.144 (1.027-1.275)	0.014
Sex, male *vs* female	0.352 (0.117-1.062)	0.064	1.184 (0.246-5.693)	0.833
IBD[1]	1.161 (0.346-3.901)	0.809	-	-
Constipation[1]	1.212 (0.329-4.466)	0.773	-	-
Grouping, RC *vs* CC	1.895 (0.645-5.569)	0.245		

[1]Without *vs* with each factor. IBD: Inflammatory bowel disease; RC: Regular colonoscopy; CC: Cap-assisted colonoscopy.

Several studies have explored patient discomfort and pain undergoing CC among unsedated patients. Both Tada *et al*[31] and Lee *et al*[22] showed that there was no difference in patient discomfort between the CC and RC groups. However, a significantly reduced pain level in the colonoscopy with cap was proved by several studies[32-34]. No study has shown a higher degree of patient discomfort or pain with CC compared with RC. The finding is consistent with this study, which found that the pain score was lower in the CC group than the RC during the TET procedure. This might be attributed to two factors: The cap method may prevent looping and there is also less need for air insufflation because the cap provides a better visual field[33,34].

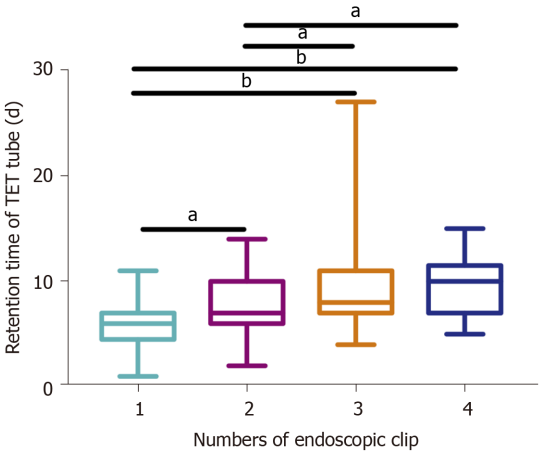

Figure 3 Relationship between the number of endoscopic clips and retention time of transendoscopic enteral tube. With the increased number of endoscopic clips, the retention time of transendoscopic enteral tube was prolonged ($P < 0.001$). After pairwise comparisons, subjects with four, three, or two clips had longer retention times than subjects with one titanium clip (4 *vs* 1, adjusted $P < 0.001$; 3 *vs* 1, adjusted $P < 0.001$; 2 *vs* 1, adjusted $P = 0.035$); and also, longer than patients with two clips (4 *vs* 2, adjusted $P = 0.011$; 3 *vs* 2, adjusted $P = 0.036$). But compared to three and four clips, there was no significant difference (adjusted $P = 1.000$). $^{a}P < 0.05$, $^{b}P < 0.001$. Data are presented as the median (range).

Our current study showed that CC had a higher cecal intubation rate than RC, though no significant difference was found. It echoes the findings by two meta-analyses[26,35]. Although it seems that colonoscopy using the cap method does not confer any significant benefit for cecal intubation, there is evidence to suggest that it may be a back-up procedure when RC fails to intubate the cecum. Lee and colleagues reported that CC achieved a higher rescue rate in cecal intubation compared with RC[22].

In our experience, the cap method may help to stabilize the colonoscope which may be useful to the procedure of fixing endoscopic clips. However, the results of this study suggested that there was no difference in the TET tube's single endoscopic clip fixation time between the two groups. This may be related to the fact that fecal matter may stick to the cap's interior, thus impeding the view and needing a longer time to be cleaned by water insufflation or simple flushing.

Our results confirmed that the transparent cap did not affect the retention time of the colonic TET tube. The retention time of the tube was significantly correlated with the endoscopic clip number. Our previous study reported that two to four endoscopic clips are recommended to ensure the fixation of the TET tube onto the colonic wall and maintain it for 7-11 d[24]. We increased the sample size in using one endoscopic clip for the fixation of TET tube in the current study, suggesting that one clip could also meet short-term treatment needs within 6 d. Therefore, it is recommended to use one endoscopic clip to fix the TET tube in patients who only need 1 to 2 FMTs and do not need a long-term intracolonic administration of drugs, because the increased number may not bring more benefits to the patient and, conversely, may increase medical costs. Although the retention time of the TET tube using four endoscopic clips was longer than that of three, the absence of statistical significance in the three to four is likely a type II error due to the small sample size.

The length of the TET tube inserted into the colon is affected by many factors. On the one hand, it may be related to age and height in physiology. On the other hand, it may be associated with the type of disease. For example, constipation may cause redundant colon or twisted colon. Nevertheless, chronic inflammatory diseases such as IBD may shorten the colon. Multivariate analysis demonstrated that height was an independent factor affecting the length of the TET tube inserted into the colon in adults. This result of our current study may be useful to guide inexperienced endoscopists to perform the TET procedure in the future. Then, the more physicians would bring more opportunities to more patients with better education and endoscopic technique[36]. Further large sample studies are still warranted to confirm this opinion, due to the lack of sample size of children in current results. Also, evidence remains to be obtained from the Western population.

There were several limitations in the current study. First, the lack of blinding of the assistant who gathered the data on pain scores may have exposed individual bias outcomes. Second, as the endoscopists had a different personal preference for the cap assisted method before, we could not exclude the possibility that the cecal intubation

time may have been affected by personal bias. However, we had used procedure randomization blocks in individual operators, and each colonoscopist would contribute equally in the two groups and the overall result should not be biased by the performance of individual colonoscopists. Third, due to the absence of withdrawal time, polyp and adenoma detection rate in this study, we still need further research to investigate the time for observation of the entire colon and the number of polyps and adenomas after placing a tube in the colon.

CONCLUSION

This study demonstrated for the first time that CC for the colonic TET procedure is a safe and less painful technique saving the cecal intubation time. However, further studies are needed in children aged 3-7 years and among the Western population.

ARTICLE HIGHLIGHTS

Research background

The design of colonic transendoscopic enteral tubing (TET) requires repeated colonoscopies, which increase procedure time and potential procedure-related risks. It is uncertain whether cap-assisted colonoscopy (CC) would facilitate the technical performance after inserting the TET tube into the intestinal lumen during the TET procedure.

Research motivation

We conducted a multicenter, prospective, and randomized controlled trial to ascertain whether CC could decrease the second cecal intubation time and bring potential benefits compared with regular colonoscopy (RC) during TET.

Research objectives

The aim of this study was to compare CC with RC in the second cecal intubation time among subjects undergoing colonic TET.

Research methods

This trial was performed at four centers. Subjects ≥ 7 years needing colonic TET were recruited from August 2018 to January 2020. All subjects were randomly assigned to the RC (n = 165) or CC (n = 166) group. Baseline characteristics including age, sex, body mass index, previous abdominal or pelvic surgery, and disease category were collected before colonic TET. The primary outcome was the second cecal intubation time. The secondary outcomes included TET success rate, maximum insertion pain score, single clip fixation time, purpose and retaining time of TET tube, length of TET tube inserted into the colon, and all procedure-related (serious) adverse events.

Research results

The median time of the second cecal intubation was significantly shorter for the CC group than RC (2.2 min *vs* 2.8 min; P < 0.001). In constipation patients, the median time of the second cecal intubation in group of CC (n = 50) was shorter than RC (n = 43) (2.6 min *vs* 3.8 min; P = 0.004). However, no difference was observed in the groups of CC (n = 42) and RC (n = 46) in ulcerative colitis patients (2.0 min *vs* 2.5 min; P = 0.152). The insertion pain score during the procedure in the group of CC (n = 14) was lower than that in RC (n = 19) in unsedated colonoscopies (3.8 ± 1.7 *vs* 5.4 ± 1.9; P = 0.015). Multivariate analysis revealed that only CC (OR = 2.250, 95%CI: 1.161-4.360; P = 0.016) was an independent factor affecting the second cecal intubation time in difficult colonoscopy. CC did not affect the colonic TET tube retention time and the length of the tube inserted into the colon. Moreover, multivariate analysis found that only endoscopic clip number (OR = 2.201, 95%CI: 1.541-3.143; P < 0.001) was an independent factor affecting the retention time. Height (OR = 1.144, 95%CI: 1.027-1.275; P = 0.014) was the only independent factor influencing the length of TET tube inserted into the colon in adults by multiple regression analysis.

Research conclusions

CC for the colonic TET procedure is a safe and less painful technique which is able to

save the cecal intubation time. Importantly, CC does not affect the safety and stability of the TET tube.

Research perspectives

Further studies are needed in children aged 3-7 years and the Western population.

ACKNOWLEDGEMENTS

We appreciate the kind help from Jie Zhang by providing data from China Microbiota Transplantation System (www.fmtbank.org), and gratitude goes to Dr. Cicilia Marcella for polishing the language in the manuscript.

REFERENCES

1 **McDonald LC**, Gerding DN, Johnson S, Bakken JS, Carroll KC, Coffin SE, Dubberke ER, Garey KW, Gould CV, Kelly C, Loo V, Shaklee Sammons J, Sandora TJ, Wilcox MH. Clinical Practice Guidelines for Clostridium difficile Infection in Adults and Children: 2017 Update by the Infectious Diseases Society of America (IDSA) and Society for Healthcare Epidemiology of America (SHEA). *Clin Infect Dis* 2018; **66**: 987-994 [PMID: 29562266 DOI: 10.1093/cid/ciy149]

2 **Costello SP**, Hughes PA, Waters O, Bryant RV, Vincent AD, Blatchford P, Katsikeros R, Makanyanga J, Campaniello MA, Mavrangelos C, Rosewarne CP, Bickley C, Peters C, Schoeman MN, Conlon MA, Roberts-Thomson IC, Andrews JM. Effect of Fecal Microbiota Transplantation on 8-Week Remission in Patients With Ulcerative Colitis: A Randomized Clinical Trial. *JAMA* 2019; **321**: 156-164 [PMID: 30644982 DOI: 10.1001/jama.2018.20046]

3 **Ding X**, Li Q, Li P, Zhang T, Cui B, Ji G, Lu X, Zhang F. Long-Term Safety and Efficacy of Fecal Microbiota Transplant in Active Ulcerative Colitis. *Drug Saf* 2019; **42**: 869-880 [PMID: 30972640 DOI: 10.1007/s40264-019-00809-2]

4 **Xiang L**, Ding X, Li Q, Wu X, Dai M, Long C, He Z, Cui B, Zhang F. Efficacy of faecal microbiota transplantation in Crohn's disease: a new target treatment? *MicrobBiotechnol* 2020; **13**: 760-769 [PMID: 31958884 DOI: 10.1111/1751-7915.13536]

5 **Ianiro G**, Masucci L, Quaranta G, Simonelli C, Lopetuso LR, Sanguinetti M, Gasbarrini A, Cammarota G. Randomised clinical trial: faecal microbiota transplantation by colonoscopy plus vancomycin for the treatment of severe refractory Clostridium difficile infection-single versus multiple infusions. *Aliment PharmacolTher* 2018; **48**: 152-159 [PMID: 29851107 DOI: 10.1111/apt.14816]

6 **Moayyedi P**, Surette MG, Kim PT, Libertucci J, Wolfe M, Onischi C, Armstrong D, Marshall JK, Kassam Z, Reinisch W, Lee CH. Fecal Microbiota Transplantation Induces Remission in Patients With Active Ulcerative Colitis in a Randomized Controlled Trial. *Gastroenterology* 2015; **149**: 102-109.e6 [PMID: 25857665 DOI: 10.1053/j.gastro.2015.04.001]

7 **Paramsothy S**, Kamm MA, Kaakoush NO, Walsh AJ, van den Bogaerde J, Samuel D, Leong RWL, Connor S, Ng W, Paramsothy R, Xuan W, Lin E, Mitchell HM, Borody TJ. Multidonor intensive faecal microbiota transplantation for active ulcerative colitis: a randomised placebo-controlled trial. *Lancet* 2017; **389**: 1218-1228 [PMID: 28214091 DOI: 10.1016/S0140-6736(17)30182-4]

8 **Quraishi MN**, Widlak M, Bhala N, Moore D, Price M, Sharma N, Iqbal TH. Systematic review with meta-analysis: the efficacy of faecal microbiota transplantation for the treatment of recurrent and refractory Clostridium difficile infection. *Aliment PharmacolTher* 2017; **46**: 479-493 [PMID: 28707337 DOI: 10.1111/apt.14201]

9 **Kassam Z**, Lee CH, Yuan Y, Hunt RH. Fecal microbiota transplantation for Clostridium difficile infection: systematic review and meta-analysis. *Am J Gastroenterol* 2013; **108**: 500-508 [PMID: 23511459 DOI: 10.1038/ajg.2013.59]

10 **Ianiro G**, Maida M, Burisch J, Simonelli C, Hold G, Ventimiglia M, Gasbarrini A, Cammarota G. Efficacy of different faecal microbiota transplantation protocols for *Clostridium difficile* infection: A systematic review and meta-analysis. *United European Gastroenterol J* 2018; **6**: 1232-1244 [PMID: 30288286 DOI: 10.1177/2050640618780762]

11 **Peng Z**, Xiang J, He Z, Zhang T, Xu L, Cui B, Li P, Huang G, Ji G, Nie Y, Wu K, Fan D, Zhang F. Colonic transendoscopic enteral tubing: A novel way of transplanting fecal microbiota. *EndoscInt Open* 2016; **4**: E610-E613 [PMID: 27556065 DOI: 10.1055/s-0042-105205]

12 **Zhang F**, Cui B, He X, Nie Y, Wu K, Fan D; FMT-standardization Study Group. Microbiota transplantation: concept, methodology and strategy for its modernization. *Protein Cell* 2018; **9**: 462-473 [PMID: 29691757 DOI: 10.1007/s13238-018-0541-8]

13 **Zhang F**, Zhang T, Zhu H, Borody TJ. Evolution of fecal microbiota transplantation in methodology and ethical issues. *CurrOpinPharmacol* 2019; **49**: 11-16 [PMID: 31059962 DOI: 10.1016/j.coph.2019.04.004]

14 **Huang HL**, Chen HT, Luo QL, Xu HM, He J, Li YQ, Zhou YL, Yao F, Nie YQ, Zhou YJ. Relief of irritable bowel syndrome by fecal microbiota transplantation is associated with changes in diversity and composition of the gut microbiota. *J Dig Dis* 2019; **20**: 401-408 [PMID: 31070838 DOI: 10.1111/1751-2980.12756]

15 **Wang JW**, Wang YK, Zhang F, Su YC, Wang JY, Wu DC, Hsu WH. Initial experience of fecal microbiota transplantation in gastrointestinal disease: A case series. *Kaohsiung J Med Sci* 2019; **35**: 566-571 [PMID: 31197926 DOI: 10.1002/kjm2.12094]

16 **Xie WR**, Yang XY, Xia HH, Wu LH, He XX. Hair regrowth following fecal microbiota transplantation in an

elderly patient with alopecia areata: A case report and review of the literature. *World J Clin Cases* 2019; **7**: 3074-3081 [PMID: 31624757 DOI: 10.12998/wjcc.v7.i19.3074]

17 **Chen HT**, Huang HL, Xu HM, Luo QL, He J, Li YQ, Zhou YL, Nie YQ, Zhou YJ. Fecal microbiota transplantation ameliorates active ulcerative colitis. *ExpTher Med* 2020; **19**: 2650-2660 [PMID: 32256746 DOI: 10.3892/etm.2020.8512]

18 **Allegretti JR**, Mullish BH, Kelly C, Fischer M. The evolution of the use of faecal microbiota transplantation and emerging therapeutic indications. *Lancet* 2019; **394**: 420-431 [PMID: 31379333 DOI: 10.1016/S0140-6736(19)31266-8]

19 **Fecal Microbiota Transplantation-standardization Study Group**. Nanjing consensus on methodology of washed microbiota transplantation. *Chin Med J (Engl)* 2020 [PMID: 32701590 DOI: 10.1097/CM9.0000000000000954]

20 **Rastogi A**. Cap-assisted colonoscopy. *GastroenterolClin North Am* 2013; **42**: 479-489 [PMID: 23931855 DOI: 10.1016/j.gtc.2013.05.008]

21 **Morgan J**, Thomas K, Lee-Robichaud H, Nelson RL, Braungart S. Transparent cap colonoscopy versus standard colonoscopy to improve caecal intubation. *Cochrane Database Syst Rev* 2012; **12**: CD008211 [PMID: 23235654 DOI: 10.1002/14651858.CD008211.pub3]

22 **Lee YT**, Lai LH, Hui AJ, Wong VW, Ching JY, Wong GL, Wu JC, Chan HL, Leung WK, Lau JY, Sung JJ, Chan FK. Efficacy of cap-assisted colonoscopy in comparison with regular colonoscopy: a randomized controlled trial. *Am J Gastroenterol* 2009; **104**: 41-46 [PMID: 19098847 DOI: 10.1038/ajg.2008.56]

23 **Kim HH**, Park SJ, Park MI, Moon W, Kim SE. Transparent-cap-fitted colonoscopy shows higher performance with cecal intubation time in difficult cases. *World J Gastroenterol* 2012; **18**: 1953-1958 [PMID: 22563177 DOI: 10.3748/wjg.v18.i16.1953]

24 **Zhang T**, Long C, Cui B, Buch H, Wen Q, Li Q, Ding X, Ji G, Zhang F. Colonic transendoscopic tube-delivered enteral therapy (with video): a prospective study. *BMC Gastroenterol* 2020; **20**: 135 [PMID: 32375675 DOI: 10.1186/s12876-020-01285-0]

25 **Mearin F**, Lacy BE, Chang L, Chey WD, Lembo AJ, Simren M, Spiller R. Bowel Disorders. *Gastroenterology* 2016; Epub ahead of print [PMID: 27144627 DOI: 10.1053/j.gastro.2016.02.031]

26 **Ng SC**, Tsoi KK, Hirai HW, Lee YT, Wu JC, Sung JJ, Chan FK, Lau JY. The efficacy of cap-assisted colonoscopy in polyp detection and cecal intubation: a meta-analysis of randomized controlled trials. *Am J Gastroenterol* 2012; **107**: 1165-1173 [PMID: 22664471 DOI: 10.1038/ajg.2012.135]

27 **Nutalapati V**, Kanakadandi V, Desai M, Olyaee M, Rastogi A. Cap-assisted colonoscopy: a meta-analysis of high-quality randomized controlled trials. *EndoscInt Open* 2018; **6**: E1214-E1223 [PMID: 30302379 DOI: 10.1055/a-0650-4258]

28 **von Renteln D**, Robertson DJ, Bensen S, Pohl H. Prolonged cecal insertion time is associated with decreased adenoma detection. *GastrointestEndosc* 2017; **85**: 574-580 [PMID: 27590962 DOI: 10.1016/j.gie.2016.08.021]

29 **Park HJ**, Hong JH, Kim HS, Kim BR, Park SY, Jo KW, Kim JW. Predictive factors affecting cecal intubation failure in colonoscopy trainees. *BMC Med Educ* 2013; **13**: 5 [PMID: 23331720 DOI: 10.1186/1472-6920-13-5]

30 **Tseng CW**, Koo M, Hsieh YH. Cecal intubation time between cap-assisted water exchange and water exchange colonoscopy: a randomized-controlled trial. *Eur J GastroenterolHepatol* 2017; **29**: 1296-1302 [PMID: 28857895 DOI: 10.1097/MEG.0000000000000954]

31 **Tada M**, Inoue H, Yabata E, Okabe S, Endo M. Feasibility of the transparent cap-fitted colonoscope for screening and mucosal resection. *Dis Colon Rectum* 1997; **40**: 618-621 [PMID: 9152195 DOI: 10.1007/bf02055390]

32 **de Wijkerslooth TR**, Stoop EM, Bossuyt PM, Mathus-Vliegen EM, Dees J, Tytgat KM, van Leerdam ME, Fockens P, Kuipers EJ, Dekker E. Adenoma detection with cap-assisted colonoscopy versus regular colonoscopy: a randomised controlled trial. *Gut* 2012; **61**: 1426-1434 [PMID: 22187070 DOI: 10.1136/gutjnl-2011-301327]

33 **Shida T**, Katsuura Y, Teramoto O, Kaiho M, Takano S, Yoshidome H, Miyazaki M. Transparent hood attached to the colonoscope: does it really work for all types of colonoscopes? *SurgEndosc* 2008; **22**: 2654-2658 [PMID: 18297353 DOI: 10.1007/s00464-008-9790-6]

34 **Harada Y**, Hirasawa D, Fujita N, Noda Y, Kobayashi G, Ishida K, Yonechi M, Ito K, Suzuki T, Sugawara T, Horaguchi J, Takasawa O, Obana T, Oohira T, Onochi K, Kanno Y, Kuroha M, Iwai W. Impact of a transparent hood on the performance of total colonoscopy: a randomized controlled trial. *GastrointestEndosc* 2009; **69**: 637-644 [PMID: 19251004 DOI: 10.1016/j.gie.2008.08.029]

35 **Morgan JL**, Thomas K, Braungart S, Nelson RL. Transparent cap colonoscopy versus standard colonoscopy: a systematic review and meta-analysis. *Tech Coloproctol* 2013; **17**: 353-360 [PMID: 23371422 DOI: 10.1007/s10151-013-0974-2]

36 **Zhong M**, Sun Y, Wang HG, Marcella C, Cui BT, Miao YL, Zhang FM. Awareness and attitude of fecal microbiota transplantation through transendoscopic enteral tubing among inflammatory bowel disease patients. *World J Clin Cases* 2020; **8**: 3786-3796 [PMID: 32953854 DOI: 10.12998/wjcc.v8.i17.3786]

Published by **Baishideng Publishing Group Inc**
7041 Koll Center Parkway, Suite 160, Pleasanton, CA 94566, USA
Telephone: +1-925-3991568
E-mail: bpgoffice@wjgnet.com
Help Desk: https://www.f6publishing.com/helpdesk
https://www.wjgnet.com